Macromolecules Containing Metal and Metal-Like Elements

Volume 4

Group IVA Polymers

Edited by

Alaa S. Abd-El-Aziz
Department of Chemistry, The University of Winnipeg, Winnipeg, Manitoba, Canada

Charles E. Carraher, Jr.
Department of Chemistry and Biochemistry, Florida Atlantic University, Boca Raton, Florida

Charles U. Pittman, Jr.
Department of Chemistry, Mississippi State University, Mississippi State, Mississippi

Martel Zeldin
Department of Chemistry, Hobart and William Smith Colleges, Geneva, New York

WILEY-INTERSCIENCE
A John Wiley & Sons, Inc., Publication

Macromolecules Containing Metal and Metal-Like Elements

Volume 4

Macromolecules Containing Metal and Metal-Like Elements

Volume 4

Group IVA Polymers

Edited by

Alaa S. Abd-El-Aziz
Department of Chemistry, The University of Winnipeg, Winnipeg, Manitoba, Canada

Charles E. Carraher, Jr.
Department of Chemistry and Biochemistry, Florida Atlantic University, Boca Raton, Florida

Charles U. Pittman, Jr.
Department of Chemistry, Mississippi State University, Mississippi State, Mississippi

Martel Zeldin
Department of Chemistry, Hobart and William Smith Colleges, Geneva, New York

WILEY-INTERSCIENCE
A John Wiley & Sons, Inc., Publication

Published by John Wiley & Sons, Inc., Hoboken, New Jersey.
Published simultaneously in Canada.

Library of Congress Cataloging-in-Publication Data:

ISBN 0-471-68238-1
ISSN 1545-438X

Printed in the United States of America

10 9 8 7 6 5 4 3 2 1

Contributors

Alaa S. Abd-El-Aziz, Department of Chemistry, The University of Winnipeg, Winnipeg, Manitoba, Canada R3B 2E9 (a.abdelaziz@uwinnipeg.ca)

Charles E. Carraher, Jr., Florida Atlantic University, Boca Raton, FL 33431 and Florida Center for Environmental Studies, Palm Beach Gardens, FL 33410 (carraher@fau.edu)

Junwu Chen, Department of Chemistry, Institute of Nano Science and Technology, Open Laboratory of Chirotechnology, and Center for Display Research, Hong Kong University of Science and Technology, Clear Water Bay, Kowloon, Hong Kong, China

Stephen J. Clarson, Department of Chemical and Materials Engineering, University of Cincinnati, Cincinnati, OH 45221-0012

Hongchen Dong, Department of Chemistry, Institute of Nano Science and Technology, Open Laboratory of Chirotechnology, and Center for Display Research, Hong Kong University of Science and Technology, Clear Water Bay, Kowloon, Hong Kong, China

Sakuntala Chatterjee Ganguly, SAKCHEM, Consultant, 357A Invermay Road, Mowbray, Tasmania, Australia and Polymer Science Group, Ian Wark Research Institute, University of South Australia, Adelaide, South Australia

Chang-Sik Ha, Department of Polymer Science and Engineering, Pusan National University, Pusan 609-735, South Korea (csha@pusan.ac.kr)

Il Kim, Department of Polymer Science and Engineering, Pusan National University, Pusan 609-735, South Korea

Jacky W.Y. Lam, Department of Chemistry, Institute of Nano Science and Technology, Open Laboratory of Chirotechnology, and Center for Display Research, Hong Kong University of Science and Technology, Clear Water Bay, Kowloon, Hong Kong, China

Guizhi Li, Department of Chemistry, Mississippi State University, Mississippi State, MS 39762

Siddarth V. Patwandhan, Department of Chemistry and Materials Engineering, University of Cincinnati, Cincinnati, OH

Charles U. Pittman, Jr., Department of Chemistry, Mississippi State University, Mississippi State, MS 39762 (cpittman@ra.msstate.edu)

Edward Rosenberg, Department of Chemistry, University of Montana, Missoula, MT 59812 (ed.rosenberg@umontana.edu)

Ben Zhong Tang, Department of Chemistry, Institute of Nano Science and Technology, Open Laboratory of Chirotechnology, and Center for Display Research, Hong Kong University of Science and Technology, Clear Water Bay, Kowloon, Hong Kong, China (tangbenz@ust.hk)

Mohammad A. Wahab, Department of Polymer Science and Engineering, Pusan National University, Pusan 609-735, South Korea

Martel Zeldin, Department of Chemistry, Hobart and William Smith Colleges, Geneva, NY

Ronghua Zheng, Department of Chemistry, Institute of Nano Science and Technology, Open Laboratory of Chirotechnology, and Center for Display Research, Hong Kong University of Science and Technology, Clear Water Bay, Kowloon, Hong Kong, China

Contents

Preface

The Group IVA elements represent the most dramatic transition from non-metallic (carbon), to metal-like (silicon and germanium), to metallic (tin and lead) of any family. Organosilicon polymers are the most widely used metal-like materials and organotin compounds are the most frequently employed organometallic materials. Polysiloxanes are widely utilized as biomaterials while organotin compounds are widely employed because of their bioactivity. Polysilanes, polygermanes, and polystannanes are being increasingly investigated because of their unique conducting properties. This volume contains comprehensive review chapters covering germanium, tin, and lead polymers as well as reviews that illustrate the breadth of materials offered by polymers containing Group IVA metals and metal-like elements. Material referring to Group IVA containing polymers, including silicon, was previously covered in Volume 1 of this series. A future volume will focus on silicon-containing macromolecules.

Alaa S. Abd-El-Aziz
Charles E. Carraher, Jr.
Charles U. Pittman, Jr.
Martel Zeldin

Series Preface

Most traditional macromolecules are composed of less than 10 elements (mainly C, H, N, O, S, P, Cl, F), whereas metal and semi-metal-containing polymers allow properties that can be gained through the inclusion of nearly 100 additional elements. Macromolecules containing metal and metal-like elements are widespread in nature with metalloenzymes supplying a number of essential physiological functions including respiration, photosynthesis, energy transfer, and metal ion storage.

Polysiloxanes (silicones) are one of the most studied classes of polymers. They exhibit a variety of useful properties not common to non-metal-containing macromolecules. They are characterized by combinations of chemical, mechanical, electrical, and other properties that, when taken together, are not found in any other commercially available class of materials. The initial footprints on the moon were made by polysiloxanes. Polysiloxanes are currently sold as high-performance caulks, lubricants, antifoaming agents, window gaskets, O-rings, contact lens, and numerous and variable human biological implants and prosthetics, to mention just a few of their applications.

The variety of macromolecules containing metal and metal-like elements is extremely large, not only because of the larger number of metallic and metalloid elements, but also because of the diversity of available oxidation states, the use of combinations of different metals, the ability to include a plethora of organic moieties, and so on. The appearance of new macromolecules containing metal and metal-like elements has been enormous since the early 1950s, with the number increasing explosively since the early 1990s. These new macromolecules represent marriages among many disciplines, including chemistry, biochemistry, materials science, engineering, biomedical science, and physics. These materials also form bridges between ceramics, organic, inorganic, natural and synthetic, alloys, and metallic materials. As a result, new materials with specially designated properties have been made as composites, single- and multiple-site catalysts, biologically active/inert materials, smart materials, nanomaterials, and materials with superior conducting, nonlinear optical, tensile strength, flame retardant, chemical inertness, superior solvent resistance, thermal stability, solvent resistant, and other properties.

There also exist a variety of syntheses, stabilities, and characteristics, which are unique to each particular material. Further, macromolecules containing metal and metal-like elements can be produced in a variety of geometries, including linear, two-dimensional, three-dimensional, dendritic, and star arrays.

In this book series, macromolecules containing metal and metal-like elements will be defined as large structures where the metal and metalloid atoms are (largely) covalently bonded into the macromolecular network within or pendant to the polymer

backbone. This includes various coordination polymers where combinations of ionic, sigma-, and pi-bonding interactions are present. Organometallic macromolecules are materials that contain both organic and metal components. For the purposes of this series, we will define metal-like elements to include both the metalloids as well as materials that are metal-like in at least one important physical characteristic such as electrical conductance. Thus the term includes macromolecules containing boron, silicon, germanium, arsenic, and antimony as well as materials such as poly(sulfur nitride), conducting carbon nanotubes, polyphosphazenes, and polyacetylenes.

The metal and metalloid-containing macromolecules that are covered in this series will be essential materials for the twenty-first century. The first volume is an overview of the discovery and development of these substances. Succeeding volumes will focus on thematic reviews of areas included within the scope of metallic and metalloid-containing macromolecules.

Alaa S. Abd-El-Aziz
Charles E. Carraher, Jr.
Charles U. Pittman, Jr.
John E. Sheats
Martel Zeldin

CHAPTER 1

Overview-Group IVA Polymers

Charles E. Carraher Jr.

Department of Chemistry and Biochemistry, Florida Atlantic University, Boca Raton, Florida

Charles U. Pittman Jr.

Department of Chemistry, Mississippi State University, Mississippi State, Mississippi

Martel Zeldin

Department of Chemistry, Hobart and William Smith Colleges, Geneva, New York

Alaa S. Abd-El-Aziz

Department of Chemistry, The University of Winnipeg, Winnipeg, Manitoba, Canada

CONTENTS

Macromolecules Containing Metal and Metal-Like Elements, Volume 4: Group IVA Polymers, edited by Alaa S. Abd-El-Aziz, Charles E. Carraher Jr., Charles U. Pittman Jr., and Martel Zeldin
ISBN: 0-471-68238-1

I. INTRODUCTION

The chemistry of Group IVA (Group 14) organometallic monomeric[1–17] and polymeric[18–24] species has been described in great detail. Reaction mechanisms for these elements have also been described.[1,2]

The trend in chemical Group IVA behavior from nonmetallic to metallic elements is clearly evident in Group IV.[3] Carbon is non-metallic. Silicon and germanium are metalloids, and their monomers and polymers represent bridges in behavior between those of metallic tin and lead and those of non-metallic carbon. While this trend from non-metallic to metallic behavior is significant from the lighter to the heavier elements in this family, there is probably no more dramatic change than that between carbon and silicon. Generally, carbon is unable to expand its valence shell beyond the octet; however, the other elements in the family are know to experience hypervalency, presumably owing to the availability of valence shell *d* orbitals in Si and Ge and *d* and *f* orbitals for Sn and Pb, which are able to accept electrons from nucleophiles.

Significantly, the tendency toward catenation decreases precipitously from carbon to lead, which is evidenced by the existence of an enormous number of linear and branched polyalkanes, numerous polysilanes, some polygermanes, a few polystannanes, and no polyplumbanes. This behavior has been explained partially in terms of the decreasing strength of the catenated bond: i.e., C–C = 347 kJ/mol, Si–Si = 220 kJ/mol, Ge–Ge = 170 kJ/mol, and Sn–Sn = 150 kJ/mol, and other thermodynamic and kinetic considerations. Furthermore, the strength of single bonds between the Group IV and the other elements also decreases from the lighter to the heavier elements (Table 1), which to some extent parallels the covalent character of these bonds.

While most of the compounds of the Group IV elements are tetravalent, the trend toward divalency increases with atomic number. For example, stable C(II) compounds are unknown; however, Moser et al.[26] have recently prepared and identified a stable divalent silicon species, **1**. This subject has been reviewed.[27]

Table 1 Electronegativities, Covalent Radii, and Some Mean Bond Energies[a] (kJ/mol) for Group IV Elements

Element	C	Si	Ge	Sn	Pb
Electronegativity (Pauling)	2.54	1.90	2.01	1.96	2.33
Covalent Radius, nm	0.077	0.117	0.122	0.141	0.154
M–H	412	318	310	300	—
M–C	347	301	242	—	—
M–Cl	338	401	339	314	—
M–Br	276	310	280	270	—
M–I	238	230	210	190	—
M–O	360	466	—	540	—

[a] Mean bond energies are taken from several sources.[25]

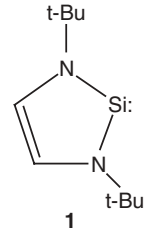

1

There is a difference between coordination number and oxidation number. For example, the general tendency is for tin in organotin compounds to have a formal oxidation number of 4. Nevertheless, it is common for inorganic and organotin compounds to have coordination numbers of 4, 5, and 6, with 4 and 6 prevailing. Furthermore, Sn(IV) compounds are more apt to form cations through ionization. Another trend for Sn(IV) compounds is their tendency in the solid state to form supramolecules in which the connective lengths between various units approximate internal covalent bonds, which qualify them as covalently bonded species that form linear, two-, and three-dimensional arrays. A similar tendency has been observed for the other non-carbon Group IV elements with an order Pb > Sn > Ge > Si that is related, at least in part, to the larger atoms being more capable of attracting neighboring atoms over a longer distance.[1–4]

While carbon readily forms (p-p) π multiple bonds with itself and other elements, this phenomenon is not achieved with the other Group IV elements beyond silicon. However, (d-p) π bonding does appear to occur for Si, Ge, and Sn. Thus for polymers such as polysiloxanes and polysilazanes unshared electrons on oxygen or nitrogen appear to "backbond" to the *3d* orbitals of silicon. This multiple bond character in Si–O and Si–N may play a significant role in the thermodynamic stability of these species. The use of vacant *d* orbitals is also indicated by some substitution reactions involving nucleophilic attack on tetrahedral metal atoms sites. For Si and Ge, reaction mechanisms analogous to the dissociative (e.g., S_N1) mechanisms in carbon compounds do not seem to occur readily. Rather, many Group IV organometals and organometalloids undergo substitution reactions via the associative pathway, which involves the formation of, for example, a five-coordinate transition state.[1,2] This subject has been recently reviewed by Eaborn.[2b] In general, most experimental and theoretical data are consistent with an order of availability of outer *d* orbitals of Pb > Sn > Ge > Si so that the larger metals are more apt to form 5- or 6-membered complexes (or transition states) as a prelude to associative interchanges.[1–4]

Hydrolysis of various silicon and germanium halides forms the synthetic basis for the formation of well-defined polysiloxanes and polygermoxanes. Most organolead halides are insoluble in water and are not as susceptible to hydrolysis. Organotin halides are often resistant to hydrolysis because of their general hydrophobic nature. Thus dibutyltin dichloride can be set in boiling water for hours with little indication that hydrolysis; however, hydrolysis does occur on addition of a wetting solvent such

as dimethyl sulfoxide (DMSO) or acetone. In such reactions, compounds with amazing structural diversity have been identified and characterized.[28]

II. GROUP IV POLYMERS

The order of commercial importance of Group IV metal-containing polymers is Si ⩾ Sn ⩾ Ge > Pb.[18–24] Although by number there are more organotin compounds used industrially, polysiloxanes represent the largest bulk use and net worldwide sales for organometallic polymers. Lead-containing polymers rank last in the Group IV series, owing to the lack of solubility of suitable monomers and, of course, their toxicity.

A general introduction of silicon-, germanium-, tin- and lead-containing polymers is presented in Chapter 6 of Volume 1 in this series.[19] A more extensive treatment of organogermanium, organotin, and organolead polymers is presented in this volume in Chapter 9, Chapter 10, and Chapter 11, respectively. The remainder of this volume (Chapters 2–8) focuses attention of special aspects and new developments in silicon-containing polymers.

Specifically, Chapter 2, by Zheng et al., is a discussion of the design and synthesis of a variety of soluble and thermally stable hyperbranched poly(silylenearylene)s via catalytic alkyne polycyclotrimerization reaction. Organosilicon hyperbranched polymers are promising candidates as functional ceramics, degradable templates, and high-temperature elastomers. The particular poly(silylenearylene)s prepared and discussed by the authors not only exhibit efficient photoluminescence with high quantum yields (~98%) but also display significant non-linear optical properties. In Chapter 3, Lam et al. discuss the synthesis, photoluminescence (aggregation-induced emission in poor solvents), and fabrication of light-emitting diodes of silole-containing conjugated polymers. In Chapter 4, Rosenberg provides a review of the synthesis, characterization, and study of the metal sequestering-ability of silica-polyamine composites. These materials can be used for metal ion recovery and remediation. Rosenberg evaluates these new composite materials in metal recovery from acid mine drainage, solvent extraction raffinates, and acid ore leaches.

Chapter 5 is a review of polyhedral oligomeric silsesquioxanes (POSS), hybrid POSS-organic copolymers, and POSS resin nanocomposites. Although silsesquioxanes have been known since the 1960s, only recently, through controlled synthesis and purification, have their structure and unique properties been determined and their useful applications been explored. This chapter is complemented by a discussion of the synthesis and properties of silica- and silsesquioxanes-containing polymer nanohybrids in Chapter 6. Chapter 7 involves a review of the preparation and characterization of siloxane-based polyviologens, polyurethanes, and divinylbenzene elastomers.

In Chapter 8, Patwardhan and Carlson delve into the use of proteins extracted from plants, such diatoms, grasses, and sponges, for the in vitro precipitation of

silica from silica precursors (e.g., tetraalkoxysilanes). Thus the extracted proteins serve as catalysts, templates, and/or scaffolds for the bioinspired synthesis of silica networks. The resulting spherical and non-spherical micro- and nano-size bioinspired silicas are compared using, for example, SEM techniques.

III. REFERENCES

1. M. Tobe, J. Burgess, *Inorganic Reaction Mechanisms*, Longman, New York, 1999.
2. (a) J. Atwood, *Inorganic and Organometallic Reaction Mechanism*, 2nd ed., VCH, New York, 1997; (b) C. Eaborn, *J. Chem. Soc.*, *Dalton Trans.* **23**, 3397 (2001); (c) R. G. Jones, W. Ando, J. Chojnowski, eds., *Silicon-Containing Polymers: The Science and Technology of Their Synthesis and Applications*, Kluwer Academic, Dordrecht, 2000.
3. F. A. Cotton, G. Wilkinson, *Advanced Inorganic Chemistry*, 5th ed., Wiley, New York, 1988.
4. G. Rayner-Canhan, *Descriptive Inorganic Chemistry*, Freeman, New York, 2000.
5. M. Henry, W. Davidson, in *Organotin Compounds*, Vol. 3, A. K. Sawyer, ed., Dekker, New York, 1972, chap. 13.
6. M. Hoch, *Applied Geochem*., **16**, 719 (2001).
7. A. Davies, *Organotin Chemistry*, Wiley-VCH, Chichester, 1997.
8. I. Omae, *Organotin Chemistry*, Elsevier, Amsterdam, 1989.
9. W. P. Neumann, *The Organic Chemistry of Tin*, Wiley, New York, 1970.
10. A. K. Sawyer, *Organotin Compounds*, Dekker, New York, 1971.
11. R. C. Poller, *The Chemistry of Organotin Compounds*, Logos Press, London, 1970.
12. J. Zuckerman, *Organotin Compounds: New Chemistry and Applications*, American Chemical Society, Washington, D.C., 1976.
13. T. Sato, *Main-Group Metal Organometallics in Organic Synthesis: Tin*, Pergamon, Oxford, 1995.
14. P. Harrison, in *Dictionary of Organometallic Compounds*, J. Macintyre, ed., Chapman & Hall, London, 1995.
15. S. Patai, *The Chemistry of Organic Germanium, Tin, and Lead Compounds*, Wiley, New York, 1995.
16. R. Ingham, H. Gilman, in *Organopolymers of Group IV Elements in Inorganic Polymers*, F. G. A. Stone, W. Graham, eds., Academic Press, New York, 1962, chap. 6.
17. M. Lesbre, P. Mazerolles, J. Satge, *The Organic Compounds of Germanium*, Wiley, New York, 1971.
18. R. Archer, *Inorganic and Organometallic Polymers*, Wiley, New York, 2001.
19. A. S. Abd-El-Aziz, C. Carraher, C. Pittman, J. Sheats, M. Zeldin, eds., *Macromolecules Containing Metal and Metal-like Elements, Vol. 1: A Half Century of Metal and Metalloid-Containing Polymers*, Wiley, Hoboken, NJ, 2003, chap. 6.
20. C. E. Carraher Jr., *Polymer Chemistry*, 6th ed., Dekker, New York, 2003.
21. M. Van Dyke, *Synthesis and Properties of Silicones and Silicone-Modified Materials*, American Chemical Society, Washington, D.C., 2003.
22. S. J. Clarson, *Silicones and Silicone-Modified Materials*, Oxford University Press, New York, 2000.
23. K. Jurkschat, M. Mehring, in *Organometallic Polymers of Germanium, Tin, and Lead*, Vol. 2, Z. Rappoport, ed., Wiley, New York, 2002, chap. 22.
24. R. Wei, L. Ya, W. Jinguo, X. Qifeng, in *Polymer Materials Encyclopedia*, J. Salamone, ed., CRC Press, Boca Raton, FL, p. 4826, 1996.

25. (a) R. T. Sanderson, *Chemical Bonds and Bond Energy*, 2nd ed., Academic Press, New York, 1976; (b) T. L. Cottrell, *The Strengths of Chemical Bonds*, 2nd ed. Buttterworths, London, 1958.

26. (a) D. F. Moser, T. Bosse, J. Olson, J. L. Moser, I. A. Guzei, R. West, *J. Am. Chem. Soc.*, **124**, 4186 (2002); (b) see also J. S. Becker, R. J. Staples, R. G. Gordon, *Cryst. Res. Techn*., **39**(1), 85 (2004).

27. (a) T. Kuehler, P. Jutzi, *Adv. Organometal. Chem*., **4**, 1 (2003); (b) N. Tokitoh, R. Okazaki, *Coord. Chem. Rev*., **210**, 251 (2000); (c) N. Tokitoh, Y. Matsuhashi, K. Shibata, T. Matsumoto, H. Suzuki, M. Saito, K. Manmaru, R. Okazaki, Renji, *Main Group Metal Chem*. **17**(1–4), 55 (1994).

28. V. Chandrasekhar, S. Nagendran, V. Baskar, *Coord. Chem. Rev*. **235**(1–2), 1 (2002).

CHAPTER 2

Hyperbranched Poly(silylenearylene)s

Ronghua Zheng, Hongchen Dong, and Ben Zhong Tang

Department of Chemistry, Institute of Nano Science and Technology, Open Laboratory of Chirotechnology, and Center for Display Research, Hong Kong University of Science and Technology, Clear Water Bay, Hong Kong, China

CONTENTS

Macromolecules Containing Metal and Metal-Like Elements, Volume 4: Group IVA Polymers, edited by Alaa S. Abd-El-Aziz, Charles E. Carraher Jr., Charles U. Pittman Jr., and Martel Zeldin
ISBN: 0-471-68238-1

I. INTRODUCTION

Hyperbranched polymers have attracted much attention because of their ease of synthesis by one-pot experimental procedures as well as their unique properties such as high solubility and excellent processibility.[1–5] Organosilicon hyperbranched polymers are organic–inorganic molecular hybrids and are promising candidates for functional ceramics, degradable templates, and high-temperature elastomers.[6–9] The hyperbranched silicon-containing polymers are usually prepared by hydrosilylation of AB_n monomers, where A and B represent functional groups of silane (Si–H) and olefin (–CH=CH_2) or acetylene (–C≡CH), respectively, with n being ≥2.

Our research group has been working on the designs and syntheses of hyperbranched polymers via alkyne polycyclotrimerizations. Through systematic investigations we have developed effective catalyst systems and optimized reaction conditions for the alkyne polycyclotrimerizations.[10–14] A large variety of functional

hyperbranched polyarylenes has been prepared by the homopolycyclotrimerizations of diynes as well as their copolycyclotrimerizations with monoynes.[15–20] These polymers are completely soluble in common solvents and are thermally very stable (up to ~500°C) and exhibit efficient photoluminescence (quantum yield up to 98%) and optical nonlinearity (strongly attenuating intense laser pulses).[10–20] In this chapter, we report on the syntheses of hyperbranched poly(silylenearylene)s by the homopolycyclotrimerizations of silylenediynes (Fig. 1). Their thermal and optical properties are also presented.

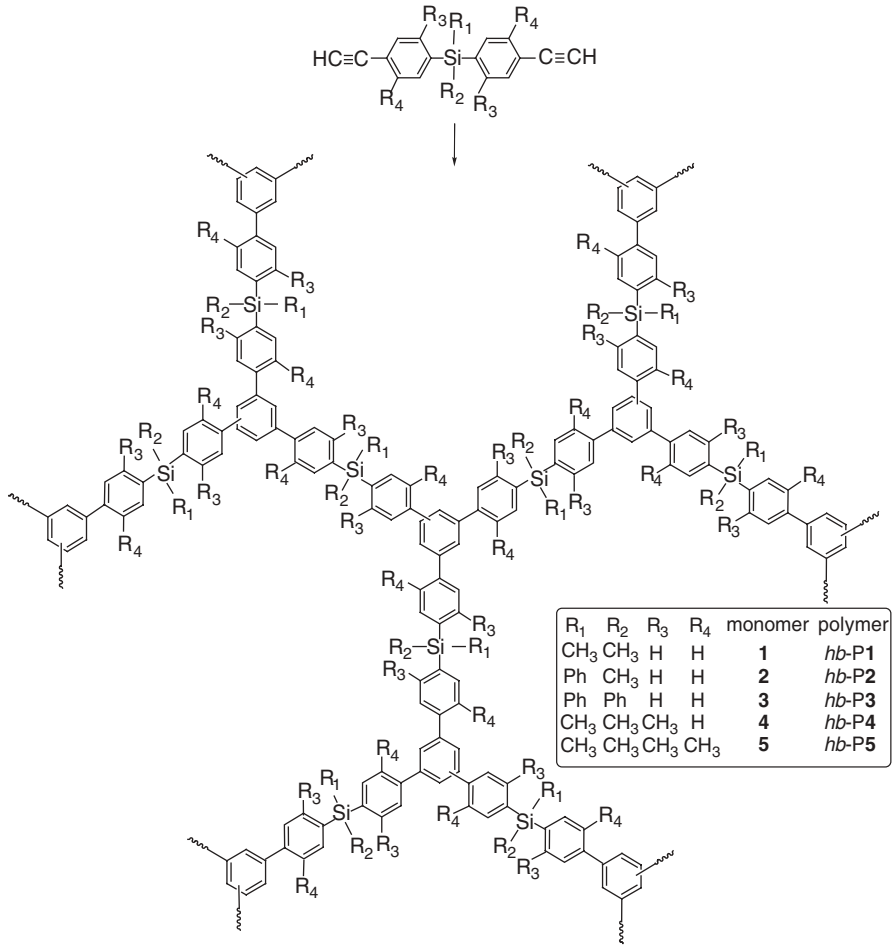

R_1	R_2	R_3	R_4	monomer	polymer
CH_3	CH_3	H	H	**1**	*hb*-P**1**
Ph	CH_3	H	H	**2**	*hb*-P**2**
Ph	Ph	H	H	**3**	*hb*-P**3**
CH_3	CH_3	CH_3	H	**4**	*hb*-P**4**
CH_3	CH_3	CH_3	CH_3	**5**	*hb*-P**5**

Figure 1 Syntheses of hyperbranched poly(silylenearylene)s.

II. RESULTS AND DISCUSSION

A. Monomer Synthesis

We prepared five monomers (**1–5**), taking the synthetic routes illustrated in Figure 2. Silylenediyne monomers **1–3** are prepared by palladium-catalyzed coupling of 1,4-dibromobenzene with trimethylsilylacetylene, followed by lithiation with *n*-butyllithium, silylation with dichlorosilanes and base-catalyzed cleavage of acetylenic trimethylsilyl group. Silylenediynes **4** and **5** are prepared by similar reactions, using substituted 1,4-dibromobenzenes as starting materials.

1,4-Dibromobenzene has two bromo groups with equal chemical reactivity. Its coupling with $(CH_3)_3SiC{\equiv}CH$ produces 33% of monosilylated compound **6** and a similar amount of disilylated derivative 1,4-bis(2-trimethylsilylethynyl)benzene. Lithiation of **6** by *n*-butyllithium gives 1-trimethylsilylethynyl-4-lithiobenzene, which is allowed to react in situ with dichlorodimethylsilane or dichloromethylphenylsilane to give **7** (78%) or **8** (69%) in high yield, although the reaction with dichloro-diphenylsilane gives **9** in a low yield (27%). The final products, i.e., monomers **1–3**, are isolated in yields of 52–86%. Monomers **1** and **3** are white powders, while **2** is a light yellow liquid. Monomers **4** and **5** are synthesized in an analogous

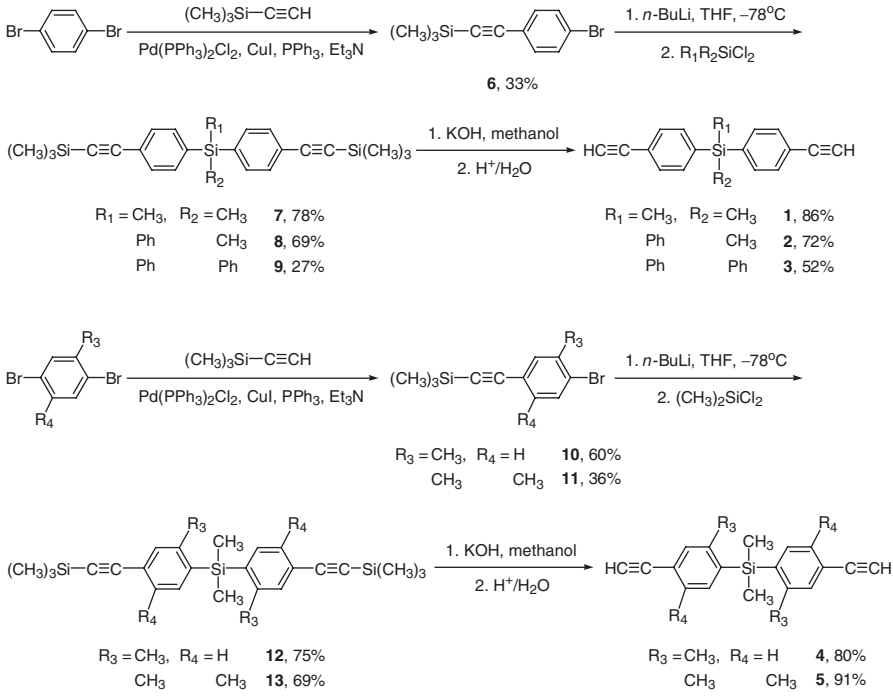

Figure 2 Syntheses of silylenediynes.

manner from 2,5-dibromotoluene and 1,4-dibromo-2,5-dimethylbenzene, respectively. Whereas the yield of **11** (36%) is similar to that of **6**, the yield of **10** is much higher (60%). The steric hinder of the ortho methyl group may have helped increase the amount of monocoupling of one of the two bromo groups with $(CH_3)_3SiC{\equiv}CH$. The desired final products (**4** and **5**) are isolated in yields of ≥80%. Monomers **4** and **5** are white and yellowish powders, respectively. All the monomers (**1–5**) are characterized by spectroscopic methods, from which satisfactory analysis data are obtained (see "IV. Experimental Section" for details).

B. Polymerization Behaviors

Table 1 summaries the results of polymerizations of **1** by different catalysts. $[Ir(cod)Cl]_2$–Ph_3P fails to catalyze the polymerization of **1**. $NbBr_5$ polymerizes **1** in a sluggish way, giving a polymer of a low molecular weight (M_w 9400) in a low yield (11%). $TaBr_5$ effectively catalyzes the polymerization of **1**: A polymer with a high molecular weight (48,600) is produced in a high yield (61%; Table 1, entry 4). The polymer is completely soluble in such common organic solvent as tetrahydrofuran (THF), toluene, dichloromethane, and chloroform. The concentration of monomer greatly affects its polymerization. When the concentration of monomer decreased from 0.1 to 0.03 M, only a trace amount of polymer is obtained (Table 1, entry 3). Increasing the catalyst concentration boosts the polymer yield to 100% but the polymer solubility is worsened (Table 1, entry 5). Addition of Ph_4Sn as a cocatalyst has little influence on the polymerization of **1** (Table 1, entry 6). At low monomer and catalyst concentrations, $CoCp(CO)_2$ does not yield any polymeric products. At higher concentrations, however, $CoCp(CO)_2$ changes to an effective

Table 1 Polymerization of Bis(4-ethynylphenyl)dimethylsilane (1)[a]

Entry Number	Catalyst	[Catalyst] (mM)	$[M]_0$ (M)	Time (h)	Yield (%)	S[b]	M_w^c	M_w/M_n^c
1	$[Ir(cod)Cl]_2$–Ph_3P	10.0	0.20	6	0			
2	$NbBr_5$	5.0	0.10	6	11	√	9,400	1.7
3	$TaBr_5$	5.0	0.03	6	Trace			
4	$TaBr_5$	5.0	0.10	6	61	√	48,600	3.2
5	$TaBr_5$	10.0	0.10	18	100	Δ		
6	$TaBr_5$-Ph_4Sn[d]	5.0	0.10	6	69	√	35,500	2.7
7	$CoCp(CO)_2$-$h\upsilon$	5.0	0.10	6	0			
8	$CoCp(CO)_2$-$h\upsilon$	15.0	0.50	24	28	√	11,800	1.4
9	$CoCp(CO)_2$-$h\upsilon$	30.6	0.58	24	28	√	5,600	3.4
10	$CoCp(CO)_2$-$h\upsilon$	15.0	0.50	24	11	√	8,100	1.8

[a] Carried out under nitrogen; solvent: toluene (entries 1–9), THF (entry 10); temperature: ~23°C (room temperature; entries 1–6), 65°C (entries 7–10).

[b] Solubility (S) tested in common organic solvents, such as THF, toluene, dichloromethane, and chloroform; symbols: √ = completely soluble, Δ = partially soluble.

[c] Measured by gel permeation chromatography (GPC) in THF on the basis of a polystyrene calibration.

[d] The molar ratio of $TaBr_5$ to Ph_4Sn is 1.0.

catalyst with the aid of UV radiation. The yield of polymer is 28% and its molecular weight is 11,800 (Table 1, entry 8). The molecular weight of the polymer decreases with a further increase in catalyst concentration. Solvent exerts some influences on the polymerization of **1**. When THF, instead of toluene, is used as polymerization solvent, the yield and molecular weight of the polymer are both decreased (Table 1, entry 10).

The polymerizations of monomers **2–5** were also investigated under different conditions, and the results are summarized in Table 2. $TaBr_5$ and $CoCp(CO)_2$-$h\upsilon$ effectively catalyze the polymerization of **2** (Table 2, entries 1, 2, 4, and 5). When the concentration of $TaBr_5$ is increased from 5.0 to 10.0 mM, the yield and molecular weight of polymer *hb*-P**2** are obviously increased (Table 2, entries 1 and 2). $NbCl_5$ polymerizes **2** to give a partially soluble polymer in 78% yield. Solvent has some effects on the polymerization of **2** catalyzed by $CoCp(CO)_2$-$h\upsilon$. The reaction carried out in toluene gives a polymer with a higher molecular weight in a higher yield, compared to that conducted in THF (Table 2, entries 4 and 5). The polymerization of monomer **3** produces high molecular weight polymer *hb*-P**3** ($M_w >$ 15,000) in the presence of $TaBr_5$ (Table 2, entries 6 and 7). The increase of $TaBr_5$ concentration from 5.0 to 10.0 mM increases the yield of the polymer from 17% to 62%.

The polymerization of monomers **4** and **5** are carried out in the presence of $TaBr_5$, $NbBr_5$, and $CoCp(CO)_2$-$h\upsilon$. The yield and molecular weight of polymer *hb*-P**4**

Table 2 Polymerization of Silylenediynes 2–5[a]

Entry Number	Monomer	Catalyst	[Catalyst] (mM)	$[M]_0$ (M)	Yield (%)	S[b]	M_w^c	M_w/M_n^c
1	**2**	$TaBr_5$	5.0	0.10	31	√	5,700	1.6
2	**2**	$TaBr_5$	10.0	0.10	80	√	42,200	3.5
3	**2**	$NbCl_5$	5.0	0.10	78	Δ		
4	**2**	$CoCp(CO)_2$-$h\upsilon$	15.0	0.50	9	√	3,500	1.4
5	**2**	$CoCp(CO)_2$-$h\upsilon$	15.0	0.50	27	√	8,300	1.8
6	**3**	$TaBr_5$	5.0	0.10	17	√	15,700	1.3
7	**3**	$TaBr_5$	10.0	0.10	62	√	23,500	1.5
8	**4**	$TaBr_5$	2.5	0.10	72	√	37,825	3.8
9	**4**	$TaBr_5$	5.0	0.10	99	√	39,200	3.4
10	**4**	$TaBr_5$	10.0	0.10	94	Δ		
11	**4**	$NbBr_5$	10.0	0.20	Trace			
12	**4**	$CoCp(CO)_2$-$h\upsilon$	15.0	0.50	16	√	4,800	2.7
13	**5**	$TaBr_5$	2.5	0.10	6	√	7,000	2.0
14	**5**	$TaBr_5$	5.0	0.10	39	√	15,100	2.2
15	**5**	$TaBr_5$	10.0	0.10	55	Δ		

[a] Carried out under nitrogen in toluene except for entry 4 (THF). For entries 1–3, 6–11, and 13–15, at room temperature for 6 h; for entries 4, 5, and 12, at 65°C for 24 h.

[b] Solubility (S) tested in common organic solvents such as THF, toluene, dichloromethane, and chloroform; symbols: √ = completely soluble, Δ = partially soluble.

[c] Measured by GPC in THF on the basis of a polystyrene calibration.

obtained from the $TaBr_5$-catalyzed polymerization under catalyst concentration of 2.5 and 5.0 mM are both high (Table 2, entries 8 and 9). Further increasing the catalyst concentration to 10.0 mM results in the formation of a partially soluble polymer (Table 2, entry 10). When $NbBr_5$ is used as the catalyst, only a trace amount of polymer is obtained. The polymerization of **4** catalyzed by $CoCp(CO)_2$-$h\upsilon$ produces a low molecular weight polymer (4800) in a low yield (16%). Monomer **5** is polymerized in the presence of $TaBr_5$ (Table 2, entries 13–15). The resultant polymers are completely soluble when the catalyst concentrations are $\leq$5.0 mM.

C. Structural Characterizations

The polymers are fully characterized by standard spectroscopic methods, including IR and ^1H, ^{13}C and ^{29}Si NMR. All the polymers give satisfactory spectroscopic data corresponding to their expected macromolecular structures (see "IV Experimental Section" for details). An example of the IR spectrum of *hb*-P**1** is given in Figure 3. The spectrum of its monomer (**1**) is also shown in the same figure for comparison. The strong band associated with ≡C–H stretching is observed at 3271 cm^{-1} in the spectrum of the monomer. This absorption band becomes weaker in the spectrum of its polymer, indicating that most of the triple bonds have been consumed by the polymerization reaction. Meanwhile, the absorption band of the aromatic –C=C– skeleton at 1595 cm^{-1} becomes stronger in the spectrum of the polymer, indicating that new aromatic rings have formed during the polymerization reaction.

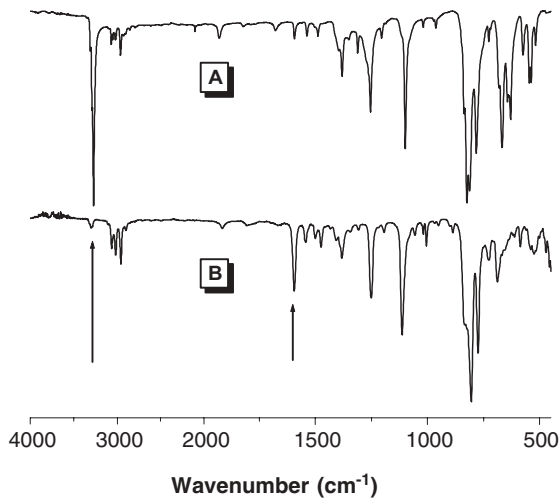

Figure 3 IR spectra of (A) monomer **1** and (B) its polymer *hb*-P**1** (sample taken from Table 1, entry 4).

Figure 4 shows the ^{1}H NMR spectra of *hb*-P**1** and its monomer (**1**). The resonance peak at δ 3.18 assigned to ≡C–H group of **1** becomes weaker in the spectrum of *hb*-P**1**, indicating that a large amount of triple bond has been consumed by the polymerization, with some triple bonds left in the polymer. The resonance peaks in the spectral region of aromatic protons become broader and intensified in the spectrum of polymer. The ^{13}C NMR spectra of the polymer and its monomer are shown in Figure 5. The resonance peaks of the triple bonds at δ 83.8 and 78.1 obviously become weaker and new peaks appear at the aromatic carbon resonance region in the spectrum of the polymer. This result is consistent with those of IR and ^{1}H NMR analyses, indicating that many triple bonds have been transformed and some small amounts of the triple bonds are left after the polymerization reaction.

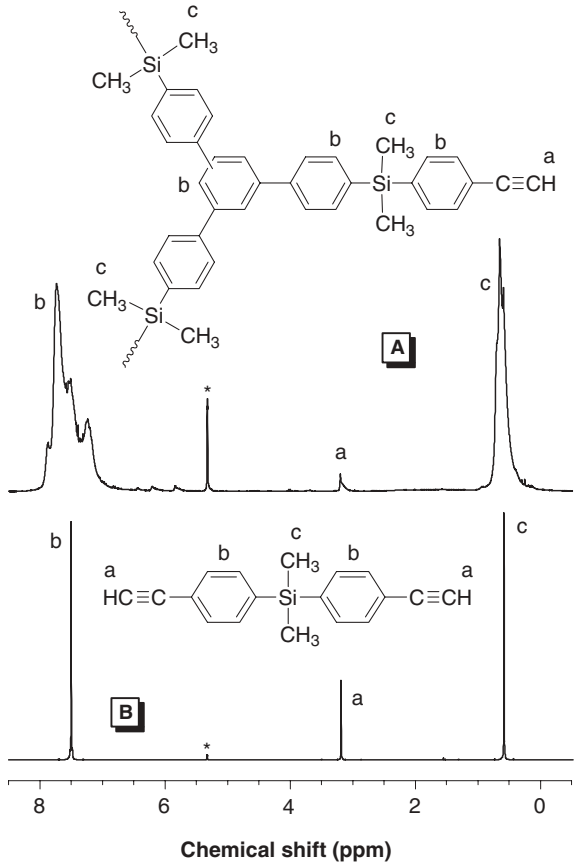

Figure 4 ^{1}H NMR spectra of dichlomethane-d_2 solutions of (A) polymer *hb*-P**1** (sample taken from Table 1, entry 4) and (B) its monomer **1**. The solvent peaks are marked with asterisks (*).

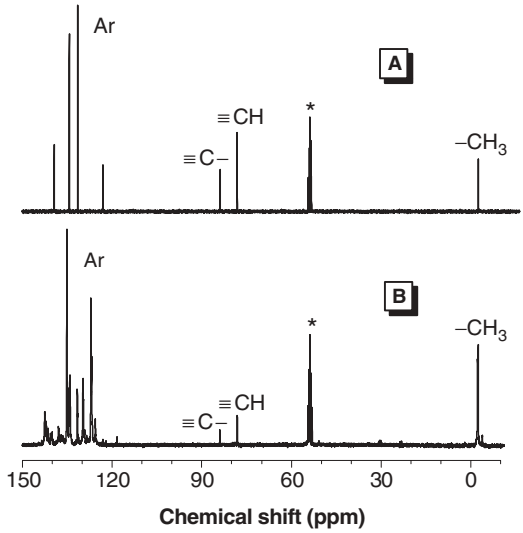

Figure 5 ^{13}C NMR spectra of dichlomethane-d_2 solutions of (A) monomer **1** and (B) its polymer *hb*-P**1** (sample taken from Table 1, entry 4). The solvent peaks are marked with asterisks (*).

^{29}Si NMR spectrum of the polymer offers more information about its structure. As can be seen from Figure 6, monomer **1** shows one peak resonating at δ – 7.26, which disappears in the spectrum of polymer *hb*-P**1**. Two broad peaks at δ – 7.54 and –7.83 are observed in the spectrum of the polymer. Based on the results of IR and NMR, it is certain that the chemical environments of the silicon atoms have been changed after the polymerization.

All the above spectroscopic data suggest that new aromatic rings have been formed during the polymerization reaction. The resonance signals of the newly formed aromatic rings in the IR and NMR spectra are, however, overlapped and disturbed by those of the "old" phenyl groups originally existing in the monomer structure. To provide more evidence for the formation of new aromatic rings in the polymer and to make the polymer structure clearer, we designed and conducted some model reactions. One is the reaction of phenylacetylene (**14**), a monoyne, catalyzed by $TaBr_5$ by the similar procedures used in the polymerizations of diynes **1**–**5** (Fig. 7). No high molecular weight polymers are precipitated when the reaction mixture is dropped into a large amount of methanol, unambiguously ruling out the possibility that the diynes may be polymerized by a metathesis mechanism in the presence of $TaBr_5$ catalyst.

The reaction products are purified by silica chromatography using hexane as eluent. The ^{1}H (Fig. 8*C*) and ^{13}C NMR spectra (Fig. 9*C*) prove that the products are a mixture of 1,2,4- and 1,3,5-triphenylbenzenes (**15**). Recrystallizations of the

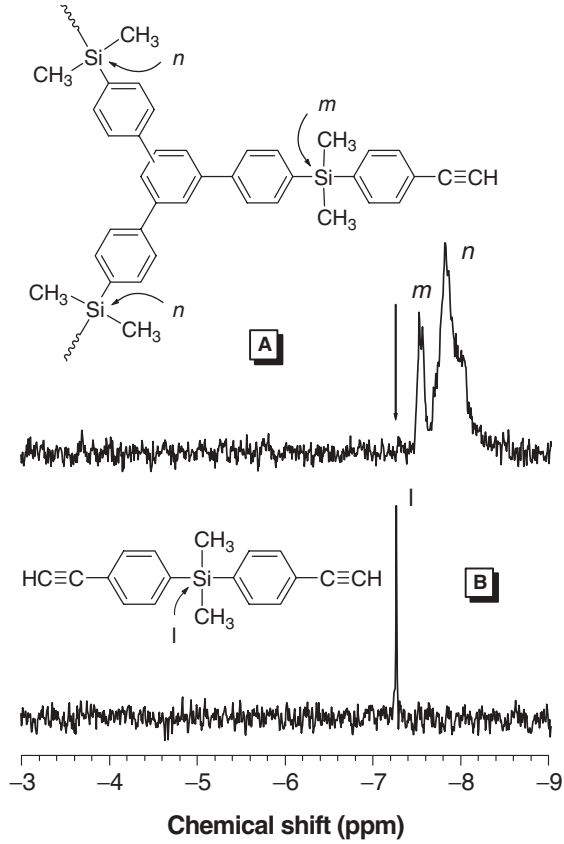

Figure 6 ^{29}Si NMR spectra of dichlomethane-d_2 solutions of (A) polymer *hb*-P**1** (sample taken from Table 1, entry 4) and (B) its monomer **1**.

products from ethanol and a mixture of ethanol/hexane give pure isomers of 1,3,5-**15** and 1,2,4-**15**, respectively. Their ^{1}H and ^{13}C NMR spectra are shown in panels *D* and *E* of Figures 8 and 9. These results verify that the $TaBr_5$-catalyzed polymerization has transformed three triple bonds into one phenylene ring through a cyclotrimerization mechanism. From the ^{1}H NMR spectra of the mixture of 1,3,5-**15** and 1,2,4-**15**, the molar ratio of 1,3,5-**15** to 1,2,4-**15** can be calculated according to equation 1. The calculated molar ratio of 1,3,5-**15** to 1,2,4-**15** is 1.0:2.0.

$$\frac{N_{1,2,4}}{N_{1,3,5}} = \frac{A_k/10}{A_g/3} = \frac{3A_k}{10A_g} \tag{1}$$

where $N_{1,2,4}$, is the number of 1,2,4-trisubstituted phenylene units; $N_{1,3,5}$, the number of 1,3,5-trisubstituted phenylene units; A_k, the integrated area of resonance peak k; and A_g, the integrated area of resonance peak g.

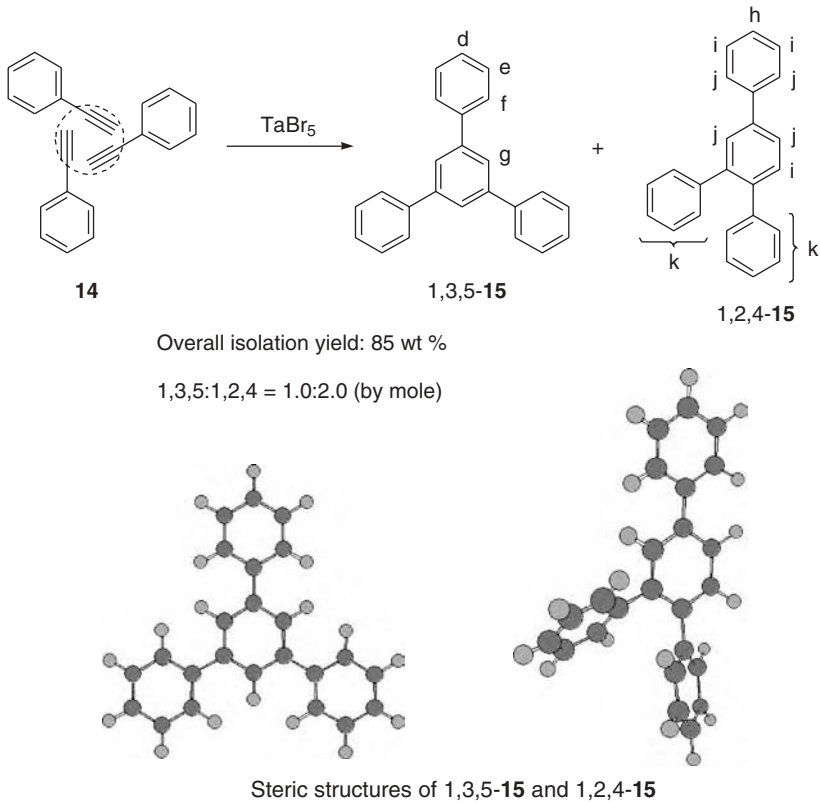

Figure 7 Cyclotrimerization of phenylacetylene (**14**) catalyzed by $TaBr_5$ and the stereochemical structures of 1,3,5- and 1,2,4- isomers of the resultant cyclic products of triphenylbenzenes (**15**).

Another model reaction we designed and conducted is the decomposition of the polymers. Strong protonic acids such as CF_3COOH, $HClO_4$, and H_2SO_4 are known to cleave Si–C bond.[21–23] When a mixture of *hb*-P**1** and CF_3COOH is heated at 60°C for 48 h, the polymer is decomposed, giving 71% yield of **15** (Fig. 10 and Table 3, entry 1). The identity of the major decomposition product of **15** is confirmed by IR, NMR, and mass spectroscopic analyses, examples of whose ^1H and ^{13}C NMR spectra are given in Figures 8*A* and 9*A*, respectively. These results further confirm that new phenylene rings have been formed in the $TaBr_5$-catalyzed polymerization of diyne **1**. Together with the results of model reaction of phenylacetylene cyclotrimerization, it can be concluded that diyne **1** has undergone alkyne polycyclotrimerization to give poly(silylenephenylene) in the presence of $TaBr_5$.

Like in the case of cyclotrimerization of the monoyne (phenylacetylene), the diyne polycyclotrimerizations should give rise to the formation of 1,3,5- and 1,2,4-substituted phenylene structures in the polymers. This is confirmed by the

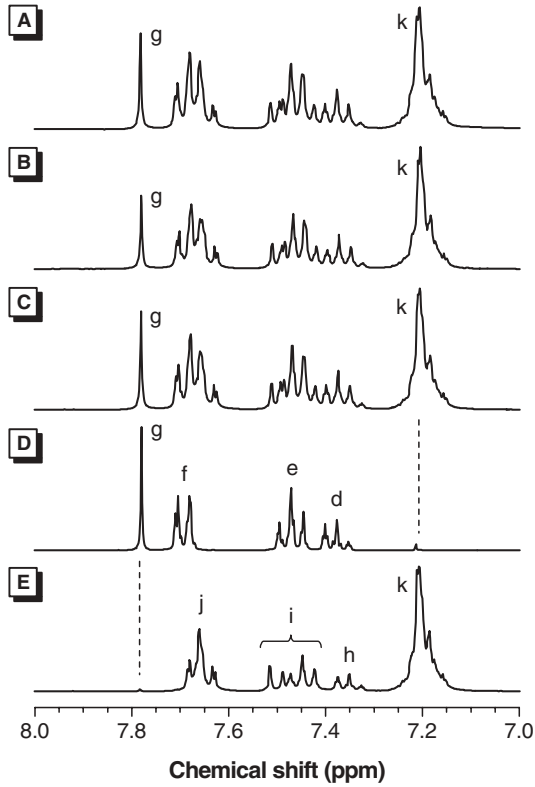

Figure 8 ^{1}H NMR spectra of (A) desilylated product of completely soluble polymer *hb*-P**1** (sample taken from Table 1, entry 4), (B) desilylated product of partially soluble polymer *hb*-P**1** (sample taken from Table 1, entry 5), (C) mixture of model compounds **15** (Fig. 7), (D) pure isomer 1,3,5-**15**, and (E) pure isomer 1,2,4-**15**.

degraded products of the polymer, which are consisted of stereoisomers of 1,3,5- and 1,2,4-triphenylbenzenes. Because most of the polymer had been decomposed in the presence of CF_3COOH, the contents of the 1,3,5- and 1,2,4-triphenylbenzenes represent those of 1,3,5- and 1,2,4-substituted phenylene structures in the polymer. From the ^{1}H NMR spectrum of the decomposition product of the soluble *hb*-P**1** (Fig. 5*A*), the contents of 1,3,5- and 1,2,4-triphenylbenzenes are calculated from equation 1. The molar ratio of 1,3,5- to 1,2,4-triphenylbenzenes is estimated to be 1.0:2.2. So the molar ratio of the newly formed 1,3,5- to 1,2,4-trisubstituted phenylene structures should be ~1.0:2.2 in *hb*-P**1**. The partially soluble *hb*-P**1** (Table 1, entry 5 and Table 3, entry 2) is also decomposed, and the degradation product **15** is isolated in 72% yield, the ^{1}H and ^{13}C NMR spectra of which are shown in Figures 5*B* and 6*B*. The calculated molar ratio of 1,3,5- to 1,2,4-triphenylbenzenes is

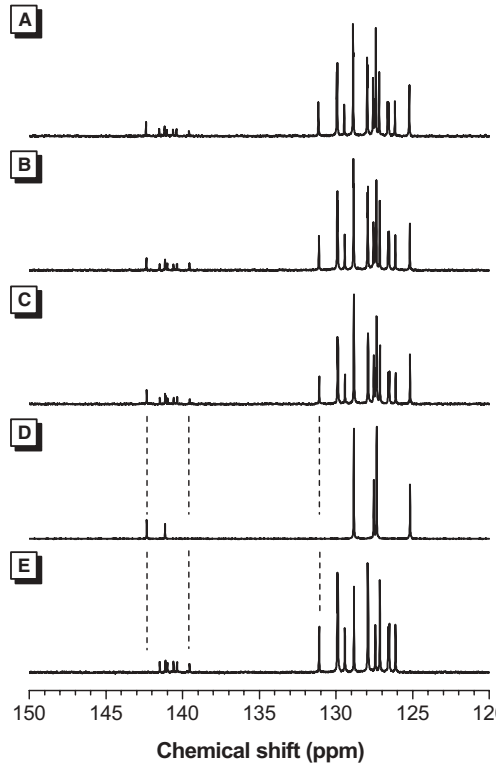

Figure 9 ^{13}C NMR spectra of (A) desilylated product of completely soluble polymer *hb*-P**1** (sample taken from Table 1, entry 4), (B) desilylated product of partially soluble polymer *hb*-P**1** (sample taken from Table 1, entry 5), (C) mixture of model compounds **15** (Fig. 7), (D) pure isomer 1,3,5-**15**, and (E) pure isomer 1,2,4-**15**.

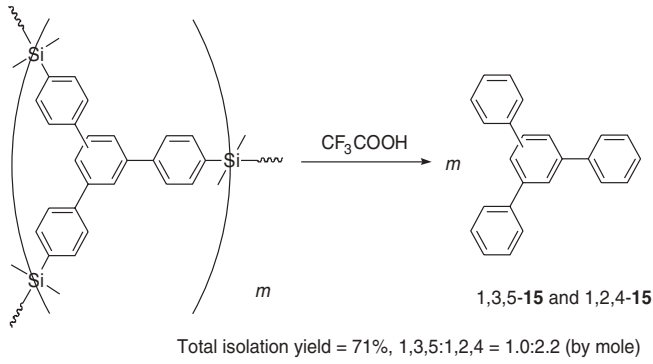

Figure 10 Decomposition of *hb*-P**1** (samples taken from Table 1, entry 4) by acid-catalyzed desilylation.

Table 3 Desilylation of Hyperbranched Poly(silylenearylene)s Catalyzed by CF_3COOH[a]

Entry Number	Polymer	W_0 (mg)	W_{15} (mg)	W_r (mg)	Yield of **15** (%)[b] Total	1,2,4-	1,3,5-
1	*hb*-P**1**(cs)	70.0	29.5	17.0	71	49	22
2	*hb*-P**1**(ps)	125.8	50.4	36.5	72	50	22

[a] *cs*, completely soluble; *ps*, partially soluble. Solubility of the polymer tested in common solvents such as THF, toluene, dichloromethane, and chloroform. W_0, initial weight of polymer used for desilylation; W_{15}, weight of desilylated product of **15**; W_r, weight of oligomeric residue.

[b] Calculated by the following equation:

$$\text{Yield} = \frac{W_{15}}{\frac{W_0 - W_r}{M_{ru}} \times M_{15}} = \frac{W_{15} \times M_{ru}}{(W_0 - W_r) \times M_{15}}$$

where M_{ru} and M_{15} are molar masses of the repeat unit of *hb*-P**1** (390.6) and model compound **15** (306.4), respectively.

1.0:2.3. The molar ratio of the newly formed 1,3,5- to 1,2,4-trisubstituted phenylene structures in the partially soluble *hb*-P**1** should thus be ~1.0:2.3, which is close to that in the soluble *hb*-P**1**.

From the above results, it becomes clear that the diynes have undergone polycyclotrimerizations to produce hyperbranched polymers. The polymer may thus contain three different units—namely, dendritic, linear, and terminal units (Fig. 11). Clearly the proton number of the newly formed phenyl ring is 3 for all three different units. The proton numbers of the triple bonds left are 0, 1, and 2 for the dendritic, linear, and terminal units, respectively. Assuming that the numbers of the dendritic, linear, and terminal units are N_D, N_L, and N_T, the total proton number of the newly formed phenyls (N_{Ph}) is $3N_D + 3N_L + 3N_T$, and that of the triple bonds left ($N_{C\equiv CH}$) is $N_L + 2N_T$. If no side reaction occurs in the polycyclotrimerization, it is easily understandable that the number of the dendritic units is equal to that of the terminal units when the molecular weight of the polymer is high enough, i.e., $N_D = N_T$.[24] The total proton number of newly formed phenyl is $3N_L + 6N_T$. The molar ratio of the total proton number of the newly formed phenyls to the total proton number of triple bonds left ($N_{Ph}/N_{C\equiv CH}$) is thus 3 (eq. 2). On the other hand, the total proton number of the newly formed phenyls represents the number of the consumed triple bonds ($N'_{C\equiv CH}$), i.e., $N_{Ph} = N'_{C\equiv CH}$. So the molar ratio of the consumed triple bonds to the unreacted triple bonds is 3, indicating that 25% of the triple bonds should be left after polycyclotrimerization (eq. 3). The ^1H NMR spectra of the polymers reveal that the numbers of the triple bonds left are evidently <25%. The number of the triple bonds left in polymer *hb*-P**1**, for example, is only 6%, as calculated from equation 4, where $UR_{C\equiv CH}$ is the molar fraction of unreacted ethynyl groups; A_{Me}, the integrated area of absorption peaks of methyl protons; A_{Ph}, the integrated area of absorption peaks of phenyl protons; and $A_{C\equiv CH}$, the integrated area of absorption peaks of ethynyl protons. This result

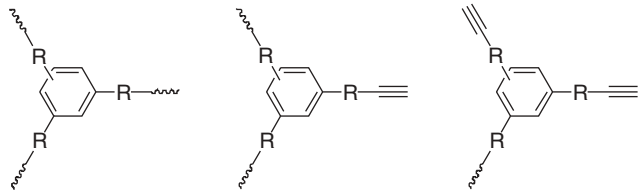

	dendritic unit (D)	linear unit (L)	terminal unit (T)
n_{Ph}[a]	3	3	3
$n_{C\equiv CH}$[b]	0	1	2

a. Number of protons of newly formed phenylene ring.

b. Number of protons of unreacted triple bond(s).

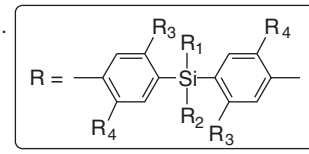

Figure 11 Dendritic, linear, and terminal units of hyperbranched poly(silylenephenylene)s.

suggests that intrasphere cyclotrimerization may be involved in the polycyclotrimerizations of the silylenediynes, which consumes the triple bonds during the polycyclotrimerizations.

$$\frac{N_{ph}}{N_{C\equiv CH}} = \frac{3N_D + 3N_L + 3N_T}{0N_D + 1N_L + 2N_T} = \frac{3N_L + 6N_T}{N_L + 2N_T} \tag{2}$$

$$\frac{N_{C\equiv CH}}{N'_{C\equiv CH} + N_{C\equiv CH}} = \frac{N_{C\equiv CH}}{N_{Ph} + N_{C\equiv CH}} = \frac{N_{C\equiv CH}}{4N_{C\equiv CH}} \tag{3}$$

$$UR_{C\equiv CH} = \frac{\frac{A_{Me}}{6}\times 2 - \left(A_{Ph} - \frac{A_{Me}}{6}\times 8\right)}{\frac{A_{Me}}{6}\times 2} = \frac{5A_{Me} - 3A_{Ph}}{A_{Me}} \tag{4}$$

Figure 12 shows possible pathways of branch growths in the silylenediyne polycyclotrimerization. The first pathway is a normal growth mode of p_1m_2 type, where p and m stand for polymer and monomer, respectively (eq. 5). The second is an intracyclotrimerization mode of p_2m_1 type, with two triple bonds from two polymer branches and one from a monomer (eq. 6). The third is another intracyclotrimerization mode of p_3 type, with three triple bonds all from polymer branches (eq. 7). The experimental results suggest that one or both of the intracyclotrimerizations must have been at play in the polycyclotrimerizations of the silylenediynes. The newly formed phenyl rings by these intracyclotrimerizations are, however, undistinguished

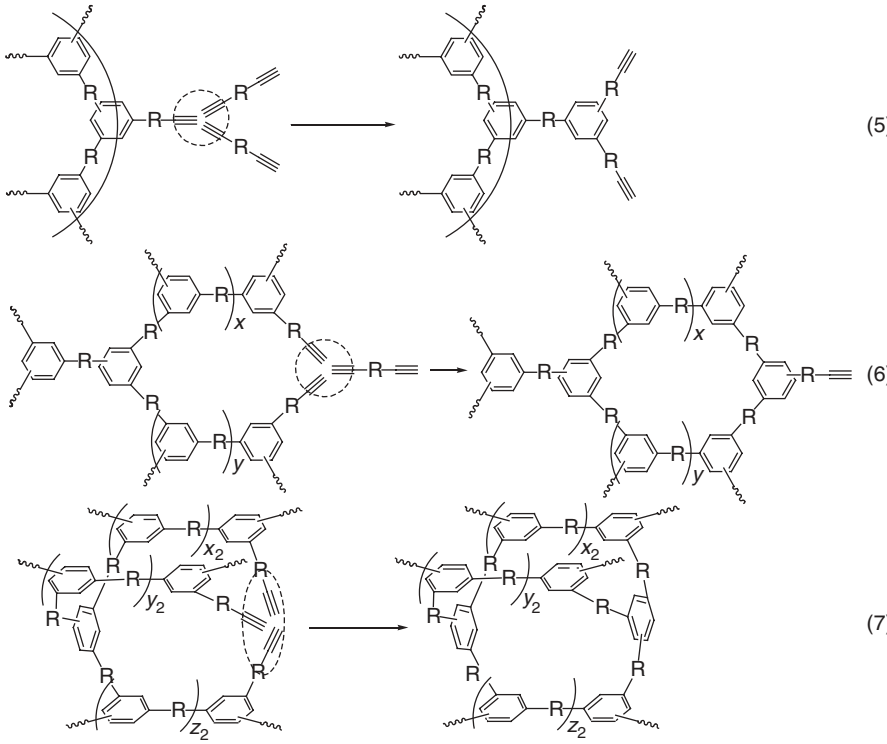

Figure 12 Propagation modes in the silylenediyne polycyclotrimerizations.

from each other and are also indistinct from those formed by the normal cyclotrimerization in the NMR spectra, making it difficult to calculate the probability of the intracyclotrimerization reactions.

To solve this problem, computational simulation method is employed. The models of the polymer structures are built, and the probabilities of the growth modes are estimated, using a Materials Studio program.[25] The models are optimized to minimize the energy of the structures, an example of which is shown in Figure 13. The structure is constructed from 72 monomers, representative of *hb*-P**1** according to its number-average molecular weight. It is found that the number of unreacted triple bonds is 15 in the model. We know that the total number of the triple bonds that might be used in the cyclotrimerization reaction is twice the consumed monomers, i.e., 144. The number of unreacted triple bonds thus accounts for 10% of the total number of the triple bonds. The ^{1}H NMR spectrum reveals that the number of the triple bonds left in the polymer is ~6% of the total number of the triple bonds. The simulated model is thus consistent with the real polymer. When the numbers of the three growth modes in the model are counted, it is found that the number of the normal cyclotrimerization reactions p_1m_2 is 28, whereas the numbers of the two

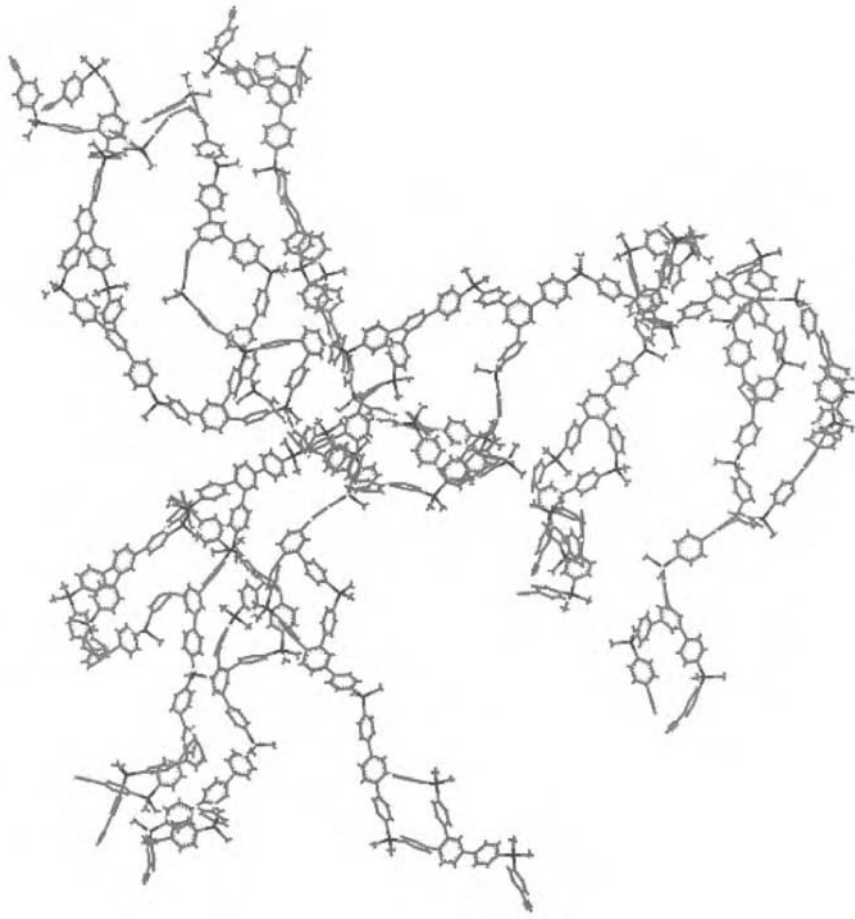

Figure 13 Three-dimensional macromolecular structure of *hb*-P**1** simulated by Materials Studio program.

intracyclotrimerizations p_2m_1 and p_3 are 15 and 1, respectively. A simple calculation thus gives the possibilities of 64%, 34%, and 2% for the growth modes of p_1m_2, p_2m_1, and p_3, respectively.

The number and size of the cycles formed via the intracyclotrimerization reactions p_2m_1 and p_3 shown in Figure 7 were counted. The total number of the cycles was found to be 16. Most of the cycles (14 cycles) are, however, small, being formed by two monomer units. The other two cycles are constructed from four and six monomer units, represented in two-dimensional space in Figure 14. The small cycles are strung together like beads on a necklace. This structure model is in good agreement with the excellent solubility of the polymer, although it contains many cyclic structures.

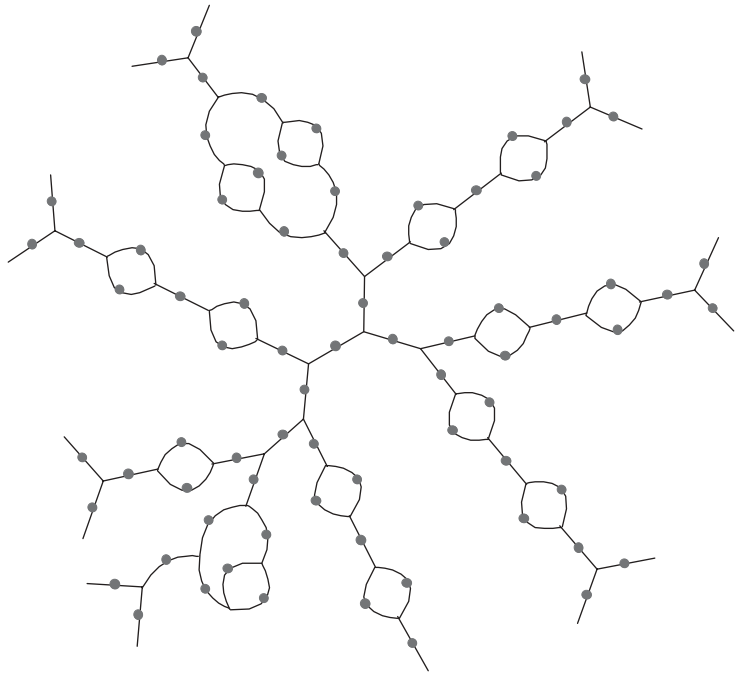

Figure 14 Simplified illustration of two-dimensional geometric structure of *hb*-P**1**.

D. Polymer Properties

The thermal properties of the hyperbranched polymers were investigated by thermogravimetric analysis (TGA). The results are summarized in Figure 15. All the polymers show excellent thermal stabilities. The weight losses of the polymers are $<5\%$ when heated to a temperature as high as 490°C. These results are consistent with their hyperbranched poly(silylenephenylene) structures, in which the polymers were knitted by the phenylene rings. Furthermore the residue weights of all the polymers are still $>59\%$ after pyrolysis at 900°C, with that of *hb*-P**2** being as high as 81%. These polymers are hence promising candidates as precursors of ceramic materials.

Figure 16 shows UV spectra of the polymers. All the monomers absorb at ~248 and 260 nm. However, the absorptions of polymers *hb*-P**1** and *hb*-P**4** shift to longer wavelength (~269 nm), probably caused by the extensive conjugation of the four phenylene rings in the repeat units of the polymers. In addition to their weak, sharp absorption peaks at ~260 nm, polymers *hb*-P**2** and *hb*-P**3** show strong, broad absorption peaks at ~269 nm, indicating the extensive conjugation of the four phenylene rings in the repeat units of the polymers. Polymer *hb*-P**5** absorbs at 258 nm,

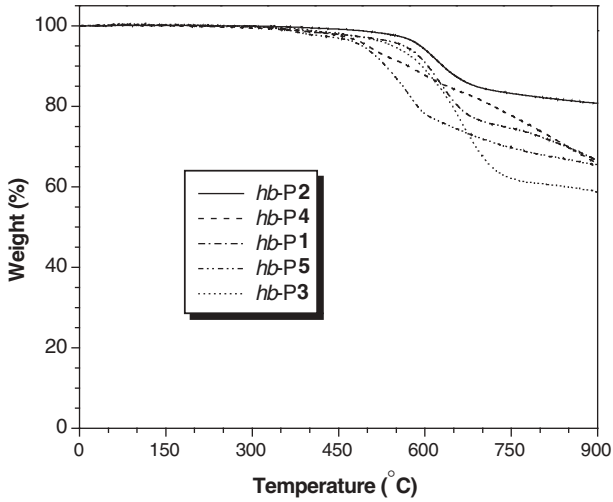

Figure 15 TGA thermograms of hyperbranched polymers *hb*-P**1** (sample taken from Table 1, entry 4), *hb*-P**2** (Table 2, entry 1), *hb*-P**3** (Table 2, entry 6), *hb*-P**4** (Table 2, entry 8), and *hb*-P**5** (Table 2, entry 14) recorded under nitrogen at a heating rate of 20°C/min.

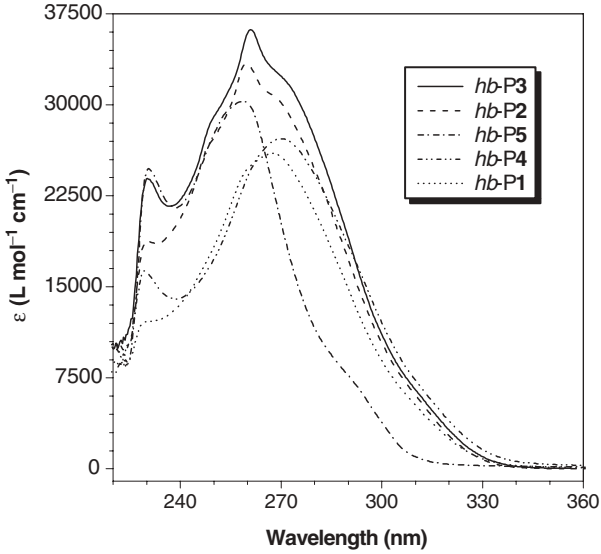

Figure 16 UV absorption spectra of dichloromethane solutions (5×10^{-5} M) of hyperbranched polymers *hb*-P**1** (sample taken from Table 1, entry 4), *hb*-P**2** (Table 2, entry 1), *hb*-P**3** (Table 2, entry 6), *hb*-P**4** (Table 2, entry 8), and *hb*-P**5** (Table 2, entry 14).

suggesting a poor conjugation of the phenylene rings in the polymer because of the steric hinder of the methyl groups. None of the polymers absorbs at wavelengths >340 nm, indicating that the conjugation is interrupted by the silicon atoms and is limited in the range of four phenylene rings.

Figure 17 shows the fluorescence spectra of the poly(silylenearylene)s. When exited at ~300 nm, the polymers emit somewhat structured photoluminescence. The emission peaks of *hb*-P**1**, *hb*-P**2**, *hb*-P**3**, and *hb*-P**4** are located at ~374 and ~392 nm. However, the emission peak of *hb*-P**5** appears at 347 nm, along with a shoulder peak at 391 nm. The difference in the emission peaks between *hb*-P**5** and other polymers may be caused by the poor conjugation of the four phenylene rings in *hb*-P**5**. The quantum yields of the polymers are 0.57–1.04% (Table 4).

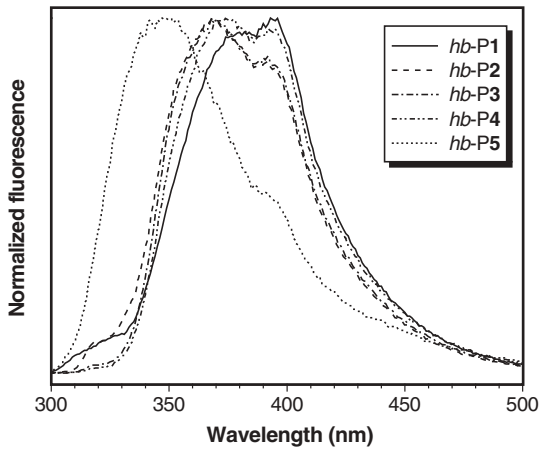

Figure 17 Fluorescence spectra of dichloromethane solutions (5×10^{-5} M) of hyperbranched polymers *hb*-P**1** (sample taken from Table 1, entry 4), *hb*-P**2** (Table 2, entry 1), *hb*-P**3** (Table 2, entry 6), *hb*-P**4** (Table 2, entry 8), and *hb*-P**5** (Table 2, entry 14).

Table 4 Optical Properties of Poly(silylenephenylene)s[a]

Entry Number	Polymer	λ_{ab} (nm)[b]	λ_{em} (nm)[c]	Φ_F (%)
1	*hb*-P**1**	231, 268	382, 393	1.04
2	*hb*-P**2**	231, 260 (*sw*), 269 (*bs*)	369, 392	0.82
3	*hb*-P**3**	230, 261 (*sw*), 269 (*bs*)	368, 392	1.02
4	*hb*-P**4**	230, 270	374, 392	0.57
5	*hb*-P**5**	231, 258	347, 391	0.96

[a] Measured in dichloromethane at room temperature; polymer concentration: 5×10^{-5} M.
[b] *sw*, sharp and weak; *bs*, broad and strong.
[c] Excitation wavelength: 299 (entry 1), 300 (entry 2), 299 (entry 3), 303 (entry 4), and 294 (entry 5).

III. CONCLUSIONS

In this work, we designed and synthesized silicon-containing diynes and their hyperbranched polymers. $TaBr_5$ effectively catalyzes the polymerizations of the diyne monomers. The resultant polymers are characterized by spectroscopic methods. It is confirmed that the polymers possess hyperbranched poly(silylenephenylene) structures formed through a polycyclotrimerization mechanism. The newly formed phenylene rings have 1,3,5- and 1,2,4-trisubstituted isomers, whose molar ratio is ~1.0:2.2. The terminal triple bonds of the hyperbranched polymers are much lower than expected because of the active intramolecular ring formation. The model of the polymer structure is simulated by Materials Studio program and the possibilities of three growth modes—p_1m_2, p_2m_1, and p_3—are estimated to be 64%, 34%, and 2%, respectively. All the polymers are thermally stable. Their weight losses are $<$5% even when heated to 490°C, and the residue weights of all the polymers are $>$59% after pyrolyzed at 900°C. The polymers are thus promising candidates as precursors to ceramic materials. When photoexcited at ~300 nm, the polymers emit UV light in the spectral region of 347–393 nm.

IV. EXPERIMENTAL SECTION

A. Materials and Instruments

Toluene and THF were distilled from sodium benzophenone ketyl before use. Tantalum bromide, niobium bromide, niobium chloride, cyclopentadienyl cobalt dicarbonyl, bis(1,5-cyclo-octadiene)diiridium(I) dichloride, tetraphenyltin, and triphenylphosphine were Aldrich products of the highest purities. All other reagents and solvents were purchased from Aldrich and used as received.

M_w and M_w/M_n were estimated by a Waters Associates GPC system in THF using monodisperse polystyrene as calibration standards. IR spectra were recorded on a Perkin-Elmer 16 PC FTIR spectrophotometer using pressed NaCl plates or dry thin films. ^1H and ^{13}C NMR spectra were measured on a Bruker ARX 300 NMR spectrometer using deuterated chloroform or dichloromethane as solvent and TMS as internal reference. ^{29}Si NMR spectra were measured on a Jeol 400 NMR spectrometer using chloroform-*d* as solvent and TMS as internal reference. UV spectra were measured on a Milton Ray Spectronic 3000 Array spectrophotometer. Fluorescence spectra were recorded in dichloromethane on a SLM 8000C spectrofluorometer. Thermogravimetric analyses were carried out on a Perkin-Elmer TGA 7 analyzer at a heating rate of 20°C/min under nitrogen.

B. Synthesis of (4-Bromophenylethynyl)trimethylsilane (6)

To a round-bottomed flask equipped with a septum and a stirring bar was placed 9.44 g (40 mmol) of 1,4-dibromobenzene. The flask was put into a glovebox and charged with 281 mg (0.4 mmol) dichlorobis(triphenylphosphine)palladium(II)

[$Pd(Ph_3P)_2Cl_2$], 19 mg (0.1 mmol) CuI, and 26 mg (0.1 mmol) triphenylphosphine [Ph_3P]. Dry triethylamine (Et_3N; 120 mL) was injected into the flask by a syringe. Under stirring, 6.73 mL (48 mmol, 4.71 g) of trimethylsilylacetylene [$(CH_3)_3$-SiC≡CH] was added. The mixture was continuously stirred at room temperature for 24 h. The formed precipitate was separated and washed with diethyl ether. The solutions were collected and the solvent was removed by evaporation. The obtained product was purified by a silica-gel column using hexane as eluent. White powdery (4-bromophenylethynyl)-trimethylsilane (**6**) was isolated in 33% yield (3.31 g). IR (thin film), ν (cm^{-1}): 2963, 2899 (CH_3 stretching), 2158 (–C≡C– stretching), 1895 (overtone band, disubstituted benzene ring), 1485, 1470 (CH_3 scissoring), 1246 (Si–CH_3 bending), 845 (Si–C stretching), 824 (Ar–*H* bending). ^{1}H NMR (300 MHz, $CDCl_3$), δ (TMS, ppm): 7.41 (*d,* 2H, Ar–H *ortho* to Br), 7.31 (*d,* 2H, Ar–H *meta* to Br), 0.24 (*s,* 9H, Si–CH_3). ^{13}C NMR (75 MHz, $CDCl_3$), δ (ppm): 133.2 (aromatic carbon *meta* to Br), 131.3 (aromatic carbon *ortho* to Br), 122.6 (aromatic carbon linked with Br), 122.0 (aromatic carbon *para* to Br), 103.8 (acetylenic carbon linked with aromatic ring), 95.5 (acetylenic carbon linked with Si), –0.02 (Si–CH_3).

C. Synthesis of (4-Bromo-3-methylphenylethynyl)-trimethylsilane (10)

Compound **10** was prepared from a reaction using 10.00 g (40 mmol) 2,5-dibromo-toluene, 281 mg (0.4 mmol) $Pd(Ph_3P)_2Cl_2$, 19 mg (0.1 mmol) CuI, 26 mg (0.1 mmol) Ph_3P, and 5.61 mL (40 mmol, 3.93 g) $(CH_3)_3SiC{\equiv}CH$ by the synthetic procedure similar to that described for the preparation of **6**. Yield: 6.41 g (60%), light yellow liquid. IR (thin film), ν (cm^{-1}): 2959, 2899 (CH_3 stretching), 2154 (–C≡C– stretching), 1474 (CH_3 scissoring), 1250 (Si–CH_3 bending), 1032 (Ar–H bending), 843 (Si–C stretching). ^{1}H NMR (300 MHz, $CDCl_3$), δ (TMS, ppm): 7.45 (*d,* H, Ar–H *ortho* to Br), 7.32 (*s,* H, Ar–H between –CH_3 and –C≡C), 7.12 (*d,* 1H, Ar–H *para* to –CH_3), 2.37 (*s,* 3H, –CH_3), 0.24 (*s,* 9H, Si–CH_3). ^{13}C NMR (75 MHz, $CDCl_3$), δ (ppm): 137.8 (aromatic carbon linked with –CH_3), 133.9 (aromatic carbon between –CH_3 and –C≡C), 132.1 (aromatic carbon *para* to –CH_3), 130.5 (aromatic carbon *ortho* to Br), 125.3 (aromatic carbon linked with Br), 122.2 (aromatic carbon *para* to Br), 104.1 (acetylenic carbon linked with aromatic ring), 94.9 (acetylenic carbon linked with Si), 22.7 (–CH_3), 0.01 (Si–CH_3).

D. Synthesis of (4-Bromo-2,5-dimethylphenylethynyl)-trimethylsilane (11)

Compound **11** was prepared from 10.56 g (40 mmol) 1,4-dibromo-2,5-dimethylbenzene, 281 mg (0.4 mmol) $Pd(Ph_3P)_2Cl_2$, 19 mg (0.1 mmol) CuI, 26 mg (0.1 mmol) Ph_3P, and 5.61 mL (40 mmol, 3.93 g) $HC{\equiv}CSiCH_3$ by the procedure similar to that for the synthesis of **6**. Yield: 4.01 g (36%), light yellow powder. IR (thin film), ν (cm^{-1}): 2959, 2896 (CH_3 stretching), 2156 (–C≡C– stretching), 1486, 1473 (CH_3 scissoring), 1249 (Si–CH_3 bending), 856 (Ar–H bending), 842 (Si–C stretching). ^{1}H NMR (300 MHz, $CDCl_3$), δ (TMS, ppm): 7.39 (*s,* H, Ar–H *ortho* to Br), 7.29 (*s,* H, Ar–H *meta* to Br), 2.37 (*s,* 3H, –CH_3 *ortho* to Br), 2.32 (*s,* 3H, –CH_3

meta to Br), 0.26 (*s,* 9H, Si–CH_3). ^{13}C NMR (75 MHz, $CDCl_3$), δ (ppm): 140.0 (aromatic carbon linked with –CH_3 and *ortho* to –C≡C), 135.3 (aromatic carbon linked with –CH_3 and *ortho* Br), 134.0 (aromatic carbon *meta* to Br), 133.3 (aromatic carbon *ortho* to Br), 125.2 (aromatic carbon linked with Br), 122.5 (aromatic carbon *para* to Br), 103.3 (acetylenic carbon linked with aromatic ring), 99.3 (acetylenic carbon linked with Si), 22.3 (–CH_3 *meta* to Br), 20.0 (–CH_3 *ortho* to Br), 0.10 (Si–CH_3).

E. Synthesis of Bis[4-(2-trimethylsilylethynyl)-phenyl]dimethylsilane (7)

To a nitrogen-flushed, round-bottomed flask equipped with a septum and a stirring bar were added 2.53 g (10.0 mmol) **6** and 100 mL THF. The flask was cooled to −78°C and a solution of *n*-butyllithium in hexane (4.2 mL, 2.5 M, 10.5 mmol) was added dropwise under vigorous stirring. After stirring for 0.5 h at −78°C, 0.6 mL (0.64 g, 5.0 mmol) dichlorodimethylsilane [$(CH_3)_2SiCl_2$] was slowly added. The mixture was then gradually warmed to room temperature and stirred overnight. After removing the solvent, a white powder was obtained. The crude product was dissolved in dichloromethane and then washed with water. The solution was collected, and the solvent was evaporated. The product was purified by silica chromatography using a mixture of hexane and chloroform (4:1 by volume) as eluent. White powdery bis(4-(2-trimethylsilylethynyl)phenyl)dimethylsilane (**7**) was isolated in 78% yield (1.57 g). IR (thin film), ν (cm^{-1}): 3066, 3011 (Ar–H stretching), 2960, 2900 (CH_3 stretching), 2159 (–C≡C– stretching), 1594, 1537, 1489 (–C=C– ring stretching), 1381 (CH_3 bending), 1251 (Si–CH_3 bending), 1106 (Si–Ph stretching), 842 (Si–C stretching), 824 (Ar–H bending). ^{1}H NMR (300 MHz, $CDCl_3$), δ (TMS, ppm): 7.41 (*s,* 8H, Ar–H), 0.52 [*s,* 6H, –$Si(CH_3)_2$], 0.25 [*s,* 18H, –$Si(CH_3)_3$]. ^{13}C NMR (75 MHz, $CDCl_3$), δ (ppm): 138.5 (aromatic carbon linked with Si), 133.8 (aromatic carbon *meta* to Si), 131.0 (aromatic carbon *ortho* to Si), 123.8 (aromatic carbon *para* to Si), 105.0 (acetylenic carbon linked with aromatic ring), 95.0 (acetylenic carbon linked with Si), 0.07 [–$Si(CH_3)_3$], −2.51 [–$Si(CH_3)_2$].

F. Synthesis of Bis[4-(2-trimethylsilylethynyl)-phenyl]methylphenylsilane (8)

Compound **8** was prepared from 3.44 g (13.6 mmol) **6**, 5.71 mL (2.5 M, 14.3 mmol) *n*-BuLi, and 1.11 mL (1.30 g, 6.8 mmol) dichloromethylphenylsilane by the procedure similar to that for the synthesis of **7**. Yield: 2.18 g (69%), colorless viscous liquid. IR (thin film), ν (cm^{-1}): 3068, 3015 (Ar–H stretching), 2959, 2899 (CH_3 stretching), 2158 (–C≡C– stretching), 1594, 1537, 1489 (–C=C– ring stretching), 1382 (CH_3 bending), 1250 (Si–CH_3 bending), 1109 (Si–Ph stretching), 864 (Ar–H bending), 843 (Si–C stretching). ^{1}H NMR (300 MHz, $CDCl_3$), δ (TMS, ppm): 7.46 (*m,* 13H, Ar–H), 0.85 (*s,* 3H, Si–CH_3), 0.28 [*s,* 18H, –$Si(CH_3)_3$]. ^{13}C NMR (75 MHz, $CDCl_3$), δ (ppm): 137.0, 135.5, 135.4, 135.3, 131.3, 130.0, 128.3, 124.5 (aromatic carbon), 105.2 (acetylenic carbon linked with aromatic ring), 95.6 (acetylenic carbon linked with Si), 0.10 [–$Si(CH_3)_3$], −3.49 (Si–CH_3).

G. Synthesis of Bis[4-(2-trimethylsilylethynyl)-phenyl]diphenylsilane (9)

Compound **9** was prepared from 2.23 g (8.7 mmol) **6**, 3.48 mL (2.5 M, 8.7 mmol) *n*-BuLi, and 0.90 mL (1.09 g, 4.3 mmol) dichlorodiphenylsilane by the procedure similar to that for the synthesis of **7**. Yield: 0.62 g (27%), white powder. IR (thin film), ν (cm^{-1}): 3069, 3013 (Ar–H stretching), 2959, 2898 (CH_3 stretching), 2158 (–C≡C– stretching), 1593, 1537, 1490 (–C=C– ring stretching), 1383 (CH_3 bending), 1250 (Si–CH_3 bending), 1107 (Si–Ph stretching), 863, 760, 700 (Ar–H bending), 843 (Si–C stretching). ^{1}H NMR (300 MHz, $CDCl_3$), δ (TMS, ppm): 7.46 (*m,* 18H, Ar–H), 0.24 [*s,* 18H, –Si(CH_3)$_3$]. ^{13}C NMR (75 MHz, $CDCl_3$), δ (ppm): 136.3, 136.1, 134.6, 133.3, 131.2, 129.8, 127.9, 124.4 (aromatic carbon), 104.9 (acetylenic carbon linked with aromatic ring), 95.5 (acetylenic carbon linked with Si), −0.07 [–Si(CH_3)$_3$].

H. Synthesis of Bis[2-methyl-4-(2-trimethylsilylethynyl)-phenyl]dimethylsilane (12)

Compound **12** was prepared from 2.67 g (10.0 mmol) **10**, 4.20 mL (2.5 M, 10.5 mmol) *n*-BuLi, and 0.61 mL (0.65 g, 5.0 mmol) dichlorodimethylsilane by the procedure similar to that for the synthesis of **7**. Yield: 1.63 g (75%), colorless viscous liquid. IR (thin film), ν (cm^{-1}): 2959, 2899 (CH_3 stretching), 2152 (–C≡C– stretching), 1595, 1533 (–C=C– ring stretching), 1383 (CH_3 bending), 1250 (Si–CH_3 bending), 947 (Si–Ph stretching), 857, 810 (Ar–H bending), 842 (Si–C stretching). ^{1}H NMR (300 MHz, $CDCl_3$), δ (TMS, ppm): 7.46 (*d,* 2H, Ar–H *ortho* to Si), 7.27 (*m,* 2H, Ar–*H para* to –CH_3), 7.23 (*s,* 2H, Ar–H between –C≡C– and –CH_3), 2.71 (*s,* 6H, –CH_3 linked with aromatic ring), 0.59 [*s,* 6H, –Si(CH_3)$_2$], 0.26 [*s,* 18H, –Si(CH_3)$_3$]. ^{13}C NMR (75 MHz, $CDCl_3$), δ (ppm): 144.2, 138.2, 135.0, 133.1, 128.5, 124.3 (aromatic carbon), 105.4 (acetylenic carbon linked with aromatic ring), 95.0 (acetylenic carbon linked with Si), 22.9 (–CH_3 linked with aromatic ring), 0.12 [–Si(CH_3)$_3$], −0.92 [–Si(CH_3)$_2$].

I. Synthesis of Bis[2,5-dimethyl-4-(2-trimethylsilylethynyl)-phenyl]dimethylsilane (13)

Compound **13** was prepared from 2.90 g (10.3 mmol) **11**, 4.34 mL (2.5 M, 10.8 mmol) *n*-BuLi, and 0.62 mL (0.67 g, 5.2 mmol) dichlorodimethylsilane by the procedure similar to that for the synthesis of **7**. Yield: 1.63 g (69%), white powder. IR (thin film), ν (cm^{-1}): 2959, 2896 (CH_3 stretching), 2149 (–C≡C– stretching), 1597, 1481 (–C=C– ring stretching), 1382 (CH_3 bending), 1249 (Si–CH_3 bending), 1015 (Si–Ph stretching), 859, 819 (Ar–H bending), 841 (Si–C stretching). ^{1}H NMR (300 MHz, $CDCl_3$), δ (TMS, ppm): 7.28 (*s,* 2H, Ar–H *meta* to Si), 7.18 (*s,* 2H, Ar–*H ortho* to Si), 2.39 (*s,* 6H, –CH_3 linked with aromatic ring and *meta* to Si), 2.06 (*s,* 6H, –CH_3 linked with aromatic ring and *ortho* to Si), 0.55 [*s,* 6H, –Si(CH_3)$_2$], 0.25 [*s,* 18H, –Si(CH_3)$_3$]. ^{13}C NMR (75 MHz, $CDCl_3$), δ (ppm): 140.6, 137.9, 136.6, 135.5, 132.9, 123.6 (aromatic carbon), 104.1 (acetylenic carbon linked with

aromatic ring), 98.5 (acetylenic carbon linked with Si), 22.2, 20.2 ($-CH_3$ linked with aromatic ring), 0.12 [$-Si(CH_3)_3$], −0.97 [$-Si(CH_3)_2$].

J. Synthesis of Bis(4-ethynylphenyl)dimethylsilane (1)

To a round-bottomed flask equipped with a septum and a stirring bar were added 1.78 g (4.4 mmol) **7**, 400 mL methanol, and 61.5 mg (1.1 mmol) KOH. The mixture was heated at 50°C for 3 h and was then poured into 1000 mL of 1 M HCl solution. The mixture was extracted by chloroform four times. The organic layer was collected and the solvent was removed by evaporation. The crude product was purified by silica column chromatography using a mixture of hexane and chloroform [3:1 (v/v)] as eluent. White powdery bis(4-ethynylphenyl)dimethylsilane (**1**) was isolated in 86% yield (0.98 g). IR (thin film), ν (cm^{-1}): 3271 (≡C–H stretching), 3068, 3021 (Ar–H stretching), 2962, 2897 (CH_3 stretching), 2105 (–C≡C– stretching), 1929, 1822 (overtone band, substituted benzene ring), 1594, 1538, 1489 (–C=C– ring stretching), 1381 (CH_3 bending), 1254 ($Si–CH_3$ bending), 1100 (Si–Ph stretching), 824 (Si–C stretching), 813 (Ar–H bending). ^{1}H NMR (300 MHz, $CDCl_3$), δ (TMS, ppm): 7.50 (*s,* 8H, Ar–H), 3.18 (*s,* 2H, ≡C–H), 0.58 [*s,* 6H, $-Si(CH_3)_2$]. ^{13}C NMR (75 MHz, $CDCl_3$), δ (ppm): 139.4 (aromatic carbon linked with Si), 134.3 (aromatic carbon *meta* to Si), 131.5 (aromatic carbon *ortho* to Si), 123.1 (aromatic carbon *para* to Si), 83.8 (acetylenic carbon linked with aromatic ring), 78.1 (acetylenic carbon linked with H), −2.57 [$-Si(CH_3)_2$]. UV (DCM, 2.5×10^{-5} mol/L), λ_{max}(nm)/ε_{max}(mol^{-1} L cm^{-1}): 247/44184, 259/51852.

K. Synthesis of Bis(4-ethynylphenyl)methylphenylsilane (2)

Monomer **2** was prepared from 2.95 g (6.3 mmol) **8** by the procedure similar to that for the synthesis of **1**. Yield: 1.47 g (72%), light yellow viscous liquid. IR (thin film), ν (cm^{-1}): 3294 (≡C–H stretching), 3068, 3011 (Ar–H stretching), 2959 (CH_3 stretching), 2104 (–C≡C– stretching), 1923, 1816 (overtone band, substituted benzene ring), 1594, 1538, 1488 (–C=C– ring stretching), 1428, 1380 (CH_3 bending), 1254 ($Si–CH_3$ bending), 1102 (Si–Ph stretching), 825 (Si–C stretching), 798 (Ar–H bending). ^{1}H NMR (300 MHz, $CDCl_3$), δ (TMS, ppm): 7.49 (*m,* 13H, Ar–H), 3.19 (*s,* 2H, ≡C–H), 0.86 (*s,* 3H, $Si–CH_3$). ^{13}C NMR (75 MHz, $CDCl_3$), δ (ppm): 137.3, 135.4, 135.3, 135.2, 131.6, 130.0, 128.3, 123.4 (aromatic carbon), 83.7 (acetylenic carbon linked with aromatic ring), 78.3 (acetylenic carbon linked with H), −3.56 ($Si–CH_3$). UV (DCM, 2.5×10^{-5} mol/L), λ_{max}(nm)/ε_{max}(mol^{-1} L cm^{-1}): 248/46048, 259/50444.

L. Synthesis of Bis(4-ethynylphenyl)diphenylsilane (3)

Monomer **3** was prepared from 1.87 g (3.5 mmol) **9** by the procedure similar to that for the synthesis of **1**. Yield: 0.70 g (52%), white powder. IR (thin film), ν (cm^{-1}): 3294 (≡C–H stretching), 3068, 3013 (Ar–H stretching), 2104 (–C≡C– stretching), 1594, 1536, 1488 (–C=C– ring stretching), 1428, 1102 (Si–Ph stretching), 700 (Ar–H bending). ^{1}H NMR (300 MHz, $CDCl_3$), δ (TMS, ppm): 7.50 (*m,* 18H, Ar–H),

3.12 (*s,* 2H, ≡C–H). ^{13}C NMR (75 MHz, $CDCl_3$), δ (ppm): 136.3, 136.1, 135.0, 133.1, 131.4, 129.9, 128.0, 123.4 (aromatic carbon), 83.5 (acetylenic carbon linked with aromatic ring), 78.3 (acetylenic carbon linked with H). UV (DCM, 2.5×10^{-5} mol/L), λ_{max}(nm)/ε_{max}(mol^{-1} L cm^{-1}): 249/50400, 261/54044.

M. Synthesis of Bis(4-ethynyl-2-methylphenyl)-dimethylsilane (4)

Monomer **4** was prepared from 2.00 g (4.6 mmol) **12** by the procedure similar to that for the synthesis of **1**. Yield: 1.06 g (80%), white powder. IR (thin film), ν (cm^{-1}): 3286 (≡C–H stretching), 2960 (CH_3 stretching), 2107 (–C≡C– stretching), 1593, 1533 (–C=C– ring stretching), 1383 (CH_3 bending), 1253 (Si–CH_3 bending), 834 (Si–C stretching), 809 (Ar–H bending). ^{1}H NMR (300 MHz, $CDCl_3$), δ (TMS, ppm): 7.48 (*d,* 2H, Ar–H *ortho* to Si), 7.31 (*d,* 2H, Ar–H *para* to –CH_3), 7.27 (*s,* 2H, Ar–H between –C≡CH and –CH_3), 3.15 (*s,* 2H, ≡C–H), 2.16 (*s,* 6H, –CH_3 linked with aromatic ring), 0.62 (*s,* 6H, –Si(CH_3)$_2$). ^{13}C NMR (75 MHz, $CDCl_3$), δ (ppm): 144.3, 138.5, 135.0, 133.3, 128.8, 123.2 (aromatic carbon), 83.9 (acetylenic carbon linked with aromatic ring), 77.8 (acetylenic carbon linked with H), 22.9 (–CH_3 linked with aromatic ring), −0.96 [–Si(CH_3)$_2$]. UV (DCM, 2.5×10^{-5} mol/L), λ_{max}(nm)/ ε_{max}(mol^{-1} L cm^{-1}): 250/41572, 261/49384.

N. Synthesis of Bis(2,5-dimethyl-4-ethynylphenyl)-dimethylsilane (5)

Monomer **5** was prepared from 1.50 g (3.3 mmol) **13** by the procedure similar to that for the synthesis of **1**. Yield: 0.94 g (91%), light yellow powder. IR (thin film), ν (cm^{-1}): 3292 (≡C–H stretching), 2956, 2865 (CH_3 stretching), 2102 (–C≡C– stretching), 1479 (–C=C– ring stretching), 1450, 1381 (CH_3 bending), 1250 (Si–CH_3 bending), 1002 (Si–Ph stretching), 833 (Si–C stretching), 817 (Ar–H bending). ^{1}H NMR (300 MHz, $CDCl_3$), δ (TMS, ppm): 7.31 (*s,* 2H, Ar–H *meta* to Si), 7.21 (*s,* 2H, Ar–H *ortho* to Si), 3.26 (*s,* 2H, ≡C–H), 2.41 (*s,* 6H, –CH_3 linked with aromatic ring and *meta* to Si), 2.09 (*s,* 6H, –CH_3 linked with aromatic ring and *ortho* to Si), 0.57 (*s,* 6H, –Si(CH_3)$_2$). ^{13}C NMR (75 MHz, $CDCl_3$), δ (ppm): 140.7, 138.1, 136.8, 135.7, 133.3, 122.7 (aromatic carbon), 82.6 (acetylenic carbon linked with aromatic ring), 81.2 (acetylenic carbon linked with H), 22.2, 20.2 (–CH_3 linked with aromatic ring), −0.97 [–Si(CH_3)$_2$]. UV (DCM, 2.5×10^{-5} mol/L), λ_{max}(nm)/ ε_{max}(mol^{-1} L cm^{-1}): 253/36836, 261/44252.

O. Diyne Polycyclotrimerization

All polymerization reactions were carried out under dry nitrogen using standard Schlenk technique. A typical example of experimental procedure for the polycyclotrimerization of 1 is given here: To a thoroughly baked and carefully evacuated 15-mL Schlenk tube with a three-way stopcock on the sidearm was placed 14.5 mg (0.025 mmol) $TaBr_5$ under nitrogen in a glovebox. Then freshly distilled toluene

(4.0 mL) was injected into the tube using a hypodermic syringe and was stirred continuously for 5 min. A solution of 130.2 mg (0.50 mmol) 1 in 1.0 mL toluene was syringed into the catalyst solution. The polymerization mixture was stirred at room temperature under nitrogen for 6 h and was then stopped by the addition of a small amount of methanol. The solution was added dropwise into 300 mL methanol through a cotton filter under stirring. The precipitate was allowed to stand overnight and was then collected by filtration. The polymer was washed with methanol and dried under vacuum at room temperature to a constant weight.

P. Polymer Characterization

i. hb-P**1**

White powder. Yield: 61%. M_w: 48,600, M_w/M_n: 3.2 (GPC, Table 1, entry 4). IR (thin film), ν (cm^{-1}): 3297 (≡C–H stretching), 3063, 3017 (Ar–H stretching), 2955, 2896 (CH_3 stretching), 1915, 1808 (overtone band, substituted benzene ring), 1595, 1543, 1498, 1475 (–C=C– ring stretching), 1382 (CH_3 bending), 1250 (Si–CH_3 bending), 1113 (Si–Ph stretching), 805 (Si-C stretching), 775 (Ar–H bending). ^{1}H NMR (300 MHz, $CDCl_3$), δ (ppm): 6.60–8.00 (Ar–H), 3.17 (≡C–H), 0.10–1.00 (Si-CH_3). ^{13}C NMR (75 MHz, $CDCl_3$), δ (ppm): 120.0–145.0 (aromatic carbons), 83.9 (–C≡CH), 78.1 (–C≡CH), –2.5 (Si–CH_3). UV (DCM, 5.0×10^5 mol/L), λ_{max}(nm)/ε_{max}(mol^{-1} L cm^{-1}): 231/12126, 268/26012.

ii. hb-P**2**

White powder. Yield: 80%. M_w: 42,200, M_w/M_n: 3.5 (GPC, Table 2, entry 2). IR (thin film), ν (cm^{-1}): 3298 (≡C–H stretching), 3067, 3016 (Ar–H stretching), 2958, 2896 (CH_3 stretching), 1919, 1813 (overtone band, substituted benzene ring), 1594, 1543, 1500 1475 (–C=C– ring stretching), 1428, 1113 (Si–Ph stretching), 1383 (CH_3 bending), 1252 (Si–CH_3 bending), 785 (Si–C stretching), 758, 735, 700 (Ar–H bending). ^{1}H NMR (300 MHz, $CDCl_3$), δ (ppm): 6.70–8.10 (Ar–H), 3.22 (≡C–H), 0.40–1.20 (Si-CH_3). ^{13}C NMR (75 MHz, $CDCl_3$), δ (ppm): 115.0–150.0 (aromatic carbons), 83.8 (–C≡CH), 78.3 (–C≡CH), –3.4 (Si–CH_3). UV (DCM, 5.0×10^{-5} mol/L), λ_{max}(nm)/ε_{max}(mol^{-1} L cm^{-1}): 231/18742, 260/33416.

iii. hb-P**3**

White powder. Yield: 62%, M_w: 23,500, M_w/M_n: 1.5 (GPC, Table 2, entry 7). IR (thin film), ν (cm^{-1}): 3295 (≡C–H stretching), 3067, 3016 (Ar–H stretching), 1594 (–C=C– ring stretching), 1428, 1110 (Si–Ph stretching), 699 (Ar–H bending). ^{1}H NMR (300 MHz, $CDCl_3$), δ (TMS, ppm): 6.80–8.00 (Ar–H), 3.20 (≡C–H). ^{13}C NMR (75 MHz, $CDCl_3$), δ (ppm): 120.0–150.0 (aromatic carbons), 83.8 (–C≡CH), 78.5 (–C≡CH). UV (DCM, 5.0×10^{-5} mol/L), λ_{max}(nm)/ε_{max}(mol^{-1} L cm^{-1}): 230/23940, 261/36196.

iv. hb-P**4**

White powder. Yield: 99%. M_w: 39,200, M_w/M_n: 3.4 (GPC, Table 2, entry 9). IR (thin film), ν (cm^{-1}): 3301 (≡C–H stretching), 2957 (CH_3 stretching), 1594, 1540

(–C=C– ring stretching), 1382 (CH_3 bending), 1251 (Si–CH_3 bending), 831 (Si–C stretching), 809 (Ar–H bending). ^{1}H NMR (300 MHz, $CDCl_3$), δ (TMS, ppm): 6.30–8.10 (Ar–H), 3.16 (≡C–H), 1.50–2.60 (Ar–CH_3), 0.10–1.00 (Si–CH_3). UV (DCM, 5.0×10^{-5} mol/L), λ_{max}(nm)/ε_{max}(mol^{-1} L cm^{-1}): 230/16348, 270/27212.

v. hb-P**5**

Light orange powder. Yield: 39%. M_w: 15,100, M_w/M_n: 2.2 (GPC, Table 2, enter 14). IR (thin film), ν (cm^{-1}): 3286 (≡C–H stretching), 2954, 2863 (CH_3 stretching), 1590, 1471 (–C=C– ring stretching), 1447, 1381 (CH_3 bending), 1249 (Si–CH_3 bending), 832 (Si–C stretching), 816 (Ar–H bending). ^{1}H NMR (300 MHz, $CDCl_3$), δ (TMS, ppm): 6.60–7.60 (Ar–H), 3.32 (≡C–H), 1.60–2.60 (Ar–CH_3), 0.30–0.90 (Si–CH_3). ^{13}C NMR (75 MHz, $CDCl_3$), δ (ppm): 120.0–150.0 (aromatic carbons), 82.9 (–C≡CH), 81.4 (–C≡CH), 22.4, 20.2 (Ar–CH_3), −0.82 (Si–CH_3). UV (DCM, 5.0×10^{-5} mol/L), λ_{max}(nm)/ε_{max}(mol^{-1} L cm^{-1}): 231/24788, 258/30298.

Q. Synthesis of Model Compounds 1,3,5- and 1,2,4-Triphenylbenzenes (15)

It was prepared from 0.55 mL (511.5 mg, 5.0 mmol) phenylacetylene, 29.0 mg (0.05 mmol) $TaBr_5$ in 5.0 mL toluene by the procedure similar to that used in the polymerization. The product was purified by silica chromatography using hexane as eluent. White powdery **15** was obtained in 85% yield. 1,3,5- and 1,2,4-isomers of **15** were separated by recrystallizations from ethanol and a 1:1 mixture of ethanol/hexane, respectively. The molar ratio of 1,3,5- to 1,2,4- was 1.0:2.0.

i. 1,3,5–**15**

IR (thin film), ν (cm^{-1}): 3058, 3033 (Ar–H stretching), 1595, 1576, 1497, 1411 (–C=C– ring stretching), 873, 762, 698 (Ar–H bending). ^{1}H NMR (300 MHz, $CDCl_3$), δ (ppm): 7.78 (*s,* 3H, Ar–H g), 7.69 (*m,* 6H, Ar–H f), 7.47 (*m,* 6H, Ar–H *e*), 7.38 (*m,* 3H, Ar–H *d*). ^{13}C NMR (75 MHz, $CDCl_3$), δ (ppm): 142.3, 141.1, 128.8, 127.5, 127.3, 125.2 (aromatic carbons). UV (dichloromethane, 2.5×10^{-5} mol/L), λ_{max} (nm)/ε_{max} (mol^{-1} L cm^{-1}): 255/41540. MS(CI): *m*/*e* 307.1 [$(M+1)^{+\cdot}$]; calculated 307.1.

ii. 1,2,4–**15**

IR (thin film), ν (cm^{-1}): 3055, 3025 (Ar–H stretching), 1599, 1575, 1490, 1474 (–C=C– ring stretching), 756, 697 (Ar–H bending). ^{1}H NMR (300 MHz, $CDCl_3$), δ (ppm): 7.66 (*m,* 4H, Ar–H *j*), 7.47 (*m,* 3H, Ar–H *i*), 7.35 (*m,* 1H, Ar–H *h*), 7.20 (*m,* 10H, Ar–H *k*) (the peak assignments were referred to their steric structure in Scheme **3,** which was calculated according to the minimized energy of the structure by the MOPAC method of the *3D ChemDraw* program). ^{13}C NMR (75 MHz, $CDCl_3$), δ (ppm): 141.5, 141.1, 141.0, 140.6, 140.4, 139.5, 131.1, 129.9, 129.8, 129.4, 128.8, 127.9, 127.8, 127.4, 127.1, 126.6, 126.5, 126.1 (aromatic carbons). UV (dichloromethane, 2.5×10^{-5} mol/L), λ_{max} (nm)/ε_{max} (mol^{-1} L cm^{-1}): 252/34988. MS(CI): *m*/*e* 307.1 [$(M+1)^{+\cdot}$]; calculated 307.1.

R. Decomposition of Hyperbranched Polymers

The polymers were decomposed via Si-C bond cleavage. A typical example of reaction procedure for the decomposition of *hb*-P**1** is given here. To a round-bottomed flask equipped with a septum and a stirring bar were added 70.0 mg *hb*-P**1** (Table 1, entry 4; whose weight is denoted as W_0) and 50 mL CH_2Cl_2. After the polymer had dissolved, 5 mL (65 mmol) CF_3COOH was added dropwise under stirring. The solution was kept stirring at 60°C for 48 h. The solution was dropped slowly into an aqueous solution of sodium carbonate (0.2 M) for neutralization. The organic layer was separated and the water layer was extracted with CH_2Cl_2. The organic solution was collected and washed with deionized water. The solvent was removed by evaporation. The crude products were separated on silica-gel column by a progressive solvent change from hexane to a mixture of hexane/chloroform (1:3, v/v) to give 29.5 mg of a mixture of 1,3,5- and 1,2,4-**15** (whose weight is denoted as W_{15}) and 17.0 mg oligomer of **1** (W_r). Characterization data for **15** were identical to those given above (cf. Section Q).

The partially soluble polymer *hb*-P**1** (Table 1, entry 5) was decomposed by a similar procedure. 50.4 mg of **15** and 36.5 mg of oligomer of **1** were obtained from 125.8 mg of polymer.

S. Structural Simulation

Polymer structures were simulated by molecular modeling technique using a Materials Studio program.[25] The polymer model consisting of 72 monomers was built by Materials Visualizer. The building strategy was based on the experimental data and the following assumptions: (1) the number-average molecular weight of the polymer was ~15,200, which was measured by GPC in THF on the basis of a polystyrene calibration; (2) the molar ratio of the newly formed 1,2,4- and 1,3,5-trisubstituted phenylene structures was ~2.2:1.0, which was measured by ^{1}H NMR spectra; and (3) the cutoff distance was 9.5 Å.

The interactions occurring in a system are described by a potential *E*, which consists of harmonic bond length, harmonic bond angle, three-fold tensional, inversion and nonbonded interactions, the last of which can be further subdivided into hydrogen bonding, van der Waals interaction, and columbic electrostatic potentials.

The potential energy of the initial structure was minimized by *Discover Minimizer* using the method of Conjugate Gradient (Fletcher_Reeves), until the maximum derivative was 0.703 kcal/mol.

V. ACKNOWLEDGMENTS

The work described in this chapter is in part supported by the Hong Kong Research Grants Council (Project Nos.: HKUST 6121/01P, 6085/02P, and 604903) and the University Grants Committee of Hong Kong through an Area of Excellence Scheme (Project No.: AoE/P-10/01-1-A). This project also benefited from the support

of the Innovation and Technology Fund of the Hong Kong Government. We thank Y. Tang and P. Gao of the Department of Chemical Engineering of our university for their assistance in the computer simulation of the polymer structures.

VI. REFERENCES

1. D. S. Thompson, L. J. Markoski, J. S. Moore, I. Sendijarevic, A. Lee, A. J. McHugh, *Macromolecules* **33**, 6412 (2000).
2. A. Sunder, R. Hanselmann, H. Frey, R. Mulhaupt, *Macromolecules* **32**, 4240 (1999).
3. H. T. Chang, J. M. J. Fréchet, *J. Am. Chem. Soc.* **121**, 2313 (1999).
4. M. H. Xu, H. C. Zhang, L. Pu, *Macromolecules* **36**, 2689 (2003).
5. J. Hao, M. Jikei, M. Kakimoto, *Macromolecules* **36**, 3519 (2003).
6. K. Yoon, D.Y. Son, *Macromolecules* **32**, 5210 (1999).
7. G. Kwak, T. Masuda, *Macromol. Rapid Commun.* **23**, 68 (2002).
8. M. Oishi, M. Minakawa, I. Imae, Y. Kawakami, *Macromolecules* **35**, 4938 (2002).
9. Q. Sun, K. Xu, H. Peng, R. Zheng, M. Häußler, B. Z. Tang, *Macromolecules* **36**, 2309 (2003).
10. M. Häußler, J. W. Y. Lam, E. Zheng, H. Peng, J. Luo, J. Chen, C. C. W. Law, B. Z. Tang, *C. R. Chim.* **6**, 833 (2003).
11. J. W. Y. Lam, J. Chen, C. C. W. Law, H. Peng, Z. Xie, K. K. L. Cheuk, H. S. Kwok, B. Z. Tang, *Macromol. Symp.* **196**, 289 (2003).
12. Z. Xie, H. Peng, J. W. Y. Lam, J. Chen, Y. Zheng, C. Qiu, H. S. Kwok, B. Z. Tang, *Macromol. Symp.* **195**, 179 (2003).
13. J. W. Y. Lam, J. Luo, H. Peng, Z. Xie, K. Xu, Y. Dong, L. Cheng, C. Qiu, H. S. Kwok, B. Z. Tang, *Chin. J. Polym. Sci.* **19**, 585 (2001).
14. B. Z. Tang, K. Xu, Q. Sun, P. P. S. Lee, H. Peng, F. Salhi, Y. Dong, *ACS Symp. Ser.* **760**, 146 (2000).
15. J. Chen, H. Peng, C. C. W. Law, Y. Dong, J. W. Y. Lam, I. D. Williams, B. Z. Tang, *Macromolecules* **36**, 4319 (2003).
16. H. Peng, J. Luo, L. Cheng, J. W. Y. Lam, K. Xu, Y. Dong, D. Zhang, Y. Huang, Z. Xu, B. Z. Tang, *Opt. Mater.* **21**, 315 (2002).
17. K. Xu, H. Peng, Q. Sun, Y. Dong, F. Salhi, J. Luo, J. Chen, Y. Huang, D. Zhang, Z. Xu, B. Z. Tang, *Macromolecules* **35**, 5821 (2002).
18. H. Peng, L. Cheng, J. Luo, K. Xu, Q. Sun, Y. Dong, F. Salhi, P. P. S. Lee, J. Chen, B. Z. Tang, *Macromolecules* **35**, 5349 (2002).
19. K. Xu, B. Z. Tang, *Chin. J. Polym. Sci.* **17**, 397 (1999).
20. R. Zheng, J. W. Y. Lam, H. Peng, M. Häußler, B. Z. Tang, *Polym. Mater. Sci. Eng.* **88**, 365 (2003).
21. C. Eaborn, K. L. Jones, P. D. Lickiss, *J. Organometal. Chem.* **461**, 31 (1993).
22. R. W. Bott, C. Eaborn, P. M. Jackson, *J. Organometal. Chem.* **7**, 79 (1967).
23. C. Eaborn, *J. Organometal. Chem.* **100**, 43 (1975).
24. D. Hölter, A. Burgath, H. Frey, *Acta Polymer* **48**, 30 (1997).
25. *Materials Studio*® is a software environment that brings together the world's most advanced materials simulation and informatics technology. It is a product of Accelrys Inc.

CHAPTER 3

Silole-Containing Conjugated Polymers

Jacky W. Y. Lam, Junwu Chen, Hongchen Dong, and Ben Zhong Tang

Department of Chemistry, Institute of Nano Science and Technology, Open Laboratory of Chirotechnology, and Center for Display Research, Hong Kong University of Science and Technology, Clear Water Bay, Hong Kong, China

CONTENTS

Macromolecules Containing Metal and Metal-Like Elements, Volume 4: Group IVA Polymers, edited by Alaa S. Abd-El-Aziz, Charles E. Carraher Jr., Charles U. Pittman Jr., and Martel Zeldin
ISBN: 0-471-68238-1

I. INTRODUCTION

Silole is a five-membered silacycle, which may well be viewed as a cyclopentadiene derivative with its carbon bridge replaced by a silicon atom, hence the name *silacyclopentadiene*. Silole enjoys a unique $\sigma^*\rightarrow\pi^*$ conjugation arising from the orbital interaction of the σ^* orbital of its silylene moiety with the π^* orbital of its butadiene fragment, which significantly lowers its LUMO energy level and increases its electron affinity.[1–3] As a matter of fact, silole has a high electron-accepting ability[4,5] and has been used as an electron-transporting and light-emitting material in the construction of electroluminescence (EL) devices.[6,7]

We have recently observed a novel phenomenon of aggregation-induced emission (AIE) in this group of molecules: The siloles are practically nonluminescent when molecularly dissolved but become emissive when aggregated in poor solvents or fabricated into thin films.[8,9] The photoluminescence (PL) quantum yield (Φ_{PL}) of the silole aggregates can differ from that of their molecularly dissolved species by two orders of magnitude (>300). Using this AIE property, we fabricated LEDs using thin solid films of siloles as active layers, which are found to exhibit outstanding EL performance.[10,11] For example, an LED device of 1-methyl-1,2,3,4,5-pentaphenylsilole exhibits maximum current efficiency (CE_{max}) and power efficiency (PE_{max}) of 20 cd/A and 14 lm/W, respectively. Its highest external quantum efficiency (η_{max}) is 8%,[10,11] approaching the limit of the possible. An LED device of its structural conger 1,1,2,3,4,5,-hexaphenylsilole also performs well and is turned on at a low voltage (~4 V), emitting intensely at a moderate bias (55880 cd/m^2 at 16 V) and showing high EL efficiencies of 15 cd/A (CE_{max}), 10 lm/W (PE_{max}), and 7% (η_{max}). Siloles are thus a group of excellent organometallic molecules for LED applications.

Low molecular weight compounds, however, have to be fabricated into thin films by relatively expensive techniques such as vacuum sublimation and vapor deposition, which are not well suited to the manufacture of large area devices.[12] One way to overcome this processing disadvantage is to make high molecular weight polymers, which can be readily processed from their solutions into thin solid films over large areas by simple spin coating or doctor blade techniques. In this chapter, we report our work on the syntheses of silole polymers through the metathesis and cyclotrimerization polymerizations of alkynes initiated by transition metal catalysts and present their novel properties originated from their unique molecular structures.

II. POLYMER SYNTHESES

We designed four acetylene-silole adducts by nucleophilic substitutions of 1-chloro-1,2,3,4,5-pentaphenylsilole with ethynylmagnesium bromide, 11-undecyn1-ol, 11-phenyl-10-undecyn-1-ol, and lithium 5-([4-(phenylethynyl)phenyl]oxy)-1-pentynylide, respectively.[13,14] Most of the monomers are prepared in high yields and give satisfactory analysis data corresponding to their expected molecular structures. Polymerizations of the monomers are effected by the mixtures of $NbCl_{5-}$, WCl_{6-}, and

$MoCl_5$–Ph_4Sn, producing polymers **1–4** (Fig. 1) with high molecular weights (M_w up to 70×10^3) in high yields (up to 80%) (Table 1).

We also prepared a silole-containing diacetylene (**5**; Fig. 2) by reacting a 1,1-dichlorosilole with ethynylmagnesium bromide.[15] Homopolycyclotrimerization of

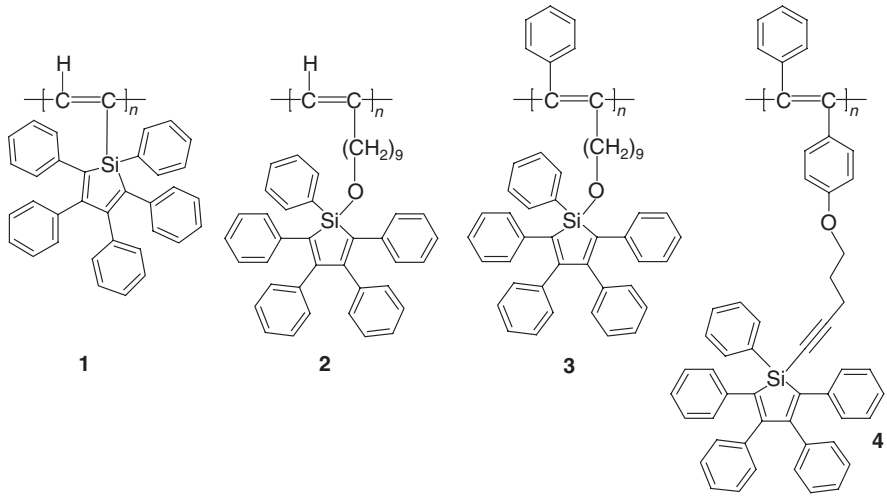

Figure 1 Structures of linear poly(silolylacetylene)s.

Table 1 Synthesis of Silole-Containing Polyacetylenes[a]

Entry Number	Catalyst	Temperature (°C)	Yield (%)	M_w	M_w/M_n
		*Poly[1-(1,2,3,4,5-pentaphenyl)silolylacetylene] (**1**)*			
1	$NbCl_5$–Ph_4Sn	60	60.0	46,400	1.7
2	$NbCl_5$–Ph_4Sn	80	78.0	68,800	1.8
		*Poly(11-{[1-(1,2,3,4,5-pentaphenyl)silolyl]oxy}-1-undecyne) (**2**)*			
3	WCl_6–Ph_4Sn	60	60.3	11,500	3.5
4	$MoCl_5$–Ph_4Sn	60	11.7	10,600	3.4
		*Poly(11-{[1-(1,2,3,4,5-pentaphenyl)silolyl]oxy}-1-phenyl-1-undecyne) (**3**)*			
5	WCl_6–Ph_4Sn	60	80.5	33,400	2.2
		*Poly(1-phenyl-2-{4-[({2-[1-(1,2,3,4,5-pentaphenyl)silolyl]ethynyl}propyl)oxy]phenyl}-acetylene) (**4**)*			
6	$NbCl_5$–Ph_4Sn	60	22.6	1,430	1.2
7	WCl_6–Ph_4Sn	80	56.4	4,810	1.7

[a] Under N_2 in toluene for 24 h; $[M]_0 = 0.1$ M; [cat.] = [cocat.] = 10 mM.

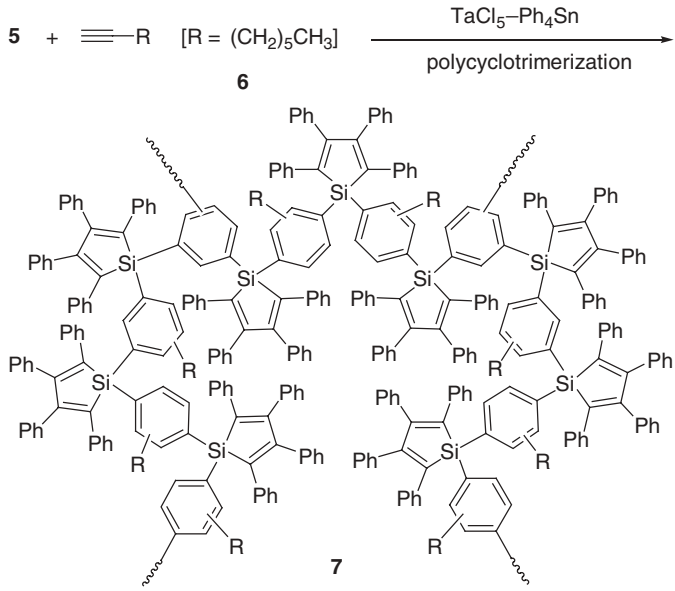

Figure 2 Synthesis of hyperbranched poly(phenylenesilolene)s (**7**).

5 and its copolymerization with 1-octyne **6** catalyzed by $TaCl_5$–Ph_4Sn proceed smoothly, giving completely soluble hyperbranched poly(phenylenesilolene)s **7** in high yields (Table 2). The weight-average molecular weight of the polymers analyzed by gel permeation chromatography (GPC) using linear polystyrenes falls in the range of 3530–5320 g/mol. These values are probably underestimated because of the hyperbranched nature of the polymers coupled with their rigid molecular structures. In our

Table 2 Synthesis and Properties of Poly(phenylenesilolene)s[a]

Entry Number	**6/5**[b]	Yield (%)	M_w	M_w/M_n	T_d[c] (°C)	F_L[d] (mJ/cm^2)	$F_{t,m}/F_{i,m}$[e]
1	0	83.0 (**7a**)	5320	1.6	395	185	0.19
2	0.5	85.3 (**7b**)	5820	1.7	378	182	0.24
3	1.0	67.6 (**7c**)	3610	1.4	355	190	0.28
4	1.5	34.0 (**7d**)	3530	1.4	343	1140	0.32

[a] By homopolymerization of diyne **5** or its copolymerizations with **6** catalyzed by $TaCl_5$–Ph_4Sn in toluene at room temperature under nitrogen for 24 h; [**5**] = 0.072 M, [$TaCl_5$] = [Ph_4Sn] = 20 mM.

[b] Molar ratio.

[c] Temperature for 5% weight loss (TGA, under nitrogen, heating rate: 20°C/min).

[d] Optical limiting threshold (incident fluence at which the nonlinear transmittance is 50% of the linear one).

[e] Signal suppression (ratio of the saturated transmitted fluence to the maximum incident fluence).

previous studies on hyperbranched polymers,[16–19] we found that the underestimation can be as large as seven fold,[17] and the actual or real molecular weight of **7** thus can be much higher than the relative value estimated from the GPC analysis.

III. THERMAL STABILITY

All the polymers give spectroscopic data that satisfactorily correspond to their expected molecular structures. Figure 3 shows their TGA thermograms and Table 2 summarizes the thermal analysis data of the hyperbranched poly(phenylenesilolene)s. All the polymers are thermally stable and lose little of their weights at a temperature as high as ~350°C. The degradation temperatures of the linear silole-containing polyacetylenes **2–4** are much higher than those of poly(dimethylalkoxysilylacetylene)s $-(HC{=}C[Si(CH_3)_2OC_mH_{2m+1}])_n-$,[20] probably due to the "jacket effect"[21,22] of the bulky silolyl pendants. Wrapping of the polyacetylene backbone in the stable silole rings may have shielded the double bonds from the harsh chemical and thermal attacks. Hyperbranched polymer **7a** shows a higher thermal stability than its structural congener **7d**. This is easy to understand: **7a** is an all-aromatic homopolymer, which should be thermally stable. The incorporation of the weak aliphatic (hexyl) moiety into **7d** should increase its thermolytic susceptibility, and the copolymer thus starts to decompose at a relatively low temperature.

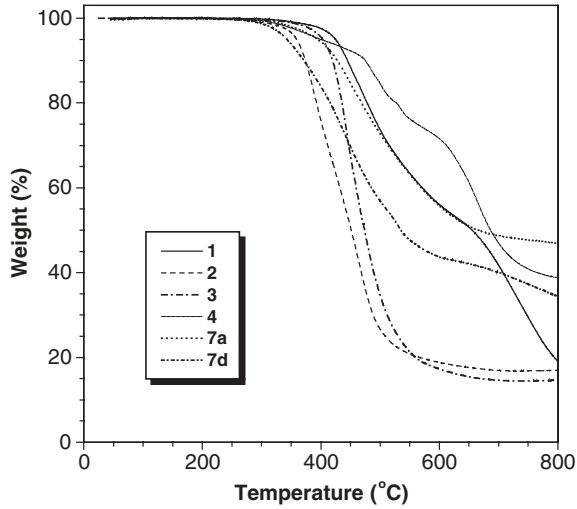

Figure 3 TGA thermograms of silole-containing linear polyacetylenes **1** (sample from Table 1, entry 2), **2** (Table 1, entry 3), **3**, and **4** (Table 1, entry 7) and hyperbranched polyphenylenes **7a** (Table 2, entry 1) and **7d** (Table 2, entry 4) recorded under nitrogen at a heating rate of 20°C/min.

IV. PHOTOLUMINESCENCE

Silole's emission is characterized by its AIE feature. Do the silole polymers behave in a similar way? The answer to this question is yes or no, depending on the molecular structure of the polymer. No emission from the silole pendants is observed when the chloroform solution of **1** is excited. Even when methanol, a poor solvent of the polymer, is added into the chloroform solution, the emission of **1** is hardly enhanced. The rigid polyacetylene backbone of **1** may not allow its directly attached silole pendants to pack well in the aggregation state, thus making the polymer AIE inactive. Thanks to the decoupling effect of the long nonanyloxy chain, **2** exhibits a pronounced AIE effect. As can be seen from Figure 4*A*, the PL spectrum of the chloroform solution of **2** is almost a flat line, with a Φ_{PL} as low as 0.15%. The Φ_{PL} starts to swiftly increase when >40% methanol is added into the mixture (Fig. 4*B*). When the methanol fraction is increased to 90%, the Φ_{PL} rises to 2.95%, which is ~20 times higher than the solution value. Polymer **3** shows a similar behavior, but its Φ_{PL} in a 90% methanol mixture is higher (9.25%), probably due to the additional contribution from its backbone emission: Its poly(1-phenyl-1-alkyne) main chain is known to luminesce in the similar spectral region.[23,24]

Unlike the solutions of **1**–**3**, the chloroform solution of **4** emits a green light at 523 nm with a Φ_{PL} of 2.8%. Because its monomer is a weak emitter when molecularly dissolved, the green light observed here thus should be associated with the backbone emission. We also checked the AIE property of **4** by adding menthol into its chloroform solution. The PL intensity can, however, barely be enhanced even when 90 vol % menthol is added. The reason **4** is AIE inactive may be similar to that

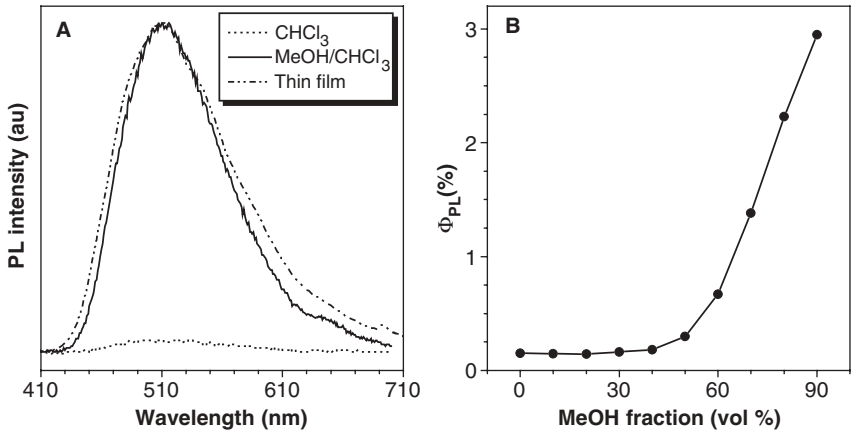

Figure 4 **A** PL spectra of **2** (Table 1, entry 3) in chloroform solution, methanol/chloroform mixture (9:1 by volume), and solid state (thin film); concentration of **2**: 10 μM; excitation wavelength (nm): 400 (solution/mixture), 325 (thin film). **B** Quantum yield (Φ_{PL}) of **2** versus solvent composition of methanol/chloroform mixture.

of **1**, in which the packing of the silole pendants is hampered by the rigid poly(diphenylacetylene) backbone. The stiff hyperbranched poly(phenylenesilolene) spheres of **7** also make the polymers AIE inactive. Their chloroform solutions emit weakly at ~500 nm with a Φ_{PL} of ~1.0%.

We carried out particle size analysis, which proves that the polymers indeed form nanoaggregates in the methanol/chloroform mixtures. Examples of the particle size histograms are shown in Figure 5. The size distribution and average size vary by polymer because of the differences in each polymer's solubility in the solvent mixture. Polymer **1** is hydrophobic and rigid and will easily associate into large nanoaggregates in the polar mixture. Polymer **2** possesses polar siloxy moieties with a better miscibility with the polar solvent and hence forms smaller aggregates under comparable conditions. Polymer **3** is a disubstituted polyacetylene with a more rigid backbone structure and its aggregates are thus understandably bigger than those of **2**.

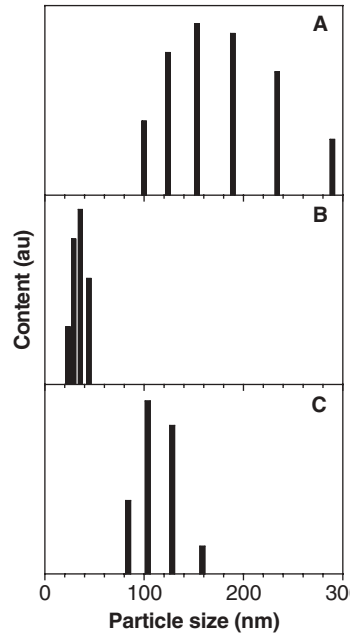

Figure 5 Particle size distribution of (**A**) **1** (sample from Table 1, entry 2), (**B**) **2** (Table 1, entry 3), and (**C**) **3** (Table 1, entry 5) in methanol/chloroform mixtures (9:1 volume). Concentration of polymers: 10 μM.

Aggregation normally quenches light emission;[25,26] what is the cause for this "abnormal" AIE phenomenon? To address this question, we designed and carried out more experiments. When a dilute dioxane solution of **3** (10 μM) is cooled, the intensity of its PL spectrum is progressively increased in a nonlinear fashion (Fig. 6*A*). When cooled from room temperature to below the melting point (11.8°C) of the solvent, the liquid solution changes to a solid "glass." The intramolecular rotations or

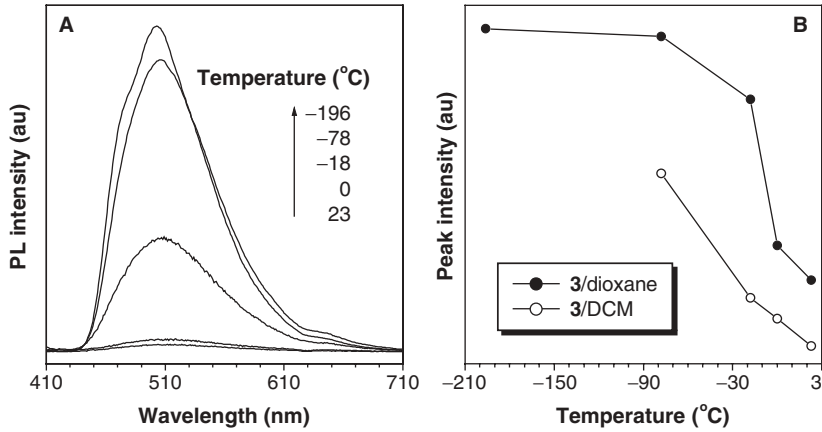

Figure 6 **A**. PL spectra of **3** in dioxane at different temperatures. **B**. Effect of temperature on the peak intensity of the luminescence of **3** in dioxane and DCM. Concentration of **3** : 10 μM; excitation wavelength: 407 nm.

twistings of the peripheral phenyl rings on the axes of the single bonds linked to the central silacyclopentadiene cores may be physically restricted by the solid environmental surroundings. This restricted rotation in some sense rigidifies the chromophoric molecule as a whole, thus making the silole pendant more emissive.

To separate the cooling effect from the "glass" effect, we choose dichloromethane (DCM), a liquid with much lower melting point, for the PL measurement. The PL intensity of the solution increases with a decrease in temperature in a nearly "linear" fashion (Fig. 6*B*). This enhancement in emission must be due to the restricted intramolecular rotation caused by cooling-induced conformation freezing because the melting point of the solvent (−95°C) is lower than the lowest temperature we tested for this solution (−78°C). Similar to **3,** polymers **2, 4,** and **7** also show much stronger emission when their solutions are cooled.

V. ELECTROLUMINESCENCE

Siloles are excellent materials for LED applications. How are their polymers? We checked the EL performances of polymers **1–4** using a single-layer device with a configuration of ITO/Polymer(∼46 nm)/LiF(1 nm)/Al. The EL spectrum of **1** peaked at 664 nm, while the emission maximums of **2**, **3** and **4** are at ∼521 nm. All the EL devices exhibit similarly low current efficiencies: 0.008 (**1**), 0.022 (**2**), 0.029(**3**), and 0.024 cd/A (**4**). This is not surprising because the injection and transportation of charges are generally not balanced in devices with a single-layer structure. We thus tried to modify the device configuration, using **3**, the most PL-active polymer, as the emitting material. We added poly(9-vinylcarbazole) (PVK) and

tris(8-hydroxyquinolinato)aluminum (Alq_3) on the anode and cathode sides, respectively, to facilitate the charge injection and to enhance the charge transport efficiencies in the EL device. Between the PVK and Alq_3 layers, we also added a layer of bathocuproine (BCP) to prevent the holes from traveling through to reach the cathode. With these modifications, an EL device with a configuration of ITO/(**3**:PVK)-(1:4)/BCP/Alq_3/LiF/Al is fabricated, which emit a strong blue light of 496 nm with a maximum luminance of 1118 cd/m^2 (Fig. 7). The maximum current and external quantum efficiencies of the device are 1.45 cd/A and 0.55%, respectively, which are comparable to some of the best results reported by other research groups for blue-emitting LEDs.[27–28]

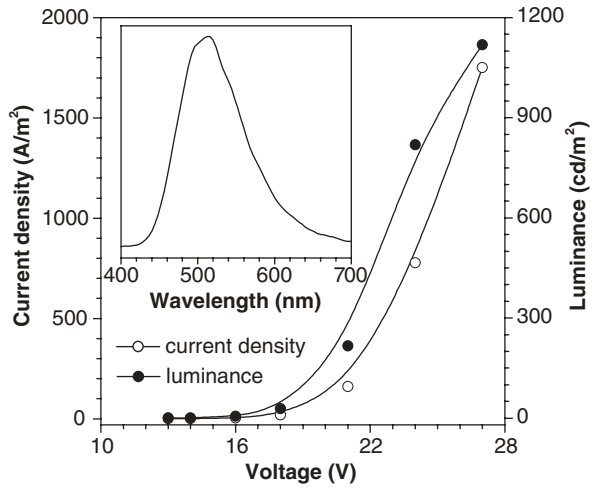

Figure 7 Changes in the current density and luminance with the applied voltage in a multilayer LED of **3** with an ITO/**3**:PVK(1:4 w/w)/BCP/Alq_3/LiF/Al device configuration. Inset: EL spectrum.

The promising device results of **3** encourage us to further investigate the EL properties of other silole-containing polyacetylenes. Table 3 summarizes their EL performances. Clearly, the devices with multilayer structures perform much better than those of single-layer configurations, demonstrating the importance of the device configuration and suggesting much room for device improvement. Among the polymers, **3** and **4** are much better EL emitters, thanks to the additional contribution from the emissive poly(1-phenyl-1-undecyne) and poly(diphenylacetylene) backbones.

Poly(fluorene)s are the best-known blue light-emitting polymers, but their EL devices suffer from such disadvantages as poor spectral stability.[29–35] Under normal conditions of device operation, a broad EL peak centered at 530–540 nm evolves with the passage of a current through the devices; as a result, the blue emission changes to an undesirable color. The LEDs of our polymers, however, enjoy excellent spectral stability. Figure 8*A* shows the EL spectra of **3** measured at different voltages. When 16 V are applied to the device, the polymer emits a blue light of 496 nm. The spectral

Table 3 Performances of Multilayer EL Devices of Polymers 1–4[a]

Polymer	λ_{max} (nm)	*CIE*[b] (*x*, *y*)	V_{on}[c] (V)	L_{max} (cd/m^2)	CE_{max} (cd/A)	QE_{max} (%)
1	632	0.47,0.39	11	9	0.17	0.09[d]
2	496	0.24,0.41	16	63	0.26	0.11[e]
3	496	0.25,0.45	14	1118	1.45	0.55[f]
4	512	0.26,0.48	13	489	0.54	0.20[g]

[a] With a device configuration of ITO/polymer:PVK (1:4 by weight) (~46 nm)/BCP (20 nm)/Alq_3 (20 nm)/LiF (1 nm)/Al. λ_{max}, EL peak maximum; V_{on}, turn-on voltage; L_{max}, maximum luminance; CE_{max}, maximum current efficiency; QE_{max}, maximum external quantum efficiency.
[b] CIE 1931 coordinates.
[c] At 1 cd/m^2.
[d] At 13 V; 25.9 A/m^2.
[e] At 18 V; 17.9 A/m^2.
[f] At 16 V; 4.29 A/m^2.
[g] At 15 V; 12.3 A/m^2.

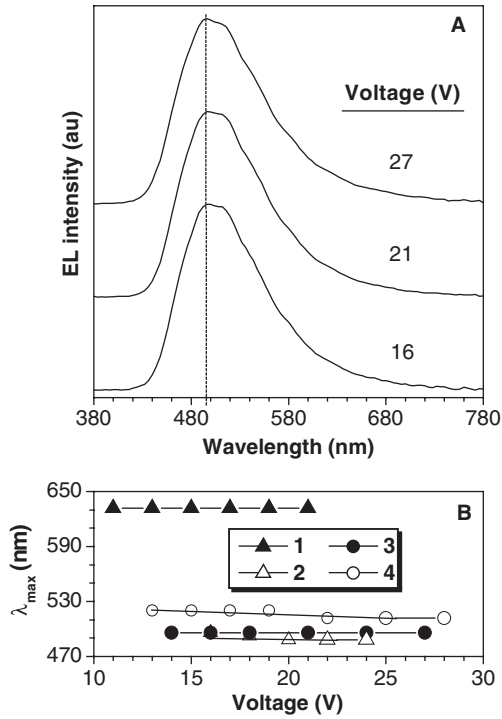

Figure 8 Stability of electroluminescence spectra in multilayer LEDs with a device configuration of ITO/LEPA:PVK (1:4 by weight) (~46 nm)/BCP (20 nm)/Alq_3 (30 nm)/LiF (0.8 nm)/Al. **A** Electroluminescence spectra of **3** under different voltages. **B** Maximum wavelength (λ_{max}) versus applied voltage for polymers **1**–**4**.

pattern remains nearly the same at 21 V. Even at 27 V, practically no change is recognizable in the EL spectrum, although the luminance of the device is increased by ~200 times (from 6 to 1118 cd/m^2) and its efficiency reaches its maximum value of 0.55%.

VI. OPTICAL LIMITING

The hyperbranched polymers **7** are not only thermally but also optically stable. Figure 9 shows the optical responses of the polymer solutions to 532 nm laser pulses, along with the data for the solutions of poly(phenylacetylene) (PPA)[36] and C_{60}.[37,38] PPA photodegrades under the attack of harsh laser shots. Our hyperbranched polyarylenes exhibit comparable linear transmittance in the low fluence region (T = 70–85%) but become opaque in the high fluence region. The polymers strongly attenuate the power of the intense laser pulses, whose optical limiting performances are superior to that of C_{60}, a best-known optical limiter.[37–40] Among the hyperbranched polymers, **7a** shows the best performance, which starts to limit the optical power at

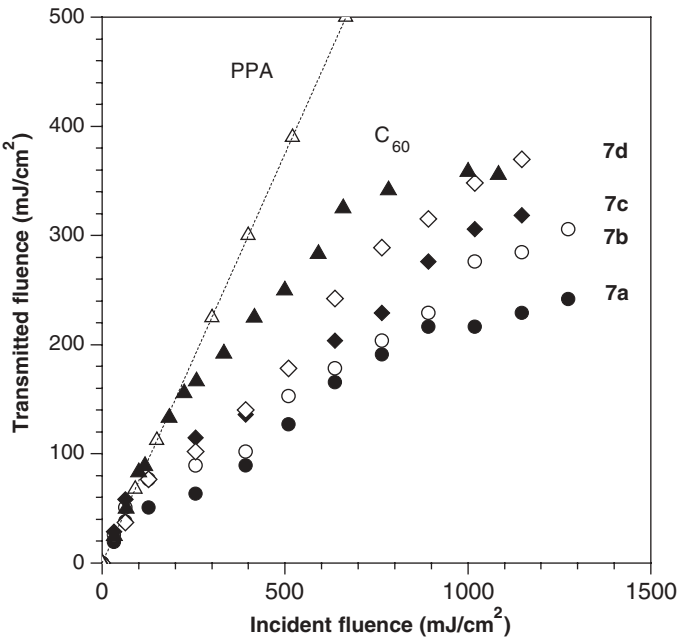

Figure 9 Optical responses to 8 ns, 10 Hz pulses of 532 nm laser light, of dichloromethane solutions (0.70 mg/mL) of hyperbranched poly(phenylenesilolene)s. Data for PPA and C_{60} solutions are shown for comparison. Linear transmittance (%): 70 (**7a**), 80 (**7b**), 82 (**7c**), 85 (**7d**), 79 (C_{60}), 75 (PPA).

a low threshold (185 mJ/cm^2) and suppresses the optical signals to a great extent (19%; Table 2, entry 1).

VII. CONCLUSIONS

In this work, we succeeded in incorporating silole ring, an organometallic chromophore with novel luminescence properties, into the linear polyacetylene and hyperbranched polyphenylene structures through metathesis and cyclotrimerization polymerizations of alkynes effected by transition-metal catalysts, respectively. The polymerizations yield completely soluble polymers of high thermal stability. Although most of the polymers are weak luminophors when molecularly dissolved, polymers **2**, **3, 4,** and **6** become emissive when aggregated in poor solvents or when cooled to low temperatures. Multilayer EL devices with a configuration of ITO/(Polymer: PVK) (1:4)/BCP/Alq_3/LiF/Al were fabricated, which emit strong light with maximum luminance, current efficiency, and external quantum efficiency of 1118 cd/m^2, 1.45 cd/A, and 0.55%, respectively. The LEDs of the silole-containing polymers enjoy excellent spectral stability, and the EL peak maximum experiences little change with the applied voltage. The hyperbranched poly(phenylenesilolene)s strongly limit intense laser pulses, whose limiting thresholds and signal suppression power are better than those of C_{60}, a well-known optical limiter.

VIII. ACKNOWLEDGMENTS

We thank the financial support of the Hong Kong Research Grants Council (Project Nos.: HKUST 6085/02P, 6121/01P and 604903) and the University Grants Committee through an Area of Excellence Scheme (Project No.: AoE/P-10/01-1-A).

IX. REFERENCES

1. V. Y. Lee, A. Sekiguchi, M. Ichinohe, N. Fukaya, *J. Organomet. Chem*. **611**, 228 (2000).
2. J. Hermanns, B. Schmidt, *J. Chem. Soc. Perkin Trans. 1*, 81 (1999).
3. S. Yamaguchi, K. Tamao, *J. Chem. Soc., Dalton Trans.* 3693 (1998).
4. S. Yamaguchi, K. Tamao, *Bull. Chem. Soc. Jpn.* **69**, 2327 (1996).
5. C. Chuit, R. J. P. Corriu, C. Reye, J. C. Young, *Chem. Rev.* **93**, 1371 (1993).
6. J. Ohshita, H. Kai, A. Takata, T. Iida, A. Kunai, N. Ohta, K. Komaguchi, M. Shiotani, A. Adachi, K. Sakamaki, K. Okita, *Organometallics* **20**, 4800 (2001).
7. S. Yamaguchi, T. Endo, M. Uchida, T. Izumizawa, K. Furukawa, K. Tamao, *Chem. Eur. J.* **6**, 1683 (2000).
8. J. Luo, Z. Xie, J. W. Y. Lam, L. Cheng, H. Chen, C. Qiu, H. S. Kwok, X. Zhan, Y. Liu, D. Zhu, B. Z. Tang, *Chem. Commun*. 1740 (2001).

9. M. Freemantle, *Chem. Eng. News* **79** (41), 29 (2001).
10. B. Z. Tang, X. Zhan, G. Yu, P. P. S. Lee, Y. Liu, D. Zhu, *J. Mater. Chem*. **11**, 2874 (2001).
11. H. Chen, J. W. Y. Lam, J. Luo, Y. L. Ho, B. Z. Tang, D. Zhu, M. Wong, H. S. Kwok, *Appl. Phys. Lett*. **81**, 774 (2002).
12. A. Ktaft, A. C. Grimsdale, A. B. Holmes, *Angew. Chem. Int. Ed.* **37**, 402 (1998).
13. J. Chen, Z. Xie, J. W. Y. Lam, C. C. W. Law, B. Z. Tang, *Macromolecules* **36**, 1108 (2003).
14. J. Chen, B. Z. Tang, unpublished data.
15. J. Chen, H. Peng, C. C. W. Law, Y. Dong, J. W. Y. Lam, I. D. Williams, B. Z. Tang, *Macromolecules* **36**, 4319 (2003).
16. H. Peng, J. Luo, L. Cheng, J. W. Y. Lam, K. Xu, Y. Dong, D. Zhang, Y. Huang, Z. Xu, B. Z. Tang, *Opt. Mater*. **21**, 315 (2002).
17. K. Xu, H. Peng, Q. Sun, Y. Dong, F. Salhi, J. Luo, J. Chen, Y. Huang, D. Zhang, Z. Xu, B. Z. Tang, *Macromolecules* **35**, 5821 (2002).
18. H. Peng, L. Cheng, J. Luo, K. Xu, Q. Sun, Y. Dong, F. Salhi, P. P. S. Lee, J. Chen, B. Z. Tang, *Macromolecules* **35**, 5349 (2002).
19. Q. Sun, K. Xu, H. Peng, R. Zheng, J. Chen, M. Häußler, B. Z. Tang, *Macromolecules* **36**, 2309 (2003).
20. M. G. Voronkov, V. B. Pukhnarevich, S. P. Sushchinskaya, V. Z. Annenkova, V. M. Annenkova, N. J. Andreeva, *J. Polym. Sci. Polym. Chem. Ed*. **18**, 53 (1980).
21. J. W. Y. Lam, J. Luo, Y. Dong, K. K. L. Cheuk, B. Z. Tang, *Macromolecules* **35**, 8288 (2002).
22. J. W. Y. Lam, Y. P. Dong, K. K. L. Cheuk, J. Luo, Z. L. Xie, H. S. Kwok, Z. S. Mo, B. Z. Tang, *Macromolecules* **35**, 1229 (2002).
23. J. W. Y. Lam, C. K. Law, Y. P. Dong, J. N. Wang, W. K. Ge, B. Z. Tang, *Opt. Mater*. **21**, 321 (2002).
24. R. G. Sun, Q. G. Zheng, X. M. Zhang, T. Masuda, T. Kobayashi, *Jpn. J. Appl. Phy*s. **38**, 2017 (1999).
25. B.-K. An, S.-K. Kwon, S.-D. Jung, S. Y. Park, *J. Am. Chem. Soc.* **124**, 14410 (2002).
26. S. H. Chen, A. C. Su, Y. F. Huang, C. H, Su, G. Y, Peng, S. A. Chen, *Macromolecules* **35**, 4229 (2002).
27. X. Z. Jiang, S. Liu, H. Ma, A. K. Y. Jen, *Appl. Phys. Lett*. **76**, 1813 (2000).
28. L. C. Palilis, D. G. Lidzey, M. Redecker, D. D. C. Bradley, M. Inbasekararn, E. P. Woo, W. W. Wu, *Synth. Met*. **121**, 1729 (2001).
29. V. N. Bliznyuk, S. A. Carter, J. C. Scott, G. Klarner, R. D. Miller, D. C. Miller, M*acromolecules* **32**, 361 (1999).
30. W.-L. Yu, J. Pei, W. Huang, A. J. Heeger, *Adv. Mater.* **12**, 828 (2000).
31. M. Leclerc, *J. Polym. Sci. A Polym. Chem.* **39**, 2867 (2001).
32. S. Setayesh, A. C. Grimsdale, T. Weil, V. Enkelmann, K. Mullen, F. Meghdadi, E. J. W. List, G. Leising, *J. Am. Chem. Soc.* **123**, 946 (2001).
33. G. Zeng, W.-Y. Yu, S.-J. Chua, W. Huang, *Macromolecules* **35**, 6907 (2002).
34. U. Scherf, E. J. W. List, *Adv. Mater.* **14**, 477 (2002).
35. F.-I. Wu, D. S. Reddy, C.-F. Shu, M. S. Liu, A. K.-Y. Jen, *Chem. Mater.* **15**, 269 (2003).
36. B. Z. Tang, H. Xu, *Macromolecules* **32**, 2569 (1999).
37. B. Z. Tang, S. M. Leung, H. Peng, N.-T. Yu, K. C. Su, *Macromolecules* **30**, 2848 (1997).
38. B. Z. Tang, H. Peng, S. M. Leung, C. F. Au, W. H. Poon, H. Chen, X. Wu, M. W. Fok, N.-T. Yu, H. Hiraoka, C. Song, J. Fu, W. Ge, K. L. G. Wong, T. Monde, F. Nemoto, K. C. Su, *Macromolecules* **31**, 103 (1998).
39. B. Z. Tang, H. Xu, J. W. Y. Lam, P. P. S. Lee, K. Xu, Q. Sun, K. K. L. Cheuk, *Chem. Mater.* **12**, 1446 (2000).
40. L. W. Tutt, A. Kost, *Nature* **356**, 225 (1992).

CHAPTER 4

Silica Polyamine Composites: Advanced Materials for Metal Ion Recovery and Remediation

Edward Rosenberg

Department of Chemistry, University of Montana, Missoula, Montana

CONTENTS

Macromolecules Containing Metal and Metal-Like Elements, Volume 4: Group IVA Polymers, edited by Alaa S. Abd-El-Aziz, Charles E. Carraher Jr., Charles U. Pittman Jr., and Martel Zeldin
ISBN: 0-471-68238-1

I. INTRODUCTION

Environmental contamination due to waste water discharges containing high concentrations of toxic ions is ubiquitous. Sources include metal plating, pickling, pigments industries, tanneries, municipal landfills and wastewater treatment facilities, nuclear weapons production facilities and nuclear power generators, and mining waste. Increasing regulation on natural resource extraction and industrial waste water discharge has caused an increased interest in removal and recovery of these ions from waste streams as well as the remediation of contaminated sites.[1] The growing scarcity of high-grade mineral ores and the environmental problems associated with pyrometallurgy has lead to a steady increase in the use of hydrometallurgical techniques.[2] By far, the most popular solution mining technique is solvent extraction.[2] However, this technique suffers from some environmental drawbacks, including the use of flammable and toxic organic solvents, the buildup of crud at the aqueous–organic interface, and an inability to extract the desired metal to low levels. Recently, there has been increased interest in the use of solid-phase adsorbents for mining and metal ion remediation applications.[3]

The materials needed to effectively and economically treat these waste waters will ideally have the following properties: (1) the ability to reduce heavy metal ion concentrations to below allowable discharge limits; (2) high adsorption capacities for the target metal ions, even in solutions containing high levels of alkali and alkaline earth metal ions; and (3) the capability of processing waste water or ore leaches at high throughput rates.[1–4] Many materials are currently being developed for these purposes, but few can be said to have all of these features. Simple methods involve the use of agricultural waste materials and other biomass.[5,6] More sophisticated methods involve the ultrafiltration of soluble metal-binding polymers and resins containing intricately designed ligands.[3,7–10] The more advanced materials incorporate ligands designed to bind only one specific metal ion or a group of similar metal ions. This is accomplished in a number of ways; in some cases, molecular species or elements that demonstrate a preference for binding to the metal of interest are used in the ligand and/or the atoms in the ligand molecule are “preformed” to match the size and coordination geometry of the metal ion.[8–10] With these considerations in

mind, materials can be synthesized that are effective at removing the target ions, but the synthesis of these materials is often complicated and costly and the resulting material chemically delicate. An alternative to this method of rendering separations is to create a material composed of a single binding element in high density that is conformationally mobile. This type of material is not intrinsically selective for a specific metal ion, but based on the stability constant of the metal–ligand complex formed, the material selectively extracts metal ions in a series retaining those ions with a high stability constants more than those with a low stability constants.

Recently, patented polyamine-silica composite materials designed to remove transition metal ions from aqueous solutions have been developed at The University of Montana in collaboration with Purity Systems Inc.[11,12] These materials consist of linear or branched water-soluble chelating polyamines covalently bound to a silica gel support. For example, the material designated as WP-1 consists of poly(ethylene imine), MW 1,200, covalently bound to porous silica gel. Poly(ethylene imine) is a highly branched, water-soluble amine polymer containing primary-, secondary-, and tertiary-degree amino groups in a ratio of 0.35:0.35:0.30, respectively. The synthetic route (Fig. 1) yields good coverage of the silica gel with an organic coating and uses a polymer for

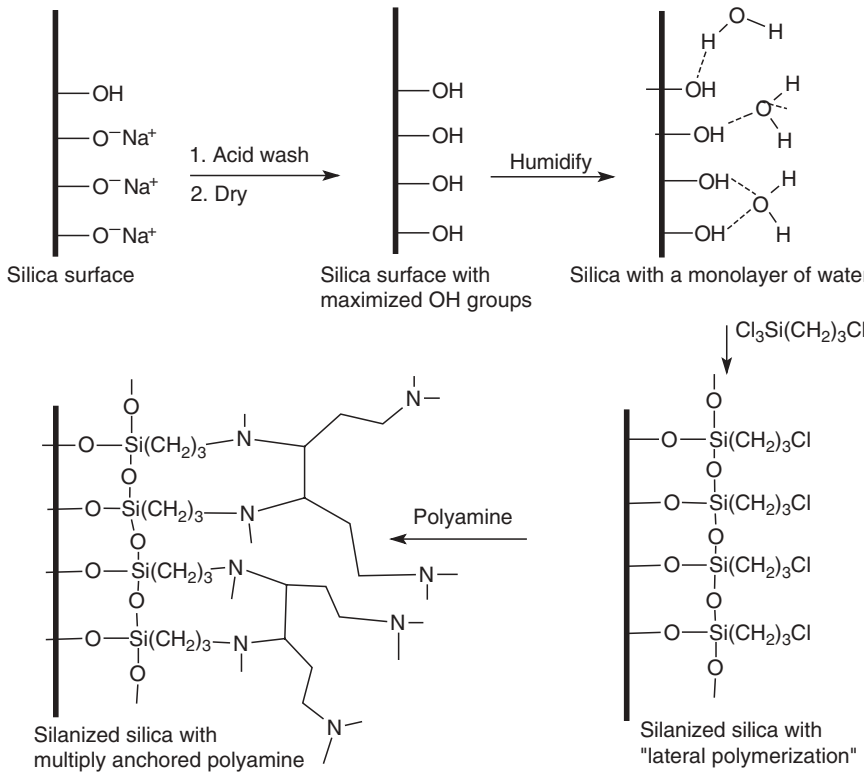

Figure 1 Synthetic scheme for making silica polyamine composites, illustrating the key features of humidification to promote "lateral polymerizan," for maximization of surface coverage.

which the chelating agent is an integral part of the matrix coating. These are key factors in creating a material that has remarkable durability.

These resins have been tested through 3000 cycles with no visible loss of physical stability and <10% loss in capacity.[12c] The copper capacity of the basic polyamine composites is in the range of 0.7–1.1 mmol/g, and depends on the polymer being used. To date we have tried three polyamines, poly(ethylene imine) (PEI), poly(vinyl amine) (PVA), and poly(allyl amine) (PAA) (Fig. 2).

These polyamine composites can be readily modified to make them selective for a given metal or group of metals over a particular pH range, in similar ways to those used for polystyrene resins.[12,13] These materials, however, offer distinct advantages over polystyrene resins (Table 1). These advantages have been demonstrated through

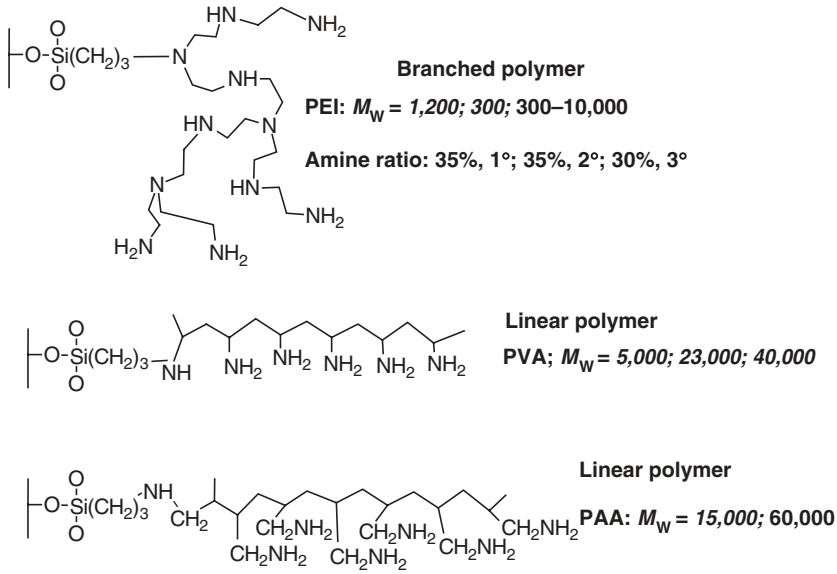

Figure 2 The polyamines used to synthesize the silica-polyamine composites, showing structures and the available molecular weights (only values in italics were used).

Table 1 Advantages of Purity Systems, Inc., Composite Resins over Polystyrene Resins

- No shrink–swell in load-strip-regenerate cycles; ideal for up or down flow fixed beds.
- Faster capture kinetics allows use of shallower beds.
- Available in four particle sizes: 200–165, 94–74, 74–38, and 38–22 mesh.
- Faster operational flow rates at higher capacities than conventional resins.
- More porous structure gives lower pressure drops at comparable particle sizes.
- Much longer usable lifetimes due to more rigid structure.
- Shipped dry (<10% water) compared with 45–50% water for polystyrene.
- Higher maximum operating temperature (110°C) compared with 70°C for polystyrene.
- More stable to radiolytic decomposition.
- Stable over a wide range of alkalinities and acidities.

studies that directly compare the properties of the polyamine composites with commercially available polystyrene resins.[12c,13]

In this chapter we provide an overview of the performance characteristics of these materials as they relate to the properties of the polymers and to the silica gels used in their synthesis as well as to some of their applications in mining and remediation problems.

II. RELATIONSHIPS BETWEEN COMPOSITE CHARACTERISTICS AND THE STARTING MATERIALS USED

A. Wide-Pore Amorphous Silica

The silica gels used in the synthesis of the polyamine composites are wide-pore amorphous silica made by controlled precipitation of sodium silicate with mineral acids. These silicas are available from a wide range of suppliers in particle sizes ranging from 30 to 1000 μm and with average pore diameters of 8–30 nm and pore volumes of 0.8–1.5 mL/g. Typical surface areas for these materials are in the range of 150–400 m^2/g. Depending on their size and method of production, the particles can be obtained in spherical or in irregular shapes. Their average bulk density is, of course, determined by a combination of all of these properties. We have synthesized silica-polyamine composite materials starting with a wide range of silica gels and found that the properties of the composite are extremely sensitive to its physical characteristics. Some generalizations, however, can be made (Table 2). First, the

Table 2 Changes in Density of Various Silica Gels Relative to Different Polyamine Composites

Entry Number	Material	Silica Gel (μm)	Polymer (M_W)	Composite Density (g/mL)	Silica Density	Pore Diameter (nm) [Pore Volume (mL/g)]
1	WP-1	Crosfield (100)	PEI (1,200)	0.49	0.29	15.0 (1.0)
2	BP-1	Crosfield (100)	PVA (5,000)	0.40	0.29	15.0 (1.0)
3	BP-1	Crosfield (100)	PVA (23,000)	0.42	0.29	15.0 (1.0)
4	BP-1	Crosfield (100)	PVA (40,000)	0.40	0.29	15.0 (1.0)
5	BP-1	Crosfield (100)	PAA (15,000)	0.45	0.29	15.0 (1.0)
6	BP-1	Nanjing (215)	PAA (15,000)	0.57	0.41	8.0 (0.8)
7	WP-1	Qingdao (110)	PEI (1,200)	0.70	0.46	9.0 (0.8)
8	WP-1	Qingdao (215)	PEI (1,200)	0.72	0.44	9.0 (0.8)
9	WP-1	Qingdao (215)	PEI (300)	0.67	0.44	9.0 (0.8)
10	WP-1	Aldrich (250)	PEI (1,200)	0.57	0.36	14.1 (1.1)

density of the composite is always greater than the starting silica gel. This means that the polymers are grafted in the silica gel pores and are not tethered to the surface of the gel. This is not all that surprising since >95% of the silica gel surface is inside the pores. The percent increase in density is relatively insensitive to the molecular weight of the polymer over the range of 5,000–40,000 (entries 2–5), but the 1200 MW branched polymer (entry 1) apparently fills the pores more efficiently. For the silica gels with larger pore diameters, the percent increase in bulk densities are about the same (38–55%; entries 2–5) but for those with smaller pore diameters the percent increase is considerably less for the larger MW polymers (entry 6 versus entries 7–9). As might be expected, the particle size has little influence on the percent increase in bulk density.

B. Particle Size and Back Pressure

The application of silica-polyamine composites to metal recovery in fixed beds usually involves a trade-off between good capture kinetics and acceptable back pressures. Smaller particle sizes can efficiently remove metals from fast-flowing streams but at the expense of higher back pressures. The relationship between these two parameters for the silica-polyamine composites is illustrated in Table 3. In all the table entries, the same polyamine was used and only the silica gel particle size (and unavoidably the pore size) was varied. It can be seen that an increase in average particle size of a factor of approximately 10 leads to a decrease in flow capacity of about a factor of 4.5 (entry 1 versus entry 4). By decreasing the flow rate by a factor of about 3 the flow capacity increases by about a factor of 2.5, with a corresponding decrease in pressure drop of about 3.5. The silica gels with average particle sizes <500 μm do not significantly increase in flow capacity on going from 2 to 0.6 column volumes per minute. This is because these materials (entries 3–5) are close to their equilibrium capacities, even at these relatively rapid flow rates. It should be pointed out that polystyrene beads normally sold in the particle size range of 250–500 μm have copper flow capacities of 0.31 mmol/g at flow rates of 2 column volumes

Table 3 Effect of Silica Gel Particle Size on Copper Flow Capacity and Pressure Drop[a]

Entry Number	Material[b] (PEI)	Density (g/mL)	Particle Size (μm)	Copper Flow Capacity[a] 2 cv/m mmol/g	Copper Flow Capacity[a] 0.6 cv/m mmol/g	Pressure Drop (psi) 2 cv/m (0.6 cv/m)
1	Tosoh	0.485	500–2000	0.18	0.41	70 (20)
2	Tosoh	0.520	500–1000	0.42	0.62	70 (20)
3	Aldrich	0.539	250–500	0.56	0.65	110 (30)
4	Crossfield	0.486	90–105	0.84	0.90	220 (60)
5	Qingdao	0.597	170–250	0.78	0.84	75 (25)

[a] Pressure drop (lb/in^2) across a 25 × 450-mm column; *cv*, column volumes/min.
[b] Silica gel supplier.

per minute.[12c] The intrinsically hydrophilic nature of the surface of the polyamine composite is thought to be responsible for their better capture kinetics at higher flow rates. We have found that for most of the applications tested so far the best compromise between back pressure and metal capturing performance are materials made with the particle size range 177–250 μm (60–80 mesh). This size gives pressure drops that are comparable to the 250–500 μm that is common for currently used polystyrene resins, yet has much better capture kinetics.

C. Capacity, Longevity, and Polymer Molecular Weight

In the course of our studies, we have synthesized silica-polyamine composites with polyamines having a wide range of molecular weights (Table 4).[14] We observed that for a given polymer type and silica particle size the copper capacity does not change. This could be due to the fact that there is a constant number of amine binding sites (chloropropyl groups) per unit area and that the larger MW polymers bind to more of these sites and take up more room in the pores. Thus the lower molecular weight polymers fit more molecules in each pore, which compensates for the smaller number of amine groups per site. The various polyamine composites were subjected to 1500 cycles (copper loading, acid stripping, and base regeneration). Although the silica gel matrix does not shrink or swell during the large pH swings (−1 to 13) occurring during the cycle test, the polymer will tend to uncoil on protonation and coil on deprotonation. This could result in considerable shearing stress on the silica gel matrix. The higher molecular weigh polymers would be expected to be more subject to this type of behavior, which could manifest itself as particle fragmentation and loss of capacity. The data in Table 4 clearly illustrate this phenomenon. Thus the composites prepared from 5,000–40,000 linear PVA show significant losses in bed volume and associated losses in capacity. The materials prepared from the lower molecular weight, branched PEI do show capacity losses associated with loss of polymer in some cases, but none shows the loss in bed volume associated with particle degradation.

Table 4 The Impact of Molecular Weight on Capacity and Longevity

Polymer (Silica Particle Size)	M_W	Flow Capacity mmol/g (SEM)	Average Capacity 1500 cycles (mmol/g)	Capacity Loss or Gain (%)	Bed Volume Loss (%)
PEI (100)	1,200	0.84 (0.01)	0.79 (0.01)	−6.0%	0.0%
PVA (100)	5,000	0.89 (0.03)	0.93 (0.04)	+4.3%	5.7%
PVA (100)	23,000	0.86 (0.05)	0.70 (0.03)	−18.6%	9.8%
PVA (100)	40,000	0.88 (0.06)	0.77 (0.03)	−12.5%	16.3%
PEI (250)	1,200	0.51 (0.02)	0.38 (0.03)	−25.5%	0.0%
PEI (250)	300	0.51 (0.01)	0.42 (0.02)	−17.6%	0.0%
PEI (250)	1,200	0.86 (0.04)	0.77 (0.03)	−10.5%	0.0%

III. COMPARISON WITH OTHER RESIN TECHNOLOGIES

Silica-polyamine composite materials have been available as chromatographic materials and as potential metal-sequestering agents for quite some time.[15–18] A variety of synthetic approaches have been taken in an attempt to produce stable and economically viable materials. These include binding a silane to a polyamine and then binding the resulting silanized macromolecule to the silica surface,[15] physically adsorbing the polyamine to the surface of silica and then crosslinking the polyamine with a second polymer,[16] and grafting a linker polymer to silica by covalent bonding and then attaching the polyamine to the linker. In addition, there is a considerable literature on using 3-aminopropyl trimethoxy silanes as platforms for attaching metal-selective ligands to silica gel.[19] The problem with all of these approaches is that little attention has been paid to the most important aspect of obtaining a high-capacity composite with a long usable life time: obtaining good coverage of the silica gel surface with the silane anchor. To address this issue, we pursued an approach used to improve the longevity of high pressure liquid chromatography columns.[20,21] There are several key steps to this approach First, the silica gel must be acid washed, dried, and then rehumidified. The rehumidification ensures lateral polymerization of the silane group, which results in more complete coverage of the silica gel surface (Fig. 1). Previous work has shown that coverage on the order of 80% can be obtained.[20,21] Second, we found that the use of trichlorosilanes instead of trialkoxy silanes in non-polar solvents helps drive the silanization to completion by out gassing the hydrochloride formed in the reaction. The impact of the hydration step on the silane–silica reaction is obvious from the ^{13}C-NMR CP-MAS spectrum of humidified and unhumidified samples of silanized silica. A sample that was not rehumidified shows a significant methoxyl peak arising from the methanolysis of unreacted chlorosilane groups (Fig. 3*A*). Rehumidification results in a spectrum that has a barely detectable methoxyl peak (Fig. 3*B*). This indicates that all of the chlorosilane bonds are reacted and suggests a much better coverage of the surface.[12a]

Perhaps the best evidence for the superior quality of the composite comes from our comparative studies with other polyamine composites and polystyrene resins. Ramsden et al. synthesized a silica-polyamine composite by reacting 3-chloropropyl trimethoxy silane with PEI, and then reacting the resulting polyamine silane with silica gel.[15] We reproduced this synthetic approach with the same silica used in our procedure (Fig. 1). The material produced had a density of 0.31 g/mL versus 0.49 g/mL for WP-1. A scanning electron micrograph of the two materials revealed a much smoother surface for WP-1 relative to the material produced by the method of Ramsden (Fig. 4).

Most significantly, we tested the two materials in exactly the same manner using a computer-controlled copper sulfate load, water rinse, acid strip, water rinse, base regenerate, and water rinse cycle. The results of these tests are summarized in Figure 5. The Ramsden composite column plugged after about 400 cycles, owing to

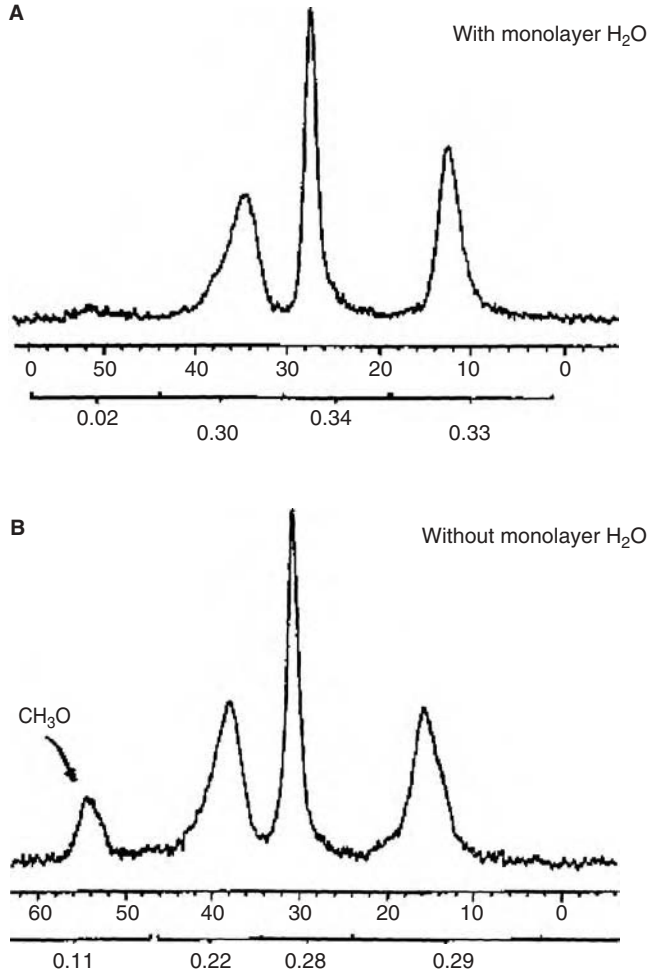

Figure 3 ^{13}C-NMR CP-MAS of the aliphatic region of silica gel silanized with 3-chloropropyl silane with hydration, (**A**) and without hydration, (**B**) showing the methoxyl peak intensity.

collapse of the gel as a result of deterioration of silica matrix. To test the impact of the rehumidification step on the Ramsden method, the silica gel was hydrated according to our procedure.[11,12] This resulted in a considerably longer lifetime for the gel, but collapse was still observed after 1000 cycles. This in turn suggests that although hydration is important in getting better surface coverage, attaching the silane to the bulky polymer first leads to a poorer coverage of the silica surface.

We also cycle tested a polystyrene chelator resin for material lifetime. Here, the column held its capacity. However, after about 1200 cycles the particles degraded,

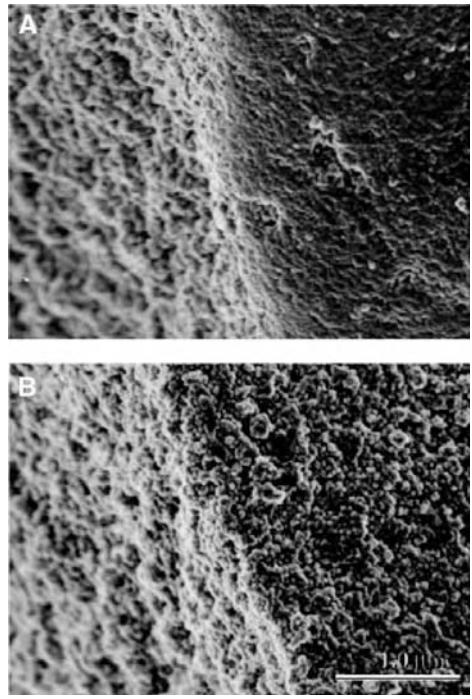

Figure 4 Scanning electron micrograph at 30,000 magnification of WP-1 (**A**) and the silica polyamine composite prepared according to the method of Ramsden (**B**)[15] both prepared from the same 100-μm silica gel.

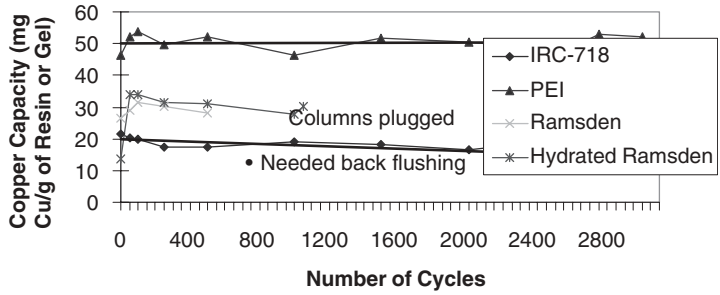

Figure 5 Results of cycle testing for WP-1 (PEI), silica-polyamine composites made according to Ramsden[15] and a polystyrene resin IRC 718.

owing to the shrink–swell cycles resulting from the large swings in pH. The process required back flushing to relieve high back pressures every 250 cycles.

The flow capacities of both the Ramsden materials and the polystyrene chelator resin were less than half that of the WP-1 for the fast flow rates at which these tests were done (two column volumes per minute). More important, after 3000 cycles there

was no back pressure buildup in the WP-1 column and no loss in the volume of the material, while both the polystyrene resin and the other silica-polyamine composites showed 20–30% losses in bed volume. Perhaps even more significant, the flow capacity of the 250–500 μm WP-1 is 0.56 mmol/g, the 500–1000 μm is 0.42 mmol/g at two bed volumes per minute, and the polystyrene resin tested with a particle size range of 300–1000 μm showed a flow capacity of 0.31 mmol/g at the same flow rate (Fig. 4, Table 3). These results clearly illustrate the superior capture kinetics of WP-1 relative to a polystyrene resin.

IV. STRUCTURAL CONSIDERATIONS

A. The Nature of the Polymer Graft to the Silica Surface

The reaction of the polyamine with the 3-chloropropyl trichlorosilane anchor undoubtedly leads to multiple point bonding on the silica surface. Indeed, it is this feature of the composite materials that adds to their durability. What is uncertain is the structural relationship between the anchor points. In the case of the linear polymers PAA and PVA, the polymer could bind to the silane using adjacent nitrogen sites, leaving a "dangling end" coming off the surface of the silica gel. Alternatively, alternating or random nitrogen sites along the entire polymer chain could bind to the anchor, creating a "looped" structure. We can gain some insight into the general composition and indirectly into the "gross" structure of the composite by doing an elemental analysis of the materials at each stage of the synthesis (Fig. 1). Thus, after reaction of the silica gel with the 3-chloropropyl trichlorosilane chlorine, analysis gives the total number of available nitrogen-binding sites. After reaction of the chloropropyl groups with the polymer, residual chorine analysis, in combination with the nitrogen analysis and the change in the carbon content, reveals the number of polymer nitrogen atoms that are bound to the anchor, if one assumes none of chlorine atoms is hydrolyzed during the polymer-binding step. Using this approach, 4 of every 10 nitrogen atoms of the polymer are bound to the silica. Subsequent reaction of the PAA composite BP-1 with picolyl chloride produces PSI's patented copper selective composite, CuWRAM.[13,22] The change in carbon and nitrogen analysis provides the average number of picolyl groups bound to the polymer nitrogen atoms, which turns out to be 4 out of 10 as well. The overall metal capacity is approximately half of the precursor, BP-1 (~0.5–0.6 and 1.0–1.1 mmol/g, respectively), but the selectivity for copper over other metals is remarkable (separation factors of 500–1000).[20,22] These facts taken together suggest that the amino groups that are bound to the anchor and the unmodified amino groups are both not accessible to the metal ions. This is more consistent with a looped structure, in which the polymer is bound to the silica surface along the entire length of the polymer chain (Fig. 6).

We subjected the branched polyamine composite that was modified with chloroacetic acid, WP-2, to a similar analytical procedure. Here, we made the assumption that the tertiary amine residues in the polymer do not participate in bonding to the

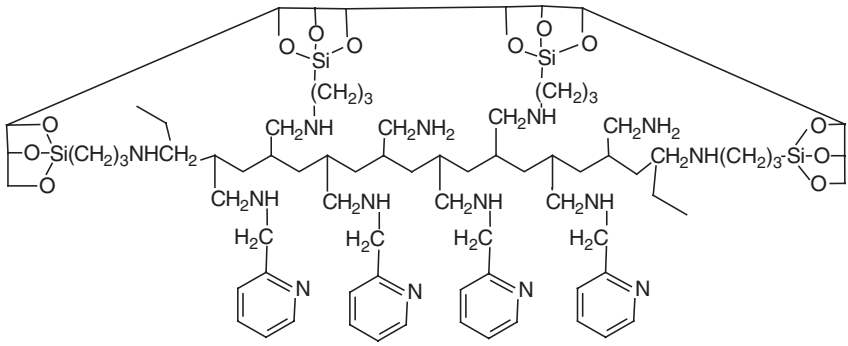

Figure 6 The structure of CuWRAM, a copper-selective silica-polyamine composite, based on elemental composition and adsorption behavior.

silane anchor or the acetic-acid-modifying ligand. It seems unlikely that any significant number of tertiary amines would undergo alkylation, because this would create a positively charged composite that would not be expected to have an affinity for cations, as observed. Correcting for this assumption we calculate that five of eight primary and secondary amines are bound to the silica anchor. Given the lower molecular weight and branched nature of the PEI used to make this composite, it seems likely that the polymer is bound flat on the silica surface. Reaction of the PEI composite, WP-1, with chloroacetic acid results in a composite that has different metal coordinating properties and lower overall metal capacities (vide infra). Therefore, it is likely that all three of the remaining amino groups have been converted into amino acetic acid residues and that the amino groups bound to the silica surface have also been converted, or that their access to the metal ions in solution have been blocked by the more accessible amino acetic acid groups not bound to the surface. Based on the observed weight gains and the changes in the elemental composition, the latter is the more likely possibility.

Thus a working structural model for the ligand-modified composites WP-2 and CuWRAM emerges where the propyl-bound amino groups do not participate in metal coordination. This accounts for their greater selectivity and lower metal ion capacities. The unmodified materials WP-1 (PEI) and BP-1 (PAA) probably use most if not all their amine groups in metal ion coordination. This working model is, of course, based on indirect evidence and must be verified by direct structural investigations with solid-state techniques such as NMR, ESR, ENDOR, and low-angle X-ray techniques.

B. Polymer Structure and Metal Ion Coordination

Although, as stated in the previous section, the basic polyamine composites WP-1 and BP-1 need to be modified to enhance their selectivity and operational pH

range, there are significant intrinsic differences in their metal-ion-coordinating properties (Fig. 7). First, it can be seen that metal capacities fall to zero simultaneously below a pH of 2 for the linear, higher molecular weight polymer (Fig. 7*B*), while there is still significant copper and nickel capacity below pH 2 for the branched polymer. This is undoubtedly due to the fact that PEI has 1º, 2º and 3º amino groups that have different basicities and therefore different binding constants for a given metal. This is also reflected in the divalent metal ion selectivity, which for WP-1 is Cu > Co > Zn > Ni at pH 3 and for BP-1 is Cu ⩾ Ni∼Co > Zn. The Irving–Williams series for the ethylene diamine ligand predicts the order Cu ⩾ Ni > Co∼Zn.[23] That nickel is unexpectedly lower for the branched polymer may reflect the tendency for this metal to adopt higher coordination numbers than the other metals, which would be more difficult for the more rigid, lower molecular weight and more surface-bound branched polymer.

Although the higher molecular weight linear polymer composites give higher metal ion batch capacities (66 mg/g for 15K PAA versus 50 mg/g for 1200 PEI at pH 3), they exhibit somewhat poorer capture kinetics under flow conditions, with silica gels having smaller average pore diameters. We recently investigated a silica gel

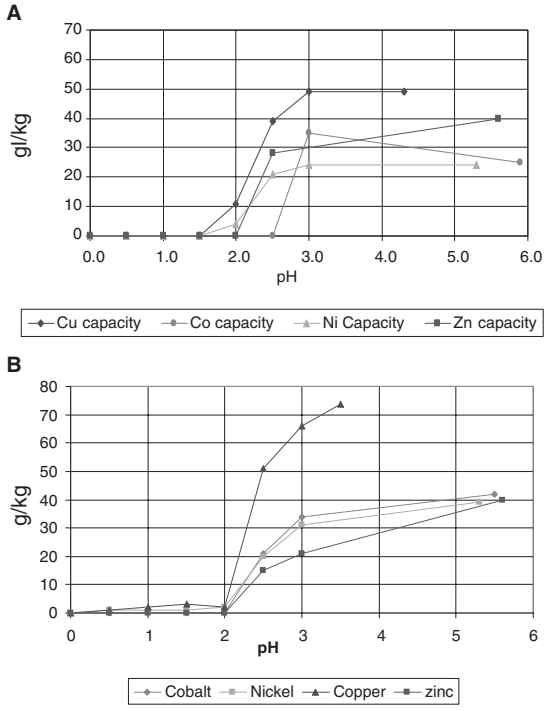

Figure 7 pH profiles for transition metal ion batch capacities for a WP-1 made with branched polymer PEI, MW = 1200 (**A**) and BP-1 made with linear polymer PAA, MW = 15,000 (**B**). The same silica gel was used for both.

with average pore diameter of about 8.0 nm with a particle size range of 177–250 µm. We found that the copper breakthrough point for the higher molecular weight PAA was at about five bed volumes, while the lower molecular weight PEI had a copper breakthrough point at nine bed volumes (Fig. 8). When a silica gel with wider average pore diameter is used, this difference disappears. The real problem occurs when we convert BP-1 to CuWRAM using the 8.0-nm pore resin. The introduction of a bulky hydrophobic modifying ligand (picolyl chloride) apparently blocks the pores completely, and the resin loses adsorptive capacity under normal flow conditions. Batch capacities remain almost unchanged relative to the wider pore silica gels.

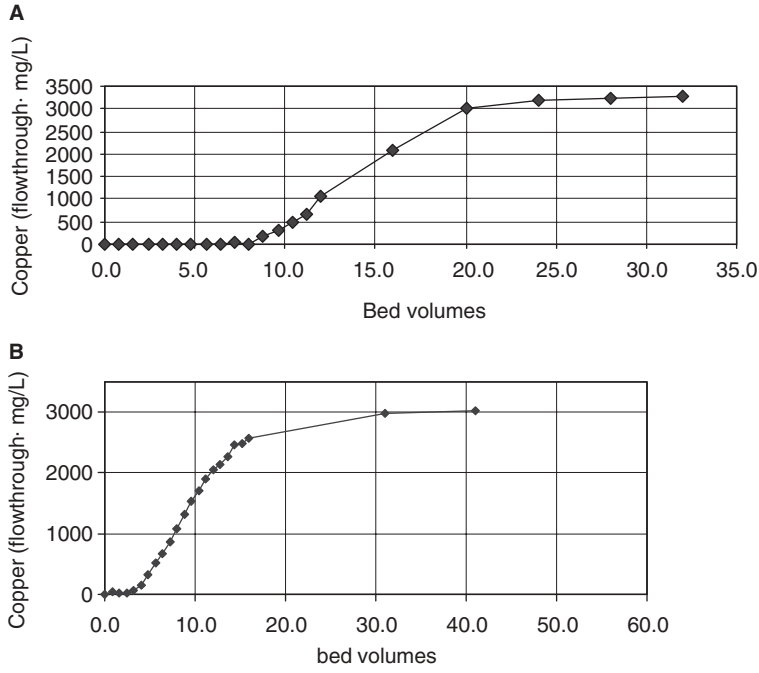

Figure 8 Breakthrough curves for a 50.0 mM solution of $CuSO_4$ run through a 5-mL column at 0.5 bed volumes per minute for WP-1 made with PEI, MW = 1,200 (**A**) and BP-1 made with PAA, MW = 15,000 (**B**). Both composites were prepared from the same silica gel with 8.0-nm average pore diameter and 177–250 µ particle size range.

C. Molecular Modeling Studies

The differences in behavior noted for the different polymers, especially in the smaller pore silica gels, prompted us to attempt some molecular modeling to understand the intrinsic conformations of the linear and branched polymers when anchored to a

fixed surface. We used the molecular mechanics program *Sybyl* 6.7 and the calculations were done on an Octane R12000 computer operating in a Silicon Graphics environment (Tripos Associates, St. Louis, MO; Silicon Graphics, Inc., Mountain View, CA).[24] The results of these studies included neither solvent interactions nor the complexation of the metal ions. Our primary goal was to view the low-energy conformations of a 10-unit segment of the picolyl modified polyamine CuWRAM in the presence and absence of the surface constraints. We started from the schematic representations of the composites based on their elemental composition and chemical behavior (Fig. 6). The silica gel surface was simulated by attaching the silane anchors to a rigid carbon skeleton. Figure 9*C* shows one of many minimum energy conformations of the 10 repeat units with unconstrained propyl silanes. In all of the low-energy conformations, the polymer tends to coil and the aromatic groups tend to stack. The high-energy conformations are all elongated (Fig. 9*D*) with the aromatic and propyl silane groups being far apart. This, of course, makes sense in light of the expected attractive polarization forces between the hydrocarbon groups. The question is, would these interactions persist in the presence of water molecules that would be expected to hydrogen bond with the amino groups? What is more important is that the

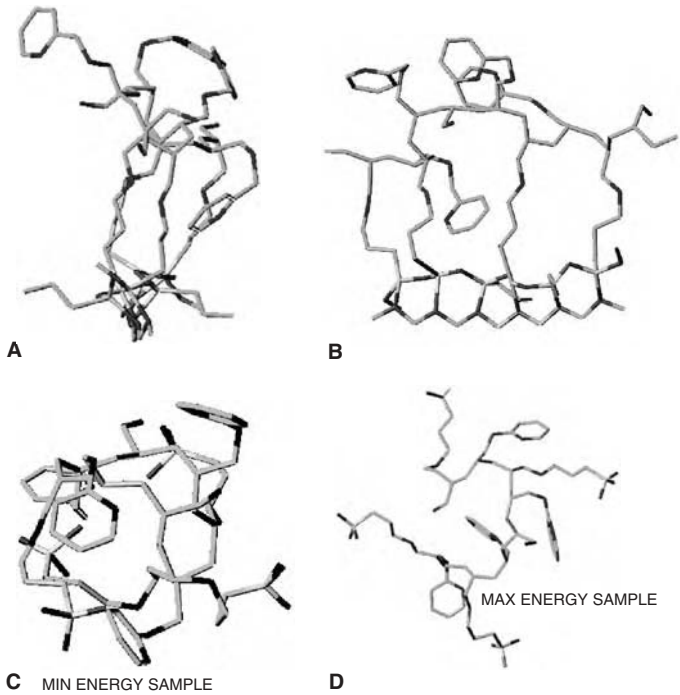

Figure 9 Sybyl generated conformations of 10 repeat units of CuWRAM. **A**, Side view minimum energy surface constrained. **B**, Front view minimum energy surface constrained. **C**, Minimum energy unconstrained. **D**, Maximum energy unconstrained.

surface-constrained situation (Fig. 9*A* and *B*), in which the silane anchors project away from the rigid surface the polymer, still tends to coil and the aromatic residues still tend to group. In the confines of the pore this intramolecular association of the polymer may persist even in the presence of a polar solvent, and this could account for poor capture kinetics observed with CuWARM and BP-1 when silica gels with smaller pore diameters are used (see Section III.B). These preliminary studies illustrate the value of molecular mechanics calculations in understanding polymer behavior. More recently, we have extended the calculations on the unconstrained polymer to a constrained 40-repeat-unit polymer, as well as adding metal ions and water molecules to get a more complete picture of the conformational behavior of these polyamines in constrained environments.

V. APPLICATIONS

A. Metal Chromatography: Separation and Concentration of Multicomponent Metal Mixtures from Acid Mine Drainage

Acid mine drainages from abandoned and operational sulfide ore mines present an environmental threat to surface waters and underground aquifers worldwide. Aquatic life is particularly vulnerable to high levels of transition metals such as copper and zinc.[25] The Berkeley Pit in Butte, MT, is one of the largest open-pit mines in the world. The pit is constantly filling with contaminated acid mine drainage and will threaten Butte's water supply by 2030. The pH of the water is 2.5 and contains an average of 1000 ppm iron, 500 ppm Mg, 150 ppm Cu, 500 ppm Zn, 200 ppm Mn, 250 ppm Al with about a $\pm$ 20% variation with depth and various other trace elements. In 1997 we performed a bench scale demonstration project, the results of which were verified by the EPA. Our approach was to do an iron/aluminum/magnesium separation using well-established precipitation techniques and then separate and recover the commercially viable metals copper, zinc, and manganese. The intent here was to offset the price of acid mine drainage remediation by recovery of the more valuable metals.

The economics of iron precipitation as a separate process was addressed in the work of Hsin-Hsiung et al.[11] Consequently, it was desirable to use an oxidizing agent that is easily handled on a laboratory scale and a base that would dissolve quickly and completely at the desired concentration. For these reasons, the initial step on the Berkeley Pit water was to precipitate the iron from the water selectively. This step removed most of the iron and aluminium, producing a test water that had a pH of 4.1 and contained the elements of interest in the following concentrations: Al = 41.1 ppm, Cu = 131.9 ppm, Mn = 214.3 ppm, and Zn = 548.6 ppm; the total iron concentration was reduced to $<$4 ppm.

Inspection of the WP-1 flowthrough concentrations (Fig. 10) readily shows that the copper and aluminium are almost totally removed from the treated Berkeley

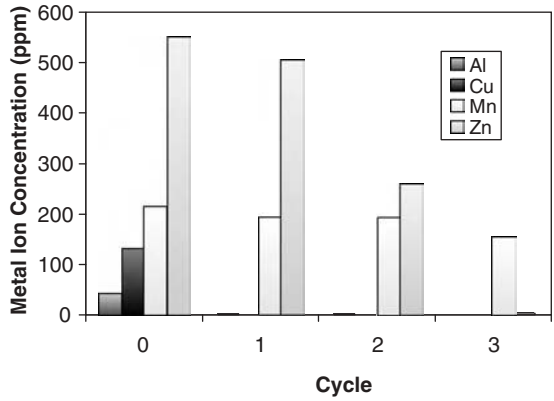

Figure 10 Metal ion concentrations in the flowthrough after three cycles of adsorption followed by stripping of three tandem columns of WP-1 (0 on the horizontal indicates the composition of the feed).

Pit water after the first cycle, while the manganese and zinc concentrations remain essentially unchanged. After cycle two, the concentration of zinc is almost reduced by half, whereas once again the manganese concentration remains unchanged. After three cycles, the zinc is almost completely removed, whereas the manganese concentration remains stable. These data indicate that WP-1 will selectively bind to copper and aluminium before binding with zinc and that there is a strong affinity for zinc over manganese. A similar test was done with WP-2. Comparison of WP-1 flowthrough concentrations with WP-2 flowthrough concentrations shows that WP-1 and WP-2 complement each other in their selectivity. While 99.0% of the copper was removed after the first pass through the WP-2 columns, 71% of the aluminium remains in the flowthrough. This demonstrates good separation of two metal ions that did not separate using WP-1. Following the concentration of metal ions in the column strips shows an even clearer picture of the selectivity. The three loaded columns are removed and individually eluted with acid. The column closest to the pump is designated column 1 and the column from which the test water exited is designated column 3. Figure 11 depicts the concentration of metal ions eluted from each of the three WP-1 columns over the three cycles. Columns 1 and 2 of cycle one show high concentrations of copper and aluminium in an approximate 4:1 ratio, with the exclusion of zinc and manganese. In column 3, there is a dramatic rise in the zinc concentration with a concurrent drop in copper concentration. The graph also shows an almost singular extraction of zinc until column 3 in cycle three, where an increase in manganese concentration occurs. The aluminum and copper concentrations in the flowthrough after cycle one are 1.9 and 0.1 ppm, respectively; coupled with the strip profile for cycle one this strongly suggests that zinc is not removed to any substantial extent until the copper and aluminum are removed to low levels. Similar conclusions can be drawn about the relationship between zinc and manganese by comparing the flowthrough and strip data of cycle three.

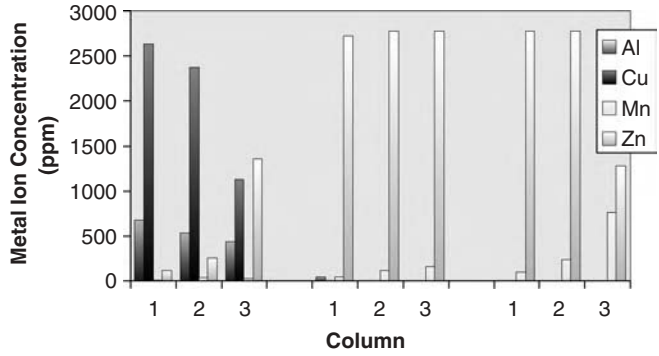

Figure 11 Sulfuric acid strip concentrations on tandem columns 1–3 after each load cycle with iron-precipitated Berkeley Pit water at pH 4.1.

The strip data can also be used to determine the percentage of each of the four metals in relation to the total concentration of the critical metals using the formula [M]/[Cu (II)] + [Al (III)] + [Mn (II)] + [Zn (II)], where M = Cu, Al, Mn, or Zn, and the concentrations are in milligrams per liter. These calculations will give an indication of the relative purity of the strip. This initial test has produced some promising results. Using WP-1 alone produced copper strips with 75% purity and zinc solutions with 95% purity. Using WP-2 alone produced copper solutions with 92% purity.

The increase in metal ion concentration in the strip from the treated water is reported as the concentration factor. The concentration factor is determined from the following equation: Concentration factor = $[M^{n+}]$ in strip / $[M^{n+}]$ in original solution. The emphasis of these tests was metal ion separation; therefore, the concentration factors reported here are far from optimal. The concentration factors for the WP-1 strip were Cu = 20, Al = 17, and Zn = 5. The concentration factors for the WP-2 strip were Cu = 19, Al = 3, and Zn = 3.

B. Selective Recovery of Copper from Solvent Extraction Circuit Waste Streams of Acid Mine Leaches

Although solvent extraction has proven to be an effective method of recovering copper from oxide ore acid leaches, the solution wastes from this process often contain significant amounts of copper (up to 1 g/L).[2] The waste streams are most often recirculated in the extraction circuit, which eventually build up undesirable metal impurities. The circuit must be periodically bled, thus wasting a large amount of copper. The silica-polyamine composite CuWRAM (Fig. 12), contains the picolyl ligand (2-methylaminopyridine) that has a particularly high binding constant for copper. Previous work has shown that this type of ligand was effective in separating copper from ferric ions, the major component in solvent extraction raffinates and acid ore leaches, when bound to a polystyrene resin.[9a]

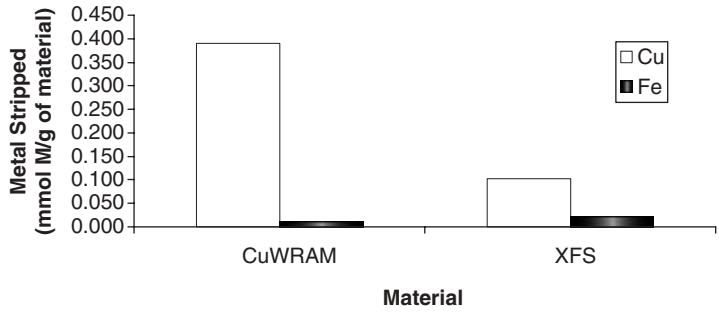

Figure 12 Sulfuric acid strips of 5-mL columns of CuWRAM and Dowex 43084 (XFS) after loading 14-bed volumes of a solution containing 3000 ppm Fe^{3+} and 1000 ppm Cu^{2+} at pH 1.5.

In this section, we present the results of our studies on the recovery of copper from an actual solvent extraction raffinate from a copper mine in the United States and compare its performance to Dowex 43084 on mock ore solutions. Fourteen bed volumes of a solution containing 3000-ppm ferric ion and 1000-ppm cupric ion at pH 1.5 were passed through a 5-mL column containing CuWRAM at 2 bed volumes per minute. The experiment was repeated using the same volume of Dowex 43084 (labeled XFS, its alternative name, in Fig. 12). The contents of the sulfuric acid strip solutions reveal that the CuWRAM is more selective and has a higher flow capacity at relatively rapid flow rates. The difference in flow capacity is partially due to the difference in particle size of the two materials (100 μm for CuWRAM and 250–500 μm for XFS). However, we have previously shown that at equal particle sizes and flow rates the silica-polyamine composites have about 80% better flow capacities at 2-bed volumes per minute and at equal particle sizes (see section I.B).[12c]

The differences in the separation factors are truly remarkable. The separation factor is equal to $q^{Cu}/c^{Cu} / q^{Fe}/c^{Fe}$ where q^{Cu} and q^{Fe} are the amounts of copper and iron adsorbed onto the extractant, respectively, and c^{Cu} and c^{Fe} are the amounts of copper and iron in solution, respectively. Under the conditions of this experiment, the separation factor for CuWRAM is 1047 while for Dowex 43084 is 60, with copper capacities of 23.5 and 11.8 g/kg resin. The batch capacity of Dowex 43084 is actually considerably higher than CuWRAM at 30 g/kg resin.

More recently, we improved the loading of the picolyl ligand and obtained batch capacities even more than those reported for Dowex 43084 (45 g/kg).[20,22] We used this improved CuWRAM to repeat our initially reported recovery of copper from solvent extraction circuit raffinates.[13]

The results of this test show that for solvent extraction raffinates the effective removal of copper from ferric ions can be accomplished. Figure 13 shows that for over 35-bed volumes copper is selectively removed to <10 ppm, while almost all of the ferric ions are passed. The graph illustrates that initially ferric ions are captured

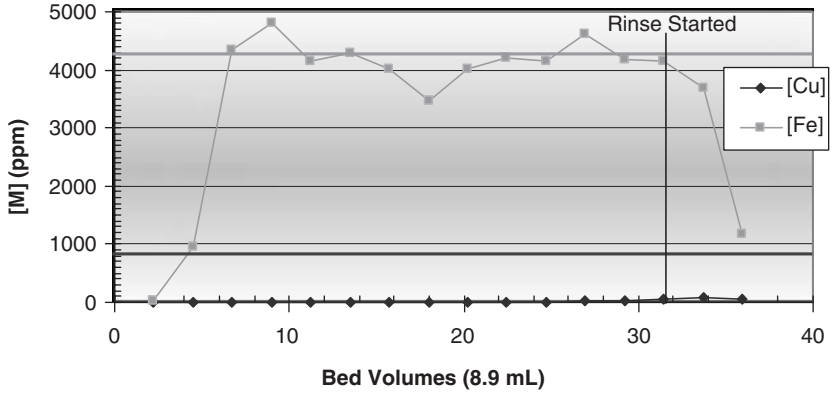

Figure 13 Breakthrough curve for a solvent extraction copper raffinate loaded onto an 8.9-mL CuWRAM column at 0.5 bed volumes per minute containing 800 ppm copper and 4300 ppm ferric ions (*horizontal lines*) at pH 0.9. *Vertical line* indicates when rinse was started. Copper loading was 29.9 g/kg.

by the resin, but they are gradually displaced by copper. When the copper concentration in the flowthrough started to rise in the column, it was rinsed with water and then stripped with concentrated sulfuric acid to yield a strip of 79,000-ppm copper that contained <5% ferric ion. This resulted in a separation factor of ~500 using the formula given above. This separation factor is even more impressive considering the low pH (0.9) at which the test was conducted. We previously showed that the Dowex 43084 performed much less adequately at pH values <1.[9a,13] The reasons for the much better performance of CuWRAM relative to its polystyrene counterpart are not entirely clear at this time. Certainly the hydrophilic nature of the silica composite surface is a factor, but there are also significant differences in the molecular architecture between the two materials that must be further elucidated before any firm conclusions can be drawn.

A separate test was done on an acid ore leach from an Australian copper mine that uses ferric iron to oxidize copper sulfide ores, and where the reduced ferrous is reoxidized by air. The resulting leach has a rather low copper content and contains significant amounts of other transition metals as well as alkaline earth metals at pH 0.95. This presented a significant challenge to CuWRAM. The same bench scale configuration was used as in the previous test, and the results are shown in Figure 14. Here, the ratio of copper to ferric iron in the feed was even lower than in the previous test (~500:7200). After 300 mL of the feed was passed through the 8.9-mL column at 0.5 bed volumes per minute, the column was rinsed and stripped. A separation factor of 127 was achieved and a concentration factor of 14 was realized for copper. Most significant, CuWRAM passed all the other metals completely, with exception of nickel and arsenic, where some co-loading of these metals was observed. The experimental details of these tests have been reported elsewhere.[13,20,22]

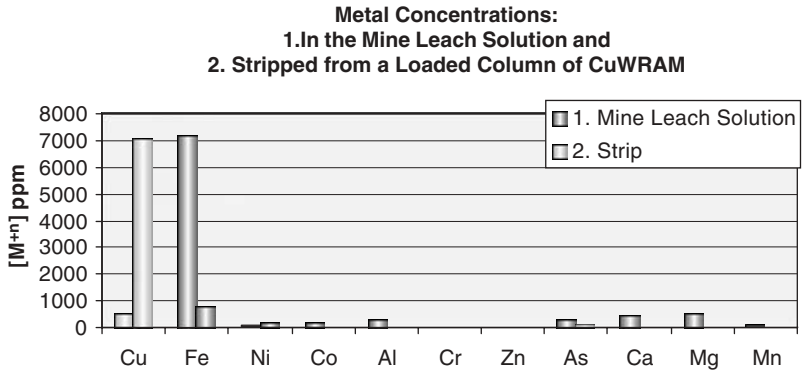

Figure 14 Feed (1; left) and strip (2 right) concentrations of the metals in a ferric acid mine leach. An 8.9-mL column was loaded with 300 mL of feed, rinsed, and then stripped with 8N sulfuric acid. Analyses were done by ICP-AA.

C. Separation of Cobalt and Copper Using Two Different Polyamine Composites in Tandem Columns

Section III.A discussed how WP-1 and WP-2 could be used as metal ion chromatographic materials. Given the selectivity of CuWRAM for copper, we thought that the use of this resin in a tandem column composed of WP-2 could be used to separate more effectively this metal from other transition metals. To test this hypothesis we obtained a sample of a copper solvent extraction waste stream from a chalcocite (Cu_2S)/cobaltite (CoAsS) ore leach from a mine in the United States. The iron in the leach had been removed by precipitation before the copper solvent extraction and contained significant amounts of copper and cobalt as well as arsenic. The goal was to separate the cobalt from the copper and to reject the arsenic.

The pH of the solution was 4. Two 5-mL columns of CuWRAM and WP-2 were loaded with 30 mL of the solution by first passing the solution through the CuWRAM column and then passing the effluent through the WP-2 column. As can be seen in Figure 15 the single pass through the CuWRAM column removed all of the copper. Two passes through the WP-2 column were required to capture all the the copper. Two passes through the WP-2 column were required to capture all the cobalt. Significantly, no detectable amounts of arsenic were present in the strip, and a perfect separation of copper from cobalt was realized. The arsenic was probably present as $H_2AsO_4^-$ at this pH and does not compete with the sulfate that is taken out with copper in the CuWRAM step. WP-2 takes out cations by exchanging them with protons and would not be expected to remove any anion. The concentration factors achieved were impressive but could be greatly improved by optimizing strip volumes and by recycling the strip solutions, a technique that we have often used.[26]

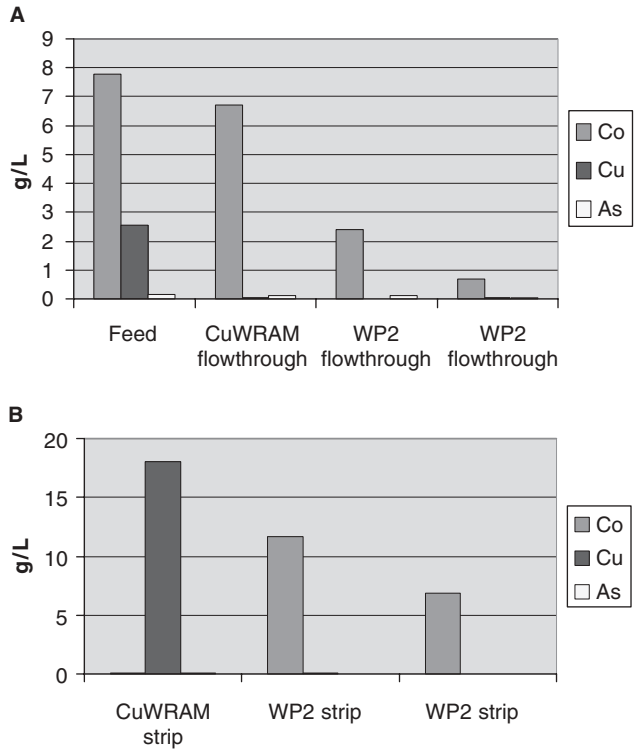

Figure 15 Flowthrough (**A**) and strip (**B**) resulting from successive loading of 5-mL CuWRAM and WP-2 columns with 30 mL of a raffinate form of a copper solvent extraction circuit after iron precipitation by adjustment to pH 4.

D. Removal of Mercury from Waste Solutions Using Sulfur-Modified Silica-Polyamine Composites

We previously reported the synthesis of thiol-modified silica-polyamine composite using ethylene sulfide.[12b] Although the reaction of ethylene sulfide with WP-1 gave a material that had excellent mercury capture characteristics, this ligand is toxic and difficult to make and handle. In addition, ethylene sulfide polymerizes with itself in the presence of nucleophiles; therefore, we could not tell if we were dealing with an amino-thiol ligand (Fig. 16*A*) or a polysulfide ligand (Fig. 16*B*).[27]

We also wanted to evaluate whether an aminothioether or dithiocarbamate ligand would work as well as the thiol functional group as the mercury selective agent. Four sulfur-containing compounds were tried, and their conversions to the corresponding sulfur-containing functional group are shown in Figure 17.

The ethylene-sulfide-modified material gave a sulfur-containing derivative that had excellent capture kinetics for removing mercury, cadmium, and lead from

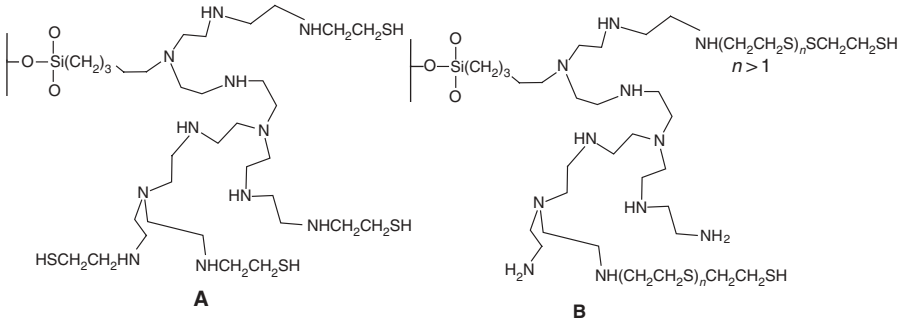

Figure 16 Possible structures for the reaction products of ethylene sulfide with WP-1. **A**, An aminothiol. **B**, A polysulfide appended to the polyamine.

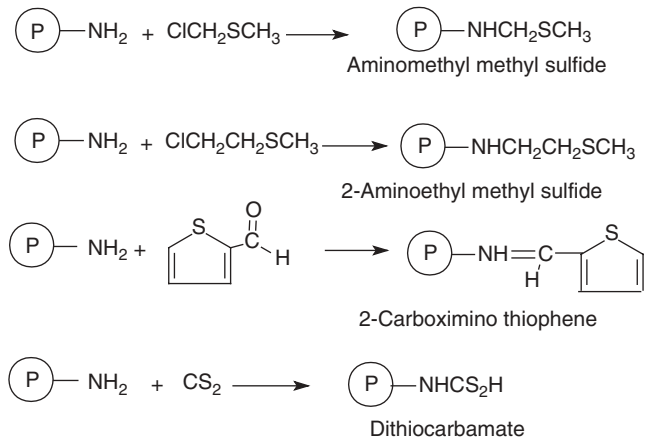

Figure 17 Structures of the modifying sulfur ligands to be used and the proposed functional groups that should result from their reaction with WP-1 and BP-1.

solutions containing the National Sanitary Foundation's recommended level of these ions (6, 30, and 150 ppb, respectively) to below their EPA recommended release levels of 2, 6 and 15 ppb, respectively.[28] The results were encouraging in that the ethylene-sulfide-modified material removed the toxic metals to safe levels for $>$600 gal of solution applied to a $\sim$50 g column at flow rates of 1.5 L/min (Fig. 18). Furthermore, in the case of mercury, the captured ions proved difficult to remove, resisting leaching with even 10 M hydrochloric acid. Thus this type of material could prove useful for immobilizing toxic metals for eventual disposal in a landfill. However, as stated above, ethylene sulfide is toxic and expensive to produce in large quantities. In addition, the functional group is unstable toward slow oxidation, which could lead to a release of mercury.

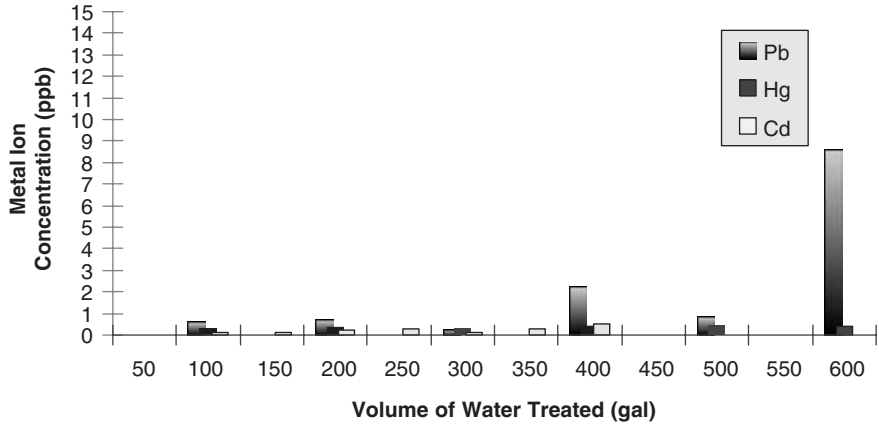

Figure 18 Removal of Hg, Cd, and Pb by the ethylene sulfide-modified resin at a flow rate of 1.5 L/min through 27-cm^3 column containing 50 g of resin.

We, therefore, set out to find an alternative to this composite material for remediation and immobilization of toxic metals. Table 5 shows the results of the elemental analyses for the various polymer composites and the materials resulting from their reaction with the listed sulfur-containing ligands. Several important conclusions can be drawn from these data. First, none of the chloroalkyl sulfide ligands

Table 5 Elemental Analyses and Mercury Capacities of Silica Polyamine Composites

Polymer	Ligand	C (%)	H (%)	N (%)	S (%)	S:N	Hg Flow Capacity (mmol/g)
PEI	—	10.70	3.15	4.63	0.29[a]	—	0.67
PVA	—	13.47	2.29	3.47	0.50[a]	—	0.94
PAA	—	14.21	2.77	3.54	0.45	—	0.67
PEI	Chloromethyl methyl sulfide	12.56	2.21	4.12	2.02	2:11	0.68
PVA	Chloromethyl methyl sulfide	14.40	2.81	3.39	1.84	1:6	0.68
PEI	2-Chloroethyl ethyl sulfide	14.95	2.82	3.79	2.10	1:5	0.71
PVA	2-Chloroethyl ethyl sulfide	12.39	2.91	3.03	2.46	2:7	0.98
PVA	Thiophene 2-carboxaldehyde	18.81	2.59	3.51	4.86	5:9	0.45
PEI	Carbon disulfide	11.89	2.24	4.34	8.38	5:8[b]	1.50
PAA	Carbon disulfide	14.77	3.28	3.54	6.03	3:4	1.50

[a] Sulfur content due to sulfate from acid wash corrected for S:N ratios.
[b] Ratio obtained for sulfur analysis was divided by 2 (because there are 2 sulfurs in CS_2).

loaded to any appreciable extent based on the calculated S:N ratios. The degree to which they loaded had no significant impact on the mercury capacity relative to the starting polyamine composites. Apparently, displacement of the halide by the amine groups on the polymer is slow relative to the hydrolysis of the halide or the expected competing elimination in the case of the 2-chloroethyl sulfide. Second, although the sulfur loading of the thiophene-2-carboxaldehyde was quite good, the mercury capture was poor even relative to the parent polyamine composites. This clearly shows that thioether ligands are not good functional groups for the surface capture of mercury ions from solution. It should be pointed out here, as well, that although the parent polyamines show decent flow capacities for mercury, the resins are readily stripped of mercury with dilute acid, making them useless for immobilization applications and probably for low level removal as well.

The polyamine composites treated with carbon disulfide show a remarkably different behavior. Sulfur loading is high, but more important, the flow capacities are significantly higher than all the other materials we have tested to date. This is not surprising in light of the fact that the dithiocarbamate ligand has a stability constant on the order 10^{68} for mercury salts.[29] The breakthrough, shown in Figure 19, reveals that the PAA polyamine composite modified with carbon disulfide (WP-3) has an even higher capacity for low level mercury removal than the ethylene sulfide-modified material.[12b] Approximately, 350 L of 500 ppb mercury solution was run through a 5-cm^3 column before mercury above the allowed release level of 2 ppb came through the column consistently. Flow capacities of 1.5 mmol/g were realized when more concentrated solutions of mercury were used.

We attempted to examine an adsorption isotherm on the PAA composite modified with carbon disulfide (WP-3). The results of these measurements are illustrated in Figure 20. Batch capacities on the order of 2 mmol/g were realized from these tests; but the K_D values (mmol adsorbed/mmol remaining in solution) unexpectedly leveled off at ~0.4. This indicates that even after the resin is fully loaded adsorption

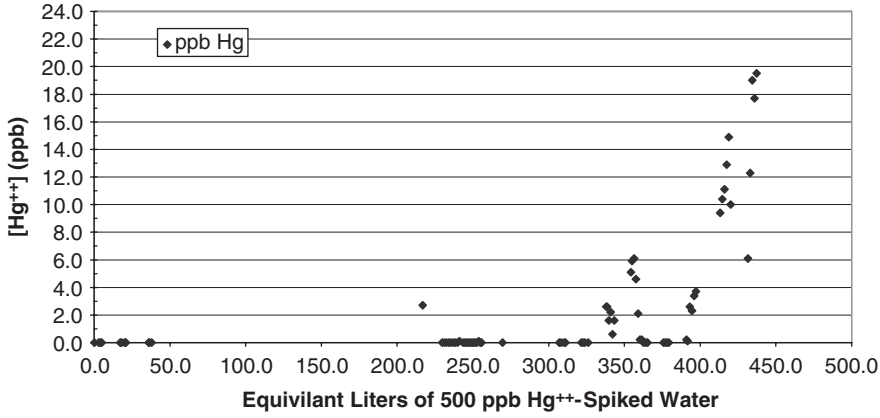

Figure 19 Breakthrough curve for the carbon-disulfide-modified PAA composite (labeled WP-3) treated with 500 ppb mercury chloride solutions at a flow rate of 0.5 column volume per minute.

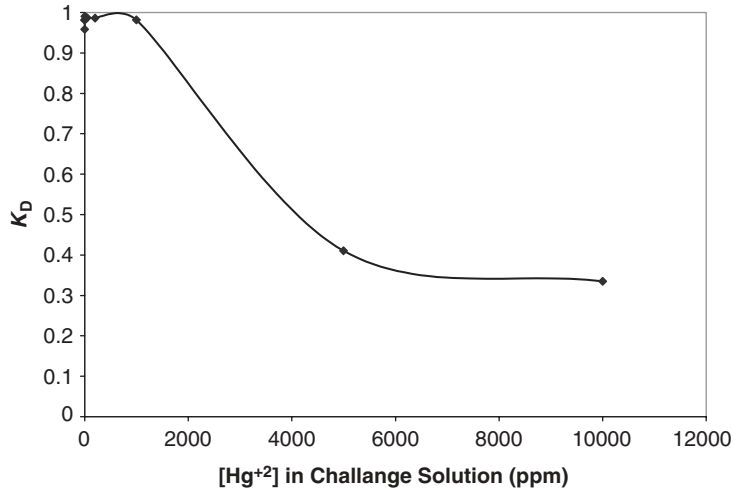

Figure 20 Adsorption isotherm for the PAA composite modified with carbon disulfide, where K_D is the fraction of mercury in mmol removed from the solution.

of mercury continues. Accompanying this phenomenon is a series of color changes from yellow to dark brown, then back to yellow. Although this is difficult to explain, one can speculate that there is a surface reaction between composite-bound mercury and solution mercury once all the adsorption sites are almost saturated.

It is well known that mercury can form polymeric structures with sulfur-containing ligands where the ratio of the ligand to mercury is less than the 2:1 found in the isolated complex, $Hg(S_2CNR_2)_2$.[30] Finally, it should be pointed out that the captured mercury on WP-3 resists leaching even with 10 M hydrochloric acid, as with WP-1, which is modified with ethylene sulfide.

The dithiocarbamate-type ligand produced from the reaction of carbon disulfide with silica-polyamine composites represents a viable alternative to the previously reported ethylene-sulfide-modified composites.[12] This material should prove useful for immobilizing mercury that is contained in aqueous waste streams. The resin is not going to be useful for applications requiring the regeneration and reuse of the resin. There are several other polystyrene and silica-based mercury removal resins available on the market, and it remains to be shown how these resins compare with WP-3.

VI. FUTURE WORK

The work done so far indicates that there are distinct advantages for using silica polyamine composites over polystyrene-based resins. These advantages arise

from the more rigid and more porous nature of the silica gel matrix as well the better capture kinetics of the surface only bound active sites and their attachment to a hydrophilic polymer. More work needs to be done on understanding the detailed relationship between silica pore size and polymer conformation and its impact on the capture kinetics of a given composite. Structural studies using solid state NMR, EPR, and ENDOR should be of use in elucidating structural details of the metal complexes on the composite surface.

The ability to modify the polyamine with metal-selective ligands has been demonstrated. The ease with which this can be done holds out the possibility for further ligand modifications that target lanthanides, actinides, platinum group metals, and other technologically important metals as well as anions such as arsenates, selenates, and borates. The approach that taken will be to borrow known ligand designs from solvent extraction lixavents and polystyrene resins and to create synthetic pathways and structural modifications that are compatible with polyamine composites. We will also investigate grafting other types of functionalized polymers to wide pore amorphous silica gel.

VII. ACKNOWLEDGMENTS

We gratefully acknowledge the National Science Foundation for support of this research in the form Phase I and Phase II SBIR Grants (9961006 and 0109983). We also acknowledge the Environmental Protection Agency for an SBIR Phase I Grant (68-D-00-260) and the Montana Board of Research and Commercialization Technology for generous support. The molecular mechanics calculations were done at the Molecular Computational Core Facility, Center for Structural and Functional Neuroscience (NIH NCRR P20 RR15583).

VIII. REFERENCES

1. A. Gupta, E. F. Johnson, R. H. Schlossel, *Ind. Eng. Chem. Res*. **26,** 588 (1987).
2. R. W. Bartlett, *Solution Mining*, Gordon & Breach, Amsterdam, 1992.
3. G. Amos, W. Hopkins, S. Izatt, R. L. Breuning, J. B. Dale, in *Environmental Improvements in Mineral Processing and Extractive Metallurgy*, M.A. Sanchez, F. Vergara, S. H. Castro, eds., University of Concepcion, Chile, 1997.
4. J. W. Patterson, R. Passino, *Metals Speciation Separation and Recovery*, Lewis Chelsea, MI, 1986.
5. K. Periasamy, C. Namasivayam, *Waste Manage*. **15,** 63 (1995).
6. (a) J. Chang, R. Law, C. Chang, *Water Res*. **31,** 1651 (1997); (b) L. Zhang, L. Zhao, Y. Yu, C. Chen, *Water Res*. **32,** 1437 (1998).
7. R. C. Gatrone, M. L. Dietz, E. P. Horwitz, *Solvent Extraction Ion Exchange* **11,** 411 (1993).
8. (a) S. Alexandratos, *Sep. Purification Method* **21,** 1 (1992); (b) S. Alexandratos, D. Quillen, *Reactive Polym*. **13,** 255 (1990); (c) R. Fish, *Reactive Polym*. **6,** 255 (1987).

9. (a) R. Grinstead, *J. Metals* **31,** 13 (1979); (b) G. D. Del Cul, *Sep. Sci. Technol*. **32,** 431 (1997).
10. A. M. Mathur, A. B. Scranton, *Sep. Sci. Technol*. **32,** 285 (1997).
11. E. Rosenberg, D. Pang, U.S. Patent 5,695,882 (1997).
12. (a) S. T. Beatty, R. J. Fischer, D. Pang, E. Rosenberg; *Sep. Sci. Technol*. **34,** 2723 (1999); (b) S. T. Beatty, R. J. Fischer, D. Pang, E. Rosenberg, *Sep. Sci. Technol*. **34,** 3125 (1999); (c) S. T. Beatty, R. J. Fischer, D. L. Hagars, E. Rosenberg, *Ind. Eng. Chem. Res*. **38,** 4402 (1999).
13. E. Rosenberg, in *Symposium Proceedings of the International Conference on Materials and Advanced Technologies*, T. White, D. Sun, eds., Material Research Society, Singapore, 2001.
14. D. Hagars, *Performance Evaluation for Heavy Metal Ion Removal Using Silica Polyamine Composites Made with Different Silica Gels and Polyamines*, Masters thesis, University of Montana, 1999.
15. H. E. Ramsden, U.S. Patent 4,540,486 (1985).
16. F. W. Regnier, W. Kopaciewicz, U.S. Patent 4,804,686 (1989).
17. L. Crane, V. Kakodkar, U.S. Patent 5,085,779 (1992).
18. R. Hammen, U.S. Patent 5,240,602 (1993).
19. J. S. Kim, J. Yi, *J. Chem. Technol. Biotechnol*. **75,** 359 (2000), and references therein.
20. Robert Fischer, *Development of a Copper Selective Silica Polyamine Composite*, doctoral thesis, University of Montana, 2002.
21. M. J. Wirth, H. O. Fatumbi, *Anal. Chem*. **65,** 822 (1993).
22. E. Rosenberg, R. Fischer, U.S. Patent **6,** 576,590 (2003).
23. D. Shriver, P. Atkins, *Inorganic Chemistry*, Freeman, New York, 1999.
24. M. Clark, R. D. Cramer, *J. Comput. Chem*. **10,** 982 (1989).
25. U.S. EPA, Office of Ground and Drinking Water, EPA-814 N 95001, *Lab. Cert. Bull*. (August 8, 1995).
26. H. Hsin-Hsiung, L. Qi, paper presented at the American Chemical Society Special Symposium, Wastewater Treatment by Separation III, Atlanta, GA, September 1993.
27. R. D. Adams, in *Catalysis by Di- and Polynuclear Cluster Complexes*, R. D. Adams, F. A. Cotton, eds., Wiley, New York, 1998.
28. Fifteenth NSF Joint Committee on Drinking Water Treatment Units, *NSF International Standard 53-1993 Drinking Water Treatment Units—Health Effects*, NSF International, Ann Arbor, MI, 1993.
29. A. Izquierdo, *Polyhedron* **4,** 897 (1985).
30. T. Alsina, *J. Chem. Soc. Chem. Commun*. 1010 (1992), and references therein.

CHAPTER 5

Polyhedral Oligomeric Silsesquioxane (POSS) Polymers, Copolymers, and Resin Nanocomposites

Guizhi Li and Charles U. Pittman Jr.

Department of Chemistry, Mississippi State University, Mississippi State, Mississippi

CONTENTS

Macromolecules Containing Metal and Metal-Like Elements, Volume 4: Group IVA Polymers, edited by Alaa S. Abd-El-Aziz, Charles E. Carraher Jr., Charles U. Pittman Jr., and Martel Zeldin
ISBN: 0-471-68238-1

I. INTRODUCTION

The term *silsesquioxane* refers to all structures with the empirical formulas $RSiO_{1.5}$ where R is hydrogen or any alkyl, alkylene, aryl, arylene, or organo-functional derivatives of alkyl, alkylene, aryl, or arylene groups. The silsesquioxanes include random structures, ladder structures, cage structures, and partial cage structures, as illustrated in Figure 1.[1] The first oligomeric organosilsesquioxanes, $(CH_3SiO_{1.5})_n$, were probably isolated along with other volatile compounds by Scott in 1946 through thermolysis of the polymeric products obtained from methyltrichlorosilane and dimethylchlorosilane co-hydrolysis.[2] Even though silsequioxane chemistry spans more than half a century, interest in this area really accelerated in the past ten years and continues to increase.

In 1995, Baney et al.[1] reviewed the structures, preparation, properties and applications of silsesquioxanes, especially the ladderlike polysilsesquioxanes shown in Figure 1b. These include poly(phenyl silsesquioxane) (PPSQ),[3–12] poly(methyl silsesquioxane) (PMSQ)[13–19] and poly(hydridosilsesquioxane) (PHSQ).[20,21] Recently, one of us found that single crystals of PPSQ could be formed from its toluene or benzene solutions at 70–80°C.[9,10] These ladderlike polymers have outstanding thermal stability, and they exhibit oxidative resistance even at temperatures of >500°C. In addition, these ladderlike polymers have good insulating properties and gas permeabilities. Therefore, the ladderlike silsesquioxane polymers have a variety of applications in areas such as photoresist coatings[22–29] for electronics and optical devices, interlayer dielectrics and protective coating films[30–35] for semiconductor devices, liquid crystal display elements,[36,37] magnetic recording media,[38,39] optical fiber coatings,[40,41] gas separation membranes,[42,43] binders for ceramics[44,45] and carcinostatic drugs.[46] However, in the past few years, much more attention has been paid to the silsesquioxanes with specific cage structures (shown in Scheme 1 c–f). These cage polyhedral oligomeric silsesquioxanes have been designated by the abbreviation POSS.

POSS compounds embody a truly hybrid (inorganic–organic) architecture that contains an inner inorganic framework made up of silicone and oxygen $(SiO_{1.5})_x$, which is externally covered by organic substituents. These substituents can be totally hydrocarbon in nature or they can embody a range of polar structures and functional groups. POSS nanostructured chemicals, with sizes from 1 to 3 nm in diameter, can be thought of as the smallest possible particles of silica possible. They may be viewed as molecular silicas. However, unlike silica, silicones, or fillers, each POSS molecule

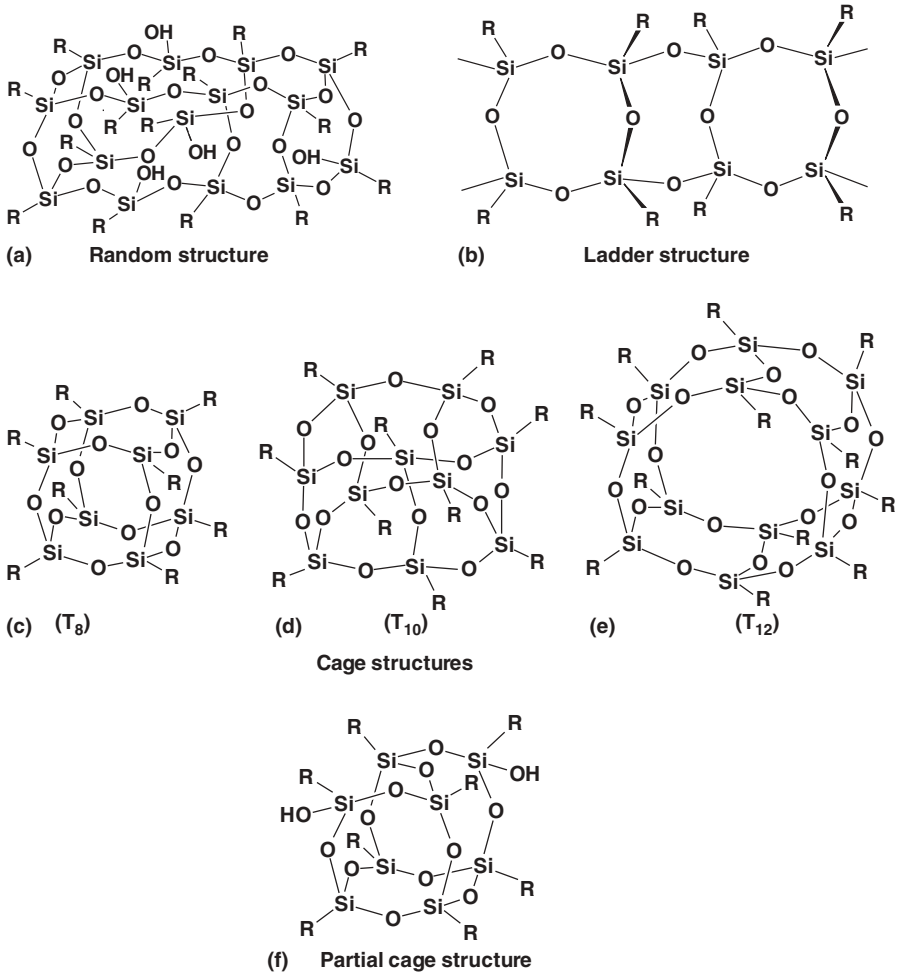

Figure 1 Structures of silsesquioxane.

contains organic substituents on its outer surface that make the POSS nanostructure compatible with polymers, biological systems, or surfaces. Furthermore, these groups can be specially designed to be either nonreactive or reactive.

A variety of POSS nanostructured chemicals have been prepared that contain one or more covalently bonded reactive functionalities that are suitable for polymerization, grafting, surface bonding, or other transformations.[47,48] Unlike traditional organic compounds, POSS chemicals release no volatile organic components, so they are odorless and environmentally friendly. A group at Edwards Air Force Base, CA, has recently developed a large-scale process for POSS monomer synthesis[47,49–52] and a number of POSS reagents. As a result of this success, monomers have recently become commercially available as solids or oils from Hybrid Plastics Company (www.hybridplastics.com), Fountain Valley, CA and Hattiesburg, MS.

A selection of POSS chemicals now exist that contain various combinations of nonreactive substituents and/or reactive functionalities. Thus POSS nanostructured chemicals may be incorporated into common plastics via the classic synthetic methods, copolymerization and grafting, or by blending.[53] The incorporation of POSS derivatives into polymeric materials can lead to dramatic improvements in polymer properties. These include, but are not limited to, increases in use temperature, oxidation resistance, surface hardening, and improved mechanical properties as well as reductions in flammability, heat evolution, and viscosity during processing. These enhancements have been shown to apply to a wide range of thermoplastics and a few thermoset systems.[52,53] It is especially convenient that the use of POSS monomers does not require dramatic changes in processing. Monomers are simply mixed and copolymerized. As long as the POSS monomer is soluble in the monomer mixture and no precipitation occurs during polymerization, POSS is incorporated in a true molecular dispersion into the copolymer. No phase separation will occur unless POSS moieties bound to polymer chains aggregate in small POSS-rich domains. This is a significant advantage over current filler technologies. POSS nanostructures have also shown significant promise for use in catalyst supports and biomedical applications as scaffolds for drug delivery, imaging reagents, and combinatorial drug development.

II. SYNTHESIS OF POLYHEDRAL OLIGOMERIC SILSESQUIOXANES

A 1982 review by Voronkov and Lavrent'yev[54] covered the methods of synthesizing POSS compounds. Feher and co-workers[55] reviewed the more recent progress on POSS synthesis in 2000. There are a great number of reactions leading to the formation of POSS and its derivatives.[20,56–58] These reactions may be divided into two major groups, depending on the nature of the starting materials employed. The first group includes the reactions giving rise to new Si–O–Si bonds with subsequent formation of the polyhedral cage framework. These reactions are complex, multistep processes leading to polymers and oligomers that include oligosilsesquioxanes and their derivatives. This class of reactions assembles polyhedral silsesquioxanes from monomers of the $XSiY_3$ type, where X is a chemically stable substituent (such as CH_3, phenyl, vinyl), and Y is a highly reactive substituent (such as Cl, OH or OR) (Eq. 1). Alternatively, POSS can form from linear, cyclic, or polycyclic siloxanes that are derived from the $XSiY_3$-type monomers.

$$n\mathrm{XSiY_3} + 1.5n\mathrm{H_2O} \rightarrow (\mathrm{XSiO_{1.5}})n + 3n\mathrm{HY} \quad (1)$$

The second major class of reactions involves the manipulation of the substituents at the silicon atom without affecting the silicon–oxygen skeleton of the molecule. As the interest in POSS derivatives has increased, efforts to synthesize POSS with a variety of both reactive and inert substituents have increased. A large number of substituents have been appended to the silicon oxygen cages $[R(SiO_{1.5})]_n$ ($n = 8$, 10, 12 and larger) by Hybrid Plastics Co. (Hattiesburg, MS). Such substituents include alcohols and phenols, alkoxysilanes, chlorosilanes, epoxides, esters, fluoroalkyls, halides, isocyanates,

methacrylates and acrylates, alkyl and cycloalkyl groups, nitriles, norbornenyls, olefins, phosphines, silanes, silanols, and styrenes. Many of the reactive functionalities are suitable for polymerization or copolymerization of the specific POSS derivative with other monomers. In addition to substituents with reactive functional groups, nonreactive organic functionalities have been varied to influence the solubility and compatibilization of POSS nanostructured cages with polymers, biological systems, or surfaces.[49–51] The synthesis of both monofunctional and multifunctional POSS chemicals and examples of such derivatives are described briefly below.

A. Monofunctional POSS Synthesis

Silsesquioxanes are synthesized by the controlled hydrolysis and condensation of organotrichlorosilanes which are commercially available.[59] The predominant reaction products are heptameric siloxanes with partially formed cages containing two or three residual silicon hydroxyl functional groups. The controlled hydrolysis/condensation of cyclohexyltrichlorosilane is shown as an example in Figure 2. The crude products vary with reaction conditions and time. In one published example,[59] 45% of the heptameric siloxane, containing three SiOH functions, was formed along with 40% of a hexamer and 15% of an octameric closed-cube silsesquioxane. Due to the difference in their solubilities, the incompletely closed heptameric siloxane was easily separated from the other two compounds. The three remaining hydroxyl groups of the heptamer are then used to attach reactive organosilicone monomers, such as triethoxysilanes ($R\text{-}Si(OEt)_3$), to the POSS molecule. This condensation produces the closed POSS cage, which is now substituted with a single specific reactive function and seven cyclohexyl substituents.

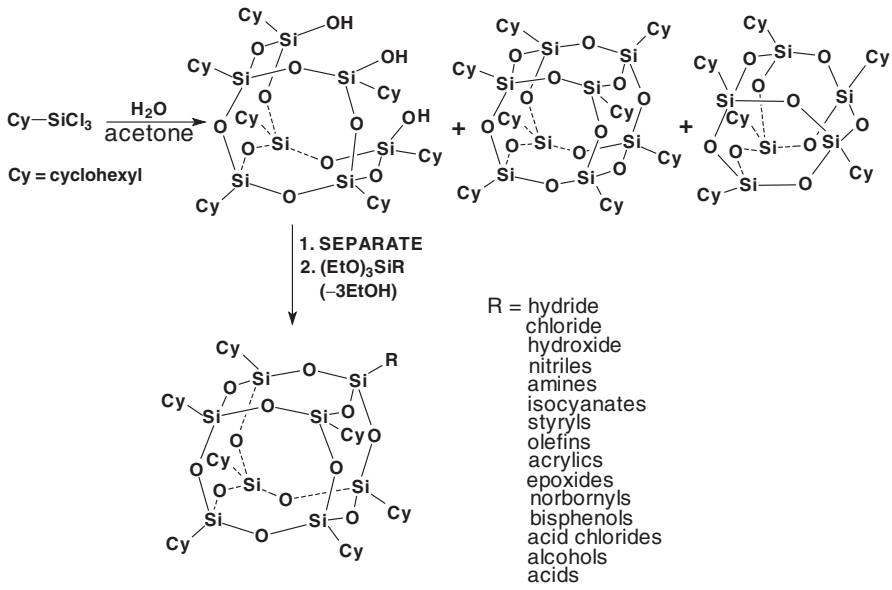

Figure 2 Synthesis of structures of monofunctional POSS macromonomers.

Virtually any reactive type of functionality (or protected function) available as R-$Si(OEt)_3$ or a related trialkoxysilane can be used to close the cage using this synthetic approach. Examples of specific reactive corner groups attached in this way include hydride, chloride, hydroxide, nitriles, amines, isocyanates, styryls, olefins, acrylics, epoxides, norbornyls, bisphenols, acid chlorides, alcohols, and acids (Fig. 2).[49,60–65] These monofunctional POSS molecules are then used for subsequent synthesis of grafted or copolymerized nanostructured polymers and composites.

B. Multifunctional POSS Synthesis

POSS $(RSiO_{1.5})_n$, where R = H and n = 8, 10, 12, 14 or 16, are unique structures generally formed by hydrolysis and condensation of trialkoxysilanes ($HSi(OR)_3$) or trichlorosilanes ($HSiCl_3$).[54] For example, $(HSiO_{1.5})_n$, where n = 8, 10, 12, 14 or 16, is prepared by hydrolysis of $HSiCl_3$ involving the addition of a benzene solution of $HSiCl_3$ to a mixture of benzene and SO_3-enriched sulfuric acid.[20] The hydrolysis of trimethoxysilane is carried out in cyclohexane-acetic acid in the presence of concentrated hydrochloric acid and leads to the octamer in low yield (13%).[20] The hydrolytic polycondensation of trifunctional monomers of the type $XSiY_3$ leads to crosslinked three-dimensional networks and *cis*-syndiotactic (ladderlike) polymers, $(XSiO_{1.5})_n$. With increasing amounts of solvent, however, the corresponding condensed polycyclosiloxanes, POSS, and their derivatives may be formed.[54] A few representative examples of polycondensations that lead to form POSS derivatives are summarized in Table 1.

Table 1 Representative Syntheses of POSS, $(XSiO_{1.5})_n$, by Condensations of $XSiY_3$ Precursors

X	n	Y	Solvent	Catalyst	Yield (%)	References
H	8	OCH_3	Cyclohexane	$HCl + CH_3COOH$	13	20,66
H	10,12, 14,16	Cl	Benzene	$H_2SO_4 + SO_3$	15–35	20
CH_3	6	OC_2H_5	Benzene	HCl	—	56
CH_3	8	Cl	Methanol	HCl	37	56 67–69
CH_3	10,12	OC_2H_5	Benzene	KOH	—	67,69
C_2H_5	6	OC_2H_5	Benzene	HCl	—	57
C_2H_5	8	Cl	Methanol	HCl	37	57,67
C_2H_5	10	Cl	Butanol	HCl	16	70
C_6H_{11}	6	Cl	Acetone	HCl	7	71
C_6H_{11}	8	OCH_3	Nitro-benzene	OH	—	67,71
$CH{=}CH_2$	8	OCH_3	Methanol	HCl	20	72
$CH{=}CH_2$	10	OCH_3	Butanol	HCl	—	72
C_6H_5	8	OCH_3	Benzene	$PhCH_2(CH_3)_3N^+ {}^-OH$	88	58 73,74
C_6H_5	10	OC_2H_5	Tetra-hydrofuran	Me_4NOH	—	74
C_6H_5	12,22, 24	OC_2H_5	Tetra-hydrofuran	Me_4NOH	—	58,74,11

The reaction rate, the degree of oligomerization, and the yield of the polyhedral compounds formed under these conditions strongly depend on the several factors. First, the concentration of the initial monomer in the solution is an important variable. Other important variables include the nature of the solvent, the identity of the substituent X in the initial monomer, the nature of the functional groups Y in the monomer, the type of catalyst, the reaction temperature, the rate of water addition, and the solubility of the polyhedral oligomers that are formed.[54] For example, POSS cages where $n = 4$ and 6 could be obtained only in nonpolar or weakly polar solvents at 0°C or 20°C but not in alcohols. However, octa(phenylsilsesquioxane), $Ph_8(SiO_{1.5})_8$, is more readily formed in benzene, nitrobenzene, benzyl alcohol, pyridine, or ethylene glycol dimethyl ether at high temperature (e.g. 100°C). A more detailed discussion of the effects of all these factors on POSS syntheses has been reviewed.[54]

Multifunctional POSS derivatives can be made by the condensation of $R'Si(OEt)_3$, as described above, where R′ is a reactive group. This reaction produces an octa-functional POSS, $R'_8(SiO_{1.5})_8$. Another approach involves functionalizing POSS cages that have already been formed. For example, this may be accomplished via Pt-catalyzed hydrosilylation of alkenes or alkynes with $(HSiO_{1.5})_8$ and $(HMe_2SiOSiO_{1.5})_8$ cages[75–77] (Figs. 3–5). In this case, $(HMe_2SiOSiO_{1.5})_8$ was synthesized following modified literature procedures.[78,79]

Another example of the synthesis of multifunctional POSS derivatives is the simple hydrolytic condensation of modified aminosilanes reported by Fasce et al.[80] *N*-(β-Aminoethyl)-γ-aminopropyltrimethoxysilane, a trifunctional aminosilane, was reacted with a stoichiometric amount of phenylglycidyl ether in sealed ampules at 50°C for 24 h. The reaction leads to the trisubstituted product plus a series of oligomers arising from the intermolecular reaction between methoxysilane groups and the secondary hydroxyls that are generated by the epoxy–amine reaction. When this product was subjected to hydrolytic condensation using a variety of catalysts (HCl, NaOH, HCOOH) and a heating cycle attaining 150°C, POSS derivatives, where $n = 8$ and 10, were obtained[80] (Eq. 2).

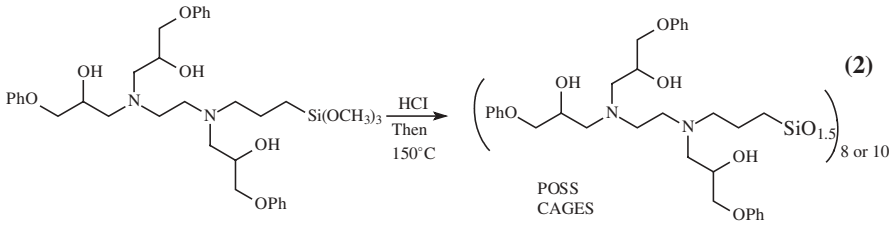

(2)

A key area of synthetic activity has been the effort to lower the cost of generating a variety of POSS structures. Thus faster rates of cage formation were needed at higher product selectivity. In recent years the prices of several POSS systems have decreased about 1000-fold. More progress is needed to allow this field to reach its commercial potential. The best synthetic conditions to make many POSS cages and to achieve various substitution patterns are proprietary at this time.

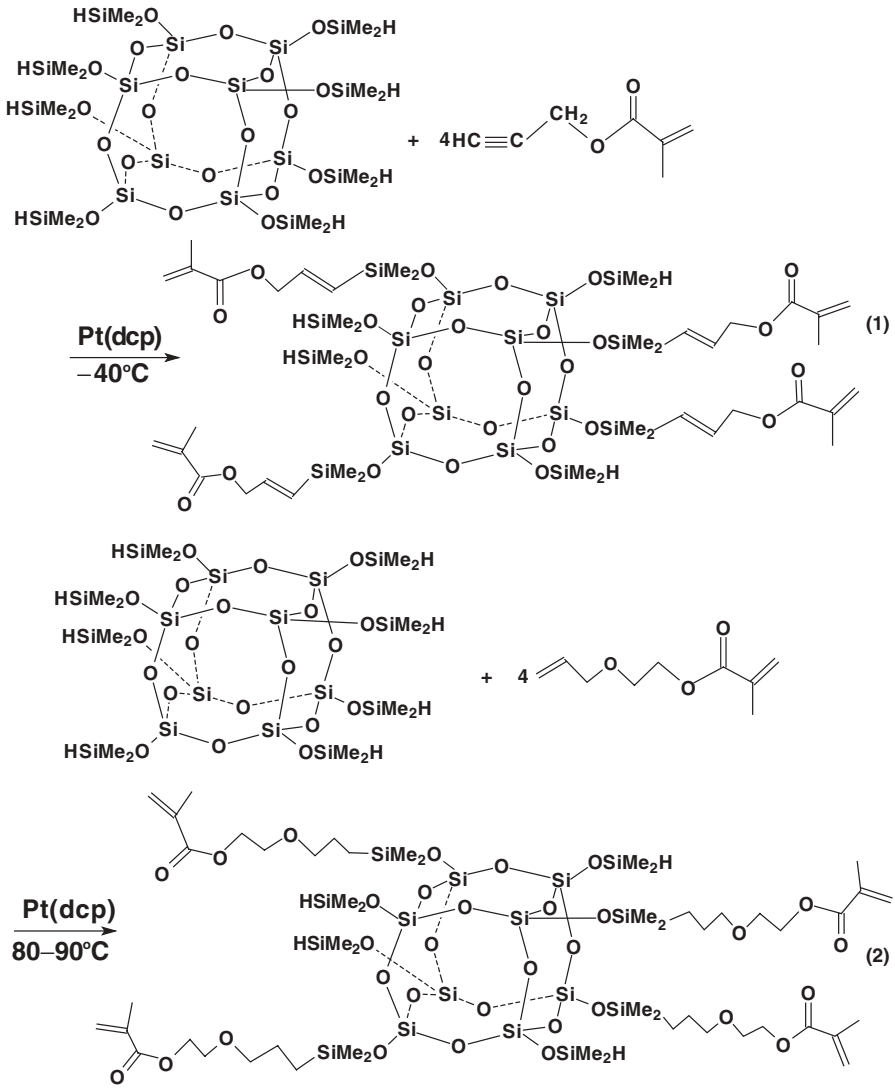

Figure 3 Synthesis of multifunctional MA-POSS.

III. POSS POLYMERS AND COPOLYMERS (THERMOPLASTICS)

POSS feedstocks, which have been functionalized with various reactive organic groups, can be incorporated into virtually any existing polymer system through either grafting or copolymerization. POSS homopolymers can also be synthesized. The incorporation of the POSS nanocluster cages into polymeric materials by copolymerization

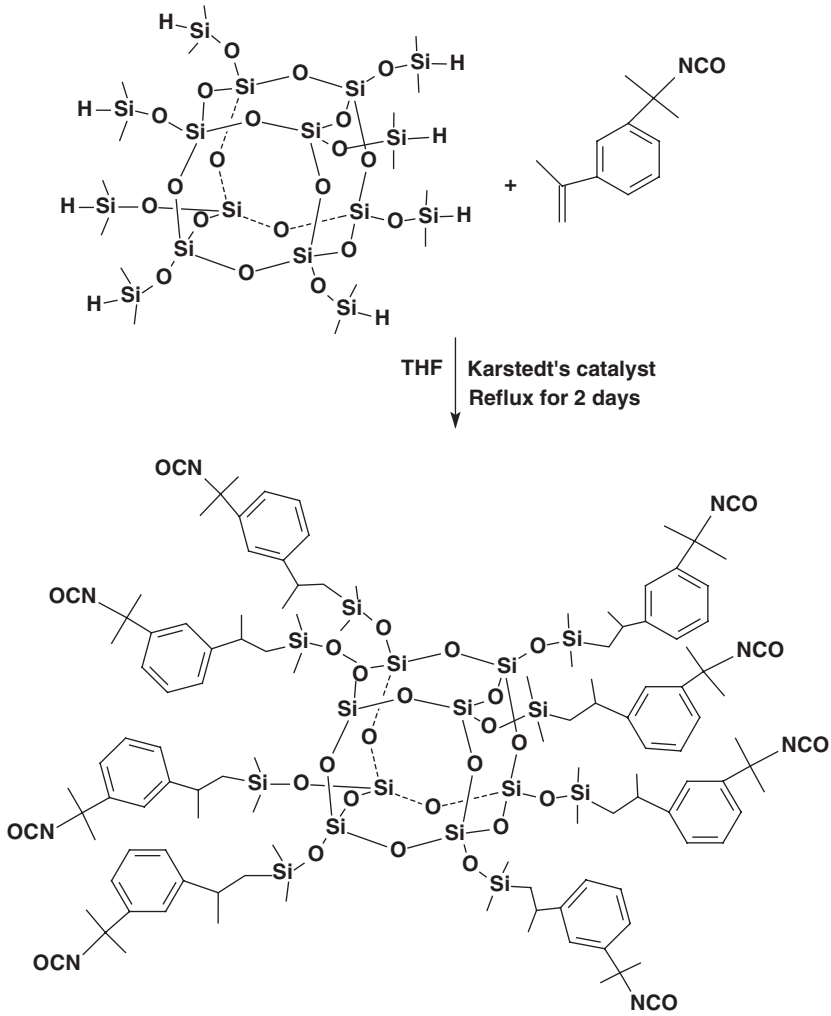

Figure 4 Synthesis of multifunctional isocyanate-POSS.

or blending can result in dramatic improvements in polymer properties, including temperature and oxidation resistance, surface hardening and reductions in flammability. Therefore, research has accelerated on POSS polymers, copolymers and nanocomposites recently. Some representative systems are now discussed.

A. Styryl-POSS Polymers, Copolymers, and Nanocomposites

Haddad and Lichtenhan[81a] synthesized the styryl-substituted POSS, $R_7(Si_8O_{12})(CH_2CH_2C_6H_4CH{=}CH_2)$, where R = either cyclohexyl, **2a**, or

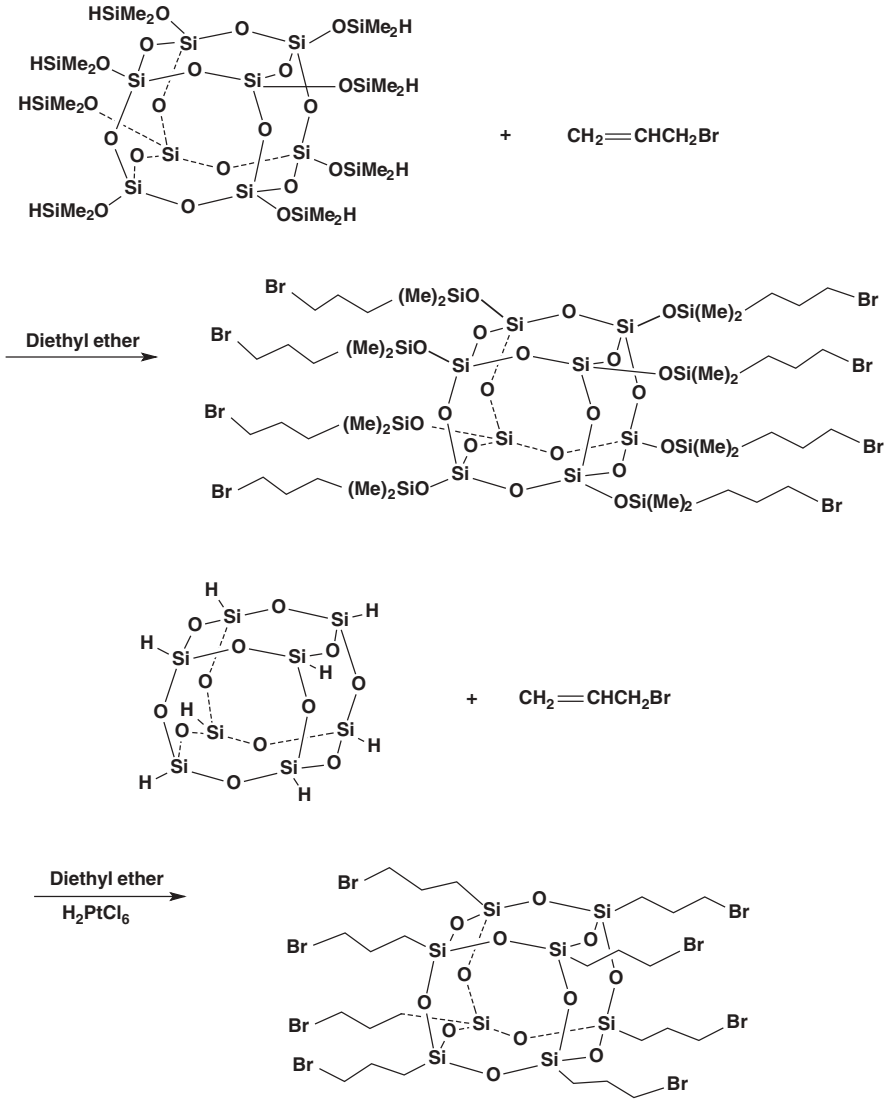

Figure 5 Synthesis of multifunctional allyl bromide-POSS.

cyclopentyl, **2b**, from incompletely condensed heptameric silsesquioxanes **1a** or **1b** by the route shown in Figure 6. The homopolymers **3a** and **3b** and their copolymers with 4-methylstyrene (**4a**–**8a** or **4b**–**8b**) were prepared by carrying out AIBN-initiated free-radical polymerization (Fig. 6).[81a] The cyclohexyl and cyclopentyl corner substituents have a great influence on the solubility and thermal properties of the corresponding styryl-POSS homopolymers. The styryl-POSS homopolymer **3a**,

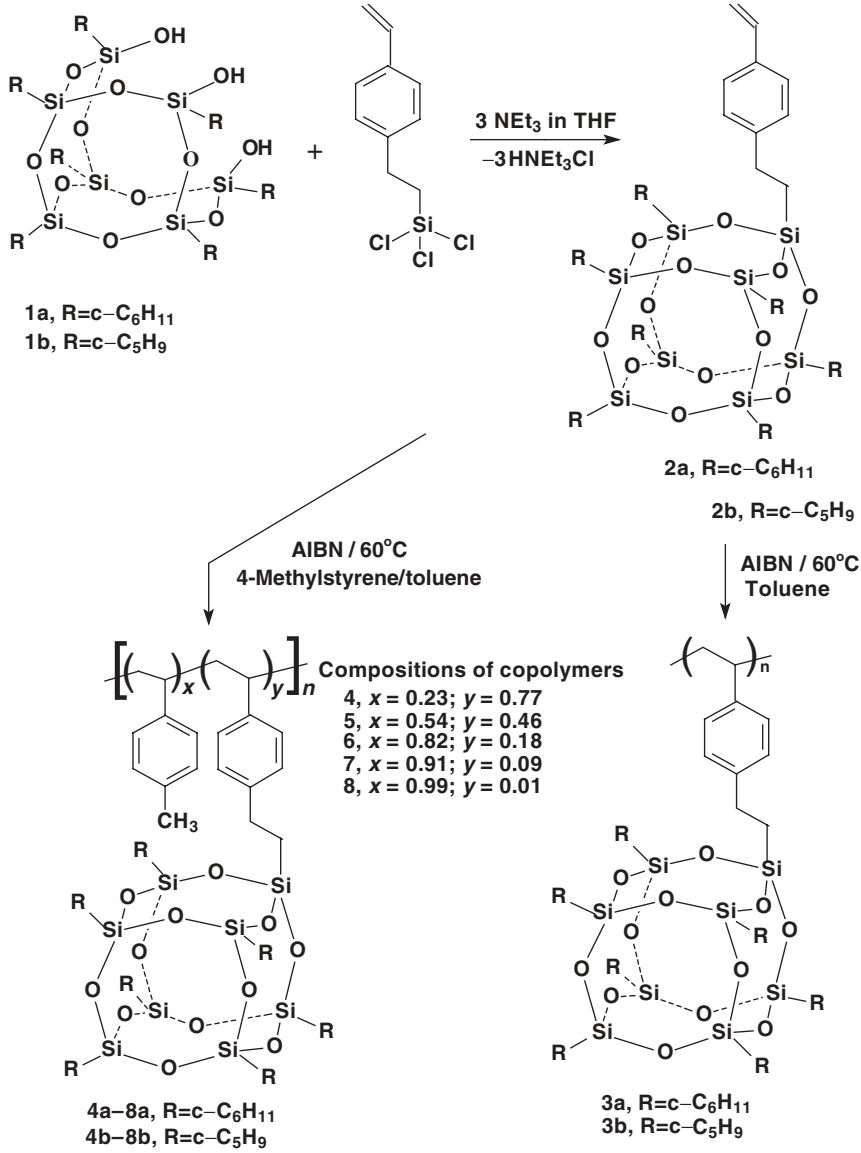

Figure 6 Styryl-POSS macromonomer synthesis and its polymerization and copolymerization.

where R = cyclohexyl, dissolved in tetrahydrofuran (THF). In contrast to **3a**, the homopolymer **3b**, where R = cyclopentyl, was insoluble in THF. The glass-transition temperature, T_g (396°C), and the decomposition temperature, T_d (445°C), of the cyclohexyl-substituted styryl-POSS homopolymer **3a** are higher than those of the cyclopentyl-substituted styryl-POSS homopolymer **3b** ($T_g = 343$°C; $T_d = 423$°C).

Poly(4-methylstyrene) has substantially lower values of T_g (116°C) and T_d (388°C) than either of the styryl-POSS homopolymers, **3a** and **3b**. The 4-methylstyrene copolymers **8a** and **8b** of the styryl-POSS monomers **2a** and **2b**, which contain only 1 mol % of the POSS monomer, exhibited lower values of T_g and T_d (**8a**, $T_g = 112$°C and $T_d = 378$°C; **8b**, $T_g = 113$°C and $T_d = 383$°C) than those of poly(4-methyl styrene). However, as the mole percent of POSS increased to 9, the copolymers **7a** and **7b** exhibited higher values of T_g and T_d (**7a**, $T_g = 132$°C and $T_d = 402$°C; **7b**, $T_g = 127$°C and $T_d = 399$°C), which are higher than those of pure poly(4-methyl-styrene). The T_g and T_d values increase with an increase in the mole percent of POSS.[81a]

Rheological differences occurred as the mole fraction of the styryl-POSS monomer was increased in styryl-POSS/4-methyl styrene copolymers. The copolymers with low POSS mole fractions (≤4 mol %, or ≤28 wt % of **2a** or ≤27 wt % of **2b**) retained melt- and solid-phase features similar to those of poly(4-methyl styrene)[81b]. Modification of the copolymers' viscoelastic behavior occurs as the POSS mole fraction increases (≥8 mol %, or ≥45 w % of **2a** or ≥42 wt % of **2b**). This leads to a rubberlike behavior at high temperatures.[81b] For example, the shear storage modulus, G′ of polymethylstyrene is 14.45 Pa at a frequency of 0.1 rad/s at a temperature of 180°C, whereas the corresponding G′ of its copolymer containing 8 mol % POSS **2a** is 1000 Pa. These results suggest that the incorporation of POSS into polymers greatly retards polymer chain motion.

An explanation of this retardation in chain motion by POSS moieties has been suggested.[81b] Interchain interactions between the massive POSS inorganic groups retards segmental motions. Furthermore, the large mass and steric bulk of the POSS units prevent rapid shifts in the physical location of these POSS units, thereby retarding segmental motion. This is akin to attaching an anchor to a jumprope and then trying to use the jumprope. Therefore, polymer chain sereptation (snakelike reptation that must occur for entangled polymer chains to undergo chain relocation) is more difficult. Higher temperatures are required to provide the requisite thermal energy for this process to occur and to achieve viscous flow. This mechanism is similar to the "sticky reptation" model conceived for hydrogen-bonded elastomers.[81b] As the fraction of chain segments (existing in amorphous regions) that are substituted with POSS substituents goes up, the T_g can broaden or go up. However, the T_g value may also remain almost unchanged or even drop at lower POSS mole fractions, while the heat distortion temperature, the melt viscosity, and the shear storage modulus can all increase. In summary, incorporation of the styryl-POSS comonomer can improve the thermal properties of poly(4-methyl styrene) and modify its rheological properties.

The other copolymers of styryl-POSS and its blend with PS (nanocomposites) have been reported.[82] Haddad et al.[82a] described the preparation of three styrene copolymers with cyclohexyl-, cyclopentyl-, and isobutyl-substituted monofunctional styryl-POSS monomers (at 30 wt % or approximately 4 mol % loadings) using free-radical bulk polymerization. The storage moduli, E′, of these three POSS copolymers and polystyrene (PS) at room temperature are similar and typical for glassy polymers. However, at 30°C above the glass-transition temperature, the moduli of

the cyclopentyl and cyclohexyl POSS copolymers are still $>10^6$ Pa. These moduli are significantly higher than that of either polystyrene or the isobutyl POSS copolymer. This illustrates how POSS units can markedly effect polymer properties at temperatures above T_g (in the rubbery region). The glass-transition temperatures of the three POSS copolymers and PS (obtained from the tanδ peak) are 120°C for isobutyl POSS copolymer, 131°C for the cyclopentyl POSS copolymer, 138°C for the cyclohexyl POSS copolymer, and 129°C for PS. The isobutyl styryl-POSS copolymer exhibited a lower T_g than that of PS. In contrast, the other two styryl-POSS copolymers, containing cyclopentyl or cyclohexyl groups, exhibited higher T_g values and much higher E′ values in the rubbery region than those of PS. Clearly, the alkyl groups substituted to POSS can exert a strong effect on the bulk properties of the POSS copolymers.[82a]

The organic groups in the outer shell of POSS monomers make up the portion that interacts with the surrounding polymer structure. As substituent groups move out from the $(SiO_{1.5})_{8 \text{ or } 10 \text{ or } 12}$ core, the tetrahedral geometry at silicon orients these functions in a specific direction. Rigid phenyl groups point directly away from the center of the cage. Groups with greater flexibility, while having more conformational freedom, are still oriented away from the cage center. Therefore, the seven R groups will interact with the surrounding polymer segments differently (on average) from the way they would, if these same functions were substituted on randomly coiling chains. Therefore, POSS units may actually act to increase the free volume in some polymers and decrease free volume in others. In many cases, POSS substituted on a polymer chain may prefer to associate with other POSS moieties, leading to aggregation of POSS units within the bulk polymer. POSS-rich domains may form. This may effect both morphology and polymer properties. Thus when the physical and engineering properties of a POSS-containing thermoplastic is examined, one must be cognizant of the fact that property changes may be due to POSS aggregation as well as the individual effects of POSS units on chain segmental motion and sereptation.

Copolymers of syndiotactic polystyrene and cyclopentyl styryl-POSS (POSS loadings up to 24 wt % and 3.2 mol %) have been synthesized.[82b] The glass-transition temperatures of the copolymers underwent only a minor increase from 98°C to 102°C over a range of 0–3.2 mol % POSS. The melting temperatures of the copolymers decreased with an increase of POSS loading, and the heat of fusion (ΔH) data revealed that the degree of crystallinity also decreased with increasing POSS content. Thermogravimetric analysis of these copolymers under both nitrogen and air showed that introducing POSS moieties improved thermal stability. Higher degradation temperatures and higher char yields were achieved, demonstrating that the inclusion of the inorganic POSS nanoparticles makes the organic polymer matrix more thermally robust. When compared at the same POSS content, syndiotactic P(S-co-styryl-POSS) copolymers exhibited higher degradation temperatures than those of the atactic poly(methyl styrene-co-styryl-POSS) copolymer.[82b]

Two copolymers of poly(*p*-acetoxystyrene-co-isobutylstyryl-POSS) (P(AS-co-POSS)) and poly(vinylpyrrolidone-co-isobutylstyryl-POSS) (P(VP-co-POSS)) were synthesized (Fig. 7).[82c] The P(AS-co-POSS) copolymers, with 0.98–4.03 mol % POSS, exhibited lower T_g values than that of pure PAS. However, the T_g value

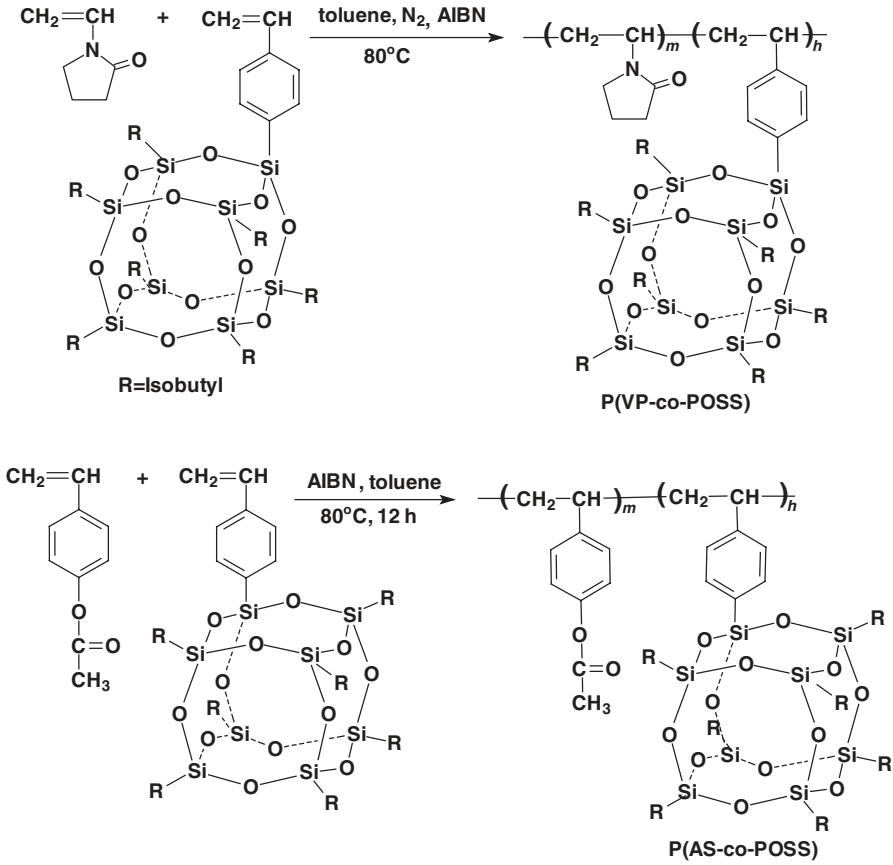

Figure 7 Synthesis of poly(vinylpyrrolidone-co-isobutylstyryl-POSS) and poly-(*p*-acetoxystyrene-co-isobutylstyryl-POSS).

(107.8°C) of the copolymer with 4.03 mol % POSS is slightly higher than that (103.2°C) of the copolymer with 3.23 mol % POSS. At low POSS contents (≤3.23%), the T_g values of these P(AS-co-POSS) copolymers decreased as POSS content went up. However, in the P(VP-co-POSS) copolymers, only the copolymer with 1.5 mol % POSS exhibited a lower T_g value (138.9°C) than that of pure PVP (149.5°C). At POSS contents ≥2.25 mol %, the T_g values are higher than that of pure PVP, and they increased with an increase of POSS content.

IR spectroscopy was applied to study interaction among these copolymers.[82c] The T_g values of these copolymers were found to depend on three factors: (1) the inert role of POSS as a diluent that reduces the self–association dipole–dipole interactions of the parent polymer molecules (a negative contribution), (2) the dipole–dipole interactions between the POSS's siloxane cage and the polar carbonyl

groups within organic polymer species, and (3) the POSS–POSS intermolecular and/or intramolecular interactions. At a relatively low POSS content, the dilution effect plays the main role and results in a T_g decrease. At a relatively high POSS content, the POSS–PAS or POSS–PAP and POSS–POSS interactions play a dominant role and T_g increases.[82c] Furthermore, Xu et al.[82d,e] prepared the terpolymers poly(acetoxystyrene-co-vinylpyrrolidone-co-isobutylstyryl-POSS) (PAS-PVP-POSS) and poly(hydroxystyrene-co-vinylpyrrolidone-co-isobutylstyryl-POSS) (PHS-PVP-POSS). The later was formed by selective removal of the acetyl protective group from the former. The PAS-PVP-POSS terpolymers with 0.8 and 2.2 mol % POSS had T_g values of 84.4°C and 98.5°C, respectively. These values are lower than those of both PAS (122.3°C) and PVP (148.4°C). These values are also lower than that of PAS–PVP (122.5°C). Only when the POSS content reached 3.2 mol %, was a slightly higher T_g value (123.9°C) observed versus the T_g of PAS-PVP. At low POSS contents, POSS acts as an inert diluent, reducing self-associations existing in the homopolymer molecules and lowering T_g values. However, at a higher POSS content, the terpolymer T_g values increase due to the rigid nature of the POSS.

The PHS-PVP-POSS terpolymers, unlike the PAS-PVP-POSS terpolymers, exhibited an increase in T_g at all levels of POSS incorporation. Overall, their T_g values are much higher than those of PAS (122.3°C) and PVP (148.4°C) and higher than PAS–PVP copolymers (194.9°C) and PAS-PVP-POSS terpolymers. PHS-PVP-POSS terpolymers with 0.8, 2.2 and 3.2 mol % POSS had T_g values of 205.8°C, 235.8°C, and 245.3°C, respectively. Clearly, the T_g values went up with any increase of the styryl POSS content. The formation of hydrogen bonds between the POSS cage's oxygens and the PHS para-hydroxyl groups in PVP-PHS-POSS forms a hydrogen bond network. This effectively restricts the polymer chain motion and causes a significant increase in T_g with even small amount of POSS.[82d]

POSS and polystyrene blends have been prepared,[82f] leading to an increase in surface hardness for the blend sample.

B. Methacrylate-POSS Polymers, Copolymers, and Nanocomposites

Methacrylate-substituted POSS macromers have been made that contain one polymerizable functional group. These macromers have been both homopolymerized and copolymerized (Fig. 8a).[62a] Propyl methacrylate-substituted POSS monomers **9** and **10**, containing seven nonreactive cyclohexyl and cyclopentyl groups, respectively, are examples. Solubility differences between the MA-POSS monomers **9** and **10** were observed in THF, toluene, and benzene. The cyclohexyl-substituted MA-POSS **9** has approximately twice the solubility of the cyclopentyl-substituted MA-POSS **10**.[62a] Furthermore, monomer **9** displayed a broad two-step thermal transition beginning at 187°C, which involves melting, thermal polymerization and decomposition, whereas **10** gave a similar thermal transition beginning at 192°C.[62a] X-ray

powder diffraction data indicated that both macromonomers **9** and **10** were crystalline. The homopolymers of **9** and **10** and **9**/**10** copolymers were synthesized by free-radical polymerization using AIBN as the initiator (Fig. 8).[62a] The homopolymer **11** and the 50/50 copolymer of **13** are soluble in common solvents. In contrast, the homopolymer **12** is insoluble in all common hydrocarbon and halogenated hydrocarbon solvents.[62a]

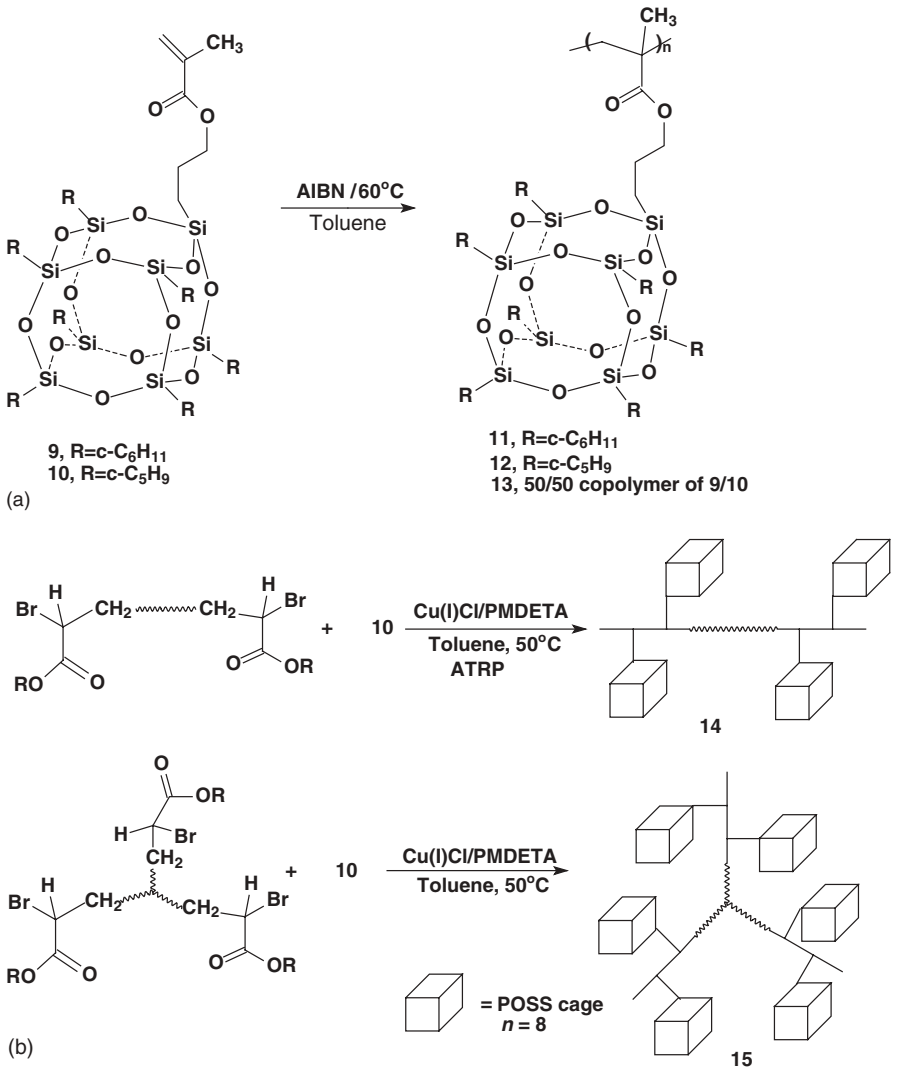

Figure 8 Synthesis of (**a**) MA-POSS homopolymers and copolymers and (**b**) P(MA-POSS)-*b*-BA-*b*-(MA-POSS) triblock and P(MA-b-(MA-POSS)) star-block copolymers.

POSS-methacrylate homopolymers **11** and **12** and the 50/50 copolymer **13**, were amorphous according to X-ray diffraction measurements. These materials appear to be transparent brittle plastics. Neither the glass nor the melting transitions of either homopolymer or copolymer was observed by DSC or DTMA from 0°C to 400°C. Apparently, incorporation of the POSS group into these linear polymers greatly reduces their segmental mobility. The absence of a noticeable glass transition in the methacrylate-POSS homopolymers **11** and **12** most likely reflects an overall rigid nature of the methacrylate polymer backbone resulting from the dominant T_8-POSS pendant groups. The thermal stability of MA-POSS homopolymers **11** and **12** and the 50/50 copolymer **13** is high. Homopolymer **11** decomposes at 388°C, while homopolymer **12** decomposes at 389°C without melting. In contrast, PMMA begins to decompose at above 200°C. Thus POSS incorporation raises T_d by 188–189°C.

The incorporation of methacrylate-POSS monomer units into methacrylate polymers causes dramatic changes in the copolymers' properties. For example, dynamic thermal mechanical analysis (DTMA) of a cyclopentyl-substituted POSS-methacrylate/butyl methacrylate copolymer, which contains only 10 mol % POSS-methacrylate **10**, has a T_g of 150°C.[62b] This is almost 130°C higher than the T_g (20°C) of atactic poly(butyl methacrylate). Moreover, the 50/50 (mol %) copolymer of cyclopentyl-substituted POSS-MA **10** with butyl methacrylate has a T_g above 220°C.[62b] This copolymer nanocomposite exhibits an increased decomposition point, increased resistance to oxidation, increased oxygen permeability, reduced flammability, reduced heat evolution, increased char yields, and enhanced miscibility. In addition, the copolymer of MMA and heptaphenyl MA-POSS copolymers has been synthesized.[62c] Thermal property measurements indicated the incorporation of POSS into PMMA increased the glass-transition temperature and thermal decomposition temperature dramatically. These thermal property enhancements were attributed to the rigid phenyl groups of POSS and its inorganic core.[62c]

Besides the enhancement of thermal stability and heat deflection temperature, the gas permeability is also affected. Oxygen permeability of cyclopentyl-substituted MA-POSS homopolymer **12**/PMMA blends increased with POSS content. For example, the O_2 permeability of the 10/90 weight ratio blend of MA-POSS homopolymer **12** with PMMA is about 9 times greater than that of PMMA.

Pyun and Matyjaszewski[83a] synthesized homopolymer **12** (Figure 8) from cyclopentyl-substituted MA-POSS monomer **10** using atom-transfer radical polymerization (ATRP). ATRP was also used to make the block copolymer of MA-POSS **10** with *n*-butyl acrylate.[83a] In this reaction, *p*-tolyl bromoisobutyrate was used as the initiator, along with a copper(I) chloride/*N,N,N′,N″,N″*-pentamethyldiethylenetriamine (PMDETA) catalyst system. A 72% conversion of monomer **10** was reached at 60°C in an appropriate time using a monomer to initiator ratio of 100:1.24 by weight. The resulting homopolymer **12** exhibited a $DP_n = 14$ and a low polydispersity ($M_w/M_n = 1.14$).

Triblock copolymers of poly(heptacyclopentyl propyl methacrylate-POSS-*b*-*n*-butylmethacrylate-*b*-heptacyclopentyl propyl methacrylate-POSS), [P((MA-POSS**10**)-*b*-BA-*b*-(MA-POSS**10**))], were prepared from both ends of a difunctional

bromine-terminated poly(*n*-butylacrylate) macroinitiator ($M_{nNMR} = 7780$) and MA-POSS **10** (Fig. 8b). In the triblock copolymer synthesis, this macroinitiator was prepared by the ATRP of *n*-BA using dimethyl 2,6-dibromheptanedioate as the difunctional initiator. Chain extension of the difunctional bromine-terminated *n*-butylacrylate macroinitiator using MA-POSS monomer **10** proceeded to higher monomer conversion ($p > 0.95$). The mole percent of each component and the molecular weight in **14** were calculated from NMR analyses. The mole percent of the poly(*n*-butyl methacrylate) was 85% versus 15% of P(MA-POSS) and $M_n = 36070$ vs. M_n(theoretical) = 41510. This block copolymer had a low polydispersity ($M_w/M_n = 1.19$). A star-block copolymer, **15,** of methyl methacrylate and MA-POSS **10** was prepared by the ATRP of methyl methacrylate using a trifunctional initiator 1,1,1-tris(4-(2-bromoisobutyryloxy)phenyl)ethane (Fig. 8b). The mole percentages of each component in copolymer **15**, calculated from NMR analyses, were 25% P(MA-POSS) and 75% poly(methyl methacrylate). Its molecular weight was $M_n = 30270$ vs. M_n(theoretical) = 34730. The polydispersity of this star-block copolymer was found to be $M_w/M_n = 1.30$ by steric exclusion chromatography. No properties of these block copolymers have been reported.

The organic–inorganic hybrid copolymers of monofunctionalized cyclopentyl MA-POSS with liquid crystalline (LC) mononer, 6-[4′-(4′-cyanophenyl)phenoxyl] hexyl methacrylate at mole ratios of 0/100, 10/90, 30/70, 50/50, 70/30 and 100/0, have been synthesized by radical addition polymerization (Fig. 9).[83b] These copolymers were soluble in common solvents, such as tetrahydrofuran, toluene, and chloroform. The decomposition temperature values, defined at 10% weight loss, of the copolymers with 0, 10, 30, 50, 70, and 100 mol % of POSS are 316°C, 343°C, 350°C, 364°C, 375°C, and 385°C, respectively. Thus their thermal stability was increased with an increasing ratio of POSS moieties. However, only the 10 mol % POSS copolymer showed liquid crystalline behavior and a higher glass-transition temperature (48°C, which is 5°C higher than that of LC homopolymer). This can be attributed to the reduction of segment mobility in the hybrid copolymer, which was caused by incorporation of hard, compact POSS moieties. The LC homopolymer showed enantiotropic behavior in which the LC phase appeared from 101°C to 106°C during the heating cycle and from 102°C to 97°C during cooling. In contrast, the 10% POSS copolymer only showed the LC transition from 82°C to 97°C during the heating cycle, indicating monotropic LC behavior.

The apparent absence of LC transition temperatures and glass-transition temperatures in the hybrid copolymers with >10 mol % POSS indicated that the presence of POSS moieties in the hybrid copolymers made it more difficult to orient or order LC mesogens as the amount of the POSS component increased. Orientation became more difficult because the rigidity and bulkiness of POSS lowered the mobility and flexibility of the hybrid copolymer. Differential scanning calorimetry (DSC) and optical polarizing microscopy showed the 10% POSS copolymer had a smectic mesophase-like fine-grained texture. Moreover, the 10% POSS LC copolymer had better thermal stability than that of the corresponding LC homopolymer.

Recently, many applications of MA-POSS copolymers have been developed.[83c] Random MMA/POSS copolymers were applied as compatibilizers for blending

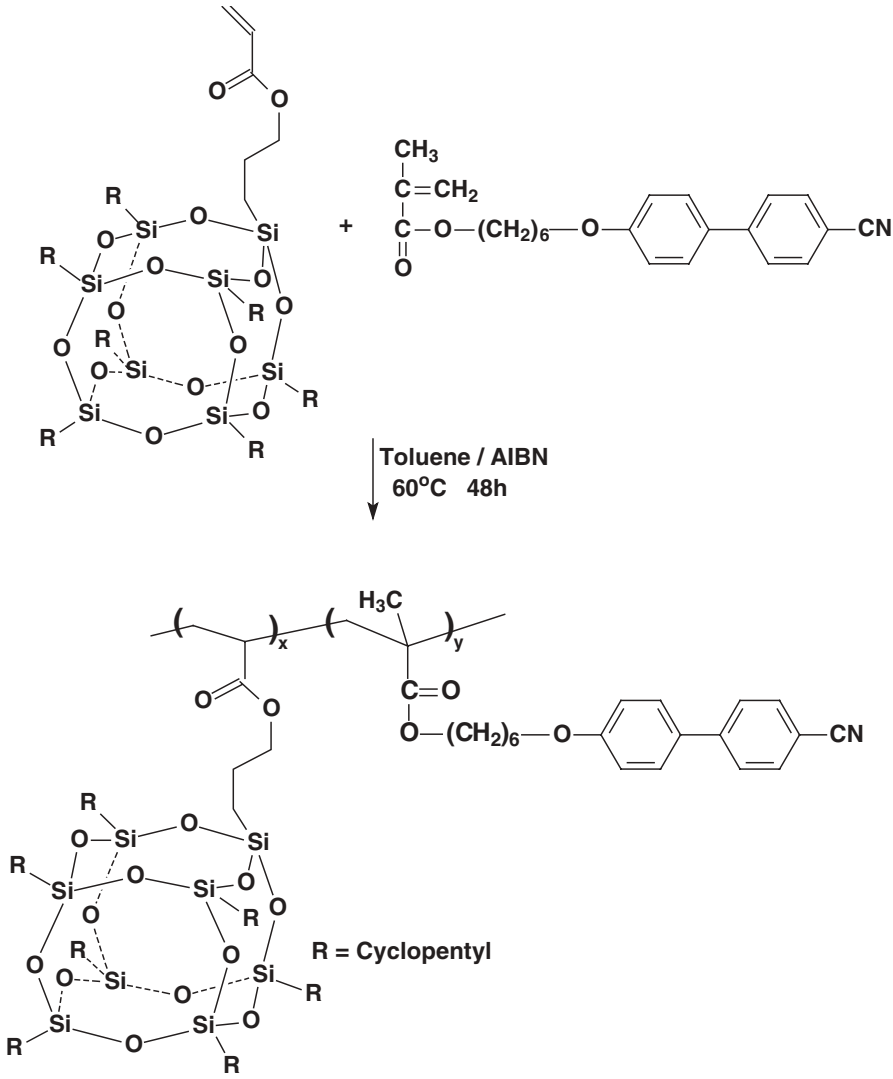

Figure 9 Synthesis of 6-[4-(4′-cyanophenyl)phenoxy]hexyl methacrylate/MA-POSS copolymers.

immiscible PS and PMMA homopolymers.[83c] These copolymers were efficient at compatibilizing these immiscible polymer blends. Compatibilization occurred when the POSS was grafted onto the MMA backbone and a favorable interaction existed between the POSS functional groups and the PS homopolymers. The consequences of this compatibilization included reduced domain size, increased interfacial width, and greatly improved fracture toughness.[83c] MA-POSS copolymers and nanocomposites

were applied as dental materials.[83d,e] The incorporation of MA-POSS into dental materials was aimed at reducing the magnitude of volume shrinkage that occurred in the neat resins (without POSS). The miscibility between the POSS component and the matrix played an important role in the improvement of the properties of the formulated thermosets.[83e]

The incorporation of MA–POSS into MA polymers enhances their reactive ion etching (RIE) resistance.[83f] While copolymers with low POSS concentrations showed little RIE resistance improvement, incorporation of 20.5 wt % of the POSS monomer into MA-based chemically amplified resists significantly improved their RIE resistances in O_2 plasmas. High-resolution transmission electron microscopy revealed the RIE resistance improved because rectangular crystallites formed. These crystallites were composed of silica cages, uniformly distributed as networks within the polymer matrix.[83f] Novel X-ray nanolithographic resists, based on terpolymer of methyl methacrylate (MMA)/*t*-Bu acrylate/MA-POSS, were synthesized[83g] by solution polymerization. They were optimized specifically for contrast enhancement. A MMA to POSS mass ratio of 85.7/14.3 led to maximum contrast (23.5) without sacrificing the sensitivity (1350 mL/cm^2). This sensitivity was comparable to that of standard PMMA. This major contrast enhancement shows that organic–inorganic nanocomposites are promising candidates for sub-100-nm lithography.

C. Norbornenyl-POSS Copolymers and Nanocomposites

Random norbornene copolymers **17a** and **17b** of heptacyclohexyl or heptacyclopentyl monofunctional norbornyl POSS monomers (**16a** or **16b**) were synthesized by Mather and coworkers under nitrogen via ring-opening metathesis polymerization (ROMP). Mo($C_{10}H_{12}$)($C_{12}H_{17}N$)(OC_4H_9)$_2$ was used as the catalyst in chloroform (Fig. 10).[84] Various weight ratios of norbornene versus norbornyl-POSS

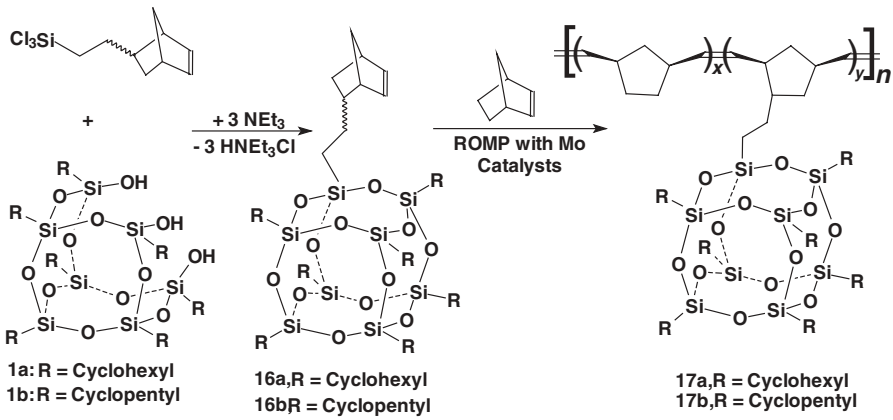

Figure 10 Synthesis of POSS-norbornyl macromers and their ring-opening metathesis copolymerization.

16a or **16b** (100/0, 90/10, 80/20, 70/30, 60/40 and 50/50) were employed.[84] Copolymerizations were designed to produce a degree of polymerization of about 500 by controlling the monomer to catalyst ratio. These living polymerization reactions were terminated by addition of benzaldehyde. The copolymers were precipitated and purified by adding the chloroform solution of the copolymer to a large excess of methanol and collecting the precipitate.

The effect of POSS incorporation into norbornene ring-opened polymers on the glas-transition temperature was investigated.[84] The T_g value of pure polynorbornene is 52.3°C. When 7.7 mol % (50 wt %) of heptacyclohexyl-substituted norbornyl-POSS 16a was present, the T_g was raised to 81.0°C. The copolymer with 8.4 mol % (50 wt %) heptacyclopentyl norbornyl-POSS, **16b**, exhibited a T_g of 69.0°C. These values were determined by DSC. The T_g values of these copolymers increased with increasing weight percent of the POSS monomer. This effect was slightly more pronounced in the cyclohexyl-substituted POSS copolymers, **17a**, than in their cyclopentyl-substituted POSS counterparts, **17b**. However, POSS copolymerization was observed to have no significant effect on the decomposition temperature. All of the copolymers exhibited a T_d of 440°C.

Norbornene copolymers of POSS **16a** and **16b** (Fig. 10) were subjected to dynamic mechanical thermal analysis.[84] DMTA data showed that the α-relaxation temperature, T_α (T_g), of the copolymers increased as the weight percent of POSS increased. A slight enhancement of the room temperature storage modulus also occurred. The magnitude of tensile loss tangent for the α transition monotonically decreased with an increasing POSS content. Unlike polynorbornene and the copolymers (**17b**) of norbornyl-POSS **16b** with norbornene, the norbornene/norbornyl-POSS-**16a** copolymers, **17a,** (with 0.9, 2.1, 3.5, 5.3 and 7.7 mol % POSS) displayed a β-relaxation transition at −78°C. This β-relaxation arises from the liberation of the cyclohexyl groups bound to the corner silicon atoms. X-ray scattering showed that the norbornene/norbornyl-POSS-**16a** copolymers preserve the amorphous character of the polynorbornene homopolymer. In contrast, the norbornene/norbornyl-POSS-**16b** copolymers, **17b**, (with 5.8 and 8.4 mol % POSS **16b**) lead to significant ordering of the POSS macromers. This is an excellent example of how changes in the "inert" organic substituents on POSS can vary properties of copolymers. In **17a**, R = cyclohexyl, whereas in **17b** R = cyclopentyl.

The effect of introducing norbornene-substituted, pendant POSS moieties onto polynorbornene chains was explored by Bharadwaj et al.[85a] using atomistic molecular dynamics simulations (AMDS). The mobility of the POSS moieties in these copolymers was addressed via the mean squared displacement of the POSS polyhydra in the norbornene copolymers of **16a** and **16b**. Computation of the torsional autocorrelation function indicated that conformational dynamics were retarded by the presence of the POSS moieties. The main chain dynamics were sensitive to the presence and the nature of the attached POSS moieties (at 10 mol % POSS). Chain dynamics were slower in the copolymer with cyclohexyl-substituted POSS pendent groups compared to the copolymer with cyclopentyl-substituted POSS pendant groups. These results are in good agreement with the mechanical properties predicted from AMDS simulations[85a] and with the observed T_g values.[84] The simulations predicted

that the tensile, bulk, and shear moduli for the POSS-containing copolymers would increase and change less dramatically with increasing temperature when compared to the same properties of the polynorbornene homopolymer. The source of this reinforcement was traced to the ponderous nature of the POSS moieties. POSS groups behave as strong anchoring points in the polymeric matrix based on their size (mass and occupied volume) rather than any specific strong intermolecular attractive interactions between the POSS moieties or between POSS groups and the polymer backbones.

The shape memory in the copolymers of norbornyl-POSS macromers, **16a** or **16b**, with norbornene were also studied by Jeon, Mather and Haddad,[85b] using thermomechanical analysis. Samples containing 50 wt % POSS macromer **16a** or **16b** were mechanically drawn at temperatures above the T_g followed by rapid quenching in liquid nitrogen. Shape-memory properties of such drawn samples were explored using DMTA by measuring the recovered strain while heating the samples back above the T_g. Incorporation of POSS comonomers into polynorbornene caused a slight decrease in the percent recovery, while improving thermal stability significantly. It is interesting that the identity of the corner groups (cyclohexyl and cyclopentyl) in the POSS macromers affected the shape-memory behavior. The cyclohexyl-substituted POSS/ norbornene copolymer **17a** gave a lower percent recovery than the cyclopentyl-substituted POSS/ norbornene copolymer **17b** due to enhanced aggregation of cyclohexyl-substituted POSS macromers within the polymer.

Coughlin and coworkers[86] synthesized several copolymers of norbornylethylPOSS, **16c**, with ethylene, propylene, cyclooctene and 1,5-cyclooctadiene (Fig. 11). Thermal characterization of poly(ethylene-co-norbornylethyl-POSS), (P(E-co-POSS)), and poly(propylene-co-norbornylethyl-POSS), (P(P-co-POSS)), are summerized in Tables 2 and 3, respectively.[86b] The P(E-co-POSS) copolymers with 0, 19, 27, 37 and 56 wt % POSS exhibited a gradual decrease in both the melting temperature and heat of fusion with an increase of POSS content. This indicates that the copolymers have fewer polyethylene crystalline domains at higher POSS concentrations. Thus the copolymer with highest POSS concentration (56 wt %) was partially soluble in hexanes at room temperature, whereas none of the other samples was. A slight increase in the onset of decomposition temperature for the P(E-co-POSS) copolymers was observed as the mole percent of the POSS increased. The temperature at which a 5% weight loss occurred was from 90°C to 104°C higher for every ethylene/norbornylethylPOSS copolymer sample compared with that of a PE control sample. Thus incorporating monomer **16c** caused a significant improvement of the thermal oxidative resistance in these poly(ethylene-co-norbornylethyl-POSS) copolymers. Dynamic mechanical thermal analysis (DMTA) of a P(E-co-norbornylethyl-POSS) sample with 19 wt % POSS-**16c** exhibited higher storage modulus values in the rubbery region than those of PE.

The copolymers of **16c** with propylene also exhibited a decrease in crystallinity and an increase in thermal stability versus polypropylene.[86b] The poly(propylene-co-norbornylethyl-POSS) copolymers had slightly lower melting temperatures and significantly smaller heats of fusion versus those of PP, indicating that the PP crystallinity decreased with an increase of POSS content. Dispite having lower T_m,

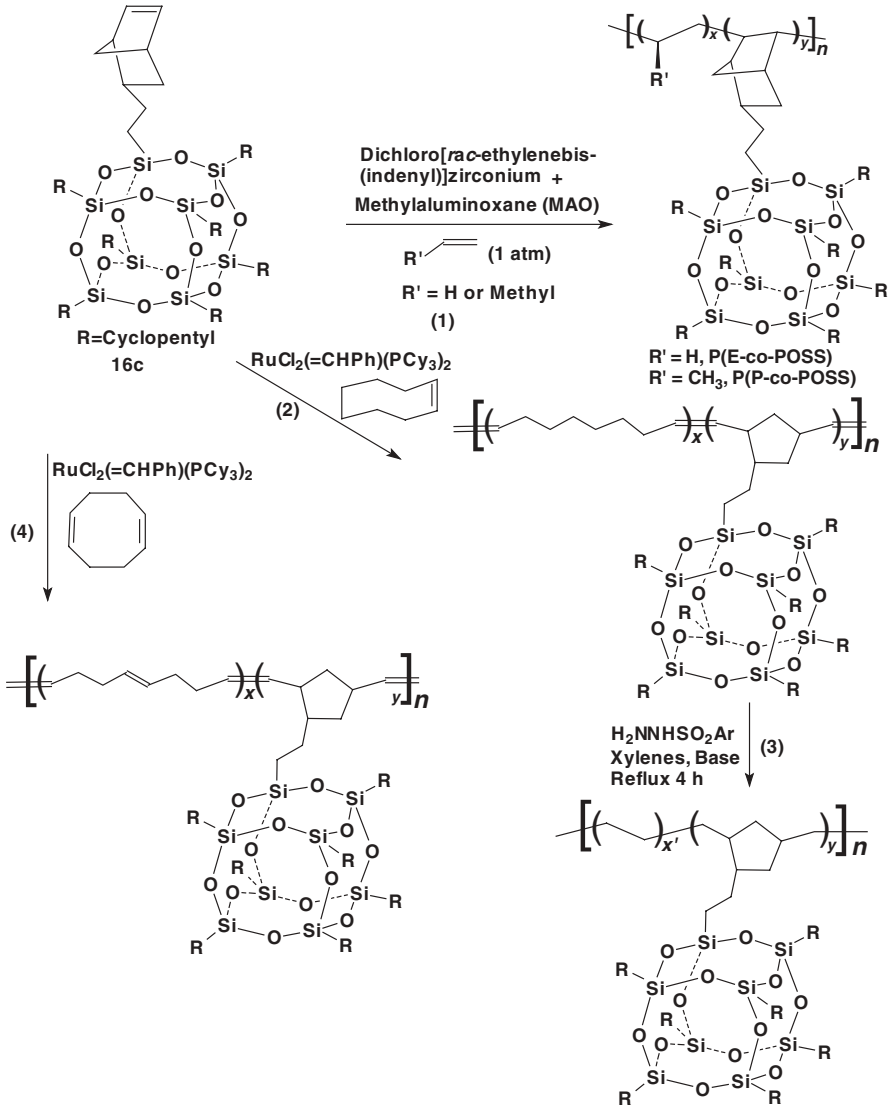

Figure 11 Synthesis of norbornenylethyl-POSS, **16c**, copolymers with ethylene, propylene, cyclooctene, and 1,5-cyclooctadiene.

crystallinity and heat of fusion values, the onset of the decomposition temperature of the P(P-co-norbornylethyl-POSS) copolymers in nitrogen increased with an increase in POSS content. However, the thermal oxidative behavior for the P(P-co-POSS) copolymers was different from that that of the P(E-co-POSS) copolymers. The 5% weight loss temperature in air for the P(P-co-POSS) copolymers did not

Table 2 Thermal Characterization of Poly(ethylene-co-norbornylethylPOSS) Copolymers[a]

Entry Number	POSS Amount (wt %)	T_m[b] (°C)	Heat of Fusion ΔH (J/g)	Onset of T_d[c] (°C)	Char Yield in N_2[c] (%)	5 wt % Loss in Air[c] (°C)	Char Yield in Air[c] (%)
1	0	136	161	437	0.5	283	0
2	19	126	112	448	2	373	7
3	27	125	91	456	2	397	9
4	37	116	65	457	2	387	10
5	56			458	4	388	7

[a] Copolymers incorporated **16c** where the $(SiO_{1.5})_8$ cage has seven cyclopentyl and one 2-norbornylethyl function attached.
[b] Data were obtained on the second melt using a heating and cooling rate of 10°C/min.
[c] Temperature ramp 20°C/min in nitrogen or air.

Table 3 Thermal Characterization of Poly(propylene-co-norbornylethylPOSS) Copolymers[a]

Entry Number	POSS Amount (wt %)	T_m[b] (°C)	Heat of Fusion ΔH (J/g)	Onset of T_d[c] (°C)	Char Yield in N_2[c] (%)	5 wt % Loss in Air[c] (°C)	Char Yield in Air[c] (%)
1	0	140	84	382	0.03	257	0
2	20	134	69	405	1	256	8
3	58	130	55	421	1	259	12
4	73	119	23	427	3	309	24

[a] Copolymers incorporated **16c** where the $(SiO_{1.5})_8$ cage has seven cyclopentyl and one 2-norbornylethyl function attached.
[b] Data were obtained on the second melt using a heating and cooling rate of 10°C/min.
[c] Temperature ramp 20°C/min in nitrogen or air.

increase until relatively high POSS concentrations (≥58 wt %, ≥3.4 mol %). The tertiary carbons in the propylene repeating units of these copolymers are more susceptible to degradation, requiring higher levels of POSS to push up the thermal oxidative stability.

The Coughlin group's wide-angle X-ray scattering (WAXS) studies indicated that the P(E-co-POSS) copolymers form a dual crystalline system, containing PE crystalline lattice regions and POSS nanocrystals.[86c] As the molar content of POSS **16c** increased from 0.64 to 3.4 mol % (19 to 56 wt %), the PE crystallinity and apparent crystalline domain sizes became progressively smaller, while the amount of POSS crystallization simultaneously increases. However, these POSS crystallites do not exhibit full three-dimensional development. Instead, they grow within spatial constraints imposed by the presence of their polymer chains, leading to anisotropic crystallite shapes. Moreover, the surfaces of PE and POSS crystalline domains are not connected directly. A disordered amorphous phase must lie within this interfacial region.

The method of precipitation/crystallization from solution and the manner in which the P(E-co-POSS) copolymers are processed and solidified from melts can

affect the overall structure and nanomorphology, this dual crystalline system.[86a] For example, precipitation of P(E-co-POSS) copolymers by adding a xylene solution of copolymer into the non-solvent acetone, produced higher PE crystallinity within the solid copolymer. However, if solid samples were subjected to melt processing and thermal annealing, more POSS nanocrystalline domains were formed. Factors that favor aggregation of the pendant POSS functions into crystalline domains tend to disrupt polyethylene crystallinity within the copolymer and vice versa. Manipulation of POSS aggregation, therefore, is a route to tailor morphology and properties of these copolymer nanocomposites. The contributions of POSS nanocrystals within the copolymers help explain such novel properties of this type of nanocomposite as better dimensional stability, extension of the high-temperature rubbery plateau, and strong thermal oxidative resistance.

Ring-opening metathesis copolymerizations of cyclooctene and norbornyl-POSS were performed with Grubbs's catalyst, $RuCl_2(=CHPh)(PCy_3)_2$ (Fig. 11).[86d] Reduction of these copolymers afforded poly(ethylene-co-norbornyl-POSS) copolymers, which have properties similar to those of the poly(ethylene-co-norbornylethyl-POSS) prepared by direct copolymerization of ethylene with no bornyl-POSS, described above. Poly(cyclooctene-co-norbornylethyl-POSS) copolymers with 0, 12, 23, 31, 45, and 56 wt % POSS (0, 1.39, 3.06, 4.62, 7.96, and 11.9 mol %) had melting temperatures of 46°C, 43°C, 38°C, 36°C, 33°C, and 30°C, respectively. Their heat of fusion values (J/g) are 56, 45, 36, 28, 24, and 19, respectively. This decrease in both melting temperatures and heat of fusion values as more POSS is incorporated shows that the random POSS moieties disrupted crystallinity. No T_g was observed for these copolymers, presumably because of their semicrystalline nature.

Poly(butadiene-co-norbornylethyl-POSS) copolymers, containing from 12 to 53 wt % POSS, were made by ring-opening metathesis copolymerization of 1,5-cyclooctadiene (Fig. 11).[86a,g] At the lower POSS weight percents, the copolymers tend to be viscous oils, much like *cis*- or *trans*-polybutadiene. However, at higher POSS incorporation levels, these copolymers become elastomeric. POSS moieties aggregate into nanocrystals in these copolymers, and the nanocrystals acted as physical cross-linking joints. Thus the segments between these nanosized aggregates can elongate in response to applied stress, but polymer flow and creep are retarded because POSS moieties from different chains are caught in the nanocrystalline aggregates. If the temperature of such a nanocomposite were raised above the melting region of the nanoaggregates, they would melt allowing the polymer to flow. In this respect, these POSS nanocomposite linear copolymers should resemble thermoplastic elastomers.

The above discussion demonstrates conclusively that POSS macromers can play an enormous role in changing polymer properties via a variety of mechanisms. The massive and pondorous POSS function moderates segmental motion, makes sereptation (hence flow) difficult and can introduce more free volume while disrupting crystallinity. Individual POSS units distributed in the polymer solid structure do that. However, POSS groups can also aggregate to form nanocrystals of varying order and properties. These, in turn, cause changes in morphology and properties.

D. POSS-Olefin Copolymers and Nanocomposites

Heptaethyldec-9-enyl POSS monomer, **18**, is a terminal α olefin monomer that has been employed by Tsuchida et al.[87] to incorporate POSS moieties into polyolefins. Copolymers of this monovinyl POSS monomer with ethene and propene (Fig. 12) were synthesized using different methylalumoxane-activated metallocene catalysts.[87] POSS comonomer incorporation levels between 17 and 25 wt % were achieved, depending on which catalyst was used in the copolymerization. Incorporation of 25 wt % (1.2 mol %) of the vinyl-POSS **18** into the ethylene copolymer, **20**, lowered the melting temperature by 18°C versus that of polyethene (PE). The thermal stability in air of vinyl-POSS **18**/ethylene copolymer (0.7 mol % POSS) and **18**/propylene copolymer

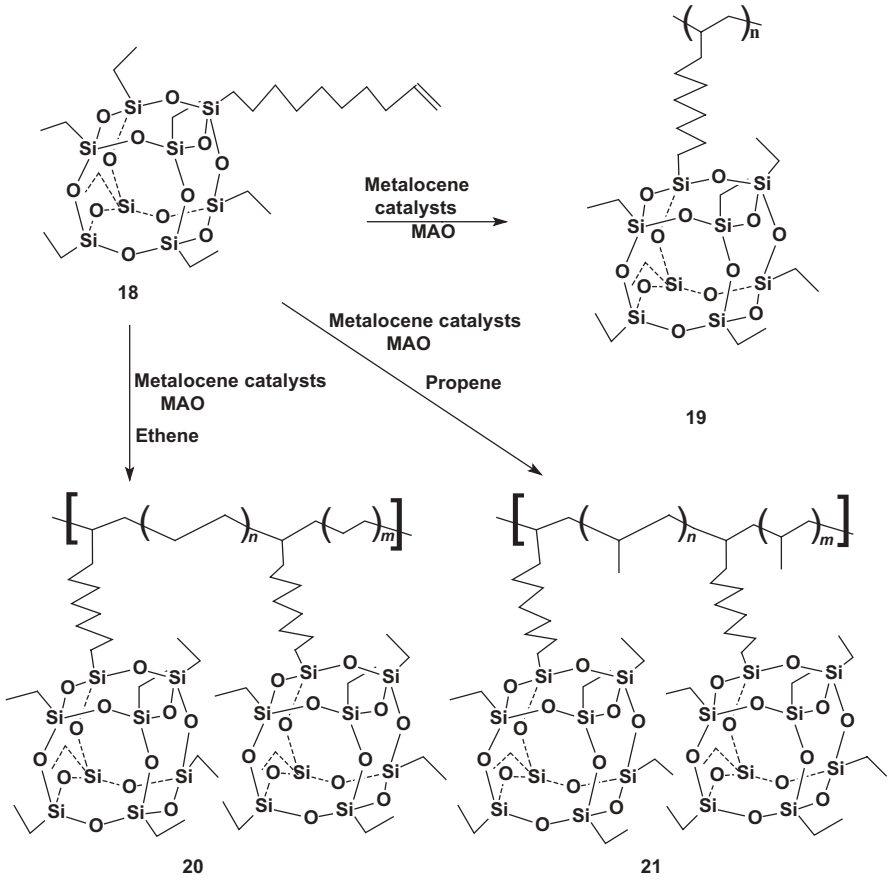

Figure 12 Homopolymerization of a decenyl-functionalized POSS and its copolymerization with ethene and propene using methylalumoxane-activated metallocene catalysts.

(1.1 mol % POSS) was better than that of either pure polyethylene or oligomeric polypropylene. For example, the T_d value (TGA) at 30% weight loss of the **18**/ethylene copolymer, **20**, was 410°C versus a value of 380°C for polyethylene. The T_d value of the **18**/propylene copolymer, **21**, was 313°C versus 261°C for oligomeric polypropylene. Thus small mole percents of POSS **18** had large effects on thermostability.

E. Siloxane-POSS Copolymers

Lichtenhan et al.[60] prepared POSS-siloxane copolymers. Two methods were employed. The first involved polycondensation of the silanol-functionalized POSS macromer **27** with a bis(dimethyl amine)-substituted silane or a siloxane comonomer (Fig. 13a).[60] Dichlorosilane or siloxane monomers could be used in this method to generate POSS-siloxane copolymers represented by **28**. The second route involved the hydrosilation polymerization of the allyl-substituted POSS macromers, ($R_7Si_8O_{12}(CH_2–CH=CH_2)$, **29a** and **29b**, where R = cyclohexyl or cyclopentyl, with poly(hydridomethyl-co-dimethyl siloxane) **30** (Fig. 13b). Thus hydrosilation places pendant POSS units along the polysiloxane backbone of the resulting polymers **31a** and **31b**. The T_g of these copolymers increased with an increase in their POSS monomer content. The T_g values range from −125°C for the pure polysiloxane to 250°C for the copolymer **31a** containing 70 wt % of POSS-**29a**. The graft polymers containing cyclohexyl-substituted allyl-POSS **29a** have lower T_g values than those grafted with cyclopentyl-substituted-POSS, **29b**. POSS-siloxane copolymers **31a** and **31b** underwent a complex depolymerization-decomposition process at high temperatures.[88a] This included the evolution of cyclic dimethyl siloxanes at 400°C, cyclohexyl hydrocarbons from 450°C to 550°C, and H_2 liberation from 700°C to 1000°C when the copolymer [$(CySi_8O_{11}$-$(OSiMe_2)_{5.4}O$-$)_n$] **31a** was heated. Loss of the silsesquioxane "cage" structure occurred upon heating from 450°C to 650°C and after the evolution of most of the pyrolysis gases.[88a] The analysis of the resulting 1000°C char composition by XPS revealed three major silicon environments, corresponding to a composition of 14.5% SiO_2, 7.5% SiO_xC_y, and 1.4% SiC.[88a] This analysis was consistent with both NMR and X-ray diffraction studies. These results suggest that POSS units promote a special type of char formation during combustion of POSS-containing organic thermoplastics or thermosets.

POSS-siloxane copolymers with varying proportions of POSS were synthesized and characterized by rheological measurements by Haddad et al.[88b] A POSS macromer, substituted on one corner with a -$OSIMe_2H$ function, was grafted onto poly(dimethylsiloxane-co-methyl vinyl siloxane). The rheological behavior of the POSS-grafted polymers was compared to the behavior of blends prepared by simply mixing equivalent amounts of POSS into PDMS.[88b] Covalently attached POSS groups (5 wt %) result in a decrease of the PDMS relaxation time by one order of magnitude. In contrast, blending the ungrafted polymers with the POSS macromer does not induce any changes in these relaxations.

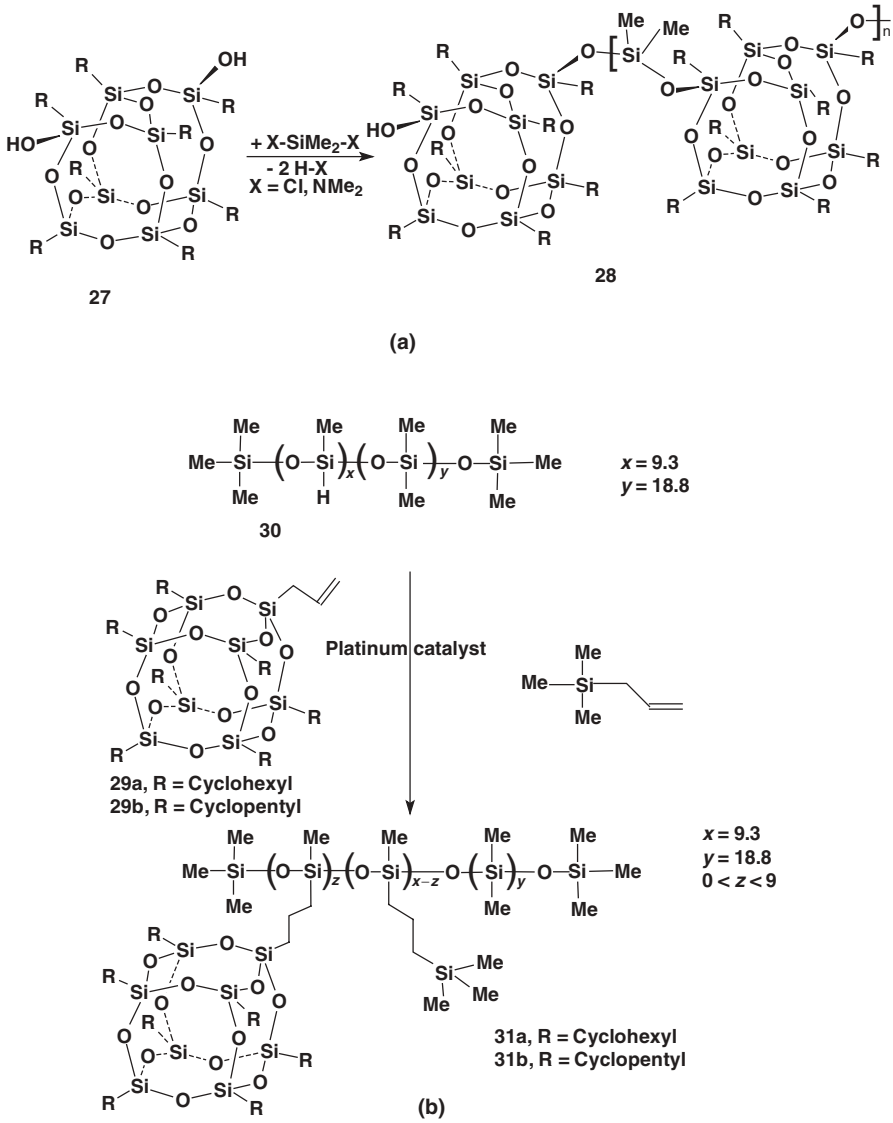

Figure 13 Synthesis of siloxane-POSS copolymers by (**a**) polycondensation and (**b**) hydrosilation polymerization.

IV. CROSSLINKED POSS-CONTAINING RESINS AND MATERIALS

POSS cages that were multifuntionalized with several vinyl groups have been used to develop new microporous and mesoporous hybrid materials, crosslinked polymers, and other three-dimensional structures by the research groups of Laine,

Morrison, Lichtenhan, and Lee.[89] Polyhedral octahydridosilsesquioxane, $(HSiO_{1.5})_8$ **22**, and $(HSiMe_2O)SiO_{1.5})_8$ **23**, were each copolymerized with stoichiometric amounts of the octavinylsilsesquioxane, $(CH_2{=}CH{-}SiO_{1.5})_8$ **24**, and $((CH_2{=}CH{-}SiMe_2O)SiO_{1.5})_8$ **25**.[89a] These polymerizations proceed via successive hydrosilations in toluene catalyzed by platinum divinyltetramethyldisiloxane, "Pt(dvs)."[89a] The chemical structures of these copolymers, **26a-d**, are presented in Figure 14. The degree of condensation of these four copolymers increased from 43% to 81% as the intercube chain lengths are increased. POSS cubes with longer spacer groups are more reactive than

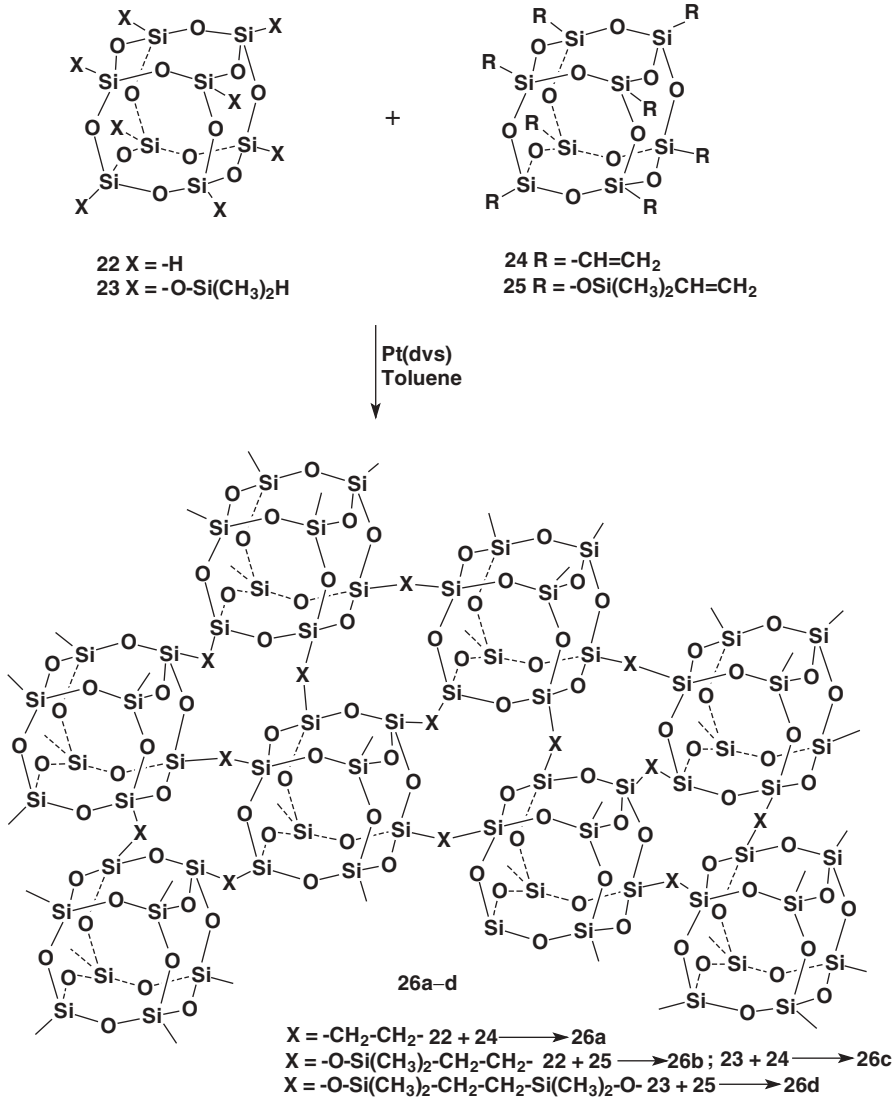

Figure 14 Copolymerization of multifunctional vinyl POSS macromers **24** and **25** by hydrosilation with POSS derivatives **22** and **23**.

those with no spacer groups. Longer intercube lengths allow more freedom of motion and more diffusional freedom for new monomers or oligomeric segments to find teactive counterpacts within the developing matrix. If the groups forming the intercube chains are short, it is difficult for POSS moieties to migrate to all eight-corner locations as the crosslinked network forms.

As the chain lengths between cubes increases, the space between the cubes should increase and visa versa. Because 100% condensation is not achieved, the structure of the material will not exhibit a regular or perfect cube order. The pores within the POSS cube interiors are ~0.3 nm in diameter, whereas pores between the cubes were reported by Mantz et al.[88a] to range from 1 to 50 nm in diameter, according to nitrogen absorption, positron annihilation lifetime spectroscopy (PALS), and small-angle X-ray scattering (SAXS) data. Nitrogen sorption analyses give specific surface areas of 380–530 m^2/g with "observable" pore volumes of 0.19–0.25 mL/g. All of these three-dimensional copolymer networks showed good to excellent thermal stability in N_2. The first mass losses in N_2 begin at about 300°C for the copolymers **26b–d**, and at 440°C for the copolymer **26a**.

Porous POSS-based network polymers have also been prepared by hydrosilation copolymerization reactions where a silyl–functionalized POSS molecule reacts with a vinyl-functionalized moiety. This path is quite similar with that shown in Figure 14.[89b] These solids possessed pore structures in the mesoporous regime. The polymers with longer organic linking groups between the cages showed flexible wall structure behavior. These polymer networks were then functionalized by reaction with triflic acid or sodium hydroxide, followed by incorporation of $CpTiCl_3$.[89b] Functionalized porous POSS polymeric materials can be further developed. In addition, Lui et al.[89c] reported that the hydrosilation polymerization using vinyl POSS compounds give products with excellent mechanical properties and thermal stability, plus remarkable fire resistance.

A. Vinyl Ester, Epoxy, and Phenolic Resins Containing POSS

An obvious extension of polyhedral silsesquioxane materials chemistry would be the incorporation of suitably functionalized POSS cages into important classes of thermoset resins, such as epoxy, phenolic, vinyl ester, styrene/divinylbenzene, acrylic resins and hydrocarbon networks. However, little has appeared in the literature, except for a few examples already discussed. This is an area in which our laboratory has become quite active. Two general types of substituted POSS monomers can be chemically incorporated into such resins. First, monofunctional monomers can be used. Alternatively, difunctional or polyfunctional POSS monomers can be used. Incorporating a monofunctional POSS monomer can actually lower the resulting resin's crosslink density if the amount of the monofunctional POSS monomers in the commercial resin's monomer mixture is held constant. The POSS cages with organic functions attached to its corners have typical diameters of 1.2–1.5 nm. Therefore, each POSS monomer occupies a substantial volume. When that POSS

monomer is monosubstituted, it cannot contribute to crosslinking. A 2 mol % loading of POSS in a resin might actually occupy 6–20 vol % of the resin and this occupied volume contains no crosslinks. Therefore, the average crosslink density per unit volume of resin will be lowered. Conversely, when a polyfunctional POSS monomer is employed, several bonds can be formed from the POSS cage into the matrix, thereby making the POSS cage the center of a local crosslinked network. Some examples of monofunctional and polyfunctional POSS monomers **32–39** are illustrated in Figure 15 together with the types of resins into which they have been chemically incorporated.

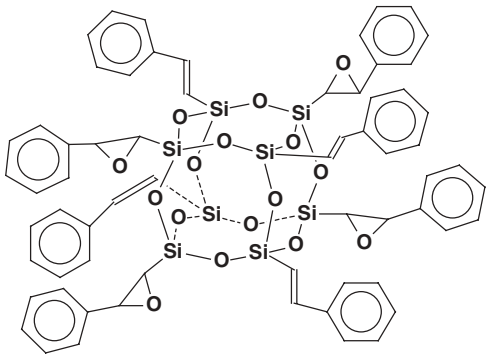

32
Tetraepoxidized octa-b-styryl-POSS
M_w = 1305
For vinyl ester, phenolic, epoxy and dicyclopentadiene (DCPD) resins

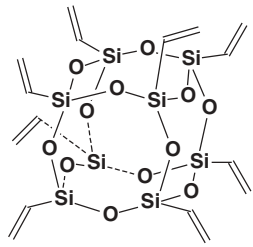

34
Octavinyl-POSS
$C_{16}H_{24}O_{12}Si_8$ M_w = 633
For DCPD resins and polyolefins (epoxy resins after epoxidation)

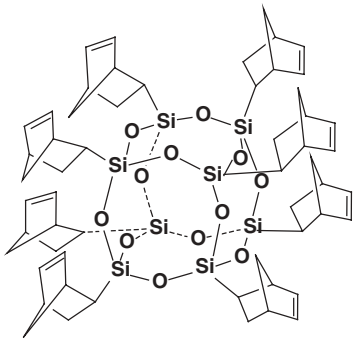

33
Octanorbornyl-POSS
$C_{56}H_{72}O_{12}Si_8$ M_w = 1162
For DCPD resin

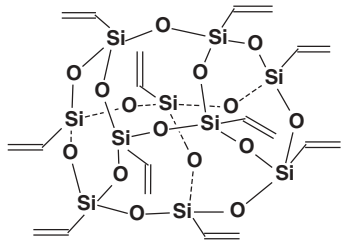

35
Decavinyl-POSS
$C_{20}H_{30}O_{15}Si_{10}$ M_w = 791
For DCPD resins and polyolefins (epoxy resins after epoxidation)

Figure 15 (*Continued*)

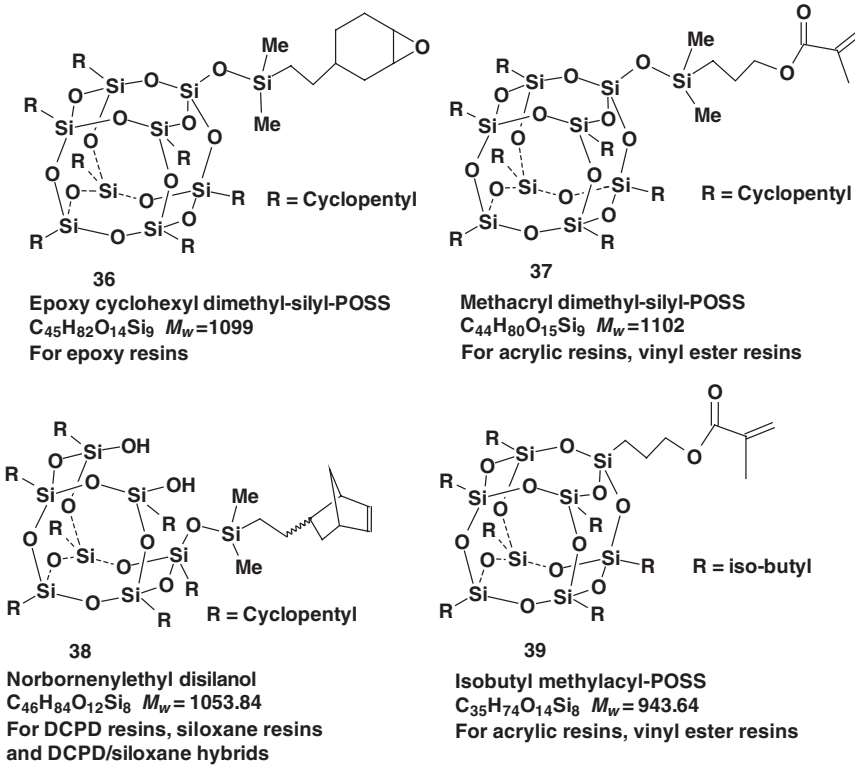

Figure 15 Polyfunctional and monofunctional POSS macromers.

Recently, Lee et al.[89d] reported that multifunctional vinyl POSS mixtures (POSS mixtures with cages of 8, 10, and 12 Si atoms) could be used to modify vinyl ester resins. The successful use of multifunctional POSS mixtures is important because it represents one approach to lower the costs of using POSS. In the original monomer syntheses, separation steps may be avoided and the atom efficiency of the overall approach is improved.

The presence of 15 wt % of the mixed vinyl-POSS macromers increased the ignition times of these vinyl ester/POSS resins and reduced the overall heat release rates.[89d] The T_g values of Derakane 441–400 vinyl ester resin (VE) and its 15 wt % mixed-POSS composites are 118°C and 125°C, respectively. Their heat distortion temperatures are 245°F, and 257°F, respectively. The decomposition temperatures (T_{dec}) of the neat VE and its 15 wt % POSS composite are 360°C and 411°C, respectively, and their char percent values are 8% and 34%, respectively. This incorporation of vinyl-POSS into vinyl ester resins certainly improved the thermal and fire-retasdant properties. However, there was little change in their mechanical properties. The tensile strength, tensile modulus, elongation, flexural strength, and flexural modulus of the 15 wt % POSS composite are 13,195 psi, 5.1×10^5 psi, 4.8%, 24,360 psi and

5.0×10^5 psi, respectively. The neat VE resin had quite similar values, 13,000 psi (tensile strength), 5.0×10^5 psi (tensile modulus), 5–6% (elongation), 24,000 psi (flexural strength), and 5.1×10^5 psi (flexural modulus).[89d]

Hybrid Plastics Co. has now developed high-POSS-content vinyl ester resins with lower viscosities than Derakane VE. These systems can then be resin transfer molded into 60 wt % glass-fiber-reinforced composites with improved fire retardancy. However, the mechanical properties of these higher POSS resins was not good as Derakane VE resin. Unlike VE resins, these high POSS systems did not exhibit a glass transition. Furthermore, they had excellent thermal stability (there was no significant degradation up 500°C).[89d]

In addition to the POSS-containing homopolymers, copolymers, and nanocomposites mentioned above, POSS monofunctional and multifunctional monomers have also been used to modify polyurethanes.[90,91]

The monofunctional epoxy-substituted POSS monomer [(c-$C_6H_{11})_7Si_8O_{12}$ ($CH_2\overline{CHCH_2O}$)] was incorporated into an epoxy resin network composed of the two difunctional epoxies, diglycidyl ether of bisphenol A (DGEBA) and 1,4-butanediol diglycidyl ether (BDGE), at a DGEBA/BDGE mole ratio of 9/1 by Lee and Lichtenhan.[92] The diamine-terminated poly(propylene oxide), Jeffamine D230, composed of an average of 38 propylene oxide molecules and a M_w of 2248, was employed as the curing agent in an amount that gave a 1:1 equivalent of epoxy to amine functions.[92,93]

The glass-transition temperatures of the neat parent epoxy resin and the resin-containing POSS monomer were defined as the deflection point in the glass-transition region in their respective DSC thermographs.[92,93] The temperatures at the onset, midpoint, and end of the glass-transition region of the neat epoxy resin (DGEBA/BDGE mole ratio = 9/1) are 66.9°C, 71.2°C, and 75.3°C, respectively. These correspond to temperatures of 67.2°C, 74.8°C, and 80.3°C for the resin-containing 5 wt % of epoxy-POSS. The resin-containing 10 wt % epoxy-POSS monomer exhibited a T_g range of 67.2°C, 78.9°C, and 83.4°C. Thus the glass-transition region was observed to broaden with an increase in weight percent of the POSS monomer. These changes occurred without increasing the degree of crosslinking. In fact, the crosslink density per unit volume of resin actually decreased as more POSS was incorporated due to the volume occupied by the POSS monomer unit. Broadening of the T_g region may be due to the nanoscopic size and mass of these POSS cages, which enhance their ability to hinder the segmental motion of molecular chains and network junctions to which the POSS is bound. The onset temperature remains low because many segments of chains are not attached to POSS moieties at the low mole percentages of POSS that were used.

The POSS-containing epoxy networks described above were subjected to thermal quenching and aging experiments at temperatures below T_g.[92] The topological constraints provided by the presence of POSS-reinforcements slowed the motion of the network junctions. Therefore, the time needed to reach structural equilibrium is dramatically increased relative to that for networks that are not modified by POSS nanoreinforcements. Stress–relaxation experiments were used at small strains to probe the viscoelastic responses of these networks during isothermal aging.[92] Surprisingly, the instantaneous modulus was not affected by incorporation of the

POSS nanoreinforcement. This suggests that, whereas POSS cages influence polymer chain motions and the motion of the molecular junctions, these nanoreinforcements did not participate in the overall deformation of the chains. This, again, may be a manifestation of the low mole fraction of POSS present, which means many chain segments are not bound to a POSS moiety.

Pittman and coworkers[94a,b] prepared aliphatic epoxy resins containing the multifunctional (tetraepoxy)POSS macromer **32** (Fig. 15). TEM studies did not observe POSS aggregation or phase separation down to a size range of ~2 nm for the resin containing 5 wt % **32**. DMTA and stress–strain studies as a function of POSS loading exhibited improved properties above the T_g and a complex T_g behavior on POSS loading.[94b]

Lee studied nanocomposites of trisilanolphenyl-POSS (structure **1** R=Ph) with several epoxy resins. DER332, a difunctional epoxy of the DGEBA variety, was cured using Jeffamine D-230, an amine-terminated poly(propylene oxide) mixture. This system was cured in nitrogen at 100°C for 12 h. T_g values determined by DMTA of POSS nanocomposites with 0, 0.20, 0.40, 0.60, 0.80, and 1.00 wt % POSS are 84.2°C, 92.1°C, 91.2°C, 90.6°C, 91.6°C, and 91.7°C, respectively. Thus the sample, which contained only 0.2 wt % POSS, exhibited a significant T_g increase. However, further POSS addition did not increase T_g any further. Nanocomposites of the 4,4′-methylenebis(*N,N*-diglycidylaniline)epoxy/Jeffamine D-230 system (cured at 150°C for 12 h), were also synthesized with 0, 0.20%, 0.40%, 0.60%, 0.80%, and 1.00 wt % trisilanolphenyl-POSS. These systems had T_g values of 136.8°C, 146.5°C, 148.8°C, 144.2°C, 145.0°C, and 148.4°C, respectively. This increase in T_g values was similar to that of the DER332 epoxy/Jeffamine D-230/POSS nanocomposites. However, if the less-flexable DytecA diamine, which has no ether-type carbon–oxygen linkages, was used as the curing agent for the two-epoxy systems, no increase in T_g was observed as trisilanolphenyl-POSS was added. With trisilanolphenyl-POSS levels of 0, 0.20, 0.40, 0.60, 0.80 and 1.00 wt %, the T_g values were 59.9°C, 58.6°C, 54.8°C, 57.5°C, 54.7°C, and 57.8°C, respectively, for the DER-332 epoxy system. Therefore, the particular diamine used to cure the thermosetting system is apparently critical to how POSS **1** addition affects T_g. Not all of the 4-amine groups of Dytic A may participate in the reaction to open up the epoxy rings, while the hydrogens in the primary and secondary amine groups of the Jeffamines are able to participate in crosslinking or opening of the epoxy rings. Thus the crosslink density would be different for the same epoxy with a different curing agent. The incorporation of POSS moieties into epoxy systems with different crosslink densities results in different influences on their properties. The composite with 1 wt % trisilanolphenyl POSS seemed to absorb more water at 45°C or 70°C than the one without POSS.

Epoxy, vinyl ester, phenolic, methacrylate, styrene-divinylbenzene, cyanate ester, and dicyclopentadiene (DCPD) resins have been made in Pittman's laboratory in which various POSS macromers have been chemically incorporated.[94] For example, a low-viscosity aliphatic epoxide resin was blended with macromer **32** (Fig. 15) and aliphatic triamine curing agents, and these blends were cured in five stages to both 120°C and 150°C.[94b] The incorporation of 5 and 25 wt % of **32** into these epoxy resins gave an increase in the storage modulus versus that of the neat epoxy.[94b] The

increases in storage moduli were most pronounced above the T_g. The T_g increased as the maximum cure temperature was increased. DMTA tanδ vs. temperature measurements exhibited a broadening and lowering of the intensity of the tanδ peak as the POSS content increased. Daulton of the Naval Research Laboratory, Stennis Space Center, performed TEM studies on Pittman's epoxy resin systems and demonstrated to a resolution of ~1 nm that no agglomeration of the POSS units was observed. This established that **32** is molecularly distributed in the 5 wt % POSS resin although some aggregation of POSS-**32** moieties could not be excluded.

Macromer **32** was also incorporated into a commercial (Borden SC-108) phenolic resin and cured in stages to a final postcure of 350°C.[94a,d] Incorporation of 5 wt % of POSS-**32** raised the T_g by 11–14°C versus that of the pure cured phenolic resin. When vapor-grown carbon fibers (VGCF) (30 % wt, 60–240 nm in diameter, 1–60 μm in length) were also incorporated, the phenolic/POSS-**32**/VGCF composite exhibited a T_g 22°C higher than with the equivalent phenolic resin/VGCF composite system without POSS and 53°C higher than the phenolic/POSS-**32** (5 wt %) resin alone. The bending storage modulus of the resin with 5 wt % POSS was 1.94 GPa higher than the parent phenolic resin at 40°C and 0.067 GPa higher at 350°C. A large number of POSS macromer have now been cured with both phenolic and cyanate ester resins including trisilanolphenyl POSS, octa(aminophenyl)T_8 POSS, 3-cyanopropyl-substituted-T_8-POSS, and 3-(dichloromethylsilyl)propyl-substituted-T_8-POSS.[94f,h] Their morphologies were studied by TEM and small angle neutron scattering and viscoelastic behavior by DMTA.[94f,h]

Macromer **32** was also dissolved in styrene and blended into the commercial vinyl ester, Derakane 510C-350 (from Dow Chemical Co.) This compatible liquid system was then cured at room temperature (24 h), 90°C (24 h), and 150°C (5 h) using a 1% methyl ethyl ketone peroxide/0.2% cobalt naphthanate catalyst system (Fig. 16).[94c] All the resins contained 50 wt % styrene. POSS-**32** was incorporated in 5 wt and 10 wt % into these thermoset resins. The flexural strength dropped from 192 to 175 and 152 MPa with 5 wt % and 10 wt % POSS added into the blends. The extent of strain at failure also decreased with increasing levels of POSS. DMTA measurements confirmed that the bending storage moduli of the vinyl ester/POSS-**32** resins were higher than that of vinyl ester resin without POSS at temperatures below the T_g. The storage moduli increased greatly with an increase in the POSS-**32** content at temperatures above the T_g. Storage modulus enhancement was larger at temperatures lower than the T_g (e.g., in the glassy region). Specifically, at 40°C, the bending storage moduli were 1.24, 1.96, and 1.58 GPa for the pure vinyl ester and the vinyl ester with 5 wt % and 10 wt % POSS, respectively. The T_g values of neat VE, the 5 wt % and 10 wt % POSS nanocomposites are 130.6°C, 131.8°C, and 131.1°C, respectively. Thus, given some experimental variations, the inclusion of multifunctional POSS-**32** into the VE had no appreciable effect on the T_g. This is, in part, a reflection that POSS functions are present in low mole percents leaving many segmental regions without a bound POSS function.

The vinyl ester/POSS-**32 90/10** composites did exhibit some discernable phase separation via TEM.[94c] Phases rich in Si were observed as domains, ranging in size from a few nanometers to about 75 nm in diameter. Elemental composition maps

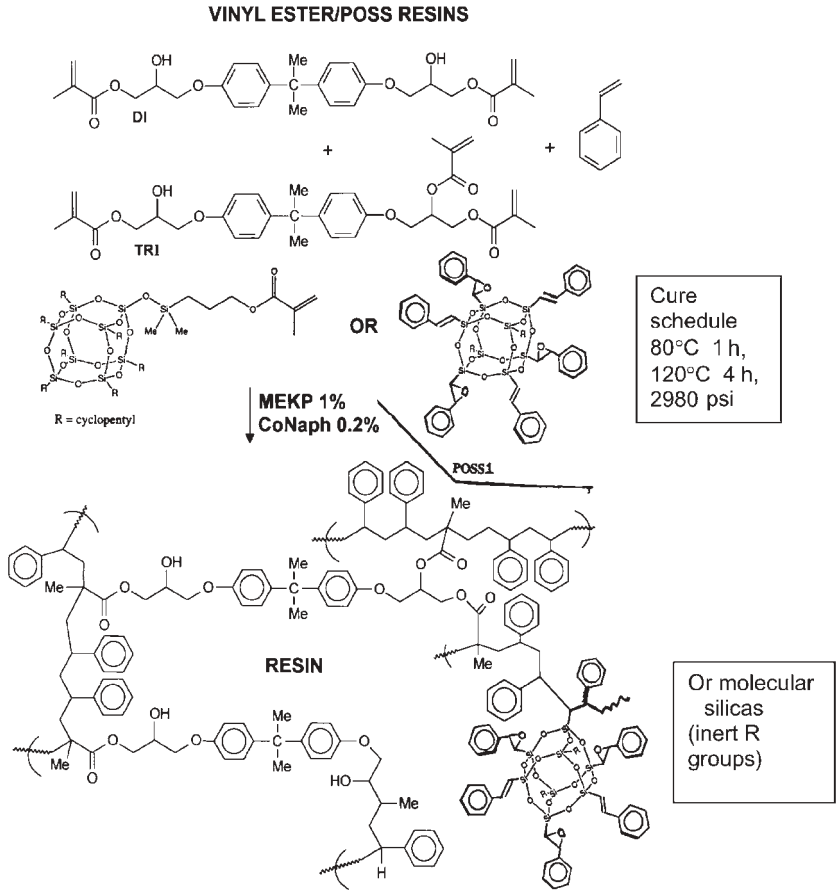

Figure 16 Vinyl ester (Derakane 510C-350)/POSS-**32** resin formation.

from EDAX and EELS studies established that POSS units were also present in the silicon-poor continuous domains and that the silicon-rich domains did not appear to have as high a silicon content as the POSS macromer **32**. The picture that emerges from this work is that during vinyl ester curing, some POSS is chemically incorporated via radical polymerization into the vinyl ester chains and network. Some POSS macromers may aggregate before polymerization is completed, since their solubility will decrease as the resin structure forms (e.g., the entropy of mixing decreases). The aggregated or separated POSS can undergo homopolymerization, and growing polymer chain ends encountering these POSS-rich regions can initiate new bond formation. Thus POSS-rich domains still contain some of the vinyl ester chains.

Swelling studies showed almost no uptake of THF or toluene by the vinyl ester/POSS-**32** composites after 50 days.[94] Furthermore, no POSS-**32** could be recovered on extensive extraction of fragmented samples. EDAX and EELS studies of

Si and Br (from a bromine-containing label used) provided evidence of some phase separation of Si-rich regions at a small size scale in the VE/POSS-**32** (10 wt %) sample. POSS-rich dispersed phases with sizes of 75 nm to 1–2 nm were observed by EELS. The epoxy/**32** resin composites appeared to exhibit mostly molecular level dispersion of chemically bound POSS-**32**, the vinyl ester/**32** (5 wt %) nanocomposites had a more complex nanomorphology. This illustrates the importance of early chemical bonding of any POSS derivative into the developing crosslinked resin's network structure during the cure. As curing occurs, the entropy of mixing term will contribute less and less to the thermodynamics of solubility of the POSS monomer. However, before phase separation of the POSS can occur due to a lowering of its solubility, the chemical bonds formed between the POSS and the developing resin matrix can lock POSS molecules into the resin structure. Thus migration and phase separation do not occur or only partial separation takes place. Partial separation is due to some phase separation late in the curing or due to POSS units, already attached to different chains or chain segments of the resin, aggregating while enough segmental mobility within the developing network structure still exists. Eventually, such mobility will be restricted as the crosslink density increases. This behavior of polymerizable POSS derivatives stands in sharp contrast to the behavior of T_8, T_{10} and T_{12} POSS molecules (Fig. 1) where none of the corner groups has a polymerizable function (e.g., R = *i*-Bu, cyclopentyl, cyclohexyl or phenyl). These molecules regularly phase separate (even when they can initially dissolve in the resin before curing). We have observed dispersed POSS particle (phase) sizes from 50 nm to 300 μm under a variety of conditions with these types of POSS derivatives in cured resins.[94]

B. Dicyclopentadiene Resins Containing POSS

Another resin system is worth noting. Dicyclopentadiene (DCPD) ring-opening methathesis polymerization (ROMP) with macromer **32** has been carried out using the Grubbs-type ruthenium carbene catalyst shown in Figure 17.[94a,d] Macromer **32** was incorporated into a series of resins with from 1 wt % to 5 wt % (0.1 mol % to 0.5 mol %) of **32** present. When co-cured in four stages (final stage 260°C, 1 h), DCPD/POSS-**32** gave a series of resins with from 1 wt % to 5 wt % (0.1 mol % to 0.5 mol %) of **32** present. The presence of 1–5 wt % of the POSS-**32** macromer increased T_g in these DCPD resins (note it did not change the T_g in the aliphatic epoxy resins).[94b] However, the dependence of the resin's T_g on the weight percent of POSS-**32** present was complex.

The bending modulus increased as the loading of **32** was raised in these DCPD/**32** resins (at temperatures both below and above the T_g). The tanδ peak intensity was reduced while the peak width was substantially broadened. The T_g value of the DCPD resin (182.5°C) increased by 5.8°C to 188.3°C when only 1 wt % of **32** was added. The DCPD/5 wt % **32** resin exhibited a bending storage modulus at 10 Hz of 1.54 GPa at 40°C and 0.032 GPa at 240°C, which may be compared to those of the pure DCPD resin, which were 1.45 GPa and 0.027 GPa, respectively. Thus, despite the fact that the volume occupied by POSS would lower the DCPD resin's

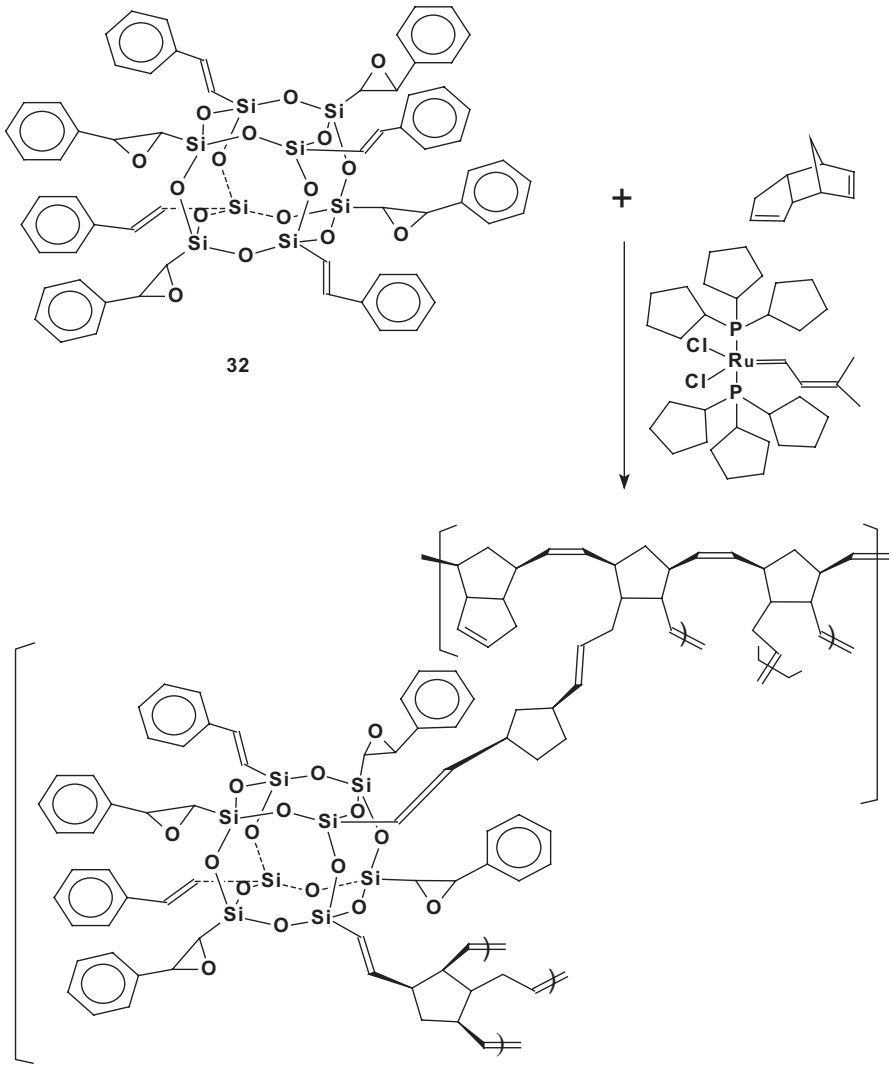

Figure 17 Copolymerization of polyfunctional POSS macromer **32** with dicyclopentadiene.

crosslink density, the storage modulus increased because POSS-**32** became chemically bound into the resin by forming more than one bond per POSS. POSS-**32** sites constitute new crosslinks (Fig. 17). All these data confirmed that POSS-**32** actually was, on average, bound into the resin by more than one chemical bond. Thus ROMP took place readily enough on the β-siloxy-substituted styrene function to multiply bond the cage into the resin.

The norbornenyl-functionalized partially opened, cage macromer **38** (Fig. 15, R = cyclopentyl) also was incorporated by ROMP into DCPD resins using the same

cure cycle (final stage 260°C, 1 h).[94a,d] From 0.4 mol % to 3.0 mol % of **38** was incorporated in this series. Residual **38** could not be extracted, despite a series of vigorous extractions by various solvents. This confirms that **38** is chemically bonded into the resin. However, **38** is only monofunctional and cannot serve as a cross-linking site. Since this monomer, like all the POSS systems, has a substantial volume, its incorporation will lower the cross-link density of the highly crosslinked DCPD resin that is generated by high-temperature curing. Indeed, this interpretation explains the lower T_g values of the POSS-**38**-containing DCPD resins versus that of the DCPD resin without POSS. The T_g values were 182.5°C for pure DCPD, 172.6°C for DCPD/5 wt % **38** and 171.1°C for DCPD/10 wt % **38**. Note that this effect is the opposite of adding between 1 wt % and 5 wt % of multifunctional POSS-**32** into DCPD resins, where it can create its own cross links. A DCPD resin with 15 wt % of POSS monomer **38** was cured via Grubbs-type ROMP and then thermally at a final temperature of 280°C for 2 h. The bending storage modulus of this resin exhibited a drop starting at 210°C (0.794 GPa) and bottoming out at 285°C (0.112 GPa). Thereafter, it rose to above 0.79 GPa at 325°C, possibly due to further crosslinking and other reactions at these high temperatures in the DMTA instrument. At such high temperatures the acidic-SiOH groups may catalyze cationic reactions in the resin.

Octanorbornyl-POSS, POSS-**33** (Fig. 15), was also incorporated into DCPD thermosetting resins.[94d] Due to the extremely limited solubility of POSS-**33** in DCPD of POSS-**33** in the resin raised the T_g by 15°C as determined by DMTA. This tiny amount of POSS addition also significantly raised the stiffness by almost 0.2 units of log E′ (Pa) at temperatures above the T_g. These were bending storage modulus values from DMTA. This behavior may be related to the fact that those norbornene groups attached to POSS metathesize readily. They probably tend to build a higher crosslink density in the DCPD/POSS-**33** resin and a very high crosslinking network emanating from the POSS cage, where up to eight linking points can bond with the resin matrix. This copolymerization is illustrated in Figure 18, where only three and four of the norbornene substituents on the POSS moieties have been represented, for the sake of clarity.

C. Styrene and Methyl Methacrylates Resins Containing POSS

Monofunctional styrylcyclopentyl POSS, **40**, at 0.4, 0.8, 1.4, and 3.2 mol % levels, was also incorporated into DCPD resins by ROMP (Fig. 19).[94d] At only 0.4 mol % POSS loading, a definite T_g increase from 182.5°C to 186.6°C was observed versus that of neat DCPD. However, as the POSS incorporation increased to 0.8 mol %, the nanocomposite exhibited an identical T_g to the corresponding neat DCPD resin. At higher POSS percentages (1.4 mol % and 3.2 mol %), the nanocomposites showed progressively lower T_g values (180.9°C and 173.7°C, respectively). The E′ values in the rubbery region dropped to much lower values than those of the neat DCPD resin (by 0.45 units of log E′ (Pa)). This indicates a crosslink density (per unit volume) in the monofunctional POSS nanocomposites with high amounts of POSS decreased. The free volume also probably increased.

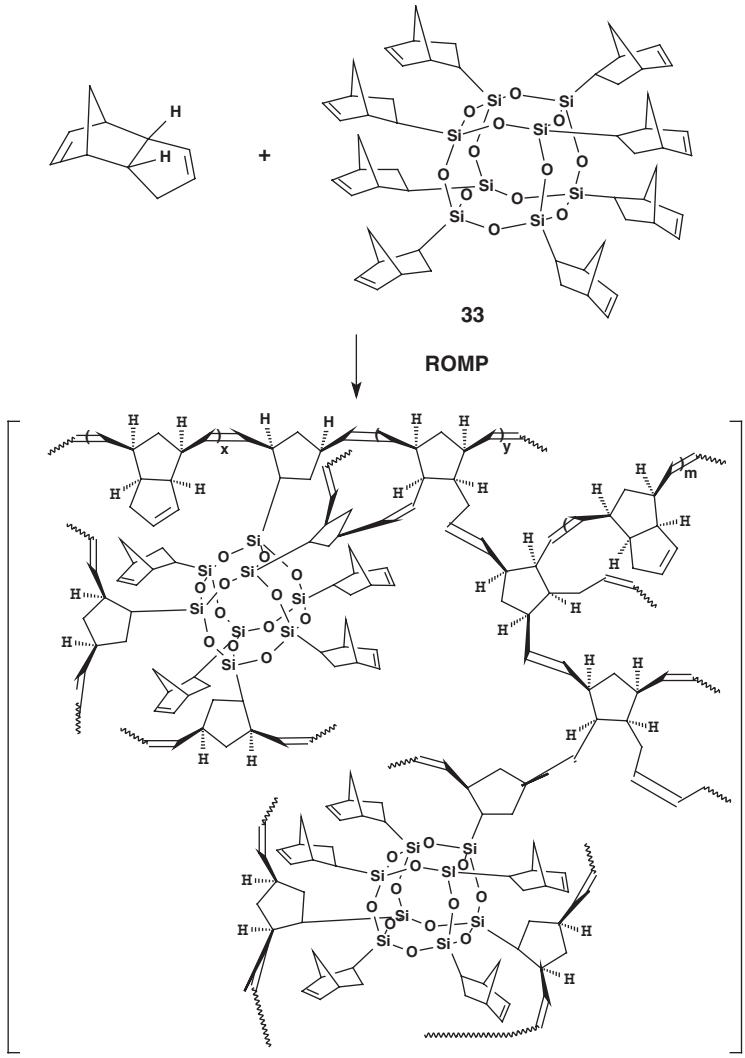

Figure 18 Synthesis of octanorbornyl POSS/DCPD nanocomposite.

The unfunctionalized POSS molecules, octaisobutyl-POSS, and dodecaphenyl-POSS (Fig. 1), T_8 and T_{12}, were blended into DCPD. No chemical bonds can form between these POSS units and the DCPD crosslinked network during curing. As the polymerization proceeds, phase-separated POSS particles are formed with size distributions in the 5–50 or 60 μm region. They appear to lower T_g, and stiffness is lost both above and below the glass-transition temperature. Perhaps this occurs because the volume they occupy does not provide any continuous bonding, so they act like inert filler particles without special adhesion to the resin.

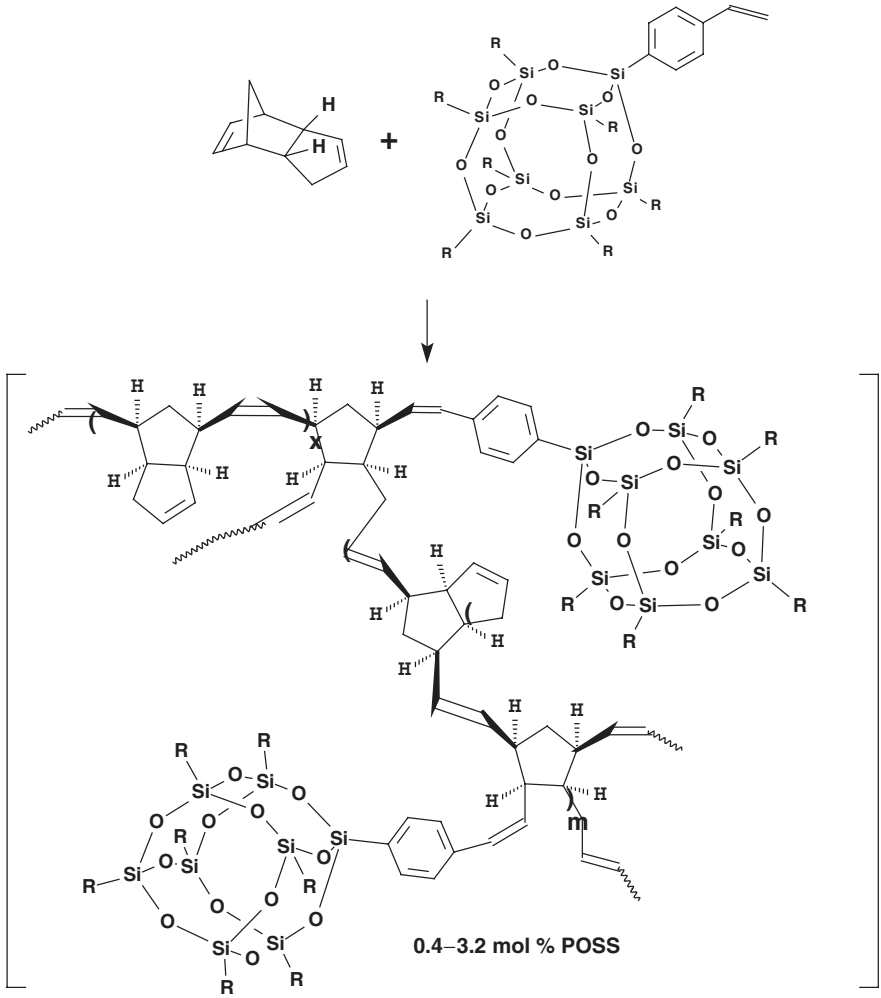

Figure 19 Synthesis of styrylcyclopentyl-POSS/DCPD resin nanocomposites.

Poly(styrene-co-divinyl benzene) thermosetting crosslinked systems are readily made with controlled cross-link densities by varying the amount of divinylbenzene (DVB) that is added. A matrix of poly(styrene-co-DVB) resins with varying densities, (0.3, 1, and 5 wt % DVB), containing styryl-POSS **40** were synthesized by radical initiated copolymerization by Pittman[94d] (Fig. 20). At each DVB level, styrylPOSS **40** was incorporated in 1, 5, 10, 15, and 20 wt % to give a total of 15 resins. At low cross-linking density (0.3 wt % DVB), all five of the POSS nanocomposites (with 1, 5, 10, 15, and 20 wt % POSS) exhibited progressively higher T_g values and E′ values, both above and below the T_g, than those of pure poly(styrene-co-DVB). Both T_g and E′ values increase with an increase of POSS content (Table 4).

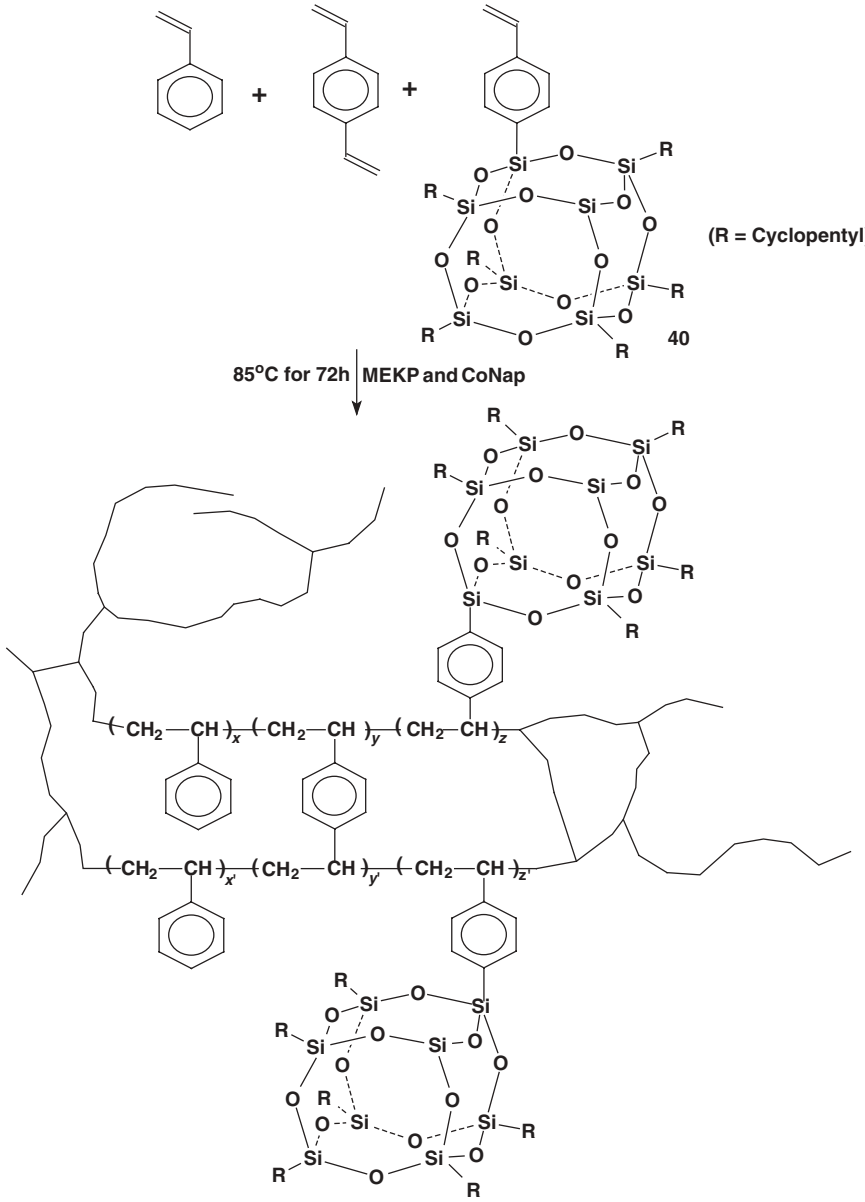

Figure 20 Synthesis of poly(styrene-co-vinylbenzene)/styryl-POSS **40** nanocomposites.

Table 4 The Effect of Incorporating Styryl-POSS (**40**) into Styrene-co-0.3% DVB Resins

Styryl-POSS **40** (wt %)	Bending Storage Moduli (E′)		Glass-Transition Temperature		Bending tanδ Peak Intensity, First Heating
	40°C (GPa)	125°C (MPa)	First Heating (°C)	Second Heating (°C)	
0	1.496	0.375	92.5	92.6	2.35
1	1.481	0.551	91.0	90.6	2.55
5	1.755	0.736	96.5	97.3	2.48
15	1.704	0.825	95.0	110.0	2.06
20	1.705	0.733	97.0	110.0	1.91

Upon raising the crosslink density to 1 wt % DVB, the addition of 5 wt % of styrylPOSS **40** also gave a slightly higher T_g values (96–97°C) and higher E′ values in the rubbery region (0.72 MPa) than those of neat poly(styrene-co-DVB) (0.48 MPa). However, at a much higher crosslink density (5 wt % DVB), the 5 wt % styrylPOSS nanocomposite exhibited a lower bending modulus above the T_g (3.65 MPa) than that of neat poly(styrene-co-5%DVB) (4.79 MPa). Examination of the entire matrix of 15 resin systems demonstrated that the influence exerted by monofunctional styrylPOSS **40** on properties of styrene/DVB networks depends on the crosslinking density present in the system.

Another example of crosslinked thermoset systems containing POSS, whose crosslinking density could also be controlled, are the acrylic systems of Pittman.[94d] Methyl methacrylates (MMA), 1,4-butane dimethacrylate (BDMA), and monofunctionalized methacrylyl heptaisobutyl-POSS (**39**) were terpolymerized, employing a MEK peroxide and a cobalt-catalyst-radical curing system at 88°C, followed by a 24-h postcure (Fig. 21). To compare the poly(MMA-co-BDMA)/POSS-**39** composites with PMMA/POSS composites, a set of P(MMA-co-MMA-POSS) copolymers was prepared without any crosslinking agent. These linear copolymers, with 5, 10, 15, 20, and 30 wt % POSS **39**, exhibited lower T_g values and E′ values in the rubbery region than PMMA. While PMMA had a T_g of 129.9°C, the T_g dropped steadily with an increase of POSS-**39** from 127.7°C with 5 wt % **39** to 121.4°C with 30 wt % **39**. Similarly, in the terpolymer resins with low cross-link densities (1, 5, and 10 wt % BDMA), the P(MMA-co-BDMA)/MMA-POSS **39** nanocomposites also exhibited lower T_g values and E′ values than those of the corresponding P(MMA-co-BDMA) resin containing no POSS. For example, the E′ values at 40°C and 180°C dropped from 1.573 GPa and 1.599 MPa, respectively, in P(MMA-co-1 wt % BDMA) to 1.136 GPa and 0.920 MPa, respectively, in P(MMA-co-1 wt % BDMA-co-20 wt % POSS-**39**).

The T_g values dropped from 132.2°C to 123.7°C in the 1 wt % BDMA crosslink methacrylate resins as the weight percent of POSS-**39** went from 0 wt % to 20 wt %. The densities of these resins also dropped as the POSS-**39** content went up. For example, P(MMA-co-5% BDMA) has $\rho = 1.188$ g/cc. This drops to 1.176 g/cc

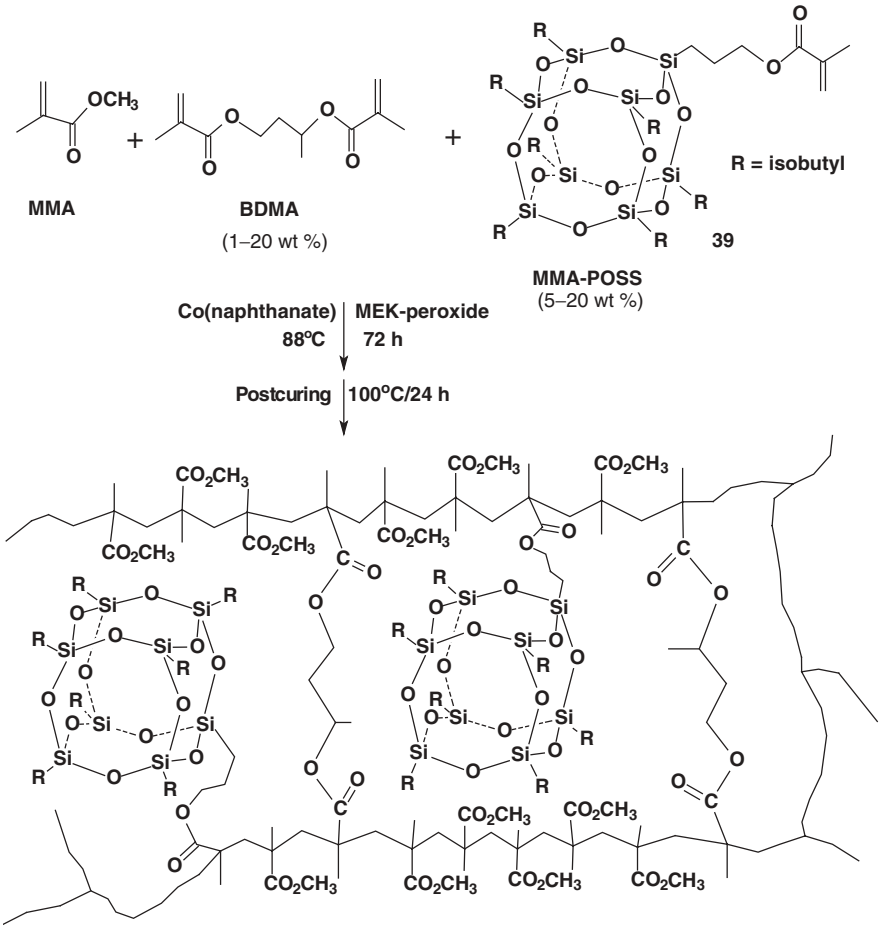

Figure 21 Synthesis of poly(MMA-co-BDMA)/MA-POSS **39** nanocomposites.

when 20 wt % POSS-**39** is present, indicating more free volume might be produced by inclusion of monofunctional POSS-**39** into the crosslinking network. However, at high crosslinking density (20 wt% BDMA), the P(MMA-co-BDMA-co-POSS-**39**) nanocomposites exhibited slightly higher T_g values as 5, 10, 15 and 20 wt % POSS was incorporated. The E′ values at 180°C in the rubbery region are slightly less (10.73–11.67 MPa) than those of P(MMA-co-BDMA) (11.99 MPa). Clearly, the influence of chemically incorporating monofunctional POSS-**39** into the thermoset crosslinked network on the resins' properties depends on the crosslink density.

Li and Pittman copolymerized POSS-**32** with styrene using a MEK peroxide/cobalt napthanate radical initiator system.[94] Swellable crosslinked gels were obtained at POSS-**32** of 0.44 mol % and 0.88 mol %. No POSS-**32** could be extracted from these systems. Therefore, all the POSS-**32** originally charged to the reaction

was chemically bound within the gel. Swelling ratios of 4.5 to 6.8 were observed in THF. The only possible site of cross-linking is the POSS-**32** monomer, so it was the crosslinking agent that caused gel formation, confirming that **32** could participate in radical polymerizations.

Overall it is becoming apparent that POSS incorporation into linear polymers or network resins in most cases can lead to nanocomposites with good thermal, mechanical, and fire-retardant properties. As a variety of POSS-containing monomers with functionalized substituents are synthesized, more nanocomposites will be developed. Furthermore, this technology will be used to modify the matrix resins used for glass or carbon fiber composites. A reduction in the cost of POSS derivatives is key to the further development of applications in this area.

V. OTHER APPLICATIONS

Besides the applications in nano-reinforced polymeric materials, there are other applications for POSS molecules. Hong et al.[95a] reported the use of a phosphine-substituted POSS, $Si_8O_{12}(CH_2CH_2PPh_2)_8$ as a core for building new types of dendritic macromolecules. A new metallodendrimer containing this octakis(diphenylphosphino)-functionalized silsesquioxane core and ruthenium(II)-based chromophores has been synthesized.[95b] Dendrimers based on a POSS core with 16 PPh_2 arms have been used as ligands for rhodium complexes, which were used to catalyze hydroformylation.[96a] These complexes gave much higher linear to branched selectivities (14:1) than their small molecular analogs (3–4:1) in the hydroformylation of oct-1-ene to 1-nonanal.[96] In addition, incompletely condensed POSS cages have been used to synthesize metal-containing, closed-cage polyhedral silsesquioxanes for use as silica-supported metal catalysts. Example gallium-containing cage silsesquioxanes **41a** and **41b**[97] and an aluminosilsesquioxane **42**[98,99] are shown in Figure 22. Additional metal-containing polyhedral silsesquioxane examples include Mg-silsesquioxane,[99] lanthanide silsesquioxane,[100] zirconium and hafnium silsesquioxane complexes,[101] and titanium-silsesquioxane.[102,103] In 2000 Lorenz et al.[104a] reviewed all the available literature on polyhedral metallasilsesquioxanes of the early transition metals and f-elements. In 1996 Murugavel et al.[104b] comprehensively reviewed all research up to that time on heterosiloxanes and metallasiloxanes derived from silanediols, disilanoles, silanetriols, and trisilanols. The discussion of hybrid organic–inorganic polymers and resins presented in a recent review emphasizes that POSS systems can be used as reagents in making improved polymers, resins, and composites for a wide range of applications.[104c] Previous reviews of various aspects of POSS polymers and nanocomposites were published by Lichtenhan et al.[49,62b,104d]

More recent applications of POSS derivatives had been developed. These applications include diffusion permeable membranes,[105a] novel electrolytes for lithium batteries,[105b] ion mobility, gas-phase conformational analysis,[105c] insertion of N_2 and O_2 into T_n ($n = 8$, 10, 12) POSS framework,[105d] surface coating,[105c] low-k dielectric films,[105f] and self-assembled films.[105g,h]

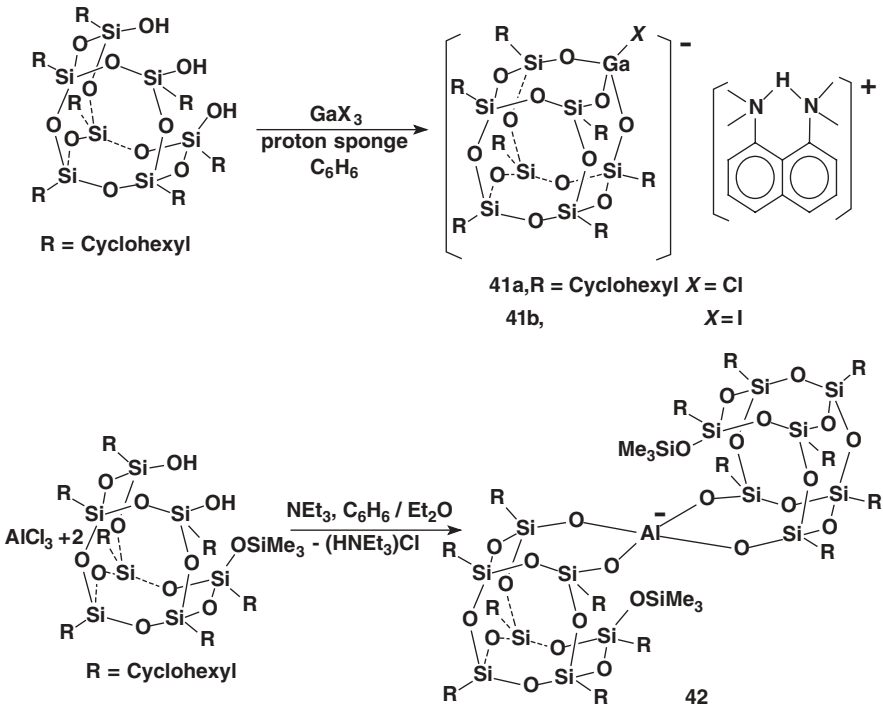

Figure 22 Synthesis of a galliumsilsesquioxane and an aluminosilsesquioxane.

Laine and coworkers[106] recently reported rediscovering the nitration of octaphenyl POSS-**43** which was first reported in 1961 by Olsson and coworkers.[107] This is exciting because Laine then successfully produced the octaaminophenyl POSS-**44** by Pd/C-catalyzed hydrogenation of **43** (Fig. 23). A green-light-emitting derivative, **45**, was obtained by Schiffs base formation upon reaction of **43** with the *ortho*-carboxaldehyde of pyridine.[106] Furthermore, the octaamino POSS-**44** was used with dianhydrides to make extremely thermally resistant polyimide cross-linked networks, **46**. These polyimides exhibited 5% mass loss temperatures in excess of 500°C.[106,108] POSS-**44** was also reacted with maleic anhydride to make the octa-*N*-phenylmaleimide, **47**,[106] which could serve as a cross-linking agent in maleimide polymer chemistry. Certainly, many exciting developments are under way in this topic. One can imagine future nanostructured materials of great variety being developed. One thought is to couple polyoxymetalate chemistry[109] with both POSS chemistry and organic chemistry to build regular three-dimensional repeating structures of POSS and polyoxymetalates or to construct polymer networks with both POSS and polyoxymetalate nanophases. Finally, one might use octafunctional POSS derivatives, like **44**, to build core-shell dendrimeric material structures.

Laine and coworkers have studied a new class of nanocomposites containing multifunctional epoxy-POSS, octakis(glycidyldimethylsiloxy)octasilsesquioxane

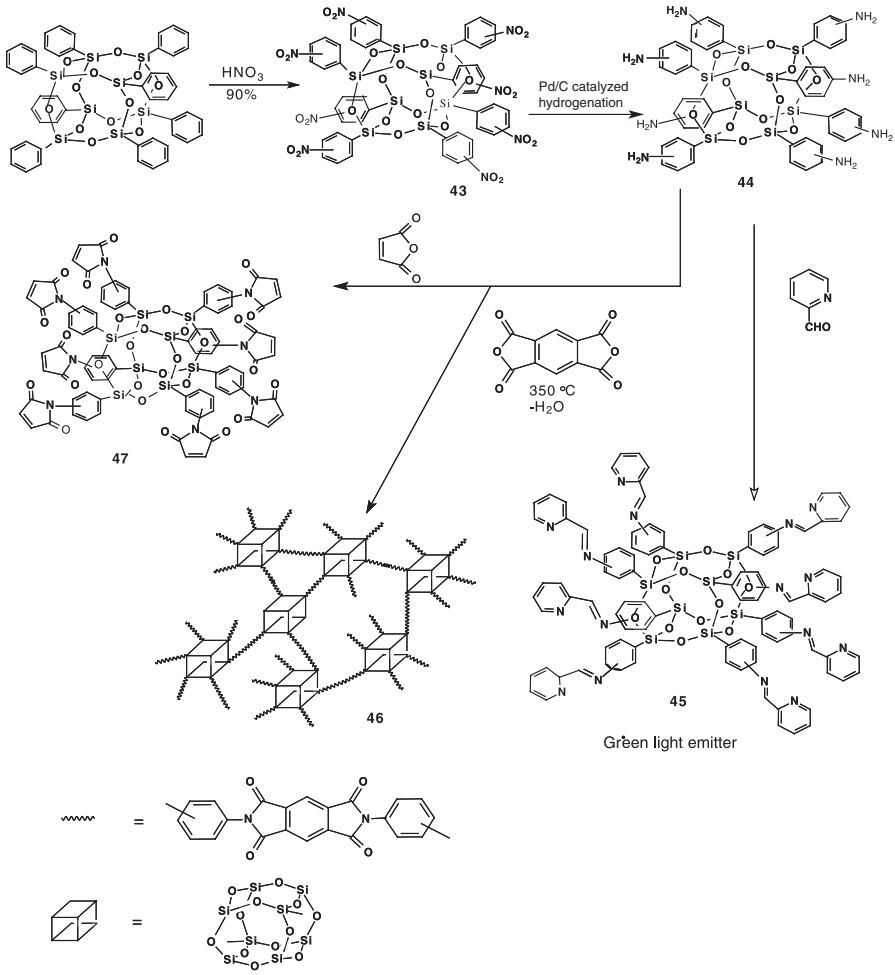

Figure 23 Preparation of octa-aminophenyl POSS, **43**, and applications.

glydicylMe$_2$SiOSiO$_{1.5}$)$_8$] (OG) or octaethylcyclohexenyl-epoxide octasilsesquioxane (OC).[110,111] Diaminodiphenyl methane (DDM) was used as the curing agent for these two systems. A commercial epoxy resin based on the diglycidyl ether of bisphenol A (DGEBA) was used as a reference material throughout these studies. For OG/DDM nanocomposites and commercial DGEBA/DDM composites, dynamic mechanical analysis and model reaction studies suggest that the maximum crosslink density is obtained at N = 0.5 (NH_2:epoxy groups = 0.5), whereas the mechanical properties are maximized at N = 1.0. The temperatures for 5% mass loss of OG/DDM and DGEBA/DDM composites at N = 1 are 344°C and 338°C, respectively, indicating that thermal stability of the POSS nanocomposite is slightly better than that of the commercial epoxy resin. However, the T_g of OG/DDM

nanocomposite at N = 1 is about 60°C and lower than that of the DGEBA/DDM composite at N = 1 (~110°C). These T_g values may reflect the fact that the NH and OH groups in the DEGBA/DDM composite at N = 1 are free to hydrogen bond with each other but are constrained from close approach in the rigid tethers of OG/DDM nanocomposite. Moreover, the glass transition is barely noticeable for OG/DDM composite at N = 0.5, suggesting that the OG/DDM composite at this formulation is much more highly crosslinked, such that the main chains are bound by crosslinks and their relaxation motion is hindered significantly. Tensile strength values of OC/DDM composites at N = 0.5 and N = 1 are higher than those of OG/DDM nanocomposites but are still slightly lower than those of the commercial DEGBA/DDM composites. Furthermore, the fracture toughness of the two POSS nanocomposites, OC/DDM and OG/DDM at N = 0.5 and 1, are worse than that of the commercial DEGBA/DDM composites. Therefore, the POSS nanocomposite in some cases showed poorer mechanical properties than that of the commercial thermosetting system.

In addition, some new copolymers containing bis(amino)-functionalized POSS and oxazoline-functionalized POSS were synthesized by Wright et al.[112] and Kim et al.,[113] respectively. Some new nanocomposites of POSS blending with PP,[114] PC,[115] PE,[116] and PET[117] have been developed by the Edwards AFB group and Ikeda's group.

VI. SUMMARY

This chapter describes the synthesis and properties of homopolymers, copolymers, and crosslinked resin nanocomposites containing inorganic–organic hybrid polyhedral oligomeric silsesquioxane (POSS) structures. Monomers such as styryl-POSS, methacrylate-POSS, norbornyl-POSS, vinyl-POSS, epoxy-POSS, and siloxane-POSS are included. Both monofunctional and multifunctional POSS macromers are discussed. Thermoplastic and thermoset systems are considered. Thermal, rheological, and dynamic mechanical properties are described. The synthesis of some POSS-macromers (monomers) is briefly described. POSS chemicals have been used to prepare nano-size designed novel composites with a variety of potential applications. This chapter is descriptive and not meant to be comprehensive. However, the major existing reviews of certain subtopics are noted, allowing the reader to gain a general introduction while providing the information to permit more comprehensive coverage.

VII. ACKNOWLEDGMENTS

This work was supported by Grant F49620-02-1-0260 from the Air Force Office of Scientific Research and an Air Force Office of scientific Research STTR

Contract No. F49620-02-C-0086. Also we thank the National Science Foundation EPSCoR Program Grant No. EPS-0132618.

VIII. REFERENCES

1. R. H. Baney, M. Itoh, A. Sakakibara, T. Suzuki, *Chem. Rev.* **95**, 1409 (1995).
2. D. W. Scott, *J. Am. Chem. Soc.* **68**, 356 (1946).
3. J. F. Brown Jr., J. H. Vogt Jr., A. Katchman, J. W. Eustance, K. W. Kiser, K. W. Krantz, *J. Am. Chem. Soc.* **82**, 6194 (1960).
4. H. Adachi, E. Adachi, O. Hayashi, K. Okahashi, *Rep. Prog. Polym. Phys. Jpn.* **28**, 261 (1985).
5. H. Hata, S. Komasaki, *Jpn. Patent* Kokai-S-59-108033 (1984).
6. X. Zhang, L. Shi, *Chin. J. Polym. Sci.* **5**, 197 (1987).
7. G. Z. Li, M. L. Ye, L. H. Shi, *Chin. J. Polym. Sci.* **12**, 331 (1994).
8. G. Z. Li, M. L. Ye, L. H. Shi, *Chin. J. Polym. Sci.* **14**, 41 (1996).
9. G. Z. Li, T. Yamamoto, K. Nozaki, M. Hikosaka, *Polymer* **41**, 2827 (2000).
10. G. Z. Li, T. Yamamoto, K. Nozaki, M. Hikosaka, *Macromol. Chem. Phys.* **201**, 1283 (2000).
11. J. F. Brown Jr., *J. Polym. Sci. C*, **1**, 83 (1963).
12. X. Zhang, L. Shi, S. Li, Y. Lin, *Polym. Degrd. Stab.* **20**, 157 (1988).
13. T. Suminoe, Y. Matsumura, O. Tomomitsu, *Jpn. Patent* Kokoku-S-60-17214 (1985).
14. Y. Matsumura, I. Nozue, O. Tomomitsu, T. Ukachi, T. Suminoe, U.S. Patent 4399266 (1983).
15. S. Fukuyama, Y. Yoneda, M. Miyagawa, K. Nishii, A. Matsuura, *Eur. Patent* 0406911A1 (1985).
16. Z. Xie, Z. He, D. Dai, R. Zhang, *Chin. J. Polym. Sci.* **7**, 183 (1989).
17. G. E. Maciel, M. J. Sullivan, D. W. Sindorf, *Macromolecules* **14**, 1607 (1981).
18. G. Engelhavdt, H. Jancke, E. Lippmaa, A. Samoson, *J. Organomet. Chem.* **210**, 295 (1981).
19. H. Adachi, E. Adachi, O. Hayashi, K. Okahashi, *Rep. Prog. Polym. Phys. Jpn.* **29**, 257 (1986).
20. C. L. Frye, W. T. Collins, *J. Am. Chem. Soc.*, **92**, 5586 (1970).
21. V. Belot, R. Corriu, D. Leclerq, P. H. Mutin, A. Vioux, *Chem. Mater*. **3**, 127 (1991).
22. A. S. Gozdz, *Polym. Adv. Technol.* **5**, 70 (1994).
23. Y. Yoneda, T. Kitamura, J. Naito, T. Kitakohji, *Jpn. Patent* Kokai-S-57-168246 (1982).
24. Y. Yoneda, S. Takeda, T. Kitamura, M. Nakajina, T. Kitakohiji, *Jpn. Patent* Kokai-S-57-168247 (1982).
25. S. Uchimura, M. Sato, D. Makino, *Jpn. Patent* Kokai-S-58-96654 (1983).
26. H. Adachi, O. Hayashi, K. Okahashi, *Jpn. Patent* Kokoku-H-2-15863 (1990).
27. H. Adachi, O. Hayashi, K. Okahashi, *Jpn. Patent* Kokai-S-60-108841 (1985).
28. H. Adachi, E. Adachi, O. Hayashi, K. Okahashi, *Jpn. Patent* Kokoku-H-4-56975 (1992).
29. (a) H. Adachi, E. Adachi, Y. Aiba, O. Hayashi, *Jpn. Patent* Kokai-H-2-222537 (1990); (b) *U.S. Patent* 5087553 (1990).
30. F. Shoji, K. Takemoto, R. Sudo, T. Watanabe, *Jpn. Patent* Kokai-S-55-111148 (1980).
31. E. Adachi, Y. Aiba, H. Adachi, *Jpn. Patent* Kokai-H-2-277255 (1990).
32. Y. Aiba, E. Adachi, H. Adachi, *Jpn. Patent* Kokai-H-3-6845 (1991).
33. E. Adachi, H. Adachi, O. Hayashi, K. Okahashi, *Jpn. Patent* Kokai-H-1-185924 (1989).
34. Y. Hayashide, A. Ishii, H. Adachi, E. Adachi, *Jpn. Patent* Kokai-H-5-102315 (1993).
35. E.Adachi, H. Adachi, H. Kanegae, H. Mochizuki, *Ger. Patent* 4202290 (1992).
36. F. Shoji, R. Sudo, T. Watanabe, *Jpn. Patent* Kokai-S-56-146120 (1981).

37. K. Azuma, Y. Shindo, S. Ishimura, *Jpn. Patent* Kokai-S-57-56820 (1982).
38. E. Imai, H. Takeno, *Jpn. Patent* Kokai-S-59-129939 (1984).
39. M. Yanagisawa, *Jpn. Patent* Kokai-S-62-89228 (1987).
40. T. Mishima, H. Nishimoto, *Jpn. Patent* Kokai-H-4-247406 (1992).
41. T. Mishima, H. Nishimoto, *Jpn. Patent* Kokai-H-4-271306 (1992).
42. Y. Saito, M. Tsuchiya, Y. Itoh, *Jpn. Patent* Kokai-S-58-14928 (1983).
43. Y. Mi, S. A. Stern, *J. Polym. Sci. B. Polym. Phys.* **29**, 389 (1991).
44. T. Mine, S. Komasaki, *Jpn. Patent* Kokai-S-60-210570 (1985).
45. T. Mine, S. Komasaki, *Jpn. Patent* Kokai-S-60-210569 (1985).
46. M. Tsutsui, S. Kato, *Jpn. Patent* Kokoku-S-63-20210 (1988).
47. (a) J. D. Lichtenhan, J. J. Schwab, F. J. Feher, D. Soulivong, *U.S. Patent* 5942638 (1999); (b) J. D. Lichtenhan, J. J. Schwab, Y. An, W. Reinerth, F. J. Feher, U.S. Patent Application No. Wo 2000-US34873 (2000); (c) B.W. Manson, J. J. Morrison, P. I. Coupar, P. Jaffres, R. E. Morris, *J. Chem. Soc. Dalton Trans.* **7**, 1123 (2001); (d) J. D. Lichtenhan, J. J. Schwab, W. Reinerth, M. J. Carr, Y. An, F. J. Feher, R. Terroba, U.S. Patent, Aplication No. Wo 2000-US21455 (2000); (e) J. D. Lichtenhan, F. J. Feher, D. Soulivong, U.S. Patent, 6100417 (2000); (f) L. Hu, Y. Sun, S. Zhao, Z. Liu, *Polym. Prepr. Am. Chem. Soc. Div. Polym. Chem.* **43**, 1114 (2002); (g) E. G. Shockey, A. G. Bolf, P. F. Jones, J. J. Schwab, K. P. Chaffee, T. S. Haddad, J. D. Lichtenhan, *Appl. Organometal. Chem.* **13**, 311 (1999).
48. J. D. Lichtenhan, J. J. Schwab, W. A. Reinerth Sr., *Chem. Innovation* **1**, 3 (2001).
49. J. D. Lichtenhan, *Comments Inorg. Chem.* **17**, 115 (1995).
50. A. Voigt, *Orgametrallics* **15**, 5097 (1996).
51. F. J. Feher, K. J. Weller, *Inorgan. Chem.* **30**, 880 (1991).
52. M. W. Ellsworth, D. L. Gin, *Polym. News* **24**, 331 (1999).
53. T. S. Haddad, R. Stapleton, H. G. Jeon, P. T. Mather, J. D. Lichtenhan, S. Phillips, *Polym. Prepr. AM. Chem. Soc. Div. Polym. Chem.* **40**, 496 (1999).
54. M. G. Voronkov, V. I. Lavrent'yev, *Topics Curr. Chem.* **102**, 199 (1982).
55. F. J. Feher, R. Terroba, R. Jin, K. O. Wyndham, S. Lucke, R. Brutchey, F. Nguyen, *Polym. Mater. Sci. Eng.* **82**, 301 (2000).
56. M. M. Sprung, F. O. Guenther, *J. Am. Chem. Soc.* **77**, 3990 (1955).
57. M. M. Sprung, F. O. Guenther, *J. Am. Chem. Soc.* **77**, 3996 (1955).
58. J. F. Brown Jr., *J. Am. Chem. Soc.* **87**, 4317 (1965).
59. F. J. Fesh, D. A. Newman, J. F. Walzer, *J. Am. Chem. Soc.* **111**, 1741 (1989).
60. J. D. Lichtenhan, N. Q. Vu, J. A. Carter, J. W. Gilman, F. J. Feher, *Macromolecules* **26**, 2141 (1993).
61. T. S. Haddad, H. W. Oviatt, J. J. Schwab, P. T. Mather, K. P. Chaffee, J. D. Lichtenhan, *Polym. Prepr. Am. Chem. Soc. Div. Polym. Chem.* **39**, 611 (1998).
62. (a) J. D. Lichtenhan, Y. A. Otonari, M. J. Carr, *Macromolecules* **28**, 8435 (1995); (b) J. J. Schwab, J. D. Lichtenhan, *Appl. Organometal. Chem.* **12**, 707 (1998); (c) J. Xiao, F. J. Feher, *Polym. Mater. Sci. Eng.* **86**, 171 (2002).
63. J. W. Gilman, D. S. Schlitzer, J. D. Lichtenhan, *J. Appl. Ploym. Sci.* **60**, 591 (1996).
64. J. D. Lichtenhan, *in Polymeric Materials Encyclopedia*, vol. 10, J. C. Salamone, ed., CRC Press, New York, 1996.
65. F. J. Feher, K. J. Weller, *Organometallics* **9**, 2638 (1990).
66. R. Muller, R. Khole, S. Sliwinski, *J. Pract. Chem.* **9**, 71 (1959).
67. A. J. Barry, *J. Am. Chem. Soc.* **77**, 4248 (1955).
68. M. M. Sprung, F. O. Guenther, *J. Am. Chem. Soc.* **77**, 6045 (1955).
69. L. H. Vogt, J. F. Brown, *Inorg. Chem.* **2**, 189 (1963).

70. M. G. Voronkov, V. I. Lavrent'yev, V. M. Kovrigin, *J. Organometal Chem.* **220**, 285 (1981).
71. J. F. Brown, L. H. Vogt, *J. Am. Chem. Soc.* **87**, 4313 (1965).
72. M. G. Voronkov, *Zh. Obshch. Khim.* **49**, 1522 (1979).
73. M. M. Sprung, F. O. Guenther, *J. Polym. Sci.* **28**, 17 (1958).
74. J. F. Brown, L. H. Vogt, P. I. Prescott, *J. Am. Chem. Soc.* **86**, 1120 (1964).
75. (a) C. Zhang, R. M. Laine, *J. Am. Chem. Soc.* **122**, 6979 (2000); (b) M. C. Gravel, C. Zhang, M. Dinderman, R. M. Laine, *Appl. Organometal. Chem.* **13**, 329 (1999); (c) D. Neumann, M. Fisher, L. Tran, J. G. Matisons, *J. Am. Chem. Soc.* **124**, 13998 (2002); (d) F. J. Feher, K. D. Wyndham, *Chem. Commun.* 323 (1998).
76. A. Sellinger, R. M. Laine, *Macromolecules* **29**, 2327 (1996).
77. A. Sellinger, R. M. Laine, *Chem. Mater.* **8**(8), 1592 (1996).
78. I. Hasegawa, *J. Sol-Gel Sci. Technol.* **1**, 57 (1993).
79. I. Hasegawa, D. Motojima, *J. Organomt. Chem.* **441**, 373 (1992).
80. D. P. Fasce, R. J. J. Williams, F. Mechin, J. P. Pascault, M. F. Llauro, R. Petiaud, *Macromolecules* **32**, 4757 (1999).
81. (a). T. S. Haddad, J. D. Lichtenhan, *Macromolecules* **29**, 7302 (1996); (b). A. Romo-Uribe, P. T. Mather, T. S. Haddad, J. D. Lichtenhan, *J. Polym. Sci. B. Polym. Phys.* **36**, 1857 (1998).
82. (a) T. S. Haddad, B. D. Viers, S. H. Phillips, *J. Inorgan. Organomet. Polym.* **11**, 155 (2001); (b) L. Zheng, R. M. Kasi, R. J. Farris, E. B. Coughlin, *J. Polym. Sci. A. Polym. Chem.* **40**, 885 (2002); (c) H. Xu, S. Kuo, J. Lee, F. Chang, *Macromolecules* **35**, 8788 (2002); (d) H. Xu, S. Kuo, J. Lee, F. Chang, *Polymer* **43**, 5117 (2002); (e) H. Xu, S. Kuo, F. Chang, *Polym. Bull.* **48**, 469 (2002); (f) R. L. Blanski, S. H. Phillips, K. Chaffee, J. Lichtenhan, A. Lee, H. Geng, *Matter. Res. Soc. Symp. Proc.* 628 (2001).
83. (a) J. Pyun, K. Matyjaszewski, *Macromolecules* **33**, 217 (2000); (b) K. M. Kim, Y. Chujo, *J. Polym. Sci. A. Polym. Chem.* **39**, 4035 (2001); (c) W. Zhang, B. X. Fu, Y. Seo, E. Schrag, B. Hsiao, P. Mather, N. Yang, D. Xu, H. Ade, M. Rafailovich, J. Sokolov, *Macromoleclues* **35**, 8029 (2002); (d) W. Jia, U.S. Patent, Application No. US2002-136031 (2002); (e) F. Gao, Y. Tong, S. R. Schricker, B. M. Culbertson, *Polym. Advan. Technol.* **12**, 355 (2001); (f) H. Wu, Y. Hu, K. E. Gonsalves, M. J. Yacaman, J. *Vacuum Sci. Technol. B Microelectron. Nanometer Struct.* **19**, 851 (2001); (g) K. E. Gonsalves, J. Wang, H. Wu, J. *Vacuum Sci. Technol. B Microelecton. Nanometer Struct*. **18**, 325 (2001).
84. P. T. Mather, H. G. Jeon, A. Romo-Uribe, *Macromolecules* **32**, 1194 (1999).
85. (a) B. K. Bharadwaj, R. J. Berry, B. L. Farmer, *Polymer* **41**, 7209 (2000); (b) H. G. Jeon, P. T. Mather, T. S. Haddad, *Polym. Int*. **49**, 453 (2000).
86. (a) E. B. Coughlin, paper presented at the POSS^{TM} Nanotechnology Conference, Huntington Beach, CA, Sept. 25–27, 2002; (b) L. Zheng, R. J. Farris, E. B. Coughlin, *Macromolecules* **34**, 8034 (2001); (c) L. Zheng, A. J. Waddon, R. J. Farris, E. B. Coughlin, *Macromolecules* **35**, 2375 (2002); (d) L. Zheng, R. J. Farris, E. B. Coughlin, *J. Polym. Sci. A. Polym. Chem.* **39**, 2920 (2001); (e) E. B. Coughlin, *Polym. Prepr. Am. Chem. Soc. Div. Polym. Chem.* **43**, 368 (2002); (f) A. J. Waddon, L. Zheng, R. J. Farris, E. B. Coughlin, *Nanoletters* **2**, 1149 (2002); (g) L. Zheng, R. J. Farris, E. B. Coughlin, *Polym. Preprin. Am. Chem. Soc. Div. Polym. Chem.* **42**, 885 (2001).
87. A. Tsuchida, C. Bolln, F. G. Sernetz, H. Frey, R. Mulhaupt, *Macromolecules* **30**, 2818 (1997).
88. (a) R. A. Mantz, P. F. Jones, K. P. Chaffee, J. D. Lichtenhan, J. W. Gilman, I. M. K. Ismail, M. J. Burmeister, *Chem. Mater*. **8**, 1250 (1996); (b) T. S. Haddad, A. Lee, S. H. Phillips, *Polym. Preprin. Am. Chem. Soc. Div. Polym. Chem.* **42**, 88 (2001).
89. (a) C. Zhang, F. Babonneau, C. Bonhomme, R. M. Laine, C. L. Soles, Hristo, A. F. Yee, *J. Am. Chem. Soc.* **120**, 8380 (1998); (b) J. J. Morrison, C. J. Love, B. W. Manson, I. J. Shannon, R. E. Morris, *J. Mater. Chem.* **12**, 3208 (2002); (c) Q. Liu, J. J. Schwab, J. D. Lichtenhan, D. Mason, A. Lee, *Polym. Mater. Sci. Eng.* **87**, 97 (2002); (d) A. Lee, paper presented at the POSS^{TM} Nanotechnology Conference, Huntington Beach, CA. Sept. 25–27, 2002.

90. J. J. Schwab, J. D. Lichtenhan, M. J. Carr, K. P. Chaffee, P. T. Mather, A. Romo-Uribe, *PMSE Prepr.* **77**, 549 (1997).

91. (a) B. X. Fu, B. S. Hsiao, S. Pagola, P. Stephens, *Polymer* **42**, 599 (2001); (b) B. X. Fu, W. Zhang, B. S. Hsiao, M. Rafailovich, J. Sokolov, G. Johansson, B. B. Sauer, S. Phillips, R. Balnski, *High Performance Polym.* **12**, 565 (2000); (c) B. S. Hsiao, X. Fu, P. T. Mather, K. P. Chaffee, H. Jeon, H. White, M. Rafailovich, J. D. Lichtenhan, J. Schwab, *Polym. Mater. Sci. Eng.* **79**, 389 (1998).

92. A. Lee, J. D. Lichtenhan, *Macromolecules* **31**, 4970 (1998).

93. A. Lee, J. D. Lichtenhan, W. A. Reinerth Sr., *Polym. Mater. Sci. Eng.* **82**, 235 (2000).

94. (a) C. U. Pittman Jr., L. Wang, H. Ni, G.Li, paper presented at the AFOSP Polymer Matrix Composites Contractor"s Review Meeting, Long Beach, CA, May 11–12, 2001; (b) G. Z. Li, L. Wang, H. Toghiani, T. L. Daulton, K. Koyama, C. U. Pittman Jr., *Macromolecules* **34**, 8686 (2001); (c) G. Z. Li, L. Wang, H. Toghiani, T. L. Daulton, C. U. Pittman Jr., *Polymer* **43**, 4167 (2002); (d) C. U. Pittman Jr., paper presented at the POSS^{TM} Nanotechnology Conference, Huntington Beach, CA, Sept. 25–27, 2002; (e) H. Ni, MS thesis, Mississippi State University, 2001; (f) K.-W. Liang, PhD Dissertation, Mississippi State University, 2005; (g) C. U. Pittman, Jr., G. Z. Li, and H. Ni, *Macromolecular Symposia,* **196,** 301 (2003); (h) C. U. Pittman, Jr., G. Z. Li, H. Toghiani, H.-S. Cho, and K. Liang, papers submitted for publication or in preparation.

95. (a) B. Hong, T. P. S. Thoms, H. J. Murfee, M. J. Lebrum, *Inorg. Chem*. **36**, 6146 (1997); (b) H. J. Murfee, T. P. S. Thoms, J. Greaves, B. Hong, *Inorg. Chem*. **39**, 5209 (2000).

96. (a) L. Ropartz, R. E. Morris, D. J. Cole-Hamilton, D. F. Foster, *Chem. Commun.* **4**, 361 (2001); (b) L. Ropartz, K. J. Haxton, D. F. Foster, R. E. Morris, A. M. Z. Slawin, D. J. Cole-Hamilton, *J. Chem. Soc. Dalton Trans.* **23**, 4323 (2002); (c) L. Ropartz, D. F. Foster, R. E. Morris, A. M. Z. Slawin, D. J. Cole-Hamilton, *J. Chem. Soc. Dalton Trans.* **9**, 1997 (2002).

97. F. J. Feher, T. A. Budzichowski, J. W. Ziller, *Inorg. Chem*. **36**, 4082 (1997).

98. F. T. Edelmann, Y. K. Gun'ko, S. Giessmann, F. Olbrich, K. Jacob, *Inorg. Chem*. **38**, 210 (1999).

99. L. Ukrainczyk, R. A. Bellman, A. B. Anderson, *J. Phys. Chem. B.* **101**, 531 (1997).

100. J. Annand, H. C. Aspinall, A. Steiner, *Inorg. Chem*. **38**, 3941 (1999).

101. R. Duchateau, H. C. L. Abbenhuis, R. A. Van Santen, A. Meetsma, S. K. H. Thiele, M. F. H. Van Tol, *Organometallics* **17**, 5663 (1998).

102. R. Duchateau, H. C. L. Abbenhuis, R. A. Van Santen, A. Meetsma, S. K. H. Thiele, M. F. H. Van Tol, *Organometallics* **17**, 5222 (1998).

103. (a) R. Duchateau, U. Cremer, R. J. Harmsen, S. I. Mohamud, H. C. L. Abbenhuis, R. A. Van Santen, A. Meetsma, S. K. H. Thiele, M. F. H. Van Tol, M. Kranenburg, *Organometallics* **18**, 5447 (1999); (b) T. Kudo, M. S. Gordon, *J. Phys. Chem. A* **105**, 11276 (2001).

104. (a) V. Lorenz, A. Fischer, S. Gießmann, J. W. Gilje, Y. Gun'ko, K. Jacob, F. T. Edelmann, *Coordination Chem. Rev.* **206–207**, 321 (2000); (b) R. Murugavel, A. Voigt, M. G. Walawalkar, H. W. Roesky, *Chem. Rev*. **96**, 2205 (1996); (c) G. Li, L. Wang, H. Ni, C. U. Pittman Jr., *J. Inorg. Organ. Polym.* **11**, 123 (2001); (d) J. D. Lichtenhan, T. S. Haddad, J. J. Schwab, M. J. Carr, K. P. Chaffee, P. T. Mather, *Polym. Prepr. Am. Chem. Soc. Div. Polym. Chem.* **39**, 489 (1998).

105. (a) A. Strachota, G. Tishchenko, L. Matejka, M. Bleha, *J. Inorgan. Organ. Polym.* **11**, 165 (2001); (b) S. L. Wunder, paper presented at the POSS^{TM} Nanotechnology Conference, Huntington Beach, CA, Sept. 25–27, 2002; (c) J. Gidden, P. R. Kemper, E. Shammel, D. P. Fee, S. Anderson, M. T. Bowers, *Int. J. Mass Spectrom.* **222**, 63 (2003); (d) B. Tejerina, M. S. Gordon, *J. Phys. Chem. B* **106**, 11764 (2002); (e) B. D. Viers, A. Esker, K. Farmer, *Polym. Preprin. Am. Chem. Soc. Div. Polym. Chem.* **42**, 94 (2001); (f) R. A. Hogle, P. J. Helly, C. Ma, L. J. Miller, U.S. Patent, Application No. 2002-121270; (g) J. B. Carroll, B. L. Frankamp, V. M. Rotello, *Chem. Commun.* **17**, 1892 (2002); (h) E. Jeoung, J. B. Carroll, V. M. Rotello, *Chem. Commun.* **14**, 1510 (2002).

106. R. M. Laine, R. Tamaki, J. Choi, C. Brick, S.-G. Kim, paper presented at the ACS Organic/Inorganic Hybrid Materials Workshop, Sonoma, CA, Nov. 2001; (b) R. Tamaki, Y. Tanaka, R. Tanaki, R. M. Laine, *J. Am. Chem. Soc.* **123**, 124167 (2001).

107. K. Olsson, C. Granwall, *Arkiv. Kemi.* **17**, 529 (1961); K. Olsson, C. Axen, *Arkiv. Kemi.* **22**, 237 (1964).

108. R. Tamaki, R. M. Laine, unpublished data.

109. Special issue, *Chem. Rev.* **98** (1998), devoted to polyoxymetalate chemistry.

110. J. Choi, J. Harcup, A. F. Yee, Q. Zhu, R. M. Laine, *J. Am. Chem. Soc*. **123**, 11420 (2001).

111. R. M. Laine, paper presented at the POSS^{TM} Nanotechnology Conference, Huntington Beach, CA, Sept. 25–27, 2002.

112. M. E. Wright, D. A. Schorzman, F. J. Feher, R. Z. Jin, *Chem. Mater*. **15**, 264 (2003).

113. K. M. Kim, D. K. Keum, Y. Chujo, *Macromolecules* **36**, 867 (2003).

114. (a) B. X. Fu, L. Yang, R. H. Somani, S. X. Zong, B. S. Hsiao, S. Phillips, R. Blanski, P. Ruth, *J. Polym. Sci. B. Polym. Phys*. **39**, 2727 (2001); (b) J. J. Schwab, W. A. Reinerth, J. D. Lichtenhan, Y. An, S. H. Phillips, A. Lee, *Polym. Preprin. Am. Chem. Soc. Div. Polym. Chem.* **42**, 48 (2001).

115. H. Saito, M. Ikeda, *Jpn. Patent*, JP2002327062.

116. B. S. Hsiao, B. Chu, X. Fu, R. L. Blanski, S. H. Phillips, U.S. Patent, 2003018109.

117. T. Okada, M. Ikeda, *Jpn. Patent*, 2002322370.

CHAPTER 6

Silica- and Silsesquioxane-Containing Polymer Nanohybrids

Mohammad A. Wahab, Il Kim, and Chang-Sik Ha

Department of Polymer Science and Engineering, Pusan, Korea

CONTENTS

Macromolecules Containing Metal and Metal-Like Elements, Volume 4: Group IVA Polymers, edited by Alaa S. Abd-El-Aziz, Charles E. Carraher Jr., Charles U. Pittman Jr., and Martel Zeldin
ISBN: 0-471-68238-1

I. INTRODUCTION

The creation of inorganic–organic nanohybrid materials is growing into an important research area because of these materials' distinguished properties, which usually arise from a synergistic effect of the properties of their organic and inorganic components in the resulting composite materials.[1–6] The advanced properties are usually obtained by distributing nanometer-scale inorganic particles evenly within a polymer matrix. Among the several routes to synthesize these nanohybrid materials, perhaps the most prominent one is the incorporation of inorganic nanoparticles into organic polymers using sol–gel reactions.[7,8] This method allows direct mixing between the inorganic and organic polymers. These nanohybrid materials have attracted much interest in the field of materials science because of the ability to control their morphologies and for their enhanced properties, such as mechanical, thermal, and electrical stability and chemical resistance, relative to their organic polymer counterparts by tailoring organic–inorganic segments into the final composite materials.[9–13] Despite the unique properties of these nanomaterials, including their optical transparency and good mechanical and thermal properties, a lack of data regarding structure–property relationships between nanoscale particles and polymer matrices has led them at present to remain only as an area of emerging research.

There are many efforts being made toward the syntheses and characterization of well-known macrocomposites or microcomposites between inorganic and organic phases, and recently this area has been expanded from the realm of hybrid microcomposites to a new class of hybrid materials called *nanocomposites* or *nanohybrids*. Nanomaterials, or nanostructured materials, in general, have characteristic length scales of <100 nm with uniform distribution, and the particles' arrangements are different from those of simple hybrid composites.[1–6,9–16] This arrangement provides the reason why nanohybrids can possess distinct properties that traditional composites do not have. Therefore, there is a general need to understand the formation mechanism of such particles and their impact on the properties of the final materials. The most important aspects of the chemistry involved in the formation of these systems are monitoring the uniformity, phase continuity, domain sizes, and molecular mixing at the phases, all of which have direct influences on the optical, physical, and mechanical properties of the resulting composites.[11–16]

The incorporation of microscale, and larger, inorganic fillers into organic polymers has been well explored scientifically; the decrease in size of the inorganic component into nano-scale dimensions and the simultaneous increase of the interfacial area result in nanohybrid materials that have extraordinary properties, which

require further investigations.[1–6] In addition, the properties of the composite hybrid materials depend on the phase morphology of the resulting hybrid composites, which must be controlled over several length scales by using appropriate processing conditions.[11] Therefore, the development of nanomaterials that exhibit exceptional properties provides a "multidisciplinary land" in the materials world, where chemists, physicists, material scientists, and engineers will work together intimately to make great progress and discoveries that may have far-reaching consequences for future generations.[11]

From a chemical point of view, the small size of the nanoparticles, which is responsible for their different electronic, optical, electrical, magnetic, chemical, and mechanical properties with respect to their bulk materials, makes them suitable for various applications.[9–24] Changing the molecular structures of nanostructured materials can change their size-dependent properties and hence their applications. The key and critical challenge for designing nanosystems is to control uniform mixing through interactions between the organic and the inorganic phases. By controlling pertinent variables, the nanohybrids approach provides great versatility and ease of preparation and a wide range of well-defined nanohybrid materials can be obtained with predictable structures.[1–3,9–14]

II. POLYMER–SILICA OR POLYMER–SILSESQUIOXANE NANOHYBRIDS

A. Key Parameters for Forming Nanohyhybrids

In this section, several key parameters are described for the formation of nanohybrids by incorporating inorganic networks of silica- or silsesquioxane-like materials into a polymer matrix. Silica is an inorganic material; when organic groups replace one or two bonds, the resulting materials are called organosilicas or silsesquioxanes. *Organic–inorganic hybrid* is a collective term used in materials science. Nanohybrids encompass a blooming research area of the materials world and have widespread use in different areas.[1–5] Within this definition, there are numerous reports describing the incorporation of inorganic silica networks into polymer matrices and studies of the corresponding properties of the resulting hybrid composites.[1–6,9–20] To prepare such hybrid materials, the incompatibility between organic and inorganic phases in the resulting materials is one of key issues that must be addressed; such incompatibility leads to phase separation and a deterioration of properties and, therefore, finding reactions for the formation of hybrid nanocomposite that do not undergo phase separation is a challenge.[1–3] Hybrid materials that have different ratios of their inorganic and organic components possess interesting structure–property relationships; for instance, a high organic content may provide composites having higher flexibility, whereas a high content inorganic content may give brittle composites.[5]

Different types of structure–property relationships can be obtained by controlling the organic and inorganic phases. To date, most hybrid composites has been prepared using silica or silicate as the inorganic component; in most cases, the organic polymer is hydrophobic, whereas silica is hydrophilic. To improve the distribution of silica particles in the organic polymer matrix, the inorganic materials usually are modified by some organic reagents and then these organically modified silicas are used with the organic polymer to prepare the hybrid composite materials.[5] There are many reports on the preparation of hybrid composite materials that have been formed by adopting this approach.[1–6,9–27] In addition to polymer/silica hybrids, other hybrid composites based on elements such as Ti, Zr, and Al have also been reported.[28–36] The synthesis of hybrid systems requires a strategy wherein the formation of good composites arises from components that are well suited to each other. In this approach, the synthesis of the hybrid materials is controlled either by the formation of hydrogen bonds between the organic polymers and silicate networks or by the formation of covalent bonds between the organic and the inorganic phases. Many studies on organic–inorganic hybrid composites have been conducted in which the properties were evaluated in terms of the phases.[1–5] The morphologies and properties of the resulting hybrid composites depend on the methodologies of the components employed. Recently, it has been demonstrated using polystyrene–silica hybrid systems that the compatibility between the organic polymer and the inorganic phases has a profound effect on the thermal, mechanical, and optical properties of the hybrid.[37] It has also been reported that the effects of steric hindrance of the organic polymer and the nature of the chemical bonding restrict the aggregation and condensation of silanols.[37]

Polysilsesquioxanes are a new class of organosilicon materials, in which at least one organic group is attached to a silicon atom; they have found various applications in different areas, such as coatings, coupling agents, surface modifiers, and metal adsorbents.[4] Figure 1 displays the yearly total number of publications and patents reported in the literature.[4] Silsesquioxanes make up a novel class of hybrid silica materials that have various structures and a wide range of chemical applications. Nowadays, silsesquioxanes are also being used for the preparation of polymer-based nanocomposites, the applications of which are spreading in different areas because they allow the formation of hybrid composites through hydrogen bonding or covalent bonding.[1–5] There are many reports on silsesquioxane-based hybrid composites having tailored properties.[4] Silsesquioxanes are also used with high-performance polymers, such as polyimide (PI), to improve the interfacial adhesion between inorganic components (e.g., between silica and PI);[1] the resulting materials exhibit improved properties. Recently, it was demonstrated that silsesquioxanes can play a vital role in the production of low-dielectric-constant materials without sacrificing their thermo-mechanical properties. The exponential increase in the rate of publication and patent generation of silsesquioxane materials in a host of different areas in both basic and applied materials sciences suggests that a wealth of discoveries have yet to be made.[4,38]

Recently, a series of thermoset organic–inorganic hybrid composites based on several types of octa-functional polyhedral oligomeric silsesquioxane (POSS) was

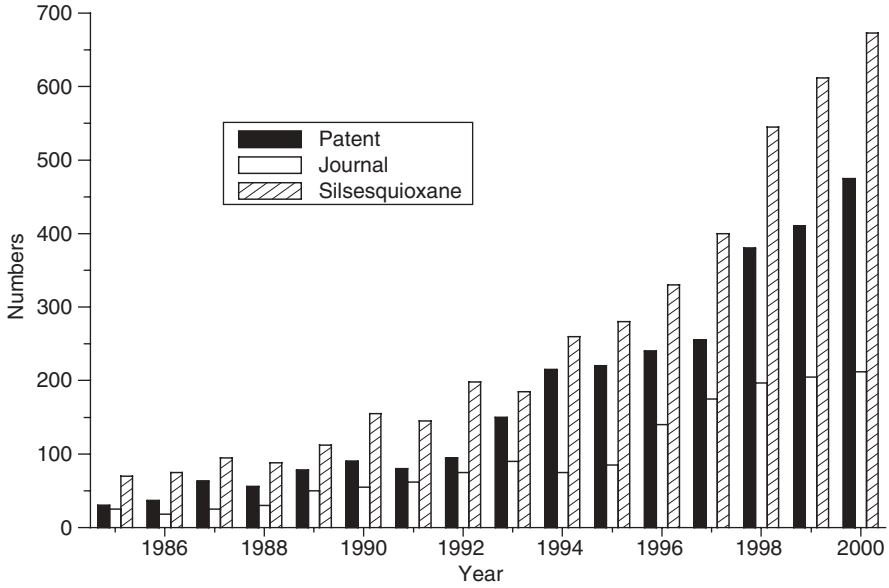

Figure 1 Yearly total citations, patents, and papers on silsesquioxanes since 1986. (Reprinted with permission from Ref. 4; American Scientific Publishers.)

prepared and studied.[39–43] In these composites, the cubic silica cores are completely defined "hard particles" with a diameter of 0.53 nm; their spherical radii, including peripheral organic units, are 1–3 nm.[39–42] The size of these cubic silsesquioxanes is on the nanometer scale, and they are monodisperse within the polymer matrix. If these hard particles are linked in a hybrid composite to an organic component with a known architecture, then a nanocomposite with a well-defined interface between the organic and the inorganic phases can be obtained. In this way, nanocomposites have been prepared based on octa(aminophenyl)silsesquioxane, which has a radius of 1.3 nm, including the rigid silica core and the eight phenyl groups.[39–42] It was found that the thermal-mechanical properties of PI–POSS nanocomposites are significantly improved relative to those of pure PI.[43]

Nanometer-scale composites prepared from layered inorganic materials, especially clay, and polymers have also attracted much attention because of their unique optical, thermal, mechanical, gas barrier, and electrical properties. There are many reports describing polymer–clay nanocomposites.[5,44–46] The clay can be, for example, a silica or silicate. In such a hybrid composite, weak dipolar and van der Waals forces provide the driving force for interactions between the layers, and they result in galleries being formed. There are three types of clay–polymer composites: conventional, intercalated, and exfoliated. Three methods are widely used for the preparation of polymer–clay hybrid nanocomposites: intercalation by in situ polymerization, direct intercalation, and polymer melt intercalation. Each of these methods has its advantages and disadvantages. For example, the in situ polymerization works only in the

presence of suitable monomers or when the intercalation of the polymer chains has quite slow kinetics arising from diffusion phenomena. In the most polymer–clay nanocomposites, a weak phase interaction between the organic and inorganic materials is observed. Much literature is available on polymer–layered silicate nanocomposites as a separate subject.[5,44–46]

B. The Sol–Gel Method and Its Related Parameters

To discuss hybrid inorganic–organic composite materials, a brief review of sol–gel chemistry is necessary. Since this section focuses on silicate and silsesquioxane chemistry, the review of sol–gel chemistry will be limited to detailing some of the nuances associated with silicate alkoxides. After the brief review of sol–gel chemistry, we will present methods for the preparation of hybrid inorganic–organic composite materials, followed by a brief discussion of polyimide-based hybrid composites.

In the past 15 years, the chemistry of sol–gel science has undergone spectacular developments. The various aspects of the sol–gel method have been scrutinized in considerable detail and have established a sound foundation for the development of new science and technologies.[7,8] In addition, this method has opened a gateway to whole classes of new materials. The sol–gel reaction is a simple and versatile process that is used widely for the preparation of inorganic ceramic-type materials based on such elements as silicon, zirconium, aluminum, and titanium. This process commonly involves the following steps: forming a solution by mixing, gelation, aging, drying, and densification. The most widely used precursors are those based on silicon, such as tetraethoxysilane (TEOS) and tetramethoxysilane (TMOS), in which the organic methoxy and ethoxy groups attached to the silicon atom are hydrolyzable. The main chemical reactions that occur in sol–gel process are hydrolysis, condensation, and polycondensation. In addition to the chosen precursors, water and a mutually soluble alcohol can also be used in suitable amounts to assist the process, which can occur under acidic or basic conditions. A basic sol–gel process begins with the metal alkoxide precursors (such as TEOS or TMOS) and water.[7,8] The hydrolyzed products, such as $Si(OH)_4$ units, interact with each other in condensation reactions. When a sufficient number of interconnected Si–O–Si bonds are formed in a region, a "colloidal particle" or "sol" is formed. As the sol–gel reaction proceeds, the colloidal particles grow in size with time and become linked together to form progressively larger aggregates. At the gel point, the viscosity increases until the sol ceases to flow and a gel forms.[7,8] Additional steps in the process, such as aging, drying, and evaporation of residual liquids, lead to the completion of network formation and shrinkage of the molded shapes. Figure 2 provides an example of the most common chemistry used for sol–gel reactions leading to the formation of siloxane bonds starting from TEOS.[3,7,8]

There are several parameters that can play vital roles in the hydrolysis and condensation reactions (sol–gel process), including the reactivity of the metal alkoxide, the water to alkoxide ratio, the solution pH, the temperature, the nature of the organic ligands, and the nature of the solvent and additive.[1–3,7,8] Another consideration is that

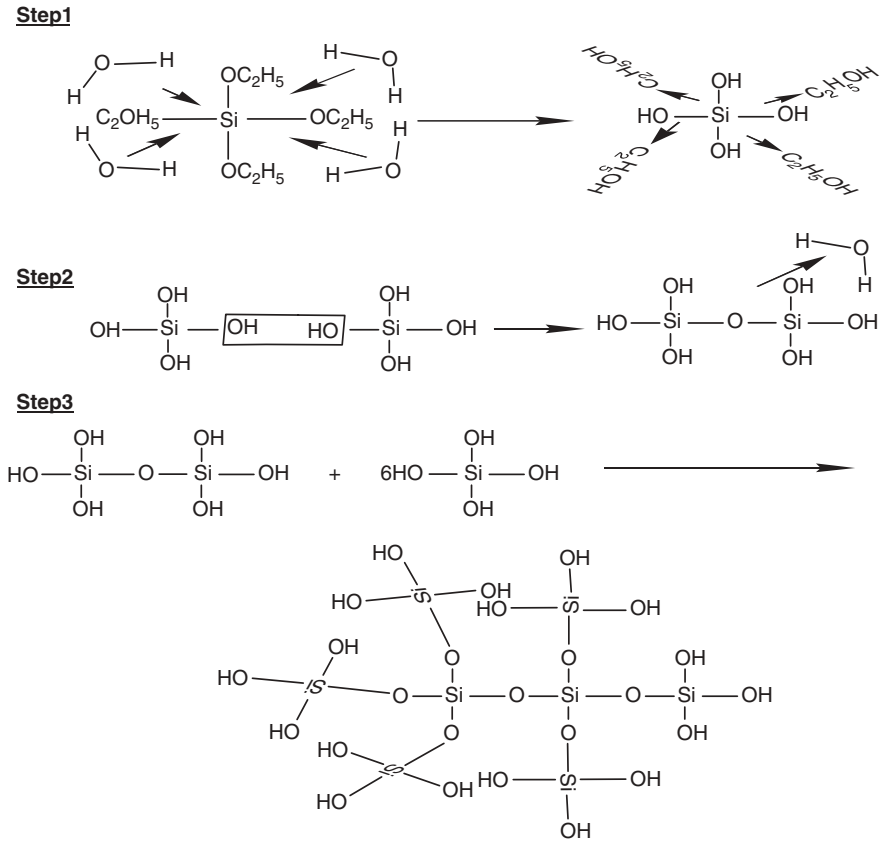

Figure 2 The sol–gel reaction of TEOS leading to the siloxane bond formation.

catalysts may also be used to control the rate and extent of hydrolysis.[1–3,7,8] By controlling these parameters, materials with different microstructures and surface chemistries can be obtained. Furthermore, the sol may produce different forms as desired. The sol–gel process is one of the most active, facile, and promising areas of materials research.[7,8] The ambient processing conditions allow the encapsulation of various organic, organometallic, and biological molecules within these sol–gel-derived inorganic phases.[1–3,7,8] The sol–gel reaction is also the most important effective way, and is extensively used to design and synthesize inorganic–organic hybrid materials that have nanometer-scale architectures.[1–3] These hybrid materials, which have many possible applications in many promising areas, often cannot be prepared by other methods.[1–3,7,8] Tremendous progress has been made in the fundamental understanding of both the sol–gel process and the newly developed organic–inorganic hybrid materials prepared this way; it has been reviewed extensively in the literature.[1–31]

C. Polymer–Silica Nanohybrids

Mixing organic polymers with preformed inorganic particles may lead to higher phase separation of products that have poor mechanical, optical, and electrical properties.[1–3,20,47–51] In addition, such silica particles not only agglomerate but also form discrete phases in the polymer matrix, which tends to weaken the mechanical or optical properties of the resulting hybrid composites. The presence of bonding between the organic polymer phase and the inorganic phase impedes phase separation and thus results in homogeneous hybrid composite materials.

A number of papers have reported the preparation and characterization of organic–inorganic hybrid composite materials by the hydrolysis of metal alkoxides, such as TEOS or TMOS, and their polycondensation with organic polymers.[51–55] Various types of organic polymer matrices, such as poly(dimethylsiloxane) (PDMS),[49] poly(tetramethylene oxide) (PTMO),[50] polyimides,[51] poly(oxyethylene),[52] poly(ether ketone),[53] and poly(ethersulfone),[54] have been used successfully with inorganic phases, such as SiO_2 or TiO_2 inorganic networks formed by sol–gel reactions. The resulting hybrid composites have also been investigated for their properties, such as improved mechanical strength and optical transparency.[49–54] Poly(methyl methacrylate) (PMMA)–SiO_2 and other acrylic polymer–SiO_2 hybrid composite materials formed by sol–gel processes have also been studied because of the commercial importance of acrylic polymers.[22,55–57] It has been found that homogeneous, transparent hybrid composites of organic polymers and inorganic phases can be prepared under certain environmental conditions. Polymers that can form an extensive number of hydrogen bonds between their carbonyl groups and the silanol units of the silicate network can produce homogeneous products with metal alkoxides.[56,58] The hydrogen bonding between the polymer and the silicate network can inhibit macroscopic phase separation in the final hybrid composites. On the other hand, the organic polymer phase can be covalently bonded to the inorganic phase by condensation of the functional groups and the metal hydroxide, which can result in homogeneous, transparent hybrid materials that have a range of desired properties.[1–3,56]

The properties of the hybrid composites are influenced by the phase of the composites.[1–3] By comparing the effects that different interactions have on the properties of hybrid composites, it has been concluded that the interactions between silica networks and polymers can be improved by using trialkoxysilyl-functionalized polymers; the hydrogen bonds and the chemical bonds formed by condensation between the hydroxyl groups and the silanols are two important sources of interactions in the hybrids.[58,59] Recent studies on organic–inorganic hybrids have been reviewed.[1–3]

D. Polymer–Silsesquioxane (SSQ) Nanohybrids

The broad objective of this section is to indicate the breadth and current status of research into silsesquioxane-based nanomaterials and their prospects in terms of their applications. The synthesis, characterization, and processing of nanostructured

materials based on SSQ are emerging and rapidly growing areas of research. Research and development in this field emphasizes scientific discoveries in the generation of materials that have controlled nanostructural characteristics, research on their processing into bulk materials that have engineered properties and technological functions, and the introduction of new device concepts and manufacturing methods related to their counterpart polymer/silica hybrids.[4,38–43] The term *silsesquioxane* refers to a wide range of structures that have the general empirical formula $RSiO_{1.5}$, where R is a hydrogen atom or an organic derivative, such as any alkyl, alkylene, aryl, or arylene group or an organofunctional derivative thereof.[38] The silsesquioxanes form various types of structures, such as random, ladder, cage, and partial-cage structures, as shown in Figure 3.[38,59,60] The first oligomeric organosilsesquioxanes, $(RSiO_{1.5})_n$, were reported by Scott in 1946 and were based on methyltrichlorosilane and dimethylchlorosilane.[59] Recently, the span of silsesquioxane chemistry has expanded unexpectedly and continues to do so because of its applications in materials science.[4,38] POSS (polyhedral oligomeric silsesquioxane) molecules embody truly hybrid inorganic–organic architectures; they bear an inner inorganic framework comprising silicone and oxygen atoms, and the silicon atoms are covalent bonded to organic substituents. Furthermore, these groups can be specially designed as needed. However, unlike silica, silicones, or inorganic fillers, POSS-like molecules have an organic group in the framework that could make the POSS nanostructure compatible with polymers, biological systems, or surfaces.[38,59,60]

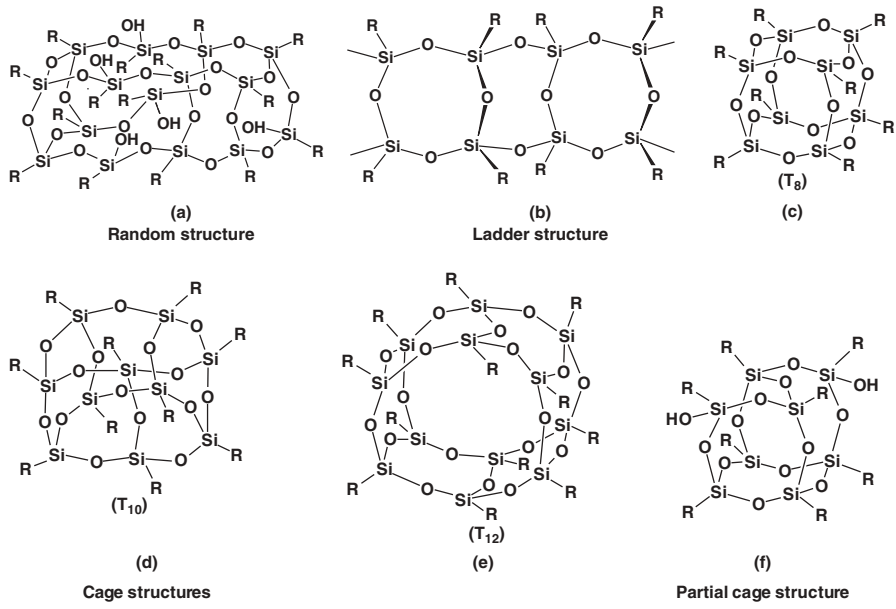

Figure 3 Various types of structures of silsesquioxane. (Reprinted with permission from Ref. 38; Plenum Publishing Co.)

Various types of SSQ monomers have been reported, such as styryl-POSS,[61] methacrylate-POSS,[62] norbornyl-POSS,[63] vinyl-POSS,[64] epoxy-POSS,[65,66] and siloxane-POSS.[67] Various types of POSS-like nanostructured materials have been prepared that contain one or more covalently bonded reactive functionalities suitable for polymerization, grafting, surface bonding, or other transformations.[38,59,60] Thus POSS-like nanostructured materials may be easily incorporated into common plastics through copolymerization, grafting, or blending. The incorporation of POSS-like derivatives into organic polymeric materials can lead to dramatic improvements in the properties of the resulting hybrid composites. These enhancements of the hybrid composites have been shown to apply to a wide range of thermoplastics and thermoset hybrids.[68,69] It is quite convenient that the use of POSS-like materials does not require dramatic changes to be made in processing conditions; the monomers are simply mixed with the organic phases. Usually no phase separation occurs after incorporating these materials into the polymer matrix, although a small degree of aggregation of POSS units bound with the polymer may occur. This lack of phase separation is an extra advantage over current filler technologies.[38] Therefore, POSS-like nanostructured materials have demonstrated significant promise in the field of organic–inorganic hybrid composites and have significantly affected applications in areas such as electronics, photonics, and other materials technologies.[4] Silsesquioxanes have a wide range of chemical reactivities, including those of alkoxy- or chlorosilanes and silanols. Many silsesquioxane hybrid materials also exhibit enhanced thermo-mechanical stability, optical transparency, gas permeability, and dielectric constant.[4,38,59,60] Recently, POSS-like materials have become widely used in conjunction with different types of polymers to improve the properties of the resulting hybrid composites.[38] The slight changes in size can result in dramatic changes in the glass-transition temperature.[38] In several reports, Kim and Chujo[70] prepared, through molecular design of systems exhibiting both hydrogen bonding and aromatic interactions, transparent polystyrene–POSS hybrids that have improved properties. Hong et al.[71] reported polymethylphenylsilsesquioxane (PMPSQ) and hydroxyl-functionalized polystyrene (PS-OH) hybrids; they found that dielectric constants increased, due to the amorphous glass-transition temperature, upon increasing the amount of the PS-OH component. It was suggested that degree of interaction and the types of interactions can bring about changes in the properties of the resulting hybrid composite materials.[1–3,38,51,60,69,70]

E. Other Metal Oxide or Metal-Like Materials Containing Polymer Nanohybrids

The incorporation of metals in polymers will not be covered in detail because only a limited number of reports exist on this subject. The major interactions that have been used for the incorporation of metals in polymers are those of functional groups that form polymer–metal oxide-based composites. The incorporation of metals leads to dramatic changes in the properties of polymers, such as an increase of the glass-transition temperature (T_g).[72] Polybutadiene or polyisoprene incorporating palladium salts can undergo crosslinking, mediated by palladium, between polymer

chains. This methodology is known as "reactive blending." The swelling properties of such crosslinked systems depend on the salt concentration: They decrease with an increase in the palladium content. In addition to the formation of such crosslinked composites, transition metal additives can also help inhibit phase separation and result in compatibilized composites. Many reports on metal-incorporating polymeric systems are available in the other chapters of this volume and the references therein.[73–78]

III. POLYIMIDE–SILICA OR POLYIMIDE–SILSESQUIOXANE NANOHYBRIDS

A. Polyimide

Polyimides are an important class of well-known high-performance step-growth polymers because of their unique physicochemical properties, such as thermal and mechanical stability, controlled dielectric behavior, good adhesion properties, and chemical resistance.[1,79–86] Polyimides are usually formed from the reaction between stoichiometric amounts of a dianhydride and a diamine, which can be either aliphatic or aromatic. For this reason, a legion of polyimides that have many different characteristics is available to satisfy the requirements of various applications. Because of these traits, PIs are used widely in a range of applications, such as in microelectronics, aerospace, and membrane science.[79–86] More recently, these materials have been used as polymeric components of hybrid organic–inorganic systems that are an important class of new-generation materials that combine the desirable combined properties of inorganic phases, such as silica or silsesquioxane, and PI.[1] Despite their many advantages, conventional PIs are insufficient for meeting the requirement of advanced applications, such as in ultra-low-dielectric-constant (i.e., low-k) applications.[87,88] In the meantime, several attempts have been made to meet the low-k requirement. PIs are also limited to additional improvements in their performance because of limitations that are inherent in all organic materials, for example, their thermo-physical properties. To overcome such limitations, incorporating inorganic components, such as silica or silica-like materials, into the polymer matrix PI may change the properties of the resulting composite materials.[1] In regard to their prospects in the various applications mentioned above, improvements in research and development in certain aspects are vital and would be of great help, for example, in relation to their mechanical and thermal strength, gas permeation, and low-k properties.[1]

B. Polyimide–Silica Nanohybrids—Their Characterization and Properties

PIs have numerous applications in the electronics industries and improvements in their properties are vital in regard to increasing such applications.

Recently, incorporating silica components, in the form of nanohybrid composites, into the PI matrix has enhanced their thermal properties and reduced their coefficients of thermal expansion compared to the pure PIs. The combination of nanoscale inorganic components and PIs has great potential for uncovering future applications and, therefore, it has attracted a lot of attention during the last few years.[1] This section focuses on the most well understood principal concepts used to incorporate inorganic components, such as silica or silica-like materials, into polyimides and the resulting properties of such nanohybrids.

Historically, in the early 1990s, attempts at combining PI with silica particles from alkoxysilanes using sol–gel chemistry often led to inhomogeneously distributed micro-size silica domains in the polyimide matrix.[1,89,90] This phenomenon led to brittle composites that featured microscopic cracks. To minimize the size of the silica particles, Nandi and co-workers[91,92] performed experiments on polyimide-based organic–inorganic hybrid composites by directly mixing a solution of a polyamic acid (PAA), typically PMDA-ODA PAA (i.e., the PAA obtained from the reaction of oxydianiline [ODA] and pyromellitic anhydride [PMDA]) in dimethylacetamide (DMAc) or *N*-methylpyrrolidone (NMP), with a metal alkoxide. The sites of coupling between the polyimide carbonyl groups and the surface of the particles may also play a role in suppressing cluster mobility, which thus prevents significant agglomeration of the metal particles and so improved properties can be obtained.[91,92] By-products and water also affect the hydrolysis and condensation of the metal oxide; water should be added in a stoichiometric amount with respect to the alkoxysilane. Silicate species containing a large number of unreacted hydroxyl groups may persist even after curing the hybrid composites at high temperatures.[93] A number of properties of these polyimide–silica hybrids, such as their thermomechanical properties, moisture uptake, and related properties, are reported to be enhanced relative to those of the host polyimide.[1] The phase compatibility between the components of the polyimide-based hybrid composites can be confirmed by recording SEM images, which can discern between the homogeneous and the heterogeneous distribution of particles in the polyimide matrix; it then becomes easy to guess the properties of the resultant hybrid composites.[1,51,87–96] Figure 4 presents a general scheme for synthesizing PAA, PAA–silica hybrid solutions, and hybrid films prepared by sol–gel reactions and thermal imidization. Here, 3,3′,4,4′-biphenyltetracarboxylic dianhydride (BPDA) and *p*-phenylenediamine (PDA) were used to prepare the PAA.

When silica, formed by the sol–gel process, is incorporated as the inorganic component into the PI matrix, phase separation is observed in the resulting hybrid composites because of the absence of adhesion between the organic and the inorganic phases. Compatibility between organic and inorganic phases is an important issue that must be addressed when attempting to improve the properties. A simple method for preparing the PI–silica nanohybrids is mixing PAA with a silicon alkoxide, such as TEOS or TMOS, followed by a step-wise sol–gel reaction involving the hydrolysis and condensation of TEOS or TMOS. Detailed sol–gel reaction chemistry is presented in Figure 2. The major advantage of the process is that relatively controlled temperatures and conditions are used for this type of processing of PI–silica

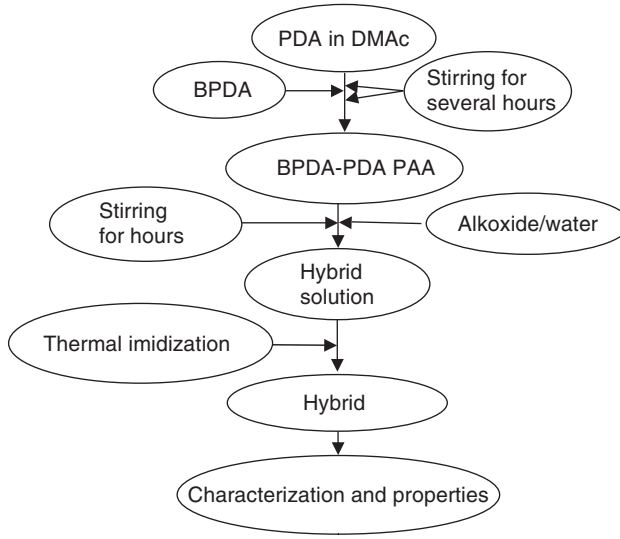

Figure 4 General synthesis scheme for polyamic acid solution (PAA), hybrid solution, and hybrid films.

nanohybrids. The product silica networks that form through the sol–gel reactions usually dictate the properties of the final composites through their morphology. In most cases, TEOS has been used as the silica component, but it leads to hybrid composites that have a high degree of phase separation.[1–3,94–101] In most cases, the incompatibility between the two phases of the PI–silica hybrids makes the dispersion of the inorganic silica particles into the polyimide matrix much more difficult. Furthermore, the morphology and interfacial properties of the two separated phases will not lead to hybrid composites possessing desirable properties. The difficulties encountered when using such an approach are the potential for incompatibilities between the moieties, which lead to phase separation, and the challenge to find reactions for the formation of the second network that can be performed in the presence of the first one without losing phase compatibility. The major problems caused by the different entities in the final composite material can be improved by introducing some type of coupling agent. This coupling agent usually improves the strength of the interactions between the organic and inorganic phases and leads to well-dispersed phase morphologies that have improved properties.[1] Most examples use a coupling agent such as 3-aminopropylsilsesquioxane (3APSSQ) to improve the properties of the resulting hybrid composites.

Figure 5 presents SEM images of the PI-based hybrid composites with or without the addition of a coupling agent.[102] In polymeric hybrid composites, the external stress transfer depends on the phase morphologies of the resulting hybrid composites and enables the properties of composite materials to be dictated. In Figure 5

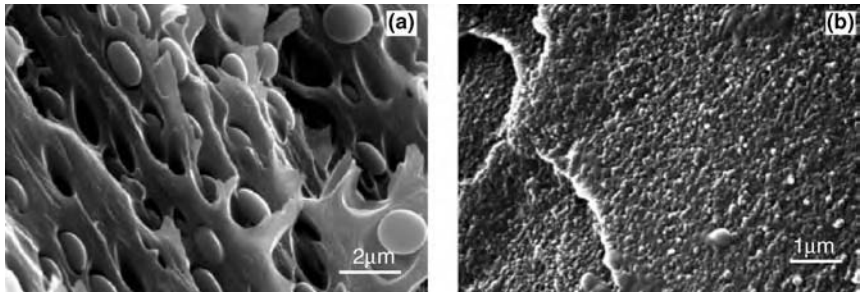

Figure 5 Polyimide–silica hybrid composites (**a**) without coupling agent and (**b**) with coupling agent. (Reprinted with permission from Ref. 102; Elsevier Science Ltd.)

TEOS or TMOS was used as a precursor for silica. Regardless of the choice of silica precursor, these micrographs display clearly the effect of 3APSSQ, which brings about a significant morphological transition from the dispersed individual silica domain phase structures in Figure 6c,d, obtained in the absence of 3APSSQ, to the fine interconnected or co-continuous well-dispersed morphologies observed in Figure 6a,b when 3APSSQ was used. For hybrid systems containing 3APSSQ (i.e., compatibilized hybrids), the size of the interconnected silica domains ranges from 40 to 55 nm, while for hybrids formed without 3APSSQ, the average diameters of the silica particles varies from 0.8 to 1.2 μm. The SEM micrographs presented in Figure 6c,d also

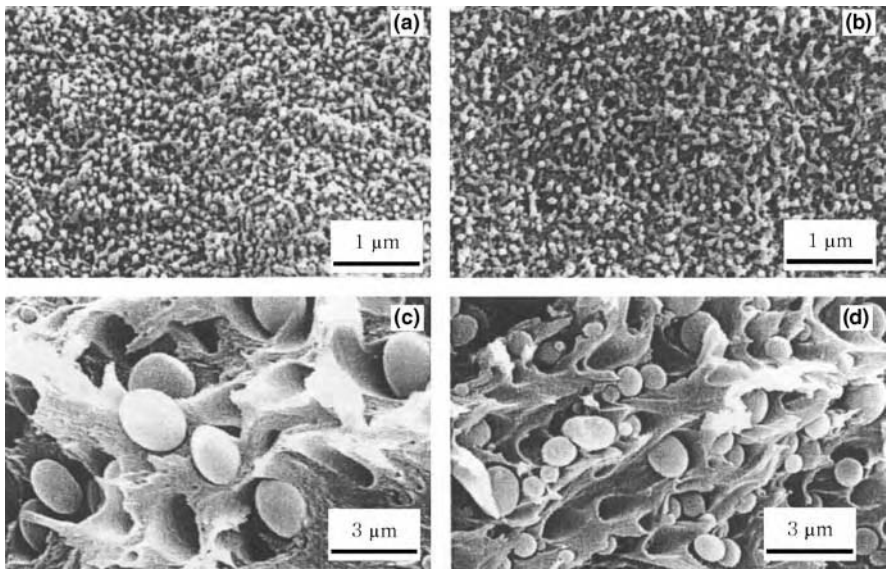

Figure 6 SEM images of the PI–silica hybrid composites. (a) PI/TEOS30. (b) PI/TMOS30. (c) PI/TEOS30-w. (d) PI/TMOS30-w. BPDA-ODA PI was used as a polymer matrix. (Reprinted with permission from Ref. 98; VSP Publishers.)

indicate that the silica particles have almost spherical shapes with smooth surfaces and seem not to be bonded to the polymer matrix, which suggests weak interfacial adhesion between the organic and the inorganic phases. Hybrid composites with such morphologies usually give inferior properties because of the weak interactions between the two phases within the composites, as evidenced by SEM micrography.

On the basis of such morphological observations, it is evident that the reduction in mechanical properties observed for the hybrid composites without a coupling agent permits the silica domains to act as individual particles and is responsible for the stress-concentration defects in the polyimide matrix, rather than acting as effective reinforcing fillers.[102] On the other hand, the improved mechanical properties of compatibilized hybrid composites are the result of both the better interfacial adhesion and the formation of co-continuous phase morphologies, which improve the efficiency of the stress transfer mechanisms between the organic and the inorganic phases.[1] The co-continuous phase morphologies are believed to be due to the presence of strong interactions or chemical bonds, such as hydrogen bonding or covalent bonding.[1,51,87,96,102,103]

Recently, γ-glycidoxypropylsilsesquioxane (GPS) was used with polyamic acid in NMP solvent when TEOS was used as the silica source.[103] Studies showed that the change in appearance of the resulting hybrid composite films, from cloudy to transparent, was a result of compatibilization effects provided by GPS being located between the organic polymer, PI, and the evolving siloxane moieties and through possible interactions involving GPS and the carbonyl groups of the polyimide.[103] Hydrogen bonding is known to occur between polyimide and silsesquioxane-like materials, such as GPS. The transparency of the hybrid PI–silica composites was improved by the presence of GPS. Moreover, the terminal GPS units hydrolyze to form hydroxyl groups that can form hydrogen bonds with the carbonyl groups in PI, which leads to the observed increase in compatibility with PI. These two factors lead to a reduction of the average silica domain sizes, to good dispersion of silica nanoscale particles in the polyimide matrix, and to improved physical properties.[103] The properties of these hybrid composites formed with or without the use of coupling agents has been reported extensively in the literature.[1,43,51,86–103]

Figure 7 displays small-angle X-ray scattering (SAXS) profiles of PI–silica hybrid composites. The images indicate that the peak intensity is affected by silica particle sizes and the degree of interpenetration.[100] Different types of silica particles can be formed during sol–gel processing, and these forms can affect the intensity of the SAXS profile. Ha and co-workers reported that atomic force microscopy (AFM) is a useful tool for interpreting the interfacial interactions and phase behavior of PI–silica hybrids.[100,101] The values of the surface roughness of the resulting hybrid composite films are highly dependent on the phase of the hybrid composites obtained. There are some reports regarding the phase behavior of hybrid composites that are interpreted in terms of the surface roughness values.[87,104,105]

The interfacial interactions and photophysical properties of PI–silica hybrid composites have also been evaluated by using fluorescence spectroscopy.[97] Figure 8 presents the wavelength of the emission peak as a function of silica content (TEOS). The figure shows that a large red shift is observed in BPDA-PDA–TEOS composites,

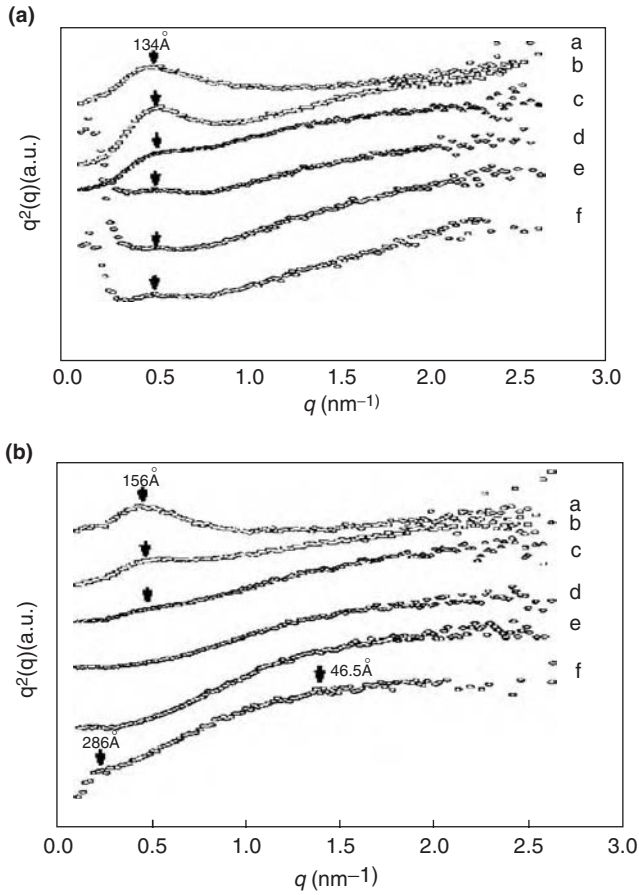

Figure 7 (**a**) Lorentz-corrected SAXS profiles of silica–BPDA-PDA composite films prepared from BPDA-PDA ES (diethyl ester). TEOS–polyimide precursor compositions are *a*, 0/100; *b*, 5/95; *c*, 10/90; *d*, 15/85; *e*, 20/80; and *f*, 30/70. (**b**) BPDA-PDA PAA. TEOS–polyimide precursor compositions are *a*, 0/100; *b*, 5/95; *c*, 10/90; *d*, 15/85; *e*, 20/80; *f*, 30/70. (Reprinted with permission from Ref. 100; Wiley Interscience, Inc.)

Figure 8 (a) Wavelengths of emission peaks of BPDA-PDA PAA–TEOS solution, PAA–TEOS as spun-film, and PI–Si film states as a function of TEOS content. The emission peaks of BPDA-PDA PAA–TEOS were obtained with the excitation wavelength at 480 nm. (b) Wavelengths of emission peaks of BPDA-ODA PAA–TEOS solution, PAA–TEOS as spun-film, and PI–Si film states as a function of TEOS content. The emission peaks of BPDA-PDA PAA–TEOS were obtained with the excitation wavelength at 480 nm. (c) The excitation spectra of BPDA-ODA PAA–HCl solution without TEOS, BPDA-ODA PAA–TEOS solution without HCl, and BPDA-ODA PAA–HCl–TEOS solution as well as BPDA-ODA PAA solution with HCl and TEOS. (Reprinted with permission from Ref. 97; American Chemistry Society.)

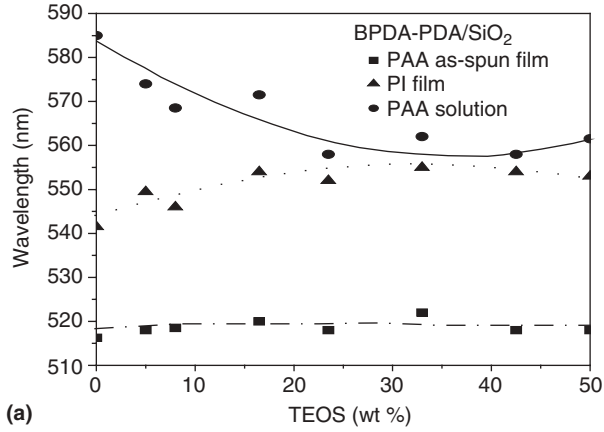
BPDA-PDA/SiO2
PAA as-spun film
PI film
PAA solution
Wavelength (nm)
TEOS (wt %)
590
580
570
560
550
540
530
520
510
0
10
20
30
40
50

(a)

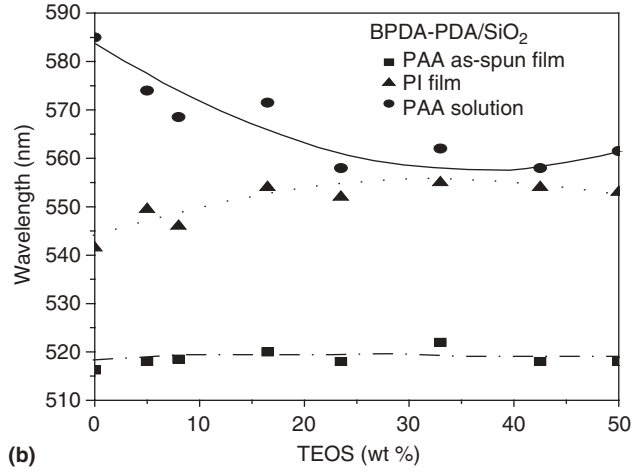
BPDA-PDA/SiO2
PAA as-spun film
PI film
PAA solution
Wavelength (nm)
TEOS (wt %)
590
580
570
560
550
540
530
520
510
0
10
20
30
40
50

(b)

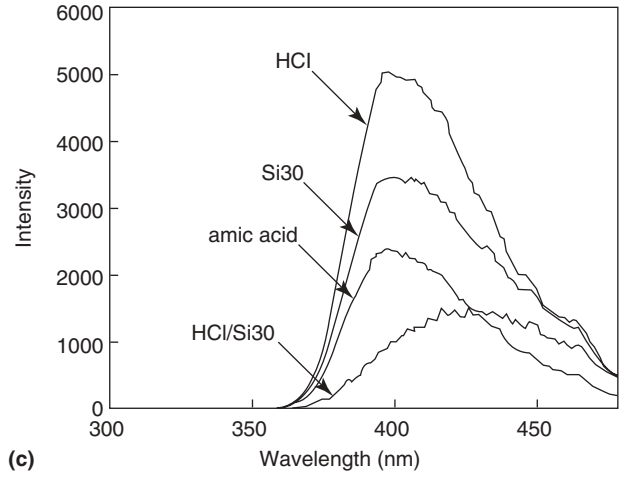
HCl
Si30
amic acid
HCl/Si30
Intensity
Wavelength (nm)
6000
5000
4000
3000
2000
1000
0
300
350
400
450

(c)

but no significant change is observed in BPDA-ODA–TEOS systems. The interaction between the PI and the silica is different and depends not only on the sample states but also on the nature of the organic moieties. The photophysical properties, the final morphology, and the physical properties of the hybrid composites can be influenced in many ways by the chemistry that occurs before and after the sol–gel reaction and during the imidization process.[97] Figure 8c indicates the systematic studies that have been conducted to determine the influencing factors in hybrid composites. Intermolecular hydrogen bonding exists between the hydroxyl groups in the hydrolyzed form of TEOS (i.e., $Si(OH)_4$) and the carboxylic acid units in BPDA in both the BPDA-PDA and BPDA-ODA composite systems. The photophysical properties of polyimide systems also depend on the nature of the diamine.

Kim and coworkers[106] studied the effects of TEOS content on the dielectric constant of PI–silica hybrid composites. They found that the values of the dielectric constant of the hybrid composite films increased monotonically upon increasing the amount of TEOS because of the inherent higher dielectric constant of silica relative to that of pure polyimide. The PI–silica hybrid films prepared from PAA possess higher dielectric constant than those of the PI–silica composite films in polyamic acid diethyl ester. This difference was ascribed to the uniformity of the distributed nanometer-scale particles in the former set of hybrid composite films.

Coefficients of thermal expansion (CTE) have been determined for PI–silica hybrid composites. Figure 9 illustrates the large reduction in CTE when the morphology is changed from particulate to co-continuous. This effect becomes more pronounced at temperatures above the T_g value of the PI and is in concordance with the greater suppression of α-relaxation that was revealed in dynamic mechanical tests.[51] In this figure, the descriptors S and SE2 denote the Ceramer and the Ceramer with a compatibilizer, respectively. It also has been reported that the CTE values increase as a result of the partial substitution of TEOS with dimethyldiethoxysilane (DEDES).[51] This result may come from the loss of continuity of the silica phase and also possibly through the reduction in its cross-linking density.

The silica domains incorporated into the polyimide matrix exhibit improved thermal stability relative to that of pure polyimide because of the inherent thermal stability of the inorganic component, silica. The compatibilized hybrid (such as the 3APSSQ-containing PI–silica) possesses much greater thermal stability because of the presence of chemical bonds, provided by the coupling agent between PI and silica. Sometimes, because of possible reactions between them at the temperatures used, the cyclization of the polyamic acid to form PI may not reach completion and this effect could reduce the thermal stability of polyimide.[87,98,107]

The glass-transition temperatures of the hybrid composites are higher than those of the pure polyimide. The increased T_g value of the hybrid composite formed in the presence of the coupling agent, relative to that of PI–silica systems, is indicative of reduced polyimide chain mobility resulting from the presence of covalent bonding in the final hybrid composites. Using this strategy, several approaches have been conducted to increase the T_g values of hybrid composites.[96,102,103] The magnitude of the tanδ peaks of the hybrids also decreases and broadens upon

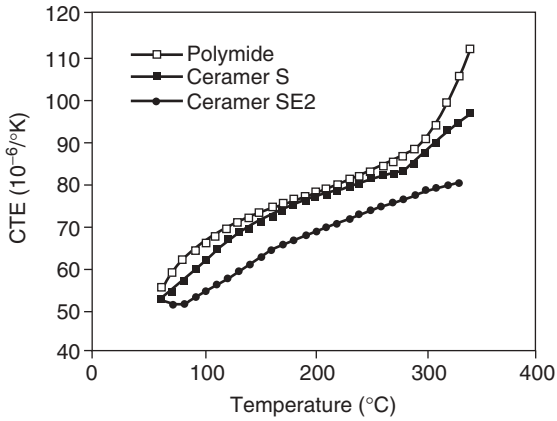

Figure 9 Effects of compatibilization on the coefficient of thermal expansion of ceramers containing 25% (w/w) equivalent SiO_2. (Reprinted with permission from Ref. 51; Elsevier Science, Ltd.)

increasing the silica content, which is a finding that suggests an increase in heterogeneity in the final hybrid composites.[108]

C. Polyimide–Silsesquioxane Nanohybrids—Their Characterization and Properties

As discussed earlier, PSSQ materials have attracted much attention among chemists, physicists, and material scientists interested in advanced technologies, such as for the preparation of low-dielectric insulators for microelectronic devices, coatings, surface modifications, and novel reinforcing elements for hybrid composites.[4,38,87,88,96] It is important that PSSQs that have an organic group in their framework have a low dielectric constant and low moisture absorption relative to those of silica; thus they have been proposed as a replacement for silicon dioxide.[99] Silica-based PSSQ is known to possess not only a low dielectric constant but also quite good thermal stability. Polyimide–PSSQ hybrid composites are new types of materials, however, and there have been only a few studies on their syntheses and properties. Silsesquioxane materials that have organic groups attached to silicon atoms are hydrolytically stable and possess three siloxane bonds; the organic part of the PSSQ plays a vital role in bringing about the change of structure and ultimately impacts the properties of the final hybrid composites. The control of microstructure, molecular weights, and the nature of the remaining functional end groups are important for determining the mechanical properties of final hybrid composites. There are several reports on the improved properties of PI–SSQ hybrid composite materials in which organic groups play a vital role in improving the properties though well-dispersed continuous phase morphologies.[87,88,96]

Although there are few reported examples, this section intends to correlate the properties with respect to the silica domains and the PSSQ content and discuss the influence that the PI–PSSQ composites have on dielectric constants, their thermal stability, phase morphology, and their effect on other properties, such as moisture absorption and optical transparency in the visible region.

The surface morphologies and the resultant properties of PI–PSSQ hybrid composites are distinguished from those of other PI–silica systems. Figure 10, for example, indicates the hybrid morphological features of the PI–poly(vinylsilsesquioxane) (PVSSQ) hybrid.[87,96,109] In this figure, BO and BP refer to BPDA-ODA PI and BPDA-PDA PI, respectively. It has been demonstrated that the homogenously distributed PSSQ domains have a co-continuous phase morphology in the hybrid composite systems. Such morphologies could arise in hybrid composite systems when the terminal hydrogen atoms of PVSSQ and the hydrogen of Si–OH provide hydrogen bonds with carbonyl groups in the polyimide matrix, which leads to an enhanced compatibility of silica with polyimide.[87,96,109] Among the two series, the BP-VSSQ series exhibited a better morphology than did the BO-VSSQ series. This difference has been ascribed to the degree of hydrogen bonding interaction between the BPDA-PDA VSSQ hybrid composites being higher than that in the BPDA-ODA VSSQ counterparts. Such morphologies could have a direct effect on the mechanical properties of the final hybrid composites.[87,96] The improvement of mechanical properties can be interpreted as arising as the result of the introduction of fine silica particles into the polyimide matrix and of better co-continuous morphologies existing through hydrogen bonding. The flexible organic group (vinyl part) in PVSSQ plays a vital role in bringing about hydrogen bonding between the carbonyl group of the PI and the terminal organic part of the PVSSQ. Such explanations of the hydrogen bonding phenomena have been published by others.[87,95,96,99,109] Such co-continuous morphologies as observed in Figure 10 can support the stress transfer mechanism between the PI and PVSSQ, whereas the nonbonded PI–silica zones act as stress concentration defects. A scheme is provided, however, for the hydrogen bonding existing between PI and PVSSQ (Fig. 11).[87,95,96,103,109] The microstructure and properties of the resulting hybrid composites are related to the nature of the silsesquioxane materials.

The surface topography and the corresponding surface roughness values can be used to investigate the phase separation of the PI–VSSQ hybrids. The surface roughness value of the hybrid composite films depends directly on the degree of the phase separation.[87,96,98,100,109]

Recently, Tsai and Whang[88] studied the dielectric constants and densities of pure polyimide and its hybrid composites and found that a proportional relationship exists between these values. The dielectric constant decreased linearly upon increasing the content of phenyltrialkoxysilane (PhSSQ) because larger PhSSQ particles may increase the free volume and decrease the density. This work is supported by the findings of a study on other PI–PSSQ hybrid systems.[87] The dielectric constants of the cured PI–PSSQ-like hybrid films are affected by the free volume in the materials and, probably, by the hydrophobicity of the PhSSQ-like domains because the phenyl moiety of PhSSQ is hydrophobic. Water absorption of the hybrid composite decreased-upon increasing the amount of PhSSQ, which is

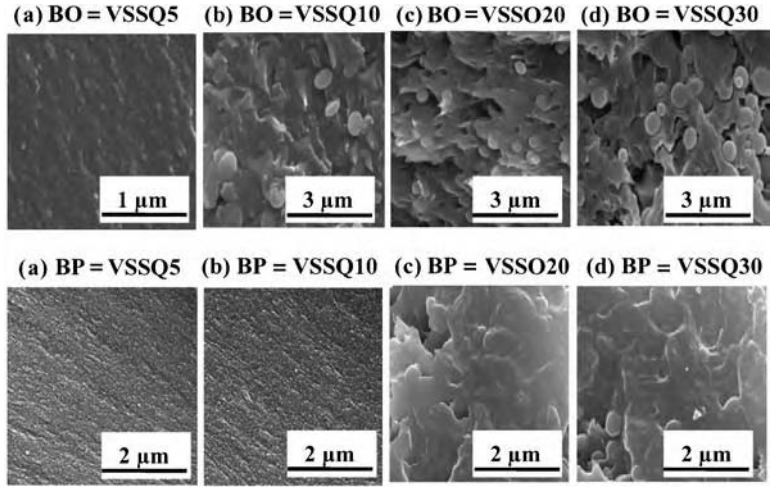

Figure 10 SEM images of fractured surfaces of PI–PSSQ hybrid composites. The samples coded are listed above the images.

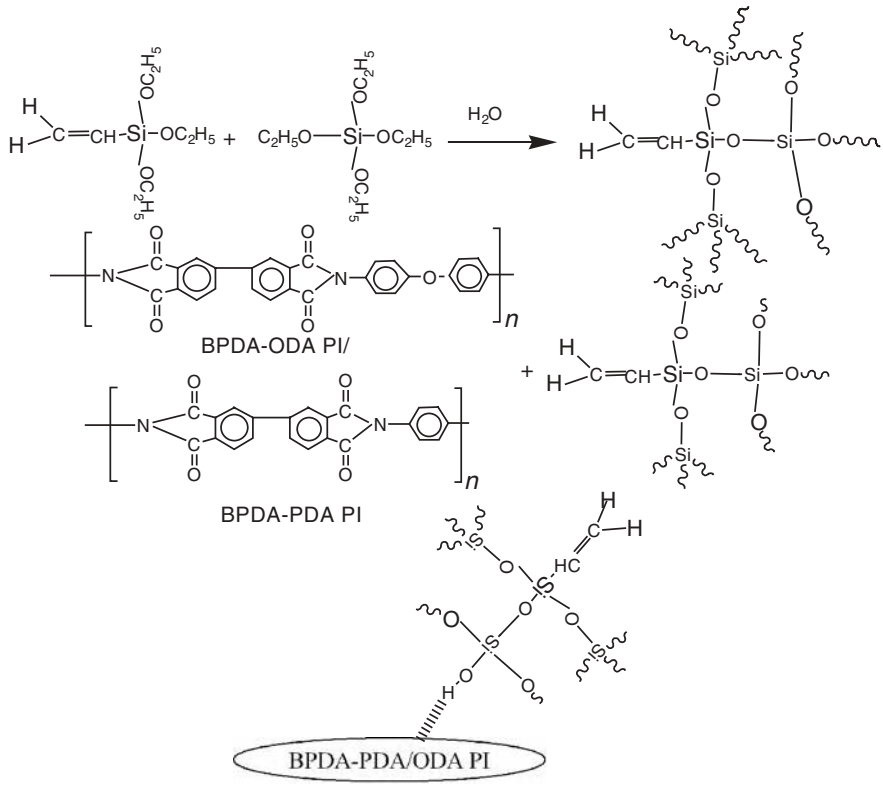

Figure 11 A diagram for the hydrogen bonding of BPDA-PDA PI and VSSQ. (Reprinted with permission from Ref. 96; American Chemistry Society.)

a finding related absolutely to the hydrophobicity of the resulting hybrid composite films. Subsequently, another study revealed the effect of vinylsilsesquioxane (VSSQ) on the dielectric constants of hybrid composite films.[87] When small amounts of VSSQ were introduced into the PI matrix, the dielectric constant decreased markedly, but it was found to increase upon increasing the loading of VSSQ.[87] This phenomenon can be explained in terms of the free volume introduced by VSSQ and the domain sizes of VSSQ. It is exceptional that PI hybrids with a VSSQ content of 20 wt % and 30 wt % possess higher values of dielectric constant, but they are still lower than that of pure polyimide. It is also true that free volume can easily be occupied by moisture, which increases the dielectric constant because of the inherently high dielectric constant of PVSSQ.[78] The presence of Si–O–Si and Si–O bonds in the cured network structures can also lead to increases in dielectric constants upon increasing the amount of PVSSQ present.[87]

Tsai and Whang described CTEs below the T_g value of pure polyimide for APTS (p-aminophenyltrimethoxysilane) containing PI; the CTE decreased upon increasing the content of APTS in the hybrid composite films, which is a phenomenon that is due to the increase in the crosslinking density of the network structure that results in increases in both the chain stiffness and the T_g value and, therefore, decreasing values of CTE.[88]

The excellent thermal stability of PI–PSSQ hybrid systems has been studied by a number of groups.[43,87,88,96] In every case, without exception, the thermal stability of the hybrids increased, as measured by the char yield at high temperatures, relative to that of pure polyimide. Tsai and Whang[88] demonstrated the improved thermal stability of hybrid composites relative to that of pure polyimide in terms of the char yield measured at 800°C. Subsequently, Ha and coworkers also reported the higher thermal stability of hybrid composites at 750°C relative to that of pure polyimide.[87,96,98] PI–PSSQ hybrid systems not only possess improved thermal stability but also higher T_g values relative to the values for pure PI reported in the literature.[87,96]

Some hybrid composites that have low contents of PSSQ do not display a significant change in T_g because such low amounts cannot contribute to the resistance of the movement of the PI chains. Improvements in the T_g values suggest strong interactions and possibly chemical bonding between the PI and PVSSQ units. The T_g values of hybrid composite films shift higher upon increasing the amount of PVSSQ. The mobility of the polyimide chain is restricted by the introduction of fairly dispersed PVSSQ domains in the polyimide matrix, as well as by the degree of crosslinking, which increases upon increasing the amount of PVSSQ.[43,87,109]

D. Polyimide–Silica–Titania Nanohybrids

Titania (Ti) is another promising partner for the polymer in hybrid composites that are useful for photonic applications because of its high refractive index. When TiO_2 is obtained by the sol–gel method, however, it is not easy to prepare hybrid composite thin films of Ti with polymers because of the fast hydrolysis reaction and thus the extremely fast gelation of titanium alkoxide. Therefore, only a few studies have been reported that describe polymer–Ti composites. Instead, attempts to form composites

of a polymer with the mixture of silica and Ti have been described.[110–114] For instance, Yoshida and Prasad[112] studied sol–gel-processed Si–Ti–poly(vinylpyrrolidone) composites as optical waveguides. The introduction of small amounts of titania significantly affects the microstructure of the PI–silica hybrid.[114]

Figure 12 displays three-dimensional AFM images of the PI–Si10 binary hybrid composite and the PI–Si–Ti ternary hybrid composites (ST(11)-0.1 g and

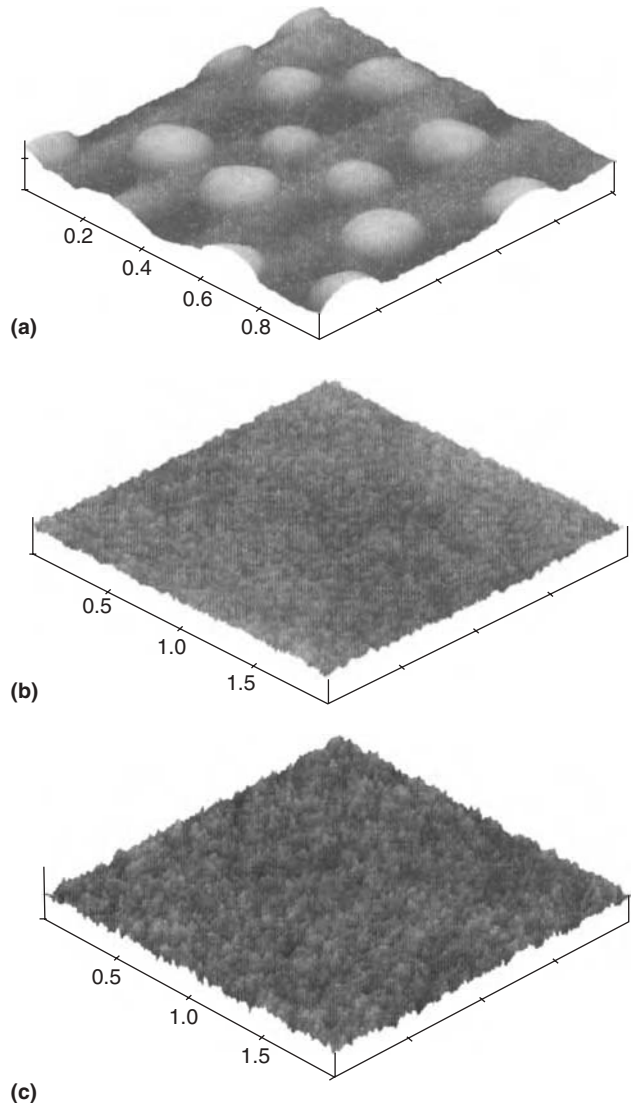

Figure 12 AFM three-dimensional images of PI–Si10 and PI–Si-Ti ternary hybrid composite films with two different ratios of Si to Ti (ST(11) and ST(21)) at constant contents (0.1 g) of the Si–Ti mixture. (Reprinted with permission from Ref. 114; Polymer Society of Korea.)

ST(21)-0.1 g), where ST refers to the mixture of silica and titania and 11 and 21 refer to ratios of Si to Ti of 1:1 and 2:1, respectively. Si particles that have diameters of 30–80 nm were observed in the PI–Si hybrid films when the Si content was 10 wt %, while the size of the Si–Ti particles was reduced significantly, to diameters < ca. 10 nm, in the PI–Si–Ti hybrid films, although the Si and Ti particles are not discernible from one another. Such fine morphologies of the PI–Si–Ti ternary hybrid composites suggests the formation of "nanocomposites," as is often stated for the composites of nanometer-scale inorganic clusters. Careful inspection of Figure 12 shows that the microstructure of the PI–Si–Ti ternary hybrid composite film containing a 2:1 ratio of Si to Ti is finer than that of the composite film containing a 1:1 ratio of these elements. This result implies that nanocomposite formation occurs more preferentially when the amount of Ti in the ternary hybrid composites is smaller than the given amount of Si.

When a small amount of $Ti(OPr)_4$ is added to TEOS, they become transformed to Ti and Si, respectively, by a sol–gel reaction such that small amounts of TiO_2 and SiO_2 particles exist together, as well as possible covalent Si–O–Ti–O–Si network particles, during molecular alignment or orientation of PAA to the PI matrix. Thus such a variety of local structural environment would be expected to give several different characteristic emission peaks. As the amount of Ti is increased, however, the system contains more complex particle systems. Some structures overlapped with others, while some structures retain their own characteristics, depending on the reactivity (relative rate of hydrolysis and condensation during the sol–gel reaction) of the Si–O–Si, Ti–O–Ti and Si–O–Ti–O–Si bonds, as well as the interactions between the PI matrix and the inorganic particles.[114]

The AFM studies have shown that the microstructure of PI–Si–Ti ternary hybrid composite films is much finer when the content of the Si–Ti mixture (ST) is relatively low or when the ratio of Si to Ti is relatively high.[114] Fluorescence behavior also has been observed to depend on the ratio of Si to Ti in the Si–Ti mixture and on the total amount of the Si–Ti mixture. This result can be interpreted as being due to the formation of different local structural environments as the Ti content increases. When the Ti content is small relative to Si, the emission spectra display several separated peaks that represent each of the chemical structural environments.[114]

IV. CONCLUSIONS

In this chapter, we discussed recent progress made in the preparation of organic–inorganic polymer nanohybrid materials that are based on silica or silsesquioxane. We focused on the physical and chemical aspects of incorporating such inorganic components into polymer matrices, the interactions between the components, and their relevant properties.

Among many kinds of polymer-based nanohybrids containing silica- or silsesquioxane-like materials, we highlighted mainly polyimide-based nanohybrids because they are well-known high-performance step-growth polymers that

have unique physicochemical properties, such as high thermal and mechanical stability, controlled dielectric behavior, good adhesion properties, and chemical resistance.

Such organic–inorganic nanohybrids can be used widely in many high-technology applications because they combine the properties of their constituent organic and inorganic materials and possess many additional advanced properties, such as excellent mechanical and thermal stability. They can be used, for example, as biosensors, structural materials, and opto-electronic materials. Thus the study of nanohybrid materials holds great promise for future advances; it demonstrates that converging physical, chemical, and, sometimes, biological approaches can result in the powerful multifunctional tools.

V. ACKNOWLEDGMENTS

The work was supported by the National Research Laboratory Program, MOST, Korea, the Center for Integrated Molecular Systems, and the Brain Korea 21 Project.

VI. REFERENCES

1. Z. Ahmad, J. E. Mark, *Chem. Mater*. **13**, 3320 (2001).
2. C. Sanchez, G. J. de. A. A. Soler-Illia, F. Ribot, T. lalot, C. R. Mayer, V. Cabuil, *Chem. Mater.* **13**, 3061 (2001).
3. J. Wen, G. L. Wilkes, *Chem. Mater*. **8**, 1667 (1996).
4. D. A. Loy, K. Rahimian, in *Handbook of Organic-Inorganic Hybrid Materials and Nanocomposites*, Vol. 1, H. S. Nalwa, ed., American Scientific Publishers, New York, 2003.
5. Y. Gao, N. R. Choudhury, in *Handbook of Organic-Inorganic Hybrid Materials and Nanocomposites*, Vol. 1, H. S. Nalwa, ed., American Scientific Publishers, New York, 2003.
6. R. Laine, C. Sanchez, E. Gianellis, C. J. Brinker, *Mater. Res. Symp. Proc.* **519**, 15 (1998).
7. C. J. Brinker, G. W. Scherer, *Sol-Gel Science: The Physics and Chemistry of Sol-Gel Processing*, Academic Press, San Diego, CA, 1990.
8. L. C. Klein, *Sol-Gel Technology*, Noyes Publications, Park Ridge, NJ, 1988.
9. D. Y. Godovski, *Adv. Polym. Sci.* **119**, 79 (1995).
10. A. D. Pomogailo, *Russ. Chem. Rev*. **69**, 53 (2000).
11. L. H. Sperling, *Interpenetrating Polymer Networks and Related Materials*, Plenum Press, New York, 1981.
12. P. Judeinstein, C. Sanchez, *J. Mater. Chem.* **6**, 511 (1996).
13. U. Schubert, N. Husing, A. Lorenz, *Chem. Mater*. **7**, 2010 (1995).
14. J. E. Mark, J. Premachandra, C. Kumudinie, W. Zhao, T. D. Dang, J. Chen, F. E. Arnold, *Mater. Res. Soc. Symp. Proc*. **435**, 93 (1996).
15. T. Saegusa, Y. Chujo, *Makromol. Chem. Macromol. Symp.* **64**, 1 (1992).
16. Y. Chujo, *Curr. Opin. Solid State Mater. Sci.* **1**, 806 (1996).
17. P. L. Shao, K. A. Mauritz, R. B. Moore, *Chem. Mater.* **7**, 192 (1995).

18. C. J. T. Landry, B. K. Coltrain, B. K. Brady, *Polymer* **33**, 1486 (1992).
19. A. B. Brennan, T. M. Miller, R. B. Vinocur, *Am. Chem. Soc. Symp. Ser.* **585**, 142 (1995).
20. P. Hajji, L. David, J. F. Gerard, J. P. Pascault, G. Vigier, *J. Polym. Sci. B Polym. Phys.* **37**, 3172 (1999).
21. T. Saegusa, Y. Chujo, *J. Macromol. Sci. Chem.* **A27**, 1603 (1990).
22. B. K. Coltrain, C. J. T. Landry, J. M. O'Reilly, A. M. Chamberlain, G. A. Rakes, J. S. Sedita, L. W. Kelts, M. R. Landry, V. K. Long, *Chem. Mater.* **5**, 1445 (1993).
23. Y. Wei, D. Yang, L. Tang, M. G. K. Hutchins, *J. Mater. Res.* **8**, 1143 (1993).
24. Y. Wei, W. Wang, D. Jin, D. Yang, L. Tartakovskaya, *J. Appl. Polym. Sci.* **64**, 1893 (1997).
25. T. Tucker, M. Rakie, C. Spang, J. D. Brennan, *Chem. Mater*. **12**, 3695 (2000).
26. R. Joseph, S. Zhang, W. T. Fard, *Macromolecules* **29**, 1305 (1996).
27. J. O. Kweon, S. T. Noh, *J. Appl. Polym. Sci*. **81**, 2471 (2001).
28. B. Wang, G. L. Wilkes, J. C. Hedrick, S. C. Liptak, J. E. McGrath, *Macromolecules* **24**, 3449 (1991).
29. I. G. Luneau, A. Mosset, J. Galey, H. Schimidt, *J. Mater. Chem.* **25**, 3739 (1990).
30. M. O. Wolf, *Adv. Mater.* **13**, 545 (2001).
31. B. Himmel, T. Gerber, H. Berger, *J. Non-Cryst. Solids* **91**, 122 (1987).
32. U. Schubert, *J. Chem. Soc. Dalton Trans.* 3343 (1996).
33. G. Trimmel, S. Gross, G. Kickelbick, U. Schubert, *Appl. Organomet. Chem*. **15**, 401 (2000).
34. G. Trimmel, P. Fratzl, U. Schubert, *Chem. Mater*. **12**, 602 (2000).
35. M. Moraru, G. Kickelbick, U. Schubert, *Eur. J. Inorg. Chem*. **5**, 1295 (2001).
36. S. Schubert, E. Aprac, W. Glaubitt, A. Helmerich, C. Chau, *Chem. Mater*. **4**, 37, 491 (1992).
37. G. H. Hsiue, W. J. Kuo, Y. P. Huang, R. J. Jeng, *Polymer* **41**, 2813 (2002).
38. G. Li, L. Wang, H. Ni, C. U. Pittman Jr. *J. Inorg. Organo. Polym.* **11**, 3 (2002).
39. J. Choi, J. Harcup, A. F. Yee, Q. Zhu, R., M. Laine, *J. Am. Chem. Soc.* **123**, 11420 (2001).
40. C. Zhang, F. Babonneau, C. Bonhomme, R. M. Laine, C. L. Soles, H. Hristov, A. F. Yee, *J. Am. Chem. Soc.* **120**, 8380 (1998).
41. C. Zhang, R. M. Laine, *J. Am. Chem. Soc*. **122**, 6979 (2000).
42. R. Tanaki, Y. Tanaka, M. Z. Asuncion, J. Choi, R. M. Laine, *J. Am. Chem. Soc.* **123**, 12416 (2002).
43. J. Huang, C. He, Y. Xiuo, K. Y. Mya, J. Dai, Y. P. Siow, *Polymer* **44**, 4491 (2003).
44. T. J. Pinnavaia, G. W. Beall, *Polymer-Clay Nanocomposites*, Wiley, New York, 2000.
45. P. C. L. Baron, Z. Wang, T. J. Pinnavaia, *Appl. Clay Sci*. **15**, 11 (1999).
46. S. S. Ray, M. Okamoto, *Prog. Polym. Sci.* **28**, 1539 (2003).
47. J. Tang, Y. Wang, D. Yu, Z. Zhou, C. Wang, B. Yang, *Mater. Lett.* **50**, 371 (2001).
48. X. Tang, T. Tang, Q. Zhang, Z. Feng, B. Buang, *J. Apply. Polym. Sci*. **83**, 446 (2002).
49. H. Huang, G. L. Wilkes, *Polym. Bull.* **18**, 455 (1987).
50. H. Huang, G. L. Wilkes, *Macromolecules* **20**, 1322 (1987).
51. L. Mascia, A. Kioul, *Polymer* **36**, 3649 (1995).
52. M. Fujita, K. Honda, *Polym. Commun.* **30**, 200 (1989).
53. J. L. W. Noell, G. L. Wilkes, D. K. Mohanty, J. E. McGrath, *J. Appl. Polym. Sci.* **40**, 177 (1990).
54. K. A. Mauritz, R. Ju, *Chem. Mater.* **6**, 2269 (1994).
55. Z. H. Huang, K. Y. Qiu, *Polymer* **38**, 52 (1997).
56. Y. Wei, R. Bakthavatchalam, C. K. Whitecar, *Chem. Mater.* **2**, 337 (1990).
57. C. J. T. Landry, B. K. Coltrain, J. A. Wesson, N. Zumbulyadis, J. L. Lippert, *Polymer* **33**, 1496 (1992).

58. I. K. Varma, A. K. Tomar, *R.* C. Anand, *J. Appl. Polym. Sci.* **33**, 1377 (1987).
59. R. H. Baney, M. Itoh, A. Sakakibara, T. Suzuki, *Chem. Rev.* **95**, 1409 (1995).
60. D. W. Scott, *J. Am. Chem. Soc.* **68**, 356 (1946).
61. T. S. Haddad, J. D. Lichtenhan, *Macromolecules* **29**, 7302 (1996).
62. J. D. Lichtenhan, Y. A. Otonari, M. J. Carr, *Macromolecules* **28**, 8435 (1995).
63. P. T. Mather, H. G. Jeon, A. Romo-Uribe, *Macromolecules* **32**, 1194 (1999).
64. A. Tsuchida, C. Bolln, F. G. Sernetz, H. Frey, R. Mulhaupt, *Macromolecules* **30**, 2818 (1997).
65. A. Lee, J. D. Lichtenhan, *Macromolecules* **31**, 4970 (1998).
66. A. Lee, J. D. Lichtenhan, W. A. Reinerth Sr., *Polym. Mater. Sci. Eng.* **82**, 235 (2000).
67. J. D. Lichtenhan, N. Q. Vu, J. A. Carter, J. W. Gilman, F. J. Feher, *Macromolecules* **26**, 2141 (1993).
68. M. W. Ellsworth, D. L. Gin, *Polym. News* **24**, 331 (1999).
69. T. S. Haddad, R. Stapleton, H. G. Jeon, P. T. Mather, J. D. Lichtenhan, S. Phillips, *Polym. Prepr.* **40**, 496 (1999).
70. K. Kim, Y. Chujo, *J. Polym. Sci. A Polym. Chem.* **41**, 1306 (2003).
71. S. Hong, S. M. Hong, S. S. Hwang, B. C. Kim, *J. Appl. Polym. Sci*. **90**, 2801 (2003).
72. B. M. Nivak, R. H. Grubbs, *J. Am. Chem. Soc*. **110**, 7542 (1998).
73. L. A. Belfiore, M. P. McCurdie, E. Ueda, *Macromolecules* **26**, 6908 (1993).
74. L. A. Belfiore, F. Bosse, P. Das, *Polym. Intl.* **36**, 165 (1995).
75. L. A. Belfiore, M. P. McCurdie, *J. Polym. Sci. B Polym. Phys.* **33**, 105 (1995).
76. L. A. Belfiore, P. Das, F. Bosse, *J. Polym. Sci. B Polym. Phys.* **34**, 2675 (1996).
77. F. Bosse, P. Das, L. A. Belfiore, *J. Polym. Sci. B Polym. Phys.* **34**, 909 (1996).
78. L. A. Belfiore, E. M. Indra, *J. Polym. Sci. B Polym. Phys.* **38**, 552 (2000).
79. G. Odian, *Principles of Polymerization*, 2nd ed., Wiley, New York, 1981.
80. J. M. G. Cowie, *Polymers: Chemistry and Physics of Modern Materials*, 2nd ed., Blackie Academic, Chapman & Hall, New York, 1994.
81. M. K. Ghosh, K. L. Mittal, *Polyimides: Fundamentals and Applications*, Marcel Dekker, New York, 1996.
82. L. H. Sperling, *Introduction to Physical Polymer Science*, Wiley, New York, 1992.
83. C. E. Sroog, *Prog. Polym. Sci.* **16**, 561 (1991).
84. C. Feger, M. M. Khojasteh, J. E. McGrath, *Polyimide: Materials, Chemistry and Characterization*, Elsevier, Amsterdam, 1989.
85. M. Navarre, *Polyimides: Synthesis, Characterization and Applications*, vols. 1–2, Plenum, New York, 1984.
86. H. Lim, Ph.D. dissertation, Pusan National University, Korea, 2002.
87. M. A. Wahab, I. Kim, C. S. Ha, *Polymer* **44**, 4705 (2003).
88. M. Tsai, W. Whang, *Polymer* **42,** 4197 (2001).
89. A. B. Brennan, Ph.D. dissertation, Virginia Polytechnic Institute and State University, 1990.
90. M. Spinu, Ph.D. dissertation, Virginia Polytechnic Institute and State University, 1990.
91. M. Nandi, J. A. Conklin, L. Salviati Jr., A. Sen, *Chem. Mater*. **2**, 772 (1990).
92. M. Nandi, J. A. Conklin, L. Salviati Jr., A. Sen, *Chem. Mater.* **3**, 201 (1991).
93. A. Morikawa, Y. Iyoku, M. Kakimoto, Y. Imal, *Polym. J.* **24**, 107 (1992).
94. Y. Kim, Ph.D. dissertation, Pusan National University, Korea, 1996.
95. A. Kioul, L. Mascia, *J. Non-Cryst. Solids* **175**, 169 (1994).
96. M. A. Wahab, I. Kim, C. S. Ha, *Polymer Prepr.* **41**, 676 (2004).
97. C. S. Ha, H. D. Park, C. W. Frank, *Chem. Mater*. **12**, 839 (2000).
98. M. A. Wahab, C. S. Ha, *Composite Interf.* **10**, 475 (2003).

99. C. Xenopoulos, L. Mascia, S. J. Shaw, *J Mater. Chem.* **12**, 213 (2002).
100. Y. Kim, W. K. Lee, W. J. Cho, C. S. Ha, M. Ree, T. Chang, *Polym. Intl*. **43**, 129 (1997).
101. C. S. Ha, W. J. Cho, *Polym. Adv. Technol*. **11**, 145 (2000).
102. P. Musto, G. Ragosta, G. Scarinzi, L. Mascia, *Polymer* **45**, 1697 (2004).
103. X. Zhang, Z. Zhu, J. Yin, X. Ma, *Chem. Mater*. **14**, 71 (2002).
104. W. C. Chen, S. J. Lee, L. H. Lee, J. L. Lin, *J. Mater. Chem*. **9**, 2999 (1999).
105. Y. Wei, D. Jin, D. J. Brennan, D. N. Rivera, Q. Zhuang, N. J. Dinardo, K. Qiu, *Chem. Mater*. **10**, 769 (1998).
106. Y. Kim, E. Kang, Y. S. Kwon, W. Cho, C. Cho, M. Chang, M. Ree, T. Chang, C. S. Ha, *Synth. Metal*. **85**, 1399 (1997).
107. Y. Chen, J. O. Iroh, *Chem. Mater*. **11**, 1218 (1999).
108. C. J. Cornelius, E. Marand, *Polymer* **43**, 2385 (2002).
109. M. A. Wahab, I. Kim, C. S. Ha, *J. Polym. Sci. A Polym. Chem*. **42**, 5189 (2004).
110. Y. Yong, Y. Li, F. Xie, M. Ding, *Polym. Intl*. **49**, 1543 (2000).
111. M. Yoshida, M. Lai, D. N. Kumer, P. N. Prasad, *J. Mater. Sci*. **2461**, 4047 (1997).
112. M. Yoshida, P. N. Prasad, *Chem. Mater*. **8**, 235 (1998).
113. P. L. Shao, K. A. Mauritz, R. B. Moore, *J. Polym. Sci. B Polym. Phys*. **34**, 873 (1996).
114. H. D. Park, K. Y. Ahn, M. A. Wahab, N. J. Jo, I. Kim, C. S. Ha, *Macromol. Res*. **11**, 172 (2003).

CHAPTER 7

Siloxane Elastomers and Copolymers

Sakuntala Chatterjee Ganguly

Sakchem Consultant, Mowbray Tasmania Australia; Polymer Science Group, Ian Wark Research Institute University of South Australia, the Level Campus Mawson Lakes, Adelaide, South Australia, Australia

CONTENTS

Macromolecules Containing Metal and Metal-Like Elements, Volume 4: Group IVA Polymers, edited by Alaa S. Abd-El-Aziz, Charles E. Carraher Jr., Charles U. Pittman Jr., and Martel Zeldin
ISBN: 0-471-68238-1

Part 1. Siloxane-Divinylbenzene Copolymers as Elastomers

I. INTRODUCTION

Silicon polymers, especially poly(dimethylsiloxane) (PDMS)-based polymers, are of interest to many research groups due to their high thermal stability, hydrophobicity, radiation stability, and applications over a wide temperature range (from −55°C to +180°C).[1–4] Silicone rubbers are specialty synthetic elastomers that have an excellent market worldwide because of their outstanding properties, such as chemical and thermal resistance, constant mechanical properties over wide temperature range, low temperature flexibility, sealing capability, and electrical performance. Furthermore, compared to organic rubbers, silicone rubbers are resistant to ozone, corona, weathering, and radiation. In addition, silicone rubbers offer outstanding biocompatibility and can be used for health care and pharmaceutical applications.

Attempts have been made by numerous research groups to offer better and relatively low cost synthetic procedures for the preperation of organic–inorganic hybrid-based silicone rubbers. Part 1 reviews the trends in the development of silicone rubbers and classifies these materials in terms of the reaction process used for crosslinking.

A. Silicone Elastomers by Radical Polymerization

High molecular weight silicone rubber may be formed by free-radical crosslinking of poly(dialkylsiloxane).[5–7] Curing proceeds heating the poly(dimethylsiloxane) with benzoyl peroxide at 150°C in the absence of air or at 250°C for 4 h in air (Scheme 1). The silicone rubbers prepared in this manner are useful at high and low temperatures, at which organic rubbers are problematic.

It has been reported that the dimethyl silicone rubber remains flexible at temperatures as low as −60°C. Partial substitution of methyl groups by phenyl groups extends the low temperature performance to −93°C due to steric hindrance of the polymer chains. Such phenyl silicone rubbers are typically used in aerospace applications at low temperatures. Crosslinking of poly(methylvinylsiloxane) is accomplished

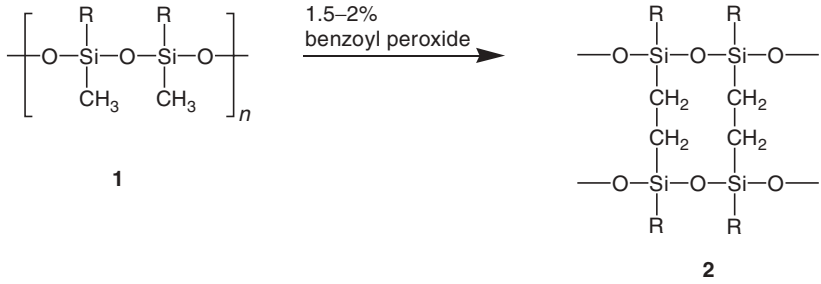

1 **2**

Scheme 1 Silicone rubber by free-radical coupling crosslinking of poly(dimethylsiloxane).

by the radical-initiated coupling reaction of two vinyl groups[8] (Scheme 2) or the vinyl group of a polymer with the methyl group on a solid silicone surface (Scheme 3).[9]

A silicone rubber may also include more than one side group, allowing for different properties. For example, a polymer containing phenyl and vinyl groups would exhibit improved crosslinking as well as low temperature flexibility.

Fluorosilicones contain polar trifluoropropyl side groups. The advantage of fluorosilicone rubbers is their excellent resistance to both oils and fuels. Moreover,

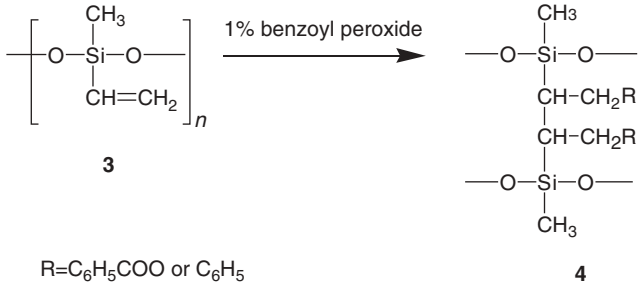

3 **4**

Scheme 2 Silicone rubber by radical crosslinking of poly(methyl vinylsiloxane).

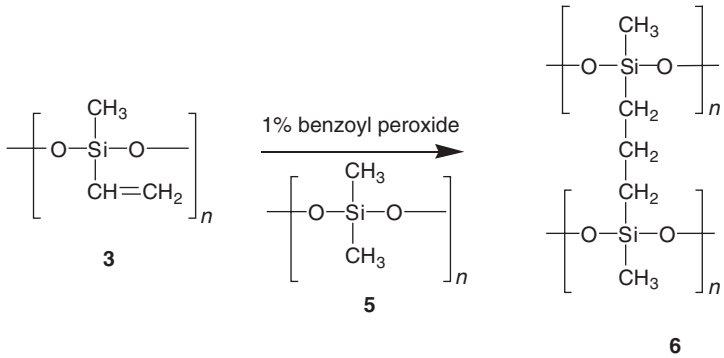

3 **5** **6**

Scheme 3 Silicone rubber by crosslinking of poly(methyl vinylsiloxane) with poly(dimethylsiloxane) by radical coupling.

these rubbers can be used over a wide temperature range from −73°C to 204°C and are resistant to harsh chemical environments. Unfortunately, at higher temperatures fluorosilicone rubbers may transform into highly corrosive hydrofluoric acid. Furthermore, fluorosilicones cannot be used with phosphate hydraulic fluids or in situations of excessive mechanical stress. Scheme 4 represents the synthesis of fluorinated organosiloxane rubber.[10]

The synthesis of a siloxane–styrene copolymer by ring-opening polymerization of a cyclic siloxane in the presence of a styrene radical that is generated by nitroxide and bromine was recently reported.[8,9] With the advancement of controlled free-radical polymerization (CFRP), block copolymers of varying architecture can be prepared. Pollack et al.[11] have synthesized a styrene–siloxane diblock copolymer (Scheme 5) using the hydrolyzed (R = OH) form **9** of Hawkers initiator[12] **8** which was lithiated

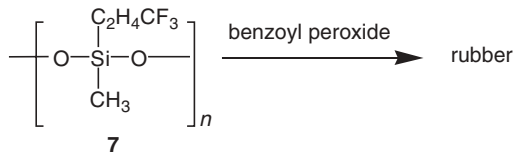

Scheme 4 Silicone rubber from fluorinated organosiloxane by radical coupling.

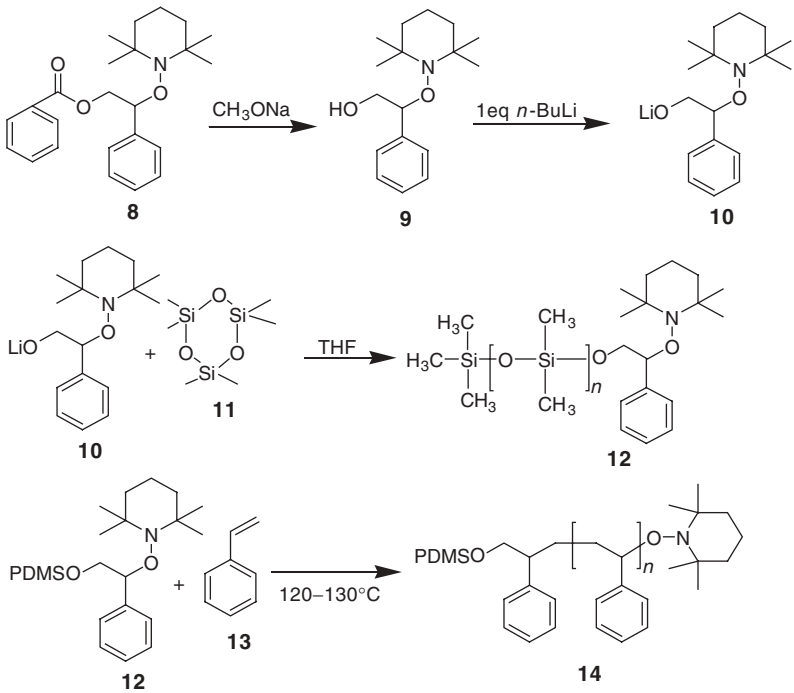

Scheme 5 Silicone rubber from siloxane–styrene copolymers via nitroxide-mediated radical polymerization.

using *n*-BuLi to an anionic initiator **10** for the ring opening polymerization of cyclosiloxane **11**. This reaction gave a polydimethylsiloxane derivative of nitroxide-mediated catalyst. Polymer **12** undergoes nitroxide-mediated free-radical polymerization with styrene **13**, resulting in poly(styrene-*b*-dimethylsiloxane) copolymer **14**. It is noteworthy to mention that copolymers rich in styrene are brittle white solids, and those rich in PDMS range from pourable white liquids to pasty white rubber-like materials.

B. Synthesis of Silicone Elastomers by Combining Radical Polymerization and Hydrosilation

Oligomeric dimethyldisiloxanes **15** when reacted with vinyl-containing dimethylsiloxanes **16** gives copolymers with the vinylsiloxyl group, which in the presence of methylstyrene **17** and chloroplatinic acid gives a silicone rubber **18** (Scheme 6).[13]

Kok et al.[14] modified the divinylbenzene (DVB) monomer with dimethylsiloxane by a hydrosilation reaction to obtain flexible prepolymers **21, 22, 23** (called DST) (Scheme 7). In this reaction, the value of *n* varies from 1 to 8. The monomers were further copolymerized with DVB through radical polymerization.

Additional work in this area has been carried out by Hill et al.[15,16] They suggested that if a second polymer radical is added to DST, a crosslink will be formed, which will ultimately cause the formation of a gel network due to the Trommsdorf effect. Accordingly, the prepolymer chain length controlled the free-radical termination reaction and resulted in materials with desirable properties. A large variety of products with commercial applications were thus obtained.

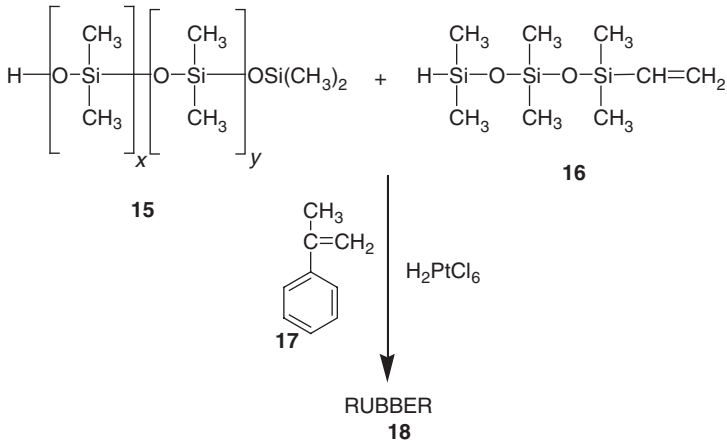

Scheme 6 Silicone rubber 18 by copolymerization of an oligomeric dimethylsiloxane 15 with a vinyl-containing siloxane 16 and styrene-based monomer 17 using chloroplatinic acid.

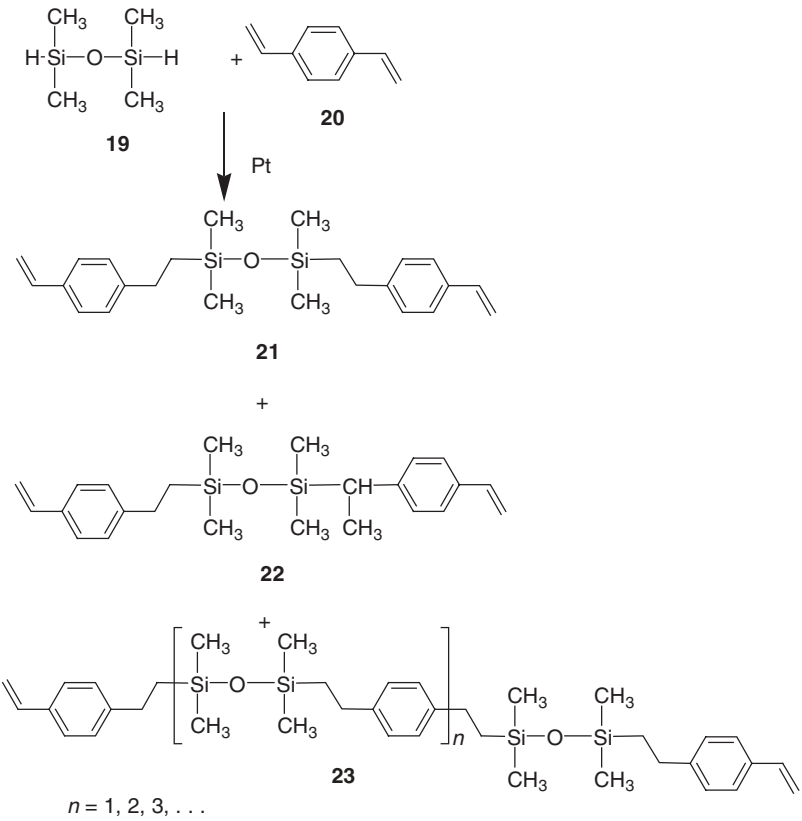

Scheme 7 Siloxane-modified divinylbenzene telomer and octamer before copolymerization with styrene and divinyl benzene to give a silicone rubber.

C. Synthesis of Silicone Elastomers by Polycondensation Reaction

As shown in Scheme 8, condensation can take place by the reaction of terminal OH groups of poly(dimethylsiloxane) with tri-**21** or tetraalkoxy-**22** silane monomers or with polyalkoxysilanes in the presence of a catalyst such as dibutyltin dilaurate or tin octanoate, which are colorless and pourable. The products from these reactions are white or beige, room temperature–vulcanized two-component system (RTV-2) silicone rubbers.[17] Polyalkoxy silane undergoes similar reaction with poly(dimethylsiloxane) to give RTV-2 silicone rubber. The reaction is isothermal and a volatile alcohol forms from the corresponding alkoxy groups.

Alcohol volitilization, unfortunately, causes a loss of mass and shrinkage of the cured rubber. Moreover, curing reactions are inhibited by the presence of

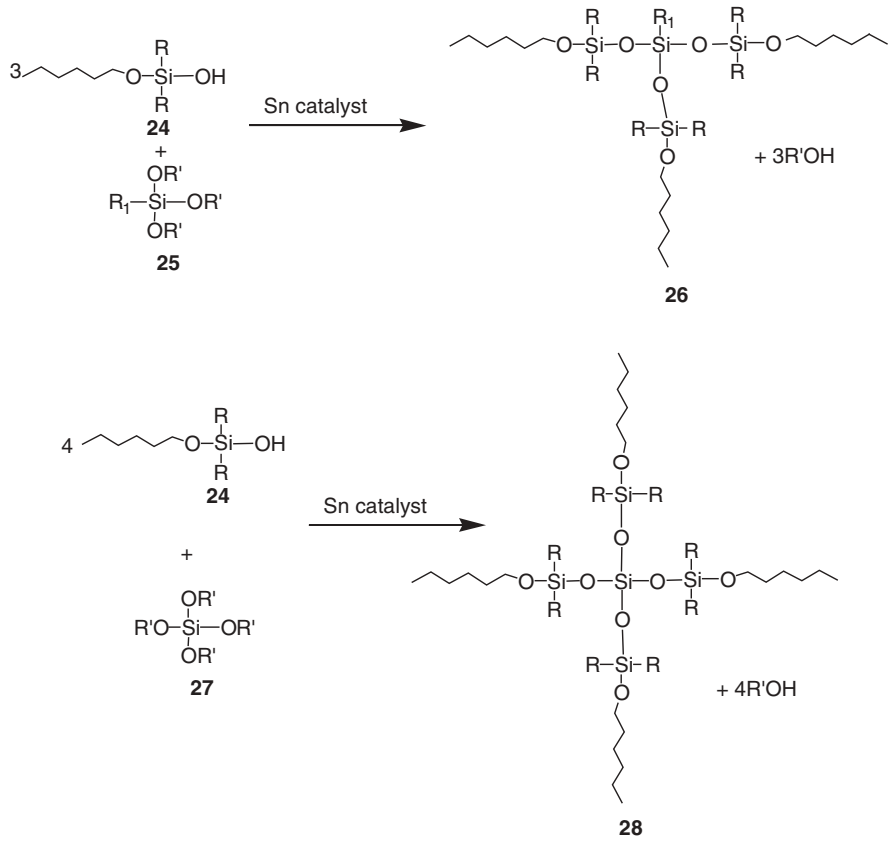

Scheme 8 Siloxane polycondensation curing for RTV silicone rubber systems.

moisture in the polymer, which reacts with the alkoxy groups at temperatures exceeding 90°C.

RTV-2 silicone rubbers were invented in the 1950s as useful materials for forming flexible negative molds. The characteristic features of RTV-2 rubbers are their excellent release properties, short-term thermal resistance to 350°C, minimal environmental effects, easy processing, and high elasticity. Scheme 9 represents the CAChe representation of a model RTV-2 silicone rubber segment.

D. Synthesis of Silicone Elastomers by Side-Chain and Main-Chain Hydrosilation Reactions

Side-chain hydrosilation is a reaction between a main-chain Si-H functional group of poly(1,3,3-trimethylsiloxane) and the vinyl group of a vinylmethyl-siloxy-containing polymer in the presence of a Pt-based catalyst[18] (Scheme 10).

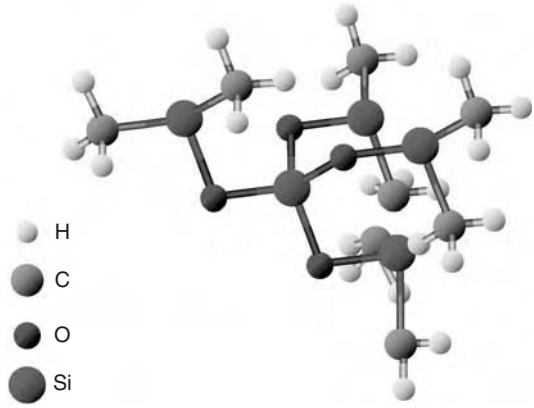

Scheme 9 CAChe representation of model RTV-2 silicone rubber segment.

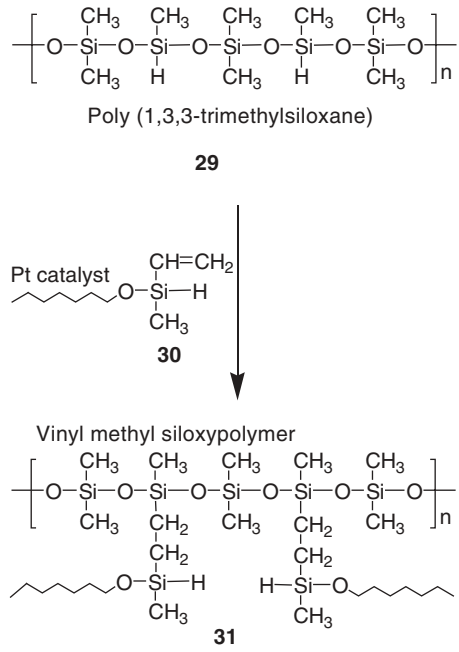

Scheme 10 Side-chain crosslinking of vinyl methyl siloxy polymers with poly-(1,3,3-trimethylsiloxane).

An alternative polymer synthesis has been carried out in our laboratory (isomeric forms **33** and **34**) (Scheme 11) using tetramethyldisiloxane (TMDS) and DVB.[19] The special feature of the new polymer is that there are no weak Si–O–C linkages, which generally undergo degradation resulting in the formation of Si-OH bonds. Scheme 12 is a CAChe representation of a poly(tetramethyldisiloxane-divinylbenzene) model segment.

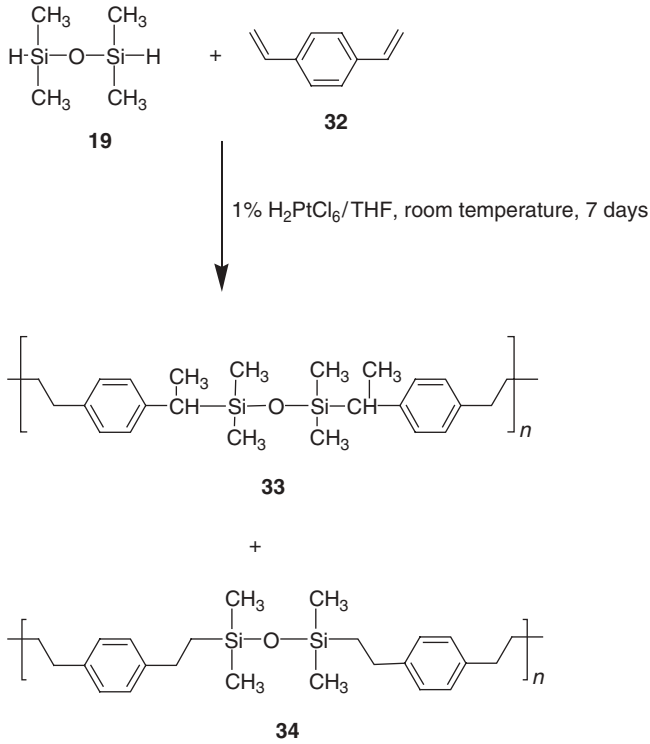

Scheme 11 Synthesis of mixed isomeric structures of 33 and 34 of poly-(tetramethyldisiloxane-divinylbenzene) by main-chain hydrosilation reaction.

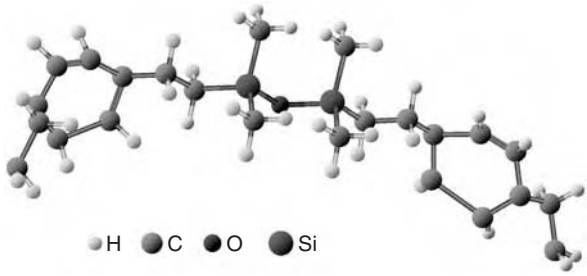

Scheme 12 CAChe representation of model poly(tetramethyldisiloxane-divinyl benzene) segment.

II. EXPERIMENTAL SECTION

A. Materials and Instruments

Platinum(0)-1,3-divinyl-1,1,3,3-tetramethyldisiloxane (Karstedt catalyst) in xylene and hexachloroplatinic acid (40 wt % Pt) as a 1% solution in THF was purchased from Aldrich chemical. 1,1,3,3-Tetramethyldisiloxane (Aldrich) was used without further purification. Divinylbenzene 960 (DVB), which is a mixture of 96% divinylbenzene (meta and para isomers) was purified from the phenolic inhibitor by stirring with 5% by weight basic alumina until the TLC showed the complete removal of inhibitor. The alumina was filtered using Whatman GF/F (0.7 μm). THF was distilled using benzophenone ketyl under a nitrogen atmosphere.

The ^{1}H- and ^{13}C-NMR spectra were recorded on a Varian Gemini Fourier Transform NMR Spectrometer at 200 Mhz and 50 Mhz, respectively. IR spectra in KBr were taken with a single-beam Nicolet Magna Model 750 spectrometer in the 4000–650 cm^{-1} region. The GPC was carried out with a Waters 2690 separation module with a 410 refractive index detector. Toluene was used as the mobile phase and measurement of molar mass was determined relative to polystyrene standards. Thermogavimetric analyses of the samples were conducted using a SDT-2960 Simultaneous DTA-TGA thermal analyzer from room temperature to 1000°C at a heating rate of 10°C/min under an atmosphere of either nitrogen or oxygen at a flow rate of 100 mL/min. The same instrument has the facilities for isothermal degradation studies. The mass loss of PTMDS-DVB was observed over 24 h at 180°C, 200°C, and 250°C under a oxygen and nitrogen atmosphere. Platinum crucibles of identical diameter were used in each experiment.

B. Synthesis of Poly(tetramethyldisiloxane-divinylbenzene) (PTMS-DVB)

In a dried flask, purified DVB (13.0 g, 0.10 mol) was dissolved in 30 mL of dry THF and stirred well with a catalytic amount of Pt(0) catalyst, Karstedt catalyst, or H_2PtCl_6 for 15 min under a nitrogen atmosphere. 1,1,3,3-Tetramethyldisiloxane (13.7 g, ~0.1 mol) in dry THF was added slowly over a 30-min period. The reaction was stirred for 2–4 days until a gel was observed. Using H_2PtCl_6, a white mass (24.6 g) was obtained, and using the Karstedt catalyst, a yellow mass (25.7 g) was obtained.

III. RESULTS AND DISCUSSIONS

The polymer synthesis was carried out in dry toluene, xylene, or THF as the solvent. THF was the preferred solvent owing to its polar nature and low boiling point. The completion of polymerization was confirmed by the formation of an insoluble but swollen product in THF. To complete the polymerization, it took 2 days using H_2PtCl_6 as a catalyst and 4 days using the Karstedt catalyst. Although the polymer

was insoluble in THF, it was soluble in toluene, chloroform, and dichloroethane. The molecular weight of the polymer was 84,600.

The FT-IR spectrum of PTMS-DVB shows absorption peaks at 1049 cm^{-1} (Si–O–Si stretching), 816 cm^{-1} (CH_3 rocking), and 2881 cm^{-1} (CH_3 stretching), which are attributed to the tetramethyldisiloxane unit in the copolymer. The stretching frequencies at 2949 cm^{-1}, 1450 cm^{-1}, and 1246 cm^{-1} are characteristics of Si–C bond in the polymer. The ^{1}H-NMR spectrum of poly(tetramethyldisiloxane-co-divinylbenzene) in $CDCl_3$ had signals at 7.2–6.9 ppm (Ar**H**), 2.6 ppm (Si–CH_2–**CH_2**–Ph), 1.4 ppm (Si–CH(**CH_3**)Ph), 0.88–0.96 ppm (Si–**CH_2**–CH_2–Ph), and 0.1 ppm (Si–**CH_3**). The ^{13}C–NMR spectrum had salient signals at 144.9 (Ar**C**), 128.4 (vinyl **C**), 31.2 (Si–C(**CH_3**)Ph) 29.4 (Si–**C**(CH_3)Ph), 20.4 (Si–CH_2–**CH_2**–Ph), 14.5 (Si–**CH_2**–CH_2–Ph) and 0.18 (Si–**CH_3**) ppm, all supportive of the proposed polymer structure.

The TGA and DTA curves of the polymer in oxygen (Fig. 1) and in nitrogen (Fig. 2) show that the polymer was initially more stable in a nitrogen atmosphere. In an oxygen atmosphere, the DTA curve showed two exothermic peaks at 456°C and 571°C, which corresponded to weight losses of 30% and 84% (maximum), respectively. A silica residue was observed in the Pt reaction pan.

In general, the polymer was thermally stable. However, under nitrogen, the mode of degradation is unclear, as the DTA curve is a straight line relative to that under oxygen. Under nitrogen, the TGA curve of the polymer indicates a major degradation at ~500°C. Generally, the polymer appears to be more stable under oxygen.

Figures 3 and 4 show the isothermal thermogravimetric curves of the polymer under nitrogen and oxygen, respectively. The mass loss of the samples were observed over 24 h at 180°C, 200°C, 220°C, and 250°C. At 250°C, a 60% weight loss takes place under oxygen, whereas a 22.5% weight loss takes place under nitrogen.

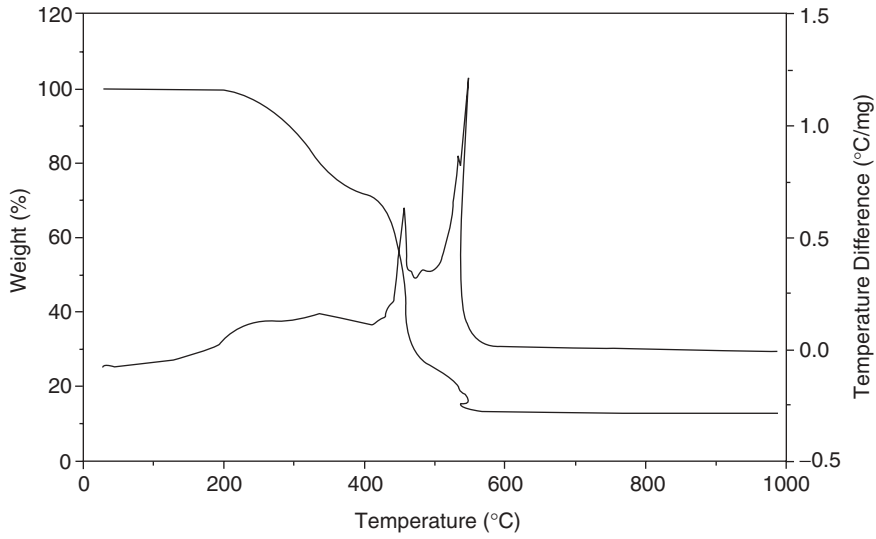

Figure 1 TGA and DTA curves of polymer in oxygen.

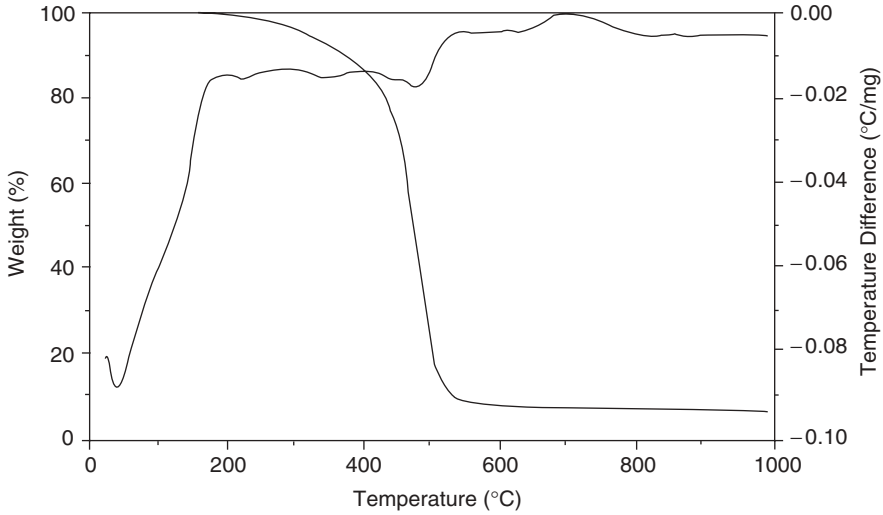

Figure 2 TGA and DTA curves of polymer in nitrogen.

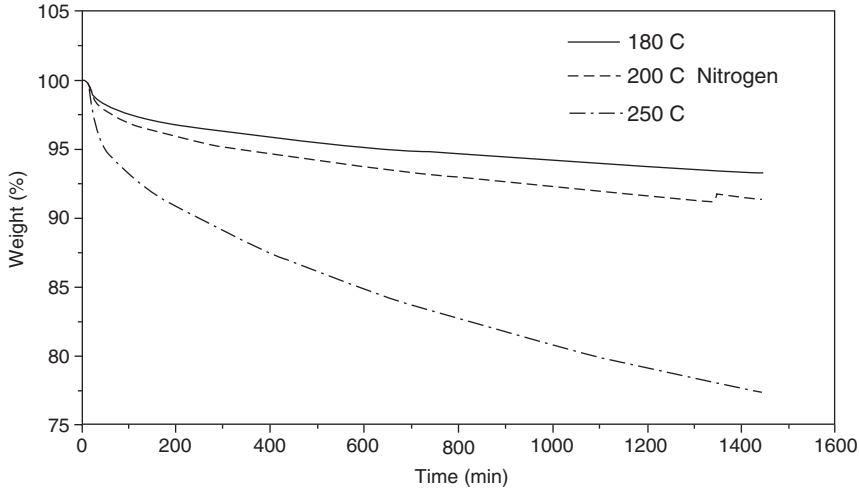

Figure 3 Isothermal thermogravimetric curves of the polymer under nitrogen.

At 180°C and 220°C under nitrogen, a 5–7% maximum weight loss takes place; under oxygen, a 25–30% maximum weight occurs. In addition, isothermal thermogravimetry reveals that the thermal degradation is a first-order reaction.[20,21]

The DSC thermogram of PTMDS-co-DVB (Fig. 5) shows one T_g at −50°C and one at ~160°C, which agrees well with the work of Feng et al.[22]

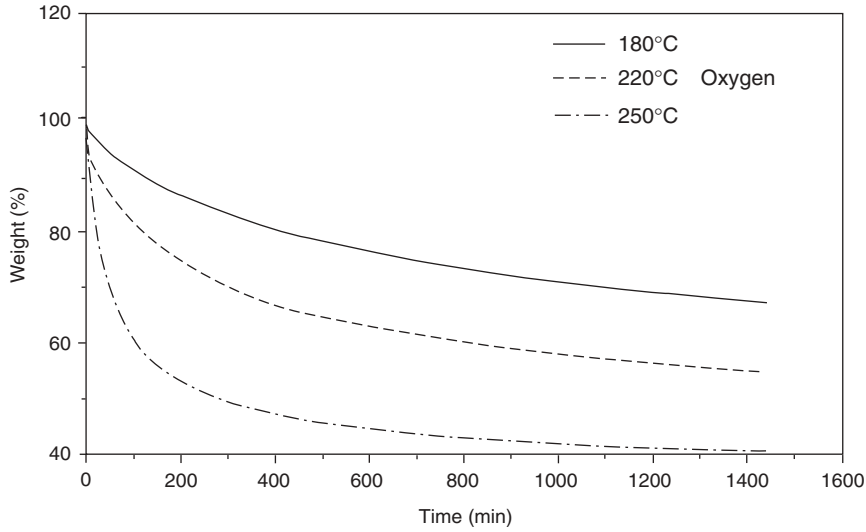

Figure 4 Isothermal thermogravimetric curves of polymer under oxygen.

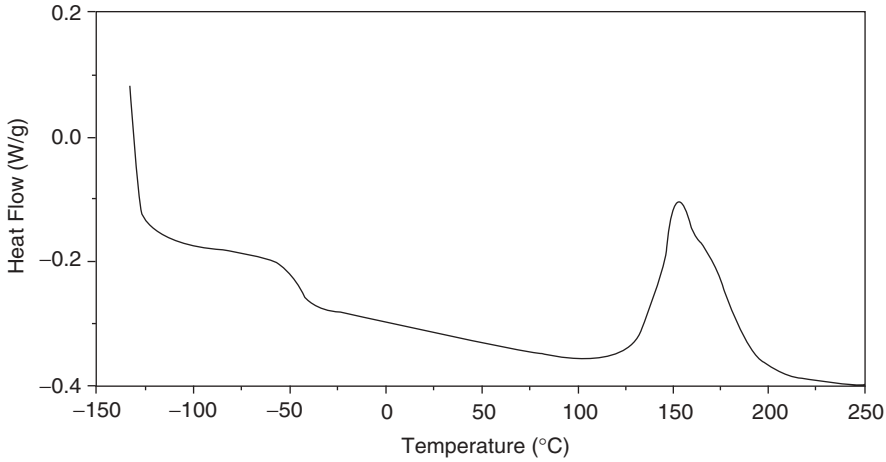

Figure 5 DSC thermogram of PTMDS-DVB.

IV. CONCLUSIONS

This section reports a room temperature, one-step hydrosilation reaction for the synthesis of a siloxane-vinylbenzene hybrid copolymer. This process supersedes other thermal polymerization methods used for vinyl monomers. An alternating ABAB-type polymer from TMDS and divinyl monomers provides a route to a wide variety of Si-based materials that are thermally stable in the oxygen free atmosphere

of space. Other important potential applications are in the sporting goods, toy and decorative furniture industries.

Part 2. Polyviologen and Siloxane-Based Polyviologen Copolymers

I. INTRODUCTION

Viologen dyes or bipyridylium dyes (Scheme 13) are a group of organic compounds based on two linked pyridine rings, which are known as paraquat and diquat. These compounds play a significant role as agricultural herbicides and are generally used as nonselective weed killers. The pyridine rings interfere with the photosynthesis of nonwoody plants, thereby inhibiting their electron-transport system and damaging chloroplasts and other cell components. The viologen dyes, as herbicides, are useful but highly toxic to animals, and their use is strictly controlled.

Attempts have been made to synthesize ionic polymers based on polyviologen[23] or quaternary ammonium salts as lateral substituents.[24] Polymeric coatings that present sustainable microorganism (i.e., bacteria, fungi, algae) free surfaces are of great importance in today's industries (e.g., food manufacturing, biomedical devices, sanitary equipment, outdoor or marine paints).

Kollmeier[25] reported the surfactant properties of siloxane-containing cationic and anionic species. The advantages of combining polyviologen and polysiloxanes have been the subject of many investigations. It is expected that such hybrids would improve coating materials. This section reports some of the major developments in the field of novel viologen and siloxane-viologen copolymers. The aim is to combine these two important classes of polymers, polysiloxanes, and polyviologen in the main chain by making an alternating copolymer. The copolymers are expected to be particularly useful in the packaging and food industries.

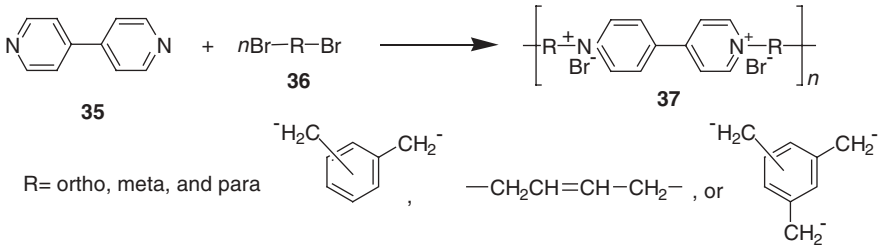

Scheme 13 Aromatic polymer containing 4,4′-bipyridinium salts.

A. Polyviologen Based on 4,4′-Bipyridinium Salts

Aromatic polymers that contain 4,4′-bipyridinium salts can be easily reduced (Scheme 14) to a dark purple radical cation.[26] These polyviologens belong to the class of ionic polymers called ionenes. These so-called polyviologens have extremely low cationic redox potentials.[27]

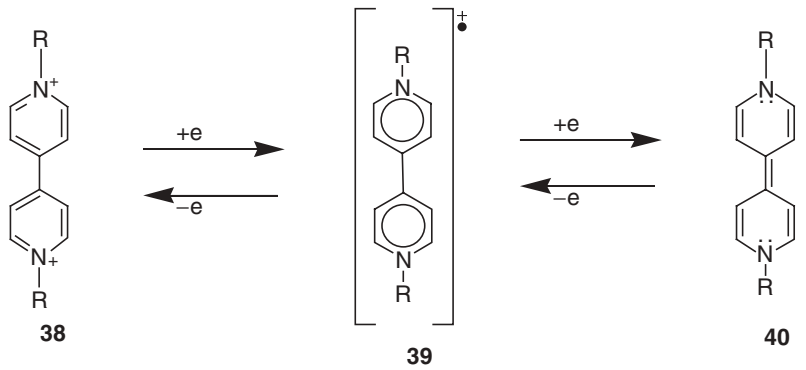

Scheme 14 The first reduction forms a deep violet radical cation; the second reduction forms a neutral red 1,1′-dialkyl-1,1′-dihydro-4,4′-bipyridyl.

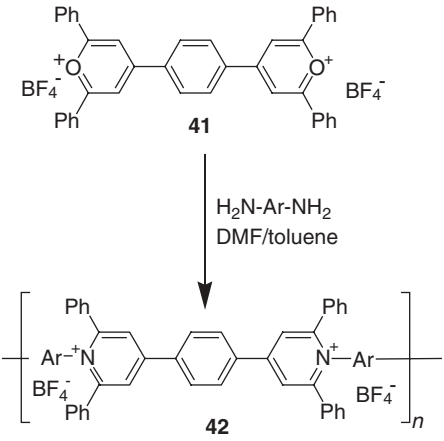

Scheme 15 Synthesis of poly(pyridium tetrafluoroborate)s(PPS).

B. Miscellaneous Polyviologens

Harris and coworkers[28–30] reported the synthesis of the monomer 4,4′-(1,4-phenylene)bis(2,6-diphenyl-pyrylium tetrafluoroborate) **41** and a novel class of high molecular weight poly(pyridinium tetrafluoroborate)s **42** salts (PPS) (Scheme 16). These phenylated heterocyclic polymers are well known for their excellent solubility in organic solvents, film-forming ability, thermal stability, ionic conductivity, ion-exchange membrane formation, and chemical stability.

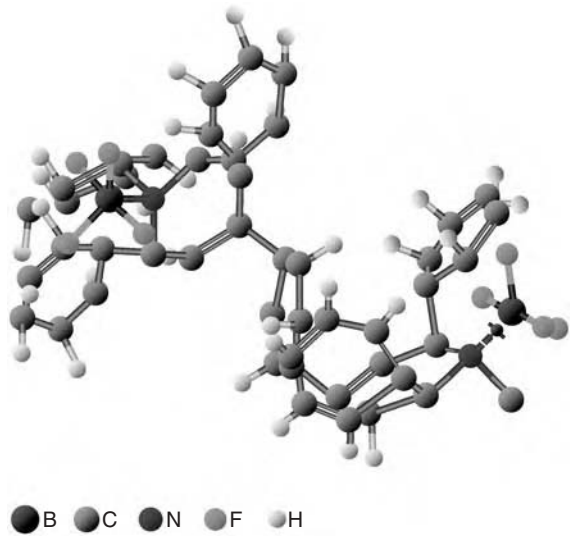

Scheme 16 CAChe representation of a PPS segment.

Beside their wide range of traditional applications, PPSs undergo dramatic changes in color and decrease in viscosity when exposed to UV light in amide solvents.[31,32] The highly colored radical cation, which forms from PPS in the presence of amide groups due to photoreduction, transforms into the original PPS by oxidation. The Harris group has been able to tune the photochromic behavior by changing the substituents on the PPS molecule.

Kamogawa and coworkers[33–35] reported a color change displayed by films of poly(*N*-vinyl-2-pyrrolidone) that contain aryl viologens and films of copolymers that contain *N,N*-dimethylacrylamide with vinyl viologen. Abruna and Bard[36] and Burgmayer and Murry[37] studied electrode films of viologen polymers, which have been prepared from preformed polymers **43** and **44** (Scheme 17). Thus electrode

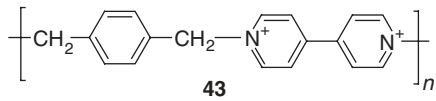

43

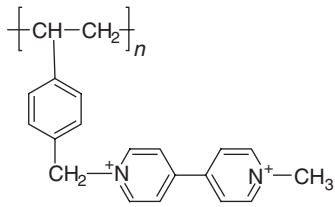

44

Scheme 17 Electrode films of viologen polymers prepared from preformed polymers **43** and **44**.

films of viologen polymers[38] can be obtained in two ways: (1) dip or spin coating of redox polymers and (2) electropolymerization, where viologens are attractive as an electron acceptor on the surface electrode in a photo-electrochemical process.

C. Modified Route to Pyridino-Terminated Oligo(dimethylsiloxane)[30]

A modified route to prepare oligo(dimethylsiloxane)s (ODMS) with pyridino-termination **48** at one chain end was investigated by Aoyagi et al.[39] In the first step, *p*-chloromethylphenyl (CMP)-terminated ODMS (CMP-ODMS) **47** was obtained. The chloromethyl group was easily quaternized by reaction with a pyridine derivative (Scheme 18). A CAChe representation for the pyridinio-terminated ODMS polymer is shown in Scheme 19.

An interesting feature of this polymer is its ability to act as a transdermal penetration enhancer. For example, the penetration profiles of indomethacin, a model

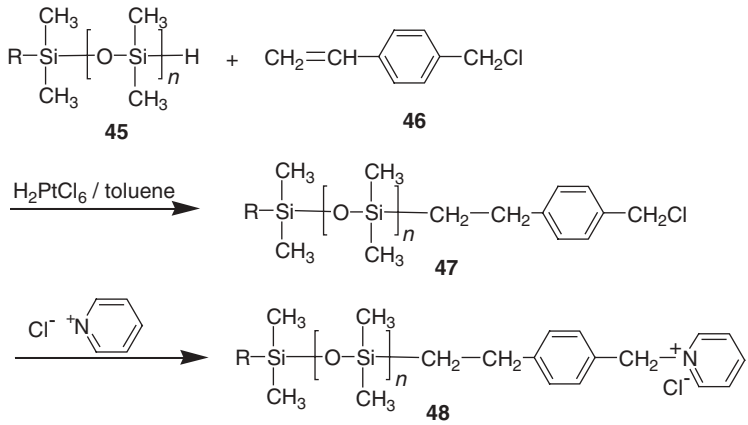

Scheme 18 The reaction scheme for the formation of CMP-ODMS **47** and the corresponding pyridino-terminated ODMS **48**.

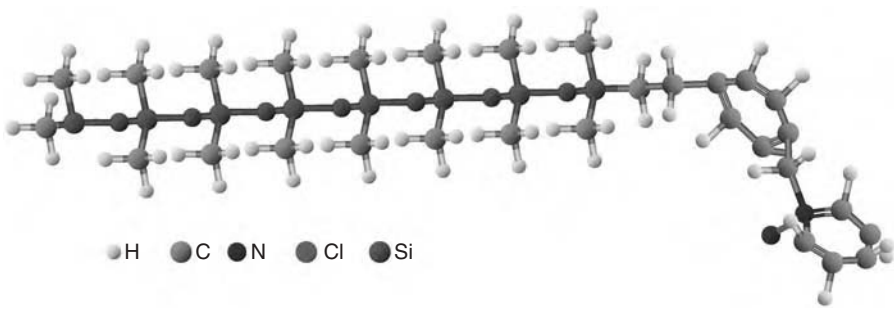

Scheme 19 CAChe representation of a pyridino-terminated ODMS structure.

drug, through the rabbit abdominal skin have been improved by the presence of pyridino-terminated ODMS.

D. Alternate Viologen Polymers from Vinylbenzyl Chloride-Modified Tetramethyldisiloxane and 4,4′-Bipyridine

Chatterjee Ganguly et al.[40] reported the two-step synthesis of viologen-TMDS from tetramethyldisiloxane (Scheme 20). In the first step, two isomers **51** and **52** of

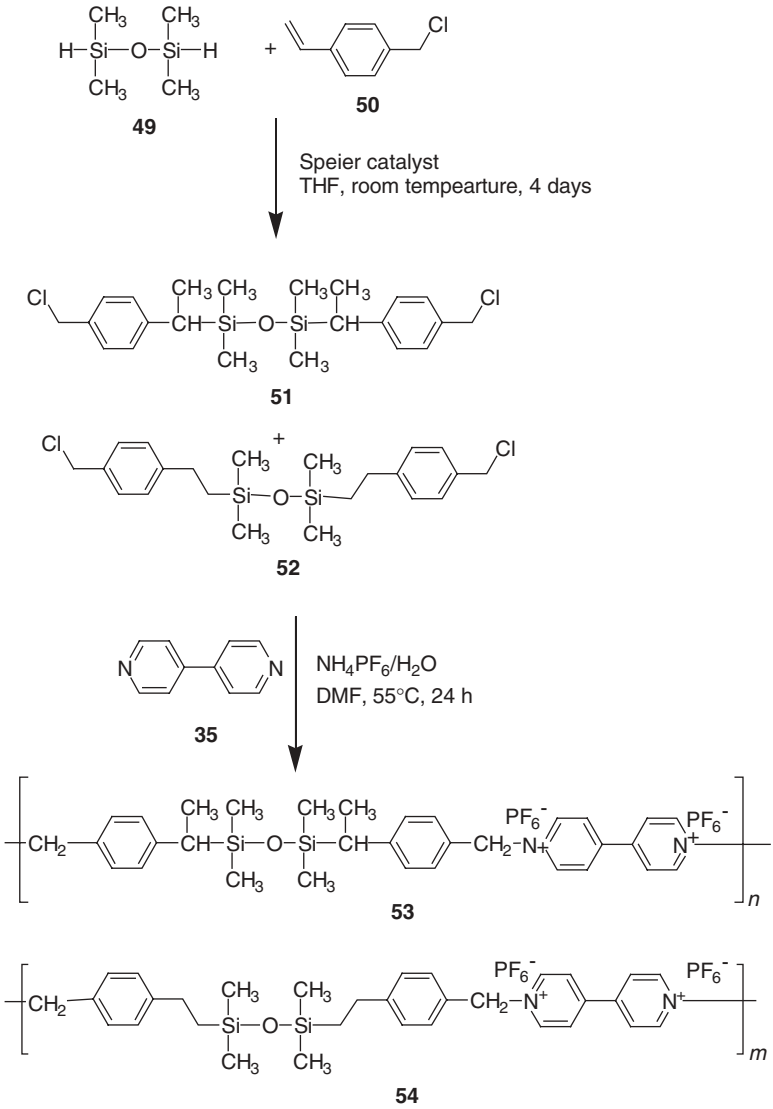

Scheme 20 Two-step synthesis of viologen polymer from vinylbenzyl chloride-modified tetramethyldisiloxane and 4,4′-bipyridine.

bis-(4-chloromethylphenylethyl)tetramethyldisiloxane (BCTD) were synthesized from tetramethyldisiloxane and vinylbenzyl chloride monomer in the presence of Pt(0) catalyst. BCTD was further reacted with 4,4′-bipyridine in dry DMF under a nitrogen atmosphere to give alternating viologen–TMDS copolymer of isomeric structures **53** and **54**. A CAChe representation for an alternating copolymer segment is shown in Scheme 21.

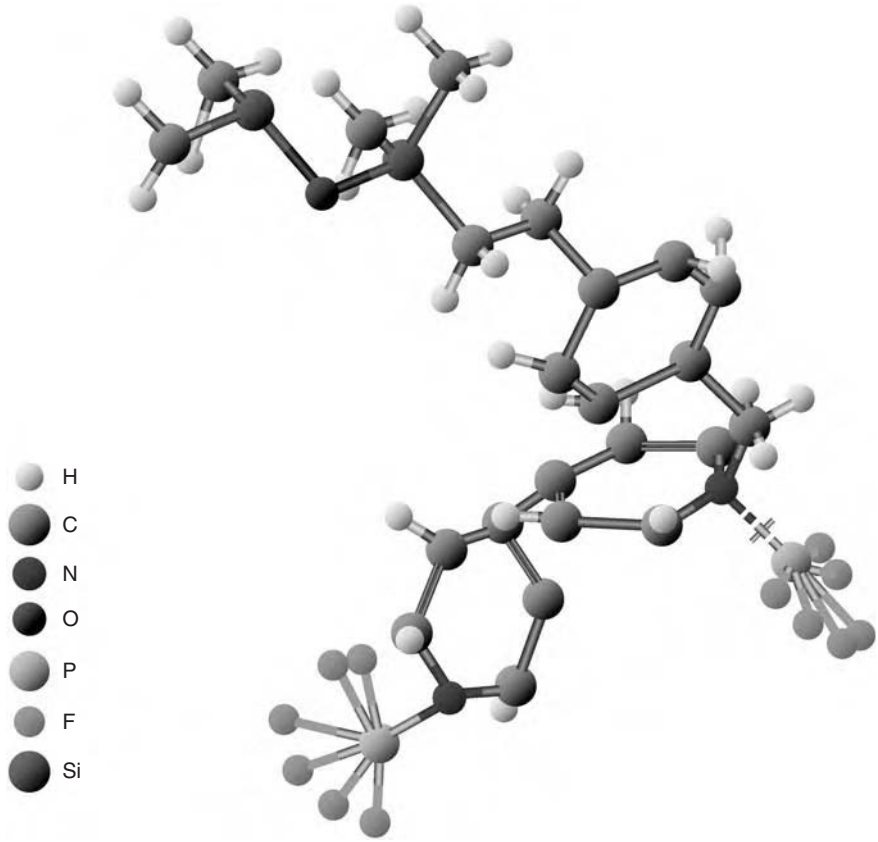

Scheme 21 CAChe representation of a viologen-TMDS copolymer segment.

II. EXPERIMENTAL SECTION

A. Materials and Instruments

Chloroplatinic acid (Sigma, 40 wt % Pt) as a 1% solution in THF was obtained from Aldrich chemical. 1,1,3,3-Tetramethyldisiloxane, vinylbenzyl chloride, ammonium hexafluorophosphate, and 4,4′-bipyridine were obtained from Aldrich chemicals and used without further purification.

DRIFT spectra were obtained with a single-beam Nicolet Magna Model 750 spectrometer in the 4000–650 cm^{-1} region using a MCT-A liquid nitrogen cooled detector. The ^{1}H-NMR spectra were recorded on a Varian Gemini Fourier Transform NMR Spectrometer at 200 MHz. Thermogavimetric analysis (TGA) of samples were conducted with an SDT 2960 Simultaneous DTA-TGA thermal analyzer from room temperature to 1000°C at a heating rate of 10°C/min. The TGA analyses were carried out under an atmosphere of either nitrogen or oxygen at a flow rate of 100mL/min. Platinum crucibles of identical diameter were used in each experiment.

B. Synthesis of Bis(4-chloromethylphenyl)-tetramethyldisiloxane (BCTD)

In a dry flask, purified vinylbenzyl chloride monomer (15.26 g, 0.10 mol) was dissolved in dry THF (30 mL) and well stirred with a catalytic amount of H_2PtCl_6 (Speier catalyst) for 15 min. 1,1,3,3-Tetramethyldisiloxane (27.4 g, 2 mol) in dry THF was added over a 30-min period. The reaction mixture was stirred for 2–4 days until a solid mass was observed. The product was pale yellow viscous oil, which solidified to a sticky mass; yield, 98%.

C. Synthesis of Viologen Polymer from BCTD and 4,4′-Bipyridine

In a dry three-necked flask, BCTD (6.59 g, 1 mmol) was stirred with dry DMF (50 mL) under nitrogen for 30 min. The flask was heated to 55°C and 4,4′-bipyridine (3.26 g, 2 mmol) in dry DMF (20 mL) was added dropwise over a 10-min period. The reaction mixture was refluxed for 24 h. The solvent was removed under vacuum, and the product was washed with dry methanol three times. The orange solid product was dried and dissolved in warm water. A saturated aqueous solution of NH_4PF_6 was added until no more precipitate formed. A light cream-colored polymer was recovered; yield, 95%.

III. RESULTS AND DISCUSSION

Dry toluene, xylene, and THF may be used as the solvent for the synthesis of BCTD. However, THF is preferred owing to its polar nature and low boiling point. BCTD was characterized by FT-IR and ^{1}H-NMR spectra and thermal analysis.[40,41] The FT-IR spectrum of BCTD in KBr showed salient absorption peaks at 1062 cm^{-1} (Si–O–Si stretching), and 673 cm^{-1}/707 cm^{-1} (C–Cl stretching). The bands at 2980, 2920, 1443, and 1266 cm^{-1} are characteristic of the Si–C bond. The FT-IR spectrum of the polymer exhibited characteristic pyridine stretching vibrations at 2923, 2859, and 1715 cm^{-1} and C–N stretching at 1655, 1443, and 1410 cm^{-1}.

The bands at 1258 cm^{-1} and 1066 cm^{-1} were assigned to Si–C and Si–O–Si stretching, respectively.

The ^{1}H-NMR spectra in $CDCl_3$ may be summarized as follows: δ (ppm), assignment: 7.2–6.9 (aromatic **H**); 4.62 (Cl–C**H**$_2$–Ph), 2.6 –2.72 (Si–CH$_2$–C**H**$_2$–Ph), 1.27–1.4 (Si–CH(C**H**$_3$)Ph), 0.96 (Si–C**H**$_2$–CH$_2$–Ph), and 0.1 (Si–C**H**$_3$). The ^{1}H-NMR spectrum of the viologen polymer of BCTD and 4,4′-bipyridine had the following assignable signals: 7.2 (all aromatic **H**), 5.5 (Py–C**H**$_2$–Ph), 2.97 (Si–CH$_2$–C**H**$_2$–Ph), 2.90 (Si–CH$_2$–C**H**$_2$), 2.90 (Si-CH(C**H**$_3$)Ph), 1.60 (Si–C**H**$_2$–CH$_2$), and 0.07 (Si–C**H**$_3$). It was noted that the positions of the C**H**$_3$, C**H**$_2$ protons changed due to the presence of bipyridinium ion.

Thermal stability studies of the polymer under oxygen (Fig. 6) and nitrogen (Fig. 7) show that in an oxygen atmosphere two sharp exothermic peaks are observed, which overlaps to a singlet and an inclined peak. In a nitrogen atmosphere, the mode of degradation is endothermic.

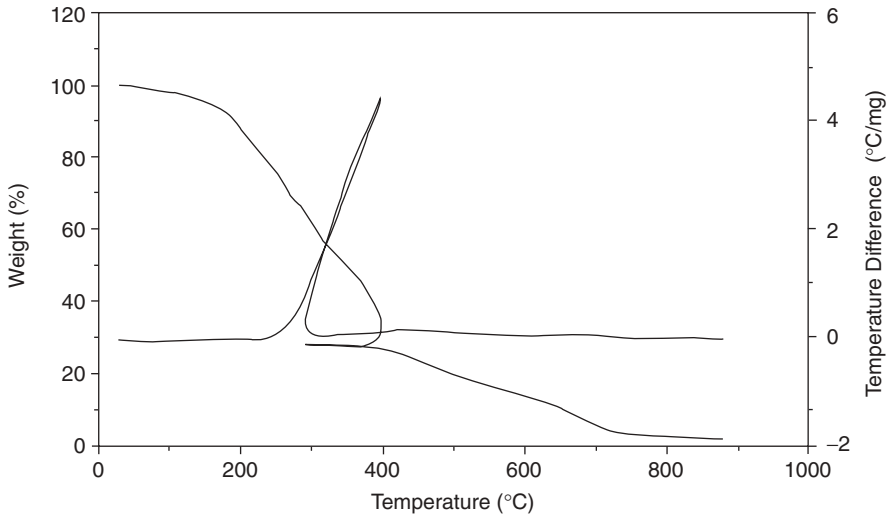

Figure 6 TGA and DTA curves of the polymer under oxygen.

IV. CONCLUSIONS

This section cited some interesting polyviologens and reported a two-step synthesis by which two classes of polymers, polysiloxanes, and polyviologens are combined to produce a hybrid copolymer. The synthesis of an AB_2-type monomer from TMDS and a vinyl monomer was achieved at room temperature. The first step of the reaction is quantitative and time dependent. The hybrid copolymer is characterized by FT-IR and ^{1}H-NMR spectroscopy. The siloxane-based polymer without the Si–O–C bond is thermally stable. Applications of the hybrid copolymer are expected in the packaging and food industries and as a new biocidal material.

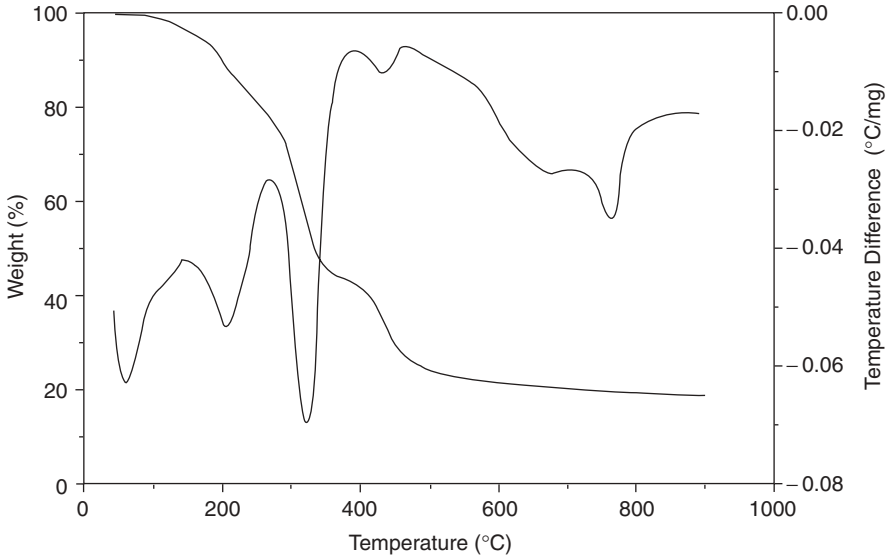

Figure 7 TGA and DTA curves of the polymer under nitrogen.

Part 3. Siloxane-Based Polyurethane Copolymers

I. INTRODUCTION

Polyurethanes and polysiloxanes are two important classes of polymers. Thermopolstic polyurethanes have excellent mechanical properties, chemical resistance, attractive abrasion properties, and hardness.[42] Siloxanes have been used as flame retardants and surfactants because of their high surface energy as well as their chemical, radiation, and thermal stability. Moreover, the relatively large Si–Si bond distance and the relatively low Si–O–Si rotational energy barrier in siloxanes are responsible for low steric hindrance between the methyl groups in polymers containing dimethylsiloxane units. Thus combining the advantages of polyurethanes with polysiloxanes has been the subject of investigations by many research groups. It is expected that such hybrid polymers would have (1) better heat resistance; (2) lower temperature flexibility; (3) better mechanical strength; (4) better resistance to ozone, corona, and weathering; (5) enhanced siloxane-containing surfaces that impart antithrombogenic character.[43] This section summarizes some of the major developments in the field of siloxane–urethane polymers.

A. Blends and Interpenetrating Networks of Silicone–Urethanes

Attempts to make blends of PDMS with thermoplastic TPUR were unsatisfactory due to the deterioration of TPUR properties.[44] However, a mixture of PDMS in THF and TPUR in dimethylacetamide has been used as a coating material.[45] Shibata et al.[46] recently reported the improvement of the ionic conductivity of poly(ether urethane) (PEU)-lithium salt complexes by blending with a polysiloxane (KF_{50}) with a polyether-modified siloxane (KF_{615A}) (Scheme 22).

Previously, it was shown that poly(ether urethane)s that are prepared from 4,4′-methylene-*bis*(phenylisocyanate)/1, 4-butanediol/poly(tetramethylene oxide) with lithium salts exhibited ionic conductivity of approximately 10^{-6} S/cm at room temperature.[47] The highest conductivity (i.e., 4.1×10^{-7} S/cm) of a PEU/electrolyte was observed in the polymer containing 10 wt % **55** (KF_{50}) with a $LiClO_4$ concentration of 1.5 mmol/g of polymer. By contrast, a 10 wt % of **56** ($KF_{615}A$) in the polymer exhibits the highest conductivity (1.3×10^{-6} S/cm), even with more than double the concentration (2.5 mmol/g) of $LiClO_4$. It is interesting to note that the PEU–KF_{50} blend exhibits two T_g values corresponding to the two components, whereas the PEU–$KF_{615}A$ blend shows only one T_g. Moreover, blending with **56** ($KF_{615}A$) shows no such behavior. Thus it appears that ether-urethane derivatives are compatible with ether-siloxanes, presumably because of the presence of the ether group in both materials.

Arkles[48] disclosed the technology for the formation of semi-IPNs involving polysiloxanes and polyurethanes in which the polysiloxane is crosslinked with a linear high molecular weight, thermoplastic polyurethane. The product is currently marketed under the trade name Rimplast by the LNP Corporation. A true

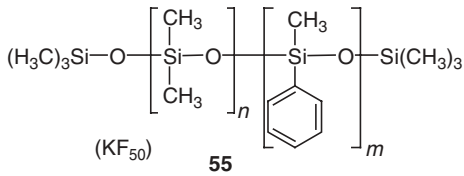

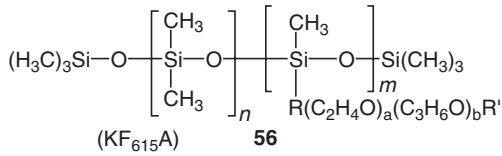

R = oxyalkyleneoxy, R' = Alkyl

Scheme 22 Structures of poly(dimethylsiloxane-co-methylphenylsiloxane (KF_{50}) and polyether-modified polysiloxane (KF_{615A}).

polysiloxane-polyurethane IPN can be described as one containing separate domains of pure siloxane and pure urethane, as previously reported by Ward and Nyilas.[49]

B. Siloxane Groups and Urethanes Linking Units into PEO

Hewitt and Jing[50] reported the synthesis of a new poly(polyethyleneoxide-co-cyanoethylmethylsiloxane) (PEO-SOCN) **60** from cyanoetyldichloromethylsilane **59**. Compound **60** finally gave tri-block copolymers **61**, incorporating PEO, polar siloxane, and urethane units, which were prepared as shown in Scheme 23. Their complexes with $LiClO_4$ exhibit high conductivity (2.6×10^{-5} S/cm at 25°C).

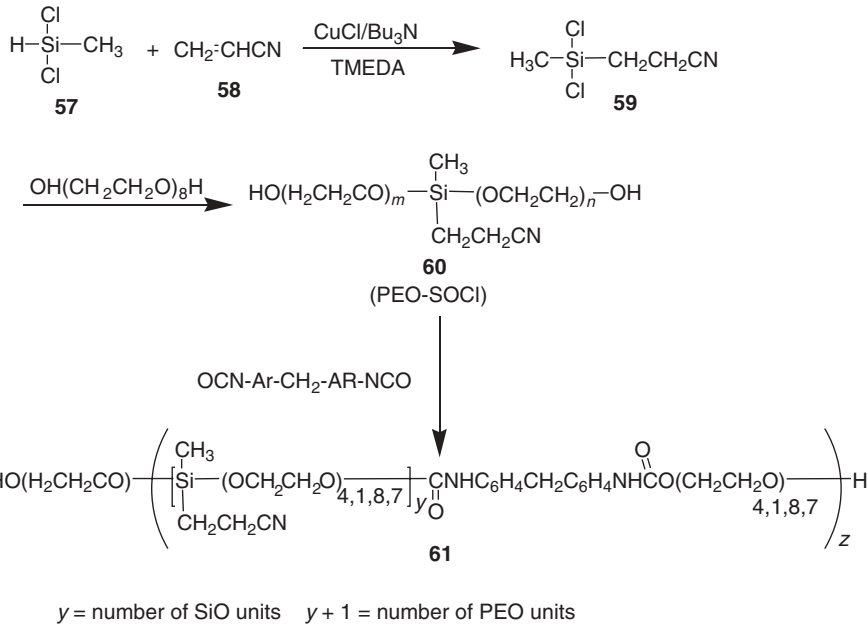

Scheme 23 Synthetic schemes for poly[urethane(ethyleneoxide)-co-cyanoethylmethylsiloxane] (U-PEO-SOCN).

C. A Side-Chain Polyurethane Based on Polysiloxanes with Pendant Primary Alcohol and Quaternary Ammonium Groups

Hazziza-Laskar et al.[51] modified polysiloxane **62** to a polysiloxane that contained a primary alcohol and quaternary ammounium group **65** side chain. Polymer **65** was modified further to a siloxane-based side-chain polyurethane[51] **66** (Scheme 24). This copolymer (3) had potential as a biocide.

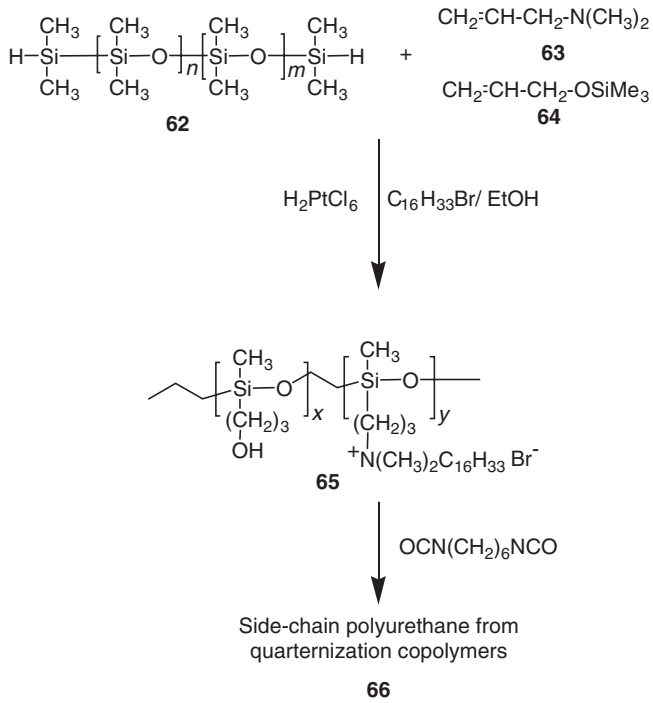

Scheme 24 Synthesis of sioloxane-based side-chain polyurethane-quaternization copolymers from poly(dimethylsiloxane-co-hydrogenmethyl siloxane).

D. End-Chain Silicone-Modified Segmented Polyurethane Membrane as Blood-Compatible Ion-Selective Electrode

Berrocal et al.[52] reported the successful fabrication of a blood-compatible ion-selective electrode from a siloxane-modified segmented polyurethane (SPU). The product is commercially known as BioSpan-S (Scheme 25). The resulting electrodes

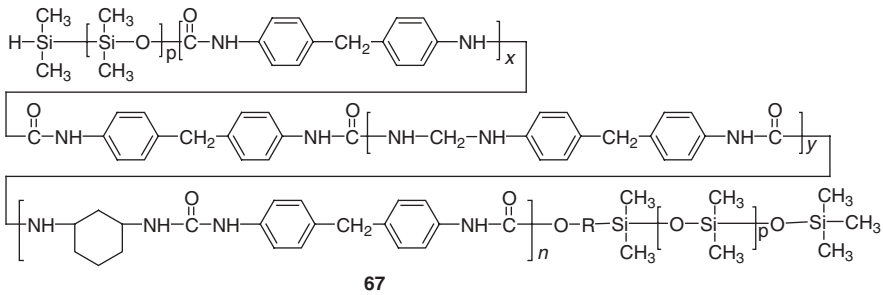

Scheme 25 Structure of BioSpan S.

exhibited good potentiometric responses with all the tested ionophores (valinomycin, sodium ionphore X, and nonactin). The selectivity coefficient obtained by them met the selectivity requirement for the estimation of sodium ion and potassium ion concentration in blood.

Williams[53] reported earlier that the above materials, show less platelet adhesion, activation, and biocompatible as well as better blood compatibility when the materials were used as implants. Moreover, BioSpan-S is a superior material to PVC in terms of platelet adhesion and it reduces thrombogenicity.

E. Polyurethane Containing Side-Chain Polyhedral Oligomeric Silsesquioxanes (POSS)

The hard segments of SPU (segmented polyurethane) usually involve interchain interactions through van der Waals forces and hydrogen bonding, which determine the macroscopic properties of those polymers. For example, Fu et al.[54] reported the synthesis of a polyurethane system containing polyhedral oligomeric silsesquioxanes (POSS), a cage-like molecule. The copolymer was made of poly(tetramethylene glycol) as a soft segment and MDI (4,4′-methylene diphenyl isocyanate) as a hard segment.

The MDI segment was chain extended using 1-[3-(propyl-bisphenol-A) propyl-dimethyl-siloxy]-3,5,7,9,11,13,15-heptacyclohexylpentacyclo [9,5,1,13,9,15,17,13] octa-siloxane (BPA-POSS) (Scheme 26). An interesting feature of this material is that the TEM image displays the POSS, a nano-scale crystal, as a dark phase that resides within or adjacent to the hard-segment domains of the polyurethane. The electron density afforded by POSS molecules is higher than that of the hydrocarbon soft segment phase. The authors suggest that the hard segment domains are initially spherical. During compression molding, these smaller domains sometimes aggregate to form large domains, which deform and coalesce into irregular shapes, mostly disk-like, with varying sizes. Scheme 27 represents the CAChe representation of model for POSS-polyurethane structure, where POSS deforms upon rotation.

F. Diphenylsilanediol-Based Polyurethanes

Lin et al.[55] also reported that the incorporation of diphenlsilanediol (DSiD) into the main chain of the polymer improves the thermal stability of the PU hybrid. They synthesized the PU-hybrid polymer in a two step-process. First, a polyurethane prepolymer **72** was synthesized using standard procedures. Second, the number of residual –NCO groups in the prepolymer was determined using di-*n*-butylamine and a stoichiometric quantity of DSiD in DMF solution was added to complete the reaction to give product **73** (Scheme 28). The activation energies at various stages of degradation for the pure PU and the silicone-containing PU were ascertained by the Ozawa[56] method—that is, the Si-PU hybrid copolymers have higher degradation activation energies than PU. Generally, the presence of a pendant siloxane moiety or a POSS on a polyurethane is better than using a siloxane oligomer as part of a main chain siloxane-urethane copolymer.

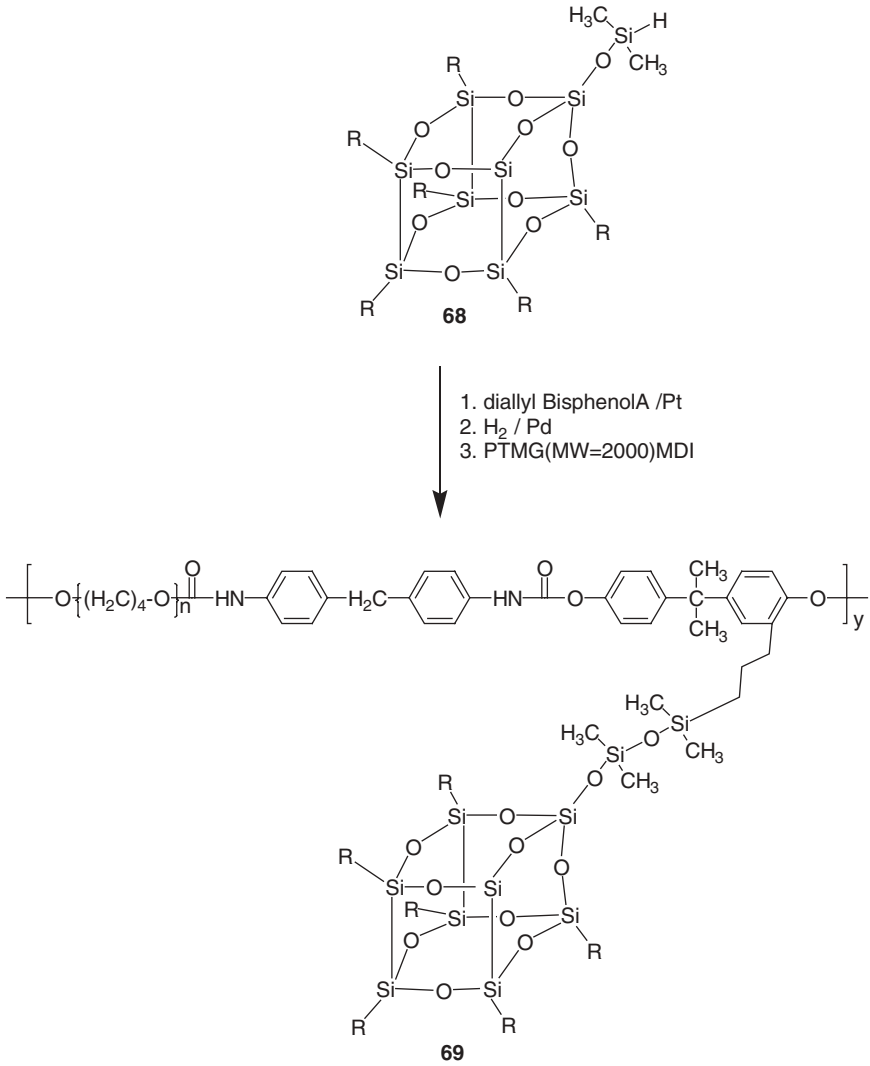

68

69

Scheme 26 Synthetic route to POSS-polyurethane.

G. Siloxane-Urethane Containing Block Copolymers

It has been observed that thermoplastic polyurethane elastomers as segmented copolymers, in which the soft segments are based on polysiloxane or polyether units and the hard segments are based on the organic aromatic diisocyanate group, exhibit a heterogeneous microstructure. The heterogeneous miscrostructure is the outcome of thermodynamic incompatibility of the soft and hard block segments.

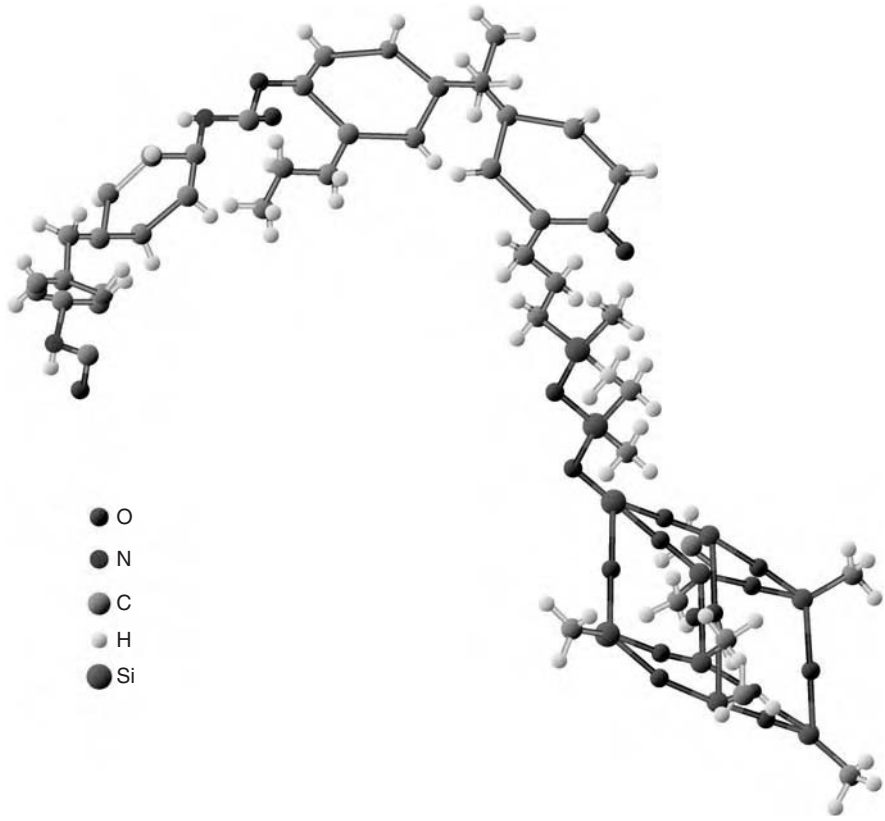

Scheme 27 CAChe representation of the POSS-polyurethane structure.

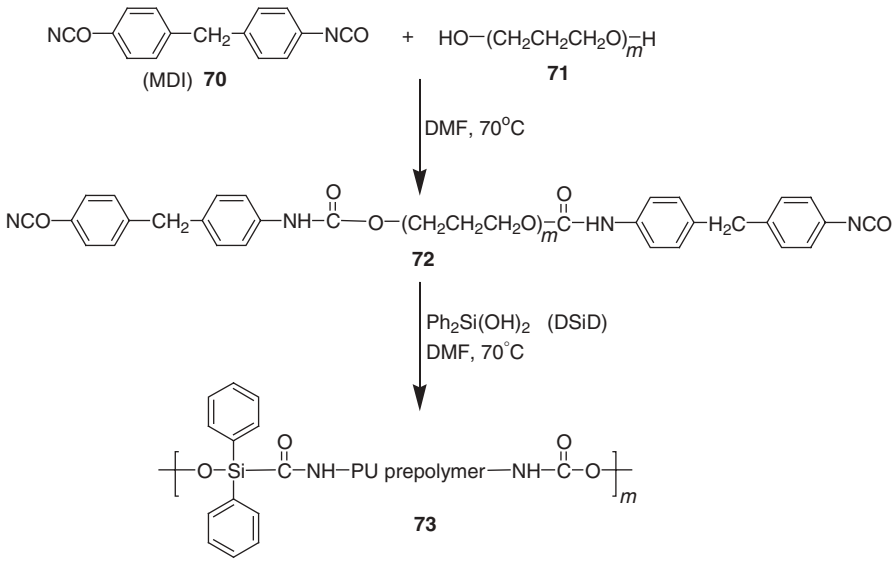

Scheme 28 Synthesis of diphenylsilanediol (DSiD) containing main chain polyurethane.

Scheme 29 illustrates the synthetic routes to three classes of silicone–urethane block copolymers that were reported by Benrashid et al.[57,58] It is interesting that the solvents from which the siloxane–urethane block coplymers were cast have a significant influence on microphase segregation. For example, films cast from THF had a higher siloxane concentration at the surface relative to polymers cast from DMAc/CH_2CI_2 or dioxane.

Kozakiewicz[59] reported that siloxane–urethane prepolymers, which were further treated with an oligomeric siloxane diol (Scheme 30) or with water (i.e., moisture-curable system), exhibited improved segment compatibility with no phase segregation. These materials have applications as biocompatible and antithrombogenic coatings. They also form flexible waterproof coatings on paper, metal, and glass; finishes for textiles and natural leather; antifriction and wear resistance materials; as binders for magnetic recording media; heat-resistant layers for thermal recording materials; printing ink binders with good adhesion to polyamide substrates; water- and oil-repellent

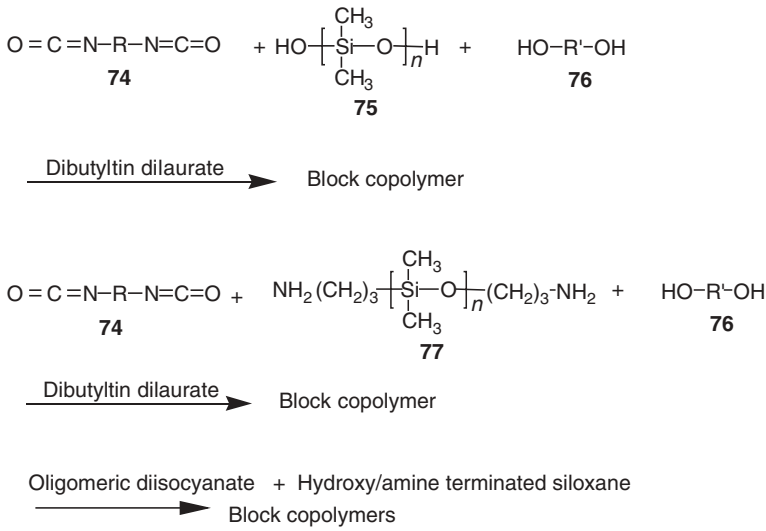

Scheme 29 Synthetic routes for three classes of siloxane-urethane block copolymers.

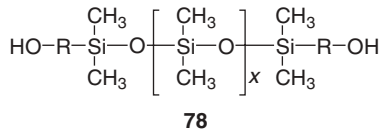

R= $(CH_2)_2O(CH_2)_3$ and —$(CH_2)_6$— x = 10 or 20

Scheme 30 Structure of the oligomeric sioloxane diol used for polymerization with poly(propylene glycol) and diisocyanates.

coatings on glass, ceramics, wood, paper, metals, leather, and textiles; and many other applications. In addition, perflorinated diols were used as chain-extending agents, as well as radiation-curable coatings, releasable coatings, and antifouling coatings. Moreover, polysiloxane–urethane block coplymers have interesting mechanical and surface-related properties. For example, the presence of a polysiloxane block allows the possibility for conversion to an insoluble silicone rubber upon hot curing.

Wang et al.[60] reported the synthesis of a complex PSU. The segment from the urethane was derived from a specially designed secondary amioalkyl-terminated poly(dimethysiloxane) along with poly(tetramethylene oxide) (PTMO), 1,4-butanediol **79** (BD) as a soft segment, and 4,4′-methylene diphenyl diisocyanate **70** (MDI). The polymerization occurred in a mixed solvent medium of *N,N*-dimethylacetamide and tetrahydrofuran (Scheme 31). Transmission electron microscopy indicates that the presence of 15 wt % of PDMS in the above polymer appears as dark domains, whereas at higher concentrations (e.g., 55 wt % of PDMS), a continuous phase is observed. The predicted properties of those polymers are low glass-transition temperatures, low surface energy, high gas permeability, good insulation capability, and thermal stability.

Kuo et al.[62] recently studied in detail the synthesis of segmented polyurethane from poly(dimethylsiloxane diol) with poly(ethylene glycol) **83** (PEG) and 4,4′-methylene diphenyl diisocyanate **70** (Scheme 32). Polymer films were prepared by casting the polymer from solution. The electrolyte was prepared by dipping the polymer films in $LiClO_4$/propylene carbonate solutions of different concentrations and for different time intervals. They obtained an ionic conductivity of 2.33×10^{-3} S/cm at 80°C. Moreover, the conductivity of the composite electrolyte increased with an increase in the content of PEG, which attracts a larger quantity of Li^+ ions.

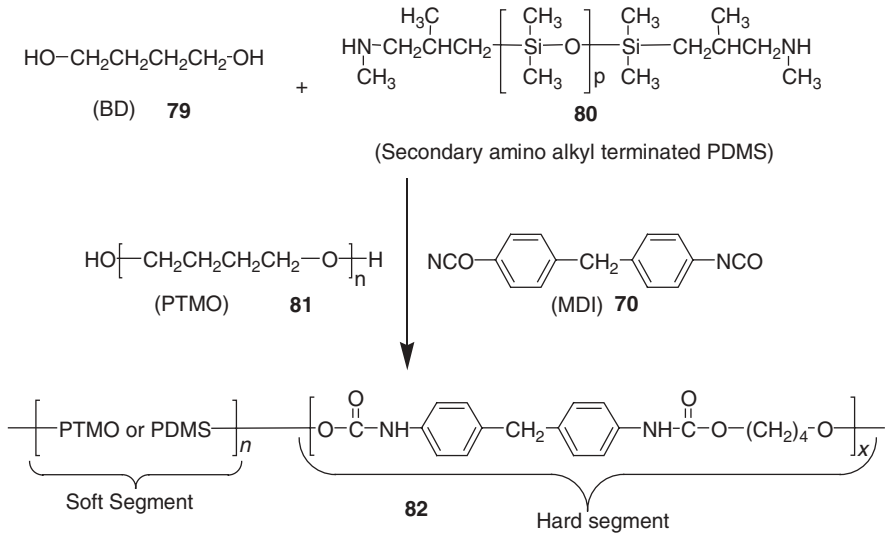

Scheme 31 Organosiloxane modified and segmented polyether–polyurethanes.

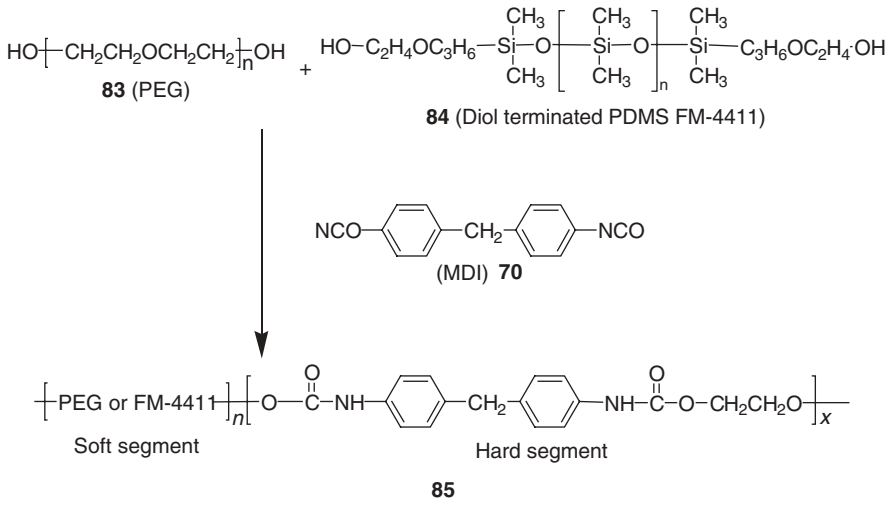

Scheme 32 Two-step addition reaction for the preparation of segmented polysiloxane-modified polyurethane.

Kuo et al.[62] also reported new polymers (PS55) in which ethylene glycol was used a chain extender. These materials were characterized by scanning differential calorimetry (DSC), ionic conductivity, and multinuclear solid-sate NMR spectroscopy. For example, the DSC measurements indicated an increase in the soft-segment T_g, which remained invariant even at high salt concentrations. In addition, a conductivity jump was observed at 310–330°K. Below this temperature, the conductivity follows Arrehnius-like behavior, implying a diffusion mechanism for the transport of the charge carriers where the charge carriers are decoupled from the segmental motion of the polymer chain. Above that temperature, a Vogel-Tamman-Fulcher behavior is observed. At high salt concentrations, the decrease in ionic conductivity is due to the formation of ion pairs and/or ion clusters.

The ^{13}C-NMR spectra together with the 2D-WISE NMR spectra of these materials suggest a significant decrease in the mobility of the soft segment, which is attributed to the added salt. Using line width changes in the ^{29}Si-NMR spectrum, it was shown that the polysiloxane backbone mobility was unaffected unless the salt concentration was high. The onset temperature of ^{7}Li motional line narrowing was correlated with the soft-segment T_g. The activation energies obtained from ionic conductivity, ^{7}Li line width, and T_1 measurements supported a strong correlation between the ionic conductivity of the solid polymer electrolyte and the mobile lithium cation.

H. Polyurethane Modified with an Aminoethylaminopropyl-Substituted Polydimethylsiloxane

Fan et al.[63] reported the syntheses and properties of a polyurethane–urea, copolymers **88** from a aminoethyl-aminopropyl poly(dimethylsiloxane) **86** (AEAPS),

with poly(tetramethylene oxide) **81** and 1,4-butanediol **79** as a soft segment and 4,4′-methylene diphenyl discarnate **70** (Scheme 33). Presence of siloxane as a side chain results in a siloxane concentration on the surface of the elastomer that is higher than that in the bulk. In fact, the Young modulus and tensile strength of the modified polyurethane increased slightly, but the ultimate elongation decreased after 1 wt % AEAPS modification.

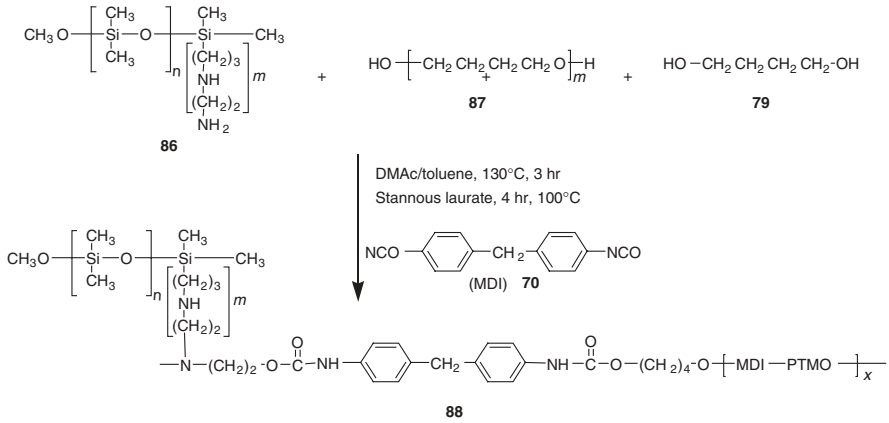

Scheme 33 Synthesis of polyurethane-modified polysiloxanes with aminoethylaminopropyl side chains (AEAPS).

On the contrary, main-chain segmented siloxane–urethane copolymers from primary or secondary amine-terminated siloxane oligomers with diisocyanates and diols of the type illustrated in Scheme 31[60,64,65] cause a surface enrichment with the siloxane chain as well as a reduction of tensile strength. These results have been attributed more to the branching of the polyurethane chain owing to more than one aminoethylaminopropyl group lying in several AEAPS molecular chains. Furthermore, surface-modified polyurethane–polysiloxanes are of great use in medical devices and prostheses owing to their excellent tensile properties, biocompatibility, and low T_g.

I. Synthesis of Waterborne Polyurethane Modified with an Aminoethylaminopropyl-Substituted Polydimethylsiloxane

Waterborne polyurethanes are of commercial importance today because of their applications in aqueous medium without evolving toxic and flammable material to pollute the air and water. Dieterich et al.[66–68] developed innovative approaches to this subject. Unfortunately, their carbon based polyurethanes had poor water resistance. Chen and coworkers[69] synthesized a waterborne PU prepolymer **91,** which was modified by AEAPS **86,** as shown in Scheme 34. According to them, the newly made PU **92** emulsions have shown stability, and the siloxane chains have been enriched on the PU surface. The water resistance of the PU film has been

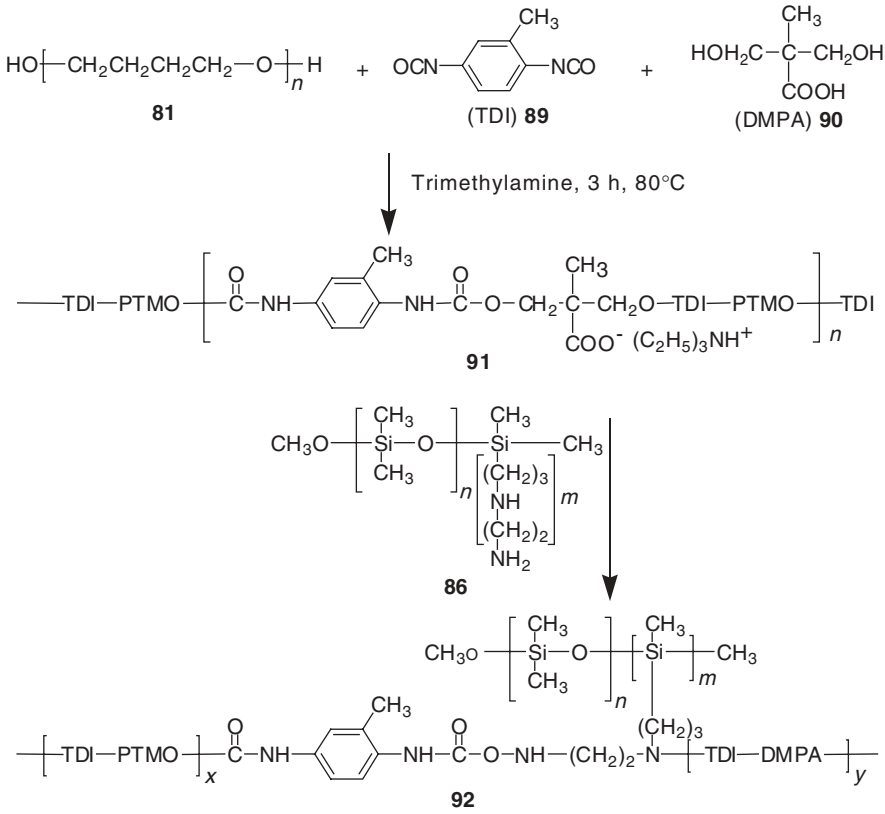

Scheme 34 Synthesis of waterborne AEAPS-modified polyurethanes.

increased, but the bulk tensile properties of the PU film has not changed significantly with a small amount of siloxane modification up to 6wt %.

J. Alternate Siloxane–Urethane Copolymer by Three-Step Reaction

Chatterjee Ganguly and Matisons[70] reported the three-step synthesis of polysiloxane–urethane from tetramethyldisiloxane (Scheme 35). In the first step *bis*(3-trimethylsiloxypropyl)tetramethyldisiloxane (BTTD) was synthesized from tetramethyldisiloxane and allyloxytrimethylsilane. BTTD was then hydrolyzed in the presence of methanol to give *bis*(3-hydroxypropyl)tetramethyldisiloxane (BHTD).

Finally, the siloxane–urethane copolymer (**22**) was obtained from BHTD and 2,5- tolyene diisocyanate (2,5-TDI) in dry DMF at 80°C. The CAChe representations of model MDI-PDMS and model TDI-TMDS structures are presented in Scheme 36 and Scheme 37, respectively.

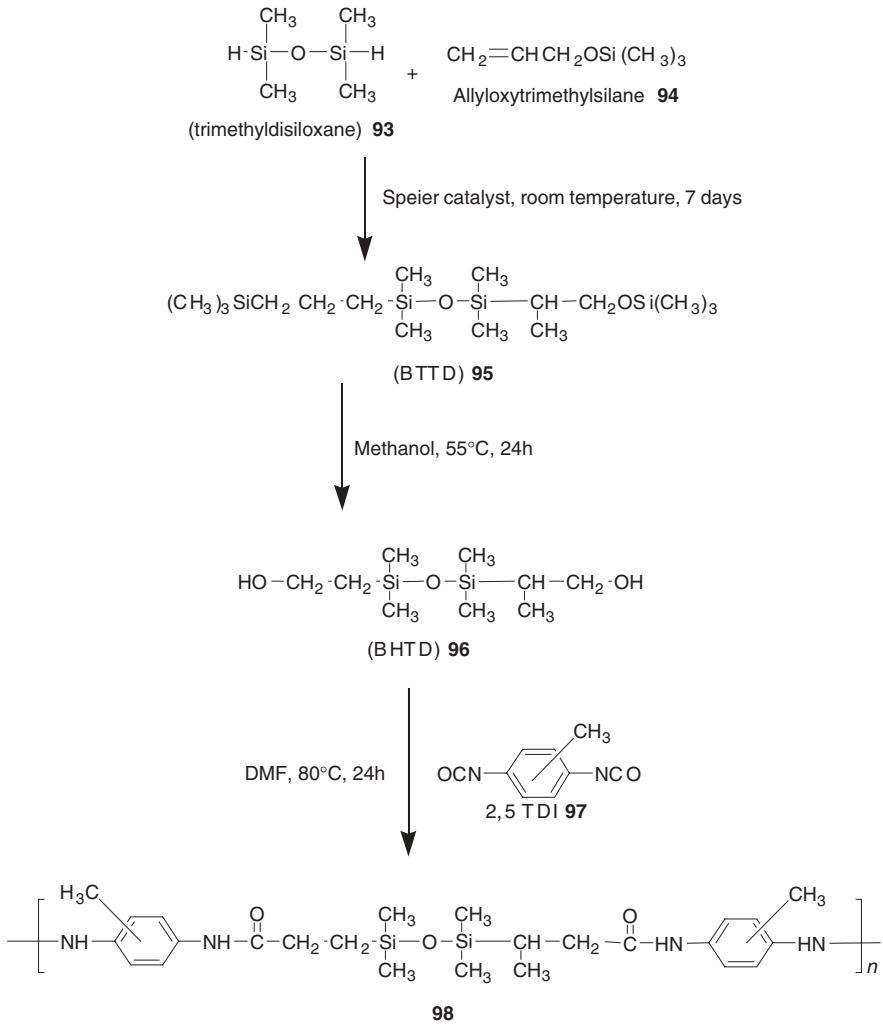

Scheme 35 Three-step synthesis of a polysiloxane–urethane copolymer (**22**)

Recently, Adhikari et al.[71] examined the effect of mixed-chain extenders on the properties and morphology of polyurethane–siloxane copolymers. In a two-step process, they made low molecular weight prepolymers with PDMS, poly(hexamethylene oxide) (PHMO) and MDI. The prepolymers were treated with 1,4-butane diol (BDO) and 1,3-*bis*(4-hydroxybutyl)-1,1,3,3-tetramethyldisiloxane (BHTD) and cured. A 60:40 molar ration of BDO:BHTD chain extender yielded a polyurethane that combined good tensile strength and flexibility.

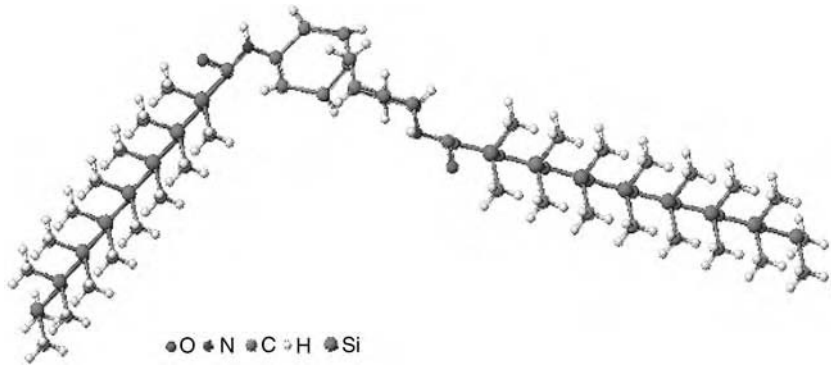

Scheme 36 CAChe representation of model MDI-PDMS structure.

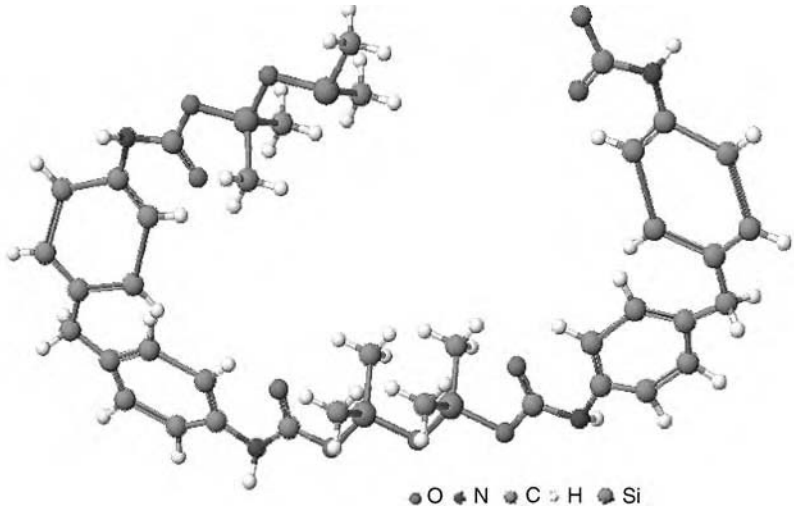

Scheme 37 CAChe representation of model TDI-TMDS-TDI structure.

II. EXPERIMENTAL SECTION

A. Materials and Instruments

Hydrogen hexachloroplatinate (IV) hydrate (choroplatinic acid) was used as a 1% solution in THF (Aldrich, 40 wt % Pt). 1,1,3,3-Tetramethyldisiloxane, allyloxytrimethylsilane, and 2,5-tolyene diisocyanate (2,5-TDI) (Aldrich) were used without further purification. DRIFT spectra were measured at room temperature using a single-beam Nicolet Magna Model 750 spectrometer with an MCT-liquid nitrogen colled detector. The ^{1}H-NMR spectra were recorded on a Varian Gemini

Fourier Transform NMR Spectrometer at 200 MHz. Thermogavimetric analysis was conducted in platinum crucibles with an SDT-2960 Simultaneous DTA-TGA thermal analyzer from room temperture to 1000°C at a heating rate of 10°C/min under nitrogen or oxygen (flow rate of 100 mL/min).

B. Synthesis of Bis(3-trimethylsiloxypropyl)tetramethyl Disiloxane (BTTD) from Allyloxytrimethylsilane

In a dry flask, allyloxytrimethylsilane (6.5 g) in dry THF (50 mL) was stirred with a catalytic amount of chloroplatinic acid at room temperature in air. 1,1,3,3-Tetramethyldisiloxane (3.3 g) in dry THF (20 mL) was added dropwise for 30 min. The reaction was stirred at room temperature for 7 days. Excess THF was removed under vacuum at −65°C. The product was a clear liquid; yield, 96%.

^{1}H-NMR ($CDCI_3$, 200 MHz), (δ ppm) assignment: 3.5-4 ($SiCH_2CH_2C\mathbf{H}_2OH$), 1.78-1.8 ($SiCH_2\mathbf{CH}_2CH_2OH$), 1.50–1.53 ($SiCH(C\mathbf{H}_3)CH_2OH$), 0.47 ($SiC\mathbf{H}_2CH_2CH_2OH$), and 0.053 ($Si\text{-}C\mathbf{H}_3$).

C. Synthesis of Bis(3-hydroxypropyl)tetramethyl Disiloxane (BHTD)

Bis(3-trimethylsiloxypropyl)tetramethyldisiloaxne (7.9 g) in dry methanol (200 mL) was refluxed[72] overnight at 55°C. Excess methanol was removed under vacuum at −65°C; yield, 99%. ^{1}H-NMR ($CDCL_3$, 200MHz), δ (ppm) assignment: 3.00 ($SiCH_2CH_2CH_2O\mathbf{H}$), 3.51–3.57 ($SiCH_2CH_2C\mathbf{H}_2OH$), 1.78–1.8 ($SiCH_2\mathbf{CH_2}CH_2OH$), 1.50–1.56 ($SiCH(C\mathbf{H}_3)CH_2OH$), 0.5 ($SiC\mathbf{H}_2CH_2CH_2OH$), and 0.00–0.05 ($SiC\mathbf{H}_3$).

D. Synthesis of a Siloxane–Urethane Copolymer from BHTD and 2,5-TDI

In a dry three-neck round bottom flask, *bis*(3-hydroxypropyl)tetramethyldisiloxane (5g, 2 mmol) was dissolved in dry DMF (25 mL). 2,5-TDI (3.48 g, 2 mmol) in dry DMF (10 mL) was added dropwise to the solution under nitrogen at room temperature. The reaction mixture was stirred at 80°C for 24 h. The solution was poured into cold methanol to precipitate the polymer. A pale yellow polymer was filtered and washed with methanol; yield 90%.

III. RESULTS AND DISCUSSION

A two-step synthesis of polysiloxane–urethane copolymers from tetramethyldisiloxane was described. The precursors, BTTD (from tetramethyldisiloxane and allymethylsilane) and BHTD (by hydrolysis of BTTD) were prepared by standard literature procedures.

The FT-IR spectra of the polysiloxane–urethane copolymers contained absorption peaks at 1092 cm^{-1} (Si-O-Si stretching), 816 cm^{-1} (CH_3 rocking), and 2854 cm^{-1} (CH_3 stretching) and were attributed to the tetramethyldisiloxane units. Absorptions at 3600 cm^{-1} (N-H stetching) and 1685–1720 cm^{-1} (C=O stretching) were typical of urethane linkages. Bands at 2954 cm^{-1} and 1232 cm^{-1} were characteristic of the Si–C bond.

The ^{1}H-NMR spectra of the copolymers contained signals at 9.1 and 8.5 ppm, which were assigned to the proton on nitrogen. Signals at 7.95 and 7.05 ppm were attributed to aromatic protons. The other salient proton signals at 5.8, 2.88, 2.72, 2.19, and 0.07 ppm have been assigned as follows: ($SiCH_2CH_2\mathbf{CH_2}$-urethane), ($SiCH_2\mathbf{CH_2}CH_2$-urethane), ($SiCH(\mathbf{CH_3})CH_2$-urethane), ($Si\mathbf{CH}_2CH_2CH_2$-urethane), and ($Si\mathbf{CH}_3$), respectively. The singlet N-H proton peaks at 9.1 and 8.5 ppm were characteristic of an asymmetric molecular structure.[72]

The TGA and DTA curves under nitrogen (Fig. 8) and oxygen (Fig. 9) indicated that the mode of degradation may have been different in the two environments. For example, under oxygen, the polymer showed 39% weight loss on heating to 200°C. A sharp exothermic peak appeared at ~330°C, with a further weight loss of 74%. This observation was analogous to that observed by Lee et al.[32] in their study of the thermal stability of polysiloxane-ether-urethane copolymers. By the time the copolymer reached 558°C, the weight loss was 99%, and only silica remained in the platinum pan.

In a nitrogen atmosphere at 347.48°C, copolymer showed two endothermic peaks, one below 200°C and one at ~374°C, which corresponded to weight losses of 25% and 77%, respectively. In this case, a silicon coating was observed.

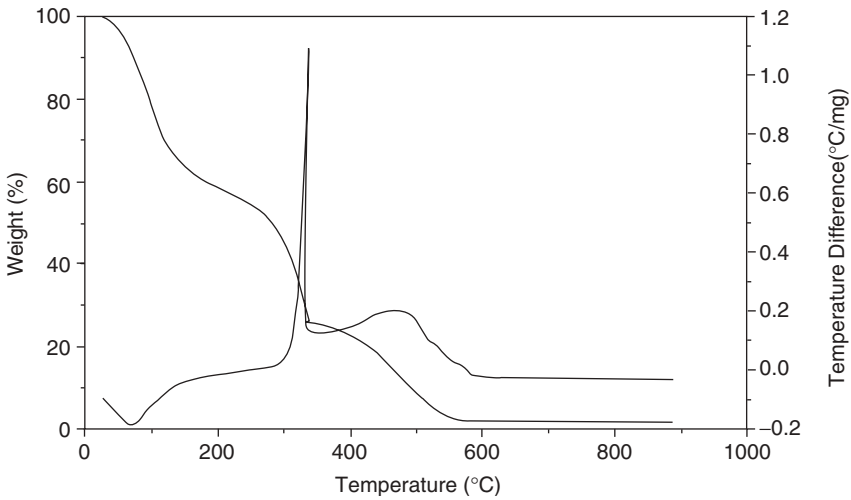

Figure 8 TGA and DTA curves of the copolymer in oxygen.

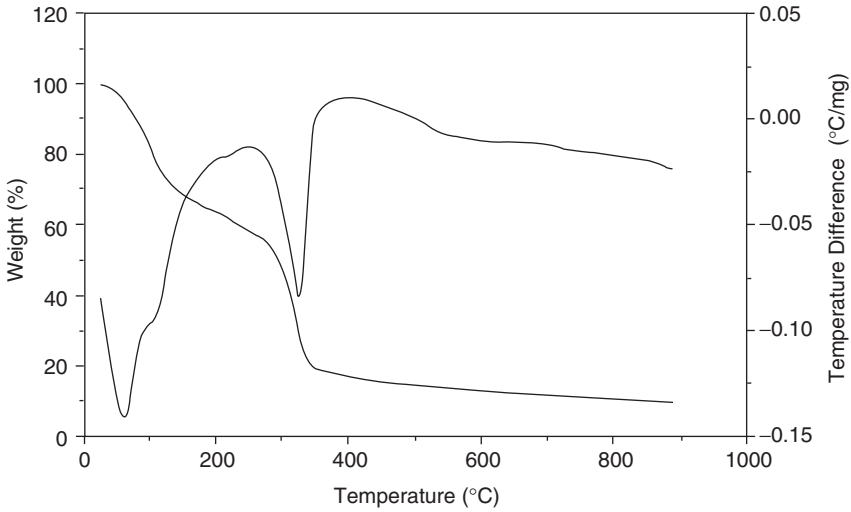

Figure 9 TGA and DTA curves of the copolymer in nitrogen.

IV. ACKNOWLEDGMENTS

The author expresses her sincerest gratitude to venerable Professor Charles E. Carraher of Florida Atlantic University for his constant encouragement and moral support to publish this work. She is highly grateful to Professors Martel Zeldin, Alaa Abd-El-Aziz, and Charles Pittman for their valuable time to improve the quality of the manuscript presentation. Thanks are due to Professors L. G. Bachas, P. L. Kuo, and B. S. Hsiao who generously supported the work by providing electronic versions of reprints of their work. Thanks are due to Ms. Amy A. Romano, assistant editor, John Wiley & Sons, Inc., for several reprints and to Master Amit Ganguly for his help in producing the manuscript.

V. REFERENCES

1. V. Harabagiu, M. Pineteala, C. C\otzur, B. C. Simionescu, J. C. Salamone, eds., *The Polymeric Materials Encyclopedia,* vol. 4, Baton Rouge, FL: CRC Press, 1996.
2. B. C. Simonescu, V. Harabagiu, C. I. Simionescu, J. C. Salamone, eds., *The Polymeric Materials Encyclopedia*, vol. 10, Baton Rouge, FL: CRC Press, 1996.
3. *Silicon Chemie und Technologies* [Symposium], Vulkan-Verlag, Essen, 1998.
4. W. Noll, Chemistry and Technology of Silicones, Academic Press, New York, 1968.
5. J. Marsden, U.S. Pat. 2,445,794 (1945).
6. (a) S. Nitzsche, M. Wick, U.S. Patent 3,127,363 (1964); (b) L. B. Bruner, U.S. Patent 3,035,016 (1962); (c) I. Ceyzeriat, U.S. Patent 3,133,891 (1964).
7. M. E. Nelson, U.S. Patent 3,020,260 (1962); (b) M. E. Nelson, U.S. Patent 3,249,581 (1966).

8. (a) C. A. Berridge, U.S. Patent 2,843,555 (1958); (b) R. A. Pike, U.S. Patent 3,046,294 (1962); (c) "RTV Silicone Rubber," Technical Brochoure No. S-3C, General Electric Co., Waterford, New York, 1964; (d) "Silicone Rubber Adhesive/Selants for Industrial Applications," Technical Brochure No. S-2D, General Electric Co., Waterford, New York, 1967.
9. H. G. O. Becker, G. Domschke, E. Fanghanel, J. Faust, M. Fischer, F. Gentz, K. Gewald, R. Gluch, R. Mayer, K. Muller, D. Pavel, H. Schmidt, K. Schollberg, K. Schwetlick, E. Seiler, G. Zeppenfield, *Organikum*, VEB Deutscher Verlag der Wissenschaften, Berlin, 1976.
10. W. J. O'Malley, *Adhes. Age* 17 (1975).
11. S. K. Pollack, D. U. Singer, A. M. Morgan, *Polym. Prepr.* **40**, 370 (1999).
12. C. J. Hawker, E. E Malmstrom, J. M. J. Frechet, M. R. Leduc, R. B. Grubbs, G. G. Barclay, in *Controlled Radical Polymerization*, K. Matyjaszewski, ed., ACS Symposium Series 685, American Chemical Society, Washington, D.C., 1998.
13. E. D. Brown, U.S. Patent 3,179,619 (1965).
14. C. Kok, H. K. Toh, J. G. Matisons, E. Joseph, Telomer Composition, WO95/00577, January 1995, PTC/Au94/00285, May 1995.
15. D. J. T. Hill, M. C. S. Perera, P. J. Pomery, H. K. Toh, *Polymer* **41**, 9131 (2000).
16. D. J. T. Hill, M. C. S. Perera, P. J. Pomery, H. K. Toh, *Eur. Polymer*. J. **36**, 241 (2000).
17. W. Hechtl, in *Silicone Chemistry and Technology*, G. Koerner, M. Schulze, J. Weis, eds., Vulkan Verlag, Essen, 1991.
18. D. Wrobel, in *Silicone Chemistry and Technology*, G. Koerner, M. Schulze, J. Weis, eds., Vulkan Verlag, Essen, 1991.
19. S. Chatterjee.Ganguly, L. Britcher, J. G. Matisons, *Polym. Mater. Sci. Eng.* **86**, 193 (2002).
20. G. Liptay, J. Nagy, Ch. Weiss, A. Borbély-Kuszmann, *J. Thermal. Anal.* **32**, 1421 (1987).
21. G. Liptay, L. Ligethy, and J. Nagy, *Thermal Analysis*, Proceedings of the Sixth ICT Conference, Birhauser Verlag, Basel, 1980.
22. D. Feng, G. L .Wilkes, J. V. Crivello, *Polymer* **60**, 1801 (1989).
23. H. C. Chang, M. Osawa, T. Matsue, I. Uchida, *J. Chem. Soc. Chem. Commun*. 611 (1991).
24. J. Hazziza-Laskar, G. Helary, G. J. Sauvet, *Appl. Polym. Sci.* **58**, 77 (1995).
25. B. J. Kollbeier, *Tenside Surf. Det.* **26**, 26 (1986).
26. A. Factor, G. E. Heinsohn, *Polym. Lett.* **9**, 289 (1971).
27. C. Bird, A. T. Kuhn, *Chem. Soc. Rev*. **10**, 3044 (1981).
28. F. W. Harris, K. C. Chuang, S. A. X. Huang, J. J. Janimark, S. Z. D. Cheng, *Polymer* **35**, 4940 (1994).
29. S. A. X. Huang, K. C. Chuang, S. Z. D. Cheng, F. W. Harris, *Polymer* **41**, 5001 (2000).
30. W. C. Yu, M. T. Shaw, X. Y. Huang, F. W. Harris, *J. Polym. Sci. B Polym. Phys.* **32**, 481 (1994).
31. F. Lin, F. W. Harris, *Am. Chem. Div. Polym. Sci. Polym. Prep.* **39**, 433 (1998).
32. F. Lin, F. W. Harris, *Am. Chem. Div. Polym. Sci. Polym. Prep.* **43**, 57 (2002).
33. H. Kamogawa, S. Satoh, *J. Polym. Sci. Polym. Chem. Ed.* **26**, 653 (1988).
34. H. Kamogawa, S. Amemiya, *J. Polym. Sci. Polym. Chem. Ed.* **23,** 2413 (1985).
35. H. Kamogawa, K. Kikushima, M. Nanasawa, *J. Polym. Sci. Polym. Chem. Ed.* **27**, 393 (1989).
36. H. D. Abruna, A. J. Bard, *J. Am. Chem. Soc.* **103**, 6898 (1981).
37. P. Burgmayer, R. W. Murray, *J. Electroanal. Chem.* **135**, 335 (1982).
38. R. W. Murray, in Electroanalytical Chemistry, vol. 13, A. J. Bard, ed., Dekker, New York, 1984.
39. T. Aoyagi, T. Akimoto, Y. Nagase, *Makromol. Chem.* **193**, 2829 (1992).
40. S. Chatterjee Ganguly, J. G. Matisons, *Am. Chem. Div. Polym. Mater. Sci. Eng.* **86**, 82 (2002).
41. Y. Nakagawa, P. J. Millerand, K. Matyjaszewski, *Polymer* **39**, 5163 (1998).
42. G. Woods, *The ICI Polyurethane Book 2*, Wiley, New York, 1990.
43. M. D. Lelah, S. L. Cooper, *Polyurethane in Medicine,* CRC, Boca Raton, FL, 1986.

44. B. Arkles, C. Carreno, *Polym. Mater. Sci. Eng.* **50**, 440 (1984).
45. W. Lemm, E. Buecherl, *Adv. Biomater.* **3**, 459 (1982).
46. M. Shibata, T. Kobayashi, R. Yosomiya, M. Seki, *Eur. Polym. J.* **36**, 485 (2000).
47. M. Seki, K. Sato, and R. Yosomiya. *Makromol Chem.* **193**, 2971 (1992).
48. (a) B. Arkles, U.S. Patent 4,714,739, 1987; (b) B. Arkles, U.S. Patent 4,970,263, 1990.
49. R. Ward, E. Nyilas, in *Organometallic Polymers*, C. E. Carraher, J. Sheats, C. U. Pittman. eds., Academic Press, 1978.
50. D. G. Hewitt, L. Jing, *J. Polym. Sci. A Poplym. Chem.* **33**, 2033 (1995).
51. J. Hazziza-Laskar,. G. Helary, G. Sauvet, *J. Appl. Polym. Sci.* **58**, 77 (1995).
52. M. J. Berrocal, I. H. A. Badr, D. Gao, L. G. Bachas, *Anal. Chem.* **73**, 5328 (2001).
53. D. F. William, *Blood Compatibility*, CRC Press, Boca Raton, FL, 1987.
54. B. X. Fu, B. S. Hsiao, S. Pagola, P. Stephens, H. White, M. Rafailovich, J. Sokolov, P. T. Mather, H. G. Jeon, S. Phillips, J. Lichtenhan, J. Schwab, *Polymer* **42**, 599 (2001).
55. M. F. Lin, W. C. Tsen, Y. C. Shu, F. S. Chuang, *J. Appl. Polym. Sci.* **79**, 881 (2001).
56. T. Ozawa, *Bull Chem. Soc. Jpn.* **38**, 1881 (1965).
57. R. Benrashid, G. L. Nelson, J. H Linn, K. H Hanley, W. R. Wade, *J. Appl. Poly. Sci.* **49**, 523 (1993).
58. R. Benrashid, G. L. Nelson, *J. Polym. Sci. A Polym. Chem*. **32**, 1847 (1994).
59. J. Kozakiewicz, *Prog. Org. Coat.* **27**, 123 (1996).
60. L. F. Wang, Q. Ji, T. E. Glass, T. C. Ward, J. E. McGrath, M. Muggli, G. Burns, U. Sorathia, *Polymer.* **41**, 5083 (2000).
61. P. L. Kuo, W. J. Liang, C. L. Lin, *Macromol. Chem. Phys.* **203**, 230 (2002).
62. C. L. Lin, H. M. Kao, R. R. Wu, P. L. Kuo, *Macromolecules* **35**, 3083 (2002).
63. Q. Fan, J. Fang, Q. Chen, X. Yu, *J. Appl. Polym. Sci.* **74**, 77 (1999).
64. I. Yilgor, G. L. Wilkes, J. E. McGrath, *Polym. Prepr.* **24**, 80 (1983).
65. L. F. Wang, J. E. McGrath, *Polym. Prepr.*, **38**, 308 (1997).
66. D. Dieterich, H. Reiff, *Adv. Urethane Sci. Technol.* **4**, 112 (1976).
67. D. Dieterich, *Prog. Org. Coat.* **9**, 281 (1981).
68. D. Dieterich, W. Keberle, H. Wtt, *Angew Chem. Int. Ed. Eng.* **9**, 40 (1970).
69. H. Chen, Q. Fan, D. Chen, X. Yu, *J. Appl. Polym. Sci.* **79**, 295 (2001).
70. S. Chatterjee Ganguly, J. G. Matisons, *Polym. Prepr.* **42**, 471 (2001).
71. R. Adhikari, P. A. Guantillake, S. J. McCarthy, G. F. Meijs, *J. Appl. Polym. Sci.* **83**, 736 (2002).
72. F. Braun, I. Willner, M. Hess, R. Kosfeld, *J. Organomet. Chem.* **366**, 53 (1989).
73. J. B. Lee, T. Kato, T. Yoshida, T. Uryu, *Macromolecules* **26**, 4990 (1993).

CHAPTER 8

Bioinspired Silica Synthesis

Siddharth V. Patwardhan* and Stephen J. Clarson

Department of Chemical and Materials Engineering, University of Cincinnati, Cincinnati, Ohio

CONTENTS

*Present address: School of Biomedical and Natural Sciences, Nottingham Trent University, Nottingham, United Kingdom.

Macromolecules Containing Metal and Metal-Like Elements, Volume 4: Group IVA Polymers, edited by Alaa S. Abd-El-Aziz, Charles E. Carraher Jr., Charles U. Pittman Jr., and Martel Zeldin
ISBN: 0-471-68238-1

I. INTRODUCTION

A. Silica

Low-valued silica sand and quartzite may be converted into specialty silica by various processes. The resulting specialty silicas are generally classified based on their properties and methods of production and include fumed silica, precipitated silica, silica gels and sols and microsilica. The value of global industrial production of specialty silica is close to $2 billion per annum, and the capacity of silica production is around 1 million tons per annum, out of which the capacity of precipitated silica (which is discussed here) is about 85%.[1] These quantities clearly illustrate the importance of the industries and processes dealing with precipitated silica.

Precipitated silica, which has applications in rubber reinforcement, moisture resistance, rheology control, as flatting agents, etc., is commercially produced by neutralizing sodium silicate with sulfuric acid to form a slurry of silica. This is filtered to recover the silica, which is then washed, dried, and size treated. The reaction takes place at ~60°C, in the presence of solvents and at extreme pH. This leads to high-energy consumption for the reaction as well as the separation steps. Organosilicon compounds may be also used as silica precursors at high or low pHs (and often in the presence of a solvent) but give poor control over the resulting silica morphology.[2]

B. Silica: Existence, Solubility, and Synthesis

Silicon is never found in nascent form in nature; however, in combination with oxygen it is abundant in the form of silica with the general formula $SiO_2 \cdot nH_2O$

and silicates. Silicon and oxygen are the major components of the earth's crust and in combination account for 78% of it. Silica is found in quartz, opal, and flint and in biological systems such as algae, sponges, and grasses.[3–5] Despite the vast scientific literature on crystalline and amorphous silica, new chemistries, structures, and applications continue to be discovered for compounds formed from these elements.

The dissolution of silica in water is slow, and its depolymerization is gradual. It follows a reversible reaction:[4]

$$\underset{\text{silica}}{(SiO_2)_x} + 2\,\underset{\text{water}}{H_2O} \leftrightarrow \underset{\text{silica}}{(SiO_2)_{x-1}} + \underset{\text{monosilicic acid}}{Si(OH)_4} \quad (1)$$

The solubility of silica in aqueous solutions depends on the following factors:[4]

1. The particle size of silica.
2. The degree of internal hydration in the silica.
3. Impurities present in the medium, such as ions, other molecules and macromolecules. These impurities alter the degree and strength of the hydrogen bonding of silica in solution, thus preventing or stimulating the dissolution of the silica, depending on the nature of the impurities.

As shown by equation 1, silica undergoes hydrolysis to form monosilicic acid. This compound is unstable and thus it can be neither isolated nor observed.[4] Thus, the term *silicic acid* is loosely used in the literature and typically indicates monosilicic acid as well as various oligomeric polysilicic acids.

The formation of a silica sol (solution of colloidal particles of sizes 1–1000 nm, in a liquid solvent) from the monosilicic acid follows three steps:[4]

1. Polymerization of $Si(OH)_4$ via condensation releasing water molecules to produce discrete nuclei/colloidal particles. The polymerization of monosilicic acid in the aqueous phase is different from the classical condensation polymerizations that are used to produce organic polymers.[4] In organic polymerizations, the polymer chains grow by a particular mechanism, but in the case of silicic acid polymerization, the growth is by nucleation and aggregation, as described below. In the early stage, siloxane (Si-O-Si) bond formation is maximized.
2. Particles grow by further polymerization of discrete colloidal particles by nucleation. The particle growth follows either Oswald's ripening (in which, smaller, unstable particles dissolve and precipitate on the surfaces of the relatively larger, insoluble, and stable particles) or condensation of intermediate size particles. Particle bridging plays an important role in this as well as the next stage of silica formation.
3. Aggregation of particles to produce larger particles and/or networks is then followed. The bridging of particles (nuclei) is maximized with only a few siloxane bonds formed at this stage.

Iler[4] described this complicated process, as shown in Figure 1.

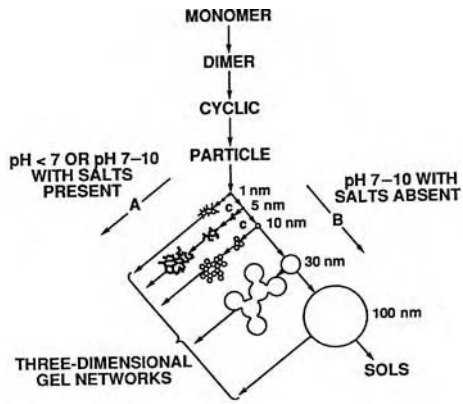

Figure 1 Polymerization behavior of silica in an aqueous medium. *A*, in the presence of salts, acidic medium; *B*, alkaline medium. (Reprinted from Ref. 4.)

i. Silica Synthesis by Sol–Gel Processing

Sol–gel processing typically uses alkoxy silane precursors that undergo hydrolysis and condensation reactions to form a sol and then a gel.[2] The process is briefly described below.

a. Hydrolysis

In the sol–gel processing of silica, a silica precursor undergoes hydrolysis. Most often, a tetraalkoxysilane is used as the silica precursor. The hydrolysis reaction can be illustrated as follows:

$$\equiv\text{Si–OR} + \text{H}_2\text{O} \rightarrow \equiv\text{Si–OH} + \text{R–OH} \tag{2}$$

The reaction follows by nucleophilic attack of oxygen from a water molecule on Si. Catalysts, solvents, and the R groups substituted on the silane precursor affect the rate and extent of hydrolysis. In the presence of catalysts, completion of the hydrolysis is observed. Typical catalysts are HF, HCl, amines, and KOH. Addition of solvent increases the rate of depolymerization and esterification reactions. Bulkier groups on the silica precursor reduce the rate of hydrolysis.[2]

b. Condensation

Hydrolysis is followed by condensation reactions liberating water or alcohol molecule(s), thus forming siloxane bonds. The two condensation reactions are represented as follows:[2]

Alcohol Condensation

$$\equiv\text{Si}-\boxed{\text{OR} + \text{H}}\text{O}-\text{Si}\equiv \rightarrow \equiv\text{Si}-\text{O}-\text{Si}\equiv + \text{ROH} \tag{3}$$

Water Condensation

$$\equiv\text{Si}-\boxed{\text{OH} + \text{H}}\text{O}-\text{Si}\equiv \rightarrow \equiv\text{Si}-\text{O}-\text{Si}\equiv + \text{H}_2\text{O} \tag{4}$$

It has been shown that these hydrolysis and condensation reactions usually follow an S_N2 mechanism. As with the hydrolysis reaction, condensation is affected by the solvent and R groups substituted on the silane precursor.[2]

ii. Silica Particle Synthesis

The sol–gel process has been used to produce various amorphous silica structures, such as tubular organogels by molecular imprinting.[6] The use of supramolecules for the synthesis of crystalline mesoporous materials via sol–gel processing is also well known.[7] Preparation of a silica sol of controlled properties was demonstrated by Stöber et al.[8] in 1968 and is discussed here.

Stöber et al. developed a process capable of forming controlled silica sols in the range from 500 nm to 2 μm. A typical reaction mixture contained tetraethoxysilane (TEOS) as the silica precursor along with water, ethanol, and ammonia in various concentrations. The silica particles produced were shown to have a narrow size distribution, and the particle sizes and size distribution could be controlled by controlling the solution pH, the composition of reactants, and the temperature. The pH of the medium was found to be the key variable and it was controlled by varying the ammonia strength. The process was typically carried out at higher temperatures (>20°C) and at higher pH (~10). This process has been widely adopted for silica particle synthesis, though it requires rather harsh process conditions. In a further detailed study on particles prepared by the Stöber route, it was found that[9] the particles were of a core-shell nature. The core was made up of highly condensed amorphous silica, and the less condensed shell contained silanol groups. This was also predicted earlier by Iler.[4] In addition, the smaller particles were found to depart from the spherical shape and were heterogeneous.

C. Biosilica: Existence and Importance

Among the interesting characteristics of biological systems are materials that exhibit a high degree of structural sophistication and the species-specific applications of ornate organic–inorganic hybrid materials formed by biomineralization.[10] In addition, biocatalysis has advantages such as mild reaction conditions, high product selectivity, and the environmentally friendliness of the process.[11] In nature, diatoms, unicellular algae found in water, are capable of forming species-specific ornate silica nano-structures, an example of which is shown in Figure 2.

Similarly, sponges and grasses form silicified structures.[5,12,13] Silicification in vivo (also called biomineralization and biosilicification, in particular) may also take place at (or very close to) neutral pH and in an aqueous phase and is predicted to be catalyzed by specific proteins. Thus biosilicification is inspirational source for in vitro studies. It is clearly important to study and understand the role and specificity of proteins involved in biosilicification. Such investigations have led to bioinspired silica synthesis. In addition, such bioinspired methodologies may help in cost reduction for industrial silica production.

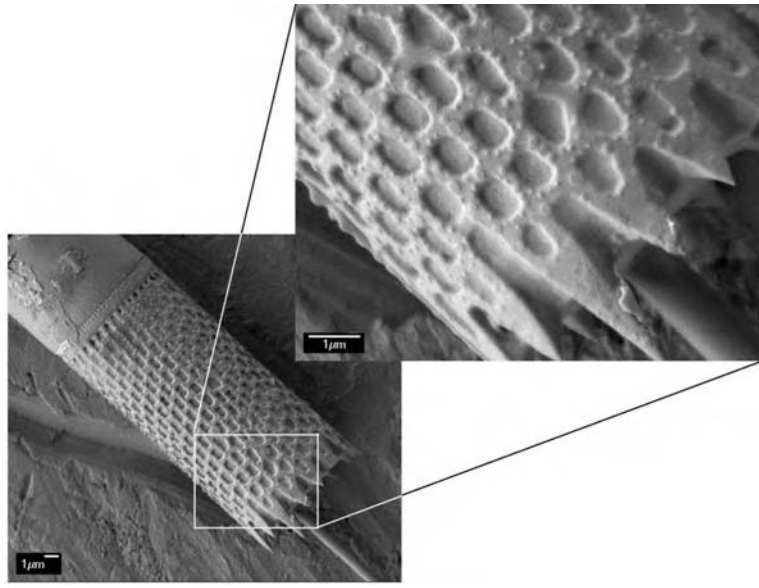

Figure 2 Representative micrograph of the elaborate biosilica structures of diatom *Aulacoseira granulata.* (Bar = 1 μm.)

II. BIOSILICIFICATION AND PROTEIN INTERACTIONS

The interactions of biological macromolecules (proteins) with silicic acid were observed in vitro and documented by Iler.[4] He described these interactions as follows: "Silicic acid precipitates gelatin . . ." and ". . . albumin combines with silicic acid." It was also reported that polyalcohols and sugars did not affect the solubility of silica, but glycine reduced its rate of dissolution. Thus it was known that macromolecules interact with silica in vivo as well as in vitro, but in an unknown fashion.

A. Diatoms

Proteins are incorporated into biosilica, and hence it is possible to selectively dissolve the biosilica and recover these biomacromolecules. Silaffin proteins (proteins having affinity towards silica) were extracted from the diatom *Cylindrotheca fusiformis* this way and were proposed to catalyze biosilicification in the diatoms.[14] The primary amino acid sequence of the silaffin proteins was also determined[14a] and was corrected twice in subsequent publications.[14b] The cDNA (*sil1* gene) corresponding to silaffin-1B encoded a polypeptide (sil1p), which was found to contain highly homologous repeating sequences (R1-R7 peptides) and is shown in Figure 3.

The silica synthesized in vitro using silaffins and an aqueous silica precursor resulted in nano-size particles (Fig. 4). The 19 amino acid sequence R5 (Fig. 3) was

Figure 3 Sequence of R1-R7 peptides derived from the diatom *C. fusiformis*. (After Ref. 14.)

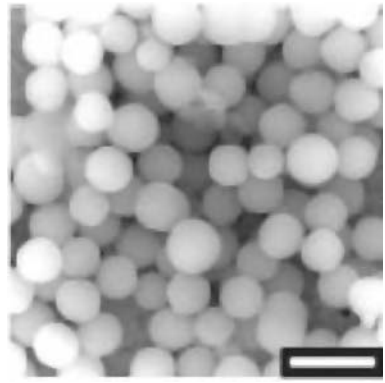

Figure 4 The silica particles synthesized in vitro using natSil protein extracted from the diatom *C. fusiformis.* Bar = 1 µm. (Reprinted from Ref. 14b.)

proposed to be a key part of the sequence; in the silaffin-1A, the lysine residues were found to be post-translationally modified. This modification is useful in maintaining a cationic charge on the protein in solution.[14a] Further studies of these proteins revealed the high levels of phosphorylation found on the serine residues.[14b] Recently, native silaffins were isolated from the diatom *C. fusiformis*, and natSil-1 was found to contain unusual amino acid modifications. Although natSil-2 did not show any

activity toward silica formation, it was shown to control silicification when present with native silaffin proteins.[15] It was proposed that these modifications may be important not only in *C. fusiformis* but also in other diatom species.

An application that used synthetic R5 polypeptide to yield an ordered precipitated array of silica onto a polymer hologram was developed.[16] Regularly spaced R5 polypeptide solution domains were produced by phase separation during the photochemical formation of a polymeric hologram. Treatment of this polypeptide patterned hologram with a pre-hydrolysed solution of tetramethoxysilane (TMOS) led to specific formation of silica nano-particles only in the region of the R5 domains (Fig. 5). These studies have put forward the technological importance of bioinspired studies in developing novel applications in addition to gaining an understanding of their roles in vivo.

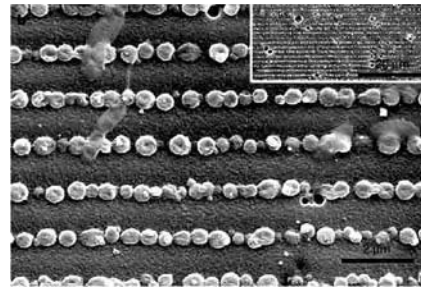

Figure 5 Two-dimensional array of ordered silica nanospheres formed within a polymeric hologram. Bar = 2 μm. (Reprinted from Ref. 16.)

Hildebrand et al.,[17] made a significant contribution toward understanding the silicification process in diatoms when they identified silicic acid transporters. It was also observed that silicon, through biosilicification and silicic acid uptake, controls the metabolism of diatoms, although the exact mechanisms of these processes are unknown.[18] In the deposition of diatom biosilica, it was recently proposed that two processes—micromorphogenesis and macromorphogenesis—might govern the silica formation.[19]

B. Grasses

Four plant materials that were silicified in various amounts were also analyzed for their protein content.[20] These plant materials were hairs from lemma of the grasses *Phalaris canariensis* L (containing 40% dry weight silica), branches from *Equisetum telmateia* (containing 20% dry weight silica), leaves from *Phragmites* sp. (containing 2% dry weight silica) and *Equisetum arvense*.[20,21] These samples were acid treated in two consecutive steps to extract the protein-containing material. It was revealed that the soluble extracts from the materials of the first two plants mainly contained amino acids with hydroxyl groups, basic amino acids, and elevated amounts of proline. Further, higher levels of basic amino acids and aliphatic amino acids were observed

in the insoluble residues obtained after HF treatment. The amino acid composition in *Phalaris* was determined: lysine, 22 mol %; histidine, 12 mol %; glutamic acid, 14 mol %; and proline, 25 mol %. A similar composition of amino acids was seen in *Phragmites*. In case of *Equisetum*, relatively higher levels of lysine and proline residues were observed.[20] It was proposed that such highly charged organic materials with rigid backbones could be regulating the nucleation of biogenic silica. In addition, the amino acids, capable of forming hydrogen bonds, may govern the particle growth, thus controlling the structure of biosilica.[20] When introduced to a silicic acid solution in vitro, these bioextracts were able to produce interesting crystalline silicas, thus highlighting the degree of control possessed by such bioextracts.[21]

C. Sponges

The marine sponge *Tethya aurantia* contains 75% dry weight silica in the form of needle-like spicules (1–2 mm in length and 30 μm in diameter) and was studied in order to isolate proteins that facilitate biosilicification.[22] It was found that each spicule contained a central filament of protein (1–2 mm in length and 1–2 μm in diameter). After various treatments to dissolve the mineral silica from the sponge,[22] three similar proteins were isolated and these silica proteins were named *silicatein* α, β, and γ. Silicatein α, which was found in large quantities as compared to silicatein β and γ and contained regular arrays of hydroxyls, was found to be highly similar to members of cathepsin L and papin family of proteases. In addition, it was found that the catalytic cysteine residues at the active site in these proteases were replaced by serine in silicatein α. Another feature of silicatein α is the hydroxy amino acid (serine, tyrosine and threonine) clusters. Using these and other findings, Cha et al.[23] proposed a mechanism for the silicon ethoxide condensation that was catalyzed by silicatein α and is based on the characteristic mechanism exhibited by the serine–histidine and the cysteine–histidine pairs of active sites of the serine- and cysteine-based proteases.

As to the role of these biomacromolecules (isolated from various biological systems) in silicification/biosilicification, Tacke[24] described how the silaffin proteins from the diatom *Cylindrotheca fusiformis* and the silicatein proteins from the sponge *Tethya aurantia* have a catalytic/templating/scaffolding role in the formation of ordered silica structures. He had also foreseen the use of such biomacromolecules in organic synthesis in vitro. These results are important from a materials science viewpoint and can be used as a methodology to synthesize organic–inorganic hybrid materials for specific applications.

III. BIOINSPIRED AND BIOMIMETIC SYNTHESIS: THE USE OF POLY (ALLYLAMINE HYDROCHLORIDE)

The growing silica nuclei/particles/sol contain negative charges at neutral pH. It is also known that the silaffins are cationically charged macromolecules, as discussed

above. Thus we have shown that various cationically charged water soluble macromolecules can be used to form silica particles and structures. Because poly(allylamine hydrochloride) (PAH) satisfies these requirements, it was used to study silica synthesis. It was also used to investigate the specificity of proteins in (bio)silica formation.

A. Synthesis of Spherical Silica Particles

PAH has been studied in detail for its role in silicification under ambient conditions and at neutral pH.[25–27] It was demonstrated that PAH can facilitate the formation of nanometer and micrometer-size spherical silica particles under mild conditions from an aqueous solution of a silica precursor (Fig. 6). It was shown by energy dispersive spectroscopy (EDS) and Fourier transform infrared spectroscopy (FTIR)[26] that the PAH was incorporated into the final silica structures. In the absence of PAH the reaction mixture gelled in 1 day. These results indicate that PAH may act as a catalyst as well as a template or structure-directing agent in silicification. In this context, the behavior of this system is consistent with how Tacke described the role(s) of macromolecules that facilitate silica formation via scaffolding (see section II).

In further investigations, various parameters that govern the silica synthesis and the morphology of the silicified products were studied. Among the important parameters were the reaction time, the precursor concentration, and the precursor prehydrolysis time.

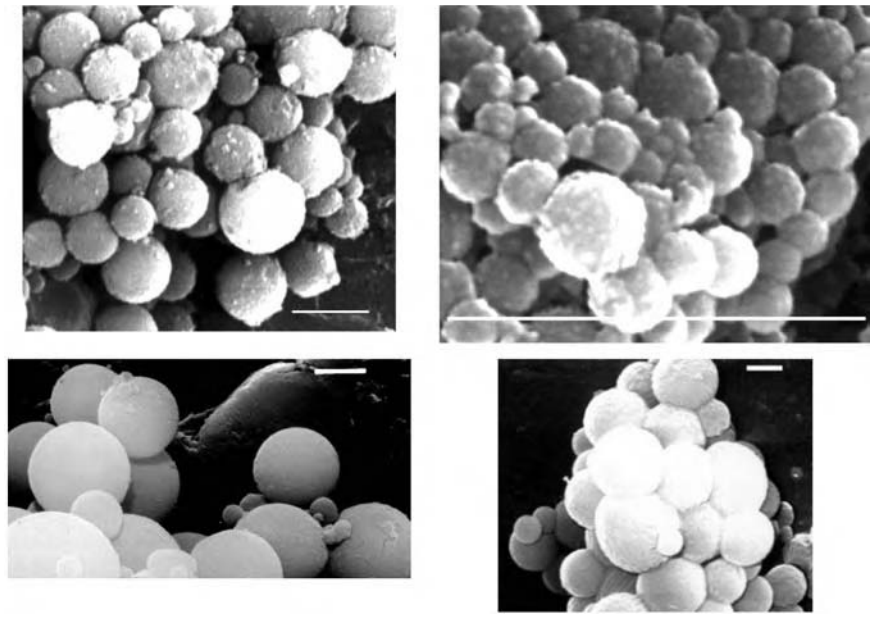

Figure 6 Representative SEM micrographs of nano- and micro-size silica particles synthesized using PAH. Bar = 1 μm.

B. Synthesis of Nonspherical Silica Structures

A shear force was externally applied to the reaction mixture by continuously stirring or flowing the reaction mixture in a tube while it was reacting; this resulted in the formation of fiber-like silica structures for the PAH system (Fig. 7).[28] One of the reasons for the departure of silica structures from a spherical morphology is due to the alteration of the orientation of the polymer in the solution under externally applied shear. Apart from fiber-like structures, various other silica structures were also synthesized, and they were found to be amorphous.[29] In a similar fashion, Naik et al.[30] have recently demonstrated how the structures of silica mediated by R5 peptide can be controlled using externally applied shear.

Figure 7 Elongated silica structures formed using PAH when the reaction mixture was stirred. (Reprinted from Ref. 28.)

Further investigations of these structures and the conditions under which they formed are in progress. One interesting thing to note in this context is that diatoms that form perfectly round structures in relatively "quiet" surroundings, may form rather elongated/ellipsoidal structures in shallow waters.[31] Thus the conditions in vitro mimic the conditions in shallow water or windy areas wherein the medium is under continuous motion.

C. Synthesis Using a Mixture of Macromolecules

When another cationically charged polymer (poly-L-lysine; discussed below) was added to the reaction mixture along with PAH, disk-like silica particles were observed rather than spherical silica particles as seen with just PAH (Fig. 8). It is postulated that the two polymers affect the chain conformations of each other, thus altering the product morphology.[29] Experiments in vitro using a mixture of polyamines and silaffins extracted from diatoms resulted in similar disk-like structures.[32]

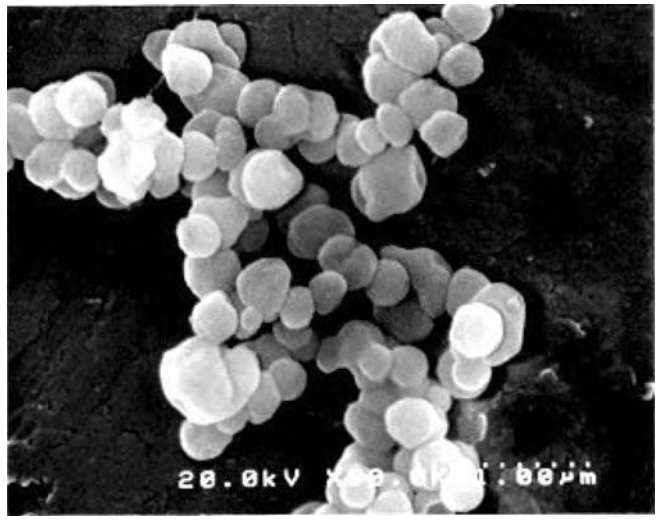

Figure 8 Disk-shaped silica particles formed on mixing PAH with PLL.

D. Electrostatically Self-Assembled Bilayers of PAAcid and PAH

A set of experiments was carried out to study the activity of PAH when it was coated on silicon and silica glass substrates. The substrates were prepared by alternate electrostatically self-assembled (ESA) adsorptions of polyacrylic acid (PAAcid) and PAH from their respective solutions to a substrate to form 10–11 bilayers.[33] These substrates were dipped into TMOS solutions, removed after 5 min, washed with deionized water, and then dried. The samples were then scanned under SEM for silica formation on the substrates. There was no evidence for the controlled formation of silica on these substrates except for a few irregular shaped silica regions, which were small in number. However, when TMOS was added to a solution of a mixture of PAH and PAAcid, silica precipitation was observed.

E. Role of Polyelectrolytes

The role of polyelectrolytes in the destabilization/stabilization of colloids was studied in detail by Heller[34] and LaMer and Healy.[35] The polyelectrolytes, due to counterions/charges, become associated with the surface of the colloids, thus destabilizing/stabilizing the colloidal particles. The effect of polyelectrolyte concentrations has also been studied. At lower concentrations, polyelectrolytes partially cover the surface of the colloids (Fig. 9a). At a certain optimum concentration, the particle surface is covered entirely, thus precipitating/flocculating the particles. At higher concentrations, the colloids redisperse due to the charges of the polyelectrolytes. A mechanism suggesting that these polyelectrolytes act as a bridge, connecting the colloidal particles has been

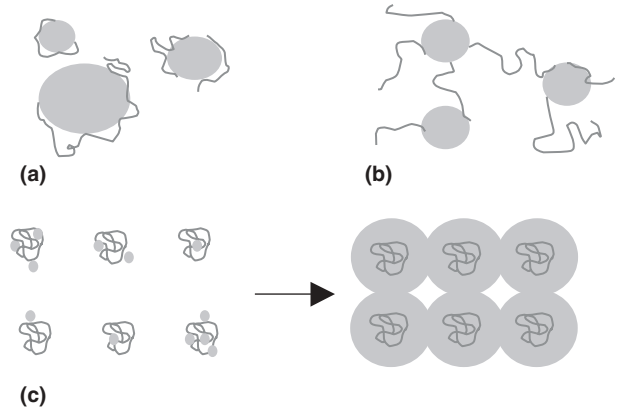

Figure 9 Polyelectrolytes and charged colloids. (Reprinted from Ref. 36 with permission from the Royal Society of Chemistry.)

proposed (Fig. 9b).[4,27,34,35] This bridging mechanism also predicts the formation of physical bonding (entanglements) and/or chemical (hydrogen) bonding between polymer molecules directly or through the flock. The polymer adsorption on the surface of the colloidal particles alters the silica–water interfacial free energy. The ability to form hydrogen bonding is considered important in the case of silicification and biosilicification. Iler[4] described the interactions of macromolecules with silica acid as follows: "The combination occurs by the formation of a multiplicity of hydrogen bonds between the relatively large molecules of proteins and polysilicic acid such that a mixed network of these molecules if formed, leading to the separation of the aggregates from the sol."

Polyelectrolytes form domains in solution with a characteristic correlation distances (i.e., spatial distribution of chains).[37] For PAH solutions this was observed using small-angle light scattering (SALS).[27] Based on our findings on the use of PAH in bioinspired silicification, the effect of phosphate ions in PAH-mediated silica synthesis was studied.[38] It was proposed that the phosphate ions play an important role in the self-assembly,[38] which is in line with our observations based on SALS.[27] The polyelectrolyte concentration, medium and the type of the monomer unit alter the correlation distance. A similar process may be taking place in vivo. The chains of proteins facilitating biosilicification may be taking a particular orientation due to the primary sequence of a variety of amino acids. In addition, proteins might also maintain a characteristic correlation distance with other chains due to the presence of the net charge on the individual protein molecules or due to the attractions/repulsions between molecules. This organization of the protein molecules may serve as a template or scaffold in addition to their showing catalytic activity. Once this organization is achieved, silica deposits specifically on the catalytically active sites, forming ordered and uniform structures. This behavior is depicted in Figure 9c.

Because particle bridging is an important factor in silica formation as discussed above, polyelectrolytes play an important role in silicification. When the

reaction is terminated after step two of the silica formation to avoid gelation, particles of nanometer and micrometer sizes are obtained. This is achieved by coagulating the particles either by intermolecular van der Waals attractions or by a species that will provide particle–particle bridging through ionic, covalent, and/or hydrogen bonding. This is achieved by using various cationically charged polymers.

IV. USE OF OTHER MACROMOLECULAR SYSTEMS TO SYNTHESIZE SILICA

It is postulated that various amino acid residues in the primary sequence of the proteins discussed in section II are important in biosilicification. These include lysine, histidine, arginine, proline, cysteine, and serine.[14,18,20,26] Homopolymers of lysine (poly-L-lysine), arginine (poly-L-arginine), histidine (poly-L-histidine), and proline (poly-L-proline) have been shown to produce silica from various silica precursors in vitro at (or close to) neutral pH.[27,29,39–47]

A. Silica Synthesis Using Polyamino Acids

Lysine is one of the important amino acids in the primary sequence of the silaffin proteins. Poly-L-lysine, PLL precipitated well-shaped silica spheres (Table 1).[29,42–44] In addition, controlled synthesis of nonspherical structures was also recently reported.[36] These new silica structures include hexagonal and petal-like two-dimensional structures. Furthermore, another investigation revealed that oligomers of lysine were able to control silicification kinetics and product properties.[47]

As seen in Figure 3, arginine residues were found in pairs in the primary sequence of the sil1p protein. Therefore, PLAr (Table 1) was used to study its ability to form silica structures.[39,42,46] PLAr was also able to precipitate well defined silica (Table 1).

In a recent investigation, we have shown that some of the silica-binding polypeptides isolated from a combinatorial phage peptide display library were able to precipitate silica in vitro when TMOS was used as a silica precursor at neutral pH.[48] From the sequence of the various phage peptide clones, it was proposed that histidine might be an important amino acid in biosilicification. Histidine was also proposed to be a key residue in silicatein α that was isolated from the silica spicules of the marine sponge *Tethya aurantia* (as discussed earlier). In these studies, TEOS was used as the silica precursor. The role of poly-L-histidine (PLHis) (Table 1) in silicification in vitro was investigated. It was found that PLHis was also able to form silica particles, similar to PLL and PLAr.

B. Silica Synthesis Using Polypeptides

Various diblock copolypeptides were used to form silica structures (Table 2).[49] Cystein–lysine block copolypeptides were successful in facilitating the silica synthesis.

Table 1 Details on Various (Macro)Molecules Used in Silicification[a]

Chemical Agent	Structure	Silica Formed[b]
Poly-L-lysine (PLL)	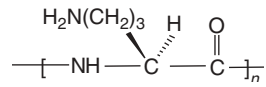	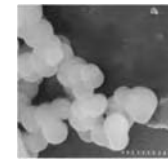
Poly-L-arginine (PLAr)	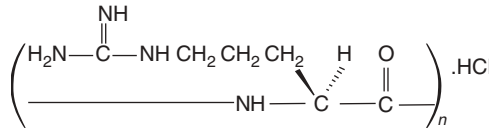	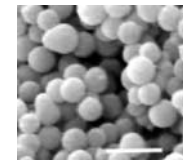
R5		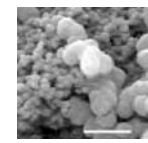
Poly-L-histidine (PLHis)	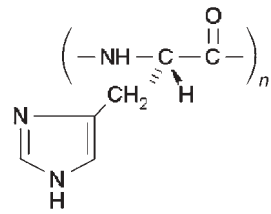	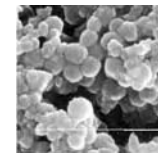
Poly(allylamine hydrochloride) (PAH)	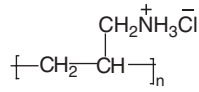	See Figure 6
Polyallylamine (PAAm)	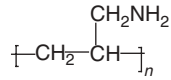	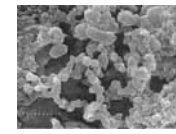
Polyethyleneimine (PEI)	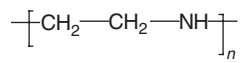	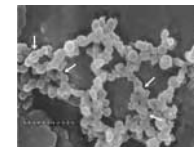
Poly(diallyldimethyl ammonium chloride) (PADA)	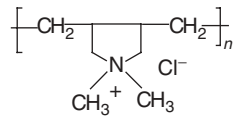	—

(*Continued*)

Table 1 (Contd.)

Chemical Agent	Structure	Silica Formed[b]
Polyvinyl alcohol (PVA)	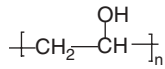	—
Polyanethole sulfonic acid (PASA)	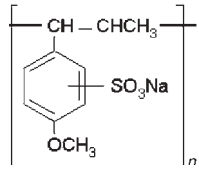	—
Polyacrylic acid (PAAcid)	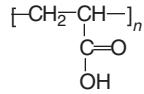	—
Polymethacrylic acid (PMA)	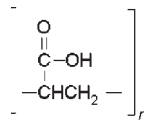	—
Poly(phenylene vinylene) (PPV) precursor	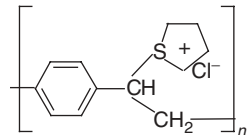	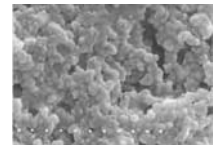
Functionalized C_{60} -fullerene	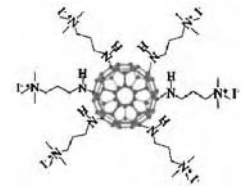	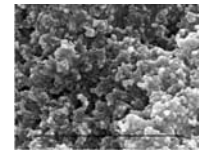

[a] Reprinted from Ref. 42.
[b] Bars = 1 μm.

It was postulated that these polypeptides self-assemble in solution and thus direct the formation of silica structures. These polypeptides were able to form spherical as well as pillar-like structures with TEOS precursor.[49]

R1, R2, and R5 peptides, three amino acid sequences found in the sil1p protein (Fig. 3), were used in vitro to study the silica formation. It was revealed that these polypeptides also form silica upon the addition of TMOS solution.[50] Another investigation made use of arginine-based surfactants to synthesize mesoporous silica.[41]

Table 2 Block Copolypeptides Used in Silicification[a]

Entry Number	Description
1	Poly[(L-alanine)$_{30}$-*b*-(L-lysine)$_{200}$]
2	Poly[(L-glutamine)$_{30}$-*b*-(L-lysine)$_{200}$]
3	Poly[(L-serine)$_{30}$-*b*-(L-lysine)$_{200}$]
4	Poly[(L-tyrosine)$_{30}$-*b*-(L-lysine)$_{200}$]
5	Poly[(L-cystein)$_n$-*b*-(L-lysine)$_m$][b]
6	Poly[(L-cystein)$_{30}$-*b*-(L-glutamate)$_{200}$]

[a] Reprinted from Ref. 49.
[b] *n*, 10, 30, or 60; *m*, 200 or 400. These polypeptides were successful in producing well defined silica structures.

C. Silica Synthesis Using Polycations

Polyallylamine (PAAm), which has a similar backbone structure to that of PAH and has a primary amine in the side chain, was found to precipitate nearly spherical silica particles.[42] Another polymer, polyethyleneimine (PEI), was used in the silicification. PEI does not have side chains but contains nitrogen in the backbone of the polymer. PEI also precipitated silica particles that were nearly spherical in shape.

Poly(diallyldimethyl ammonium chloride) (PADA) has a quaternary amine but does not have any hydrogen atoms attached to the nitrogen. The nitrogen atom in PADA is also in a five-membered ring. It did not precipitate silica but gelled in 1 day instead. This suggests the importance of the hydrogen on the active sites of the polymer, which forms hydrogen bonds that govern the chain conformation of the macromolecule in solutions and the affinity for the growing silica. The presence of the nitrogen in the ring may also alter its ability to form silica, either by altering the net charge (electronegativity) of nitrogen or by steric factors.

To study the importance of nitrogen in the silica precipitating species, polyvinyl alcohol (PVA) was used. It was expected that PVA would also form silica structures, as oxygen is capable of forming hydrogen bonds in solution. In contrast, when a solution of PVA was added to the prehydrolyzed TMOS solution, gel formation was observed. This result clearly distinguishes macromolecules that just bind with silica (hydroxyl-containing macromolecules like PVA, polysaccharides) and the macromolecules that facilitate catalysis/scaffolding (e.g., PLL, PLAr, silaffin). Hence, the panning technique recently used[48,51] for the identification and study of polypeptides that bind to the substrates or reactants (silica in this case) may be ambiguous as to the precise mechanisms and consequences of the binding.

D. Silica Synthesis Using Polyanions and Other Systems

In a similar intention as discussed for PVA, we investigated the effect of PASA (Table 1) on the silica synthesis.[42] In presence of PASA, the silica precursor solution gelled. This might be due to the negative charges of PASA, which repel the growing silica sol species, which are also negatively charged.

Further, to demonstrate that negatively charged polymers will not catalyze silica formation under these conditions, in the way discussed above for PASA, and that there might be some specificity of the cationic charge in the polymers, we used PAAcid and PMA (Table 1). As expected, neither of the polymers facilitated the precipitation of silica and they each formed gel in 1 day.

PPV precursor (Table 1) precipitated silica and did not gel, but the silica produced did not have a well-defined structure. However, the ability of PPV to precipitate silica and not gel can be used. The precipitate can be dried and can be powdered for suitable applications in photovoltaic devices. The precipitate, when left in a test tube, was seen to change its color from white to light blue in 3–5 days and then to bluish green in 5–7 days. The conversion of the PPV precursor to PPV within the inorganic–organic hybrid system and the optical properties of this hybrid are currently being investigated.

A water-soluble C_{60}-fullerene (Table 1) was studied for its ability to form silica.[52] The functionalized C_{60}-fullerene did not precipitate silica, and neither did it gel in 24 h. Fullerene-silica hybrid materials find applications in photovoltaic devices and related opto-electronic applications.

V. SUMMARY

Organisms of various kingdoms have been reported to deposit a variety of different minerals through biomineralization.[53] Key features of biomineralization are the precise hierarchical control over structural growth of biominerals, species specificity of the biomineral morphology, and ambient conditions (temperature and pH) for formation. The deposition of amorphous silica to form ornate frustules through biosilicification in diatoms is one example. In addition, biomineralization is facilitated and controlled by various characteristic proteins in each biological system. The entrapment of the catalyzing/templating/scaffolding biomacromolecules enables them to be recovered by selective dissolution of the biomineral. Study of these proteins is thus of interest in understanding biomineralization. The proteins extracted from the diatom *Cylindrotheca fusiformis* (silaffins) and the sponge *Tethya aurantia* (silicateins) and higher plants have been shown to precipitate silica from silica precursors in vitro. Furthermore, this understanding helps us design biomimetic materials, new processes, and new applications based on the aforesaid minerals in a bioinspired synthetic manner in vitro. The identification of synthetic macromolecules that can act as catalysts/templates/scaffolds for silica formation gives exciting possibilities for bioinspired silica synthesis.

VI. FUTURE WORK

Precipitated silica is widely used as a reinforcing agent in a wide variety of organic–inorganic hybrid materials. The properties of such materials to date are characteristically isotropic due to the use of spherical silica particles. The use of

biomacromolecules provide novel routes to preparing oriented silica structures and present the fascinating possibility of preparing novel organic–inorganic hybrid materials for the first time where the properties are highly anisotropic.[54]

It should be noted that (bio)macromolecules typically facilitate (bio)mineralization via ionic bridges and hydrogen bonding with the growing minerals. These interactions facilitate the self-organization of the (bio)macromolecules (also referred to as the *organic matrix* in the literature) that create appropriate scaffolds for structure direction of the growing (bio)minerals. In addition, catalytic residues/sites become available for facilitating the growth of the mineral phase (e.g. cationic residues in the case of silaffin proteins catalyzing the biosilica formation in diatoms). This mechanism can be further exploited not only for silica synthesis but also for synthesis and nano-patterning of various other systems based on aluminium, boron, tin, germanium, silver, gold, iron, calcium, and so on.[36,55–57] Research in the field of biomineralization and biomimetic materials synthesis based on these concepts will be highly fruitful.

VII. ACKNOWLEDGMENTS

We thank Professor Miriam Steinitz-Kannan (Northern Kentucky University) for kindly providing us with diatom samples. We also thank Professor Carole Perry (Nottingham Trent University) for various helpful discussions. The expertise of Dr. Niloy Mukherjee (UC) in carrying out our SEM and EDS analysis is much appreciated.

VIII. REFERENCES

1. T. Kendall, *Ind. Minerals*, 49 (2000).
2. C. J. Brinker, G. W. Scherer, *Sol-Gel Science: The Physics and Chemistry of Sol-Gel Processing*, Academic Press, Boston, 1990.
3. C. S. G. Phillips, R. J. P. Williams, *Inorganic Chemistry*, vol. 1, Oxford University Press, 1965.
4. R. K. Iler, *The Chemistry of Silica: Solubility, Polymerization, Colloid and Surface Properties, and Biochemistry*, Wiley, New York, 1979.
5. T. L. Simpson, B. E. Volcani, eds., *Silicon and Siliceous Structures in Biological Systems*, Springer-Verlag, New York, 1981.
6. J. H. Jung, Y. Ono, S. Shinkai, *Langmuir* **16**, 1643 (2000).
7. R. Szostak, *Molecular Sieves: Principles of Synthesis and Identification*, 2nd ed., Blackie, London, 1998.
8. W. Stöber, A. Fink, E. Bohn, *J. Colloid Interface Sci*. **26**, 62 (1968).
9. C. A. R. Costa, C. A. P. Leite, E. F. de Souza, Galembeck, F., *Langmuir* **17**, 189 (2001).
10. P. Calvert, S. Mann, *J. Mater Sci.* **23**, 3801 (1988).
11. A. M. Thayer, *C&EN*, **79**, 27 (2001).
12. D. Evered, M. O'Connor, eds., *Silicon Biochemistry*, Ciba Foundation Symposium, 121, Wiley, Chichester, UK, 1986.

13. W. E. G. Müller, ed., *Silicon Biomineralization*, Springer Verlag, 2003.
14. (a) N. Kröger, R. Deutzmann, M. Sumper, *Science* **286**, 1129 (1999); (b) N. Kröger, S. Lorenz, E. Brunner, M. Sumper, *Science* **298**, 584 (2002).
15. N. Poulsen, M. Sumper, N. Kröger, *Proc. Natl. Acad. Sci. USA* **100**, 12075 (2003).
16. L. L. Brott, D. J. Pikas, R. R. Naik, S. M. Kirkpatrick, D. W. Tomlin, P. W. Whitlock, S. J. Clarson, M. O. Stone, *Nature* **413**, 291 (2001).
17. M. Hildebrand, B. E. Volcani, W. Gassmann, J. I. Schroeder, *Nature* **385**, 688 (1997).
18. V. Martin-Jezequel, M. Hildebrand, M. A. Brzezinski, *J. Phycol.* **36**, 821 (2000).
19. M. Hildebrand, in *Silicon Biomineralization*, W. E. G. Müller, ed., Springer Verlag, 2003.
20. C. C. Harrison, *Phytochemistry* **41**, 37 (1996).
21. C. C. Perry, T. Keeling-Tucker, *Colloid Polym. Sci.* **281**, 652 (2003).
22. K. Shimizu, J. Cha, G. D. Stucky, D. E. Morse, *Proc. Natl. Acad. Sci. USA* **95**, 6234 (1998).
23. J. N. Cha, K. Shimizu, Y. Zhou, S. C. Christiansen, B. F. Chmelka, G. D. Stucky, D. E. Morse, *Proc. Natl. Acad. Sci. USA* **96**, 361 (1999).
24. R. Tacke, *Angew. Chem. Int. Ed.* **38**, 3015 (1999).
25. S. V. Patwardhan, S. J. Clarson, *Polym. Bull.* **48**, 367 (2002).
26. S. V. Patwardhan, N. Mukherjee, S. J. Clarson, *Silicon Chem.* **1**, 47 (2002).
27. S. V. Patwardhan, Ph.D diss., Department of Materials Science and Engineering, University of Cincinnati, 2003.
28. S. V. Patwardhan, N. Mukherjee, S. J. Clarson, *J. Inorg. Organomet. Polym.* **11**, 117 (2001).
29. S. V. Patwardhan, N. Mukherjee, S. J. Clarson, *J. Inorg. Organomet. Polym.* **11**, 193 (2001).
30. R. R. Naik, P. W. Whitlock, F. Rodriguez, L. L. Brott, D. D. Glawe, S. J. Clarson, M. O. Stone, *Chem. Commun.* **2**, 238 (2003).
31. M. Steinitz-Kannan, personal communication.
32. N. Kröger, R. Deutzmann, C. Bergsdorf, M. Sumper, *Proc. Natl. Acad. Sci. USA* **97**, 14133 (2000).
33. S. V. Patwardhan, M. F. Durstock, S. J. Clarson, in *Synthesis and Properties of Silicones and Silicone-Modified Materials*, Oxford University Press, 2003.
34. W. Heller, *Pure Appl. Chem.* **12**, 249 (1966).
35. V. K. La Mer, T. W. Healy, *Rev. Pure Appl. Chem.* **13**, 112 (1963).
36. S. V. Patwardhan, N. Mukherjee, M. Steinitz-Kannan, S. J. Clarson, *Chem. Commun.* **10**, 1122 (2003).
37. R. Borsali, in *Handbook of Polyelectrolytes and Their Applications*, vol. 2, S. K. Tripathy, K. Kumar, H. S. Nalwa, eds., American Scientific, 2002.
38. E. Brunner, K. Lutz, M. Sumper, *Phys. Chem. Chem. Phys.* **6**, 854 (2004).
39. T. Coradin, O. Durupthy, J. Livage, *Langmuir* **18**, 2331 (2002).
40. S. V. Patwardhan, S. J. Clarson, unpublished data.
41. T. Coradin, C. Roux, J. Livage, *J. Mater. Chem.* **12**, 1242 (2002).
42. S. V. Patwardhan, S. J. Clarson, *Silicon Chem.* **1**, 207 (2002).
43. S. V. Patwardhan, S. J. Clarson, *J. Inorg. Organomet. Polym.* **12**, 109 (2002).
44. S. V. Patwardhan, S. J. Clarson, *Mat. Sci. Eng. C Bio. S.* **23**, 495 (2003).
45. S. V. Patwardhan, S. J. Clarson, *J. Inorg. Organomet. Polym.* **13**, 49 (2003).
46. S. V. Patwardhan, S. J. Clarson, *J. Inorg. Organomet. Polym.* **13**, 193 (2003).
47. D. Belton, G. Paine, S. V. Patwardhan, C. C. Perry, *JMC* **14**, 2231 (2004).
48. R. R. Naik, L. L. Brott, S. J. Clarson, M. O. Stone, *J. Nanosci. Nanotechnol.* **2**, 95 (2002).
49. J. N. Cha, G. D. Stucky, D. E. Morse, T. J. Deming, *Nature* **403**, 289 (2000).
50. P. W. Whitlock, S. V. Patwardhan, S. J. Clarson, unpublished data.

51. R. R. Naik, S. J. Stringer, G. Agarwal, S. E. Jones, M. O. Stone, *Nature Mater.* **1**, 169 (2002).
52. S. V. Patwardhan, N. Mukherjee, M. F. Durstock, L. Y. Chiang, S. J. Clarson, *J. Inorg. Organomet. Polym.* **12**, 49 (2002).
53. H. A. Lowenstam, *Science* **211**, 1126 (1981).
54. V. P. Taori, M. Hassan, S. V. Patwardhan, J. E. Mark, S. J. Clarson, *Polym. Preprin.* **45,** 694 (2004).
55. S. V. Patwardhan, S. J. Clarson, unpublished data.
56. S. V. Patwardhan, K. Shiba, C. Raab, N. Hüsing, S. J. Clarson, *Silicon Chemistry*, in press.
57. S. V. Patwardhan, K. Shiba, S. J. Clarson, *Polym. Preprin.* **45**, 612 (2004).

CHAPTER 9

Organogermanium Polymers

Charles E. Carraher Jr.

Department of Chemistry and Biochemistry, Florida Atlantic University, Boca Raton, Florida

Charles U. Pittman Jr.

Department of Chemistry, Mississippi State University, Mississippi State, Mississippi

Martel Zeldin

Department of Chemistry, Hobart and William Smith Colleges, Geneva, New York

Alaa S. Abd-El-Aziz

Department of Chemistry, The University of Winnipeg, Winnipeg, Manitoba, Canada

CONTENTS

Macromolecules Containing Metal and Metal-Like Elements, Volume 4: Group IVA Polymers, edited by Alaa S. Abd-El-Aziz, Charles E. Carraher Jr., Charles U. Pittman Jr., and Martel Zeldin
ISBN: 0-471-68238-1

I. INTRODUCTION

Group IVA consists of a nonmetal, carbon; followed by metalloids; silicon and germanium; and metals, tin and lead. The bond energy of Si–Si bonds is 222 kJ/mol, while the C–C bond energy is 346 kJ/mol.[1] In contrast, Si-O bonds are more stable (452 kJ/mol) and have properties that lend themselves well to practical applications. Germanium acts as the bridge between silicon with its metalloid properties and tin and lead with their metallic properties. The Ge–Ge bond strength is only about 170 kJ/mol, which is far less than that of C–C or Si–Si but greater than that of Sn–Sn (about 150 kJ/mol). The rarity and high cost of germanium and its compounds slowed the development of this area of research compared to other group IVA elements.

In 1864, Newlands first speculated that germanium was a missing element between silicon and tin.[1] A few years later, Mendeleev stated that the missing element in the periodic table was germanium and predicted its general properties based

on similarities to silicon and tin.[1] While the preferred oxidation state of the group IVA elements is +4 and involves covalent bonding, tin and lead also form stable ionic and covalent compounds with a +2 oxidation state. Carbon, silicon, and germanium can also have formal oxidation states of −4 when they are bonded to more electropositive elements.

There are examples of polymers containing each of the Group IVA metalloids and metals; however, polymers containing silicon are the most prevalent. The lack of available organogermanium monomers as well as the high cost associated with the some of the existing monomers are the main reasons why only a small number of polymers have been prepared containing germanium compared to silicon.

The topic of organometallic-containing polymers has been reviewed in the past as part of the coverage of other Group IVA-containing polymers.[2,3] The vast majority of reports on organolead polymers deal with materials, which in the solid state, are called polymeric because of the similarity of connective bond distances to those of covalently bonded atoms. Unlike for organolead polymers, few if any reports exist of similar solid state monomeric organogermanium products that form poilymeric arrays. This may also be responsible for the poor solubility of many lead monomers and, conversely, the general good solubility of organogermanium compounds.

II. POLYGERMANES

Linear polymers of the general formula -MR_2- can be considered analogs of polymeric hydrocarbons; however, the electronic properties of polymetallanes are unlike those of the saturated hydrocarbon polymers, being rather more like those of unsaturated hydrocarbon polymers. Experimental and theoretical studies are consistent with an intense low-energy electronic absorption maximum that shifts to higher wavelengths with increasing chain length. This phenomena is the result of σ-delocalization that occurs along the polymetallane backbone.

Coupling of polysilanes, polygermanes and polystannanes with arenes or acetylenes involves their σ-delocalization and their σ-π delocalization. In exhibiting electrical conductivity germanium and tin show more typical "metallic" bonding behavior. Some polystannanes have been referred to as "molecular metals."[4] Conductivity is increased by doping,[5] illumination,[6] and application of an electric field.

Both polysilanes and polygermanes contain a metal–metal backbone, which emits in the near UV spectral region, exhibits high hole mobility, and exhibits high nonlinear optical susceptibility. This makes these materials candidates for a variety of optoelectronic applications.[7]

The optoelectronic properties result from σ-σ* delocalization and confinement of the conjugated electrons along the backbone. Polygermanes resemble polysilanes in this regard. The latter have been studied in more detail. Polysilanes exhibit UV absorption[8–10] and their λ_{max} exhibits a red shift as the silicon chain becomes longer. The UV spectra of some polysilanes were found to be thermochromic.[11] This is due to conformational changes in the backbone. Conformational dependence of

polysilanes (and polygermanes) has been explained by an avoided crossing of the two lowest-energy valence excited states of B symmetry.[12] This has been experimentally verified by using constrained tetrasilanes.[13–15] Studies of conformationally constrained hexasilanes demonstrated that an *anti* turn effectively extends the σ-conjugated system, while a *syn* turn at the temini does not.[14] Recent UV studies of the σ-σ* transition in *anti*, *cisoid* alternating oligosilanes has provided definitive evidence for the suppression of conjugation by a *cisoid* turn.[16] The notation for main-chain conformers, which is currently adopted, is given in a review by Michl and West.[17]

The absorption maximum wavelengths of alkyl oligosilanes steadily shift toward longer wavelengths as silicon chains lengthen, due to the elongation of the successive *anti* (e.g., *transoid*) segment lengths. Based on the close correspondence between polygermanes and polysilanes, this explanation should also hold for polygermanes.

Molecular orbital calculations at the CIS/6-31G* level have been carried out[11] on possible conformers of oligosilanes for peralkylated systems, which can rotate, and for conformationally constrained systems. The σ-σ* excitations for all *anti* conformations decrease in energy (HOMO-LUMO gap gets closer in energy) as the chain gets longer. When *anti* and *cisoid* conformations alternate along the backbone, the HOMO-LUMO gap decreases more slowly. Thus σ-conjugation does not effectively extend through a small Si-Si-Si-Si- dihedral angle such as a *cisoid* turn but is effectively transmitted through dihedral angles close to the 180° associated with the *anti* (*transoid*) conformation. It has been demonstrated that the band gap decreases in the order Si > Ge > Sn, which is a result of the increasing M–M bond length.

Due to the limited number of well-defined polygermanes that have been prepared and made available, few demonstrated applications have appeared. However, polygermanes have possible applications as photocondustors,[6,18] photoresists,[19–20] and nonlinear optical materials.[21–25] Applications should be pursued.

A. Wurtz Reactions

The successful preparation of high molecular weight (MW) polysilanes suggested that catenated germanium analogous might also be accessible. Like silicon, germanium derivatives form cyclic and acyclic catenates. Soluble, high MW, substituted germanium homopolymers and silicon–germanium copolymers have been made by the Wurtz-type reaction of dichlorogermanium precursors with sodium dispersions (Scheme 1).[26,27] As frequently found in polysilane synthesis, polygermanes resulting from the Wurtz reaction seem to exhibit bimodal molecular weight distributions. The charge transfer spectra of the tetracyanoethylene (TCNE) adducts of permethylated polygermane have been described by Mochida and co-workers.[6] The spectra of the charge transfer complexes were red shifted with increasing polymer chain length. More over, the polygermanes inserted into TCNE to produce 1:1 adducts at 50°C.

Mochida and Chiba[28] carried out the synthesis of dibutyl and dihexyl polygermanes via Wurtz-like couplings using a variety of conditions. The weight average

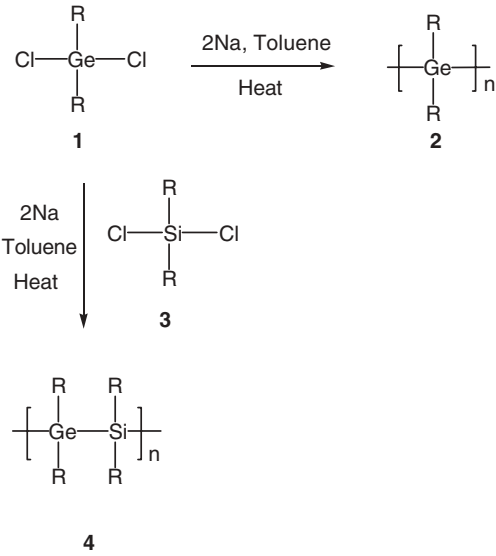

Scheme 1

molecular weights (MW_A) of the resulting polygermanes ranged from 3,000 to 10,000, with polydispersity (M_w/M_n) values ranging from 1.06 to 1.5. Clearly, molecular weight varies but these products are less polydisperse than most typical polymers. The yields of polygermanes ranged from 20% to 50%. Poly(dibutylgermane), which is obtained by heating dibutyldichlorogermane and a sodium metal dispersion in refluxing toluene, had a narrow molecular weight range but also low molecular weight. Addition of a sodium metal dispersion to a toluene solution of dibutyldichloridegermane (the inverse reaction to the first one described) gave lower yields and shorter chain lengths. Thus order of addition has an effect on the reaction. Addition of 18-crown-6 ether gave lowered chain sizes and yields. Similar results were reported by Miller and Sooriyakumaran.[27] Addition of small amounts of the co-solvent hexamethylphosphoramide (HMPA) gave greater yields but slightly decreased chain lengths. Using lithium or a sodium-potassium alloy gave much lower yields than using only sodium metal. Lithium appears to encourage formation of oligomeric cyclic products, while the sodium-potassium alloy encourages polymer degradation. Thus the Wurtz-type synthesis depends on many variables.

The use of the sodium-potassium alloy induced chain cleavage and produced branched polygermanes from trichloroorganogermanes in 11–41% product yields.[29,30] By comparison, employing sodium metal and trichlorophenylgermane gave only 6% yield with smaller chain lengths.[31] For trichlorobutyl- and trichlorohexylgermane, higher yields (39% and 50%, respectively) were achieved with sodium metal.[31] SmI_2 has also been employed as the reducing agent giving chain lengths and yields similar to those obtained by sodium metal.[32] The advantage of the SmI_2 is that polymerization occurs under milder conditions. Furthermore, SmI_2 is safer to use.

B. Catalytic Routes

Several catalytic routes have been employed to synthesize polygermanes.[33–35] The following is a brief description of some of these systems.

Catalytic dehydrogenative coupling of germanes has been induced by the Ti and Zr metallocenes. A poorly characterized product was produced from phenylgermane using dimethyltitanocene as the catalyst, **5**.[33] A somewhat three-dimensional product was formed by reacting phenylgermane in the presence of zirconocene dichloride as a catalyst.

$$\underset{\mathbf{5}}{PhGeH_3} \rightarrow \underset{\mathbf{6}}{[(PhGeH)_n(PhGe)_m]_1}$$

Highly branched polygermanes have also been isolated in high yields by the demethanative coupling of $HGeMe_3$ using catalytic amounts of $Ru(PMe_3)_4$ $(GeMe_3)_2$.[36] The molecular weights of these polymers were on the order of 10^4–10^5. High molecular weight linear polygermanes, **8**, have also been prepared by reaction of a germanium dichloride complex of 1,4-dioxane with alkyllithium compounds (Scheme 2).[37–39] This methodology gave better yields than the traditional Wurtz-type coupling reactions. These polymers displayed intense UV absorptions as a result of σ-conjugation along the polymer backbone, and they were photosensitive.[38] Upon UV absorption, chain cleavage can occur, giving two germanium-centered free radicals. The same process occurs upon photolysis of polysilanes.

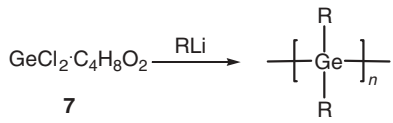

7 **8**

Scheme 2

C. Ligand Substitution

Ligand substitution polymerization is based on the tendency of diorganogermylenes to form Ge–Ge bonds. Thus stable dihalogermanes react with Grignard or organolithium compounds to give R_2Ge (germylenes) type intermediates that subsequently polymerize to give linear[28,38] or cyclic oligogermanes.[40] The tendency to form the linear products is increased with bulky substituents; that is, bulky substituents stabilize the product.[38,41–45]

The reaction of butyllithium with dichlorogermane (**9**) in diethylether at −78 °C gives poly(dibutylgermane), **11**, with a bimodal molecular weight distribution, a MW_A of about 18,000, a polydispersity index of 2.9, and a yield of 43% (Scheme 3). The same reaction carried out at higher temperatures produced only short chains.[38]

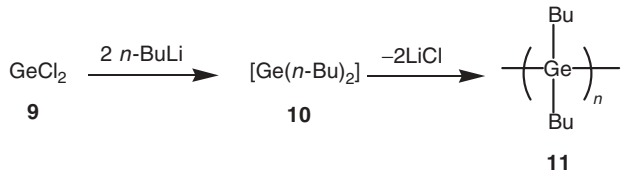

9 **10** **11**

Scheme 3

D. Electrochemical Synthesis

Electrochemical synthesis is becoming popular because of the method's safety and the mild conditions. The main drawback is the attrition of electrodes. In addition, the results depend on the nature of the electrodes.[46,47]

The electroreductive coupling of dichlorosilanes at the mercury electrode, reported in 1976,[48] gave disilane; but this was not effective for the preparation of polysilane.[49,50] However, electroreductions at Mg electrodes promotes many unique reactions.[51–55] The synthesis of high molecular weight, monomodal polysilanes using Mg electrodes suggested that polygermanes could be made in a similar fashion.[51] This proved to be true, and both Ge-Ge and Ge-Si bond formation were demonstrated.[52] The synthesis of poly(phenyl butylgermane), **13**, and germane-silane copolymers, **15**, was achieved (Scheme 4).[56]

The germane–silane copolymers, **15**, are not block copolymers. They were prepared with germanium mole fractions of 0.16 (M_n = 17,000) and 0.45 (M_n = 20,600) and exhibited λ_{max} values at 330 nm and 335 nm, respectively.[56] An almost linear correlation exists between λ_{max} and the germanium mole fraction, when compared to polygermane (λ_{max} = 355 nm) [26,27,57] and polysilane (λ_{max} = 325 nm).[9,58]

There appears to be only minimal differences in the structures of polygermanes produced by the Wurtz and electrochemical processes. In general, short alkyl and phenyl substituents give low current efficiencies and short chain lengths. Larger alkyl substituents such as butyl, pentyl, and hexyl give relatively high yields and longer chain lengths.[59] Molecular weights are in the range of 10,000–15,000 for the longer alkyls.

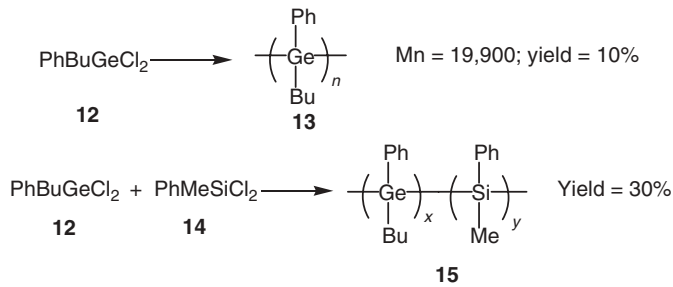

12 **13** **12** **14** **15**

Scheme 4

The synthesis of three-dimensional copolymer networks containing both Ge and Si, has also been accomplished from the reaction of trichlorophenylgermane and trichlorocyclohexylsilane using the electrochemical method. For comparison, the same reaction was carried out employing the Wurtz approach. The electrochemical method produced a narrower bimodal distribution.[59,60]

Analogous linear copolymers have also been produced using the electrochemical method. These included mixed metal, Ge and Si, as well as mixed germane monomers. Reactants included dihexylgermane-co-dihexylsilane, dibutylgermane-co-diphenylgermane, and dibutylgermane-co-dihexylgermane. Molecular weights vary from 1,000 to 5,300, which are lower than the corresponding homopolymerizations. The copolymer composition generally exists as alternate units of the two monomers.[61] Block copolymers with -Si-Ge-Si- units were prepared using bis(chlorodimethylsilyl)diphenylgermane.[62] Product yield for one composition was 25%, with an average molecular weight of 1,100 and a polydispersity of 1.3.

E. Chemical Properties

Polygermanes are generally colorless solids that are soluble in a wide range of solvents, including THF, toluene, hexane, and chloroform. They are moderately resistant toward oxidation and hydrolysis with thermal stabilities $>100°C$. TGA analysis shows that weight loss begins above 200°C.[61] For reasons unspecified, a weight retention of 50% to 500 °C was obtained.[19,31,35]

Polygermanes should be handled in the dark. The Ge–Ge backbone has an intense UV chromophore in the range of 290–360 nm, which results in the degradation of the Ge–Ge backbone. Thus polygermanes have been studied as UV photoresists. This photodegradation has been widely examined.[5,19,20,28,31,38]. Photodegradation occurs rapidly when polygermane films are laid on quartz plates.[19,20]

F. Physical Properties

As already noted, polygermanes exhibit intense adsorption bands in the range of 290–360 nm. The position of the adsorption maxima depends on the nature of the polygermane, molecular weight, temperature, and polymer phase. Generally the wavelength maximum increases with increased alkyl substituent chain length. This is believed to be due to differences in the germane backbone chain conformation with the larger alkyl substituents favoring a greater fraction of the chain segments having anticonformations relative to gauche conformations.[21,63,64] Theoretical studies have also been carried out.[64,65]

Figure 1 illustrates the gauche, top, and anticonformations for a polygermane chain. Polydiphenylgermanes give significant red shifts relative to the alkyl polygermanes. This phenomenon is also observed in polysilanes. Branched oligomeric polygermanes are yellow and exhibit a λ maxima of about 200 nm, with tailing into the visible region.

As noted above, λ_{max} varies with the conformational distributions of the polygermane. Thus in solution polydihexylgermane has a λ_{max} of 327 nm while the

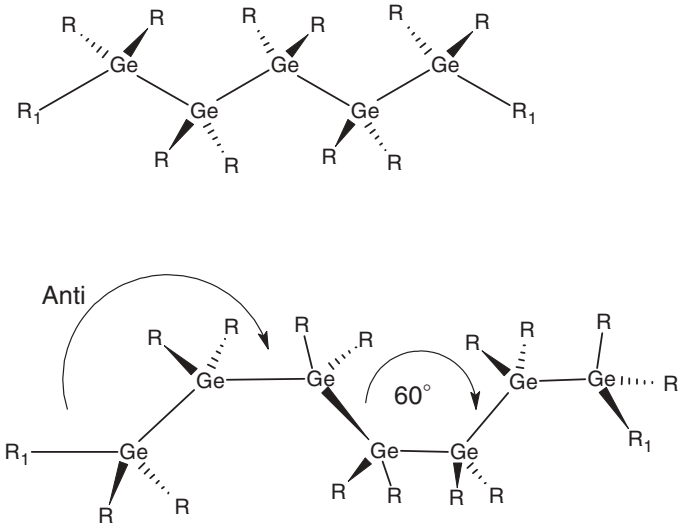

Figure 1.

solid film deposited on a quartz surface exhibits two λ_{max} at 317 and 339 nm.[20] The λ_{max} of polydibutylgermane increases from 281 nm for a MW_A of 1,300, to 290 nm for a MW_A of 2,200, to 325 nm for a MW_A of 6,800, and to 328 nm for a MW_A of 15,000.[20] Some polygermanes show thermochromic behavior in solution. Thus the UVmax for poly(dihexylgermane) in pentane increased from 340 nm at room temperature to 350 nm at –60 °C. This change is reversible.[28,31] Other materials, such as poly(diethylgermane) and poly(methylphenygermane), do not exhibit thermochromic behavior.[21,27,64]

Branched oligogermanes with alkyl or aryl substituents have found applications in micro-patterning as a result of their UV light sensitivity.[31]

G. Miscellaneous

Amorphous polygermynes $(GeR)_n$ (**16**) formed by Wurtz coupling of organotrichlorogermanes are light brown and display weak photoluminescence at 560 nm.[66]

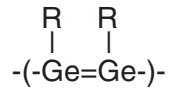

16

Vogg, et al.[67] synthesized two-dimensional (2D) layered polygermane-like materials called polygermynes, **19**, from $CaGe_2$, **17**, and HCl, **18** (Scheme 5). The 2D nature of the materials was attributed to the presence of double bonds in the backbone. They used epitaxial films of $CaGe_2$, which were grown from the reactive deposition of calcium onto crystalline germanium substrates. Polymer formation was achieved by immersion of the $CaGe_2$ films in concentrated hydrochloric acid. The crystalline

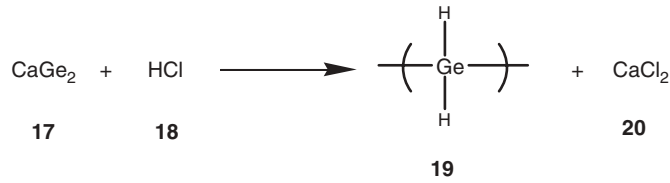

Scheme 5

polygermyne has a slight reddish tint but exhibits intense photoluminescence in the near infrared with maximum luminescence occurring at 1.35 eV (920 nm). The quantum efficiency is about 1%. The product also shows a light reddish luminescence band at 1.9 eV (650 nm), which is probably caused by partial surface oxidation. The polymer is a semiconductor with an activation energy of about 0.65 eV, which corresponds to half the energy of the photoluminescence maximum. It is believed that the electrical conductivity is of a direct bandgap semiconductive type. The layers are stacked in a sixfold sequence with a separation of 0.565 nm.

Polymeric materials containing alternating germanium and tin atoms in the backbone were synthesized[68] from the reaction of bifunctional reactants such as $R_2Sn(NR'_2)_2$ (**21**) and Ph_2GeH_2 (**22**), forming product **23** (Scheme 6). Dimethylgermanium selenides of variable ring sizes have been used to form polymeric structures with Ge–Se linkages in the backbone as noted in **24**.[69] These are probably only oligomeric products.

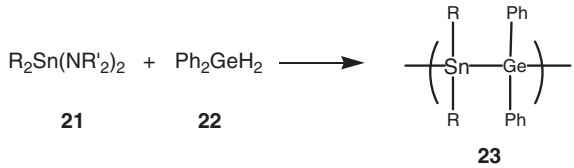

Scheme 6

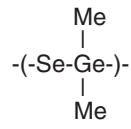

III. ORGANOGERMANIUM–CARBON BACKBONE POLYMERS

In this section we review organogermanium polymers that contain Ge–C bonds in the backbone.

A. Organogermanium Polymers Containing σ-π Conjugation

The polygermanes show interesting electrical properties because of σ-conjugation in their backbone. Unsaturated carbon-based polymers can exhibit conductive properties due to extended π-conjugation. The combination of both σ- and π-bonding in organogermanium polymers has been investigated. A theoretical investigation of silicon and germanium-containing linear chain polymers of the type in **25** and **26** is consistent with the electronic properties of both being similar.[70] The calculated energy gaps between the HOMO and conducting bands for the germanium products are in the range of 2.9–3.2 eV. The highest energy occupied band corresponds to a delocalized σ interaction, which occurs along the polymer backbone; the lowest unoccupied band is related to a C-C π* antibonding interaction with the sigma of the Ge.

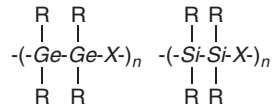

25 **26**

where R = H, Me, F

and X = -CH=CH-, 1,2-acetylene, 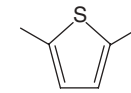

Organogermanium polymers (**27**, **28**) containing thiophene rings have also been prepared.[71–74] Related structures have been also synthesized. For example, the materials illustrated in Scheme 7 were obtained by Wurtz couplings of *bis*(halodiorganogermanium)ethane, -thiophene, and -benzene.[70–74] These products have average molecular weights from 21,000 to 33,000. Comparable structures[70–74] are given in Scheme 8.

In a similar manner, digermanylene polymers, **34**, were prepared by the reaction of di-Grignards (**32**) with 1,2-dichlorotetramethyldigermane (**33**) (Scheme 9).[72] The molecular weights of these materials ranged from 2,600 to 4,700, which are considerably lower than for the digermanylene products **25.**

Poly(germanylene)diacetylenes, **37**, containing diyne units in the backbone have been synthesized, in reasonable yields (50–90%), through either a di-Grignard reagent or dilithiobutadiyne with diorganogermanium dibromides.[75,76] These polymers, shown in Scheme 10, are cream-colored and soluble in typical organic solvents. They are stable to ~150°C, and their GPC molecular weights are in the range 2,300–3,100.[75,76] These materials are insulators with conductivities between 10^{-12} and 10^{-15} S/cm. Doping with iron(III) chloride significantly increased conductivities to 10^{-4}–10^{-5} S/cm, which is comparable to values obtained for conjugated organic materials.[75,76]

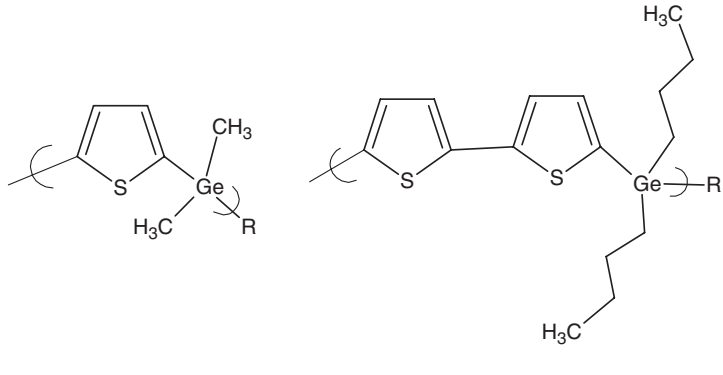

27 **28**

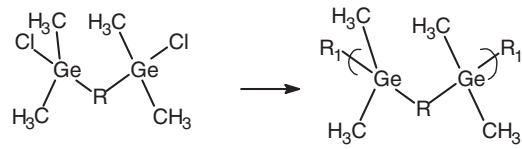

29 **30**

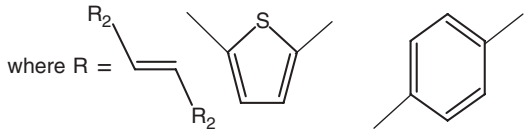

Scheme 7

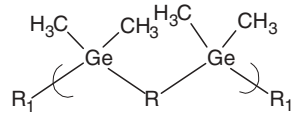

31

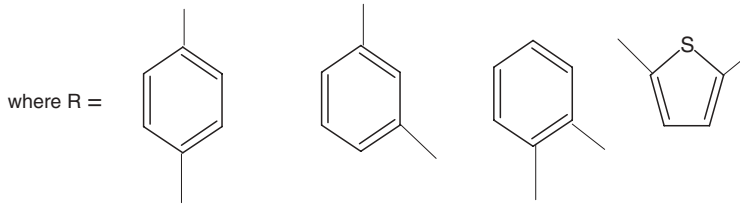

Scheme 8

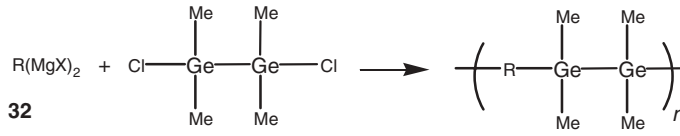

32 **33** **34**

Scheme 9

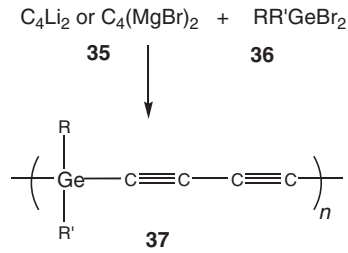

Scheme 10

Pyrolysis of the poly(germanylene)diacetylenes was studied under inert conditions.[75] Cross-polymerization through the triple bonds occurred at 150°C to 250°C. Heating the polymer to 1200°C resulted in the formation of germanium clusters along with large amounts of free carbon (40–60%). Under an ammonia atmosphere at 750°C, germanium nitride and metallic germanium were formed.

The synthesis of polygermole has been accomplished by the Wurtz-type polycondensation of dichloro(tetraphenyl)germol and by catalytic dehydrocoupling polycondensation of dihydro(tetraphenyl)germol with Wilkinson's catalyst, $Rh(PPh_3)_3Cl$, or $Pd(PPh_3)_4$.[76] The catalytic route gives polygermole in high yields (80–90%) and affords molecular weights of 4000–6000, which is in the range produced by the Wurtz coupling, although the latter gives lower yields (~30%). These reactions are summarized in Scheme 11.

In silole-germol alternating copolymers (Scheme 12), every silicon or germanium atom along the polymer chain is part of a silole or germole ring. These were

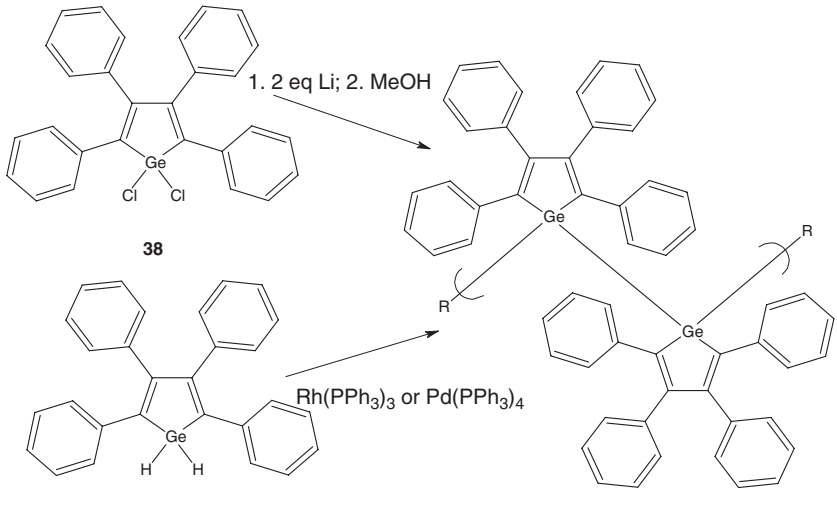

Scheme 11

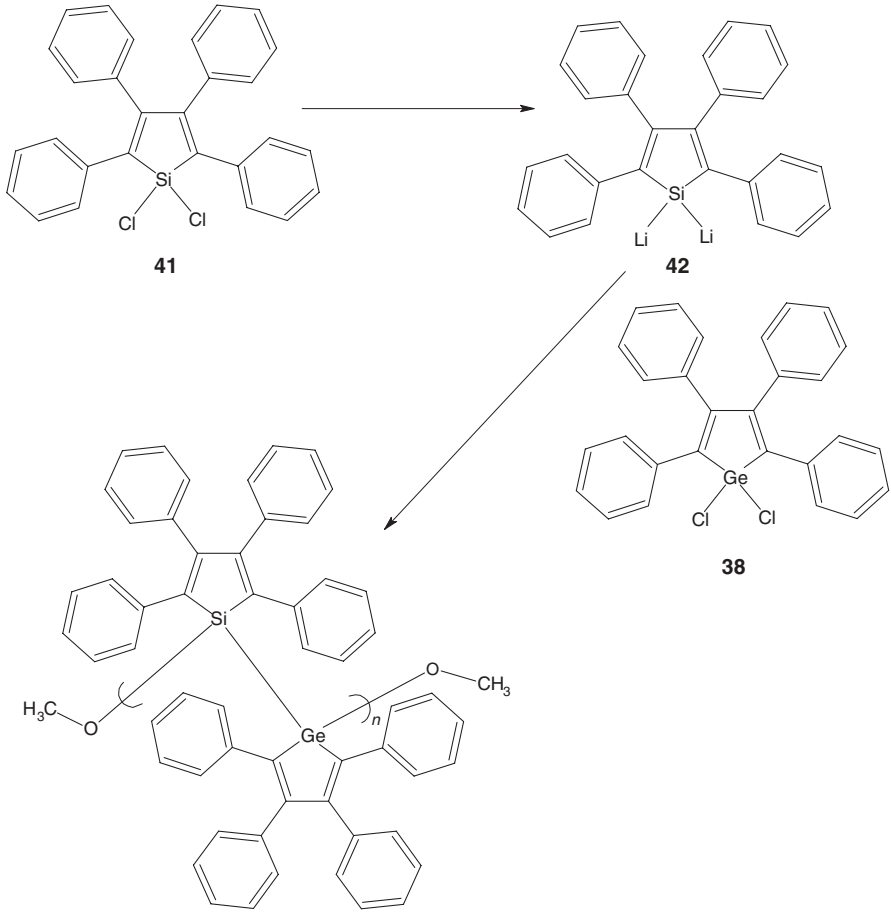

Scheme 12

obtained by coupling dichloro(tetraphenyl)germol with dilithio(tetraphenyl)silole.[76] The dilithio reagent was prepared in 39% yield from dichlorotetrahenylsilole upon reduction with lithium metal. The silole–germole copolymer exhibited a MW_w of 5500 and a MW_n of 5000 as determined by SEC versus polystyrene standards. Thus all these polymetalloles are extended oligomers with degrees of polymerization in the order of 10–16. These materials can be cast into thin films.

A series of germole-silane alternating copolymers were also synthesized (Scheme 13) by polycoupling of the germole dianion, $(Ph_4C_4Ge)Li_2$, with the corresponding dichlorosilanes.[76] These reactions were generally performed in refluxing THF for 72 h. Low molecular weights (4000–6000) were found. These polymers were soluble in THF, diethylether, toluene, and chloroform.

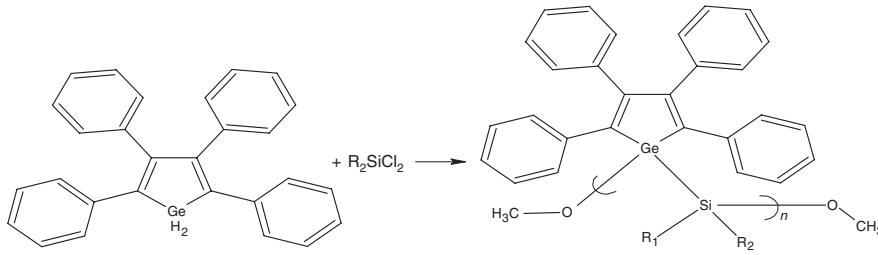

39 **44**

Where R_1 = H, R_2 = Me
=H, = Ph
= H, = Me, Ph
= Ph = Ph

Scheme 13

The UV spectra of polymers **40**, **43**, and **44** exhibit a λ_{max} at ~370 nm.[76] This absorption was assigned to the metallole π^*–π^* transition. These absorptions are red-shifted by about 89–95 nm relative to that of oligo[1,1-(2,5-dimethyl-3,4-diphenylsilole]. The shifts are due to the increasing main-chain length and partial conjugation of phenyl substituents to the silole or germole rings. Polymer **40** exhibits a single emission band at about λ_{max} = 486–513 nm when excited at 340 nm.[76] Polymers **43** and **44** exhibit two emission bands with λ_{max} = 480–510 nm and 385–402 nm, respectively. The ratios of emission intensities are not concentration dependent, indicating that these transitions do not result from an excimer.

The photoluminescent properties of polymers **40**, **43**, and **44** and other poly(tetraphenyl)siloles were of interest for use as chemical sensors to detect nitroaromatic explosives in ultratrace analytes. Explosives are important species to detect for forensic investigations, mine field detection, mapping munition remediation sites, and homeland security applications. The fluorescence lifetimes of polymetalloles and polymetallolsilanes were measured in the presence and absence of TNT, and the fluorescence lifetimes were invariant, requiring that photoluminescence quenching takes place by a static mechanism.[76] Copolymer **44** was more sensitive to TNT than organic pentiptycene-derived polymers in toluene solutions. Each metallole polymer exhibits a unique ratio of quenching efficiency to each analyte (TNT, DNT, nitrobenzene, picric acid). Furthermore, each analyte gives a variety of different responses to different metallole polymers. These properties can be used to specify the exact identity of the analyte by pattern recognition methods. Moreover, these properties might be coupled with the robust nature and insensitivity of polymetalloles to organic solvents and inorganic acids to produce useful sensors.

Scheme 14 is a summary of what is believed to occur. Light is introduced into the metallole copolymer and the exit light appears at a different wavelength, depending on the presence or absence of quenching molecules such as TNT.

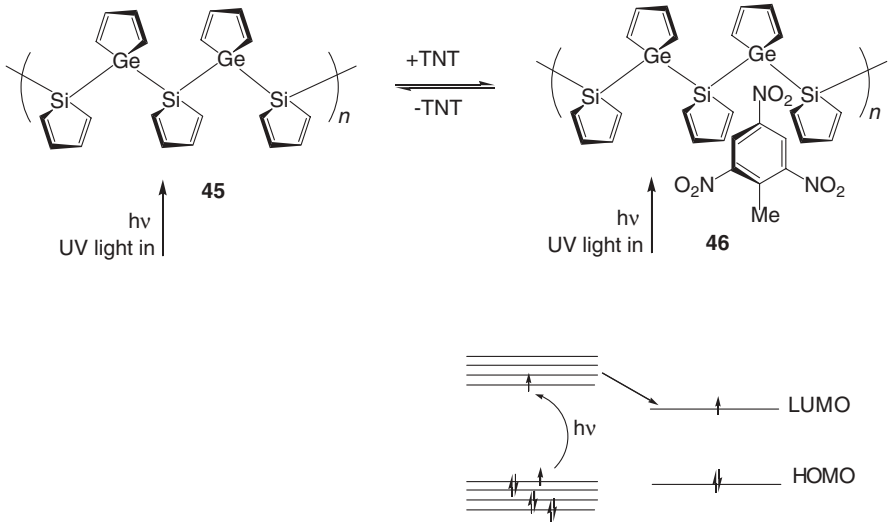

Electron-transfer mechanism for quenching photoluminescense of polymetalloles by TNT

Scheme 14

Lucht et al.[77] described the incorporation of a germole ring into polymers to investigate the novel charge-transporting properties of these materials. Zirconium-containing bis-dienyl compound **47** is converted to its $GeCl_2$ and $GeBr_2$ germole ring analogs by treatment with $GeCl_2$ and $GeBr_2$, respectively. The synthesis of the dibromogermole monomer, **48**, is illustrated in Scheme 15. The conversion of **48** to its dimethyl analog, **49**, was achieved with methyllithium. Then conjugated polymers were prepared by Ni-catalyzed coupling reactions of chloro- and bromo-substituted monomers. The MW_n of polymer **50** was 20,000 with a polydispersity of 2.9 for polymerization of the bromo-substituted monomer (Scheme 15). The optical properties of the polymers were examined. The λ_{max} values for the absorption and emission of polymer **50** were 442 nm and 500 nm, respectively, and were red-shifted relative to the monomer **49**, which had a λ_{max} of 376 nm and 464 nm, respectively. In comparison with other conjugated polymers, such as poly(*p*-phenylene), the germole-containing polymers had a greater degree of delocalization. The higher level of conjugation may be a result of the low-lying LUMO of the germole ring. Higher molecular weight polymers possessed higher emission quantum yields. For example, a polymer with $MW_n = 4700$ had a quantum yield of 0.52, while a polymer with $MW_n = 20{,}000$ had a quantum yield of 0.79. The cyclic voltammogram (CV) of the monomer showed an irreversible reduction at -3.02 V vs. Fc/Fc^+, while the CV of the polymer showed a quasi-reversible reduction at -2.66 V. The difference between monomer and polymer redox potentials and their reversibility is consistent with the expected drop in the

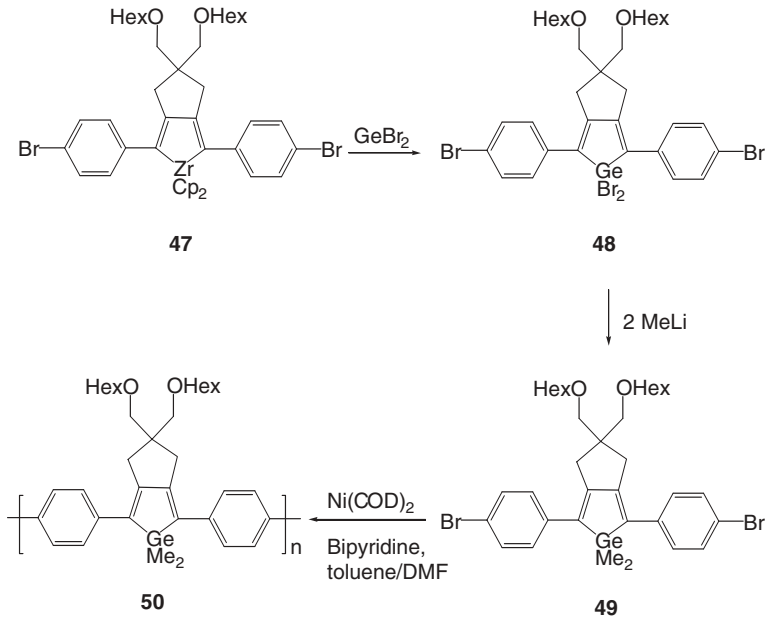

Scheme 15

HOMO–LUMO gap accompanying an increase in conjugation upon polymer formation. Both the monomers and polymers oxidized at approximately 0.6 V.[77]

Gomez and Wagener[78] reported the synthesis of organogermanium polymers, such as **54** (Scheme 16) via acyclic diene metathesis polymerization (ADMET). These ADMET polymerizations were catalyzed using the Grubbs or Schrock catalysts to give

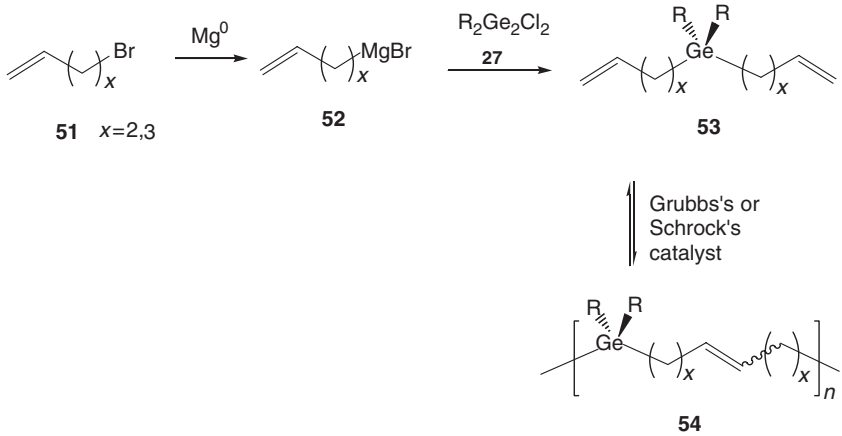

Scheme 16

71–84% *trans* polymers as determined by ^{13}C-NMR. The MW_n values were in the range 5,000–18,000 with polydispersities from 1.4 to 1.8. These polymers were 100% amorphous, with T_g values from −89°C to −98°C.[78]

Organogermanium polymers were prepared by Kobayashi[79] and coworkers via the reaction of a germylene (**55**) with acetylene monomers (**56**) in the presence of a rhodium catalyst (Scheme 17). Polymer **57** contained a larger mole fraction of polyacetylene units than germanium units in the backbone.

Kobayashi's group also conducted an oxidation-reduction polymerization (Scheme 18), where the germylene acts as a reductant and the *p*-benzoquinone as an oxidant.[80,81] The polymerization occurs at −78 °C to give high MW polymers ($>10^6$) within 1 h. These copolymers (**60**) were stable at room temperature and resistant to moisture and air. The mechanism of this synthesis was studied by ESR and found to proceed via a biradical mechanism involving germyl and semiquinone radicals.[81]

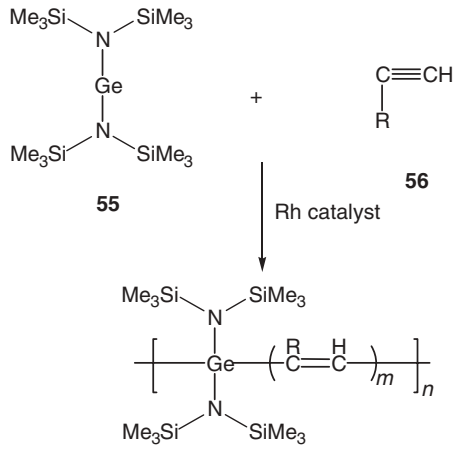

57

Scheme 17

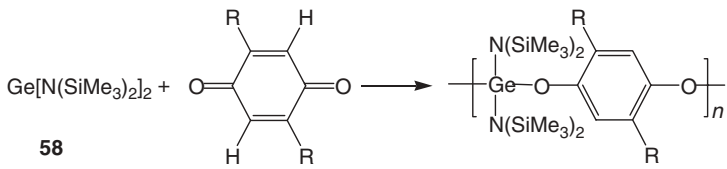

Scheme 18

B. Simple Ge-C Polymers

There have been a number of polymer syntheses based on the ring expansion of germacyclobutanes, germacyclopropane, and other cyclic strained rings. One of the early reports is the formation of **62** by heating dialkylgermacyclobutanes in the presence of chloroplatinic acid (Scheme 19).[82] In a related process, unsaturated polycarbogermanes were formed by the anionic ring-opening polymerization (ROP) of monomers such as 1,1-dimethyl-1-germacyclopent-3-enes (e.g., **63**) to form polymer **64** (Scheme 20).[83]

Similar polycarbogermane and polycarbostannane block copolymers were prepared by the pyrolysis of organogermanium and organotin-bridged *p*-cyclophanes followed by deposition polymerization of the *p*-xylene monomers to give complex bridged structures.[84]

Small et al.[85] described the synthesis of pentacoordiante and hexacoordinate spiropolygermylate ionomeric materials where germanium is contained in the polymer backbone. These materials are air stable, nonhygroscopic, amorphous powders. The hypervalent germanium functionality was verified by Ge and ^{13}C solid-state and solution NMR, proton solution NMR, and IR spectra. The powders are stable to about 325°C.

Over 30 years ago, Scheroder et al.[86] described the synthesis of a number of germanium derivatives of icosahedral orthocarboranes, metacarboranes, and paracarboranes, including their polymers. A sample polymer structure appears as **65** (Scheme 21). They also reported on the synthesis of Ge–N containing products **66** from reactions of **65** with ammonia (Scheme 22).

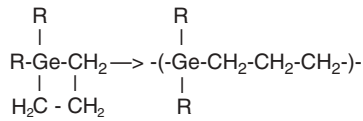

61 **62**

Scheme 19

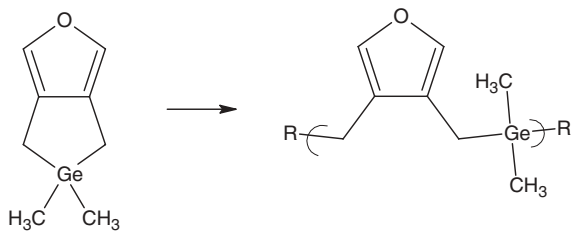

63 **64**

Scheme 20

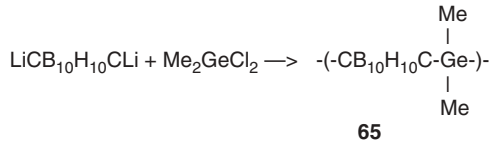

65

Scheme 21

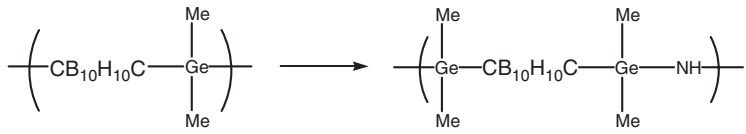

65 **66**

Scheme 22

Copolymers derived from dimethyltin dichloride with dimethylgermanium dichloride were also reported, **67**.[86] The molecular weights of these oligomers were in the range of 1500–6000. Addition of GeI_2 to ethylene was reported to give polymers **41**, when heating in a sealed tube at 150 °C (Scheme 23).[87]

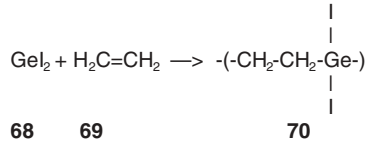

68 **69** **70**

Scheme 23

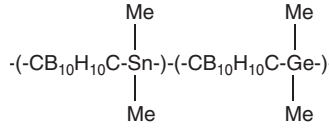

67

IV. POLYFERROCENEYLGERMANES

The thermal ROP of [1]germaferrocenophanes has resulted in the production of a number of high molecular weight (MW = 10^6) poly(ferrocenyl germanes).[88–92] The transition metal-catalyzed homopolmerization and copolymerization of germanium-bridged ferrocenophanes was accomplished using platinum and palladium catalysts.[89,90] It was also recently reported that polyferrocenylenesilylene(germylene) copolymers went from insulators to conductors upon doping with iodine.[92] Scheme 24 shows some of the poly(ferrocenyl germanes) (**72**) that have been synthesized, where R and R′ are most often methyl, hydrogen, and phenyl.[88–92]

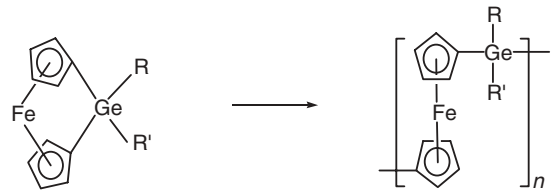

71 **72**

Scheme 24

V. POLYMERS CONTAINING OXYGEN, NITROGEN, SILICON, AND SULFUR IN THE BACKBONE

A wide variety of Ge-O, Ge-N, Ge-Si, and Ge-S polymers have been synthesized. Some of these will be reviewed here.

A. Ge–O Polymers

Germanium polyesters, **74**, were reported by Carraher and Dammeier[93–95] in 1971. The materials were made by a classical interfacial polycondensation process where salts of the dicarboxylic acids are dissolved in water and the organic phase contains diorganogermanium dihalides. The products are formed within seconds in 10–50% yield and have a MW_n of 2000–3000, which represents a number average degree of polymerization of 7–12 (Scheme 25).

The order of polymerization rates for these Group IVA polyester formation reactions is Sn > Ge > Si. This may be due to the relative rates with which the organometallic halides reach the polymerization site versus hydrolysis rates or to changes in the metalloid's electron density. The variables are complex. For instance, while the relative rate of simple movement is probably Si > Ge > Sn, the solubility in the organic solvent may be different, thus reflecting a difference in the "surface" availability of monomer on the interfacial layers. The germanium-containing polyesters exhibited better solubilities relative to organotin polyesters.

In addition, analogous ferrocene products, **75**, were synthesized,[72] where the R′ in **73** is a 1,1′-ferrocene unit. Product yields were about 50%; the reaction is completed within several seconds.

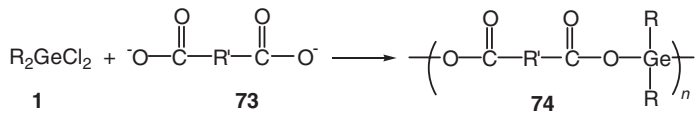

1 **73** **74**

Scheme 25

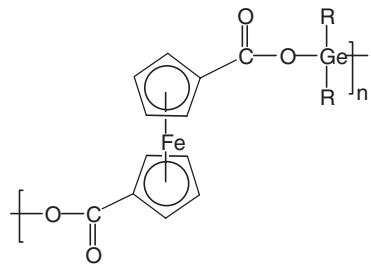

75

Other Group IVA oligomeric ferrocenyl polymers were made. In general, yields decrease as the complexity of the aliphatic substituent on the Group IVA metal increases; yields also decrease in the order Sn > Ge > Si and I > Br > Cl.

Another route used to give germanium-contai ning polymers is the oxidation-reduction copolymerization. This has been extensively studied by Kobayashi and coworkers.[37,38,79–81,96,97] While diorganogermylene-containing substituents such as methyl, ethyl, and phenyl spontaneously polymerize, the presence of bulky groups allows controlled polymerization. Kobayashi formed a number of Ge–O containing polymers based on the use of thermally stable monomeric germylenes, which were stabilized through the use of bulky substituents. This approach allowed the use of p-benzoquinone derivatives,[80,81,96,97] cyclic α,β-unsaturated ketones,[97,98] aldehydes,[99] and cyclic sulfides[99] to give polymers with molecular weights $>10^5$. The reaction occurs under mild conditions and yields a one-to-one repeat unit.

Five- and six-membered cyclic germylenes have also been reacted with *p*-benzoquinones in a 2 to 1 ratio to give the organogermanium polymers with Ge-Ge-O bonds in their backbones (Scheme 26, **78**).[37,96] The MWs of these materials were approximately 10^5, with polymer yields around 90%. The polymers had lower thermal stabilities than their linear analogues with only Ge-O and not Ge-Ge-O bonds due to the instability of the Ge-Ge bonds. Their decomposition temperatures are around 150°C, while the melting temperatures of the polymers with acyclic germylenes are about 235°C.[96]

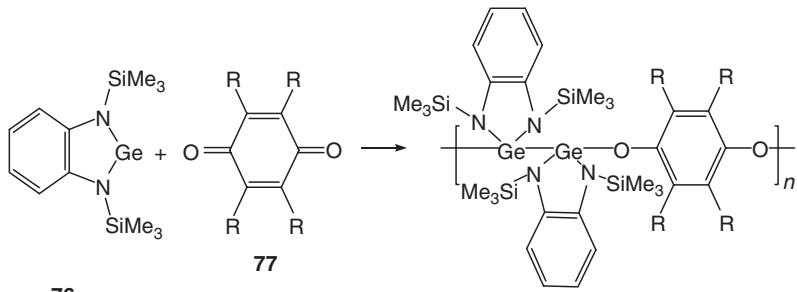

76 **77** **78**

Scheme 26

This approach has been expanded to the synthesis of other materials, for example, **79** and **80**.[73–76] While the product structures appear similar with respect to reactants, the mechanisms offered to transverse this journey are varied.

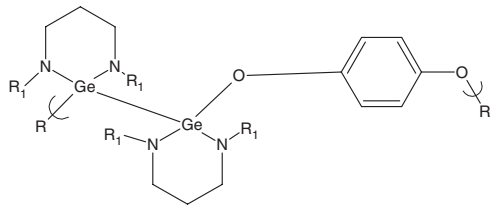

where R_1 = $SiMe_3$

79

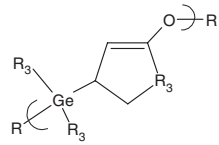

where R_3= $N(SiMe_3)_2$ and
R_2 = $(CH_2)_n$ with n= 2-4

80

A poly(germanium enolate) has been synthesized (Scheme 27, **83**).[37,97] To form a polymeric material, a *trans*-α,β-unsaturated carbonyl compound was required to react with a germylene in the presence of a lithium catalyst such as LiCl or LiR. It was speculated that initial formation of a germyl anion species was achieved by coordination of the Li catalyst to the germylene compound. Thus a nucleophilic attack of the germyl anion on the β-carbon of the cyclic ketone formed a lithium enolate that coordinated to the germylene and regenerated a germyl anion. The organogermanium polymer was stable in aqueous solution and had a $MW_w > 10^5$; T_g, 40 °C; and T_m, 221 °C.

Poly(germyl ether)s (**86**) were synthesized by Nishikubo et al.[100] via the reaction of dimethyldiphenoxygermane (**84**) with *bis*-epoxides (**85**) (Scheme 28). The reactions were catalyzed by tetrabutylphosphonium chloride, TBPC, to give the organogermanium polymers in good yields and moderate molecular weights. The analogous poly(silyl ether)s had much higher molecular weights and were not as sensitive to water and wet solvents as their germanium analogs.

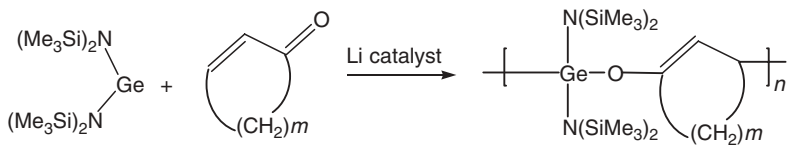

81 **82** **83**

Scheme 27

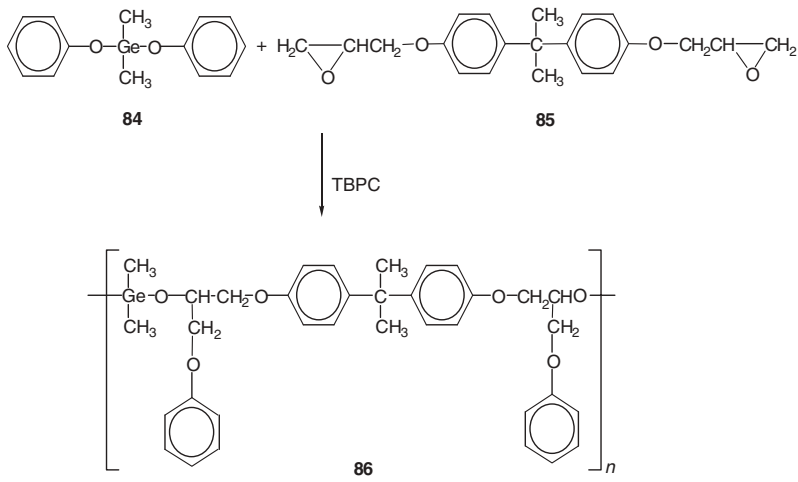

84 **85** **86**

Scheme 28

Oligomeric Ge–O products, such as **87**, were formed from the reaction of germanium-containing combinations germanium halides and hydride–halides with crotonic acid.[101] These products were described as useful in the treatment of cacohymia, malum cordis, dermatosis, allergosis, renal function disorder, and other medical problems.

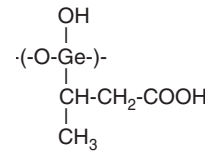

87

Polymers were reported from the addition of germanium hydrides to vinyl methylketone and allylacetone, but these products were poorly characterized.[102,103] Product **88** is a suggested structure for this reaction, where diphenylgermane was employed. A similar product was reported for the Et_2GeH_2.[104]

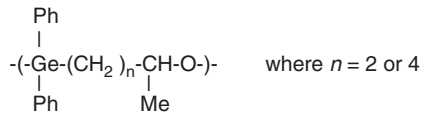

88

B. Ge–N Polymers

A number of polymers that contain Ge–N bonds in the backbone have been reported. For example, Yoder and Zuckermann[105] synthesized germanium imidazolidines using transamination between dimethyl-*bis*-(diethylamino)-germane and

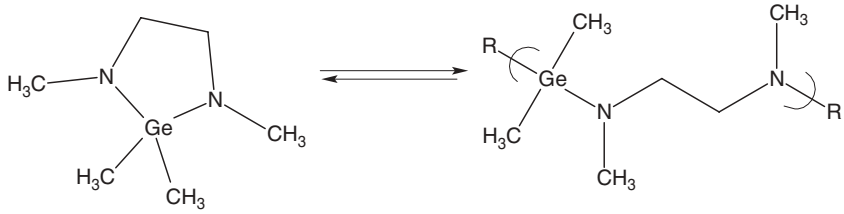

89 **90**

N,N′-dimethylethylenediamine.[105] Germanium imidazolines are stable; however, in the presence of Bronsted acids, such as ammonium sulfate, they undergo a ROP to generate polymers such as **90**. The polymerization is reversible, with the monomer being regenerated. A similar reaction was carried out using piperazine to form polymer **93** (Scheme 29).[106]

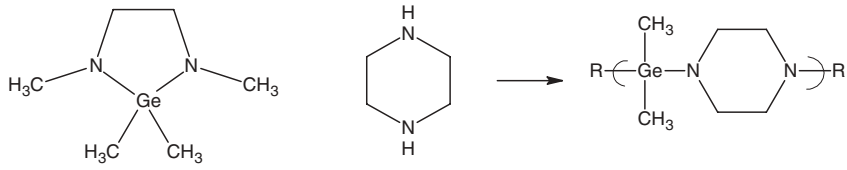

91 **92** **93**

Scheme 29

The reaction of the dimethyl-*bis*-(diethylamino)germane with diethylamine at 120 °C produced a paste that was reported to be polymeric and contained several different repeat units, some of which are shown in Scheme 30.[106]

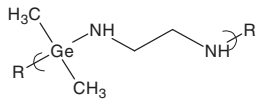

94

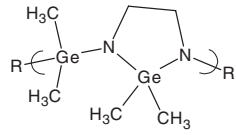

95

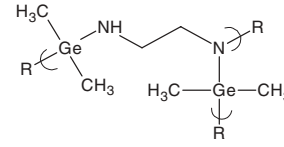

96

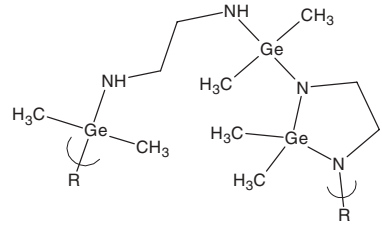

97

Scheme 30

C. Ge–S Polymers

The reaction of dithiols with dihalogermanes was reported to give gums with degrees of polymerization in the order of 50–60.[107] The structures of the polymers from *p,p′*-oxybis-(thiolmethylbenzene) and 1,5-pentane-dithiol with diphenyldichlorogermane are given as **98** and **99**.

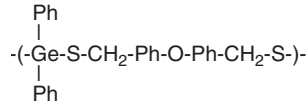

98

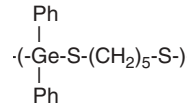

99

A number of Ge-S polymers (**102**) have been made using the redox approach of Kobayashi and co-workers[7,39,108] (Scheme 31). It is interest that the reaction with sulfides occurs without the use of a catalyst, dehydrating agent, or acid scavenger.

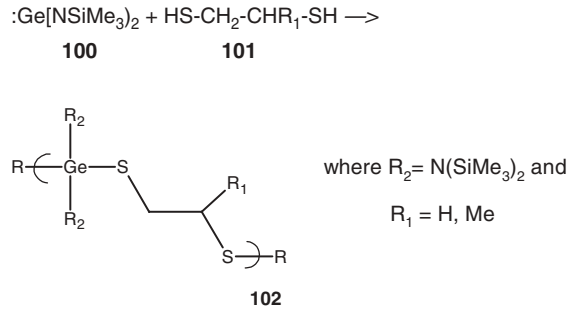

Scheme 31

Copolymers with a one-to-one repeat structure are also produced from the reactions of thietanes with germylenes. The products contain the -C-Ge-S- moiety in the backbone (Scheme 32).[39,108]

D. Ge–Si Polymers

In the past 10 years, there has been an increased interest in the design of new polymeric materials containing germanium. A monomeric system developed by Sakurai et al.[109] permitted the formation of a silane-germole copolymer in which the silane portion of the polymer is electron donating. Thus monomer **108**, derived from **107**, reacted with a catalytic amount of butyllithium to undergo a highly regioselective anionic polymerization to give polymer **109** (Scheme 33). This polymer had a MW_n of 11,000 and a polydispersity index of 1.8.

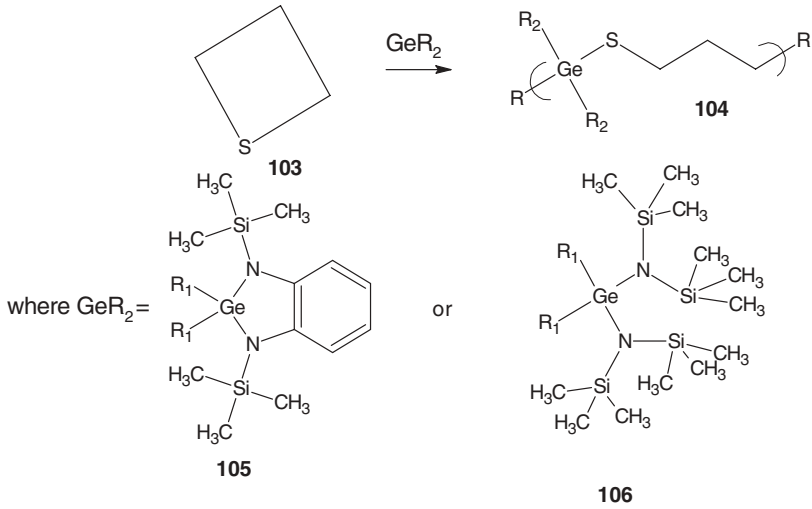

Scheme 32

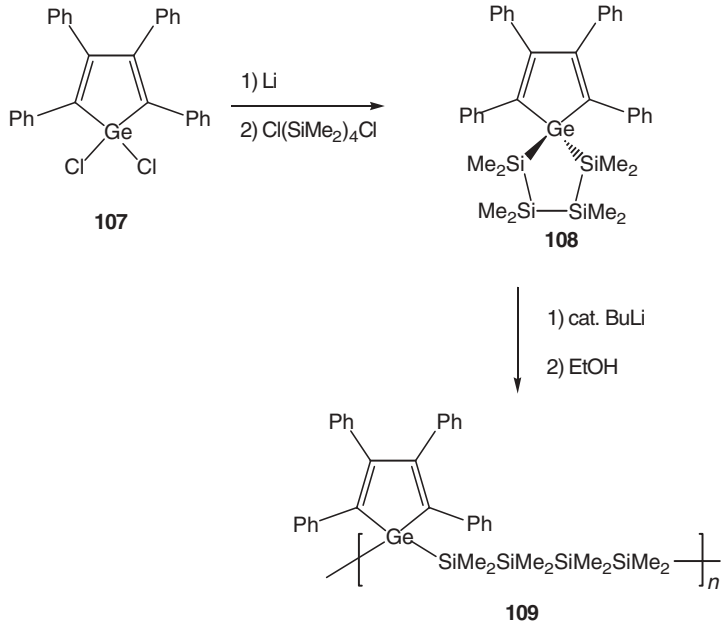

Scheme 33

E. Other Mixed-Bonded Polymers

The syntheses of polyesters, polycarbonates, and polyamides containing germane units in the polymer backbone were reported by Tagle and coworkers.[110,111] Scheme 34 shows the phase-transfer catalyzed polymerization of phosgene (**110**)

with **111** to produce the germanium-containing polycarbonate **112**.[110] Polymer yields were not high. The authors attempted the reaction in the absence of catalyst and found that no reaction occurred.[110]

Several early reports used organometallic hydrides as an approach to forming polymers.[112,113] The platinum-catalyzed addition of Si-H across carbon–carbon double

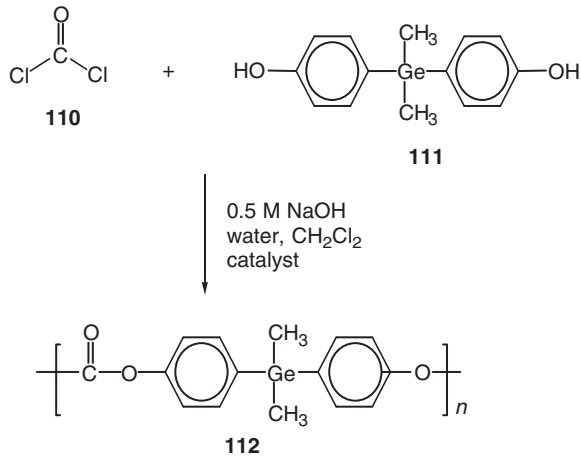

Scheme 34

bonds of vinylgermanium compounds was used in to prepare polymers **115** (Scheme 35). In the presence of chloroplatinic acid, the addition is regiospecific and is

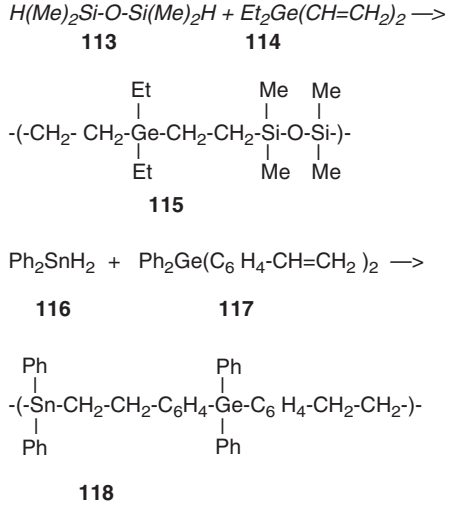

Scheme 35

anti-Markownikow. Similarly, diphenylstannane undergoes anti-Markovnikov addition to *bis*-styryl derivatives of germnium to give polymers **118**.[114]

VI. ANCHORED ORGANOGERMANIUM PRODUCTS

Many solid-phase catalytic systems have been developed. A number of systems include an immobile phase to which is tethered the active site. Germanium-containing catalytic sites have been reported.[115–119] Because the toxicity of organogermanium compounds is generally low, they make good species for use in organic syntheses. However, these materials are relatively expensive. Therefore, their use becomes feasible only when their catalytic activity is great and/or the organogermanium compound is recovered.

In one related approach, one might use organogermanium moieties bonded to a polymer support as reducing agents, not catalysts because they are stoichiometric reducing agents, for organic halides. Such materials were developed with poly-(styrene-co-divinylbenzene) beads.[115] Two such structures are **119** and **120**. These products were characterized by NMR, IR, and XPS. Several octyl and phenyl halides were reduced using these supports by simply heating the reaction mixture with free-radical initiators. The corresponding polymer-bound halides are also formed. The reactivity of the germanium hydrides increased by increasing the spacer length. The best results were obtained in the reduction of 1-octyl bromide and 1-octyl iodide using a spacer where $n = 2$. The octane yield was 60%. The polymer supports could be recycled by reducing the Ge-X moieties back to the Ge-H functions, with

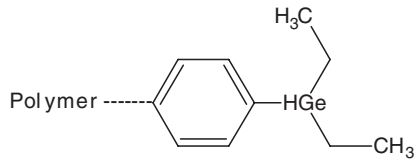

119

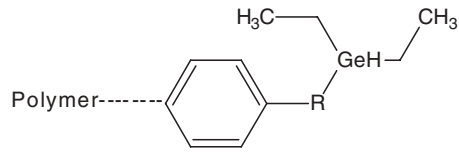

where R = $(CH_2)_n$

120

only some loss of activity. These free-radical reductions occur readily due to the relative weakness of the Ge-H bond. Thus carbon-centered radicals can readily be terminated by H-atom abstraction.

Germanium-containing materials have also been employed to immobilize organic groups.[116,117] Thus monoaryltrialkylgermanium compounds are stable toward bases and nucleophiles. On the other hand, the germanium–aryl bond is readily broken by a number of electrophilic reagents. The general order for cleavage by electrophilic agents is Sn > Ge > Si. Since germanium compounds are less toxic than some organotins, they offer an attractive alternative to organotin products. A method for the synthesis of organohalides from alcohols is illustrated in Scheme 36, where electrophilic cleavage of the aryl carbon-to-germanium bond occurs.[116,117] Spivey and coworkers discussed this reaction more fully in subsequent publications.[117,119]

Another approach (Scheme 37) was developed by Ellman,[116] which illustrates the solid-phase synthesis of a number of 1,4-benzodiazepine derivatives. Here, use of an organogermanium-tether is superior to an organosilicon bond because a larger number of functional groups can be used. Furthermore, demetallation using trifluoroacetic acid or bromine is easier. The organogermanium species also allows the efficient cleavage of the benzodiazepine products from the resin. In all these studies the anchored organogermanium compounds were used in so-called traceless linkage strategies.

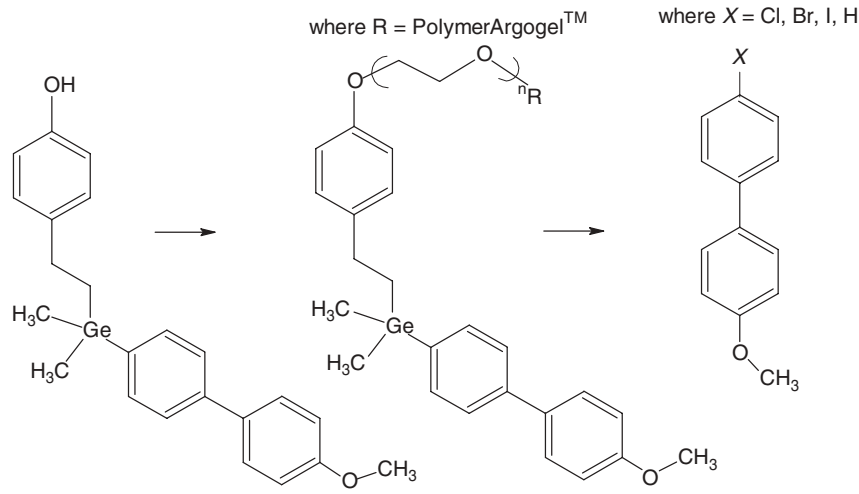

121 **122** **123**

Scheme 36

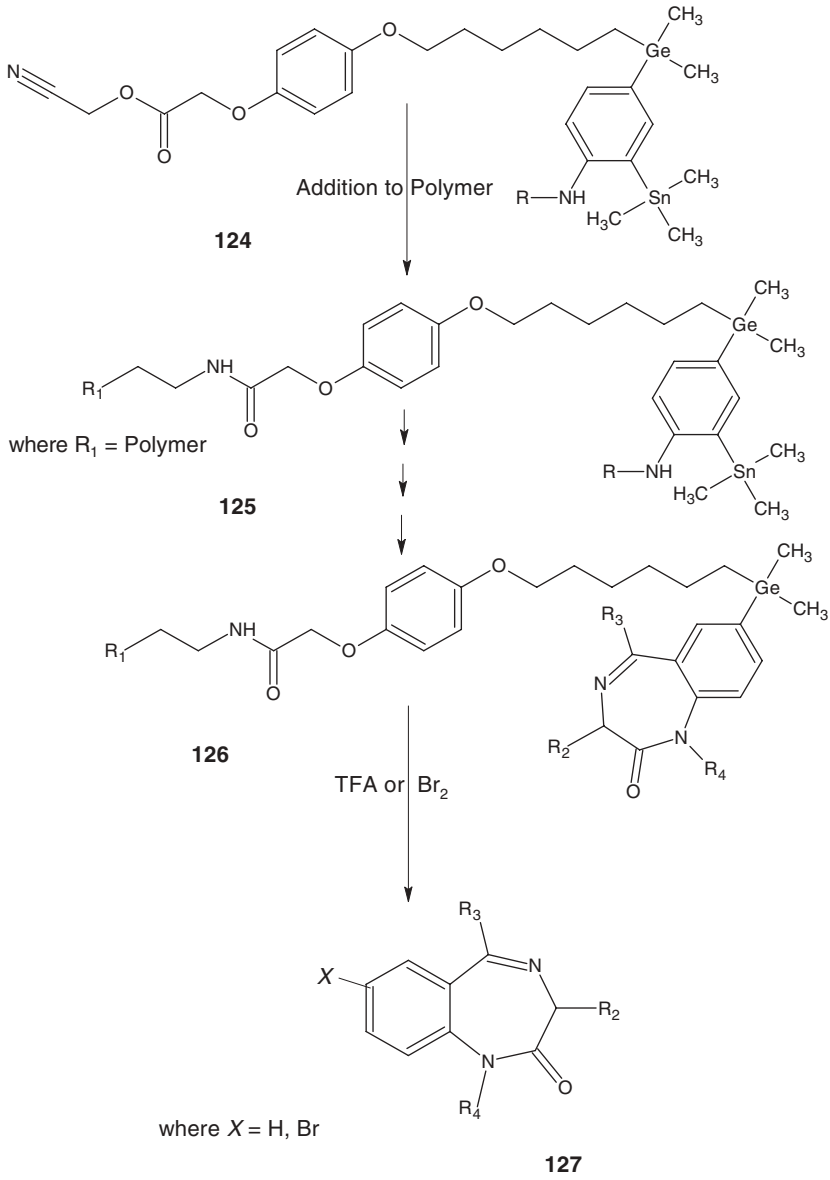

Scheme 37

VII. STACKED PHTHALOCYANINE POLYMERS

Phthalocyanine complexes of Ge were prepared by Marks et al.[120] and converted to stacked polymers under dehydrative conditions. The degree of polymerization for

the germanium-stacked polymer was found to be >70. The conducting properties of this polymer were tested by doping, irreversible oxidation with Ge-O bond cleavage resulted. These shishkabob structures are rigid-rod polymers because the large parallel planar phthalocyanine units will sterically interfer with each other if the Ge-O-Ge bond angle is bent. Thus the rings are stacked face to face, as shown in Scheme 38.

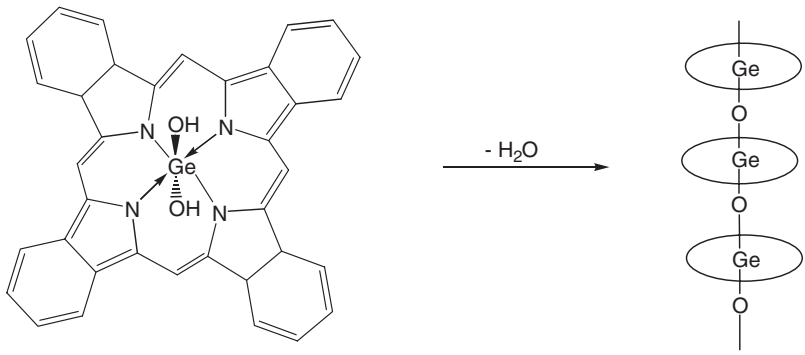

128 **129**

Scheme 38

VIII. HYPERBRANCHED MATERIALS

Little has been reported on the formation of organogermanium dendrites and related hyperbranched products. Recently, Tang et al.[121] described the synthesis of hyperbranched materials based on the diacetylene 1,1-diethynyl-2,3,4,5-tetraphenylgermole, **130**. The homopolymerization of **130** to homopolymer **131** and and copolymerization with 1-octyne, **132,** to copolymer **133** was accomplished (Scheme 39).

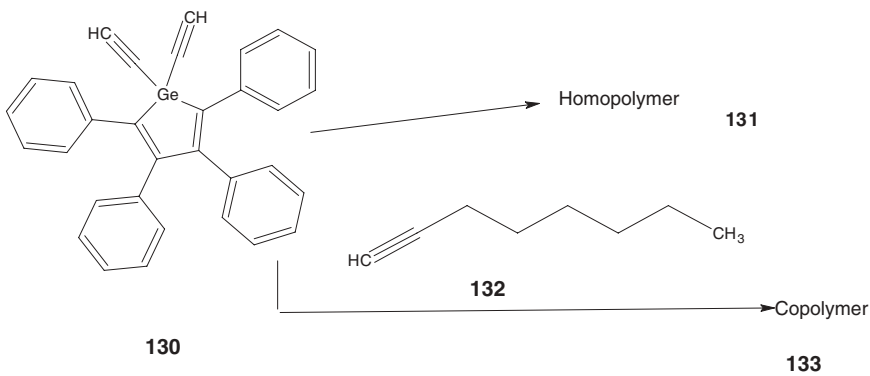

Scheme 39

The copolymerization, product was hyperbranched with the germole units dispersed throughout the product. A product yield of about 50% with a MWA of about 5200 was obtained. The hyperbranched material (Scheme 40) is soluble in organic solvents such as toluene. TGA analysis shows no weight loss to about 350°C and 60% residue to 800°C, which is consistent with ceramization upon pyrolysis.

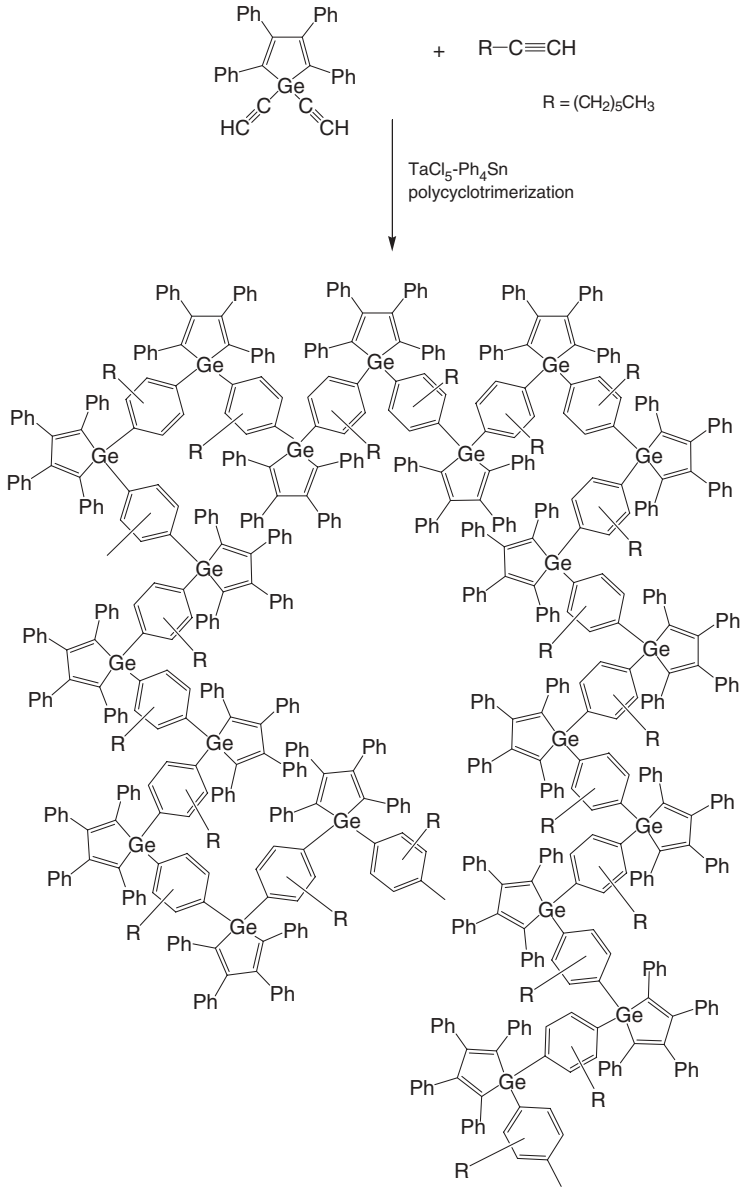

Scheme 40 Hyperbranched polyphenylenegermolene

When a chloroform solution of the copolymer with 1-octyne or the homopolymer was photoexcited at 410 nm, a blue emission at 474 nm occurs with a 1% quantum yield, which is larger than that of the corresponding silole. While the hyperbranched germoles are luminescent, they are, in general terms, only weak emitters. The extent of emission is solvent related. Thus methanol–THF solutions are much weaker emitters compared to the chloroform solutions. On cooling to −18°C, emission intensity increases. However, upon continued cooling to −196°C, emission intensity remains unchanged. This is consistent with the emission being associated with the radiative decay of singlet excitons rather than triplet species.

If reasonable molecular weight homopolymers were progressively pyrolyzed under an inert argon atmosphere, the graphitization process might result in some form of a germanium-doped graphite being produced. No such experiments have yet appeared in the literature, but the electrical properties of these a material would be of theoretical interest.

IX. SUMMARY

In summary, a wide variety of germanium-containing polymers has been synthesized. Most of the emphases has focused on the synthesis and characterization of the polygermanes. This emphasis will continue. Because of the cost and lack of ready availability of suitable germanium monomers, research with germanium-containing polymers will continue to lag behind that of silicon- and tin-containing polymers.

X. REFERENCES

1. F. A. Cotton, G. Wilkinson, *Advanced Inorganic Chemistry*, 5th ed., Wiley, New York, 1988.
2. K. Jurkschat, M. Mehring, in *Organometallic Polymers of Germanium, Tin, and Lead*. vol. 2, Z. Rappoport, ed., Wiley, New York, 2002.
3. M. Lesbre, P. Mazerolles, J. Satge, *The Organic Compounds of Germanium*, Wiley, New York, 1971.
4. K. Shibata, C. Weinert, L. Sita, *Organometallics* **17**, 8049 (1998).
5. K. Mochida, H. Chiba, M. Okano, *Chem. Lett.* **109** (1991).
6. K. Mochida, C. Hodota, R. Hata, S. Fukuzumi, *Organometallics* **12**, 586 (1993).
7. R. West, in *Comprehensive Organometallic Chemistry II,* A. G. Davies, ed., Pergamon, Oxford, 1995.
8. M. Kumada, K. Tamao, *Adv. Organometal. Chem.* **6**, 19 (1968).
9. R. Miller, J. Michl, *Chem. Rev.* **89**, 1359 (1989).
10. R.West, in *The Chemistry of Organo Silicon Compounds*, S. Patai, Z. Rappoport, eds., Wiley, New York, 1989.
11. S. S. Bukalov, L. Leites, R. West, *Macromolecules* **34**, 6003 (2001).
12. H. Teramas, J. Michl, *Chem. Eur. J.* **2**, 529 (1996).

13. R. Imhof, H. Teramae, J. Michl, *Chem. Phys. Lett.* **270**, 500 (1997).
14. K. Tamo, H. Tsuji, M. Terada, M. Asahara, S. Yamaguchi, A. Toshimitsu, *Angew. Chem. Int. Ed.* **39**, 3287 (2000).
15. H. Tsuji, A. Toshimitsu, K. Tamao, J. Michl, *J. Phys. Chem. A.* **105**, 10246 (2001).
16. H. Tsuji, M. Terada, A. Toshimtsu, K. Tamao, *J. Am. Chem. Soc.* **125**, 7486 (2003).
17. J. Michl, R. West, *Acc. Chem. Res.* **33**, 821 (2000).
18. A. Watanabe, O. Ito, K. Mochida, *Organometallics* **14**, 4281 (1995).
19. K. Mochida, S. Nagano, H. Kawata, M. Wakasa, H. Hayashi, *Appl. Organomet. Chem.* **11**, 949 (1997).
20. K. Mochida, S. Nagano, H. Kawata, H. Hayashi, *J. Organomet. Chem.* **542**, 75 (1997).
21. K. Mochida, S. Nagano, S. Maeyama, T. Kodaira, A. Wananabe, *Bull. Chem. Soc. Jpn.* **70**, 713 (1997).
22. R. Miller, F. Schellenberg, J. Baument, H. Looser, P. Shukla, W. Torruellas, G. Bjorklund, S. Kano, Y. Takashi, *ACS Symp. Ser.* **455**, 636 (1991).
23. R. Miller, J. Baumert, G. Bjorklund, J. Jundt, M. Jundt, H. Looser, J. Rabolt, R. Sooriyakumaran, J. Swalen, R. Twieg, *Polym. Preprin. ACS* **31**, 304 (1990).
24. J. Baumert, G. Bjorklund, D. Jundt, M. Jurich, H. Looser, R. Miller, J. Rabolt, R. Sooriyakumaran, J. Swalen, R. Twieg, *Appl. Phys. Lett.* **53**, 1147 (1988).
25. T. Kodaira, A. Watanabe, O. Ito, M. Matsuda, S. Tokura, M. Kira, S. Nagano, K. Mochida, *Adv. Mater*. **7**, 917 (1995).
26. P. Trefonas, R. West, *J. Polym. Sci. Polym. Chem. Ed.* **23**, 2099 (1985).
27. R. D. Miller, R. Sooriyakumaran, *J. Polym. Sci. Polym. Chem. Ed.* **25**, 111 (1987).
28. K. Mochida, H. Chiba, *J. Organomet. Chem.* **473**, 45 (1994).
29. W. Szymanski, G. Visscher, P. Bianconi, *Macromolecules* **26**, 869 (1993).
30. P. Bianconi, D. Smith, C. Freed, W. Szymanski, G. Visscher, *Polym. Preprin. ACS* **31**, 267 (1990).
31. K. Mochida, T. Ohkawa, H. Kawata, A. Watanabe, O. Ito, M. Matsuda, *Bull. Chem. Soc. Jpn.* **69**, 2993 (1996).
32. Y. Yokoyama, M. Hayakawa, T. Azemi, K. Mochida, *J. Chem. Soc. Chem. Commun.* 2275 (1995).
33. C. Aitken, J. Harrod, A. Malek, E. Samuel, *J. Organomet. Chem.* **349**, 285 (1988).
34. J. Reichi, C. Popoff, L. Gallagher, E. Remsen, D. Berry, *J. Am. Chem. Soc.* **118**, 9430 (1996).
35. N. Choi, M. Tanaka, *J. Organomet. Chem.* **564**, 81 (1998).
36. J. Reichi, C. Popoff, L. Gallagher, E. Remsen, D. Berry, *J. Am. Chem. Soc.* **118**, 9430 (1996).
37. S. Kobayashi, S. Shoda, S. Iwata, M. Hiraishi, S. Cao, *Macromol. Symp.* **98**, 91 (1995).
38. S. Kobayashi, S. Cao, *Chem. Lett.* 1385 (1993).
39. S. Kobayashi, S. Iwata, H. Kim, S. Shoda, *Macromolecules* **29**, 486 (1996).
40. W. Neumann, *Chem. Rev.* **91**, 311 (1991).
41. G. Wagner, R. Berger, A. Schier, H. Schmidbaur, *Organometallics* **20**, 418 (2001).
42. P. Jutzi, S. Keithemeyer, B. Neumann, A. Stammler, H. Stammler, *Organometallics* **20**, 42 (2001).
43. G. Ossig, A. Meller, C. Bronneke, O. Muller, Mschafer, R. Herbst-Immer, *Organometallics* **16**, 2116 (1997).
44. S. Benet, C. Cardin, D. Cardin, S. Constantine, P. Heath, H. Rashid, S. Teixeira, J. Thrope, A. Todd, *Organometallics* **18**, 389 (1999).
45. R. Simons, L. Pu, M. Olmstead, P. Power, *Organometallics* **16**, 1920 (1997).
46. S. Aeiyach, P. Lacaze, J. Satge, G. Rima, *Synth. Met.* **58**, 267 (1993).
47. L. Martins, S. Aeiyach, M. Jouini, P. Lacaze, J. Satge, G. Rima, *Appl. Organomet. Chem.* **11**, 583 (1997).

48. E. Hengge, G. Litscher, *Angew. Chem. Int. Ed. Engl.* **15**, 370 (1976).
49. E. Hengge, G. Litscher, *Monatsh. Chem.* **109**, 1217 (1978).
50. E. Hengge, H. Firgo, *J. Organomet. Chem.* **212**, 155 (1981).
51. T. Shono, S. Kashimura, M. Ishifume, R. Nishida, *J. Chem. Soc. Chem. Commun.* 1160 (1990).
52. T. Shono, S. Kashimura, H. Murase, *J. Chem. Soc. Chem. Commun.* 896 (1992).
53. T. Shono, H. Masuda, H. Murase, M. Shimomura, S. Kashimura, *J. Org. Chem.* **57**, 1061 (1992).
54. S. Kashimura, Y. Murai, M. Ishifune, H. Masuda, H. Murase, T. Shono, *Tetrahedron Lett.* **36**, 4805 (1995).
55. T. Shono, M. Ishifune, H. Kingasa, S. Kashimura, *J. Org. Chem.* **57**, 5561 (1992).
56. S. Kashimura, M. Ishifune, N. Yamashita, H. Bu, M. Takebayashi, S. Kitajima, D. Yoshiwara, Y. Kataoka, R. Nishida, S. Kawaski, H. Murase, T. Shono, *J. Org. Chem.* **64**, 6615 (1999).
57. A. Castel, P.Riviere, S. Stage, J. Malrieu, *J. Organomet. Chem.* **247**, 149 (1983).
58. R. D. Miller, *Angew. Chem. Int. Ed. Engl. Adv. Mater*. **28**, 1733 (1989).
59. M. Okano, K. Takeda, T. Toriumi, H. Hamano, *Electrochim. Acta* **44**, 659 (1998).
60. H. Kishida, H. Tachibana, M. Matsumoto, Y. Tokura, *Appl. Phys. Lett.* **65**, 1358 (1994).
61. M. Okano, T. Torjuimi, H. Harmano, *Electrochim. Acta* **44**, 3475 (1999).
62. M. Ishifune, S. Kashimura, Y. Kogai, Y. Fukuhara, T. Kato, H. Bu, N. Yamashita, Y. Murai, M. Murase, R. Nishida, *J. Organometal. Chem.* **611**, 26 (2000).
63. V. Hallmark, C. Zimba, R. Sooriyakumaran, R. Miller, J. Rabolt, *Macromolecules* **23**, 2346 (1990).
64. K. Takeda, K. Shiraishi, N. Matsumoto, *J. Am. Chem. Soc.* **112**, 5043 (1990).
65. K. Takeda, K. Shiraishi, *Phys. Rev. B.* **39**, 11028 (1989).
66. T. Tada, R. Yoshimura, *J. Phys. Chem.* **97**, 1019 (1993).
67. G. Vogg, M. S. Brandt, M. Stutzmann, *Adv. Mat.* **12**, 1278 (2000).
68. H. Creemers, J. Noltes, *J. Organometal. Chem.* **7**, 237 (1967).
69. I. Ruidisch, M. Schmidt, *J. Organometal. Chem.* **1**, 160 (1963).
70. F. Mercuri, N. Re, A. Sgamellotti, *J. Mol. Struct. Thermochem.* **489**, 35 (1999).
71. K. Mochida, S. Maeyama, M. Wakasa, H. Hayashi, *Polyhedron* **17**, 3963 (1998).
72. T. Hayashi, Y. Uchimaru, N. Reddy, M. Tanaka, *Chem. Lett.* 647 (1992).
73. J. Hockenmeyer, A. Castel, P. Riviere, J. Satge, K. Ryder, A. Drury, A. Davey, W. Blau, *Appl. Organomet. Chem.* **11**, 513 (1997).
74. S. Ritter, R. Noftle, *Chem. Mater.* **4**, 872 (1992).
75. J. Brefort, R. Corriu, P. Gerbier, C. Guerin, B. Henner, *J. Organomet. Chem.* **464**, 133 (1994).
76. H. Sohn, M. J. Sailor, D. Magde, W. C. Trogler, *J. Am. Chem. Soc.* **125**, 3821 (2003).
77. B. L. Lucht, M. A. Buretea, T. D. Tilley, *Organometallics* **19**, 3469 (2000).
78. F. J. Gomez, K. B. Wagener, J. *Organomet. Chem.* **592**, 271 (1999).
79. S. Kobayashi, S. Cao, *Chem. Lett.* 25 (1993).
80. S. Kobayashi, S. Iwata, M. Abe, S. Shoda, *J. Am. Chem. Soc.* **112**, 1625 (1990).
81. S. Kobayashi, S. Iwata, M. Abe, S. Shoda, *J. Am. Chem. Soc.* **117**, 2187 (1995).
82. P. Mazerolles, J. Dubac, M. Lesbre, *J. Organometal. Chem.* **5**, 35 (1966).
83. X. Zhang, Q. Zhou, W. Weber, R. Horvath, T. Chan, G. Manuel, *Macromolecules* **21**, 1563 (1988).
84. G. Gerasimov. E. Popova, E. Nikolaeva, S. Chvalun, E. Grigoriev, L. Trakhtenberg, V. Rozenberg, H. Hopf, *Macromol. Chem. Phys.* **199**, 2179 (1998).
85. J. Small, K. Shea, D. Loy, G. Jamison, *ACS Sym. Ser. (Hybrid Organic-Inorganic Composites)* 585 (1995).

86. H. Schroeder, S. Papetti, R. Alexander, J. Sieckhaus, T. Heying, *Inorganic Chem.* **8**, 2444 (1969).
87. M. Lesbre, P. Mazerolles, G. Manuel, *Compt. Rend. C* **257**, 2302 (1963).
88. D. A. Foucher, M. Edwards, R. A. Burrow, A. J. Lough, I. Manners, Organometallics **13**, 4959 (1994).
89. N. P. Reddy, H. Yamashita, M. Tanaka, *J. Chem. Soc. Chem. Commun.* 2263 (1995).
90. T. J. Peckham, J. A. Massey, M. Edwards, I. Manners, D.A Foucher, *Macromolecules* **29**, 2396 (1996).
91. R. N. Kapoor, G. M. Crawford, J. Mahmoud, V. V. Dementiev, M. T. Nguyen, A. F. Diaz, K. H. Pannell, *Organometallics* **14**, 4944 (1995).
92. L. Espada, K. H. Pannell, V. Papkov, L. Leites, S. Bukalov, I. Suzdalev, M. Tanaka, T. Hayashi, *Organometallics* **21**, 3758 (2002).
93. C. E. Carraher, Jr., R. L. *Dammeier, Makromol. Chem.* **141**, 245 (1971).
94. C. E. Carraher, R. Dammeier, *J. Polymer Sci.* A!, **10**, 413 (1972).
95. C. E. Carraher, *Angew. Makromol. Chemie* **31**, 115 (1973).
96. C. E. Carraher, S. Jorgensen, P. Lessek, *J. Appl. Polym. Sci.* **20**, 2255 (1976).
97. S. Kobayashi, S. Iwata, M. Hiraishi, *J. Am. Chem. Soc.* **116**, 6047 (1994).
98. S. Kobayashi, S. Iwata, K. Yajima, K. Yagi, S. Shoda, *J. Am. Chem. Soc.* **114**, 4929 (1992).
99. S. Kobayashi, S. Shoda, *Adv. Mater.* **5**, 57 (1993).
100. R. Riviere, M. Riviere-Baudet, J. Satge, *J. Organomet. Chem.* **97**, C37 (1975).
101. T. Nishikubo, A. Kameyama, Y. Kimura, T. Nakamura, *Macromolecules* **29**, 5529 (1996).
102. I. Akira, *Japanese Pat.* 57145888, 1982.
103. J. Satge, P. Riviere, *J. Organometal. Chem.* **16**, 71 (1969).
104. J. Satge, P. Riviere, M. Lesbre, *Compt. Rend.* (*C*) **265**, 494 (1967).
105. M. Massol, J. Satge, J. Barrau, *Compt. Rend.* (*C*) **268**, 1710 (1969).
106. C. Yoder, J. J. Zuckermann, *J. Amer. Chem. Soc.* **88**, 2170 (1966).
107. C. Yoder, J. J. Zuckermann, *J. Amer. Chem. Soc.* **88**, 4831 (1966).
108. W. Davidson, K. Hills, M. Henry, *J. Organometal. Chem.* **3**, 285 (1965).
109. S. Shoda, S. Iwata, H. Kim, M. Hiraishi, S. Kobayashi, *Macromol. Chem. Phys.* **197**, 2437 (1996).
110. T. Sanji, M. Funaya, H. Sakurai, *Chem. Lett.* 547 (1999).
111. L. H. Tagle, J. C. Vega, F. R. Diaz, D. Radic, L. Gargallo, P. Valenzuela, *J. Macromol. Sci. A. Pure Appl. Chem.* **37**, 997 (2000).
112. L. H. Tagle, F. R. Diaz, D. Radic, A. Opazo, J. M. Espinoza, *J. Inorg. Organomet. Polym.* **10**, 73 (2000).
113. A. Polyakova, N. Chumaevskii, *Dokl. Akad. Nauk SSSR* **130**, 1037 (1960).
114. V. Korshak, A. Polyakova, V. Mironov, A. Petrov, *Dokl. Akad. Nauk SSSR* **128**, 960 (1959).
115. J. Noltes, G. van der Kerk, *Rec. Trav. Chim.* **80**, 623 (1961).
116. K. Mochida, H. Sugimoto, Y. Yokoyama, *Polyhedron* **16**, 1767 (1997).
117. N. Pluckett, J. Ellman, *J. Org. Chem.* **62**, 2885 (1997).
118. A. Spivey, C. Diaper, A. Rudge, *Chem. Commun.* 835 (1999).
119. O. Cho, Y. Kim, K. Choi, S. Choi, *Macromolecules* **23**, 12 (1990).
120. A. Spivey, C. Diaper, H. Adams, *J. Org. Chem.* **65**, 5253 (2000).
121. The original papers of T. J. Marks and coworkers are reviewed in *Inorganic and Metal-Containing Polymeric Materials*, J. E. Sheats, C. E. Carraher Jr., C. U. Pittman Jr., M. Zeldin, B. Currell, eds., Plenum Press: New York, 1990.
122. C. Law, J. Chem, J. Lam, H. Peng, B. Z. Tang, *Inorg. Organomet. Polym.* In press.

CHAPTER 10

Organotin Polymers

Charles E. Carraher Jr.

Department of Chemistry and Biochemistry, Florida Atlantic University, Boca Raton, Florida

CONTENTS

Macromolecules Containing Metal and Metal-Like Elements, Volume 4: Group IVA Polymers, edited by Alaa S. Abd-El-Aziz, Charles E. Carraher Jr., Charles U. Pittman Jr., and Martel Zeldin
ISBN: 0-471-68238-1

I. INTRODUCTION

The first organotin compound was prepared by Sir Edward Frankland in 1849.[1] The topic of organotin polymers has been reviewed elsewhere.[2,3]

There are a larger number of organotin compounds in commercial use than for any other metal.[4] This has resulted an increase in worldwide production of organotin compounds over the last few decades. This production exceeded 50,000 tons in 1992 and accounts for about 7% of the tin metal use.[4]

Organotin polymers are important industrially serving as poly(vinyl chloride), PVC, heat stabilizers, in film for food packaging, and in PVC articles.[2,3] They are also used as antiseptic, antifouling, and antimildew agents in industry and agriculture and as additives in paint formulations. Films have excellent transparency. Table 1 contains a brief listing of industrial uses of organotin compounds.

PVC is unstable under exposure to light and heat, resulting in discoloration and embrittlement. In the early 1940s it was found that this degradation could be prevented by addition of certain organotin derivatives. Presently, about 70% of the commercial organotin compounds are employed as PVC stabilizers in the form of monoalkyltin and dialkyltin derivatives. Today, many of these stabilizers are based on organtin polymers made by Carraher and co-workers.[2]

Much of the more recent drive toward inclusion of organotin into polymers is the result of federal legislation that prohibited the use of so-called unbound or

Table 1 Commercial uses of organotin compounds

Use	Function	General Compounds
PVC stabilizers	Stabilize against decomposition by light and heat	Polymeric; monomeric R_2SnX_2 & $RSnX_3$
Antifouling coatings	Biocide	Polymer bound; R_3SnX R = Bu, Ph
Agrochemicals	Fungicide, insecticide, miticide, antifeedant	R_3SnX; R = Bu, Ph, Cy
Wood preservative	Insecticide, fungicide	Bu_3SnX
Material protection (paper, leather)	Fungicide, algicide	Bu_3SnX
Textile impregnation	Insecticide, antifeedant	Ph_3SnX
Poultry farming dewormer		Bu_2SnX_2

monomeric organotin compounds in paints and coatings. Organotin monomeric compounds were widely used as antifouling and antimold agents, but through migration they inhibited and killed nearby plant and animal life. Chemically bound organotin was permitted in the legislation. Thus there is activity to create non-migrating chemically bound organotin materials—namely polymers that contain organotin moieties.

Commercially, organotin halide derivatives are made using one of four routes: the Grignard, Wurtz, Aluminum-alkyl, and direct routes.[4] The tetraorganotin, R_4Sn, is formed in the first three routes. The tetraorganotin then undergoes a redistribution reaction with SnX_4 resulting in the formation of the various halides, R_3SnX, R_2SnX_2 and $RSnX_3$.

II. MECHANISMS

Compared with carbon, the chemistry of tin varies considerably. The mechanistic behavior of tin has been reviewed.[5]

Here we will focus on substitution reactions involving organotin compounds. For tin, nucleophillic substitution mechanism—namely S_N1 and S_N2—are important as are interchange mechanisms. Following is a brief description of some of the mechanistic considerations involving organotin compounds, focusing on those containing both halides and carbon–Sn bonding.

The reactivity trend for hydrolysis of organotin chlorides, R_3SnCl, has rate constants decreasing in the order R = Me > Ph > 1-naphthyl, which is consistent with an S_N2 rather than S_N1 mechanism.

Further, in the case of electronic effects, an electron-releasing group discourages nucleophilic approach and reduces reactivity in an S_N2 process, but facilitates generation of an R_3M^{+1} moiety in an S_N1 process. An electron withdrawing group will have the opposite effect. For nucleophilic attack on various $(4\text{-}X\text{-}C_6H_4)_3SnCl$ compounds,

the rate constants decrease as the electron release by the para-substituent "X" increases consistent with a S_N2 reaction mechanism.

Thus it is likely that Lewis acid–base reactions occurring at the ogranotin metal atom site are often of the S_N2 variety.

III. STRUCTURES

Tin exists in the +2 state, called the lower valence state, and the +4 state, called the higher valence state. While most of these compounds are tetrahedral, some form octahedral and, less often, trigonal bipyramid organometallic structures.

Here we will focus on the structures about the tin (IV) atom in polymers described in this review.

Following are some structures that exemplify products that will be encountered in this review. The polyamines (structures drawn with a dibutyltin central moiety; **1**), polyethers, **2**, polythioethers, and other related polymers feature a tetrahedral tin.

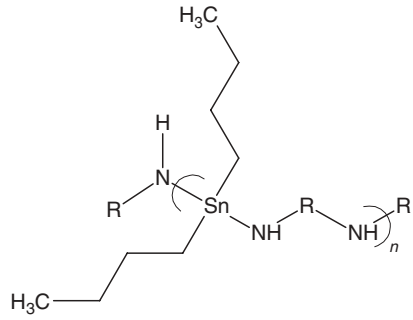

1

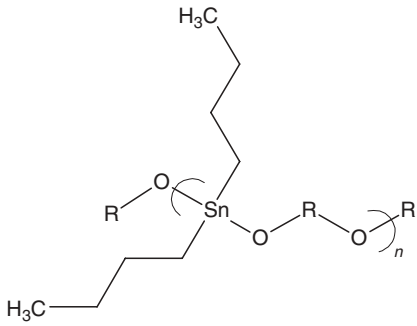

2

Polyesters can have either a nonbridged tetrahedral structure (a dimethyltin center; **3**), or a bridged octahedral structure with bond formation between the carbonyl oxygen and the organotin, **4**.

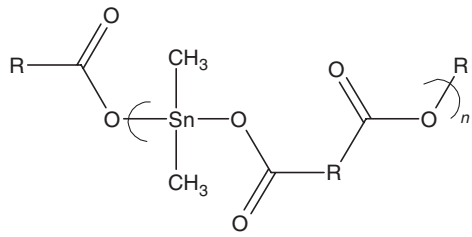

3

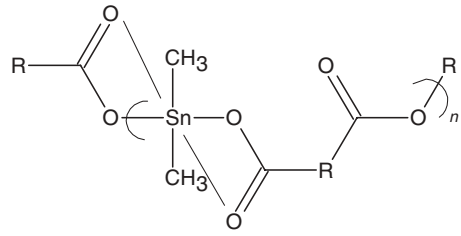

4

Structure assignments are generally based on the locations of carbonyl infrared bands. Bridging structures have a strong asymmetrical stretching band at about 1580 cm^{-1} and a weaker band assigned to symmetrical stretching near 1400 cm^{-1}. Nonbridging structures exhibit a strong asymmetrical stretching band near 1650 cm^{-1} and a weaker symmetrical stretching band near 1360 cm^{-1}.

For polyesters, the tendency for octahedral formation is Pb > Sn > Ge > Si presumably due to a greater availability of vacant *d* orbitals to accommodate back-bonding by the carbonyl oxygen.[6]

In studies of organotin products derived from poly(acrylic acid) or copolymers of acrylic acid and ethylene, we found that the organotin moiety was always present as a tetrahedral and not present in a trigonal bipyramid or octahedral structures.[6–13]

For reactions with dissimilar reacting groups such as ampicillin, where the connective groups are an amine and an oxygen, there are three possible repeat units designated as **5–7.**[10]

-NH-Sn-NH-	-NH-Sn-O-C(O)-	-(O)C-O-Sn-O-C(O)-
5	**6**	**7**

Based on the idea that organotin esters will form octrahedral structures when two esters groups are present, as in structure **7**, but not when only one ester group is present, we have been able to describe the presence and proportion of each of these three repeat units in products containing dissimilar reactants when one of them is an ester. Using this type of logic, the products from ampicillin are predominately of the nonbridging type containing mainly units as described by structure **6** and as described for the dimethyltin product, **8**.

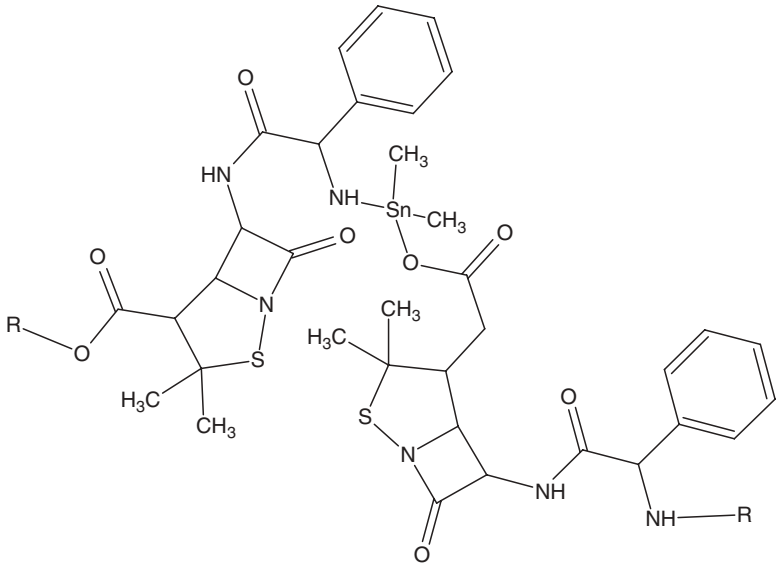

8

IV. ORGANOTIN POLYMERS

A number of organotin polymers have been synthesized. Following is a brief review of this activity. In general the presence of organotin in polymers can be divided by its presence as an appendage in/on a polymer and its presence within the main backbone of the polymer.

V. ORGANOTIN APPENDAGES

Organotin appendages generally occur from reaction on already formed polymers, such as poly(acrylic acid) and cellulose, or by introduction through polymerization of organotin-containing monomers.

A. Vinyl Introduction

i. Organoesters and Ethers

The organotin moiety can be introduced either through polymerization of a vinyl monomer that already contains the tin, or it can be introduced by reaction with already formed polymers. The former ensures that organotin units are present whenever the organotin vinyl group is included in the polymer chain. Thus homopolymerization of organotin vinyl acrylates will give a polymer where each unit contains the organotin grouping. Reaction of already formed polyacrylates is more difficult with a loading factor generally no greater than 0.7–0.8 organotin units per repeat unit.

Three general approaches are most used for the preparation of unsaturated organotin ester monomers. The first approach involves the reaction of the salt of the acid with the organotin halide shown for reaction with R_3SnX (eq. 1)

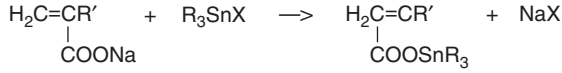

(1)

9

The second approach involves the reaction of organotin oxides and hydroxides with the organic acids as shown in equations 2 and 3.

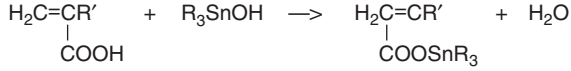

(2)

10

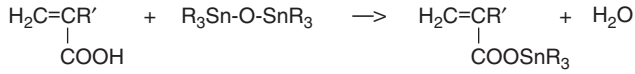

(3)

11

The third approach involves the use of the tetraaryltin with the vinyl acid (eq. 4).

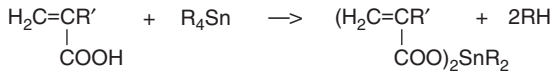

(4)

12

While the hydrogen on the nonorganotin ester carbon can be another grouping, polymerization readily occurs only when it is hydrogen.

Polymerizations of the organotin acrylate or methacrylate can be accomplished using heat, free-radical catalysts, or mercaptanpersulfate initiators and has been accomplished using bulk, solution, and water-emulsion techniques.[3]

In 1958, Montermoso and co-workers in the United States made one of the earliest reports of the synthesis of organotin-containing polymers using organotin-containing vinyl reactants.[14,15]

Some of the earliest work on the chemical inclusion of organotin into polymers was by Russian scientists in the late 1950s and early 1960s. Kochkin et al.[16a] in 1959 synthesized triethylstannic methacrylate and made homopolymers and copolymers of it through reaction with acrylonitrile, methyl methacrylate, methacrylic acid, styrene, divinylbenzene, pentaerythritol ester, methacrylic acid, and cyclopendiene. The organotin ester was made from reaction of dialkyl or diaryl stannic oxide with the respective acids, **13**.[16]

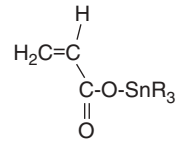

13- Trialkyltin ester

Shortly thereafter similar products were reported but the organotin ester formed from reaction of the vinyl acid, such as methacrylic acid, and R_3SnOH or $R_3Sn\text{-}O\text{-}SnR_3$.[17–19]

Adrova in 1962 reported the synthesis of polytributylin-4'-vinyl-biphenylcarboxylate, **14**, using a similar process.[20,21] The products were colorless and soluble in toluene. As seen in structure **14**, these products are similar to those previously made, except that the biphenylene spacers have been introduced.

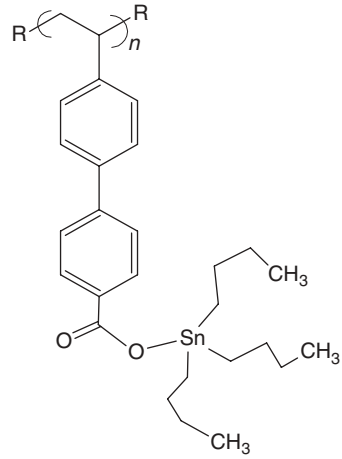

14

Leebrick[22a] prepared a similar series of polyesters, except that only one phenyl group was used to separate the polymer backbone from the organotin ester, **15**. Some of these polymers were crosslinked when diorganotin reactants were employed as shown for structure **15**.

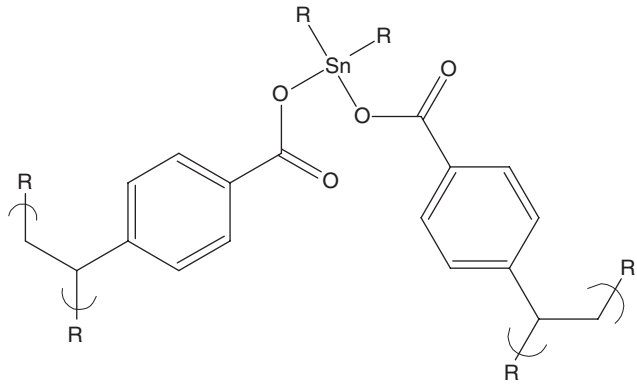

15

Polytributyltin *p*-vinylbenzoate was reported to be a brown rubbery material when polymerized using a peroxide initiator and a strong tacky rubber when produced

using emulsion polymerization. Thus the particular physical properties depended on the particular polymerization technique employed.[22]

Rzaev's group[23–30] and Kochkin's group[16] produced a series of organotin copolymers and terpolymers using the observation that tributyltin oxide reacted with maleic anhydride forming disubstituted organotin esters. Thus the terpolymer of maleic anhydride, styrene, and the organotin diester of maleic anhydride was formed. Depending on the reaction conditions, the product could contain unreacted anhydride units, unsubstituted acid groups, or the diorganotin esters as shown for structure **16**. In that structure, we have in order from left to right the lone organotin ester and acid derived from a single maleic anhydride unit, the styrene unit, and two organotin ester units from a single maleic anhydride unit.

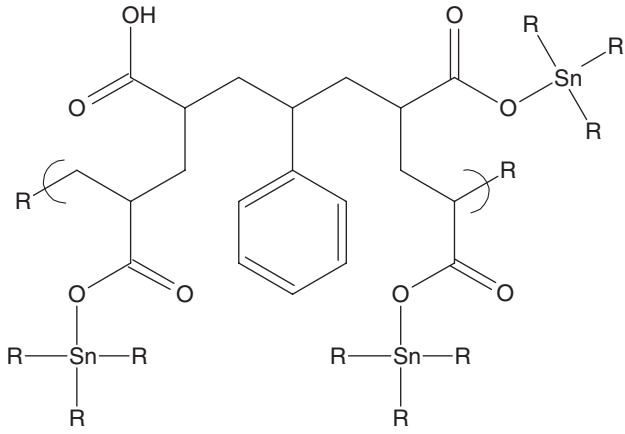

16

One of the early leaders in the inclusion of organotin into polymers through numerous routes is Subramanian. His group synthesized a number of crosslinked organotin-containing systems aimed at inclusion of the tin for its biological activity, mainly for antifouling applications. They were able to extend the life time of submerged wood to >20 years without noticeable degradation through pressurized embedding of organotin monomers followed by chemically connecting these units to the wood. They also successfully introduced tri-*n*-butyl acrylate copolymers into epoxy systems retaining the desired biological activity.[31–43]

Structure **17**, is a representative structure of the network polymer obtained by reaction of the epoxy group containing resins with amines, where the organotin, generally tributyltin, moiety is contained within a poly(acrylic acid) chain. Yeager and Castelli[44] produced similar materials to overcome the national prohibition for use of monomeric organotin compounds, through chemical bonding using varieties of methyl vinylether-co-maleic acid, crosslinked poly(methacrylic acid) and copolymers of methacrylate and methyl methacrylate. These materials offered good antifouling properties while being easily incorporated into various paint formulation.

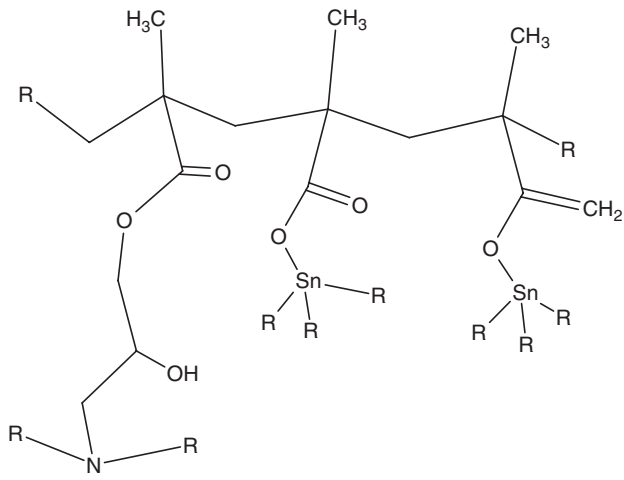

17

Such coatings were studied using NMR, Mossbauer, and IR by a variety of groups,[45–47] their hydrolysis properties were studied,[48,49] and their biological properties were reviewed.[50]

Radwan[51] produced tributyltin-containing polymers from the polymerization and copolymerization of vinyl monomers as tri-*n*-butyltin α-bromoacrylate, **18**. Similar products are made from the copolymerization of tributyl α-chloroacrylate with 2-hydroxyethyl methacrylate or 2-hydroxypropyl methacrylate. These polymers are subsequently crosslinked using one of a series of diisocyanates.[52]

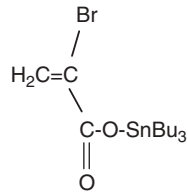

18 Tri-*n*-butyltin α-bromoacrylate

Al-Diab and co-workers have reported a number of copolymers and terpolymers. For instance, they reported the synthesis of *N*-(tri-*n*-butyltin) maleimide, **19**, copolymers with methyl methacrylate, styrene, and *N*-vinyl-2-pyrrolidinone using free-radical polymerization.[53–59] This group also described the polymerization and co-polymerization of di(tri-*n*-butyltin)citraconate,[54] tributyltin *m*-acrylamidobenzoate,[55] and *p*-(tributyltin)styrene.[58] They also reported the synthesis of biologically active organotin-platinum-imine and organotin-platinum-amine complexes containing trans-[$PtCl_2(PPh_3)$ units.[59]

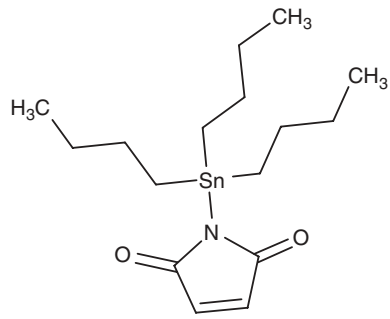

19, N-(Tributyltin) maleimide

Liepins and co-workers[60] reported that homopolymers, copolymers, and terpolymers of tributyltin methacrylate, and trimethyltin methacrylate were made piezoelectric active in thin films by preferential dipole-orienting solvent or by poling procedures. For instance unpoled tributytin methacrylate copolymers exhibited d3 piezoelectric activity of 1.5×10^{-12} C/N, while poled film exhibited g31 activity of 1.6×10^{-2} Vm/N. This is good piezoelectric activity, and it is surprising that this work has not been followed up. These materials also showed good antifouling properties and paint formulation characteristics.[60]

Examples of other organotin polymers produced from monomer introduction reactions are available.[61–66]

ii. Organotin Carbon

Here we will look at some organotin polymers where the organotin is only bonded to carbon. Most organotin polymers connected through only carbon bonds are difficult to make. When a tin atom is attached directly to a vinyl group back, donation of the pi electrons from the vinyl group to the tin deactivates the vinyl group sufficiently to make polymerization difficult. Thus Korshak[67] was able to make only trimers with trialkylvinyltin monomers even using pressures of 6000 atm., 120ºC, for 6 h. Minoura[68] had similar results but was able to produce several copolymers. Thus, even if it was not possible to homopolymerize vinylorganotin, it is possible to copolymerize with styrene and methyl methacrylate and a free-radical initiator. The rate of addition of styrene or methyl methacrylate to its own radical is much greater than that of the organotin monomer adding to the styrene or methyl methacrylate growing chains, producing primarily block copolymers as in structure **20** for methyl methacrylate, where $n > m$.

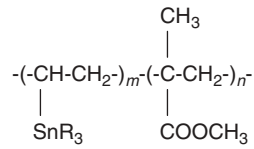

20

As expected, moving the organotin away from the vinyl group allows more ready homopolymerization. A number of polymers have been made using monomers as depicted in structure **21**.[69–91] Plate and coworkers also reported the inclusion of triphenytin moieties through replacement of the chloride in poly(vinyl chloride).[71,72]

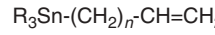

21

Zhao and coworkers synthesized a number of trialkyltin methacrylate homopolymers and copolymers.[74–91] They extensively studied the homopolymerization and copolymerization of tributyltin methacrylate with methyl methacrylate (**22**). Along with the tributyltin methacrylate copolymers with methyl methacrylate, they also synthesized a number of other related homo copolymers, including copolymers, derived form two tin-containing methacrylates such as triphenyltin methacrylate, and triethyltin methacrylate.[79]

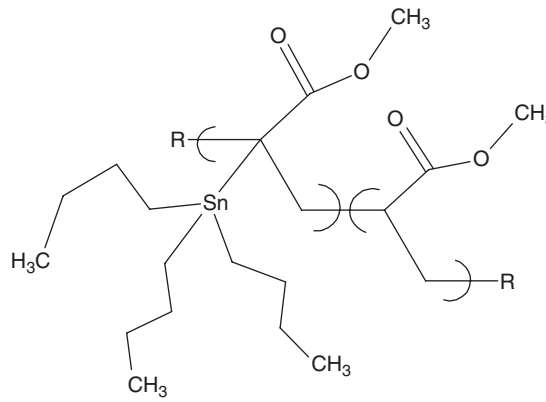

22

Organotin-containing polymers, **23**, have been made from 2-tributyltin-1,3-butadiene.[92] The polymerization is slow, but using a bulk process and azo-bis-isobutyronitrile at 60ºC, a clear colorless liquid product is formed after about 24 days.

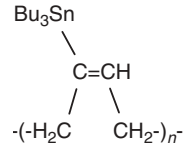

23

Organotin polystyrene copolymers of *p*-triphenyltin styrene and styrene and vinyl toluene have been prepared and their kinetics studied.[93,94] Kolditz and Furcht[95] prepared a series of organotin-containing polymer ion-exchange products from organotin halides and the Grignard derivative of *p*-bromostyrene. They prepared three different cationic ion exchange materials. Sulfonation of the polystyryltin polymer-introduced sulfonic acid groups that could exchange cations. Phosphorylation of the polystyryltin material gave a phosphate cation exchange material. Finally, polymerization of tetrastyryltin and maleic acid gave a carboxylic acid ion exchanger.

Anionic exchanger materials were also created.[95] Bis(*p*-dimethylaminophenyl)distytyltin and *p*-dimethylaminophenyl tristyryltin were polymerized, and the product treated with methyl iodide to give ion exchangers with $-N^{+}(Me)_3$ groups. Polytetrastytyltin was chloromethylated and then aminated, giving an ion exchanger with a $-CH_2N^{+}(Me)_3$ functional group.

B. Preformed Polymer

Migdal and co-workers were one of the first to chemically bond organotin moieties to existing polymers. Polyesters and polyethers with attached organotin groups were prepared by treating these polymers with an organotin oxide, hydroxide, halide, or acetate. They also looked at naturally derived materials with the appropriate functional groups, including methyl cellulose, starch, hydroxyethyl cellulose, nitrocellulose, and cellulose acetate. Some of these materials exhibited inhibition of selected microorganisms.[96–101]

Chlorostannane resins, **24**, have been developed with the chlorostannane attached to a Merrifield resin for use in solid-phase organis synthesis by Zhu et al.[102] The resin had the chlorotin functional groups shown in structure **24**, which could be subsequently coupled with RZnX, where R = aryl, heterocyclic, benzyl, and styryl and X = I and Br. The coupling in THF occurred in better than 95% yield.[102]

Merrifield resin-O-CH_2-CH_2-CH_2-$SnBu_2Cl$

24

Organotin polymers were prepared by adding tri-*n*-butyltin chloride to polybutadiene with lithium living chain ends.[103] Triple resonance $^{1}H/^{13}C/^{119}Sn$ three-dimensional (3D) methods were used to show the relative abundances of precise organotin end group structures and to compare these results with the internal additions. For instance, it was found that the number of vinyl-1,2-butadiene units, **26**, at the chain ends is essentially the same as the percentage of these units in the main chain. But the percentage of *trans*-1,4-butadiene units, **25**, increases at the chain end relative to the percentage of these units in the main chain. This work illustrates the use of tin itself in the structural analysis.

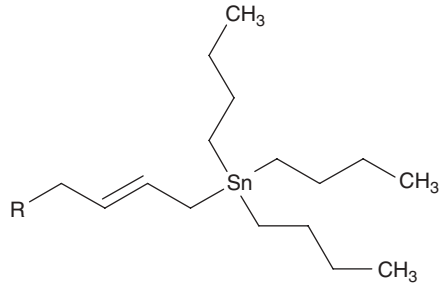

25 *Trans* end group

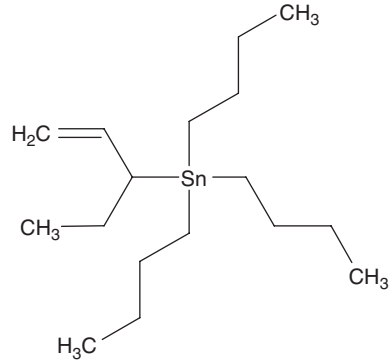

26 Vinyl end group

Labadie et al.[104] synthesized a number of organotin polymers and reported their resist properties. These products included homopolymers of stannylalkyl methacrylates that crosslinked upon e-beam exposure. It is interesting that copolymers containing methyl methacrylate units degraded on e-beam exposure. Polymers containing tin in the backbone were prepared by condensation of aminostannanes with α,ϖ-diynes followed by crosslinking upon e-beam exposure. A 15 wt % tin content was required to obtain etch rate selectivities of ≥15:1 relative to the corresponding non-tin polymer.

We have synthesized a number of organotin-containing polymers using preformed polymers, both natural and synthetic. Products from natural sources include those from cotton (cellulose),[105–107] dextran,[108–117] xylan,[118,119] lignin.[120–123]

Products from synthetic polymers include those from poly(vinyl alcohol),[124,125] polyacrylonitrile,[126,127] polyethyleneimine,[128–130] and poly(acrylic acid) and ionomers.[6–13,131]

For illustrative purposes for natural polymers we will use dextran. Dextran is an extracellular polysaccharide synthesized by certain bacteria when grown on sucrose. The polymer consists mainly of branched chains of α(1->6)-linked *D*-glucosepyranose units. Reaction with organotin dihalides (here dimethyltin

dihalide) results in a complex of units, including unreacted units, those where the organotin forms preferred five-member rings (**27a**), units where one organotin moiety is bonded to another glucosepyranose unit (**27b, 27c**), or more than one organotin moiety can be associated with a single glucosepyranose unit (**27d**).

Reaction with monohalo organotins (here trimethyltin halide) again gives a mixture of products, but it does not increase the crosslinking, so these products are soluble. The mixture contains unreacted units, units containing one organotin moiety (**28**), and units containing more than one organotin moiety per unit (**29**).

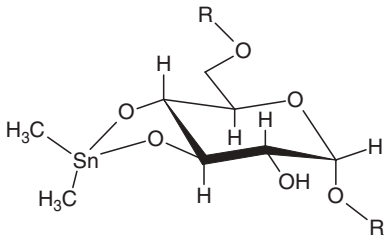

27a

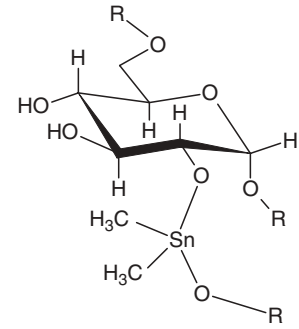

27b

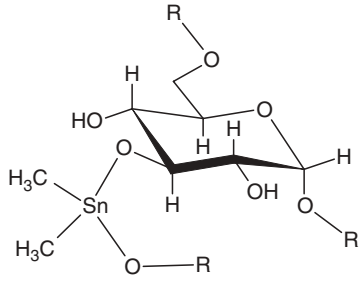

27c

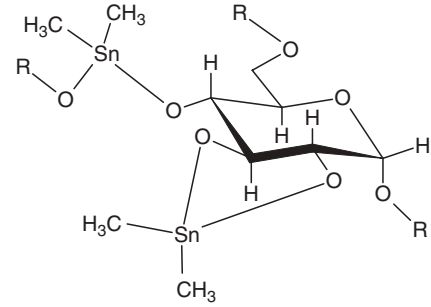

27d

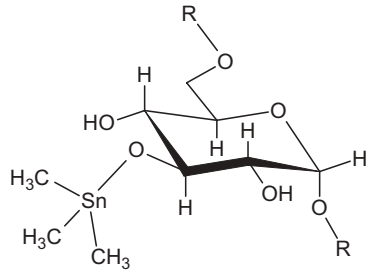

28

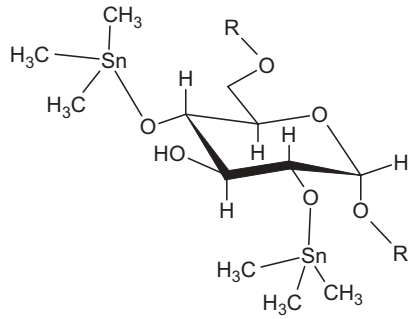

29

The situation is similar for synthetic polymers where monohalo organotin products will be linear, **30**, and not contribute to crosslinking, while dihaloorganotin reactants with two functional groups will be crosslinked, as shown for polyethyleneimine, **31** and poly(acrylic acid), **32**.

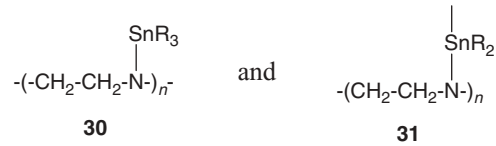

30 and **31**

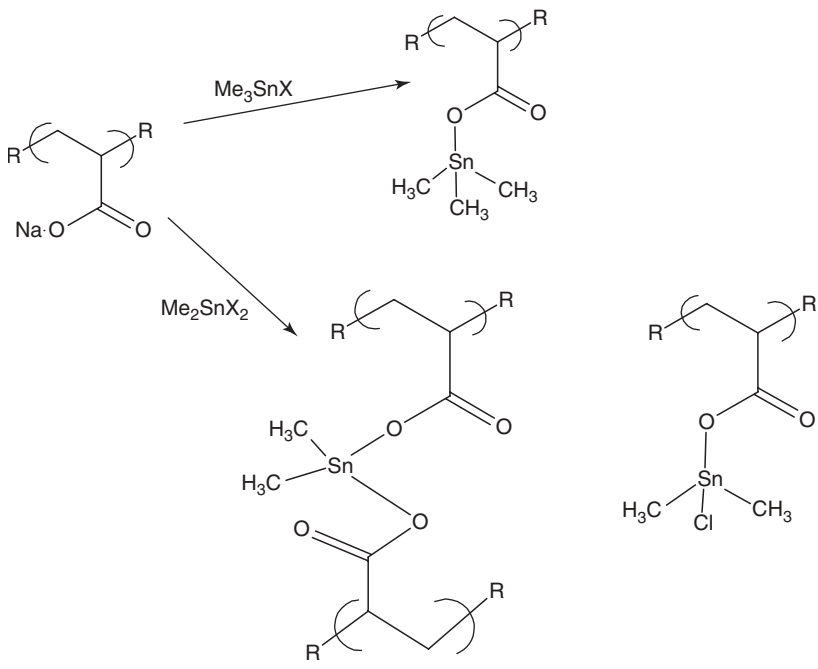

32

The activity with natural reactants is a move toward the use of natural feedstocks for the production of organotin-containing products with potential industrial uses as insulation, films, and building materials. Thus cellulose and starch are readily abundant, as is lignin. Lignin constitutes about 25% of the dry weight of wood, and most of it is discarded to return to the earth though natural degradation. It contains hydroxyls and is sheet-like, making it an ideal material for reactions involving a Lewis base. Carbohydrates are the most abundant (weight-wise) organic material, constituting three-fourths of the dry wight of the plant world. About 400 billion tons of sugar are produced yearly through photosynthesis, dwarfing the production of most other materials, with the exception of lignin.

Our work with organotin and tin-containing ionomers involved understanding how ionomers work.[9–13] In general ionomeric behavior is described as being related to two major factors. The first is movement provided by the metal atoms that supposedly act as ball-bearings as pressure and heat are applied. The behavior is also due to the low T_g of the ethylene portions, which also are mobile when heat and pressure are applied. We made a series of organotin and metallic tin compounds from poly(acrylic acid)-co-ethylene materials. All of the materials were able to be reformed—that is be pressed into various shapes—on application of pressure and heat. Many of these materials are crosslinked with the tin atom chemically bonded through primary sigma bonds to the acrylic acid portion of the polymer. This is consistent with the ethylene portion of the polymers alone being sufficient to provide the needed movement to allow shaping through application of pressure and heat.

C. Crosslinked Mixtures

We have examined some of these materials in the prior section, but here we will focus on additional examples. Organotin catalysts for use in polyurethane systems have been produced using reactions of R_2Sn and R_2SnCl_2 in the presence of polyfunctional molecules such as in structure **33**. These products are presumably crosslinked because of the trifunctional nature of the nonorganotin reactant.[132] The products are used in cationic electrodepositable polyurethane compounds.

$$HS\text{-}CH_2\text{-}CH(OH)\text{-}CH_2OH$$

33

Tributyltin hydrides and modified organotin monohydrides that contain allylic ether groups were polymerized with diallylidenepentaerithritol, producing crosslinked products containing organotin and acetal groups.[133] Moriya and co-workers also synthesized organotin polymers from diallyl terephthalate and tributyltin hydride, Bu_3SnH. The products contained both ester and organotin units.[134] Similar polymers and copolymers were formed from the reaction of diallyl carbonates with tri-*n*-butyltin hydride.[135]

Highly conducting organotin films were prepared by plasma polymerization of mixtures of tetramethyltin and oxygen. These films presumably are highly crosslinked. They were characterized by electron microscopy, ESCA, and X-ray spectroscopy.[136]

Another example of introducing organotin as part of a crosslinked system is available.[129]

We synthesized a number of organotin-containing materials from reaction with simple sugars such as sucrose.[137,138] As expected these products are crosslinked, with the primary sites of reaction being the ring-hydroxyls as shown for a dimethyltin-containing moiety, **34**.

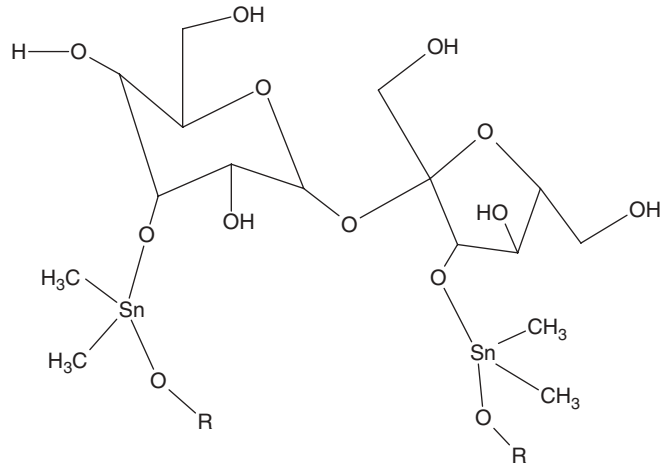

34

In general, controlled-release formulations can offer longer shelf life, sustained-release of the active agent, and greater retention of the active agent due to lowered solubility of the polymer. The co-reactant, if it is an organotin, can offer additional properties, such as antifungal-activity. All of these result in a greater effect of the controlled-release formulation with less active agent in the environment.

We have been interested in the use of polymers as controlled-release agents for biomedical applications. The focus is the delivery of the biologically agent drug. It is difficult to determine if polymers such as the organotin products truly would or could deliver the drug in its active form. Thus we moved to the use of plant growth hormones to test if delivery of the biologically active material could be proven. Our use of plant growth hormones (PGHs) also involved another activity of ours, that of increasing the food supply through the use of polymers. Organotin compounds are of particular interest to us because of the added potential benefit of inhibiting unwanted microorganisms that might impair food crop seed from properly germinating.

The PGH initially investigated was gibberellic acid (GA3).[139–143] Gibberellic acids encompass a number of similar structures, but only one of these, GA3, has found commercial application. Most of the gibberellic acids are inactive, but GA3 is active and is typically the most active of the gibberellins. GA3 is known to play

a key role in seed germination. The most direct effect of GA3 is in inducing the expression of the gene for α-amylase in germinating seeds.

GA3 has three groups that will react with diorganotin dichlorides—two alcohol and one acid group, **35**. Thus the products are crosslinked and should be insoluble.

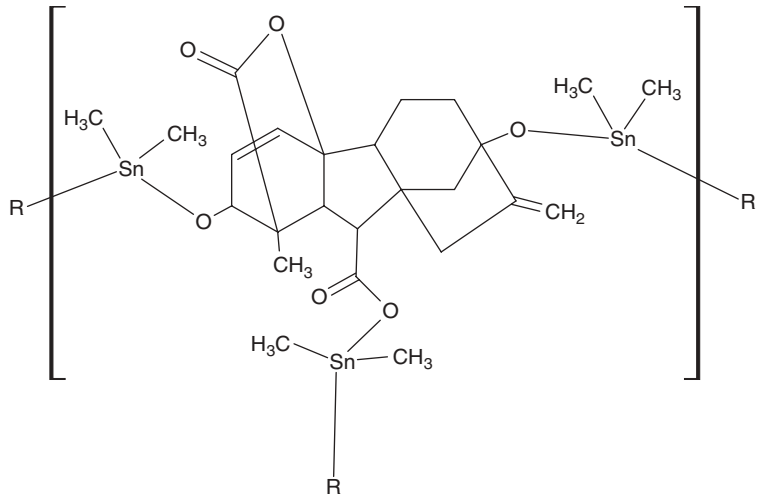

35

The dimethyl derivative was chosen for initial study because it is the least hydrophobic of the group of organostannanes under study (i.e., dimethyl, diethyl, dipropyl, and dibutyl) and should hydrolyze the most rapidly.

The argument is that if GA3 polymers exhibit PGH effects, then release of the biologically active form of GA3 occurred. The evidence for degradation is circumstantial and is based on the ability of the polymer to influence the germination and growth of the food seeds and—as part of our Everglades restoration work—sawgrass and cattail seeds. Furthermore, while there are many gibberellins, only a few are active so that in order for the polymer to exhibit activity, it must degrade, giving the GA3 moiety in an "active" form. GA3-containing organotin polymers were able to increase the germination rate of compromised, old, and damaged food crop seeds as well as increase the germination rate of sawgrass seeds.

The Florida Everglades is called the River of Grass. The grass is actually the sedge sawgrass (*Cladium jamaicense Crantz*). Historically, about 80% of the Everglades was covered with sawgrass. Today, this has been greatly reduced. Sawgrass seeds typically germinate to an extent of about 0–2%. We were able to increase the germination percentage to 10% with the use of minute (~0.1 ppm) dimethyltin-GA3 polymer.[140]

Sample results for the increase in the percentage of germination for food seeds can be seen: 9% for untreated wheat seeds to 27% for organotin-GA3 treated seeds; from 3% for untreated peas to 20% for seeds treated with organotin polymer.[139]

VI. ORGANOTIN-CONTAINING BACKBONES

A. Noncarbon-Linked Organotin Polymers

One of the earlier reports for incorporation of organotin units into polymer backbones involves the synthesis of organotin polymers using organotin hydrides.[21] The proposed structure is given as **36**. The molecular weight of the dibutyltin product is about 8500, giving a degree of polymerization of about 25.[21]

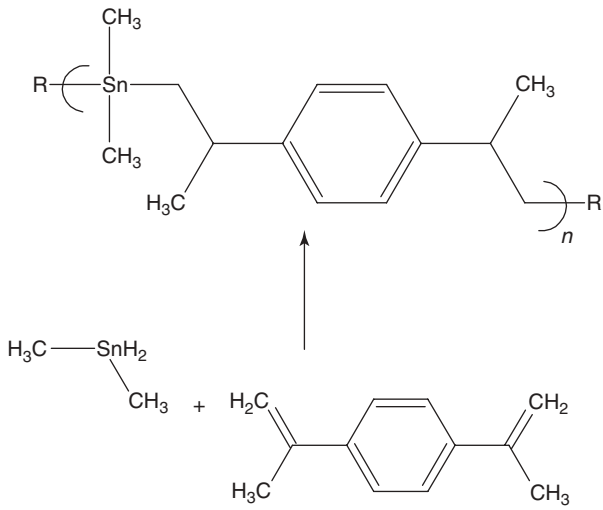

36

Copolymers containing organotin and organosilane units were prepared from the Wurtz coupling reaction of dichloromethylphenylsiland and dichloro-*n*-butylstannane, **37**. The copolymer had a molecular weight approaching 10,000 or a degree of polymerization of about 28.[144–148]

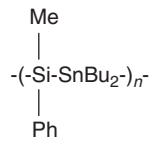

37

This group also synthesized a number of insoluble polymer-supported organotin reagents with a number of potential industrial uses, including as clean reducing agents.[144–156] They also described the deuteration of organotin molecules for tin-119 NMR analysis.[149,150]

Che et al.[157] synthesized a series of bis(β-alkoxycarbonylalkyl)tin polythioethers from the interfacial polymerization of bis(B-alkoxycarbonylalkyl)tin dichlorides with organic dithiolalcohols.

Our group and others [158–219] have synthesized a series of organotin-containing polymers from reaction with various Lewis bases, including dialcohols, diamines, diacid salts, dithiols, urea, and thiourea using various interfacial polycondensation systems, mainly the classical aqueous interfacial system. General repeat units along with references for these materials are given as structures **38–47**. The naming of these general classes of linear polymers follows the idea that the organotin moiety is an alkane rather than an acid chloride.

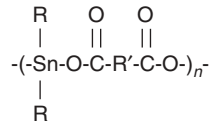

38 Organotin polyester[2,97,101,165–176]

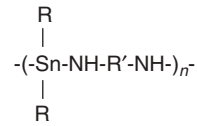

39 Organotin polyamine[2,160,178–186]

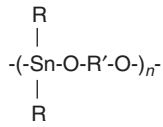

40 Organotin polyether[2,161,192–205]

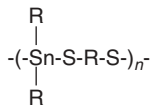

41 Organotin polythiolether[159]

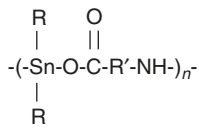

42 Organotin polyaminoester[161,190,199]

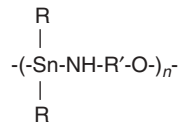

43 Organotin polyaminoether [207]

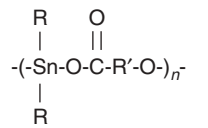

44 Organotin polyetherester[161,200–206]

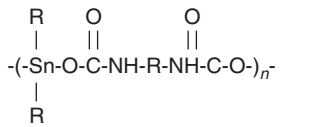

45 Organotin polyurethanes[208,209]

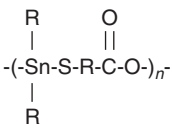

46 Organotin thioesters[210,211]

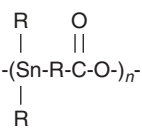

47 Organotin acetates[212]

Each of these have been prepared from reaction of an organotin dihalide with the appropriate Lewis base. While they have not been prepared from the analogous reaction with R_2Sn, similar products should be forthcoming using it in place of the organotin dihalides.

Along with the straightforward products, we have also synthesized organotin products that contain other metals. Organotin ferrocene polyesters, shown for the dimethyl moiety **48**, have been synthesized in good yield using the classical interfacial

system.[214–216] Similarily, cobalticinium polyesters were also prepared of structure **49**, for the dimethyltin moiety. Here solubility and other properties could be varied by changing the nature of the accompanying anion either for the starting cobalticinium reactant or subsequent to polymer formation. The cobalt is a net plus one, which is balanced by the hexafluorophosphate, which is a net minus one.[217–219]

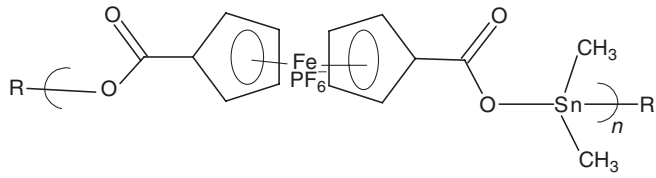

48

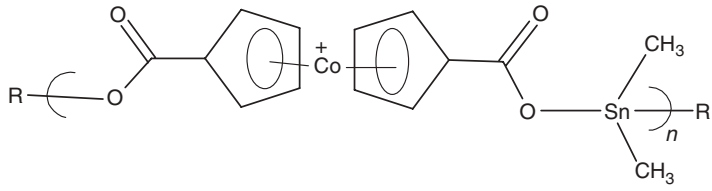

49

We also synthesized a number of organotin polymers using as the Lewis bases known organic dyes.[201–204] These materials were referred to as simply *polydyes*. The structure for one of the polydyes derived from fluorescein, **50**, is shown.

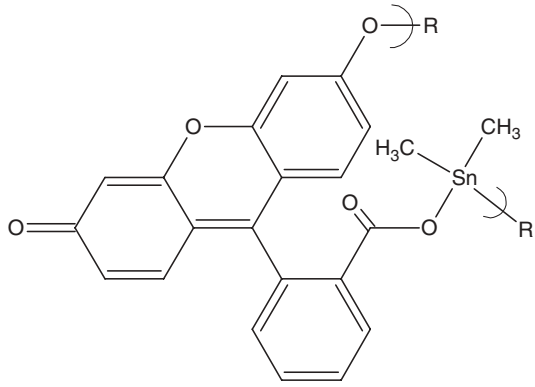

50

A number of other dyes were used, including sulphonephalein (**51**). Depending on the type of laser light these materials were exposed to, these polydyes could greatly influence the stability impregnated film and plastic. Han et al.[203] reported the

synthesis of similar organotin polydyes derived from fluorescein, eosine Y, phloxine B, erythrosine B, and rose Bengal, also employing the interfacial system.

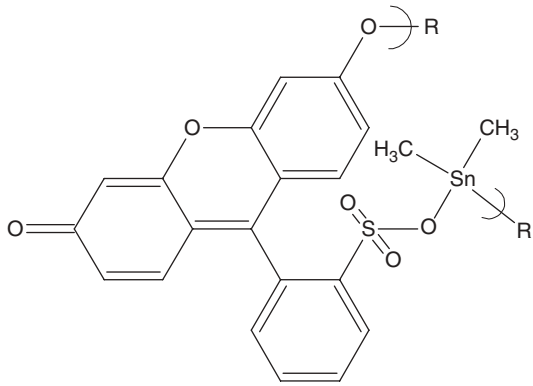

51

Along with the work on GA3 we worked with kinetin as part of the Everglades restoration and to increase food availability. Unlike GA3, which has three functional groups, kinetin has only two, so that the products are linear and soluble. The repeat unit for the product derived from dimethyltin dichloride is as structure **52**. The product is then an organotin polyamine. The use of these materials allowed the sawgrass seed germination rate to increase from the 0–2% range to >20%. We have now systems that will give sawgrass germination rates of >60% which makes wholesale seed distribution by air boat or airplane a practical way of seeding large areas in need of sawgrass restoration.[183–186]

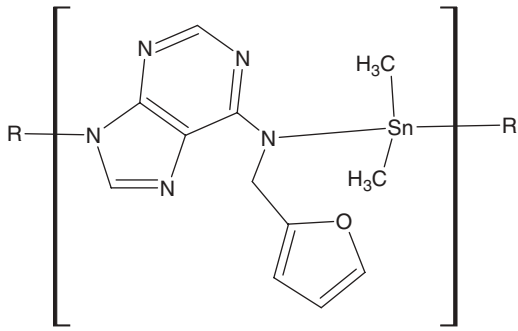

52

More recently, we have been emphasizing the inclusion of known drugs, working toward the inhibition of unwanted microorganisms through a coupled attack, the organotin moiety and the known drug. We have included such drugs as ampicillin (the structure of which was given earlier) [69, 192–196] cephalexin,[196] Norfloxacin,[197–199] and ciprofloxacin.[129] While these materials exhibit good antibacterial activity, they

also form the basis for drugs for the treatment of cancer. This topic will be dealt with in another chapter. We recently included in our arsenal of organotin-containing drugs the antivirial agent acyclovir[208] as shown in equation 5 (**53**).

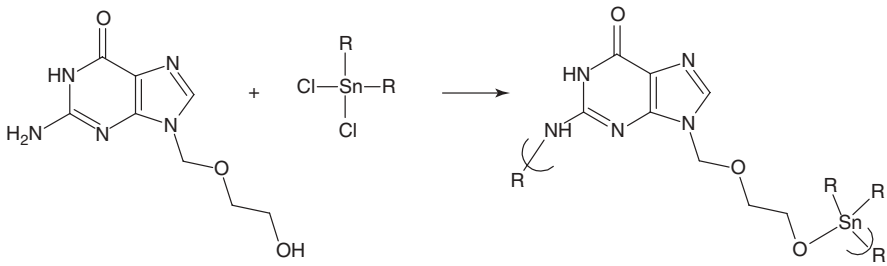

53

Organotin-containing copolymers have been produced from the reaction mixture of a bisphenol A and a mixture of a diorganotin dihalide and an acyl halide of a dicarboxylic acid. The products probably contain various arrangements of groupings connecting the bisphenol A moiety. The materials are said to be useful as wood preservatives, in the treatment of textiles for imparting insect resistance, and as surface coatings.[177] Similar products were also reported by Janson and Fields.[178]

B. Organotin Polyolefins

A number of miscellaneous organotin polyolefins have been produced. Treatment of tin halides or organotin halides with olefins, aluminum, and hydrogen at elevated temperatures produced materials of the general form as structure **54**.[220] Addition reactions involving organotin dihydrides and diolefins have been used to produce organotin polyolefins of structure **55** (eq. 6).[221–223]

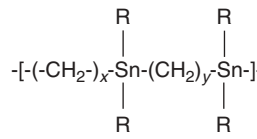

54

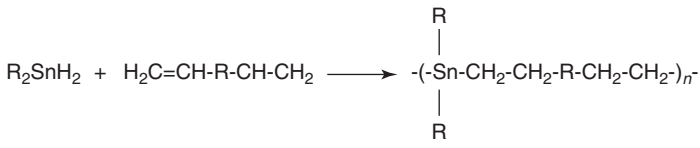

55

Aluminum catalysts such as di-isobutyl aluminum hydride have been used in these hydrostannations to give other similar products. Trihydrides of tin, $RSnH_3$, and diolefins react to give various products of the general structure of **56**.[224,225] A similar reaction sequence has been used to possibly prepare block polymers containing

organotin in the backbone.[226,227] Thus organotin hydrides were reacted with butadiene or isoprene followed by a further copolymerization with ethylene, acrylic esters, styrene, acrylonitrile, etc.

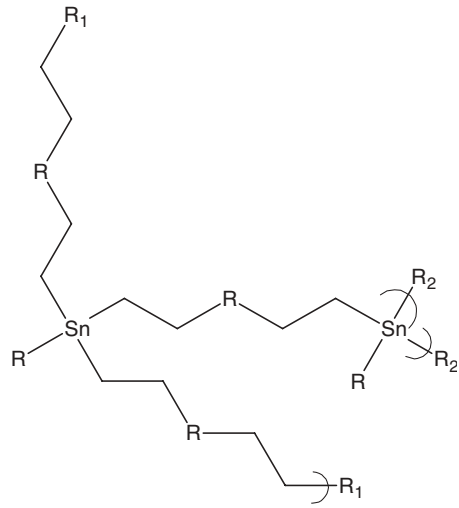

56

Stanno-neocarborane polymers have been synthesized by reaction of dilithium-stannces, giving materials with degrees of polymerization of 1–20 with the general structure of **57**. Softening temperatures ranged from about 50ºC to 260 º C.[228]

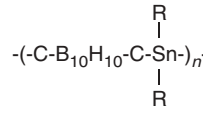

57

A similar reaction of diethynyl dilithium salts with organotin dihalides gives materials of the structure of **58**, which were reported to have interesting electrical properties.[229,230] Because of potential for whole-chain resonance present in these materials, they may be candidates for further investigation particularly if the "R" group allows this whole-chain resonance.

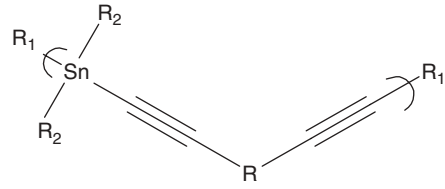

58

Bromine has been added to the triple bonds, giving a saturated structure with some of the resulting organotin polymers stable to >300ºC. Photoconductivity applications have been described for these materials.[67,231–234]

The reaction between tin tetrahalides and tetraalkyl tin compounds can give linear organotin alkylenes of structure **59**. These material have been reported to be stabilizers and catalysts.[73]

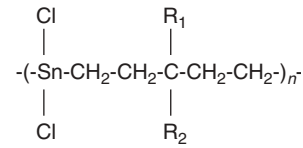

59

VII. POLYSTANNANES

Carbon has an unique ability to form strong single, double, and triple bonds to itself. Because of the relatively high bond energies (C-C single bonds are of the order of 80 kcal/mole) compounds containing carbon in their backbone do not readily cleave. By comparison, fellow members of the IVA main group family have only recently been formed because of the low bond energies (generally of the order of 20–30 kcal/mol).

Polystannanes have been generally synthesized using one of four methods:[235–239] reductive coupling, dehydrogenative coupling, "masked" dienes, and anionic ring opening. Many of these materials show better sigma conductivity than the corresponding polysilanes and have been used as light-emitting diodes.[240]

Much of the interest in the polysilanes, polygermanes, and polystannanes involves their s-delocalization and their σ–π delocalization when coupled with arenes or acetylenes. This is not unexpected since silicon exists as a covalent network similar to diamond. In exhibiting electrical conductivity, germanium and tin show more typical "metallic" bonding. Some polystannanes have been referred to as *molecular metals*.[241] Conductivity is increased by doping,[242] illumination,[243] and application of an electric field.

VIII. ORGANOTIN ALUMINOXANES AND TITANOXANES

A number of stannoxy-aluminoxane[244] polymers containing organotin side groups have been prepared from monomers of the type **60**. These materials have good thermal stability. They are formed through heating with or without pressure and in the presence of an alkali metal alcoholate catalyst. A sample structure is given as **61**.

These materials range from liquids to solids. Similar polymers and copolymers can be made from monomers such as **62**. Suggested uses for there materials are as laminating, molding, varnish, embedding, and elastomeric resins.

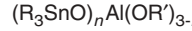

60

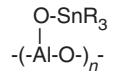

61

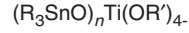

62

IX. GROUP VA-CONTAINING ORGANOTIN POLYMERS

A number of polymeric stannylimidophosphines, stannylimidoarsines, and stannylimidostibines have been synthesized with most of them based on the reaction of organometallic azides with trisubstituted phosphines, arsines, and stibines as shown in equation 7 for phosphines, **63**.[245] These polymers have been described as being useful as transformer oils, greases, lubricating oils, and hydraulic fuels. They are also described as imparting thermal, UV, and oxidative stability to materials impregnated with them.

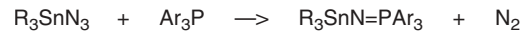

(7)

63

Polymeric organotin arsonates, **64**, are formed from the reaction of dialkyltin dihalides and disodium salts of organoarsonic acids or similarity by reaction with silver arsenate.[246] This was one of the first papers by Nobel-winner Alan MacDiarmid.

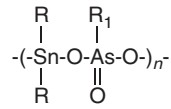

64

Freireich et al.[247] described the synthesis of poly(organotin phosphonates) from the reaction of dialkyltin dichlorides, tetralkyldichlorodistannoxanes, or hexaalkydichlorotristannoxanes with the disodium salt of phenylphosphonic acid, **65**.

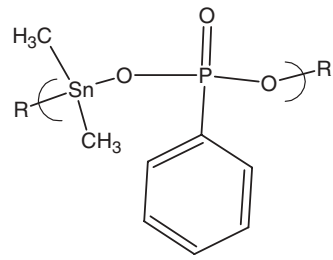

65

X. STANNOXY TITANOXANE POLYMERS

A number of stannoxy titanoxane polymers have been synthesized. Polymers with alternating tin-oxygen-titanium polymers has been formed as shown in equation 8 (**66**).[244] These materials are suggested to be useful as reinforcing agents and fillers. They can also be treated with chelating agents, forming organotin-chelated titanium oxide copolymers.[248]

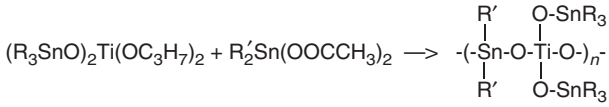

(8)

66

XI. STANNOXANE POLYMERS

While the polysiloxanes play an important role in today's society, the organotin analogs do not. Even so, oligomeric to polymeric stannoxanes have been prepared.[99,100,249–252] They have the general formula as shown by structure **67**. Sample preparations include the reaction of dialkyltin diacetates in the presence of alkoxytin compounds, organotin diacetates and organotin dioxides, and the hydrolysis of various chlorides.

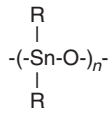

67

XII. BIOACTIVITY

Because of the increased worldwide production of organotin compounds for commercial use, considerable amounts of organotins have entered various ecosystems. Inorganic tin compounds are often said to be nontoxic, but in fact their toxicity ranges from being nontoxic to moderately toxic. Organotin compounds offer varied toxicities from mildly toxic to highly toxic, with most of the compounds falling in the mildly to moderately toxic range. The toxicity and ecosystem relationships have been reviewed.[4] While organotin-containing polymers offer a wide variety of biological activities we will focus on their use in the inhibition of bacterial and yeast.

The general microorganism biological activities of organotin compounds has been studied since the 1950s. As noted above, generally inorganic tin compounds are nontoxic or only slightly toxic toward mammals, insects, bacteria, and fungi, whereas organotin compounds show varying biological activities. For alkylorganostannanes, toxicity varies, depending on the alkyl group. In general, an increase in the alkyl chain length gives a decrease in toxicity.[253] The particular pattern for methyl, ethyl, propyl, and butyl varies with test organism. For tri-*n*-alkyltin acetates, the methyl organotin compounds are the most active for insects and mammals; for fungi and bacteria the propyl and butyl compounds are the most active. Further, activity decreases as the number of alkyl groups decreases as follows $R_4Sn > R_3Sn > R_2Sn > RSn > Sn$ all for tin IV compounds. For most cases, our findings are consistent with these general trends, and long alkyl chains such as n-octyl are generally biologically inactive with respect to bacterial inhibition.[106,107,125,129,193,197,254–270]

The organotin materials are suitable for treatment of infections (here mainly topical), for treatment of contaminated sites, a preventative agents, and in the treatment of water sources. The organotin-containing drugs are rapidly (generally within 30 s) synthesized in good yield employing readily available reactants. Thus ready availability on a gram to tons scale of target drugs is achievable. They can be used internally or topically as additives to creams, cleaning detergents and soaps, coatings (paints), plastics, paper, etc.[265] They can be handled without need for gloves or other protective ware and have shelf lives in excess of several years.

Agents successfully inhibited by the compounds cited in the review include *E. coli*,[254,255] *B. subtilis*,[254,256] *B. catarrhalis*,[254] *S. epidermidis*,[254] *E. aerogenes*,[254] *N. mucosa*,[254] *K. pneumoniae*,[254] *A. calcoacetius*,[254] *A. flavus*,[107,116,256] *A. niger*,[107,258] *A. fumagatus*,[116,258] *Penicillin* sp.,[129] *T. reesei*,[106,107] *C. globosum*,[106,107] *P. aeruginosa*,[120,125] *S. aireis*,[255,259] *C. albicans*,[125,259] *T. mentagrophytes*,[258] and Staph MRSA. [260,261] Most of these products can be incorporated into paper, plastics, textiles, and the like with only some loss in biological activity.[265]

The products from PVA and some from lignin deserve special mention because of their ability to inhibit *Candia albicans*, the microorganism most responsible for yeast infections.[125,259,268,270] This inhibition is selective, leaving much of the natural flora in tact. The organotin-modified PVA products dramatically outperformed commercial preparations.[270]

As in structure **68**, products from dihaloorganotin are crosslinked, while those from monohaloorganotin reactants are linear and soluble. Flexible films and fibers can be made from the linear products and ionomeric materials.

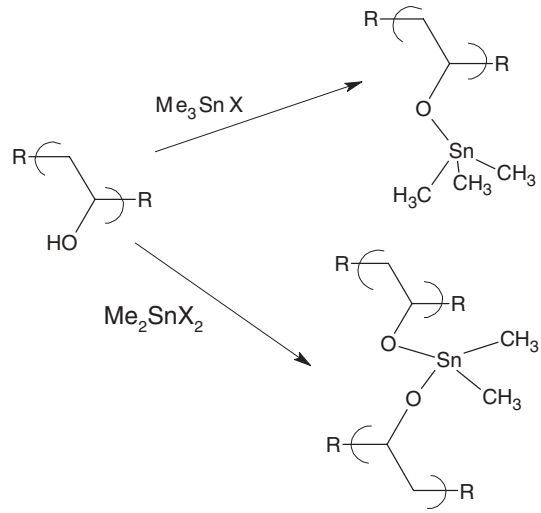

68

With the appearance of new resistant strains of common bacteria, the need for new treatment rationales increases. As part of our efforts we have looked at particularly dangerous microorganisms, where the "cure" is either extreme or not available. The most insidious microorganism involved in nosocomial infections is methicillin-resistant *S. aureus*, MRSA (also called Staph MRSA). This microbe commonly colonizes patients who are seriously ill and in high-risk areas, such as intensive-care and burn units. It is also a significant risk factor in surgical wound infections. The incident of MRSA infection in hospitals is increasing at an alarming rate. It can be carried in the anterior nares of otherwise healthy health-care givers and transferred to the patient during routine attendance at the patient's bedside. Other areas suspected of harboring the organism are air-handling duct work, linens, and general room contamination. We developed a number of organotin-containing polymeric materials that inhibited MRSA and that could be incorporated into soaps, cleaning agents, coatings, etc. for the purposes of prevention and decontamination.[260,261] These include products derived from dextran, cellulose, and lignin.

The ability of these organotin-containing polymers to successfully inhibit a wide number of microorganisms, including such resistant bacteria as MRSA, makes them prime candidates in the war on biological terrorism for the treatment of such microorganisms as *Bacillus anthracis*, responsible for anthrax; *Yersinia bub*, responsible for bubonic plague; and *Francisella tularensis*, responsible for tuleramia. Some of these products are also active against a number of fungi that cause mildew and rot and against the microorganisms responsible for ringworm and athlete's foot.[258]

A number of organotin-containing polymers have been studied as anticancer drugs.[135,192,193,197,258] The results have been most promising but are not covered in this review. Related to this is the work of Pellerito and others on the synthesis of monometic analogs of compounds similar to those synthesized by Carraher and Siegmann-Louda, except using sufficiently different reaction conditions to produce only the monomeric materials.[258d–258h] These materials have been extensively characterized, and a comparison between the bioactivities of these monomeric materials and the polymeric analogs should prove interesting.

The structures for many of the products from Pellerito's group are complex and vary with the nature of the organotin (that is being initially a dihalo or monohalo reactant). It also varies with the particular pencillin or other related drug used to react with the organotin halide. For instance, for the product formed from reaction between amoxicillin, **68a**, and monochlorotin, R_3SnCl, the amoxicillin coordinated the organotin moiety through the lactamic carbonyl, and the overall structure about the tin is trigonal bipyramidal in the solid state based on Mossbauer and infrared spectroscopes.[258b] For products derived from the dihalotin reactant, R_2SnCl_2, the coordination geometry about the tin is believed to be a skew-trapezoidal bipyridine with the two chelating amoxicillin residues acting as bidentate ligands in the trapezoidal plane, and the organic groups in the axial positions.

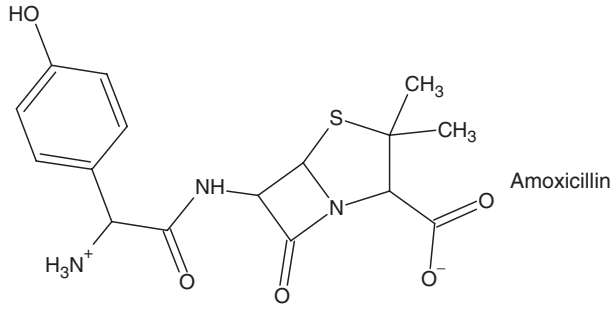

68a

XIII. GENERAL PHYSICAL PROPERTIES

A. Solubility

Crosslinked organotin materials are, as expected, insoluble. Once the product is dried, the organotin polymers are only poorly soluble in dipolar aprotic liquids such as HMPA, DMSO, DMA, and DMF; only partially soluble (presumably the shorter chains are preferably more soluble); or not soluble at all. The overall poor solubility may be due to a number of factors. First, there is often present in the organotin polymers an unusual combination of polar and nonpolar regions. Second, the polar groups are generally sufficient to produce at least partially crystalline regions. Third, many of the products are derived from Lewis bases that are themselves rigid,

producing a product that is often rigid-rod like or at least stiff. This discourages solution to occur.

Linear organotin polymers produced in rapidly stirred systems are often soluble in acetone and other polar liquids if the liquid is added just after recovery and before allowing the mixture to become dry. This is presumably due to the presence of entrapped solvent molecules that prevent close-chain interactions causing the chains to be more easily approached by the solvent molecules. Thus such metastable states allow the organotin polymers and many other metal-containing linear polymers to be dissolved. We need to remember that it generally takes more energy to dissolve a polymer chain than to maintain it in solution. Thus a polymer can be maintained in a solution where the polymer itself cannot be dissolved.

B. Stability

Solid organotin polymers are stable in air and under room conditions for over several decades. As noted elsewhere, the organotin polymers show greater stability in acids than bases. This forms the basis for certain biomedical applications. This tendency for overall great stability in acid than in base can also serve as a means of the delivery of both the organotin and often drug portion of the chain.

C. Physical Nature

Most are solids, but a few are gummy in nature, probably because entrenched solvent has not been entirely removed. They are generally white but can become colored if the matrix in which the organotin moiety is located is a color site, such as the polydyes.

D. Molecular Weight

The polymers synthesized by us using the interfacial polycondensation process are typically oligomeric, with degrees of polymerization from light scattering photometry of about 5–100. Higher molecular weight products can be made using other synthetic approaches. Thus the general degree of polymerization for organotin polyesters is about 5–50, but using a solution synthesis process employing alkoxides produces much higher chain lengths, generally >100.[188]

E. Thermal Properties

Most of the organotin products show good long-term room temperature stability as solids. When heated, they begin to degrade around 100ºC. As a general rule, organotin polymers undergo degradation without melting.

Here we will look at the organotin polyamines to illustrate general behavior. The organotin polyamines begin degrading in both air and nitrogen between 100ºC

300ºC.[185] This is followed by a large loss of weight, generally 20–80% over the next 100º range. Most then continue to about 900ºC with little additional weight loss. The relative stabilities in air and nitrogen are somewhat similar.

Using DSC, the energy changes are similar to about 300ºC, after which there is a major difference. In air, there is a large exotherm after 300ºC, consistent with oxidation occurring at the tin atom site. In nitrogen, the transitions are generally endothermic and less energetic. Weight losses coincide with the energy transitions. Temperature ranges in which there is little weight loss are referred to as stability plateaus. They are present for most organotin polymers and are believed to be due to the different kinds of bonding present in the materials. By comparison, simple organic polymers generally do not contain stability plateaus because overall thermal stability is governed by a single bond, the carbon–carbon bond.

Some of the products retain >50% of their weight to 900ºC. The nature of this residue is not well understood but is believed to contain the metal in some highly complex crosslinked matrix. The generally lesser stabilities in air are believed to be due to the availability of low-lying *d*-orbitals on the tin that are susceptible to attack by oxygen leading to oxidative degradation of the organotin chain.

F. Electrical Properties

As noted before the polystannanes are good conductors and conductivity has been found for a number of other tin-containing polymers.

While most organotin polymers made by our group are nonconductors, some of the organotin products are semiconductors. For many of the products made by our group, bulk resistivities on the order of 10^5 ohm-cm are not unusual. All results are for nondoped samples, so it would be of interest to see what doping would do to their conductivities. Preliminary evidence indicates that some of the organotin products made by our group exhibit pizoelectrical properties.

G. Mass Spectral Behavior

Because many of our organotin products are not very soluble, we have looked at avenues for physical characterization that do not require the material to be in solution. We have used a number of mass spectral techniques to characterize these materials. Here we will describe for illustrative purposes some results for the product derived from the reaction of dimethyltin dichloride and norfloxacin.[198,199]

Table 2 contains the most abundant ion fragments derived from this product using HR-EI MS. Ion fragments are present, derived from both norfloxacin and the dimethyltin moiety. The presence of ion fragments containing O-Sn-O, O-Sn-pip, and pip-Sn-pip bonding are present. Also present are ion fragments derived from one unit, **69**, as shown in equation 9.

Table 2 Most Abundant Ion Fragments Derived from the HREI Mass Spectrometry of the Product of Dimethyltin Dichloride and Norfloxacin

Temperature			
300ºC	425ºC	450ºC	(Possible) Assignment
57	57	56	pip minus 2 CH_2
71	70		pip minus CH_2
83	84		pip
97			
107			
120			
135			Sn-O
		149	MeSn-O
155			O-Sn-O
165	165	163	Sn-OCO
	176	178	MeSn-OCO
185	185		O-Me_2Sn-O
		191	Me_2SnOCO
205		206	Sn-pip
	219	219	O-Sn-pip
	233	235	Nor minus pip
	275	275	Nor minus CO_2
	289	288	Nor minus Et
	303	303	Nor minus F
381			Unit minus pip

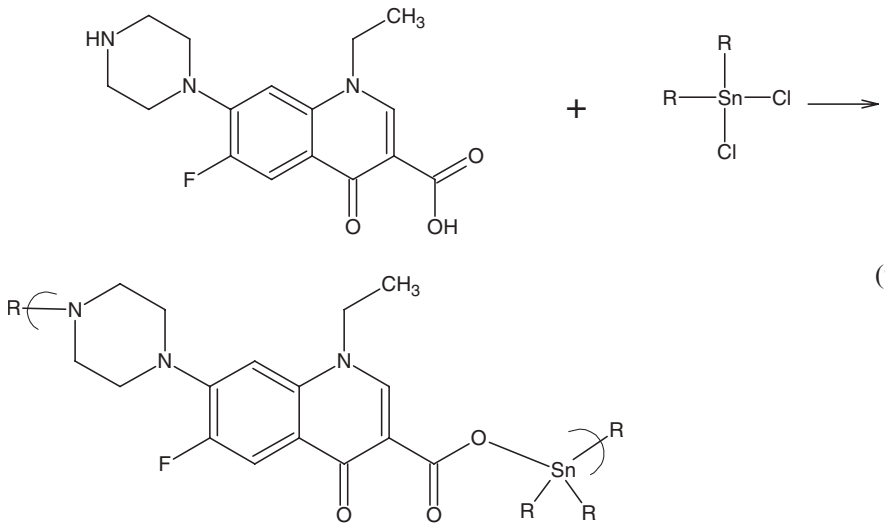

(9)

69

Tin contains 10 naturally occurring isotopes with 7 of them present in a reasonable abundance to allow identification by MS. Table 3 contains isotopic ion abundance matches for selected tin-containing ion fragments. The matches are reasonable and consistent with the presence of tin in these ion fragments.

More recently we have begun using matrix-assisted laser desorption/iodization MS, MALDI. MALDI allows molecular weight determination for reasonably soluble polymers in suitable solvents. The organotin polymers generally do not meet this requirement but we have used MALDI to investigate high molecular weight ion fragments from dilute solution–insoluble polymer mixtures. Representative results are given here, again using the product from dimethyltin dichloride and norfloxacin.

Results for the product derived from reaction of dimethyltin dichloride and norfloxacin appear in Table 4. Only the molecular weight of the most abundant ion

Table 3 Isotopic Abundance Values (425ºC) for Products Formed From Reaction between Dimethyltin Dichloride and Norfloxacin

m/z = 1	116	117	118	119	120	122	124
Nat Ab. (%)	14	8	24	9	33	56	
Sn-OCO	161	162	163	164	165	167	169
Found (%)	15	10	22	9	33	57	
O-Me_2Sn-O	181	182	183	184	185	187	189
Found (%)	13	7	26	10	34	46	

Table 4 Major Ion Fragment Clusters for the Product of Dimethyltin Dichloride and Norfloxacin for Ion Fragments >600 Daltons

Mass (Daltons)	(Tentative) Assignment[a]
600	Unit-Sn minus Me
634	Unit-Sn-OH
680	Nor-Sn-nor minus pip, Me
786	Unit-nor
844	2 Units-OH minus pip, 2 Me
954	2 Units-Cl minus Me
996	2 Units-Nor minus Me, pip
1207	2 Units-Nor minus 3 Me
1477	3 Units-pip
1691	3 Units-Nor minus 2 Me
1900	4 Units-Cl
2107	HO-4 Units-Sn-pip
2338	5 Units-Cl minus 2 Me
2541	HO-5 Units-Sn-pip minus 2 Me
2702	6 Units minus pip, Me
3394	Cl-7 Units-pip
3753	HO-8 Units
3873	Cl-8 Units-pip
4923	10 Units-nor minus pip
5367	11 Units-nor minus pip

[a] Sn, dimethyltin moiety; nor, norfloxacin moiety; pip, piperazinyl; Me, methyl radical.

fragment within the cluster is noted. The bands are generally broader than often found in MALDI because of the presence of isotopes of tin. A series of clusters of bands occur to 2540. These correspond to various DPs from 1 unit through 8 units. Bands appear to about 3750 (all values are e/m = 1; Daltons) corresponding to a DP of about 8. Taken as a whole, there appears to be two "weak" bonding sites. One of these is the tin–methyl linkage. This is consistent with observations of ion fragments derived employing simple electron impact techniques where numerous ion fragments contain tin minus one or more of the organic groups. The second weak site is the linkage that connects the two ring systems of norfloxacin. For purposes of simplicity, these two ring systems are designated as simply the one-ring and the two-ring structures.

End group analysis for ends derived from norfloxacin are hard to determine since the difference between bond scission and the presence of a proton is only 1 Dalton. By comparison, organotin end groups will contain either a chloride atom or hydroxide atom. Ion fragments containing tin end groups contain both hydroxyl groups and chloride atoms consistent for at least these ion fragments that chain scission did not occur.

Unlike HREI MS, the particular mass spectrometry employed for the MALDI studies is not highly accurate, making isotopic abundance studies difficult. Nevertheless, some matches were made, and selected ones are included in Tables 5 and 6. Reasonable matches are the exception rather than the rule. Further, results that reflect the relative isotopic abundance are leveled as the number of units, and consequently the isotopic characteristics are lost. Thus MS is a useful tool for structural identification, including, sometimes, end groups. It also allows an insight into the thermal stability of certain groups.

Table 5 Isotopic Abundance Values for a Single Tin-Containing Ion Fragment, Nor-Sn-Nor Minus pip, Me

m/z = 1	116	117	118	119	120	122	124
Standard	14	8	24	9	33	5	6
m/z = 1	676	677	678	679	680	680	684
Found	11	15	23	14	25	4	9

Table 6 Isotopic Abundances for Two Tin-Containing Ion Fragments

m/z = 1	234	235	236	237	238	239	240	242	244
Calculated	8	7	18	11	20	7	17	7	5
HO-Sn-Nor-Sn minus two methyl groups									
m/z = 1	574	575	576	577	578	579	580	582	584
Found	7	11	17	14	20	9	10	7	2
Sn-R-Sn minus one methyl									
m/z = 1	596	597	598	599	600	601	602	604	606
Found	7	9	14	11	30	—	19	9	—

H. Miscellaneous

Other useful structural reports on the structural analysis of organotin products not given elsewhere are found in literature for ^{13}C,[271] fluorescence,[204] photodegradation by UV light,[272] size exclusion chromatography,[152–156] and NMR and chromatographic.[147,153,155,156,273,274]

XIV. INTERFACIAL POLYMERIZATION

By far the majority of organotin polymers made from reactions involving attack by Lewis bases occurred using the interfacial polycondensation process. The topic of interfacial synthesis has been reviewed.[275–277]

There are several interfacial systems that have been employed in the production of organometallic polymers. Briefly, the three most used systems are as follows:

1. Classical system in which the Lewis base, generally along with an added base, is dissolved in water. The second phase consists of the Lewis acid, here the organotin-containing reactant, dissolved in a suitable organic liquid. This system is the one that was popularized by Morgan and co-workers at Dupont.
2. Nonaqueous two-phase systems employ two liquids that are largely immiscible in one another, such as dissolving the Lewis base in acetonitrile, nitrobenzene, or 2,5-hexadione and the acid chloride, here the organotin reactant, in a nonpolar organic liquid such as hexane, decane, or carbon tetrachloride.
3. Nonorganic solvent systems in which the Lewis base is dissolved in water and a liquid Lewis acid, such as tripropyltin chloride, is used neat.

By far the most widely used is the classical aqueous system.

Other modifications to the interfacial systems have been employed to assist the reaction, such as salting out and the use of phase transfer agents. As the name implies, interfacial systems require that there be two largely immiscible liquids, each containing one of the reactants. Reaction occurs at or near the interface. Morgan notes that for most organic acid chloride systems with diols and diamines the reaction occurs in the organic layer. We have found that for organotin systems employing neutral Lewis bases such as diols and diamine the reaction appears to occur within the organic phase. But for charged Lewis bases, such as salts of diacids, reaction occurs even closer to the interface and possibly at the interface, due to the poor solubility of the ionized salt in the organic phase. The site also varies with the nature of the Lewis acid. Thus organotin chlorides are highly hydrophobic so that there is less of a tendency for them to enter the aqueous phase, whereas Group IVB metallocene dihalides readily hydrolyze, forming a species that reacts by inserting the metallocene moiety. Here reaction with acid salts occurs in the aqueous phase, but reaction with diols and diamines still occurs in the organic phase.

We also made one of the few kinetic studies of the rapidly stirred interfacial systems using dimethyldichlorosilane and ethylene glycol. A model that assumes that ethylene glycol droplets reside in the organic phase predicts that the rate of reaction is

proportional to the spherical surface area of the glycol droplets, or the 2/3 power of the mass of ethylene glycol, leading to the expression

$$\text{Rate} = k\,[\text{ethylene glycol}]^{2/3}\,[\text{silane}] \tag{10}$$

which is in agreement with the kinetic data.[278,279]

This points out two other needs: the need for more well characterized reaction systems and the importance of having the reactants at the surface of the droplets. In fact, the reactants are not equally distributed throughout a solution. Since like-likes-like the best, there is a molecular-level segregation of the solute and solvent. As the solute to surface ratio decreases there comes a point at which the surface is preferentially occupied by the solute, here the reactants. This situation occurs for interfacial systems, both unstirred (expected) and highly stirred (unexpected) where the surfaces of the two different liquid droplets, the interface, is especially high in the reactants. Thus, as the Lewis base meets the surface droplet holding the Lewis acid, it sees at the surface a greater than expected amount of Lewis acid. This may be a major reason why polymer formation can occur instead of hydrolysis because on a molar basis the number of water molecules that can hydrolyze the Lewis acid severely outnumber the Lewis bases within the entire phase, but not necessarily at the interface surface. (For a reaction employing for one phase 5 mmol of reactant dissolved in 50 mL of water, the ratio of water molecules to reactant molecules is 600: 1.)

This leads us to a brief discussion of hydrolysis rates. While organic acid chlorides hydrolyze rapidly when introduced to water, organotin dihalides are relatively stable in water unless wetted. Thus dibutyltin dichloride can be placed in boiling water for some time without noticeable hydrolysis occurring.

The interfacial polymerization requires so-called high-energy reactants, such as organic acid chlorides. Although the organotin polymer groups are named as though the organotin moiety were similar to an alkylene, organotin halides are more similar to acid chlorides in their reactions and activation energies with respect to reactions involving traditional Lewis bases. Thus the activation energies for the reactions of organotin halides with amines, alcohols, and salts of acids is believed to be on the order of 20–30 kcal/mol, similar to the analogous reactions of organic acid halides with amines and alcohols. Thus polymers are formed though a chain-wise kinetic process rather than a step-wise process. Polymer is formed throughout the polymerization process rather than in polymer formation cumulating at the end of the polymerization.

The classical rope trick has as the polymer-forming step the pulling of the nylon rope from the system. Polymerization is rapid, and in rapidly stirred systems (as generally used) we use, the polymer is formed almost instantaneously and completed within several seconds to minutes. Stirred systems increase the interfacial area and consequently the reaction rate. The use of simple emulsifying jars as the reaction vessel allows the interfacial surface to be increased hundreds of thousands of times when employing rapid stirring. In general, interfacial surface increases with increasing stirring rate and, up to some limit, so does reaction rate. There comes a limit where the amount of reactant to coat the droplets is too small to accomplish this objective. At this point, increased stirring rate does not increase reaction rate. We generally use rapid stirring in the range of 18,000 rpm no load. This is several times

the speed of a model airplane propellor and is easily accomplished by most commercial blenders. Because of the possibility of spark formation and subsequent fire, we employ blender systems that resist this. We have run thousands of reactions and have never had a spark fire due to the malfunctioning of the blender system. This stirring rate is about 70% the speed where large molecules are sheared.

Added base is normally employed to convert generated acid into a salt and for diamines and diols to prevent formation of non-Lewis bases. Thus amines react with acids, forming salts; the lone pair on the nitrogen is no longer free to react with the Lewis acid (eq. 11).

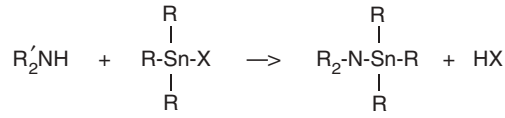

(11)

70

The acid comes from the reaction of the organotin halide and the diol or diamine.

(12)

71

Of interest is the lack of acid formation for the analogous reaction, except employing a salt.

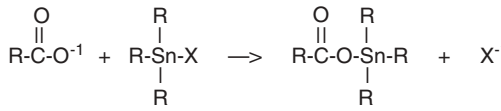

(13)

72

Here, acid is not needed to be added after the reaction because only enough base was originally added to neutralize the acid reactant.

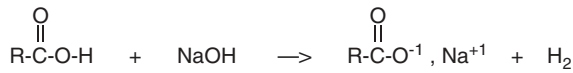

(14)

73

The base is also believed to assist in the removal of the proton on the amine or diol during the reaction sequence (eq. 15).

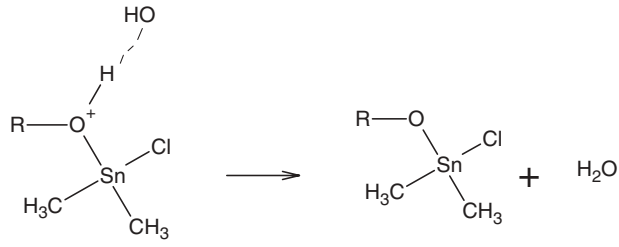

(15)

74 **75**

Many of the products are base unstable and acid stable. In cases where added base is required, there is often a race between polymer formation and base-induced degradation. Base degradation is stopped once the base is neutralized. This occurs by simple addition of dilute acid such as hydrochloric acid after several seconds to minutes. Base degradation can also be limited through the use of various base systems where the pH is maintained at a low level. This can be accomplished though the use of only slightly soluble bases, such as calcium hydroxide and barium hydroxide. It can also be lowered using organic bases as trimethylamine. Sterically hindered bases are often used since the amine competes with the desired Lewis base reactant. The use of any base will be competitive with the desired reaction and results in chain termination and the presence of the associated base as an end group. Thus organotin reactions employing triethylamine generally have amine end groups that are readily identified through the use of infrared spectroscopy and looking at bands in the 2900–2700 1/cm region. The pH control can also be accomplished through the use of buffer systems such as combinations of phosphate salts. The precipitation from the reaction solution probably also assists in protecting especially base sensitive products allowing them to be recovered.

This base instability and acid stability is useful in medical applications in which medications given by mouth are initially subjected to stomach acid; if delivery of the drug is to be after the stomach, then acid stability is desirable. There are certain places in the body that are mildly basic, and if the delivery site is there then the stability pattern is doubly advantageous. Most reactions are carried out at room temperature, minimizing undesired migration and rearrangement reactions. This is particularly important when employing certain stereoregular drugs.

High concentrations of reactants and poor solvents are often employed since there is an advantage to using reactants that are not highly soluble in the particular phase so that the tendency to coat the interface and move into the other phase is encouraged. There is often an upper maximum at which higher concentrations actually cause markedly lower product yields. Thus, while relatively high concentrations are often desired, this must be moderated and experimented with to see what is the best concentration level for the particular reaction. For many of the organotin systems, we employ about 3–5 mmol in 30–50 mL liquid for each phase (ca. 0.5 M).

There may also be a downside to employing poor solvents as the organic liquid. Such systems also cause rapid precipitation of the product and thus may limit molecular weight. We believe that this may be one cause for the limited chain lengths generally observed. We used to use such organic liquids as carbon tetrachloride and chloroform since both of these liquids are generally poor solvents for the organotin halides employed. These liquids are no longer environmentally acceptable, especially for large-scale preparations. We have moved toward the use of alkane liquids such as hexane and octant, which offer only moderately poor solubility for the organotin reactants but are inexpensive, readily available, and readily recyclable. A downside is that they are somewhat volatile and can ignite.

XV. SUMMARY

A wide variety of organotin polymers have been synthesized and partially characterized. The biological properties will continue to draw attention to organotin materials but other properties should also be investigated. Alternate synthesis using tin (II) should also be studied to see if in fact they give products analogous to the tin (IV) products. Since many of the products are made from organotin dihalides, this would save having to convert the organotin to the higher energy dihalide. It would also eliminate the need to neutralize the formed acid and the need to make sure that it has been removed from the product. For medical applications, removal of unwanted acid is especially important.

XVI. REFERENCES

1. E. Franklin, *J. Chem. Soc*. **2**, 263 (1849).
2. R. Wei, L. Ya, W. Jinguo, X. Qifeng, in *Polymer Materials Encyclopedia*, J. Salamone, ed., CRC Press, Boca Raton, FL.
3. M. Henry, W. Davidson, in *Organotin Compounds*, vol. 3 A. K. Saywer, ed., Dekker, New York, 1972.
4. M. Hoch, *Applied Geochem*. **16**, 719 (2001).
5. A. Davies, *Organotin Chemistry*, Wiley-VCH, Chichester, 1997.
6. C. Carraher, F. He, D. Sterling, F. Nounou, R. Pennisi, J. W. Louda, L. Sperling, *Polym. P.* **31**, 430 (1990).
7. C. Carraher, F. He, D. Sterling, *Polym. P*. **37**, 426 (1996).
8. C. Carraher, F. He., D. Sterling, *Polym. Mater. Sci. Eng.* **72**, 114 (1995).
9. C. Carraher, F. He., D. Sterling, "Synthesis, Characterization, and Theory of Polymeric Networks and Gels", Plenum, 1992.
10. C. Carraher, F. He, D. Sterling, *Polym. Mater. Sci. Eng.* **66**, 54 (1992).
11. C. Carraher, F. He, D. Sterling, *Polymer Modification*, Plenum, New York, 1997.
12. C. Carraher, F. He, D. Sterling, *Polym. Mater. Sci. Eng.* **75**, 180 (1996).
13. C. Carraher, F. He, L. Sperling, J. Fay, D. Sterling, *Polym. Mater. Sci. Eng.* **67**, 272 (1992).
14. (a) J. Montermoso, L. P. Mssrinelli, T. M. Andrews, U.S. Patent 3,016,369 (1962); (b) J. Montermoso, T. Andrews, L. Marinelli, *J. Polymer Sci.* **32**, 523 (1958).
15. L. Marinelli, T. Andrews, J. Montermoso, U.S. Patent 3012018 (1961).
16. (a) D. Kochkin, V. Kotrelev, M. Shostakovskii, S. Kalinina, G. Kuznetsova, V. Borisenko, *Vysokomolek. Soedin*. **1**, 482 (1959); (b) *Dokl, Akad. Nauk. SSSR*. **135**, 857 (1960).
17. (a) M. Shostakovskii, S. Kalinina, V. Kotrelev, D. Kochkin, G. Kusnetsova, L. Laine, A. Borisova, V. Borisenko, *Doklady*, 1960; (b) *Angew Chem*. **72**, 1711 (1960); (c) *Vysokomolekul. Soden.* **3**, 1131 (1961); (d) *J. Polymer Sci.* **52**, 223 (1961); (e) Russian Patent 172,777 (1965).
18. M. Shostakovskii, K. Zapunnaya, G. Skvortsova, S. Tyrinna, S. Stepoanova, M. Andriyankov, *Vysokomol. Soedin., Ser. A*. **10**, 679 (1968).
19. M. Shostakovskii, V. Kotreler, G. Kuznetsova, S. Kalinia, L. Laine, A. Borisova, *Vysokomol. Soedin*. **3**, 1128 (1961).
20. N. A. Adrova, M. Koton, E. Moskvina, *Izv. Akad. Nauk. SSSR Otdel. Khim. Nauk*, 1804 (1962).

21. N. Adrova, M. Kuton, V. Klages, *Vysokomol. Soedin*. **3**, 1041 (1961).
22. (a) J. Leebrick, U.S. Patent 3,167,532 (1965); (b) additional references are found in the following patents: U.S. Patent 3,711,524 (1978); Br. Patent 1,250,498 (1971); U.S. Patent 3,382,264 (1969); U.S. Patent 3,382,264 (1968); U.S. Patent 3,234,032 (1966).
23. Z. Rzaev, D. Kochkin, *Dokl. Akad. Nauk. SSSR.* **172**, (1967).
24. V. Zubov, Z. Rzaev, *Vysokomol. Soedin. Ser. A*, **34**, 73 (1992).
25. V. Zubov, W. Wulf, Z. Rzaev, *Vysokomol. Soedin. Ser. A*, **31**, 1846 (1989).
26. Z. Rzaev, S. Manedova, F. Saykhova, F. Rustanov, S. Mamedov, *Issled, v Obl. Sinteza Monomer. Polim. Prod., Baku*, 1007 (1987).
27. A. Talal, I. Aliev, R. Bagirov, Z. Rzaev, *Dokl. Akad. Nauk. Az SSSR* **43**, 47 (1987).
28. V. Dzhafarov, S. Mamedova, Z. Rzaev, *Issled. Obl. Sinteza Monomer. Polim. Produktov. Baku.* 96 (1987).
29. Z. Rzaev, S. Mamedova, G. Yusifov, F. Rustamov, *J. Polym. Sci., A. Polym. Chem.* **26**, 849 (1988).
30. Z. Rzaev, S. Manedova, N. Rasulov, U. Agaev, *Vysokomol. Soedin., Ser. A*, **29**, 352 (1987).
31. R. V. Subramanian, B. Garg, J. Jakubowski, J. Corredor, J. Montemarano, E. Fischer, *Org. Coat. Plast. Chem*. **32**, 660 (1976).
32. R. V. Subramanian, B. Garg, J. Corredor, in *Organometallic Polymers*, C. Carraher, J. Sheats, C. Pittman, eds., Academic Press, New York, 1978.
33. R. Subramanian, *Ann. N. Y. Acad. Sci.* **446**, 134 (1985).
34. R. Subramanian, J. Mendoza, B. Garg, *Holzforschung* **35**, 263 (1981).
35. D. Anderson, J. Mendoza, R. V. Subramanian, *Bioactive Polymers, ACS Sym. Ser.* **186**, American Chemistry Society, Washington, D.C., 1982.
36. R. Williams, R. V. Subramanian, *Polymer* **22**, 934 (1981).
37. R. V. Subramanian, R. Williams, *J. Appl. Polym. Sci.* **26**, 1681 (1981).
38. R. V. Subramanian, R. Williams, K. Somasekharan, *Org. Coat. Plast. Chem*. **41**, 38 (1979).
39. R. V. Subramanian, K. Somasekharan, *J. Macromol. Sci., Chem*. **A16**, 73 (1981).
40. R. V. Subramanian, B. Garg, K. Somasekharan, *Org. Coat. Plast. Chem*. **39**, 572 (1978).
41. K. Somasekharan, R. V. Subramanian, *Modification of Polymers, ACS Symp. Ser.* **121**, American Chemistry Society, Washington, DC, 1980.
42. R. V. Subramanian, B. Garg, *Polym. Plast. Technol. Eng*. **11**, 81 (1978).
43. B. Garg, J. Corredor, R. V. Subramanian, *J. Macromol. Sci., Chem.* **A11**, 1567 (1977).
44. W. Yeager, V. Castelli, *Organometallic Polymers*, Academic Press, New York, 1978.
45. J. Hoffman, K. Kasppel, L. Frenzel, M. Good, *Organometallic Polymers* Academic Press, New York, 1978.
46. K. Molloy, K. Quill, *J. Chem. Soc. Dalton Trans*. **7**, 1417 (1985).
47. R. Barbieri, L. Pellerito, A. Silvestri, G. Ruisi, J. Noltes, *J. Organomet. Chem*. 210, **43** (1981).
48. V. Mishchenko, V. Zubov, Y. Eremenko, *Vysokomol. Soedin. Ser. B* **27**, 341 (1985).
49. V. Mishchenko, V. Zubov, *Vysokomol. Soedin. Ser. B* **24**, 184 (1982).
50. Z. Rzaev, *Chemtech*. **9**, 58 (1979).
51. M. Radwan, *Pigment and Resin Tech*. **28**, 83 (1999).
52. R. Joshi, S. Gupta, *Prog. Org. Coat*. **19**, 245 (1991).
53. S. Al-Diab, N. Al-Muaikel, A, Al-Obeid, *Int. J. Chem.* **9**, 15 (1999).
54. N. Al-Muaikel, S. Al-Diab, H. Al-Khathian, *J. King Saud Univ. Sci*. **12**, 25 (2000).
55. N. Al-Muaikel, S. Al-Diab, A. Al-Salamah, A. Zaid, *J. Appl. Polym. Sci.* **77**, 740 (2000).
56. N. Al-Muaikel, S. Al-Diab, H. Alkhathlan, Al-Obied, *J. Saudi Chem. Soc*. **4**, 43 (2000).
57. N. Al-Muaikel, S. Al-Diab, H. Al-Khathian, *Asian J. Chem*. **11**, 1259 (1999).
58. S. Al-Diab, *J. Chem. Res., Synop*. **3**, 90 (1987).

59. I. Al-Najjar, S. Al-Diab, *Asian J. Chem*. **3**, 307 (1991).
60. R. Liepins, M. Timmons, N. Morosoff, J. Suries, in *Metal-Containing Polymeric Systems*, J. Sheats, C. Carraher, C. Pittman, eds., Plenum, New York, 1985.
61. A. Mahmoud, M. Azab, N. Messiha, *Eur. Polym. J*. **29**, 1125 (1993).
62. A. A. Mahmoud, A. Shaaban, M. Azab, N. Messiha, *Polym. Int.* **28**, 245 (1992).
63. V. Zubov, Z. Rzaev, *Vysokomol. Soedin. Ser. A* **34**, 73 (1992).
64. A. Mahmoud, *Eur. Polym. J*. **28**, 1115 (1992).
65. V. Zubov, V. Vul'f, V. Konsulov, *Vysokomol. Soedin. Ser. A* **32**, 1144 (1990).
66. A. Shaaban, A. Mahmoud, N. Messiha, *J. Appl. Polym. Sci*. **36**, 1191 (1988).
67. V. V. Korshak, *Izv. Akad. Nauk. SSSR Otdel. Khim. Nauk*. **174** (1959).
68. Y. Minoura, *J. Polym. Sci*. *A1* **4**, 2757 (1966).
69. C. Carraher, F. Li, C. Butler, *J. Polym. Mater*. **17**, 377 (2000).
70. N. A. Plate, Russian Patent 176,408 (1965).
71. K. Minsker, Y. Purinson, T. Zavarova, N. Plate, G. Fedoseeva, V. Kargin, *Vysokomol. Soedin. Ser. A* **10**, 1336 (1968).
72. Y. Purinson, N. Plate, S. Davydova, Z. Nurkeeva, V. Kargin, *Vysokomol. Soedin. Ser. B* **10**, 257 (1968).
73. R. Polster, Swiss Patent 413,372 (1966).
74. B. Zhao, W. Chem, D. Chen, L. Yan, Q. Zhu, Z. Li, *Gaofenzi Xuebao* **1**, 97 (1997).
75. Z. Ha, Y. Chang, Z. Lu, P. Wu, *Gaofenzi Xuebao* **6**, 725 (1995).
76. B. Zhao, D. Chen, M. Tian, K. Chen, K. Hu, Q. Zhu, Z. Han, *Fushe Yanjiu Yu Fushe Gongyi Xuebao* **10**, 170 (1992).
77. Z. Han, Y. Chen, J. Lin, P. Wu, *Gaofenzi Xuebao* **1**, 44 (1991).
78. Z. Han, S. Li, Z. Zhu, Q. Zhu, *Gaofenzi Xuebao* **5**, 600 (1989).
79. Z. Han, Y. Gao, *Gaofenzi Cailiao Kexue Yu Gongcheng* **6**, 19 (1990).
80. Z. Xu, C. Su, Y. Chen, Z. Han, R. Qian, Z. Song, *Gaofenzi Xuebao* **2**, 129 (1989).
81. M. He, Z. Han, L. Pu, S. Li, *Gongneng Gaofenzi Xuebao* **1**, 32 (1988).
82. Z. Xu, Z. Han, S. Li, J. Yang, C. Su, *Gongneng Gaofenzi Xuebao* **1**, 25 (1988).
83. B. Zhao, X. Zhu, Murat, Z. Han, *Fushe Yanjiu Yu Fushe Gongyi Xuebao* **5**, 24 (1987).
84. Z. Han, Y. Gao, J. Li, P. Wu, *Gongneng Gaofenzi Xuebao* **1**, 19 (1988).
85. Z. Hu, Z. Han, L. Bo, Y. Pan, Z. He, X. Zhang, *Zhongguo Kexue Jishu Daxue Xuebao* **18**, 534 (1988).
86. Z. Han, Y. Gao, *Shiyou Huagong* **16**, 851 (1987).
87. Z. HanQ. Zhang, K. Chen, H. Shen, *Zhongguo Kexue, Jishu Daxue Xuebo* **17**, 51 (1987).
88. Z. Han, *Shiyou Huagong* **16**, 313 (1987).
89. B. Zao, X. Zhu, Z. Han, *Fusshe Yanjiu Yu Fushe Gongyi Xuebao* **4**, 23 (1986).
90. Z. Han, Z. Yu, M. Yu, K. Chen, *Gaofenzi Tongxun* **4**, 317 (1986).
91. Z. Han, Z. Yu, W. Liu, *Hecheng Xiangjiao Gongye* **9**, 111 (1986).
92. C. Aufdermarsh, R. Pariser, *J. Polym. Sci. A* **2**, 4727 (1964).
93. S. Sandler, K. Tsou, *J. Phys. Chem*. **68**, 300 (1964).
94. S. Sandler, J. Dannin, K. Tsou, *J. Polym. Sci. A* **3**, 3199 (1965).
95. L. Kolditz, G. Furcht, *Z. Chem*. **6**, 381 (1966).
96. S. Migdal, D. Gertner, A. Zilkha, *Isr. J. Chem*. **5**, 163 (1967).
97. S. Migdal, D. Gertner, A. Zilkha, *Eur. Polym. J*. **4**, 465 (1968).
98. D. Wagner, D. Gertner, A. Zilkha, *Can. J. Chem*. **46**, 3612 (1968).
99. S. Migdal, D. Gertner, A. Zilkha, *Can. J. Chem*. **46**, 2409 (1968).

100. D. Gertner, S. Migdal, A. Zilkha, Bri. Patent 1107929, 1968.
101. M. Frankel, D. Gertner, D. Wagner, A. Zilkha, *J. Organomet. Chem*. **9**, 83 (1967).
102. X. Zhu, B. Blough, F. Carroll, *Teth. Lett.* **41**, 9219 (2000).
103. W. Liu, A. Halasa, J. Visintainer, P. Rinaldi, *Polym. P*. **41**, 26 (2000).
104. J. Labadie, S. MacDonald, C. G. Wilson, *J. Imaging Sci*. **30**, 169 (1986).
105. C. Carraher, J. Schroeder, C. McNeely, D. Giron, J. Workman, *Org. Coat. Plastics Chem.* **40**, 560 (1979).
106. C. Carraher, W. Burt, D. Giron, J. Schroeder, M. Taylor, H. M. Molloy, T. Tiernam, *J. Appl. Polym. Sci*. **28**, 1919 (1983).
107. C. Carraher, D. Giron, J. Scheroder, C. McNeely, U.S. Patent 4,312,981 (1982).
108. (a) C. Carraher, T. Gehrke, *Org. Coat. Plast. Chem*. **45**, 558 (1981); (b) C. Carraher, T. Gehrke, *Org. Coat. Plast. Chem.* **46**, 258 (1982).
109. Y. Naoshima, C. Carraher, *Polym. Mater. Sci. Eng.* **50**, 403 (1984).
110. Y. Naoshima, C. Carraher, T. Gehrke, M. Kurokawa, *J. Macromol. Sci. Chem*. **A23**, 861 (1986).
111. Y. Naoshima, C. Carraher, G. Hess, M. Kurokawa, S. Hirono, *Bull. Okayama U. Sci*. **20A**, 33 (1985).
112. C. Carraher, Y. Naoshima, *Biotechnology and Polymers*, Plenum, 1991.
113. Y. Naoshima, C. Carraher, S. Iwamoto, H. Shudo, *Appl. Organomet. Chem*. **245**, 1 (1987).
114. C. Carraher, T. Gehrke, *Modification of Polymers*, Plenum, 1983.
115. Y. Naoshima, C. Carraher, *Chemical Reactions on Polymers*, ACS, Washington, DC, 1988.
116. C. Carraher, T. Gehrke, D. Giron, D. Cerutis, H. M. Molloy, *J. Macromol. Sci. Chem.* **A19**, 1121 (1983).
117. C. Carraher, T. Gehrke, *Polymer Applications of Renewable-Resource Materials*, Plenum, New York, 1983.
118. Y. Naoshima, H. Shudo, M. Uenishi, C. Carraher, *Polym. Mater. Sci. Eng.* **58**, 553 (1988).
119. Y. Naoshima, H. Shudo, M. Uenishi, C. Carraher, *J. Macromol. Sci. Chem*. **A25**, 895 (1988).
120. C. Carraher, D. Sterling, C. Butler, T. Ridgway, *Biotechnology and Bioactive Polymers*, Plenum, New York, 1994.
121. C. Carraher, D. Sterling, C. Butler, T. Ridgway, J. W. Louda, *Polym. Mater. Sci. Eng.* **62**, 241 (1990).
122. C. Carraher, D. Sterling, T. Ridgway, W. Reiff, B. Pandya, *Interpenetrating Polymer Networks*, ACS, Washington, DC, 1994.
123. C. Carraher, D. Sterling, C. Butler, T. Ridgway, *Polym. Mater. Sci. Eng.* **66**, 343 (1992).
124. C. Carraher, J. Piersma, *Angew Makromol. Chem.* **28**, 153 (1973).
125. C. Carraher, L. Reckleben, C. Butler, *Polym. Mater. Sci. Eng.* **63**, 704 (1991).
126. C. Carraher, J. Piersma, L-S. Wang, *Org. Coat. Plastics Chem*. **31**, 254 (1971).
127. C. Carraher, L-S. Wang, *Makromol. Chem.* **152**, 43 (1972).
128. C. Carraher, M. Fedderson, *Angew Makromol. Chem.* **54**, 119 (1976).
129. C. Carraher, D. Girone, W. Woelk, J. Schroeder, M. Feddersen, *J. Appl. Polym. Sci*. **23**, 1501 (1979).
130. C. Carraher, J. Schroeder, W. Venable, C. McNeely, D. Giron, W. Woelk, M. Feddersen, *Additives for Polymers*, vol. 2, Academic Press, New York, 1978.
131. C. Carraher, J. Piersma, *J. Appl. Polym. Sci*. **16**, 1851 (1972).
132. J. Nichols, J. Dickerson, Eur. Patent Appl. 90-119604 19901012 (1991).
133. O. Moriya, Y. Urata, T. Endo, *J. Polym. Sci. A Polym. Chem*. **29**, 1501 (1991).
134. O. Moriyak, T. Endo, *J. Appl. Polym. Sci.* **41**, 2095 (1990).
135. O. Moriya, S. Arai, T. Endo, *J. Polym. Sci. A Polym. Chem.* **26**, 2573 (1988).
136. R. Sadhir, W. James, *Org. Coat. Appl. Polym. Sci*. **48**, 668 (1983).

137. C. Carraher, P. Mykytik, H. Blaxall, R. Linville, T. Tiernan, S. Coldiron, *Polymer Applications of Renewable-Resource Materials*, Plenum, New York, 1983.
138. Y. Naoshima, C. Carraher, S. Hirono, T. Bekele, P. Mykytiuk, *Renewable Resource Materials*, Plenum, New York, 1986.
139. C. Carraher, H. Stewart, S. Carraher, D. Chamely, W. Learned, J. Helmy, K. Abby, A. Salamone, *Functional Condensation Polymers*, Kluwer, New York, 2002.
140. C. Carraher, A. Gaonkar, H. Stewart, S. Miao, S. Carraher, *Tailored Polymeric Materials for Controlled Delivery Systems*, ACS, Washington, DC, 1998.
141. C. Carraher, A. Gaonkar, H. Stewart, S. Miao, S. Carraher, *Polym. Mater. Sci. Eng.* **80**, 367 (1999).
142. C. Carraher, A. Gaonkar, H. Stewart, S. Miao, D. Mitchell, C. Barosy, M. Colbert, R. Duffield, *Polym. P.* **38**, 572 (1997).
143. C. Carraher, A. Gaonkar, H. Stewart, S. Miao, M. Colbert, S. Casanova-Clark, T. Hale, D. Sterling, *Polym. Mater. Sci. Eng.* **76**, 580 (1997).
144. G. Dumartin, G. Ruel, J. Kharboutli, B. Delmond, M. Connil, B. Jousseaume, M. Pereyre, *Synlett* **11**, 952 (1994).
145. B. Delmond, G. Dumartin, *Phys. Organometal. Chem*. **2**, 445 (1999).
146. G. Dumartin, J. Kharboutli, B. Delmond, Y. Frangin, M. Pereyre, *Eur. J. Org. Chem*. **4**, 781 (1999).
147. G. Dumartin, M. Pourcel, B. Delmond, O. Donard, M. Pereyre, *Tet. Lett*. **39**, 4663 (1998).
148. G. Ruel, K. Ngo, G. Dumartin, B. Delmond, M. Pereyre, *J. Organometal. Chem.* **444**, C18 (1993).
149. J. Quintard, M. Degueil-Castaing, G. Dumartin, B. Barbe, M. Petraud, *J. Organomet. Chem*. **234**, 27 (1982).
150. J. Quintard, M. Degueil-Castaing, M. Dumartin, A. Rahm, M. Petraud, *J. Chem. Soc. Chem. Commun.*, **21**, 1004 (1980).
151. W. Mandeers, J. Bellama, R. Johannesen, E. Parks, F. Brinckman, *J. Polym. Sci. A Polym. Chem.* **25**, 3469 (1987).
152. E. Parks, W. Manders, R. Johannesen, F. Brinckman, *J. Chromatogr*. **351**, 475 (1986).
153. E. Parks, W. Manders, R. Johannesen, F. Brinckman, *NTIS Report NBSIR-83-2802*, National Bureau of Standards, Washington, DC, 1984.
154. E. Parks, R. Johannesen, F. Brinckman, *NTIS Report NBSIR-82-2577*, National Bureau of Standards, Washington, DC., 1982.
155. E. Parks, R. Johannesen, F. Brickman, *J. Chromatogr*. **255**, 439 (1983).
156. E. Parks, R. Johannesen, F. Brinckman, *NTIS Report NBSIR-81-2424*, National Bureau of Standards, Washington, DC.
157. R. Che, R. Wei, L. Ya, J. Wu, Chin. *J. React. Polym*. **3**, 74 (1994).
158. R. Wei, Y. Liang, Q. Xue, S. Lu, H. Shen, *Chin. J. React. Polym*. **2**, 23 (1993).
159. R. Wei, Y. Liang, S. Lu, B. Han, T. Gao, *Huaxue, Gongye, Yu Gongcheng*, **14**, 46 (1997).
160. R. Che, R. Wei, L. Yu, J. Wu, *Chin. J. Reactive Polym*., **3**, 74 (1994).
161. R. Wei, Y. Liang, R. Che, *Lizi Jiaohuan Yu Xifu* **10**, 412 (1994).
162. R. Wei, Y. Liang, Q. Xue, R. Che, *Gaofenzi Xuebao* **5**, 541 (1994).
163. R. Wei, Y. Liang, Q. Xue, *Gaofenzi Xuebao* **4**, 403 (1992).
164. R. Wei, Y. Liang, Q. Xue, S. Lu, H. Shen, *Acta Polym. Sinica* **4**, 403 (1992).
165. R. Wi, Y. Liang, *Tinjin Hua Gong* **1**, 4 (1991).
166. C. Carraher, *Angew. Makromol. Chem.* **31**, 115 (1973).
167. M. Frankel, D. Gertner, D. Wagner, A. Zilkha, Israeli Patent 23, 197 (1969).
168. S. Migdal, D. Gertner, A. Kilkha, *J. Organometal. Chem*. **11**, 441 (1968).
169. M. Frankel, G. Gertner, D. Wagner, A. Zilkha, *J. Organometal. Chem*. **9**, 3383 (1965).
170. M. Frankel, D. Getner, D. Wagner, A. Zilkha, *J. Appl. Polym. Sci*. **9**, 3838 (1965).
171. S. Buick, *J. Polym. Sci. B* **4**, 933 (1966).

172. C. Carraher, R. Dammeier, *Polym. P*. **11**, 606 (1970).
173. C. Carraher, R. Dammeier, *J. Polym. Sci. A-1* **8**, 3367 (1970).
174. C. Carraher, R. Dammeier, *Makromol. Chem.* **135**, 107 (1970).
175. C. Carraher, R. Dammeier, *J. Polym. Sci. A-1* **10**, 413 (1972).
176. M. Frankel., et. al. Fr. Patent 1,484,693 (1966).
177. T. M. Andrews, *J. Am. Chem. Soc*., **80**, 4102 (1958).
178. E. Janson, E. Fields, U.S. Patent 3,247,167 (1966).
179. C. Carraher, D. Winter, *Makromol. Chem.* **141**, 237 (1971).
180. C. Carraher, D. Winter, *Makromol. Chem.* **152**, 55 (1972).
181. C. Carraher, D. Winter, *Makromol. Chem.* **141**, 259 (1971).
182. C. Carraher, D. Winter, *J. Macromol. Sci. Chem.* **A7**, 1349 (1973).
183. C. Carraher, M. Nagata, H. Stewart, S. Miao, S. Carraher, A. Gaonkar, C. Highland, F. Li, *Polym. Mater. Sci. Eng.* **79**, 52 (1998).
184. C. Carraher, H. Stewart, S. Carraher, M. Nagata, S. Miao, *J. Polym. Mater*. **18**, 111 (2001).
185. C. Carraher, M. Nagata, H. Stewart, S. Miao, C. Butler, A. Gaonkar, C. Barosy, R. Duffield, F. Li, *Polym. Mater. Sci. Eng.* **78**, 36 (1998).
186. D. Siegmann-Louda, C. Carraher, D. Chamely, A. Cardoso, D. Snedden, *Polym. Mater. Sci. Eng.* **86**, 293 (2002).
187. C. Yoder, J. Zuckerman, *J. Am. Chem. Soc*. **88**, 4831 (1966).
188. C. Carraher, G. Scherubel, *Makromol. Chem.* **160**, 259 (1972).
189. C. Carraher, G. Scherubel, *Makromol. Chem.* **152**, 61 (1972).
190. C. Carraher, G. Scherubel, *J. Polym. Sci. A-1* **9**, 983 (1971).
191. C. Carraher, F. Li, D. Siegmann-Louda, C. Butler, S. Harless, F. Pflueger, *Polym. Mater. Sci. Eng.* **80**, 363 (1999).
192. D. Siegmann-Louda, C. Carraher, J. Ross, F. Li, K. Mannke, S. Harless, *Polym. Mater. Sci. Eng.* **81**, 151 (1999).
193. D. Siegmann-Louda, C. Carraher, F. Pflueger, D. Nagy, J. Ross, *Functional Condensation Polymers*, Kluwer, New York, 2002.
194. (a) C. Carraher, F. Li, *Polym. Mater. Sci. Eng.* **83**, 405 (2000); (b) C. Carraher, F. Li, *Polym. Mater. Sci. Eng.* **83**, 407 (2000).
195. C. Carraher, F. Li, D. Siegmann-Louda, J. Ross, *Polym. Mater. Sci. Eng.* **77**, 499 (1997).
196. C. Carraher, H. Luing, *Polym. Mater. Sci. Eng.* 82, 81 (2000).
197. D. Siegmann-Louda, C. Carraher, M. Graham, R. Doucette, L. Lanz, *Polym. Mater. Sci. Eng.* **87**, 247 (2002).
198. C. Carraher, L. Lanz, *Polym. Mater. Sci. Eng.* **87**, 245 (2002).
199. C. Carraher, L. Lanz, *Polym. Mater. Sci. Eng.* **87**, 243 (2002) and unpublished data.
200. C. Carraher, A. Zhao, *Polym. Mater. Sci. Eng.* unpublished data.
201. C. Carraher, V. Foster, R. Linville, D. Stevison, *Polym. Mater. Sci. Eng.* **56**, 401 (1987).
202. C. Carraher, L. Tisinget, G. Solimine, M. Williams, S. Carraher, R. Strother, *Polym. Mater. Sci. Eng.* **55**, 469 (1986).
203. Z. Han, Z. Wang, H. Zhuang, *Gongneng Gaofenzi Xuebao* **2**, 309 (1989).
204. Z. Han, Z. Wang, *Gongneng Gaofenzi Xuebao* **3**, 72 (1990).
205. C. Carraher, R. Venkatachalam, T. Tiernan, M. taylor, *Org. Coat. Appl. Polym. Sci*. **47**, 119 (1982).
206. C. Carraher, R. Linville, D. Stevison, V. Foster, M. Williams, M. Aloi, *Polym. Mater. Sci. Eng.* **58**, 85 (1988).
207. C. Carraher, A. Taylor, F. Medina, R. Linville, E. Randolph, J. Kloss, D. Stevison, *Polym. P*. **34,** 166 (1993).

208. R. Bleicher, C. Carraher, *Polym. Mater. Sci. Eng.* **86**, 289 (2002).
209. J. Leebrick, Fr. Patent 1,400,617 (1965).
210. M & T Chemicals, Inc. Dutch Patent 6,405,137 (1964).
211. C. Glosky, Fr. Patent 1,386,988 (1964).
212. S. Midgal, D. Gertner, A. Zilkha, *Can. J. Chem*. **45**, 2987 (1967).
213. D. DePree, R. Cordova, U.S. Patent 3,161,664 (1964).
214. C. Carraher, S. Jorgensen, P. Lessek, *J. Appl. Poly. Sci*., **20**, 2255 (1976).
215. C. Carraher, P. Lessek, *Angew. Makromol. Chem.* **38**, 57 (1974).
216. C. Carraher, P. Lessek, *Org. Coat. Plast. Chem*. **33**, 420 (1973).
217. C. Carraher, G. Peterson, J. Sheats, T. Kirsch, *Makromol. Chem.* **175**, 3089 (1974).
218. C. Carraher, G. Peterson, J. Sheats, T. Kirsch, *J. Macromol. Sci. Chem*. **A8**, 1009 (1974).
219. C. Carraher, G. Peterson, J. Sheats, *Org. Coat. Plast. Chem*. **33**, 427 (1972).
220. B. Rudner, M. Moores, U.S. Patent 3,178,375 (1965).
221. (a) J. Noltes, G. van der Kerk, *Rec. Trav. Chim*. **80**, 623 (1961); (b) **81**, 41 (1962); (c) *Chimia* **16**, 122 (1962).
222. G. van der Kerk, J. Nolts, *Ann. N. Y. Acad. Sci*. **125**, 25 (1965).
223. BASF, Dutch Patent 6,514,261 (1966).
224. W. Neumann, H. Nierman, B. Schneider, *Ann*. **707**, 15 (1967).
225. W. Neuman, B. Schneider, *Ann*. **707**, 20 (1967).
226. J. Frielink, G. van der Beek, Dutch Patent 6,514,261 (1966).
227. H. Naarmann, E. Kastning, Fr. Patent 1,455,503 (1966).
228. (a) S. Bresadola, F. Rossetto, G. Tagliavini, *Chem. Commun*. **17**, 623 (1966); (b) *Eur. Polym. J*. 475 (1968).
229. Br. Pat. 1,027,021 (1966).
230. Sladkov, Tezisy Dokladov *XV Konferentsii po Vysokomolekulyarnym soedin. Posvyansch. Poluch. Khim. Novykh Vesh.*, Moska, Yanvar, 1965.
231. A. A. Berlin, *Usp. Khim*. **29**, 1189 (1960).
232. I. Kotlyarenskii, *Izv. Akad. Nauk. USSR Otdel. Khim. Nauk*. 956 (1960).
233. (a) L. Luneva, A. Sladkov, V. Korshak, *Vysokomol. Soedin*. **7**, 427 (1967); (b) **A9**, 910 (1967).
234. V. Mylnikov, *Dokl. Akad. Nauk. SSSR* **144**, 840 (1962).
235. T. Imori, T. Tilley, *J. Chem. Soc. Commun.* 1607 (1993).
236. N. Devylder, M. Hill, K. Molloy, C. Price, *Chem. Commun.* 711 (1996).
237. V. Lu, T. Tilley, *Macromolecules* **29**, 5763 (1996).
238. J. Reichi, C. Popoff, L. Gallagher, E. Remsen, D. Berry, *J. Am. Chem. Soc.,* **118**, 9430 (1996).
239. T. Tilley, T. Imori, U.S. Patient Appl., 94-265447 19940624 (1996).
240. M. Fujino, T. Hisaki, N. Matsumoto, *Macromolecules*, **28**, 5017 (1995).
241. S. Adams, J. Drager, *Angew. Chem. Int. Ed. Engl.* **26**, 1255 (1987).
242. J. Mark, H. Allcock, R. West, *Inorganic Polymers*, Prentice Hall, New York, 1992.
243. H. Suzuki, H. Meyer, J. Simmerer, J. Yang, D. Naarer, *Adv. Mater.* **5**, 743 (1993).
244. J. Rust, G. Denault, US Patent 3,178,375 (1965).
245. (a) R. Washburn, R. Baldwin, US Patent 3,112,331 (1963); (b) US Patent 3,311,646 (1963); (c) US Patent 3,341,477 (1967).
246. B. Chamberlain, A. G. MacDiarmid, *J. Chem. Soc.* 445 (1961).
247. S. Freireich, D. Gertner, A. Zilkha, *J. Organometal. Chem.* **25,** 111 (1970).
248. H. Takimoto, J. Rust, US Patent 3,244,645 (1966).
249. M. Koton, T. Kiseleva, *Dokl. Akad. Nauk. SSSR* **130**, 86 (1960).

250. (a) S. Zhivukhim, *Zhur. Obshchei Khim* **32**, 3059 (1962); (b) **35**, 1029 (1965).

251. (a) A. G. Davies, *J. Organometal. Chem*. **7**, 13 (1967); (b) **10**, 33 (1967).

252. (a) A. G. Davies, *J. Chem. Soc*., 5439 (1963); (b) 5744 (1964).

253. I. Omae, *Organotin Chemistry*, Elsevier, Amsterdam, 1989.

254. C. Carraher, C. Butler, Y. Naoshima, V. Forste, D. Giron, P. Mykytiuk, *Applied Bioactive Polymeric Materials*, Plenum, New York, 1990.

255. C. Carraher, C. Butler, D. Sterling, V. Saurino, *Polym. Mater. Sci. Eng.* **66**, 352 (1992).

256. Y. Naoshima, H. Shudo, M. Uenishi, C. Carraher, *J. Polym. Mater*. **8**, 51 (1991).

257. C. Carraher, V. Saurino, C. Butler, D. Sterling, *Polym. Mater. Sci. Eng.* **72**, 192 (1995).

258. (a) D. Siegmann-Louda, C. Carraher, F. Pflueger, J. Coleman, S. Harless, H. Leuing, *Polym. Mater. Sci. Eng.* **82**, 83 (2000); (b) L. Pellerito, F. Maggio, M. Consiglio, A. Pellerito, G. Stocco, S. Grimaudo, *App. Organomet. Chem*. **9**, 227 (1995); (c) F. Maggio, A. Pellerito, L. Pellerito, S. Grimaudo, C. Mansueto, R. Vitturi, *Appl. Organomet. Chem*. **8**, 71 (1994); (d) R. Vitturi, C. Mansueto, A. Gianguzza, F. Maggio, A. Pellerito, L. Pellerito, *Appl. Organome. Chem*. **8**, 509 (1994); (e) H. Baratne Jankovics, L. Nagy, F. Longo, T. Fiore, L. Pellerito, *Magyar Kemiai Foly*. **107**, 392 (2001); (f) R. Vitturi, B. Zava, M. Colomba, A. Pellerito, F. Maggio, L. Pellerito, *App. Organomet. Chem*. **9**, 561 (1995) and references therein; (g) L. Pellerito, F. Maggio, T. Fiore, A. Pellerito, *App. Organomet. Chem*. **10**, 393 (1966); (h) A. Pellerito, T. Fiore, C. Pellerito, A. Fontana, R. Di Stefano, L. Pellerito, M. Cambria, C. Mansueto, *J. Inorganic Biochem.* **72**, 115 (1998).

259. C. Carraher, C. Butler, US Patent 5,043,463 (1991).

260. C. Carraher, C. Butler, US Patent 5,840,760 (1998).

261. C. Butler, C. Carraher, *Poly. Mater. Sci. Eng.* **80**, 365 (1999).

262. C. Carraher, C. Butler, Y. Naoshima, D. Sterling, V. Saurino, *Biotechnology and Bioactive Polymers*, Plenum, New York, 1994.

263. C. Carraher, C. Butler, *Biotechnological Polymers*, Technomic, Lancaster, PA, 1993.

264. C. Carraher, C. Bytler, Y. Naoashima, D. Sterling, V. Saurino, *Industrial Biological Polymers*, Technomic, Lancaster, PA, 1995.

265. C. Carraher, C. Butler, V. Foster, B. Pandya, D. Sterling, *Polym. Mater. Sci. Eng.* **68**, 255 (1993).

266. C. Carraher, C. Butler, Y. Naoshima, V. Foster, D. Giron, P. Mykytiuk, *Applied Bioactive Polymeric Materials*, Plenum, New York, 1988.

267. C. Carraher, Y. Naoshima, C. Butler, V. Foster, D. Gill, M. Williams, D. Giron, P. Mykytiuk, *Polym. Mater. Sci. Eng.* **57**, 186 (1987).

268. Yeast C. Carraher, C. Butler, L. Reckleben, *Cosmetic and Pharmaceutical Applications of Polymers*, Plenum, New York, 1991.

269. C. Carraher, T. Rigdway, D. Sterling, C. Butler, *Industrial Biotechnological Polymers*, Technomic, Lancaster, PA, 1995.

270. C. Carraher, C. Butler, L. Reckleben, A. Taylor, V. Saurino, *Polym. P*. **33**, 539 (1992).

271. J. Dharia, R. Joshi, S. Gupta, *India Polym. Mater. Sci. Eng*. **61**, 233 (1989).

272. K. Takahashi, Y. Ohyagi, *Shikizal Kyokaishi* **60**, 381 (1987).

273. D. Xu, Y. Wang, Z. Xu, Z. Han, *Gongneng Gaofenzi Xuebao* **4**, 259 (1991).

274. D. Xu, Y. Wang, Z. Xu, Z. Han, *Gongneng, Gaofenzi Xuebao* **3**, 48 (1990).

275. F. Millich, C. Carraher, *Interfacial Synthesis*, vols. I and II, Dekker, New York, 1977.

276. P. Morgan, *Condensation Polymers by Interfacial and Solution Methods*, Wileys Interscience, New York, 1965.

277. C. Carraher, J. Preston, *Interfacial Synthesis, III*, Dekker, New York, 1982.

278. C. Carraher, *Polym. P.* **10**, 418 (1969).

279. C. Carraher, *J. Polym. Sci. A-1* **7**, 2359 (1969).

CHAPTER 11

Organolead-Containing Polymers

Charles E. Carraher Jr.

Department of Chemistry and Biochemistry, Florida Atlantic University, Boca Raton, Florida

CONTENTS

Macromolecules Containing Metal and Metal-Like Elements, Volume 4: Group IVA Polymers, edited by Alaa S. Abd-El-Aziz, Charles E. Carraher Jr., Charles U. Pittman Jr., and Martel Zeldin
ISBN: 0-471-68238-1

I. INTRODUCTION

Compared to the other Group IVA metals and metalloids, there are fewer organometallic polymers of lead. This is probably due to a combination of factors including the following. First, many of the monomers analogous to Si, Ge, and Sn are less soluble. Second, while some desired properties are known for lead, other metal sites offer similar properties. Relative to tin, which has the greatest number of organometallic compounds employed commercially, few organolead compounds are employed industrially. Further, relative to tin, organolead compounds are generally more toxic. Most of us are aware of the particular toxicity toward children and babies that the intake of lead though ingestion of lead-containing coatings has. For acute organolead toxicity, symptoms are fatigue, loss of sleep, constipation, colic, diarrhea, neuritis, anemia, and metallic taste. For chronic exposure, symptoms are anemia, central nervous system, renal, and reproductive disorders. Metabolism and mode of action include mitotic abnormalities in bone marrow cells, chromosomal aberrations, affinity for nucleic acids, effect on immune mechanism, and inhibition of red-cell pigment heme. Other reasons why lead is not used may be the generally lower stability of organolead compounds and the instability of the Pb–Pb bond.

Several early and recent reviews of lead-containing polymers have been published. Most of these include a review of the Group IVA polymers, including tin and germanium and sometimes silicon.[1–5]

The use of organolead for specific applications has been described in some detail. Here I will focus on earlier suggested applications suggesting that the potential uses have been know for many years. The use of polymers containing organolead has been described in various articles and patents. In 1965 an article in *Paint Manufacture*[6] described the (potential) use of organolead polymers as potential raw materials for surface coatings. The catalytic activity of organolead compounds in polyurethane formation was described in 1966.[7] Here bivalent lead and trialkyl lead mixed with aliphatic monocarboxylic acids were mixed with poly(diethylene glycol adipate) with 2,4-tolyene diisocyanate. The production of polyurthane was increased to a greater extent in comparison to dibutyltin dilurate, which was, at that time, a widely employed monomeric catalyst. These lead compounds were monomeric but illustrate the early recognition of the catalytic activity of lead compounds.

Organolead compounds have been suggested for a variety of other applications including (emphasizing early applications) as additives for lubricating oils,[8] metal sources in electroplating,[9–22] low speed photographic reproduction chemicals,[12] liquid scintillation systems,[13,14] antifogging agents,[15] increased electron scattering,[16] heat stabilizers,[18] corrosion stabilizers,[19] etc. The use of tetraethyllead as an additive to gasoline is well know though it is now prohibited for use in newer automobiles and trucks. This application was recognized early.[18]

The use of organolead compounds as paint biocides was also widely recognized, but these lost out to the less toxic and better accepted organotin monomers and polymers.[19]

Many papers report the formation of lead-containing polymers but the formulations do not necessarily produce lead covalently bonded as part of a polymer. For instance, Honda and Kaetsu[20] described the production of a transparent, easily moldable polymer useful for protection against radiation by dissolving a specified amount of an organolead compound in a specified monomer mixture. Thus lead acetate is dissolved in a monomer mixture containing methyl methacrylate, methacrylic acid, and α-methyl styrene, and free-radical's polymerization carried out. The resulting mixture is sandwiched between glass plates to obtain the desired product.

II. POLYMERIZATION AND COPOLYMERIZATION OF VINYL LEAD COMPOUNDS

While vinyl lead itself, C=C–Pb, has not been polymerized, there have been reports of its copolymerization. Korshak et al.[21] reported that both diethyldivinyllead and triethylvinyllead decompose to lead metal under the action of peroxide polymerization catalysts at 120–130ºC, but that copolymers are formed when reacted in the presence of styrene or α-methylstyrene, giving products with about 4–6% lead content.

In 1959 Koton et al.[22–24] reported the synthesis of triphenyl-*p*-styrenyllead. This compound was discussed at the 1969 IUPAC Symposium on Macromolecular Chemistry in Moscow. It was prepared from reaction of triphenyllead chloride and *p*-styrenylmagnesium chloride (eq. 1). It homopolymerized readily, more readily than styrene itself. It also forms copolymers with styrene or methyl methacrylate in conversions of >25%, giving transparent plastic films (eq. 2).

$$Ph_3PbCl + p\text{–}CH_2 + CHMgCl \rightarrow Ph_3PbC_6H_4CH{=}CH_2 \quad (1)$$

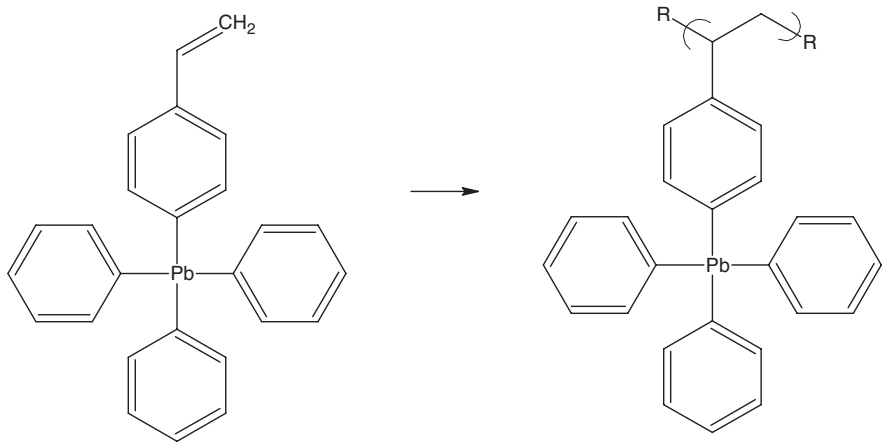

1 **2** (2)

The synthesis and polymerization of triphenyl-*p*-styrenyllead, as well as triethyl-*p*-styrenyllead, was described by Pars et al.[25] 1960. In comparison to the triphenyl-*p*-styrenyllead, isolation of triethyl-*p*-styrenyllead was difficult because of its tendency to polymerize.

Also in 1960, Nolts et al.[26,27] studied triphenyl-*p*-styrenyllead; diphenyldi-*p*-styrenyllead; and other compounds, including the polymerization of *p*-trimethyllead derivatives of styrene and α-methylstyrene. These compounds polymerize easily in free-radical initiators such as 2,2′-azobis-isobutyronitrile at 70–90ºC, giving clear, colorless solids. Of interest, the rates of polymerization decreased in the order of Pb > Si > C > Ge > Sn. The unusually fast rate of polymerization of lead compounds was attributed to the formation of homolytic lead–carbon bond cleavage during polymerization, thus giving additional chain initiators. This is consistent with the low solubility of the lead polymers in agreement with the formation of some crosslinking.

In 1959 Korshak and co-workers also studied the same compounds and the previously unknown triethyl-*p*-α-methylstyrenyllead.[28,29] This compound was prepared according to equation 3. Compound (**3**) was polymerized at 80ºC under pressure, giving a colorless, hard material (**4**) that was soluble in toluene and benzene (eq. 4). If the monomer was not purified, the resulting product was rubbery. The corresponding germanium polymer was more stable but the tin polymer was less stable.

$$\begin{aligned} &BrC_6H_4COCH_3 + CH_3MgI \rightarrow BrC_6H_4C(CH_3)_2OH \rightarrow \\ &\quad BrC_6H_4C(CH_3)=CH_2 \rightarrow Et_3PbC_6H_4C(CH_3)=CH_2 \end{aligned} \tag{3}$$

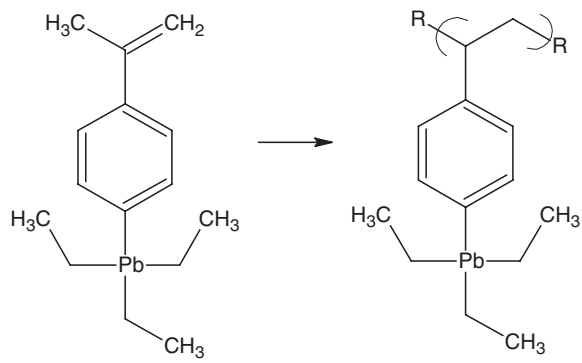

3 **4** (4)

In 1965, Noltes's group[30] reported the homopolymerization of similar compounds—namely trimethyl-*p*-styrenlylead and trimethyl-*p*-α-methylstyrenyllead. The products swelled rather than dissolved, consistent with some crosslinking.

Other similar studies have been carried out using styrenyllead compounds including tetrakislead compounds.[31–36]

III. CHELATION POLYMERS AND COPOLYMERS DERIVED FROM POLY(ACRYLIC ACID)

One of the first uses of lead-containing polymers involved the use of acrylic acid soil conditioners. The most typical metal-containing acrylic soli conditioners involved sodium and calcium but Mello et al.[37] worked with lead. In general, absorbed sodium ions are exchanged at the soil particle surface. Consequently, sites are formed on the soil with a vinyl group attached to the soil particle via a lead or calcium bridge. These then are of the same general structure as those reported by others later from reaction of the sodium salt of poly(acrylic acid) and ionic lead. Depending on the charge on the lead, the products can be as shown in scheme 1 for the Pb^{+2} products, or for the Pb^{+4} additional bonding will occur giving a complex of crosslinked structures. For the Pb^{+2}, there are possible various Pb derivatives as lead hydroxide and linkages between chains and within the same chain as pictured in scheme 1.

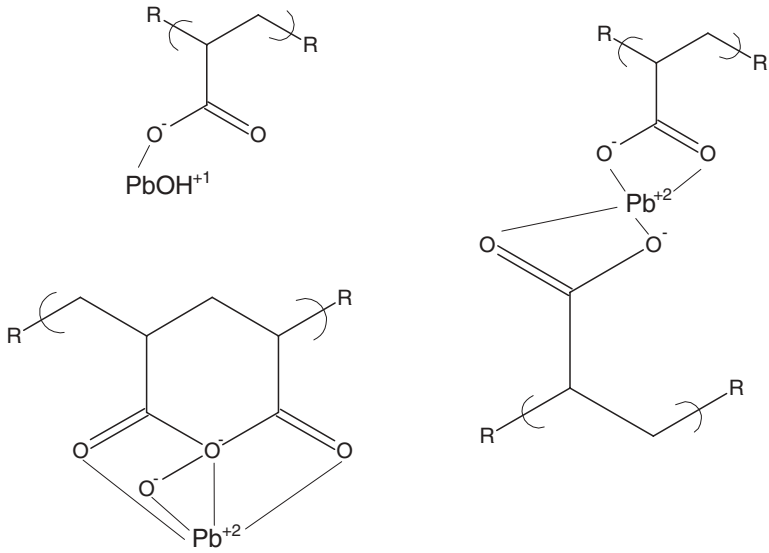

Scheme 1

Other structures were also formed using the sodium salt of acetic acid. These are not polymers of poly(acrylic acid) but rather are bridged structures, as **5**.

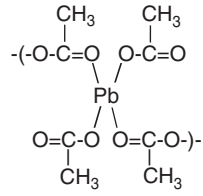

5

Along with the inclusion of organotin as part of polymers and co-polymers employing organotin bonded through acid groups, organolead polymers have been synthesized. Kochkin, et al.[38] reported the bulk polymerization of vinyl acids-containing organolead with itself or with various acrylates, including methyl methacrylate. Minimal characterization was reported but did include thermal and infrared spectral results. A product structure for the polymerization of a vinyl acid-containing the trimethyllead moiety is given as **7**.

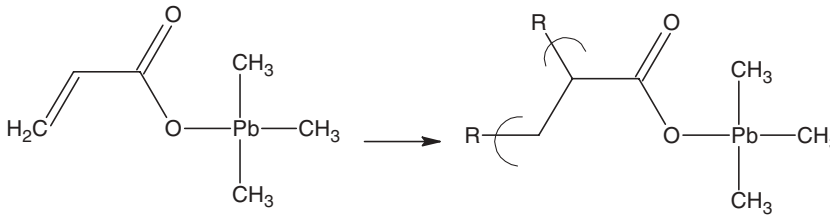

6 **7** (5)

Similar products were reported by Kochkin et al.,[39] except employing the copolymerizatin of maleic anhydride or maleic acid, styrene, and lead or tin acrylates or by esterification of maleic anhydride with trialkyl(aryl)stannols or trialkyl(ary)-plumbanols followed by the copolymerization of the intermediates with other vinyl monomers. These products were reported to form transparent films that had good fungi resistance.

IV. ARYLENE-BRIDGED PRODUCTS

A number of organolead polymers have been described that are, at best, poorly structurally characterized. For instance, Rudner and Moores[40] described the formation of complex alkylene-bridged lead polymers. Thus alkylated metallanes and alkylenedimethallane polymers were formed from lead employing high pressure and heat. Presumably the lead is held through bonding with pi-electrons on the alkylene group.

V. SOLID-STATE PRODUCTS

There is a strong tendency of lead compounds, including organolead compounds, having electron withdrawing substituents to self-assemble in the solid state. The coordination chemistry of such supramolecular compounds is less investigated than the coordination chemistry of organotin compounds. The large atomic size of lead allows coordination polymers with high-coordination-number environments at the lead atom to give coordination products different from those of the analogous tin

products. Many of these products are polymeric only in the solid state and do not conform to traditional definitions of polymers. Even so, they will be included as examples in the following discussion.

A lot of effort, including most of the most recent efforts, involves synthesis of insoluble materials that are characterized using solid-state instrumentation including Raman, IR, MS, solid-state NMR, X-ray and other related instrumentation. Following is a brief review of this effort.

Self-assembly structures have been reported[41–104] for lead (IV) and lead(II) nitrogen-containing ligands,[41–58,97–105] alkoxides,[59–61] lead(II) phosphonates,[62–64] lead(II) phosphinates,[65,66] and lead(II) carbonates.[67–78]

A. Nitrogen-Coordinated Products

A number of nitrogen-coordinated products have been reported, including those described in this section. Recently, some studies were directed at the coordination of inorganic lead salts with organic ligands. The ligands included coordination polymers of lead(II) halides, thiocyanate, and nitrate with aliphatic and aromatic nitrogen bases.[41–58,97–105] Following is a brief review of some of these efforts.

Brimah et al.[41] synthesized a series of organolead(IV) polymers of the general form $(Me_3Pb)_4M(CN)_6$ with various water of hydrations, where M = Fe and Ru. Thus aqueous solutions of Me_3PbCl and $K_4[M(CN)_6]$ (4:1; M = Fe or Ru) form infinite, puckered layers whose built-in -M-CN-Pb-OH_2 units are probably held together by hydrogen bonding between the layers. These layered systems are sensitive to even modest influences, including grinding, and tend to lose water. The strictly anhydrous materials strongly resemble their Me_3Sn homologs in exhibiting strongly temperature-dependent ^{13}C solid-state NMR and no ion-exchange activity. The presence and amount of water influence the overall structure of these compounds.

Shi et al.[42–44] and others[45–50] have been working on the synthesis and study of a variety of PbX_2-based organic–inorganic hybrides using the lead(II) ion as the building block with the belief that lead has a variable coordination number and varied coordination geometry that would allow the formation of varying polymeric networks. Formation of PbX_2 products from reaction with co-ligands such as 2,2-bypyridine, 4,4-bipridine, and pyrazine give one and two dimensional structures where the PbX_2 chain or layer perseveres. The one dimensional structures can be single or double stranded. Coordination polymers based on the lead pseudo-halide $Pb(SCN)_2$ have also been prepared. Again, these products are insoluble.

Britton's group[97,98] produced several lead-containing macromolecular products from organolead cyanides. Trimethyllead cyanide, Me_3PbCN gives Pb-N-coordinated structures,[97] which are orthorhomibic and in which the trimethhllead groups are planar and linked by disordered cyanide groups aligned along the lead–lead grouping.

A series of dimethyl Group IVA dicyano products were studied.[98] The silicon and germanium compounds are approximately tetrahedral, forming linear chains through weak acid–base N–metal interactions. The tin and lead products show similar structures but with stronger N–Pb interactions. Planer sheets are formed where

each "normally" tetrahedral molecule is distorted to nearly an octahedral arrangement by the formation of two nearly equivalent nitrogen–metal interactions.

The crystal structure of trimethyllead azide, Me_3PbN_3, was studied.[99,105] The lead atom is connected to the terminal nitrogen of the azido group, forming zigzag structures as in **8**. The lead atoms exist as an almost perfect trigonal bipyramidal coordination sphere with the trimethyllead units ordered in a skew conformation.

Mixed-metal cobalt–lead products of the formulas $[(Me_3Pb)_3M(CN)_6]_n$ (where M = Fe, Co and $[(Me_3Pb)_4M(CN)_6]_n$, where M = Fe, Ru have been formed through addition of a saturated aqueous solution of Me_3PbCl to concentrated solutions of $K_3[M(CN)_6]$ or $K_4[M(CN)_6]$.[100–104]

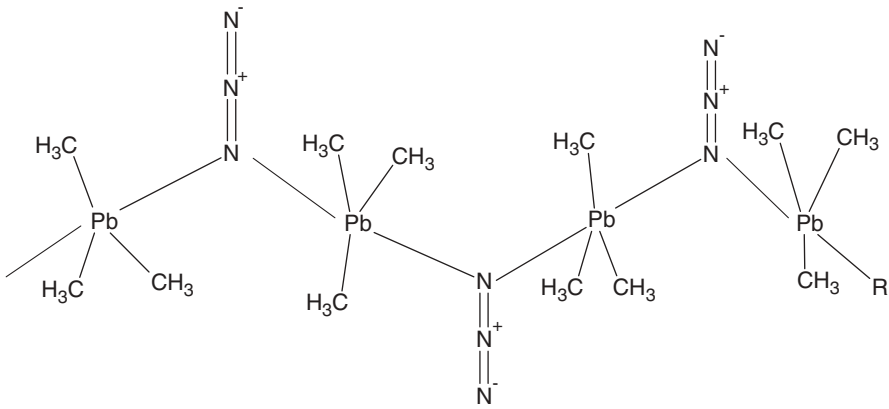

8

Another study looked at $[(Me_3Pb)_3Co(CN)_6]_n$.[103] The supramolecular sequence contains a three-dimensional network with a -Co-CN-Pb-NC- sequence. The network contains Me_3Pb^+ cations and parallel channels whose walls contain the methyl groups of the Me_3Pb^+ cation. A second structure characterized contains water as part of its structure. Its formula is $[(Me_3Pb)_4Fe(CN)_6 \cdot 2H_2O]_n$, and it exists as puckered layers. The sequences -Fe-CN-Pb-OH_2, within each layer, form hydrogen bridges between adjacent layers. A representative structural unit is given in **9**.

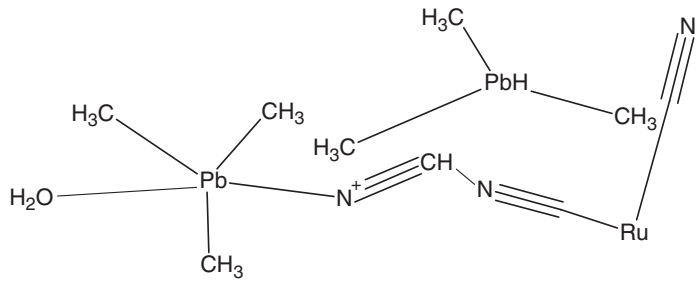

9

The anhydrous analogs were obtained after prolonged drying under vacuum at 60–80ºC.[102] These compounds do not contain the ability to exchange ions as do the analogous tin products. Thus a suspension of $[(Me_3Pb)_4Fe(CN)_6]_n$ stirred with an aqueous solution of Et_4NCl did not give $[(Et_4N)(Me_3Pb)_3Fe(CN)_6]$ and Me_3PbCl, whereas a suspension of $[(Me_3Sn)_4Fe(CN)_6]$ and Et_4NCl almost immediately gives $[(Et_4N)(Me_3Sn)_3Fe(CN)_6]$.

Various heterocyclic five-membered ring donors are completely or partially oxidized within the cavities of the three-dimensional host polymer $[(Me_3Pb)_3Fe(III)(CN)_6]_n$, giving polymeric intercalated or charge transfer complexes.[100] The structure and physical properties of these complexes depend on the time of reaction, exposure to light, presence/absence of atmospheric oxygen or moisture, degree of grinding, and nature of the heterocyclic moiety. Pyrrole, *N*-methylpyrrole, pyrrolidine, and 2,5-dimethhlpyrrole polymerize within this cavity, forming the corresponding neutral semiconducting diamagnetic polymeric intercalated complex; the host network is fully reduced to its anionic homolog $[(Me_3Pb)_3Fe(II)(CN)_6^-]_n$. If a few drops of water are added, there is a large increase in the conductivity and the products become good semiconductors. By contrast, thiazole and thiphene do not polymerize under these conditions but give paramagnetic charge transfer complexes.

B. Sulfur-Coordinated Products

A number of sulfur–lead products have been described as supramolecular polymeric arrays. These include bis(O-methyldithiocarbonato)lead(II), $[Pb(S_2COMe)]_n$.[77] The lead atom occupies a position on a crystallographic twofold axis and is chelated by two methyldithiocarbonato ligands related to each other across this axis. The sulfur atoms are also coordinated to an adjacent lead atom generating a polymeric structure with each lead atom being 6-coordinated. The lead atom exists in a distorted octahedral environmental with the two nonbonding sulfur atoms occupying approximately axial positions and the basal plane defined by the four bridging sulfur atoms.

The terms *weak* and *strong polymer formation* are sometimes employed and are based on the similarity between recognized primary bond lengths of units within the structure and bond lengths for bonds holding the "polymer" together. If the bond lengths are similar, then the products are termed strongly polymeric, and if some connective bond lengths are less the compound is termed weakly polymeric. Svensson and Albertsson[79] reported a structure for $(Pb[S_2P(Et_2]_2)_n$ with each lead atom surrounded by four sulfur atoms from the two diethyldithiophosphinate ligands in the form of a pyramid, with lead at the apex and two more sulfur atoms on the "free" side of the lead atom. The latter Pb–S interactions result in a weak polymer formation.

Haidus's group[80,81] reported the crystal and molecular structure of a number of sulfur–lead bonded polymeric materials. Bis(diphenyl)dithiophospphinato)lead(II), $[Pb(SSPPh_2]_n$, exists such that its monomeric units contains distorted square pyramidal PbS_4 units. Further, each lead atom has two weak Pb–S contacts with neighboring molecules, lying on the free side of the PbS_4 unit. This gives molecular pair units that are repeated in a chain. The coordination polyhedron about lead is a strongly distorted octahedron with axial positions occupied by a sulfur atom of a neighboring

molecule and a sulfur atom. A representation for the monomeric units is given in **10**. This paper contains references to many other similar products.

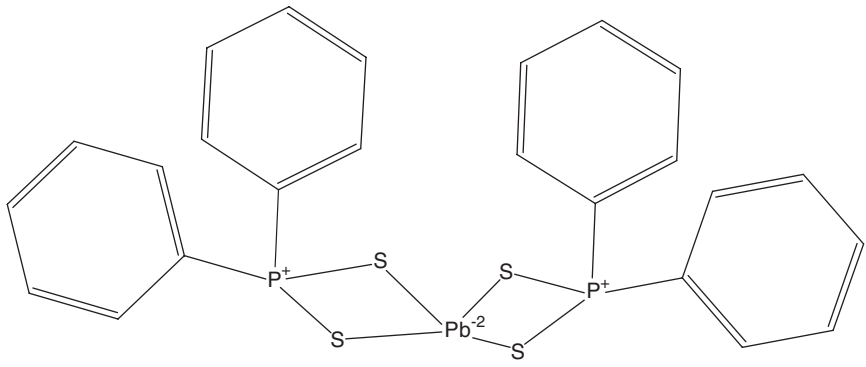

10

Haidus's group also reported on the synthesis and crystal and molecular structure of dimeric $[Pb(S_2PMe_2)_2]_2$ associated into polymeric chains through intermolecular Pb–S interactions. The dimers are associated into supramolecular polymeric chains through interdimer Pb–S secondary interactions. The overall coordination geometry about the lead atom is described as distorted pentagonal bipyramidal with two short Pb–S and two long Pb–S interactions, and the lone electron pair of lead, located between the sulfur atoms and involved in secondary interactions, is in a equatorial position, with two sulfur atoms in axial positions. A representative structure for the dimer is given in **11**. Note that each lead atom has a net minus two charge, which is omitted from the structure.

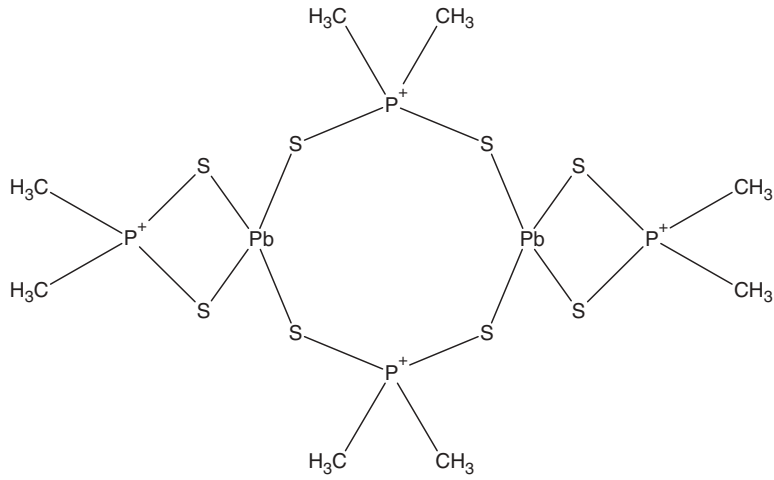

11

Triphenyllead pyridine-4-thiolate (4-$Ph_3PbSC_5H_4N$) is a chain polymer resulting from intermolecular Pb–S interactions.[86] The cyclic dithiolate

2,2-diphenyl-1,3,2-dithiaplumbolane self-assembles in the solid state, forming chain structures as shown in **12**. The intramolecular Pb–S bond lengths are nearly the same, 2.54 and 2.49 A, but the intermolecular Pb–S bond length is much larger, 3.55 A.

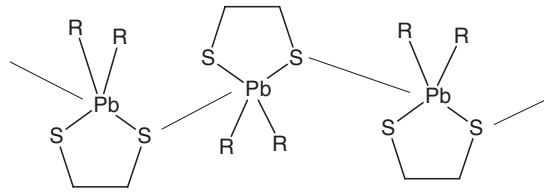

12

Triphenyllead dimethyldithiophosphinate also forms polymeric structures.[83] Here, the dithiophosphinate unsymmetrically bridges two lead atoms of adjacent units, giving a polymeric chain with pentacoordinated lead atoms (**13**). The coordination is best described as being distorted trigonal bipyramid with the phenyls in the equatorial and the sulfur in the axial positions. The lead–sulfur distances are 2.708 and 3.028 A.

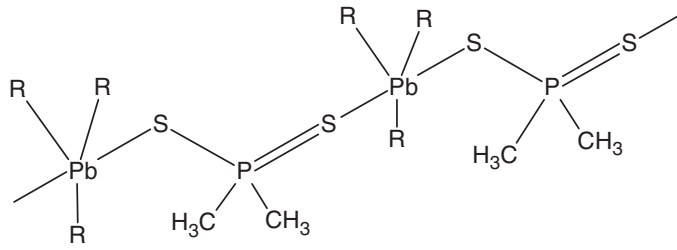

13

C. Halide-Coordinated Products

Infrared and Raman spectroscopy initially suggested that triorganolead halides are usually associated in the solid state, forming supramolecular assemblies.[84,85] This was later confirmed by X-ray crystallography.[86–89] Lead is usually pentacoordinated with the halogen atoms located in the axial positions of a trigonal bipyramid and infinite -Pb-S- chains with unsymmetrical X-Pb-X links (**14**). The two lead–halide bond distances differ significantly. For instance, for trimethyllead(IV) iodide, the Pb–I bond distances are 3.038 and 3.360 A, and in triphenyllead bromide they are 2.852 and 3.106 A.[86] The structures show a zigzag chain conformation. The Pb-X-Pb bond angle depends on the nature of the organic groups.

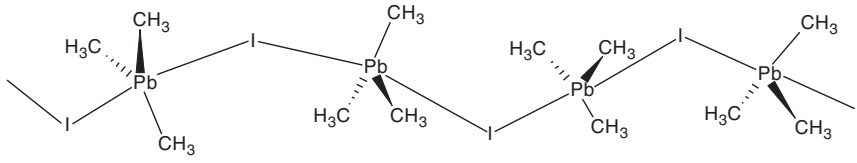

14

Diphenyllead(IV) dichloride was reported[90] to form one-dimensional chains, as shown in **15**, with the chloride atoms symmetrically bridging adjacent lead atoms. The lead atoms are octahedrally coordinated, with the phenyl groups mutually trans and the octahedra connected via opposite edges to give the chain coordination polymer. Vibrational studies were consistent with the iodine product being pentacoordinated and the chloride and bromide products being hexacoordinated.[95]

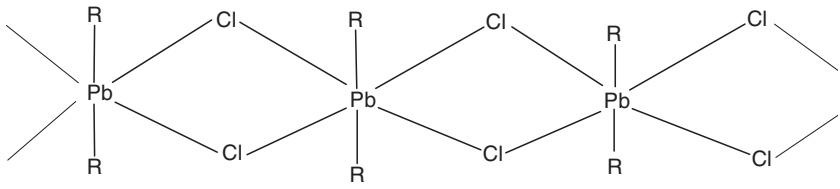

15

D. Oxygen Coordinated Products

The bimetallic compound $(Pb[CO)_9Co_3(CCOO)_2])_n$, which is a chain array, results from the bridging carboxylate ligands.[58] One central unit of this material is shown in **16**, but without the associated carbonyl groups on the cobalt. Pyrolysis gives a bimetallic product that is a stable heterogeneous catalyst for the hydrogenation of 1,3-butadiene.

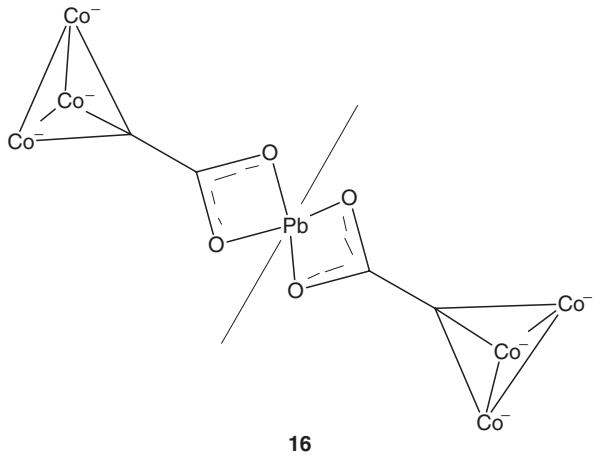

16

Crown ethers are noted for the stability of their lead(II) complexes. Poly(ethylene oxide) is often employed as a crown ether-like material. Thus poly(ethylene oxide) complexes of lead(II) nitrate and bromide were reported.[58] Oligometic ethylene oxides were employed, mostly with four to seven repeat units. The reaction with five repeat ethylene oxide units (four donor ether oxygens) resulted in the

identification of six crystalline materials. The hexaethylene and heptaethylene glycol complexes contained discreet ions. Only the heptaethylene glycol expanded the lead(II) coordination number from eight to nine. The purpose of this study was to study the selective removal of the lead(II) ion from aqueous solutions.

Triphenyllead hydroxide has the analogous structure to that of the organotin analog, forming zigzag chains where the triphenyllead is linked by hydroxide groups.[92] The unsymmetrical O-Pb-O bond length are 2.37 and 2.44 A. A representative structure is given in **17**.

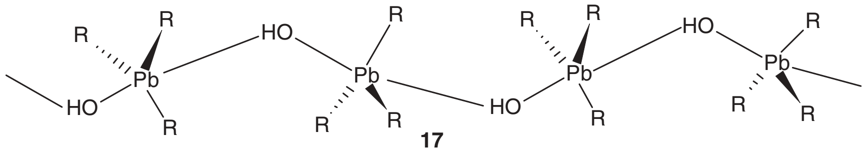

17

Triphenyllead 2-fluoro-4-nitrosophenolate forms a one-dimensional zigzag chain with pentacoordinated lead.[93] A similar structure is found for trimethyllead acetate, which is shown in **18**.[94]

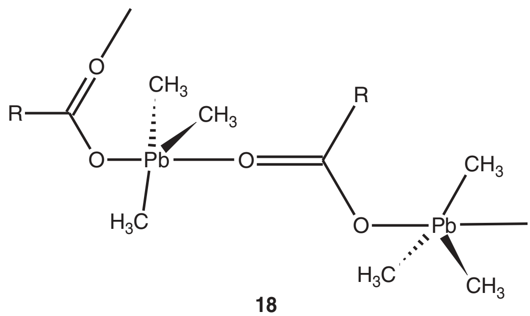

18

Of interest is that the structures of the hydrated and nonhydrated diphenyllead diacetate are different.[95] The monohydrate is a dimer, where the lead atoms are heptacoordinated with the phenyl groups occupying the axial positions of two pentagonal bipyramids. The equatorial positions in the first pentagonal bipyramide have four oxygens of two chelating acetate groups and a water molecule. The equatorial positions of the second pentagonal bipyramid are occupied by four oxygen atoms of two chelating acetate units and a weak Pb–O interaction of an adjacent acetate group chelating the first lead. Further, the coordinated water forms a hydrogen bond to an adjacent acetate group. By comparison, the nonhydrate forms a one-dimensional polymeric chain containing octahedrally configured lead atom sites. One acetate group bridges the units connecting the chain with the second acetate unit and chelates in a symmetrical fashion (**19**). By

contrast, the di-o-tolyllead diacetate and phenyllead triacetate are monomeric in the solid state.[92]

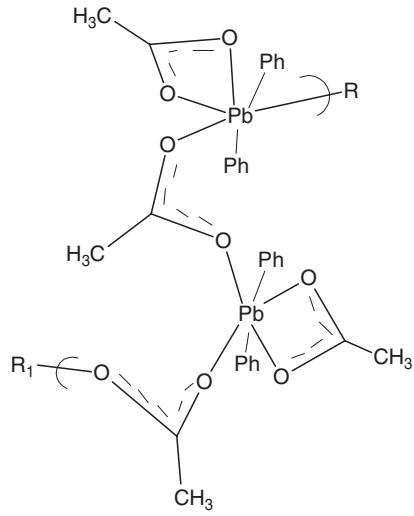

19

VI. CONDENSATION PRODUCTS

As noted before, the lack of suitable solubility and stability of organolead monomers is one reason for the low number of lead-containing polymers reported. We worked extensively to find suitable interfacial systems that would accommodate organolead dihalides but were unable to achieve polymer synthesis. Organolead compounds are soluble in 2,5-hexanedione and acetonitrile solutions when saturated with LiBr or LiCl, but no polymer was formed when these were mixed with aqueous solutions containing Lewis bases, such as salts of organic diacids. We then experimented with DMSO solution systems where the aqueous solution of the diacid salt was added to DMSO solutions containing the organolead halide. Again, no product. Eventually, we developed systems that contained 50/50 mixes of DMSO containing sodium hydroxide and the salt of the diacid with DMSO solutions of organolead dihalide. This allowed the formation of oligomeric lead products as in structure, **20**. Product yield was in the range of a few percent to about 90%. The reaction is rapid, generally reaching a plateau at about 20 seconds of stirring time.

The reaction appears general, occurring with both aliphatic and aromatic diacids and dialkyl and diaryllead dichlorides.[106–110] Aliphaltic silanes and stannanes react to give a greater yield with a given carboxylate anion than do the analogous aromatic compounds. This is also found for the plumbanes. Pi-bonding is believed to occur between the phenyl-pi electrons and empty d-orbitals on the Group IVA metal atom. Such pi-bonding is invoked to explain many kinetic and spectral trends involving Group IVA organometallic compounds. This pi-bonding may cause a reduction in the electronegativity of the metal atom and/or a reduction of the availability of the

d-orbitals to participate in accepting the carboxylate ion via an associative reaction pathway. Either or both of these would result in a decrease in product formation rate and may be responsible for the observed yield trend.

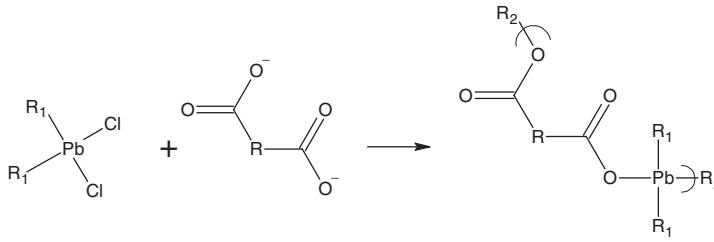

(6)

20

Reaction yields for substituted terephthalic acids are consistent with the Hammett coefficients, such that the more nucleophilic acid salt is favored in the reaction with the electron-poor lead chloride moiety. This is consistent with a nucleophilic attack (probably associative) on the lead atom as being the critical (rate-determining) step.

Yield increases with increase in stirring rate to 21,000 rpm. Above 21,000 rpm foaming becomes significant and restricts good mixing. Regions where yield increases with the stirring rate are called *diffusion-controlled regions*, and they are characteristic of reactions possessing relatively low (generally 40 kJ/mol and lower) activation energies. This is consistent with the reaction being fast and energetic. Nucleophilic attacks by anions on electron-poor sites (as is the lead atom) are fast and occur with low activation energies. This is consistent with the Hammet results.

Yield increases over the range tested as the concentration of reactants increases and is consistent with the idea that the greater the amount of reactant, the greater the amount within the reaction site(s), thus the greater yield. The reaction was also studied as a function of monomer ratio, with the results consistent with a need to have the reactants present in a 1 to 1 ratio.

The lead center can exist as an octahedron (**21**) or as a tetrahedron (**22**). The general tendency for octahedron formation for group IVA metal polyesters is Pb > Sn > Ge > Si. This trend was based on IR data, which in turn was based on X-ray diffraction data of monomeric compounds. Octahedral formation is referred to as

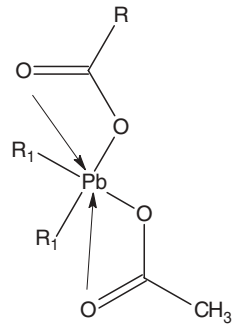

21

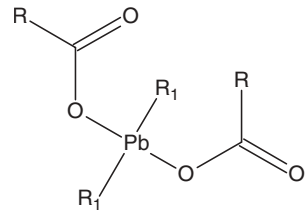

22

bridging, whereas tetrahedral formation is called nonbridging. Bridging assymetric carboxylate carbonyl absorptions are found about 1570 cm^{-1}, whereas nonbridging carboxylate carbonyl absorptions are found about 1610–1650 cm^{-1}. There is also a corresponding difference in the bridging symmetric carboxylate carbonyl bands found around 1410–1430 cm^{-1} and the nonbridging band found around 1350–1370 cm^{-1}. The lead polyesters are of the bridging variety.

TGA thermograms were obtained in air and nitrogen. Weight retention was generally greater for compounds run in nitrogen. Weight loss begins about 275–350ºC, depending on the particular compound. DSC thermograms are markedly different in air and nitrogen and are consistent with degradation in air occurring via an oxidative route, with degradation in air being highly exothermic and nitrogen changes mildly endothermic. An important aspect in evaluating the thermostability of organometallic compounds is the amount of organic moiety present at elevated temperatures, because the formation of metal oxides may represent most of the residue. For the lead polyesters, for the product from tetrafluoroterephthalic acid, and for diethyllead dichloride there is 88% weight retention at 770ºC, of which only 46% could be lead IV oxide.

VII. MISCELLANEOUS

A number of heterocyclic products have been formed from reaction of triorganolead hydroxide with the appropriate heterocyclic compound. Willemsens[111] reported pentacoordinated compounds (**23**) for some of these products. This is probably not the true structure. The formation of oligomeric and polymeric intermediates has been suggested from the disproporationation reactions of hexaethyldilead producing products (**24**).[112,113] Sidgwick[114] reported the formation of plumboxanes from diaryllead dihydroxides, shown as **25** (eq. 7). Kochkin et al.[115] reported the

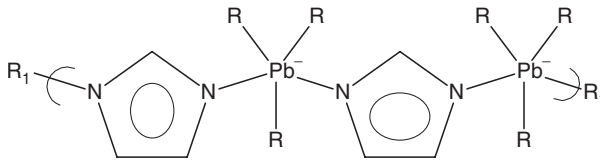

23

formation of similar product plumboxanes from the reaction of diphenyllead dichlorid and alcohol with alcoholic potassium hydroxide.

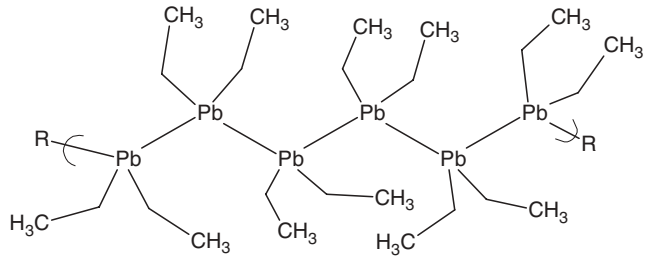

24

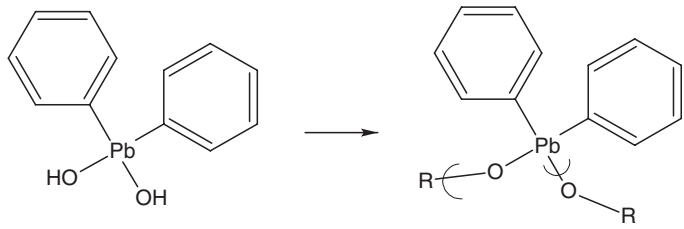

(7)

25

There are probably a number of products that are polymeric in nature but not recognized by the authors as such. In the same way there are materials that have been suggested as being polymeric that are not. Davidson et al.[116] reported the reaction of thioglycolic acid with diphenyllead dihalide as probably being polymeric because it was a high melting solid and insoluble in organic solvents. Additional information is needed before its polymeric structure is accepted or rejected.

Fischer's group[102] reported the synthesis of organolead polymers from combining aqueous solutions of Me_3PbCl and $K_4[M(CN)_6]$ (where M = Fe, Ru), giving supramolecular assemblies. Edelmann et al.[83] also reported supramolecular assemblies of triphenyllead(IV) dimethylphosphinodithiolate, giving a linear structure as noted in **26**. It was reported that the phosphinodithioate ligands were bridging with nearly linear S-Pb-S segments.

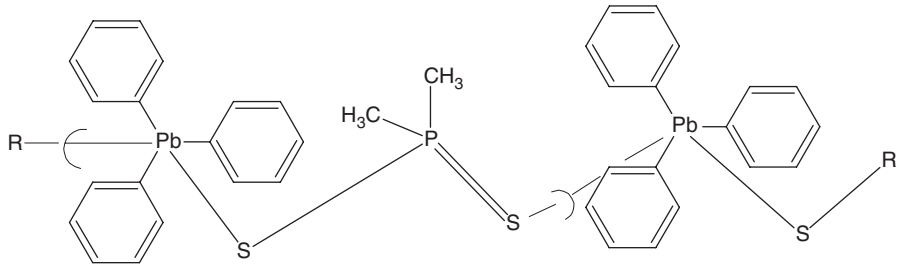

26

VIII. SUMMARY

Numerous lead-containing polymers have been made using both lead(II) and lead(IV). Almost without exception, these materials are not soluble. The potential of lead-containing polymers to be a player in the twenty-first century is there, but much more work needs to be done to even enter the marketplace.

IX. REFERENCES

1. M. Henry, W. Davidson, *Ann. NY Acad. Sci.* **125**, 172 (1965).
2. D. Braun, *Angew. Chem.* **73**, 197 (1961).
3. R. Ingham, H. Gilman, in *Inorganic Polymers*, F. Stone, W. Graham, eds., Academic Press, New York, 1962.
4. T. Wojnarowski, *Polimery* **7**, 165 (1962).
5. K. Jurkschat, M. Mehring, in *The Chemistry of Organic Germanium, Tin, and Lead Compounds*, vol. 2, Z. Rappoport, ed., Wiley, New York, 2002.
6. *Paint Manufacture* **35**, 36 (1965).
7. G. Marchenko, S. Goldobin, G. Smertin, *Vysokomolek. Soedin.* **8**, 2087 (1966).
8. M. Antler, US Patent 3,058,912 (1962).
9. H. Langer, US Patent 3,120,550 (1964).
10. N. Chakravarty, *Indian J. Technol.* **1**, 181 (1963).
11. R. Hatton, L. Stark, Fr. Patent 1,356,569 (1964).
12. H. Shapiro, J. Capinjola, Ethyl Corp., unpublished data.
13. E. Andreeshchev, E. Baroni, N. Kursonova, I. Rosman, *Pribory Tekhn. Eksperim.* **6**, 151 (1961).
14. J. Ktopp, M. Burton, *J. Chem. Phys.* **37**, 1752 (1962).
15. Horizons Inc., Neth. Appl. 6,409, 367 (1965).
16. K. Keck, *Physik*, **178**, 120 (1964).
17. S. Leshchenko, E. Finkel, N. Sheverdina, L. Abramova, V. Karpov, USSR Patent 138,043 (1960).
18. S. Curry, 9th International Symposium of Combustion, Ithaca, New York, 1962.
19. (a) D. Kochkin, *Obrastanie Biokorroziya Vod. Srede.* **164** (1981); (b) C. Skinner, *Paint Varnish Prod.* **64**, 43 (1974).
20. T. Honda, I. Kaetsu, Jpn. Patent 5,222,132 (1993).
21. V. Korshak, A. Polyakova, E. Tambovtseva, *Vysokomol. Soedin.* **2**, 13 (1960).
22. M. Koton, T. Kiseleva, F. Florinskii, *Izvest. Akad. Nauk SSSR, Otdel. Khim. Nauk* 948 (1959).
23. M. Koton, T. Kiseleva, F. Florinskii, *J. Polym. Sci.* **52**, 237 (1961).
24. M. Koton, L. Dokukina, *Vysokomol. Soedin.* **6**, 1791 (1964).
25. H. Pars, W. Graham, E. Atkinson, C. Morgan, *Chem. Ind.* 693 (1960).
26. J. Noltes, H. Budding, G. van der Kerk, *Rec. Trav. Chim.* **79**, 408 (1960).
27. J. Noltes, H. Budding, G. van der Kerk, *Rec. Trav. Chim.* **79**, 1076 (1960).
28. V. Korshak, A. Polyakova, E. Tambovtseva, *Vysokomol. Soedin.* **1**, 1021 (1959).
29. A. Polyakova, V. Korshak, E. Tambovtseva, *Vysokomol. Soedin.* **3**, 662 (1961).
30. A. Leusink, J. Noltes, H. Budding, G. van der Kerk, *AFML Report TR-65-192, R & TD,* Air Force Systems Command, WPAFB, OH, 1965.

31. S. Sandler, J. Dannin, K. Tsou, *J. Polym. Sci.*, A, **3**, 3199 (1956).
32. A. Leusink, J. Noltes, H. Budding, G. van der Kerk, *Rec. Trav. Chim.* **83**, 609 (1964).
33. J. Noltes, G. van der Kerk, *Rec. Trav. Chim.* **80**, 623 (1961).
34. J. Noltes, G. van der Kerk, *Chimia* **16**, 122 (1962).
35. G. Drefahl, G. Plotner, D. Lorenz, *Angew. Chem.* **72**, 454 (1960).
36. E. Baroni, S. Kilin, T. Lebsaddze, I. Rozman, V. Shonuma, *At. Energ. USSR* **17**, 497 (1964).
37. V. de Mello, E. Hauser, T. Lambe, US Patent 2,651,619 (1953).
38. D. Kochkin, G. El'khanov, Z. Smutkina, P. Zubov, *Zhurnal Fizicheskoi Khimii* **44**, 2984 (1970).
39. D. Kochkin, I. Novoderezhkina, P. Zubov, N. Voronkov, *Kinet. Mech. Polyreactions Int. Symp. Mascromol. Chem.* **1**, 175 (1969).
40. B. Rudner, M. Moores, US Patent 3,314,980 (1967).
41. A. Brimah, P. Schwarz, R. Fischer, N. Davies, R. Harris, *J. Organometal. Chem.* **568**, 1 (1998).
42. Y. Shi, Y. Xu, Y. Zhang, Z. Xue, X. You, S. Peng, G. Lee, *Inorg. Chem. Commun.* **5**, 678 (2002).
43. Y. Shi, L. Li, Y. Li, Y. Xu, X. Chem, X. You, *Inorg. Chem. Commun.* **5**, 1090 (2002).
44. Y. Shi, L. Li, Y. Li, X. Chem, Z. Xue, X. You, *Polyhedran* **22**, 917 (2003).
45. G. Bowmaker, J. Harrowfield, H. Miyamae, T. Shand, B. Skelton, A. Soudi, A. White, *Aust. J. Chem.* **49**, 1089 (1997).
46. L. Engelhardt, J. Patrick, C. Whitaker, A. House, *Aust. J. Chem.* **40**, 2107 (1987).
47. H. Miyamae, Y. Numahata, M. Nagata., *Chem. Lett.* 663 (1980).
48. V. Kozozay, A. Sienkiewicz, *Polyhedron* **14**, 1547 (1995).
49. Y. Cui, J. Ren, G. Zhen, W. Yu, Y. Qian, *Acta Crystallogr. C* **56**, E552 (2000).
50. J. Casas, E. Castellano, J. Ellena, M. Gracia-Tasende, A. Sanchex, J. Sordo, M. Vidarte, *Main Group Met. Chem.* **24**, 455 (2001).
51. J. Harrowfield, D. Kepert, H. Miyamae, B. Skelton, A. Soudi, A. White, *Aust. J. Chem.* **49**, 1147 (1996).
52. J. Harrowfield, H. Miyamae, B. Skelton, A. Soudi, A. White, *Aust. J. Chem.* **49**, 1121 (1996).
53. J. Harrowfield, H. Miyamae, T. Shand, B. Skelton, A. Soudi, A. White, *Aust. J. Chem.* **49**, 1043 (1996).
54. J. Harrowfield, H. Miyamae, B. Skelton, A. Soudi, A. White, *Aust. J. Chem.* **49**, 1165 (1966).
55. J. Harrowfield, H. Miyamae, B. Skelton, A. Soudi, A. White, *Aust. J. Chem.* **49**, 1157 (1996).
56. J. Harrowfield, H. Miyamae, B. Skelton, A. Soudi, A. White, *Aust. J. Chem.* **49**, 1029 (1996).
57. H. Zu, Y. Xu, Z. Yu, Q. Wu, K. Fun, Z. You, *Polyhedron* **18**, 3491 (1999).
58. R. Rogers, A. Bond, D. Roden, *Inorg. Chem.* **35**, 6964 (1996).
59. S. Goel, M. Chiang, W. Buhro, *Inorg. Chem.* **29**, 4640 (1990).
60. H. Keller, H. Riebe, *Z. Anorg. Allg. Chem.* **550**, 102 (1987).
61. P. Klufers, J. Schuhmacher, *Z. Anorg. Allg. Chem.* **621**, 19 (1995).
62. A. Cabeza, M. Aranda, S. Bruque, *J. Mater. Chem.* **9**, 571 (1999).
63. S. Ayyappan, G. de Delgado, A. Cheetham, C. Rao, *J. Chem. Soc. Dalton Trans.* 2905 (1999).
64. D. Poojary, B. Zhang, A. Cabeza, M. Aranda, S. Bruque, A. Clearfield, *J. Mater. Chem.* **6**, 639 (1996).
65. P. Colamarino, P. Orioli, W. Benzinger, H. Gillman, *Inorg. Chem.* **15**, 800 (1976).
66. V. Chandrsekhar, A. Chandrasekaran, R. Day, J. Holmes, R. Holmes, *Phosphorus Sulfur Silicon Related Elements* **115**, 125 (1996).
67. X. Lei, M. Shang, A. Patil, E. Wolf, T. Fehlner, *Inorg. Chem.* **35**, 3217 (1996).
68. D. Iacopino, L. Menabue, M. Saladini, *Aust. J. Chem.* **52**, 741 (1999).
69. D. Miernik, T. Lis, *Acta, Crystallogr. C* **52**, 1171 (1996).
70. L. Archer, M. Hampton-Smith, E. Duesler, *Polyhedron* **15**, 929 (1996).

71. S. Sobanska, J. Wignacourt, P. Conflant, M. Drache, M. Langrenee, E. Holt, *New J. Chem.* **23**, 393 (1999).
72. A. Ilyukhin, A. Poznyak, V. Segienko, L. Stopalyanskaya, *Kristallografiya* **43**, 812 (1998).
73. G. Kiosse, O. Bolga, I. Filippova, N. Gerbeleu, V. Lozan, *Kristallografiya* **42**, 1041 (1997).
74. S. Norberg, G. Svensson, J. Albertsson, *Acta Crystallogr. C* **55**, 356 (1999).
75. G. Svensson, S. Olson, J. Albertsson, *Acta, Chem. Scand.* **52**, 868 (1998).
76. M. Kourgiantakis, M. Matzapetakis, C. Raptopoulou, A. Terzis, A. Salifoglou, *Inorg. Chim. Acta* **297**, 134 (2000).
77. M. Tahir, D. Ulku, E. Movsumov, *Acta Crystallogr. C* **52**, 2436 (1996).
78. G. Battistuzzi, M. Borsari, L. Menabue, M. Saladini, M. Sola, *Inorg. Chem.* **35**, 4239 (1996).
79. G. Svensson, J. Albertsson, *Acta Chem. Scand.* **45**, 820 (1991).
80. K. Ebert, H. Breuning, C. Silvestru, I. Stefan, I. Haiduc, *Inorg. Chem.* **33**, 1695 (1994).
81. C. Silverstru, I. Haiduc, R. Cea-Olivares, S. Hernandez-Ortega, *Inorg. Chim. Acta* **233**, 151 (1995).
82. N. Furmanova, Y. Struchkov, D. Kravtsov, E. Rokhina, *J. Struct. Chem.* **20**, 897 (1979).
83. F. Edelmann, I. Haiduc, C. Silvestru, H. Schmidt, M. Noltemeyer, *Polyhedron* **17**, 2043 (1998).
84. R. Clark, A. Davies, R. Puddephatt, *J. Am. Chem. Soc.* **90**, 6923 (1968).
85. R. Clark, A. Davies, R. Puddephatt, *Inorg. Chem.* **8**, 457 (1969).
86. H. Preut, F. Huber, *Z. Anorg. Allg. Chem.* **435**, 234 (1977).
87. R. Hillwig, F. Kunkel, K. Harris, B. Neumuller, K. Dehnicke, *Z. Naturforsch* **52b**, 149 (1997).
88. U. Fahrenkampf, M. Schurmann, F. Huber, *Acta Crystallogr. Ser. C* **50**, 1252 (1994).
89. D. Zhang, S. Dou, A. Weiss, Z. *Naturforsch.* **46a**, 337 (1990).
90. M. Mammi, V. Busetti, A. Del Pra, *Inorg. Chim. Acta* **1**, 419 (1967).
91. I. Wharf, R. Cuenca, E. Besso, M. Onyszchuk, *J. Organomet. Chem.* **277**, 245 (1984).
92. C. Glidewell, D. Liles, *Acta Crystallogr. B* **34**, 129 (1978).
93. (a) N. Bokii, A. Udelnov, Y. Struchkov, D. Kravtsov, V. Pachevskaya, *Zh. Struckt. Khim.* **18**, 1025 (1977); (b) N. Bokii, A. Udelnov, Y. Struchkov, D. Kravtsov, V. Pachevskaya, *J. Struct. Chem.* **18**, 814 (1977).
94. G. Sheldrick, R. Taylor, *Acta Crystallogr. B* **31**, 2740 (1975).
95. C. Graffney, P. Harrison, T. King, *J. Chem. Soc., Dalton Trans.* 1061 (1982).
96. M. Schurmann, F. Huber, *J. Organomet. Chem.* **530**, 121 (1997).
97. Y. Chow, D. Britton, *Acta Crystallogr. B* **27**, 856 (1971).
98. J. Konnert, D. Britton, Y. Chow, *Acta Crystallogr. B* **28**, 180 (1972).
99. J. Muller, U. Muller, A. Loss, J. Lorberth, H. Donath, W. Massa, *Z. Naturforsh.* **40b**, 1320 (1985).
100. A. Ibrahim, T. Soliman, S. Etaiw, R. Fisher, *J. Orgnomet. Chem.* **468**, 93 (1994).
101. A. Ibrahim, S. Etaiw, T. Soliman, *J. Organomet. Chem.* **430**, 87 (1992).
102. A. Brimah, P. Schwarz, R. Fischer, N. Davies, R. Harris, *J. Organomet. Chem.* **568**, 1 (1998).
103. U. Behrens, A. Brimah, T. Soliman, R. Fischer, D. Apperley, N. Davies, R. Harris, *Organometallics* **11**, 1718 (1992).
104. A. Ibrahim, S. Etaiw, *Polyherdon* **16**, 1585 (1997).
105. R. Allmann, A. Waskowska, R. Hohlfeld, J. Lorberth, *J. Organomet. Chem.* **198**, 155 (1980).
106. C. Carraher, C. Deremo Reese, *Organometallic Polymers*, Academic Press, New York, 1978.
107. C. Carraher, C. Deremo Reese, *Coat. Plastics* **37**, 162 (1977).
108. C. Carraher, C. Deremo Reese, *Angew. Makromol. Chem.* **65**, 95 (1977).
109. C. Carraher, C. Deremo Reese, *J. Polym. Sci.* **16**, 491 (1978).

110. (a) C. Carraher, R. Dammeier, *Makromol. Chem.* **135**, 197 (1970); (b) C. Carraher, R. Dammeier, *Makromol. Chem.* **141**, 245 (1971); (c) C. Carraher, R. Dammeier, *Makromol. Chem.* **141**, 251 (1971); (d) C. Carraher, R. Dammeier, *Makromol. Chem.* **141**, 259 (1971).
111. L. Willemsens, paper presented to the International Lead Zinc Research Organization, New York, 1964.
112. G. Razuvaev, N. Vyazankin, Yu. Dergunov, *Dokl. Akad. Nauk. SSSR* **132**, 364 (1960).
113. G. Razuvaev, N. Vyazankin, Yu. Dergunov, *Zh. Obshch. Khim.* **30**, 1310 (1960).
114. N. Sidwick, *Chemical Elements and Their Compounds*, Oxford Press, London, 1950.
115. D. A. Kochkin, L. Lukijanova, E. Reznikova, *Zh. Obshch. Khim.* **33**, 1945 (1963).
116. W. Davidson, K. Hills, M. Henry, *J. Organometal. Chem.* **3**, 285 (1965).

Index

C

Q

R